

**SCOPE OF MICROPOROUS AND MESOPOROUS MOLECULAR
SIEVES IN THE OXIDATION OF HIGHER ALKANES
WITH OZONE**

Submitted in fulfilment of the academic requirements for the degree of Doctor of Philosophy in
the School of Chemistry, University of KwaZulu-Natal, Westville campus, Durban, South Africa.



By

V. S. R. RAJASEKHAR PULLABHOTLA

3 March 2008

**SCOPE OF MICROPOROUS AND MESOPOROUS MOLECULAR
SIEVES IN THE OXIDATION OF HIGHER ALKANES
WITH OZONE**

By

V. S. R. RAJASEKHAR PULLABHOTLA

Submitted in fulfilment of the academic requirements for the degree of Doctor of Philosophy in
the School of Chemistry, University of KwaZulu-Natal, Westville campus, Durban.

3 March 2008

**DEDICATED TO
MY BELOVED FAMILY MEMBERS**

ABSTRACT

Alkane-rich fractions including n-paraffins are the most important chemical feedstock used in the petrochemical industry. Alkanes, the saturated hydrocarbons, are known to exhibit extremely low reactivity, and reactions are achievable only at high temperature and pressure conditions. The reaction of saturated organics with ozone is at the focus of current research. The main objective of the study is to investigate the scope of the ozone as the oxidant for the conversion of saturated higher hydrocarbons, C₁₂, C₁₄ and C₁₆ alkanes to value added products at moderate reaction conditions.

Ozonation products of these higher hydrocarbons were studied under varied conditions as function of time. Major products of the uncatalysed reaction were their corresponding 4-, 3-, and 2- ketone isomers. With longer ozonation, while the percentage conversion increased, a further oxidation of the keto isomers was observed, resulting in corresponding carboxylic acids. The abstraction of hydrogen from the secondary carbon atom at 4- or 3- or 2-positions of the n-alkane and the formation of alkyl radical, hydrotrioxide, alkyl hydroxide, and alkyl dihydroxy intermediates are proposed in the mechanism of ozonation of higher n-alkanes. The selectivity towards 4-ketone is much higher and 3- and 2-ketones were the minor products. The product ratio of 3-ketone and 2-ketones, increased with the decrease in the chain length of the n-alkane (n-C₁₆ < n-C₁₄ < n-C₁₂). The oxidation products were separated using a column and characterized by gas chromatography-mass spectroscopy, Fourier-transform infrared spectroscopy, ¹H NMR, melting point and boiling point analyses.

Activated charcoal as a catalyst in the ozone initiated oxidation of higher alkanes to facilitate the decomposition of ozone, showed poor activity. The suitability of variety of materials as catalysts of oxidative ozonation was investigated. The catalyst materials investigated are silica gel, vanadium phosphorous oxides (VPO), Pd/γ-Al₂O₃, Ni/γ-Al₂O₃, V/γ-Al₂O₃, Pd/γ-Al₂O₃ (N₂ calcined), Ni/γ-Al₂O₃ (N₂ calcined) and V/γ-Al₂O₃ (N₂ calcined), microporous uni-dimensional and 3-dimensional zeolite material viz. U/Na-Y, U/ZSM-5 Si/Al-30, U/silica, Pd/Na-Y, Pd/Na-Y (N₂ calcined), Pd/ZSM-5 Si/Al-30, Pd/ZSM-5 Si/Al-30 (N₂ calcined), Ni/Na-Y, Ni/Na-Y (N₂ calcined), Ni/ZSM-5 Si/Al-30, Ni/ZSM-5 Si/Al-30 (N₂ calcined), V/Na-Y, V/Na-Y (N₂ calcined), V/ZSM-5 Si/Al-30, V/ZSM-5 Si/Al-30 (N₂ calcined), mesoporous Al-MCM-41 Si/Al-90 and Al-MCM-41 Si/Al-60. These materials were employed to improve the activity on conversion and selectivity of the catalytic ozonation of higher alkanes.

In the catalytic ozonation reactions, 5% w/v catalyst was charged. Pd/ γ -Al₂O₃ N₂ calcined, Pd/ γ -Al₂O₃ catalysts gave higher conversion on longer duration of ozonation (18-24 h). The activity towards conversion of n-hexadecane with the Pd loaded γ -Al₂O₃ was higher than that of the Ni and V metal impregnated γ -Al₂O₃. The order of catalytic activity with the metal supported on Al₂O₃ was found to be Pd > Ni \approx V. The percentage conversion and selectivities using different catalyst systems varied between 27 to 56 and 37 to 55 respectively.

The zeolite-X, Al-MCM-41 and VPO catalytic systems were synthesized. The commercially available zeolites, Na-Y, Zeolite Beta and ZSM-5 were modified to increase the acidic sites by impregnating different metals namely U, Ni, V and Pd on microporous zeolite supports. The catalysts were characterized by powder X-ray diffraction, Scanning electron microscopy, Diffuse reflectance ultraviolet-visible spectroscopy (DR UV-VIS), Fourier-transform infrared spectroscopy, Thermal analysis (TG-DTA), and BET surface area analysis.

The X-ray diffractograms of the zeolite supports and metal loaded zeolites showed the crystalline structure of micro and mesoporous materials, the structure of ZSM-5, Na-Y and Al-MCM-41 catalysts remained intact after the impregnation conditions. All the zeolite supports and metal loaded zeolites showed the characteristic bands in the FT-IR spectra, which were in good agreement with the literature. Regarding the catalysts morphologies, SEM images clearly pointed out the homogeneity in shapes for all samples. All samples were highly crystalline in nature. The total surface areas (BET) of all samples were high as it was expected. The samples maintained the high surface area even after calcination. The results are in agreement with the BET surface area measurements that showed a little decrease in the surface area upon metal (U, Ni, V and Pd) impregnation. The BET observations signified that there was a decrease in the surface area of the samples calcined under N₂ flow conditions.

Diffuse reflectance spectroscopy was employed to investigate the symmetry and the valence of the supported metals. The DR UV-Vis spectra of Ni-, V- and Pd-loaded catalysts displayed their characteristic bands, which were attributed to Ni²⁺, V⁵⁺ and Pd²⁺ cations in different zeolites. In the thermal analysis of synthesized Al-MCM-41 catalysts followed a three-stage weight loss, which is a characteristic of mesoporous materials.

It was observed that the acidity (Si/Al ratio) had no effect on the conversion of n-hexadecane. The ozonation studies on higher n-alkanes with microporous and mesoporous catalysts reveals

that Ni/Na-Y, Ni/ZSM-5, Ni/ZSM-5 N₂ calcined, V/Na-Y, Al-MCM-41 Si/Al-60 and Al-MCM-41 Si/Al-90 catalysts conversion activity was above 50%. U loaded ZSM-5 was highly active catalyst in the ozonation of n-hexadecane (55%). A plausible mechanism for the ozonation of higher alkanes with U/ZSM-5 zeolite catalyst is proposed.

The catalytic ozonation reactions, the catalysts which yielded higher conversions, showed poor selectivity towards the major product 4-hexadecanone and vice-versa. U/ZSM-5, Pd/ γ -Al₂O₃ N₂ calcined and Al-MCM-41 (Si/Al-60 and 90) are the promising catalysts for better conversions (55%, 56% and 52% respectively) in the ozonation of higher alkanes. The selectivity in favour of 4-hexadecanone with 5%Ni/HB150 (55%), Ni/Na-Y N₂ calcined (54%), HBeta-40 (53%) and Pd/Na-Y N₂ calcined (52%) catalysts were appreciable. The 3D zeolites Na-Y and HB150 showed highest selectivity towards the 4-hexadecanone compound.

Calcination of the catalysts under N₂ flow conditions had no effect on the activity of the catalysts towards the conversion and selectivity. Catalysts with 3-dimensional pore geometry showed better activity towards the conversion and selectivity. With different Si/Al ratios of the Al-MCM-41 catalysts, same rate of conversion was observed after 24 h ozonation.

The efficiencies of microporous and mesoporous catalysts on ozonation of higher alkanes (n-hexadecane), with respect to the conversion, reaction products, yields and selectivity were compared. The oxidation of the long chained alkanes to their keto products at moderate conditions is of significance, in that hitherto unreactive n-alkanes can be functionalised via ozonation, catalytically or non-catalytically.

DECLARATION

I hereby certify that this thesis is my own work, except where specifically acknowledged in the text. Neither the present thesis nor any part there of, has been submitted by any other University for a degree.

Author:

V. S. R. Rajasekhar Pullabhotla

PREFACE

The experimental work described in this thesis was carried out at the School of Chemistry, University of KwaZulu-Natal, Westville campus, Durban, from March 2003 to December 2005, under the supervision of Professor S.B. Jonnalagadda and Dr. C. Southway.

These studies represent original work by the author and have not otherwise been submitted in any form for any degree or diploma to any tertiary institution. Where use has been made of the work of others it is duly acknowledged in the text.

V. S. R. Rajasekhar Pullabhotla

ACKNOWLEDGEMENTS

I would like to express my deep sense of gratitude and sincere thanks to Professor S.B. Jonnalagadda for his valuable guidance and encouragement throughout this study. I am grateful to him for all the freedom he has given me in the entire course of this work.

I would also like to mention my sincere gratitude to my Co-supervisor, Dr. Colin Southway, School of Chemistry, Pietermaritzburg campus, University of KwaZulu-Natal for the instrumental facilities and fruitful discussions.

I would like to thank National Research Foundation, Pretoria, the School of Chemistry and the School of Pharmacy at Westville campus, University of KwaZulu-Natal for funding me through the fellowship and teaching assistantship for my PhD studies.

I acknowledge the kind support received from the Post Doctoral Fellows Dr. L. K. Uppalla for his keen moral support and suggestions during the experimental work. I also thank Dr. A. Ramakrishna and Dr. Ateeq Rahman for their support in finalizing the thesis and nice company throughout their stay at UKZN.

I would also like to thank Prof. P. Selvam, from the Department of Chemistry, Indian Institute of Technology-Bombay, India, for giving me opportunity to work in his laboratories and his research group under his able guidance.

I sincerely acknowledge the kind support received from Prof. John Dunlevy (School of Geological Sciences, Westville campus, UKZN) especially for his encouragement and help in the XRD analysis and interpretation.

I would like to thank the faculty staff members, School of Chemistry (Westville) and others for their kind support and encouragement. I am very grateful to Prof. F. O. Shode, Mr. Silver Naidoo and Dr. J. A. Nevines for their constructive suggestions.

This thesis would not have been possible without the help provided by a lot of people. My sincere thanks to Dr. K. Vidya (IIT-Bombay, India) her help during the initial stages of the catalysis work. I wish to thank Miss. Tutusa from EM Unit, Westville campus, UKZN.

It may not be possible to mention here the names of all technical staff at UKZN who have helped me during course of this study. I am grateful to all of them, in particular, I would like to thank Mr. Raj Suchipersadh, Mr. Logan Naidoo, Mrs. Shoba Sooklall, Miss. Indrani, Mr. Shannon, Mrs. Malini Padayachee, Miss. Sayuree Chellakootty and Mrs. Ria Singh. My sincere thanks due to Mr. Bret Parel and Mr. Dilip Jagjivan for their help in GC-MS and NMR analysis.

It is a nice opportunity to thank all my labmates, Mr. Viren Chunnillall, Mr. Srinivasu Nadupalli, Miss. Favorite Zuma. I wish to thank all my friends from IIT-Bombay laboratory and Hostel especially, Mr. Kuppu Swamy, Mr. Ranga, Mr. Rahul Nandurikar, Ms. K. Vidya and Mr. Vilas Rawat, friends who made life much easier and cheerful through their personal association, moreover boosting the morale during hard times.

I am very fortunate to be blessed with some brilliant teachers of per excellence whose teaching, inspiration and encouragement have paved the path of my life to where I stand today. I thank them from the core of my heart.

I am very thankful to my good friend Mr. Sarangapani Baruri for his constant moral support, perseverance and encouragement throughout my stay here.

Last but not the least my parents Mr. V. Subbaraya Sastry Pullabhotla and Mrs. Kanchanamala Pullabhotla, whose immense crave for higher studies made me motivated in the field of research. Any word would be less to describe their sacrifice and contribution in my life. Their encouragement, love, blessings, trust and constant support have been out of the world. The freedom of thought that they have given me is just awesome. I take this opportunity to thank my brothers Mr. Chandrasekhar Pullabhotla and Mr. Madhusudhan Pullabhotla, without whom I am nothing. No words can express the gratitude and thanks to the person who has been at every step of my thoughts - my life partner Mrs. Rajani Pullabhotla. Her whole personality has been of great influence to me. Lastly, everything goes waste without thanking the chemist of the chemists, whose laboratory is our mother Earth!

V. S. R. Rajasekhar Pullabhotla

Communications

1. V. S. R. Rajasekhar Pullabhotla, Colin Southway and Sreekanth B. Jonnalagadda, ***“Oxidation of Higher Aliphatic Hydrocarbon, n-Hexadecane using Ozone.”*** Oxidation Communications, **2008**, 31 (In Press).
2. V. S. R. Rajasekhar Pullabhotla, Colin Southway and Sreekanth B. Jonnalagadda, ***“Ozone Initiated Oxidation of Hexadecane with Metal Loaded γ -Al₂O₃ Catalysts.”*** Catalysis Letters, **2008** (In Press). <http://dx.doi.org/10.1007/s10562-008-9434-4>
3. V. S. R. Rajasekhar Pullabhotla, Colin Southway and Sreekanth B. Jonnalagadda, ***“Oxidation of n-Hexadecane with Uranyl Loaded/Anchored Microporous Zeolites and Ozone.”*** Catalysis Communications, **2008** (In Press).
4. V. S. R. Rajasekhar Pullabhotla, Colin Southway and Sreekanth B. Jonnalagadda, ***“Oxidation of Higher Alkanes at Moderate Reaction Conditions with Ozone in presence of Mesoporous Materials.”*** Communicated to Journal of Advanced Oxidation Technologies, **2008**.
5. V. S. R. Rajasekhar Pullabhotla, Colin Southway and Sreekanth B. Jonnalagadda, ***“Ozone Initiated Oxidation of Three Higher n-Alkanes in presence of Activated Charcoal or Silica Gel.”*** Communicated to Reaction Kinetics and Catalysis Letters, **2008**.

Presentations at conferences

1. Oral presentation entitled ***“Oxidation of Higher Aliphatic Hydrocarbons with Ozone”*** in the South African Chemical Institute (SACI) research colloquia at University of KwaZulu-Natal, Pietermaritzburg, South Africa, June **2004**.
2. Oral presentation entitled ***“Catalytic Degradation of Higher Hydrocarbons (n-Hexadecane) with Ozone.”*** Research Day colloquia at University of KwaZulu-Natal, Westville, Durban, South Africa, August **2004**.
3. Oral presentation entitled ***“Ozonation of Higher Aliphatic Hydrocarbons”*** in the SACI research colloquia at University of KwaZulu-Natal, Durban, South Africa, May **2005**.
4. Oral presentation entitled ***“Catalytic Degradation of Higher Hydrocarbons (Hexadecane) with Ozone.”*** Research Day colloquia at University of KwaZulu-Natal, Howard campus, Durban, South Africa, September **2005**.
5. Oral presentation entitled ***“Catalytic Oxidation of the Higher Hydrocarbons with Ozone”*** at Carman National Physical Chemistry conference, Johannesburg, South Africa,

November **2005**.

6. Poster presentation entitled ***“Scope of Microporous and Mesoporous Zeolites in the Ozonation of Higher Alkanes”*** at Catalysis Society of South Africa (CATSA) conference, Mosselbay, South Africa, November **2006**.
7. Poster presentation entitled ***“Oxidation of Higher Alkanes at Moderate Reaction Conditions with Mesoporous Catalysts and Ozone”*** at The 38th National Convention of the South African Chemical Institute, Durban, South Africa, December **2006**.
8. Poster presentation entitled ***“Oxidation of Higher Aliphatic Hydrocarbon, n-Hexadecane with Ozone using Various Catalyst Materials”*** at The International Symposium on Relations between Homogeneous and Heterogeneous Catalysis, Berkeley, California, USA, July **2007**.
9. Oral presentation entitled ***“Oxidation of Higher Alkanes with Uranyl Anchored Microporous Zeolites and Ozone”*** in the SACI research colloquia at University of Zululand, South Africa, September **2007**.
10. Oral presentation entitled ***“Oxidation of Higher Alkanes with Uranyl Loaded Microporous Zeolites”*** at Catalysis Society of South Africa (CATSA) conference, Richardsbay, South Africa, November **2007**.
11. Oral presentation entitled ***“Scope of Microporous and Mesoporous Zeolites in the Ozonation of Higher Alkanes”*** at International Conference on Catalysis in Membrane Reactors (ICCMR8) Calcutta, India, December **2007**.

CONTENTS

CHAPTER I: INTRODUCTION AND LITERATURE REVIEW

1.0	Introduction.	1
1.1.	Discovery of ozone.	2
1.2.	Atmospheric ozone.	3
1.3.	Industrial uses of ozone.	3
1.4.	Methods for generation of ozone.	4
1.4.1.	Photochemical ozone generation.	4
1.4.2.	Electrolytic ozone generation.	5
1.4.3.	Radiochemical ozone generation.	5
1.4.4.	Ozone generation by Corona discharge method.	5
1.5.	Properties of ozone.	7
1.5.1.	Physical properties of ozone.	7
1.5.2.	Chemistry of ozone.	9
1.5.2.1.	Molecular ozone reactivity.	10
1.5.2.1.a.	Cyclo addition (Criegee mechanism).	10
1.5.2.1.b.	Electrophilic reaction.	11
1.5.2.1.c.	Nucleophilic reaction.	12
1.5.3.	Decomposition of ozone: (aqueous solution as the medium).	13
1.5.3.1.	Initiators, promoters and inhibitors of free-radical reactions.	15
1.5.4.	Solvent effect and the carrier gas effect in the ozonation reactions.	16
1.5.5.	Importance of oxygen in O ₃ -O ₂ mixture.	22
1.6.	Mechanisms for the reaction of ozone with hydrocarbons.	23
1.7.	Reaction of ozone with saturated compounds.	24
1.7.1.	Mechanism of saturated hydrocarbons ozonation.	24
1.7.2.	Complex formation in between ozone and saturated hydrocarbons.	27
1.7.3.	Formation of singlet oxygen from hydrotrioxides in the ozonation of hydrocarbons.	28
1.7.4.	Mechanism for decomposition of the hydrotrioxide.	31
1.8.	Ozonation of cycloalkanes (cyclohexane and cyclodecane).	39
1.9.	Ozone in the treatment of water and wastewaters.	42
1.9.1.	Drinking water treatment.	43
1.9.1.a.	Disinfection.	45
1.9.1.b.	Oxidation of inorganic compounds.	46
1.9.1.c.	Oxidation of organic compounds.	46
1.9.1.d.	Particle removal processes.	50
1.9.2.	High purity water systems.	50
1.9.3.	Ozonation in wastewater treatment.	50
1.10.	Chemical oxidation.	51
1.10.1.	Advanced Oxidation Processes (AOPs).	52
1.10.1.1.	Ozone + catalyst (Catazone).	56
1.10.1.1.a.	Activated carbon.	57
1.10.1.1.b.	Ozonation with silica gel.	58
1.10.1.1.c.	Formation of ketones in ozonation of 3-methylpentane.	59
1.10.1.1.d.	Catalytic ozonation processes.	61
1.10.1.1.e.	Catalytic ozonation with Al ₂ O ₃ .	64
1.10.1.1.f.	Metal oxides as catalysts in ozonation reaction.	68

1.10.1.1.g.	Metal on support.	71
1.10.1.1.h.	Zeolites in oxidation of higher hydrocarbons.	72
1.11.	Zeolites as catalysts in the ozonation of hydrocarbons.	75
1.11.1.	Oxyfunctionalisation of alkanes with catalysts.	76
1.11.2.	Zeolites as catalysts.	79
1.11.3.	Classification of zeolite molecular sieves.	79
1.11.3.1.	Framework structure.	81
1.11.4.	Adsorption and separation.	82
1.11.5.	Ion exchange.	83
1.11.6.	Zeolites and the environment.	84
1.11.7.	Significance of Si/Al ratio.	88
1.11.8.	Uranium loaded catalysts.	91
1.11.9.	Limitation of microporous molecular sieves.	92
1.11.10.	Mesoporous molecular sieves.	92
1.12.	Objectives of the study.	93

CHAPTER II: MATERIALS AND METHODS

2.0.	Introduction.	94
2.1.	Ozonator instrument calibration.	95
2.1.1.	Ozone concentration determination.	95
2.1.2.	Preparation of solutions and standardization.	95
2.2.	Ozonation of n-hexadecane with different solvents.	102
2.3.	Reaction in absence of solvent at room temperature.	104
2.4.	Thin Layer Chromatography (TLC).	105
2.5.	Gas Chromatography-Mass Spectroscopy (GC-MS).	105
2.5.1.	Gas Chromatography (GC).	106
2.6.	Sodium bicarbonate extraction procedure.	106
2.7.	Product separation by column chromatographic technique.	107
2.8.	Catalytic ozonation.	107
2.8.1.	Zeolites synthesis and impregnation techniques.	107
2.9.	Synthesis of mesoporous molecular sieves: Hydrothermal synthesis.	108
2.10.	MCM-41.	110
2.10.1.	Al-MCM-41.	113
2.11.	Calcination.	114
2.12.	Metal Impregnation.	115
2.13.	Calcination under N ₂ flow conditions.	116
2.14.	Characterisation.	116
2.14.1.	Powder X-ray diffraction (XRD).	116
2.14.2.	Fourier transform-infrared (FT-IR) spectroscopy.	116
2.14.3.	Diffuse reflectance ultraviolet-visible (DR UV-VIS) spectroscopy.	117
2.14.4.	Thermogravimetry-Differential Thermal Analysis (TG-DTA).	117
2.14.5.	Scanning Electron Microscopy (SEM).	117
2.14.6.	Brunauer-Emmett-Teller (BET) surface area analysis.	118
2.15.	Ozonation reactions with microporous and mesoporous molecular sieves.	118

CHAPTER III: CATALYSTS CHARACTERISATION

3.0.	Introduction.	122
3.1.	X-ray diffraction studies.	122
3.1.1.	XRD results for Ni-impregnated zeolites.	122
3.1.2.	XRD results for V-impregnated zeolites.	125
3.1.3.	XRD results for Pd-impregnated zeolites.	129
3.1.4.	XRD results for mesoporous MCM-41 catalysts.	131
3.2.	Diffuse reflectance UV-Visible spectroscopy.	132
3.2.1.	Ni Loaded zeolites DR UV-Visible spectroscopy.	132
3.2.2.	DR UV-Visible spectroscopy for V-containing zeolites.	135
3.2.3.	Pd containing zeolites DR UV-Visible spectroscopy.	138
3.3.	Thermal analysis of mesoporous catalysts (TG-DTA).	140
3.4.	FT-IR analysis of zeolites.	142
3.4.1.	IR spectra for Na-Y zeolite.	143
3.4.2.	IR Spectra for ZSM-5 Si/Al-30.	144
3.4.3.	IR Spectra for zeolite- β .	145
3.4.4.	IR analysis for Ni Loaded zeolites.	146
3.4.5.	IR analysis for V loaded zeolites.	147
3.4.6.	IR analysis for Pd loaded zeolites.	148
3.4.7.	IR analysis for U loaded catalysts.	150
3.4.8.	FT-IR analysis for as-synthesized Al-MCM-41 catalysts.	152
3.5.	Scanning Electron Microscopy (SEM) technique.	155
3.6.	BET surface area determination.	160

CHAPTER IV: OXIDATION OF HIGHER n-ALKANES WITH OZONE, UNCATALYSED AND IN PRESENCE OF ACTIVATED CHARCOAL

4.0.	Introduction.	162
4.1.	Scope of CCl_4 as solvent for ozonation of n-hexadecane.	162
4.2.	Scope of tetrahydrofuran as solvent for ozonation of n-hexadecane.	166
4.3.	Product analysis for ozonation of n-hexadecane in the absence of solvent.	168
4.3.1.	Gas chromatography analysis of product mixture.	168
4.3.2.a.	FT-IR analysis of the product mixture.	171
4.3.2.b.	FT-IR analysis of the isolated products.	172
4.3.3.	^1H NMR analysis of 4-, 3- and 2-hexadecanone products.	173
4.4.	Mechanism of the ozone initiated oxidation of higher alkane.	175
4.4.1.	Formation of alkyl, hydrotrioxide, alkyl hydroxide and alkyl hydroxyl oxide.	176
4.4.2.	Formation of carboxylic acids during the ozonation (further oxidation of the products formed).	177
4.5.	Ozonation of n-hexadecane in flat bottom flask under solvent free conditions.	179
4.6.	Ozonation of n-hexadecane in long column reactor.	181
4.7.	Ozonation of n-tetradecane under similar conditions as for n-hexadecane.	183
4.8.	Ozonation of n-dodecane under similar conditions as for n-hexadecane.	185
4.9.	Ozonation of n-hexadecane with activated charcoal as catalyst.	186
4.9.1.	Comparison of uncatalysed n-hexadecane ozonation reaction and reactions in presence of activated charcoal.	188
4.10.	Ozonation of n-tetradecane with activated charcoal as catalyst.	189
4.10.1.	Comparison of uncatalysed n-hexadecane ozonation reaction and reactions in presence of activated charcoal.	190

4.11.	Ozonation of n-dodecane with activated charcoal as catalyst.	191
-------	--	-----

CHAPTER V: OZONATION OF HIGHER n-ALKANES WITH SILICA GEL, VPO AND METAL SUPPORTED γ -Al₂O₃ CATALYSTS

5.0.	Introduction.	195
5.1.	Ozonation in presence of silica gel or VPO catalysts.	195
5.1.1.	Ozonation of n-hexadecane with silica gel.	195
5.1.2.	Ozonation of n-hexadecane with VPO.	197
5.1.3.	Ozonation of n-tetradecane with silica gel.	198
5.1.4.	Ozonation of n-tetradecane with VPO.	200
5.1.5.	Ozonation of n-dodecane with silica gel.	201
5.1.6.	Ozonation of n-dodecane with VPO.	202
5.2.	Ozonation of n-hexadecane with 0.5% metal (Pd, Ni and V) loaded on γ -alumina catalysts.	204
5.2.1.	Ozonation of n-hexadecane with 0.5% Pd loaded on γ -Al ₂ O ₃ catalysts.	204
5.2.2.	Ozonation of n-hexadecane with 0.5% Ni loaded γ -Al ₂ O ₃ catalysts.	208
5.2.3.	Ozonation of n-hexadecane with 0.5% V loaded γ -Al ₂ O ₃ catalysts.	211
5.3.	Comparison of conversion and selectivity of n-hexadecane with silica gel, VPO and 0.5% metal loaded γ -Al ₂ O ₃ .	214

CHAPTER VI: SCOPE OF MESOPOROUS AND MICROPOROUS MATERIAL IN OZONE INITIATED OXIDATION OF HIGHER HYDROCARBONS

6.0.	Introduction.	220
6.1.	Ozonation of n-hexadecane with 0.5% Pd loaded zeolites.	220
6.2.	Ozonation of n-hexadecane with 0.5% Ni loaded zeolites.	225
6.3.	Ozonation of n-hexadecane with 0.5% V loaded zeolites.	229
6.4.	Ozonation of n-hexadecane with 0.5% U loaded zeolites.	232
6.4.1.	Proposed mechanism for the ozonation of n-alkanes with U/ZSM-5.	235
6.5.	Ozonation of n-hexadecane using Al-MCM-41 with different Si/Al ratios.	239
6.6.	Ozonation of higher alkanes (n-C ₁₆ H ₃₄ , n-C ₁₄ H ₃₀ and n-C ₁₂ H ₂₆) with zeolite beta (H form) catalyst.	241
6.7.	Ozonation of higher alkanes (n-C ₁₆ H ₃₄ and n-C ₁₄ H ₃₀) with zeolite-X catalyst.	244
6.8.	Ozonation of n-hexadecane with 5% metal loaded zeolite catalysts.	246
6.8.1.	Ozonation of n-hexadecane with 5% Ni on different zeolite supports.	246
6.8.2.	Ozonation of n-hexadecane with 5% metal on HB150 zeolite.	249
6.9.	Comparison of the efficiency of n-hexadecane conversion with different 5% metal loaded zeolite catalysts.	252
6.9.1.	Comparison of the selectivity for 4-hexadecanone with different 5% metal loaded zeolite catalysts.	253
6.10.	Mechanism for ozone decomposition on catalyst sites.	255
6.10.1.	Mechanism of heterogeneous catalytic ozonation.	255
6.11.	Comparison of the efficiency of n-hexadecane conversion with different metal loaded ZSM-5 (Si/Al-30) catalysts.	255
6.11.1.	Comparison of the selectivity for 4-hexadecanone with different metal loaded ZSM-5 (Si/Al-30) catalysts.	257
6.12.	Comparison of the efficiency of n-hexadecane conversion with different metal loaded Na-Y catalysts.	259
6.12.1.	Comparison of the selectivity for 4-hexadecanone with different	

metal loaded Na-Y catalysts.	260	
CHAPTER VII: CONCLUSIONS	263	
REFERENCES	266	
LIST OF TABLES		
Table 1.1.	Solubility of ozone in water.	8
Table 1.2.	Physical properties of ozone.	8
Table 1.3.	Relative oxidation potentials.	9
Table 1.4.	Stoichiometry of some ozone-paraffin reactions.	27
Table 1.5.	Reactivities of some alkanes towards ozone and some radical species.	29
Table 1.6.	Secondary hydroxylation of straight chain alkanes by H ₂ O ₂ (or H ₂ O ₃) formed in their ozonolysis in superacids.	37
Table 1.7.	Typical initiators, promoters and inhibitors for decomposition of ozone by radical type chain reaction, encountered in natural waters and wastewaters.	44
Table 1.8.	Degree of removal of the trace organic compounds during ozonation.	49
Table 1.9.	Oxidizable compounds by hydroxyl radicals.	53
Table 1.10.	Second order rate for ozone and hydroxyl radical •OH for a variety of compounds.	54
Table 1.11.	Product distribution from ozonation of 3-methylpentane at various temperatures.	59
Table 1.12.	Comparison of average rates of decomposition of aqueous ozone on different metal loaded γ-Al ₂ O ₃ .	66
Table 1.13.	Mechanisms for decomposition of ozone.	66
Table 1.14.	Average rates of the decomposition of aqueous ozone on solid phase.	70
Table 1.15.	Product distribution in the oxidation of linear alkanes.	78
Table 1.16.	Classification of molecular sieves on the basis of pore size.	81
Table 1.17.	Characteristic properties of selected aluminosilicates.	91
Table 2.1.	Determination of ozone concentration at room temperature (20 ± 1 °C) and different applied voltages.	98
Table 2.2.	Determination of ozone concentration at 120 V and different temperatures.	99
Table 2.3.	Specifications of the various starting materials used for the synthesis of various molecular sieves.	119
Table 2.4.	Specifications of the various reagents and gases used for the ozonation reactions.	120
Table 3.1.	X-ray diffraction data for Ni-impregnated Zeolites.	125
Table 3.2.	X-ray diffraction data for V-impregnated Zeolites.	126
Table 3.3.	X-ray diffraction data for Pd-impregnated Zeolites.	129
Table 3.4.	XRD data for Al-MCM-41 samples.	132
Table 3.5.	The DR UV spectra of vanadium oxides from reference compounds, oxidation state and coordination environment.	138
Table 3.6.	BET surface area analysis.	160

Table 4.1.	Percentage conversion and selectivity in the uncatalysed ozonation of n-hexadecane in flat bottom flask.	180
Table 4.2.	Percentage conversion and selectivity in the uncatalysed ozonation of n-hexadecane in long column.	181
Table 4.3.	Uncatalysed ozonation of n-tetradecane.	184
Table 4.4.	Uncatalysed ozonation of n-dodecane.	185
Table 4.5.	Ozonation of n-hexadecane with activated charcoal.	187
Table 4.6.	Ozonation of n-tetradecane with activated charcoal.	189
Table 4.7.	Ozonation of n-dodecane with activated charcoal.	192
Table 5.1.	Percentage conversion and selectivities in the ozonation of n-hexadecane with silica gel as catalyst.	196
Table 5.2.	Percentage conversion and selectivities in the ozonation of n-hexadecane with VPO as catalyst.	197
Table 5.3.	Percentage conversion and selectivities in the ozonation of n-tetradecane with silica gel as catalyst.	199
Table 5.4.	Percentage conversion and selectivities of the products formed in ozonation of n-tetradecane with VPO as catalyst.	200
Table 5.5.	Percentage conversion and selectivities in the ozonation of n-dodecane with silica gel as catalyst.	201
Table 5.6.	Percentage conversion and selectivities in the ozonation of n-dodecane with VPO as catalyst.	203
Table 5.7.	Ozonation of n-hexadecane with 0.5% Pd/ γ -Al ₂ O ₃ catalyst.	204
Table 5.8.	Ozonation of n-hexadecane with 0.5% Pd/ γ -Al ₂ O ₃ N ₂ calcined catalyst.	206
Table 5.9.	Ozonation of n-hexadecane at higher temperature (~140 °C) with 0.5% Pd/ γ -Al ₂ O ₃ N ₂ calcined catalyst.	207
Table 5.10.	Ozonation of n-hexadecane with 0.5% Ni/ γ -Al ₂ O ₃ catalyst.	209
Table 5.11.	Ozonation of n-hexadecane with 0.5% Ni/ γ -Al ₂ O ₃ N ₂ calcined catalyst.	210
Table 5.12.	Ozonation of n-hexadecane with 0.5% V/ γ -Al ₂ O ₃ catalyst.	211
Table 5.13.	Ozonation of n-hexadecane with 0.5% V/ γ -Al ₂ O ₃ N ₂ calcined catalyst.	212
Table 5.14.	Percentage conversion in n-hexadecane ozonation with silica gel, VPO and 0.5% metal loaded γ -Al ₂ O ₃ catalysts.	215
Table 5.15.	Percentage selectivity for the main product, 4-hexadecanone with silica gel, VPO and different 0.5% metal loaded γ -Al ₂ O ₃ catalysts.	216
Table 5.16.	Normalised percentage selectivity for the main product, 4-hexadecanone with silica gel, VPO and different 0.5% metal loaded γ -Al ₂ O ₃ catalysts.	216
Table 6.1.	Ozonation of n-hexadecane with 0.5% Pd/ZSM-5 zeolite.	221
Table 6.2.	Ozonation of n-hexadecane with 0.5% Pd/ZSM-5 N ₂ calcined zeolite.	222
Table 6.3.	Ozonation of n-hexadecane with 0.5% Pd/Na-Y zeolite.	222
Table 6.4.	Ozonation of n-hexadecane with 0.5% Pd/Na-Y N ₂ calcined zeolite.	222
Table 6.5.	Ozonation of n-hexadecane with 0.5% Ni/ZSM-5 zeolite.	226
Table 6.6.	Ozonation of n-hexadecane with 0.5% Ni/ZSM-5 N ₂ calcined zeolite.	226
Table 6.7.	Ozonation of n-hexadecane with 0.5% Ni/Na-Y zeolite.	226
Table 6.8.	Ozonation of n-hexadecane with 0.5% Ni/Na-Y N ₂ calcined zeolite.	227
Table 6.9.	Ozonation of n-hexadecane with 0.5% V/ZSM-5 zeolite.	229
Table 6.10.	Ozonation of n-hexadecane with 0.5% V/ZSM-5 N ₂ calcined zeolite.	230
Table 6.11.	Ozonation of n-hexadecane with 0.5% V/Na-Y zeolite.	230
Table 6.12.	Ozonation of n-hexadecane with 0.5% V/Na-Y N ₂ calcined zeolite.	230
Table 6.13.	Ozonation of n-hexadecane with 0.5% U/Silica.	233

Table 6.14.	Ozonation of n-hexadecane with 0.5% U/Na-Y zeolite.	233
Table 6.15.	Ozonation of n-hexadecane with 0.5% U/ZSM-5 zeolite.	233
Table 6.16.	Ozonation of n-hexadecane with Al-MCM-41 Si/Al-90.	239
Table 6.17.	Ozonation of n-hexadecane with Al-MCM-41 Si/Al-60.	239
Table 6.18.	Ozonation of n-hexadecane with zeolite beta (H form) catalyst.	242
Table 6.19.	Ozonation of n-tetradecane with zeolite beta (H form) catalyst.	242
Table 6.20.	Ozonation of n-dodecane with zeolite beta (H form) catalyst.	243
Table 6.21.	Ozonation of n-hexadecane with zeolite-X catalyst.	245
Table 6.22.	Ozonation of n-tetradecane with zeolite-X catalyst.	245
Table 6.23.	Ozonation of n-hexadecane with 5% Ni/ZSM-5 zeolite.	247
Table 6.24.	Ozonation of n-hexadecane with 5% Ni/Na-Y zeolite.	247
Table 6.25.	Ozonation of n-hexadecane with 5% Ni/HB150 zeolite.	247
Table 6.26.	Ozonation of n-hexadecane with 5% Mo/HB150 zeolite.	249
Table 6.27.	Ozonation of n-hexadecane with 5% Mn/HB150 zeolite.	250
Table 6.28.	Ozonation of n-hexadecane with 5% Co/HB150 zeolite.	250
Table 6.29.	Conversion of n-hexadecane with different 5% metal loaded zeolite catalysts.	252
Table 6.30.	Selectivity for the 4-hexadecanone with different 5% metal loaded zeolite catalysts.	254
Table 6.31.	Conversions of n-hexadecane with different metal loaded ZSM-5 (Si/Al-30) catalysts.	256
Table 6.32.	Selectivity for the 4-hexadecanone with different metal loaded ZSM-5 (Si/Al-30) catalysts.	258
Table 6.33.	Conversion of n-hexadecane with different metal loaded Na-Y catalysts.	259
Table 6.34.	Selectivity for the 4-hexadecanone with different metal loaded Na-Y catalysts.	260

LIST OF FIGURES

Figure 1.1.	Ozone generation by Corona discharge method.	6
Figure 1.2.	Resonance structures of ozone.	7
Figure 1.3.	Scheme of reactions of ozone added to an aqueous solution.	9
Figure 1.4.	Dipolar cyclo addition of ozone on unsaturated bonds.	10
Figure 1.5.	Criegee mechanism.	10
Figure 1.6.	Electrophilic reaction of ozone with aromatic compounds.	11
Figure 1.7.	Organic groups open to attack by ozone.	12
Figure 1.8.	Scheme of ozonation of aromatic compounds.	13
Figure 1.9.	Ozone decomposition (Initiation, propagation & break in chain reaction steps).	14
Figure 1.10.	Ozone decomposition mechanism.	15
Figure 1.11.	Mechanism of ozone decomposition - initiation, promotion and inhibition of radical-type chain reaction.	16
Figure 1.12.	Desired and undesired effects of ozone.	45
Figure 1.13.	Classification of molecular sieves based on chemical component.	80
Figure 1.14.	Schematic diagram of zeolite frameworks.	82
Figure 1.15.	The shape of <i>para</i> -xylene means that it can diffuse freely in the channels of silicalite.	83
Figure 1. 16.	Sodium zeolite A, used as a water softener in detergent powder.	83
Figure. 1.17.	Pentasil zeolites (ZSM-5) structure with emphasized channel systems.	86
Figure 1.18.	Chemical composition of zeolites.	87
Figure 1.19.	Topologies of the internal voids of zeolites.	90
Figure 1.20.	Members of M41S family: (a) hexagonal MCM-41 (b) cubic MCM-48 and (c) lamellar MCM-50.	93
Figure 2.1.	Ozone concentration vs ozonator voltage at room temperature (20 ± 1 °C).	100
Figure 2.2.	Ozone concentration at different temperatures vs oxygen flow rates (120 V).	101
Figure 2.3.	Schematic diagram of ozone generation and ozonation reaction in flat bottom flask.	103
Figure 2.4.	Long column dimensions.	104
Figure 2.5.	Schematic diagram of a stainless steel autoclave (dimensions in mm).	109
Figure 2.6.	Flow chart for the preparation of siliceous MCM-41 and MCM-48 molecular sieves.	110
Figure 2.7.	Flow chart for the preparation of Al substituted MCM-41 molecular sieves.	113
Figure 2.8.	Schematic diagram of tubular furnace set-up.	115
Figure 2.9.	Schematic diagram of catalytic ozonation reaction setup.	121
Figure 3.1.a.	XRD patterns of Ni loaded γ -Al ₂ O ₃ catalysts.	123
Figure 3.1.b.	XRD patterns of Ni loaded Na-Y zeolite catalysts.	123
Figure 3.1.c.	XRD patterns of Ni loaded ZSM-5 zeolite catalysts.	124
Figure 3.2.a.	XRD patterns of V loaded γ -Al ₂ O ₃ catalysts.	127
Figure 3.2.b.	XRD patterns of V loaded Na-Y zeolite catalysts.	128
Figure 3.2.c.	XRD patterns of V loaded ZSM-5 zeolite catalysts.	128
Figure 3.3.a.	XRD patterns of Pd loaded γ -Al ₂ O ₃ catalysts.	129
Figure 3.3.b.	XRD patterns of Pd loaded Na-Y zeolite catalysts.	130

Figure 3.3.c.	XRD patterns of Pd loaded ZSM-5 zeolite catalysts.	130
Figure 3.4.a.	XRD patterns of as-synthesized MCM-41.	131
Figure 3.4.b.	XRD patterns of as-synthesized Al-MCM-41(90).	131
Figure 3.4.c.	XRD patterns of as-synthesized Al-MCM-41(60).	132
Figure 3.5.a.	DR UV spectra of Ni loaded γ -Al ₂ O ₃ catalysts.	133
Figure 3.5.b.	DR UV spectra of Ni loaded γ -Al ₂ O ₃ catalysts (baseline function corrected).	133
Figure 3.5.c.	DR UV spectra of Ni loaded Na-Y zeolite catalysts.	134
Figure 3.5.d.	DR UV spectra of Ni loaded Na-Y zeolite catalysts (baseline function corrected).	134
Figure 3.5.e.	DR UV spectra of Ni loaded ZSM-5 zeolite catalysts.	135
Figure 3.6.a.	DR UV spectra of V loaded γ -Al ₂ O ₃ catalysts.	136
Figure 3.6.b.	DR UV spectra of V loaded Na-Y zeolite catalysts.	136
Figure 3.6.c.	DR UV spectra of V loaded ZSM-5 zeolite catalysts.	137
Figure 3.7.a.	DR UV spectra of Pd loaded γ -Al ₂ O ₃ catalysts.	139
Figure 3.7.b.	DR UV spectra of Pd loaded Na-Y zeolite catalysts.	139
Figure 3.7.c.	DR UV spectra of Pd loaded ZSM-5 zeolite catalysts.	140
Figure 3.8.a.	TG-DTA of as-synthesized Al-MCM-41(90).	140
Figure 3.8.b.	TG-DTA of as-synthesized Al-MCM-41(60).	141
Figure 3.8.c.	TG-DTA of as-synthesized MCM-41.	141
Figure 3.9.a.	FT-IR spectrum of Na-Y catalyst.	143
Figure 3.9.b.	FT-IR spectrum of ZSM-5 catalyst.	144
Figure 3.9.c.	FT-IR spectrum of HBeta Si/Al-40 catalyst.	145
Figure 3.9.d.	FT-IR spectrum of HBeta Si/Al-150 catalyst.	146
Figure 3.10.	FT-IR spectrum of Ni/ZSM-5 catalyst.	147
Figure 3.11.	FT-IR spectrum of V/Na-Y catalyst.	148
Figure 3.12.a.	FT-IR spectrum of Pd/Na-Y N ₂ calcined catalyst.	149
Figure 3.12.b.	FT-IR spectrum of Pd/ZSM-5 N ₂ calcined catalyst.	149
Figure 3.13.a.	FT-IR spectrum of U/Na-Y catalyst.	150
Figure 3.13.b.	FT-IR spectrum of U/Na-Y catalyst from 1300-1700 cm ⁻¹ .	151
Figure 3.13.c.	FT-IR spectrum of U/ZSM-5 catalyst.	151
Figure 3.13.d.	FT-IR spectrum of U/ZSM-5 catalyst from 1300-1700 cm ⁻¹ .	152
Figure 3.14.a.	FT-IR spectrum of as-synthesized Al-MCM-41 (90) catalyst.	153
Figure 3.14.b.	FT-IR spectrum of as-synthesized Al-MCM-41 (60) catalyst.	153
Figure 3.14.c.	FT-IR spectrum of as-synthesized Al-MCM-41 (90) catalyst.	154
Figure 3.14.d.	FT-IR spectrum of as-synthesized Al-MCM-41 (60) catalyst.	154
Figure 3.15.a.	SEM image of Al-MCM-41 Si/Al-60.	155
Figure 3.15.b.	SEM image of Al-MCM-41 Si/Al-90.	155
Figure 3.16.a.	SEM image of γ -Al ₂ O ₃ support.	156
Figure 3.16.b.	SEM image of Ni/ γ -Al ₂ O ₃ support.	157
Figure 3.16.c.	SEM image of Ni/ γ -Al ₂ O ₃ N ₂ calcined.	157
Figure 3.16.d.	SEM image of Pd/ γ -Al ₂ O ₃ support.	157
Figure 3.16.e.	SEM image of Pd/ γ -Al ₂ O ₃ N ₂ calcined.	157
Figure 3.16.f.	SEM image of V/ γ -Al ₂ O ₃ support.	158
Figure 3.16.g.	SEM image of V/ γ -Al ₂ O ₃ N ₂ calcined.	158
Figure 3.17.a.	SEM image of ZSM-5 support.	158
Figure 3.17.b.	SEM image of Ni/ZSM-5 support.	158
Figure 3.17.c.	SEM image of 5% Ni/ZSM-5 support.	159
Figure 3.17.d.	SEM image of V/ZSM-5 support.	159
Figure 3.17.e.	SEM image of U/ZSM-5 support.	159
Figure 3.18.	SEM image of Ni/Na-Y N ₂ calcined.	159

Figure 4.1.	Chromatogram of CCl ₄ solvent (a) before ozonation (b) after ozonation.	163
Figure 4.1.c.	MS of ozonated CCl ₄ .	164
Figure 4.2.	Chromatogram of n-hexadecane in CCl ₄ solvent (a) before ozonation (b) after ozonation.	165
Figure 4.3.	IR spectra of THF solvent (a) before ozonation (b) after ozonation.	167
Figure 4.4.	Chromatogram of n-hexadecane (a) before ozonation (b) after ozonation.	168
Figure 4.4.c.	MS of 4-hexadecanone product.	169
Figure 4.4.d.	MS of 3-hexadecanone product.	169
Figure 4.4.e.	MS of 2-hexadecanone product.	170
Figure 4.5.1.	IR spectra of extracted (a) organic layer (b) aqueous layer.	171
Figure 4.5.2.	IR spectra of isolated (a) 4-hexadecanone (b) 3-hexadecanone.	172
Figure 4.5.2.c.	IR spectrum of isolated 2-hexadecanone.	173
Figure 4.6.	¹ H NMR spectrum for 4-hexadecanone.	174
Figure 4.7.	n-Hexadecane ozonation in flat bottom flask.	180
Figure 4.8.	n-Hexadecane ozonation in long column.	182
Figure 4.9.	Comparison of ozonation reaction in flat bottom flask and long column.	183
Figure 4.10.	Uncatalysed ozonation of n-tetradecane.	184
Figure 4.11.	Uncatalysed ozonation of n-dodecane.	186
Figure 4.12.	Ozonation of n-hexadecane with activated charcoal.	187
Figure 4.13.	Comparison of uncatalysed and activated charcoal ozonation reactions of n-hexadecane.	189
Figure 4.14.	Ozonation of n-tetradecane with activated charcoal.	190
Figure 4.15.	Comparison of uncatalysed and activated charcoal ozonation reactions of n-tetradecane.	191
Figure 4.16.	Ozonation of n-dodecane with activated charcoal.	192
Figure 5.1.	Ozonation of n-hexadecane with silica gel as catalyst.	196
Figure 5.2.	Ozonation of n-hexadecane with VPO as catalyst.	198
Figure 5.3.	Ozonation of n-tetradecane with silica gel as catalyst.	199
Figure 5.4.	Ozonation of n-tetradecane with VPO as catalyst.	200
Figure 5.5.	Ozonation of n-dodecane with silica gel as catalyst.	202
Figure 5.6.	Ozonation of n-dodecane with VPO as catalyst.	203
Figure 5.7.	Ozonation of n-hexadecane with 0.5% Pd/γ-Al ₂ O ₃ catalyst.	205
Figure 5.8.	Ozonation of n-hexadecane with 0.5% Pd/γ-Al ₂ O ₃ N ₂ calcined catalyst.	206
Figure 5.9.	Ozonation of n-hexadecane with 0.5% Pd/γ-Al ₂ O ₃ N ₂ calcined catalyst at 140 °C.	208
Figure 5.10.	Ozonation of n-hexadecane with 0.5% Ni/γ-Al ₂ O ₃ catalyst.	209
Figure 5.11.	Ozonation of n-hexadecane with 0.5% Ni/γ-Al ₂ O ₃ N ₂ calcined catalyst.	210
Figure 5.12.	Ozonation of n-hexadecane with 0.5% V/γ-Al ₂ O ₃ catalyst.	212
Figure 5.13.	Ozonation of n-hexadecane with 0.5% V/γ-Al ₂ O ₃ N ₂ calcined catalyst.	213
Figure 5.14.	Conversion vs. silica gel, VPO and 0.5% metal loaded γ-Al ₂ O ₃ catalysts in the ozonation of n-hexadecane.	217
Figure 5.15.	4-Hexadecanone selectivity vs. silica gel, VPO and 0.5% metal loaded γ-Al ₂ O ₃ catalysts.	218
Figure 6.1.	Conversion of n-hexadecane with different 0.5% Pd loaded zeolite catalysts.	223
Figure 6.2.	Selectivity for the 4-hexadecanone with different 0.5% Pd loaded zeolite catalysts.	223
Figure 6.3.	Conversion of n-hexadecane with different 0.5% Ni loaded zeolite	

	catalysts.	227
Figure 6.4.	Selectivity for the 4-hexadecanone with different 0.5% Ni loaded zeolite catalysts.	228
Figure 6.5.	Conversion of n-hexadecane with different 0.5% V loaded zeolite catalysts.	231
Figure 6.6.	Selectivity for the 4-hexadecanone with different 0.5% V loaded zeolite catalysts.	231
Figure 6.7.	Conversion of n-hexadecane with different 0.5% U loaded zeolite catalysts.	234
Figure 6.8.	Selectivity for the 4-hexadecanone with different 0.5% U loaded zeolite catalysts.	234
Figure 6.9.	Conversion of n-hexadecane with mesoporous Al-MCM-41 catalysts with different Si/Al ratio.	240
Figure 6.10.	Selectivity for the 4-hexadecanone with mesoporous Al-MCM-41 catalysts with different Si/Al ratio.	240
Figure 6.11.	Conversions in ozonation of higher alkanes ($n\text{-C}_{16}\text{H}_{34}$, $n\text{-C}_{14}\text{H}_{30}$ and $n\text{-C}_{12}\text{H}_{26}$) with zeolite beta (H form) catalyst.	243
Figure 6.12.	Selectivity for the 4-ketone in the ozonation of $n\text{-C}_{16}\text{H}_{34}$, $n\text{-C}_{14}\text{H}_{30}$ and $n\text{-C}_{12}\text{H}_{26}$ with zeolite beta (H form) catalyst.	244
Figure 6.13.	Conversion and selectivity in the ozonation of higher alkanes ($n\text{-C}_{16}\text{H}_{34}$ and $n\text{-C}_{14}\text{H}_{30}$) with zeolite-X catalyst.	246
Figure 6.14.	Conversion of n-hexadecane with different 5% Ni loaded zeolites.	248
Figure 6.15.	Selectivity for the 4-hexadecanone with different 5% Ni loaded zeolites.	248
Figure 6.16.	Conversions with different 5% metal loaded HB150 (5% Mo/HB150, 5% Mn/HB150 and 5% Co/HB150) zeolites.	251
Figure 6.17.	Selectivity for the 4-hexadecanone with different 5% metal loaded (HB150 with 5% Mo/HB150, 5% Mn/HB150 and 5% Co/HB150) HB150 zeolites.	251
Figure 6.18.	Conversion of n-hexadecane with different 5% metal loaded zeolites.	253
Figure 6.19.	Selectivity for the 4-hexadecanone with different 5% metal loaded zeolites.	254
Figure 6.20.	Conversions of n-hexadecane with different metal loaded ZSM-5 (Si/Al-30) catalysts.	257
Figure 6.21.	Selectivity for the 4-hexadecanone with different metal loaded ZSM-5 (Si/Al-30) catalysts.	258
Figure 6.22.	Conversion of n-hexadecane with different metal loaded Na-Y catalysts.	260
Figure 6.23.	Selectivity for the 4-hexadecanone with different metal loaded Na-Y catalysts.	261

LIST OF SCHEMES

Scheme 1.1.	Presence of FeCl ₃ in ozonation of alkane in acetone solvent.	17
Scheme 1.2.	Decomposition of alkyl hydrotrioxides.	19
Scheme 1.3.	Isobutane ozonation in superacids.	20
Scheme 1.4.	Ozonation of pentane in presence of magic acid-SO ₂ ClF at -78 °C.	21
Scheme 1.5.	Hydrocarbon-ozone complex transition state represented by penta-coordinated ions.	21
Scheme 1.6.	Ozone attack at different hydrogens in ethyl ethoxyacetate.	22
Scheme 1.7.	Benzaldehyde ozonation mechanism in absence and presence of oxygen.	23
Scheme 1.8.	Transition state five-membered ring after ozone insertion into the C-H bond.	25
Scheme 1.9.	Different paths involved in the ozonation of cyclohexane.	26
Scheme 1.10.	Intermediates formation in ozonolysis of dimethylacetylene.	32
Scheme 1.11.	Benzaldehyde ozonation as a source for singlet oxygen formation.	32
Scheme 1.12.	Cyclic tetroxide intermediate in acetaldehyde ozonation.	33
Scheme 1.13.	The electrophilic attack of protonated ozone into the C-C or C-H σ bonds of the alkanes.	33
Scheme 1.14.	Ozonation of alkanes in strong acid media (superacids).	34
Scheme 1.15.	C-H Bond ozonolysis.	35
Scheme 1.16.	C ₁ -C ₂ Bond ozonolysis.	36
Scheme 1.17.	Propane ozonation mechanism.	38
Scheme 1.18.	Ozonation products of cyclodecane.	39
Scheme 1.19.	Hydride transfer from the alkane forming hydrotrioxide.	39
Scheme 1.20.	Dissociation, dismutation and rearrangement of hydrotrioxide.	40
Scheme 1.21.	Analogous reaction of ozone with cyclodecanol.	40
Scheme 1.22.	Radical nature of transition state in the ozonation of saturated hydrocarbons.	42
Scheme 1.23.	Primary reactions of ozone with a compound S.	48
Scheme 1.24.	Product distribution from ozonation of 3-methylpentane.	58
Scheme 1.25.	Transition state of dipolar structure and intermediate in ozonation of alkane.	60
Scheme 1.26.	Scheme of catalytic ozonation.	63
Scheme 1.27.	Brønsted and Lewis acid sites as catalytic centers of alumina.	65
Scheme 1.28.	Possible mechanism for ozonation process in the presence of Me-support (metal oxide) catalyst.	72
Scheme 2.0.	Formation of MCM-41 and MCM-48 mesoporous molecular sieves.	111
Scheme 2.1.	Schematic representation of the pore channels in MCM-41 and MCM-48.	112
Scheme 2.2.	Formation mechanism of as-synthesized Al-MCM-41.	114
Scheme 4.1.	Initial intermediates in ozonation of alkanes.	175
Scheme 4.2.	Ozonation mechanism of higher n-alkanes (C ₁₆ H ₃₄ , C ₁₄ H ₃₀ and C ₁₂ H ₂₆).	177
Scheme 4.3.	Oxidation of ketones to carboxylic acids with ozone.	178
Scheme 4.4.	Mechanism of alkane reactions.	194
Scheme 5.1.	γ -Al ₂ O ₃ ozonation mechanism.	218
Scheme 6.1.	Proposed mechanism in the oxidation of n-alkane with U/ZSM-5.	236

APPENDIX

Figure a. MS of tetrachloroethene from ozonated CCl ₄ sample.	279
Figure b. MS of 4-hexadecanone.	280
Figure c. MS of 3-hexadecanone.	281
Figure d. MS of 2-hexadecanone.	282
Figure e. IR spectrum of pure n-hexadecane.	283
Figure f. IR spectrum of ozonated n-hexadecane.	284
Figure g. ¹ H NMR spectrum of 3-hexadecanone.	285
Figure h. ¹ H NMR spectrum of 2-hexadecanone.	286
Figure i. MS of Propanoic acid.	287
Figure j. MS of Tridecanoic acid.	288

ABBREVIATIONS

To avoid the repetition of terms NaY / Na-Y and ZSM-5 Si/Al-30 / ZSM-5 were used in the text, as the same.

0.5% metal loaded catalysts can be read as Ni-, V-, Pd- zeolite.

5% metal loaded catalysts are denoted with 5%M-zeolite, one can read the 0.5% as the M-zeolite.

To compare respective changes of intensity and absorptions in the XRD and DR UV-Visible spectra, the patterns were plotted one above the other. But, one can consider the units on the Y-axis are arbitrary.

Al-MCM-41(60) and Al-MCM-41(90) can be read as Al-MCM-41 Si/Al-60 and Al-MCM-41 Si/Al-90 respectively.

1°	-	primary
2°	-	secondary
3°	-	tertiary
Å	-	Angstrom
A cm ⁻²	-	Amperes per square centimetre
ALPOs	-	aluminophosphates
AOPs	-	Advanced Oxidation Processes
atm. pressure	-	atmospheric pressure
BDOC	-	biodegradable dissolved organic carbon
BET	-	Brunauer-Emmett-Teller (BET) surface area
BHT	-	2,6-tert-butyl-4-methylphenol
BTEX	-	Benzene, Toluene, Ethylbenzene and Xylene
C _{act}	-	activated carbon
CFCs	-	chlorofluorocarbons
COD	-	chemical oxygen demand
CT	-	charge transfer
CTAB	-	cetyltrimethylammonium bromide
DBPs	-	disinfection by-products
°C	-	degrees centigrade
ΔH	-	enthalpy change
ΔH _f ^o	-	standard enthalpy of formation
DOC	-	dissolved organic carbon
DRS	-	Diffuse Reflectance Spectra
DR UV-Vis	-	Diffuse Reflectance UV-Visible (DR UV)
E _{act}	-	energy of activation
EDTA	-	ethylene-diamine-tetra-acetic acid
EFAI	-	extra framework aluminium species

EPA	-	Environmental Protection Agency
eV	-	electron Volts
FAU	-	Faujasite family of zeolites
FCC	-	fluid catalytic cracking
g	-	grams
Gb	-	billion barrels
g L ⁻¹	-	gram per Litre
h	-	hour
HY zeolite	-	zeolite-Y (H form)
ICDD	-	International Centre for Diffraction Data, Pennsylvania, USA
I _{rel}	-	relative intensity
IUPAC	-	International Union of Pure and Applied Chemistry
J kg ⁻¹ K ⁻¹	-	Joules per kilogram per Kelvin
K	-	Kelvin
kcal	-	kilo calories
kcal mol ⁻¹	-	kilo calories per mol
kg	-	kilogram
kg m ⁻³	-	kg per cubic metre
K min ⁻¹	-	Kelvin per minute
kJ mol ⁻¹	-	kilo joule per mol
kV	-	kilo Volts
Late group	-	unidentified products
LPM	-	Litre per minute
μA	-	micro ampere
μg L ⁻¹	-	microgram per litre
μm	-	micrometer or micron
M41S (family)	-	MCM-41, MCM-48 and MCM-50 catalysts.
MCM-41	-	Mobil Composite Material-41
MFI zeolites	-	pentasil group zeolites
m ² g ⁻¹	-	square meter per gram
mg m ⁻³	-	milligram per cubic metre
mg L ⁻¹	-	milligram per Litre
mg L ⁻¹ .min ⁻¹	-	milligram per litre minute
min.	-	minute
mL g ⁻¹	-	milli Litre per gram
mL min ⁻¹	-	milli Litre per minute
MMbpcd	-	million barrels per calendar day
MPa	-	megapascal
M ⁻¹ s ⁻¹	-	per mol sec
MTBE	-	Methyl tertbutylether
N ₂ calcined	-	catalysts calcined under Nitrogen flow conditions
Na-Y zeolite	-	zeolite-Y (Na form)

nm	-	nano metres
N m ⁻¹	-	Newton per metre
NOM	-	Natural Organic Matter
n-C ₁₂	-	n-Dodecane
n-C ₁₄	-	n-Tetradecane
n-C ₁₆	-	n-Hexadecane
NO _x	-	nitrogen oxides
O ₃ /GAC	-	Ozone-granulated activated carbon systems
Pa s	-	Pascal second
ppb	-	parts per billion
ppm	-	parts per million
s	-	second
SCR	-	Selective Catalytic Reduction
t-BuOH	-	tertiary butanol
TG-DTA	-	thermogravimetry-differential thermal analysis
THF	-	tetrahydrofuran
THMs	-	trihalomethane
TLC	-	Thin Layer Chromatography
TOC	-	Total Organic Carbon
tons cm ⁻²	-	tons per square centimetre
TS-1 and TS-2	-	Titanium Silicates
u	-	mass units
VOCs	-	volatile organic compounds
VPO	-	Vanadium Phosphorous Oxides
v/v	-	volume / volume
WAO	-	Wet Air Oxidation
w/v	-	weight / volume
w/w	-	weight / weight
XRD	-	X-ray diffraction

CHAPTER - I

INTRODUCTION AND LITERATURE REVIEW

1.0. Introduction:

Petroleum accounts for 40 percent of the world's total primary energy demand and economic conditions are governed to a large degree by its availability. Petroleum products are the most widely used chemicals in society today. It has been estimated that the original recoverable oil in the earth was 2,330 billion barrels¹ (Gb). The global refining process capacity for the year 2004 was 82.05 million barrels per calendar day (MMbpcd) and the world product consumption is forecasted to increase by 2-4 million barrels each year². Oil demand is roughly a function of population and level of development. Seven countries, the United States, Japan, China, Germany, Russia, Italy and France, accounted for 52 percent of the global oil demand¹.

In the petroleum industry fluid catalytic cracking (FCC), hydroprocessing (hydrocracking) and catalytic reforming are building block processes in petroleum refineries to produce high quality gasoline. Petroleum fractions rich in the higher hydrocarbons like naphtha, kerosene, diesel oil, gas oil and vacuum residuals are feed stocks for these processes. These processes involve high reaction temperature and pressure conditions (over 350 °C and 50-200 atm. pressure) and reactions of n-alkanes (liquid phase) at moderate conditions is difficult.

Saturated hydrocarbons, alkanes, are known to exhibit low reactivity in reactions with variety of reagents and in many cases the yields of the products are negligible. In last decade, new methods of alkane functionalization with participation of various transition metal complexes in solutions have been discovered and developed. The main problem for these procedures is the use of metals and organic solvents, which require disposal of wastes and the high reaction temperature and pressure condition. A “green chemistry” perspective requires metal-free oxidation procedures. Ozone has been used for the oxidation of cycloalkanes³ and the subsequent formation of hydrotrioxides has been reviewed. The selective oxidation of alkanes at room temperature is one of the most important objectives of synthetic chemistry⁴. Ozone is known to act as an electrophile towards pi systems, heteroatoms and in some special cases also toward carbon³. Barletta *et al*⁵ reported the selective formation of cyclodecanone by ozonation of cyclodecane in water at pH 3.

Alkanes are the most important chemical feedstocks in petrochemical industry and used as gasoline components. Reactions of ozone with unsaturated hydrocarbons have been investigated very extensively. Little work has been reported on the reactions of ozone with saturated hydrocarbons. Reactions of saturated organic compounds with ozone are the focus of current

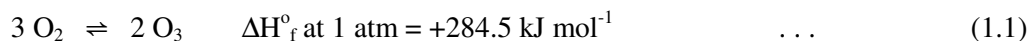
study. The selective oxidation of alkanes at room temperature and pressure conditions is one of the most important objectives of organic chemistry.

1.1. Discovery of ozone:

Ozone is known to accompany electrical storms, since the ancient times. In 1840, the German chemist C. F. Schonbein reported that the odour produced during sparking was caused by an unknown compound that he called ozone, from the Greek ozein (to smell). In 1856, Thomas Andrews showed that ozone was formed only by oxygen, and in 1863 Soret established the relationship between oxygen and ozone by finding that three volumes of oxygen produce two volumes of ozone⁶.

Harries introduced ozone to organic chemistry during the period 1903-1916 in Kiel, Germany. He established experimental procedures for ozonolysis, demonstrated the generality of the reaction of unsaturated compounds with ozone, and showed that ozone could be used for the synthesis of a variety of sensitive compounds⁶. Ozone presented a number of fascinating challenges: (1) determination of its composition, (2) its isolation as a pure substance, (3) the study of its chemistry, and (4) understanding the contrast between its behavior and that of ordinary oxygen. First it was a chemical curiosity of great interest, and then a reagent for organic synthesis and an extremely useful tool for structure determination of natural products, the number of double bonds in a molecule could also be determined from the oxygen content of the corresponding ozonide, providing a complement to such determinations by catalytic hydrogenation. Ozonolysis was also useful in determining whether two isomeric alkenes were cis-trans isomers, and more recently a component of smog and a key ingredient of the upper atmosphere. Three methods were described by Schonbein, arcing air or oxygen, electrolyzing aqueous acid solutions, and exposing phosphorus to moist air, were used by investigators in the early days of ozone research.

Formation of ozone is an endothermic reaction:



Ozone is thermodynamically unstable and spontaneously reverts back into oxygen.

Ozone is a strong oxidizing agent and capable of participating in many chemical reactions with inorganic and organic substances. Ozone has strong odour that can be detected at concentrations as low as 0.01 ppm⁷.

1.2. Atmospheric ozone:

Ozone in upper levels of the atmosphere protects the earth's surface against harmful UV radiation, but on the ground level it is toxic in high concentrations and is an air contaminant^{8, 9}. Tropospheric ozone is an important greenhouse gas that dominates tropospheric chemistry and influences climate. Ozone in the boundary layer is a cause for concern as it can damage crops and imposes human health risks. Troposphere ozone is known to have increased a factor of two in the past 100 years¹⁰. Ozone in concentration > 0.1 ppm causes severe health problems to humans like headaches, throat irritation and damage to the mucous membranes¹¹. Low concentrations of ozone (< 2 ppm) appear in the atmosphere due to ultraviolet radiation and electric discharges. In the Earth's stratosphere, it occurs naturally (with concentrations between 5 and 10 ppm), protecting the planet and its inhabitants by absorbing ultraviolet radiation of wavelength 290-320 nm¹². However, photocopier machines, laser printers and plasma reactors produce ozone in higher concentrations up to 2000 ppm¹².

1.3. Industrial uses of ozone:

Commercially, ozone has been used as a reagent in synthesis, for potable water purification, as a disinfectant in sewage treatment, and for the bleaching of natural fibers¹². Ozone is widely used in the industrial and environmental processes such as semiconductor manufacturing, deodorization, disinfection and water treatment. Ozone is an environment friendly oxidant since it decomposes to O₂ without producing self-derived byproducts in the oxidation reactions, in contrast with organoperoxides. The reactivity of ozone toward organic compounds has been extensively studied both in the liquid phase¹³ and in the gaseous phase¹⁴. Ozone reacts directly with alkenes to form ozonide compound in homogeneous media, which are subsequently transformed to alcohols, ketones and carboxylic acids in contrast with alkenes, ozone shows low activities toward alkanes and aromatic compounds^{13, 14}. Therefore, catalytic oxidation with ozone (catalytic ozonation)¹⁵⁻²¹ has been applied for the decomposition of volatile organic compounds (VOCs) in the gaseous phase. In the catalytic ozonation processes, ozone decomposes to form highly reactive active oxygen species that can oxidize the organic compounds. Einaga and Futamura²⁰ compared the catalytic activities of the oxides of Mn, Fe, Co, Ni, Cu and Ag on alumina in the oxidation of benzene and cyclohexane with ozone, and have reported that Mn

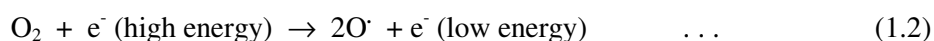
oxide shows the highest activity for benzene oxidation. Mn oxides have the steady-state activity for cyclohexane oxidation, one of the most effective constituents for catalytic ozonation.

1.4. Methods for generation of ozone:

The economic benefit of using ozone largely depends on the methods with which ozone is generated. Ozone dissolved in liquid oxygen up to 30% w/w is relatively safe, while spontaneous explosions occur at above 72% w/w of ozone in liquid oxygen. Ozone has a tendency to separate and concentrate during evaporation due to the higher volatility of oxygen. When this occurs, the composition becomes unavoidably explosive. Conservation of ozone in liquefied freons has been attempted, but application of the process to water treatment is a problem²². Ozone decomposes, even when dissolved in a liquefied matrix.

In 1857, von Siemens developed the first industrial ozone generator, which was based on corona discharges. Two concentric glass tubes were used; a layer of tin covered the outer tube externally, and a layer of tin covered the inner tube internally. Air was circulated through the annular space. This technology was later improved by the addition of circulating cooling fluids along the discharge air or oxygen gap, resulting in lower generation temperatures and less thermal destruction of the ozone.

The generation of ozone involves the intermediate formation of atomic oxygen radicals, which react with molecular oxygen.



All processes that can dissociate molecular oxygen into oxygen radicals are potential ozone generation reactions. Energy sources that make this action possible are electrons or photons quantum energy. Electrons can be used from high-voltage sources in the silent corona discharge, from chemonuclear sources, and from electrolytic processes. Suitable photons quantum energy includes UV light of wavelengths lower than 200 nm and γ -rays²².

1.4.1. Photochemical ozone generation:

The formation of ozone from oxygen exposed to UV light at 140-190 nm was first reported by Lenard in 1900, and fully assessed by Goldstein in 1903. It was recognized that the active

wavelengths for technical generation are below 200 nm. In the present technologies, the 254 nm wavelength is transmitted along with the 185 nm wavelength in mercury-based UV-emission lamps, and photolysis of ozone is simultaneous with its generation. Moreover, the relative UV-emission intensity is 5 to 10 times higher at 254 nm compared to the 185 nm wavelength. Due to concomitant thermal decomposition with ozone formation, UV process is found not ideal²³. The main reason for this failure is that is with ozone formation. Except for small-scale uses or synergic effects, the UV-ozone process (the UV-photochemical generation of ozone) has not reached maturity. Important phases requiring additional development include the development of new lamp technologies^{24, 25} with less aging and higher emission intensity at wavelengths lower than 200 nm.

1.4.2. Electrolytic ozone generation:

The simplicity of the equipment makes this process attractive for small scale users or users in remote areas^{24, 25}. Many potential advantages are associated with electrolytic generation, including the use of low voltage DC current, no feed gas preparation, reduced equipment size, possible generation of ozone at high concentrations, and generation in the water, eliminating the ozone to water contacting processes. Problems and drawbacks of the method include, corrosion and erosion of the electrodes, thermal overloading due to anodic over voltage and high current densities, need for special electrolytes or water with low conductivity, and with the in-site generation process, incrustations and deposits are formed on the electrodes, and production of free chlorine is inherent to the process when chloride ions are present in water or the electrolyte used^{24, 25}.

1.4.3. Radiochemical ozone generation:

High irradiation of oxygen by radioactive rays can promote the formation of ozone. Even with the favorable thermodynamic yield of the process and the interesting use of waste fission isotopes, the cheminuclear ozone generation process has not yet become a significant application due to its complicated process requirements²⁶.

1.4.4. Ozone generation by Corona discharge method:

Corona discharge in a dry process gas containing oxygen is presently the most widely used method of ozone generation^{24, 25}. A classical production line is composed of gas source (compressors or liquefied gas), dust filters, gas dryers, ozone generators, contacting units, and off gas destruction.

It is of utmost importance that a dry process gas is applied to the corona discharge. Limiting nitric acid formation is also important in order to protect the generators and to increase the efficiency of the generation process. In normal operation of properly designed systems, a maximum of 3 to 5 g nitric acid is obtained per kilogram ozone produced with air. If increased amounts of water vapor are present, larger quantities of nitrogen oxides are formed when spark discharges occur. Hydroxyl radicals are formed that combine with oxygen radicals and ozone, reducing the ozone generation efficiency. Consequently, the dryness of the process gas is of relevantly important to obtain a yield of ozone. Moreover, with air, nitrogen oxides can form nitric acid, which can cause corrosion. The presence of organic impurities in the feed gas should be avoided^{24, 25}.

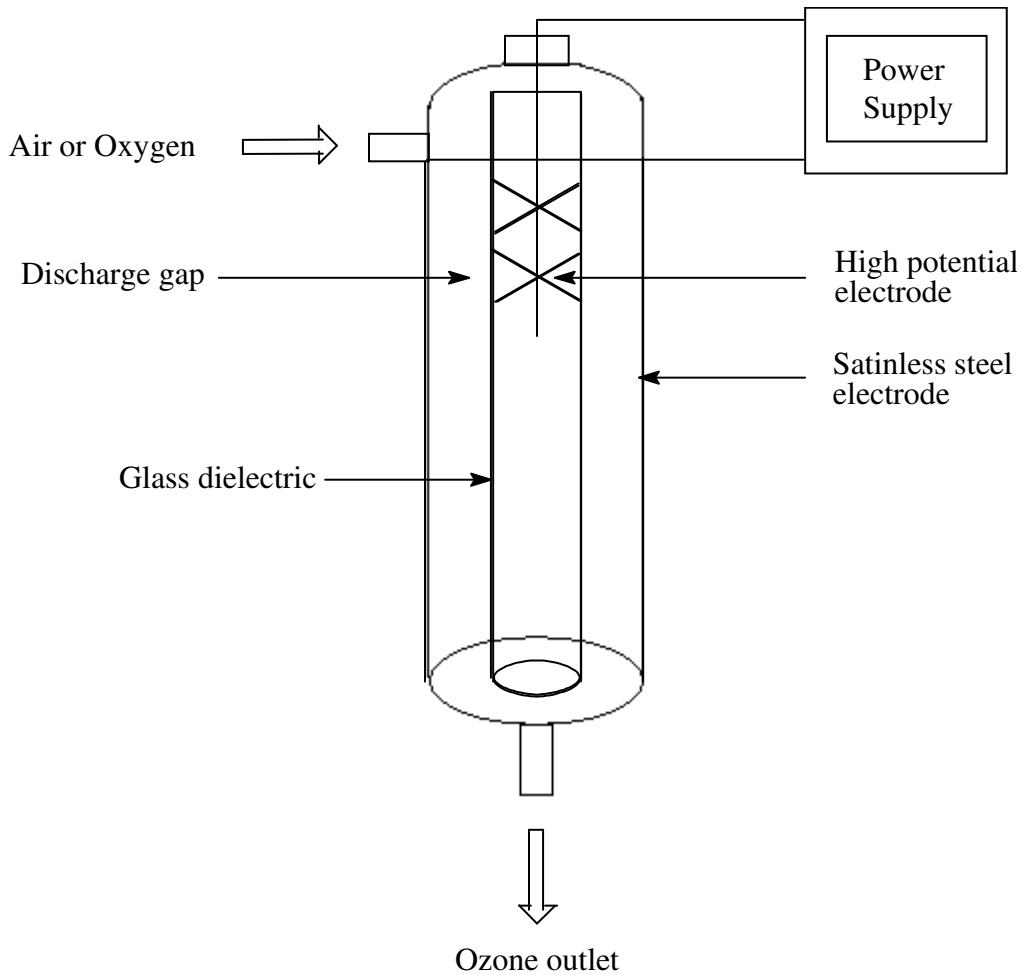


Figure 1.1. Ozone generation by Corona discharge method^{24, 25}.

The formation of ozone through electrical discharge in a process gas is based on the non-homogeneous corona discharge in air or oxygen (Fig. 1.1). There are numerous distributed microdischarges by which the ozone is effectively generated. It appears that each individual microdischarge lasts only several nanoseconds, lasting about 2.5 to 3 times longer in air than in oxygen^{24, 25}. The current density ranges between 100 and 1000 A cm⁻².

By using oxygen or enriching the process oxygen in air, the generating capacity of a given ozone generator can be increased by a factor ranging from 1.7 to 2.5 versus the production capacity with air, depending on the design parameters. The yield obtained when using an oxygen enriched process gas is increased with a smaller gas space and higher electrical current frequency. Since all variations result in energy loss in the form of heat, cooling of the process gas is very important. The most efficient form of cooling is the both-side cooling system, which is a system that has cooling on both the high voltage side and on the ground side. However, in case of accidental breakage of the dielectric, the cooling liquid (for example, water) enters the discharge gap and causes short-circuiting of the entire system. Therefore cooling only the groundside is the safer design.

1.5. Properties of ozone:

1.5.1. Physical properties of ozone:

Ozone is a pale blue gas, heavier than air, very reactive and unstable, cannot be stored and transported, so it has to be generated “*in situ*”. It is explosive and toxic, even at low concentrations¹².

By analysis of the electronic structure, the molecule is considered to have the resonance structures as shown in Fig. 1.2 characterized by end oxygen atoms with only six electrons. This fact defines the electrophilic nature that ozone shows in most of its chemical reactions.

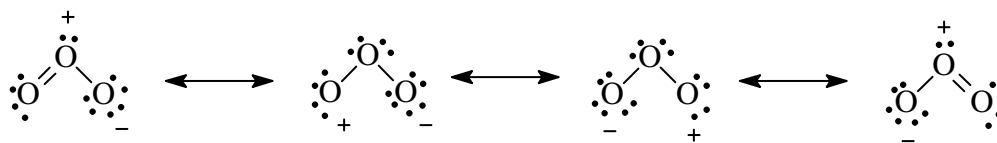


Figure 1.2. Resonance structures of ozone^{24, 25}.

Ozone is soluble in many substances, forming either stable or metastable solutions. In aqueous solutions ozone is about 14 times more soluble than oxygen, but forms a metastable solution. The stability is influenced by the presence of sensitizing impurities, such as heavy-metal cations and metal oxides, and by temperature and pressure; generally, an increase of the pressure or decrease of the temperature enhances the solubility of ozone in the aqueous phase. Mostly the solubility determinations have been performed with dilute ozone, and the values extrapolated to 100 percent ozone. Table 1.1 lists the solubility of 100 percent ozone in pure water, as a function of temperature. The solubility decreases with the increasing temperatures¹².

Table 1.1. Solubility of ozone in water¹².

Temperature (°C)	Solubility (kg m ⁻³)
0	1.09
10	0.78
20	0.57
30	0.40
40	0.27
50	0.19
60	0.14

Table 1.2. Physical properties of ozone¹².

Physical properties	Value
Molecular weight	48.0 u
Boiling point (101 kPa)	-111.9 °C
Melting point	-192.7 °C
Critical temperature	-12.1 °C
Critical pressure	5.53 Mpa
Density, gas (0 °C, 101 kPa)	2.144 kg m ⁻³
Density, liquid (-112 °C)	1358 kg m ⁻³
Surface tension (-183 °C)	3.84 x 10 ⁻² N m ⁻¹
Viscosity, liquid (-183 °C)	1.57 x 10 ⁻³ Pa s
Heat capacity, liquid (-183 to -145 °C)	1884 J kg ⁻¹ K ⁻¹
Heat capacity, gas (25 °C)	818 J kg ⁻¹ K ⁻¹
Heat of vaporization	15.2 kJ mol ⁻¹

Table 1.3. Relative oxidation potentials¹².

Species	Oxidation Potential, eV
Fluorine	3.06
Hydroxyl radical	2.80
Nascent oxygen	2.42
Ozone	2.07
Hydrogen peroxide	1.77
Perhydroxyl radical	1.70
Hypochlorous acid	1.49
Chlorine	1.36

The important physical properties of ozone are given in Table 1.2. The chemistry of ozone is largely governed by its strongly electrophilic nature. It has higher oxidation potential than chlorine, hypochlorous acid, perhydroxyl radical and hydrogen peroxide. Table 1.3 compares the oxidation potential of ozone with other strong oxidizing agents. Ozone is a stronger oxidizing agent than the normally used reagents such as peroxides, chlorine and hypochlorous acid¹².

1.5.2. Chemistry of ozone:

In an aqueous solution, ozone reacts with various compounds (M) in two ways²⁷⁻²⁹:

- By direct reaction with the molecular ozone, and
- By indirect reaction with the radical species that are formed when ozone decomposes in water.

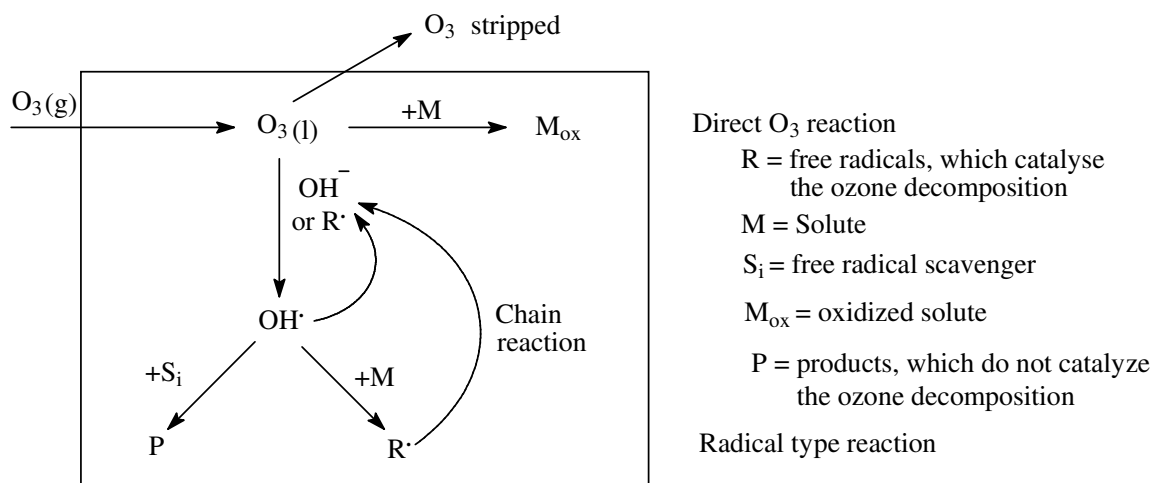


Figure 1.3. Scheme of reactions of ozone added to an aqueous solution²⁹.

The two basic reactions of ozone in water are illustrated as in Fig. 1.3. In non aqueous solutions, the molecular ozone is the predominant species.

1.5.2.1. Molecular ozone reactivity:

The extreme forms of resonance structures in ozone molecules are shown in Fig. 1.2. These structures illustrate that the ozone molecule can act as a dipole, as an electrophilic agent, and as a nucleophilic agent^{24, 25}.

1.5.2.1.a. Cyclo addition (Criegee mechanism):

As a result of its dipolar structure, the O_3 molecule may lead to 1-3 dipolar cyclo addition on unsaturated bonds, with the formation of primary ozonide as shown in Fig. 1.4.

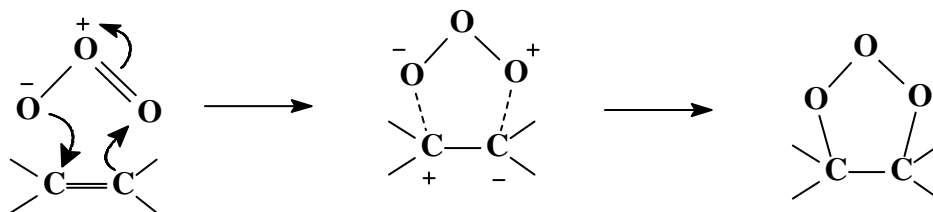


Figure 1.4. Dipolar cyclo addition of ozone on unsaturated bonds^{3, 13}.

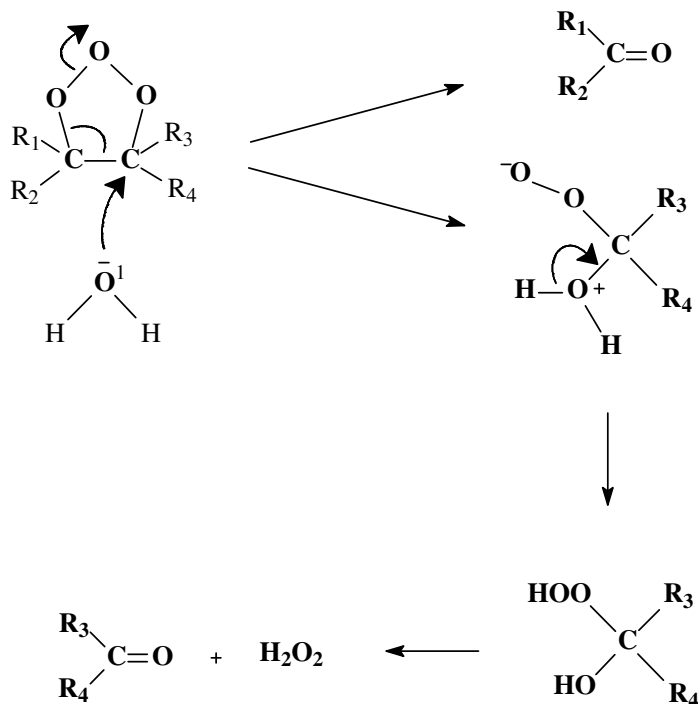


Figure 1.5. Criegee mechanism^{3, 13}.

In a protonic solvent such as water, this primary ozonide decomposes into a carbonyl compound (aldehyde or ketone) and zwitterions that quickly leads to a hydroxy-hydroperoxide stage that, in turn, decomposes into a carbonyl compound and hydrogen peroxide as shown in Fig. 1.5.

1.5.2.1.b. Electrophilic reaction:

The electrophilic reaction is restricted to molecular sites with a strong electronic density and, particularly to certain aromatic compounds. Aromatics substituted with electron donor groups (OH, NH₂ and similar compounds) show high electronic densities on carbons located in the ortho and para positions, and so are highly reactive with ozone at these positions. On the contrary, the aromatics substituted with electron-withdrawing groups (-COOH, -NO₂) are weakly ozone reactive. In this case, the initial attack of the ozone molecule takes place mainly on the least deactivated meta position. The result of this reactivity is that the aromatic compounds bearing the electron donor groups D (for example, phenol and aniline) react quickly with the ozone^{24, 25}. This reaction is schematically represented in Fig. 1.6.

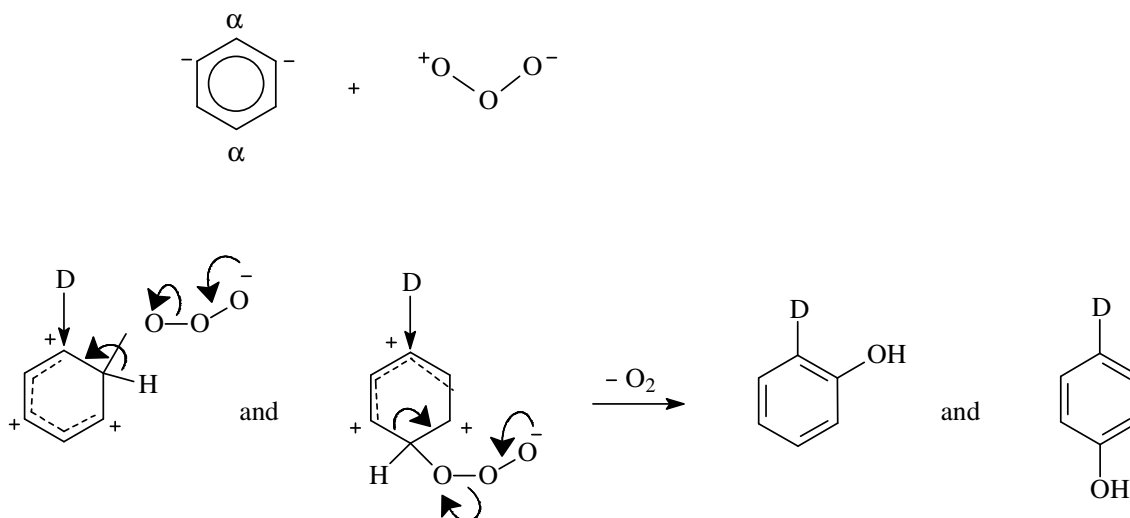


Figure 1.6. Electrophilic reaction of ozone with aromatic compounds^{24, 25}.

This initial attack of ozone molecule leads first to the formation of ortho- and para- hydroxylated by-products. These hydroxylated compounds are highly susceptible to further ozonation. The compounds lead to the formation of quinoid and, due to the opening of the aromatic cycle, to the formation of aliphatic products with carbonyl and carboxyl functions.

1.5.2.1.c. Nucleophilic reaction:

The nucleophilic reaction is found locally on molecular sites showing an electronic deficit and, more frequently, on carbons carrying electron-withdrawing groups. The molecular ozone reactions are extremely selective and limited to unsaturated aromatic and aliphatic compounds as well as to specific functional groups. Some of the organic groups readily undergo reaction with ozone are shown in Figs. 1.7. Further, Fig. 1.8 summarises the scheme of ozonation of selected organics as described by Langlais *et al*^{24, 25}.

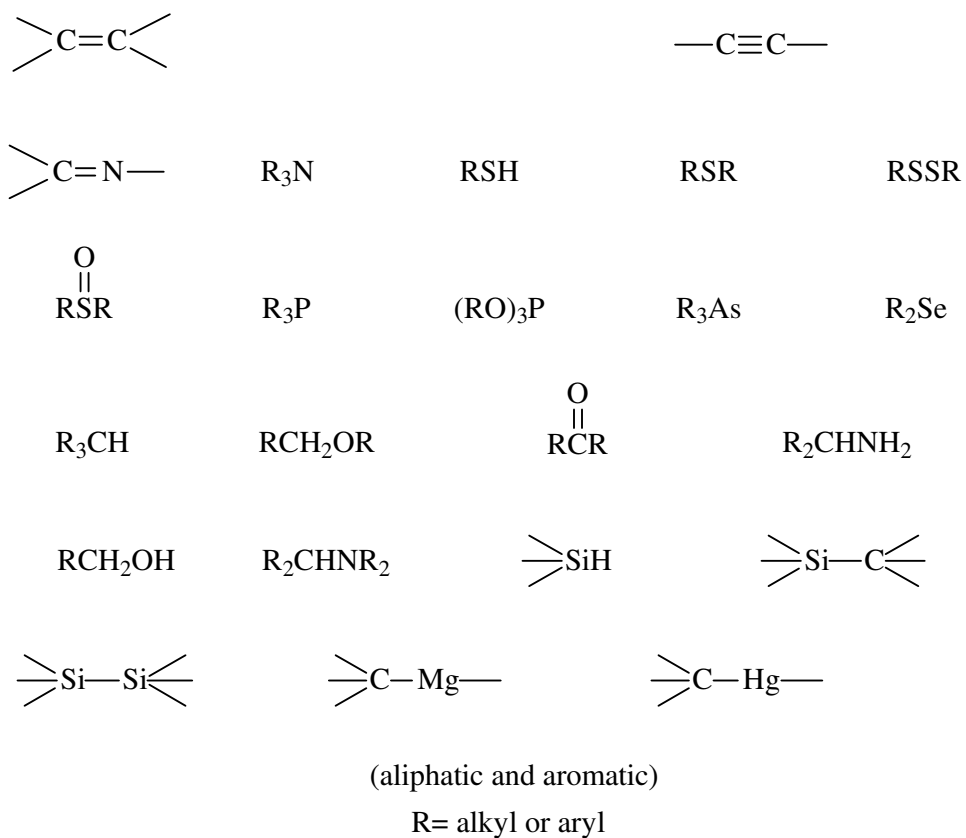


Figure 1.7. Organic groups open to attack by ozone³⁰.

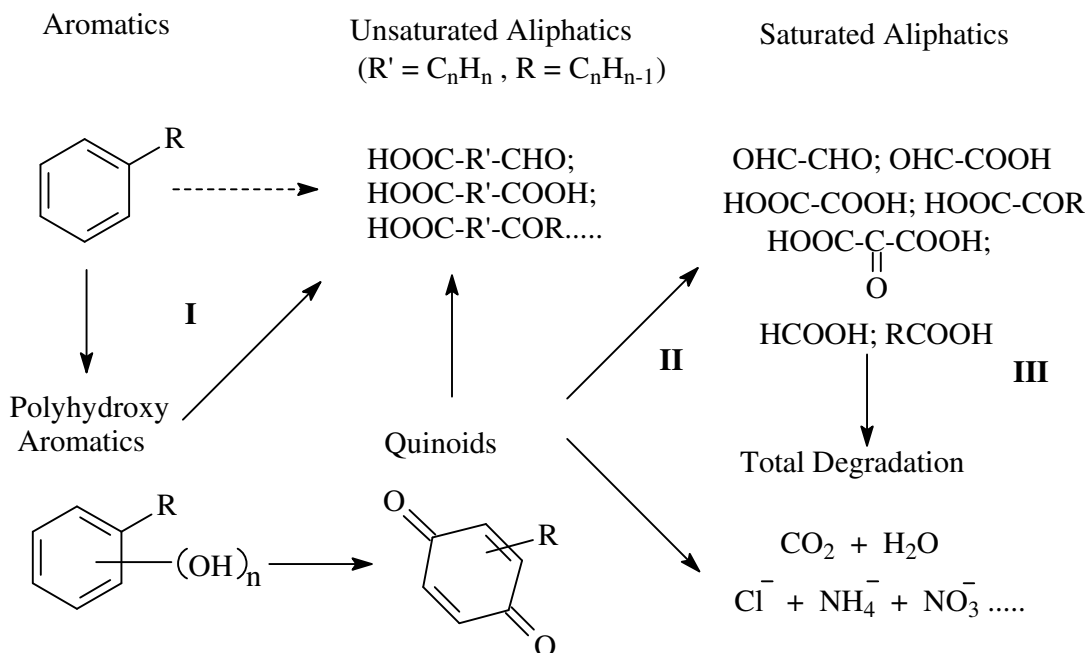


Figure 1.8. Scheme of ozonation of aromatic compounds^{24, 25}.

1.5.3. Decomposition of ozone: (aqueous solution as the medium)

The stability of dissolved ozone in water is affected by pH, ultraviolet light, ozone concentration, and the concentration of radical scavengers. The decomposition rate, measured in the presence of excess radical scavengers, which prevent secondary reactions, is expressed by a pseudo first-order kinetic equation of the following configuration³¹:

$$-\left(\frac{d[O_3]}{dt} \right)_{pH} = k' [O_3] \quad \dots \quad (1.4)$$

where k' = pseudo first-order rate constant for a given pH value. It is a linear function of pH. This evolution reflects the fact that the ozone decomposition rate is first order with respect to both ozone and hydroxide ions, in aqueous solution resulting in an overall equation of the following from:

$$-\left(\frac{d[O_3]}{dt} \right)_{pH} = k [O_3] [OH^-] \quad \dots \quad (1.5)$$

where $k = k' / [OH]$

Ozone decomposition occurs in a chain process that can be represented by the fundamental reactions as shown in Fig. 1.9, based on the two most important models^{32, 33}, which includes the initiation [1-2], propagation [3-7], and break in chain reaction steps [8-12].

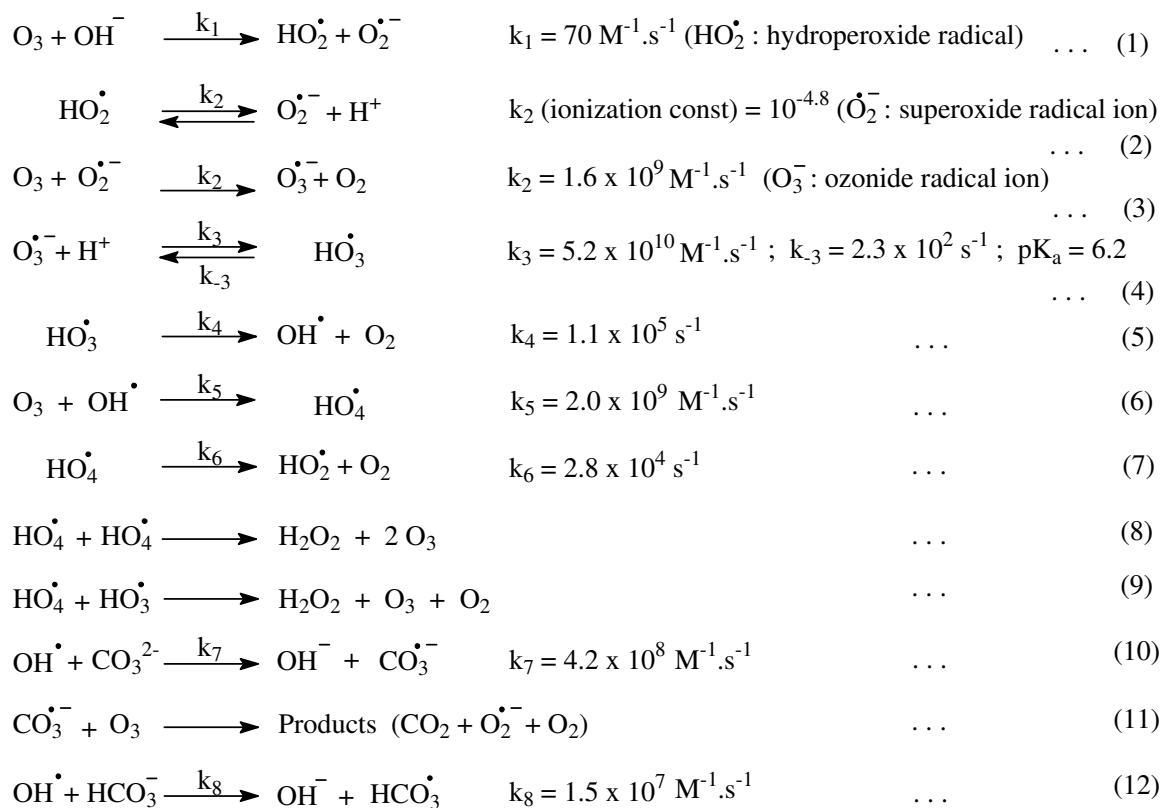


Figure 1.9. Ozone decomposition (Initiation, propagation & break in chain reaction steps)^{32, 33}.

The overall pattern of the ozone decomposition mechanism is illustrated in Fig. 1.10. The fundamental element in the reaction diagram and in the rate constant values is that the free-radical initiating step constitutes the rate-determining step in the reaction. The second is that the regeneration of the superoxide radical ion $\text{O}_2^{\bullet-}$, or its protonic form HO_2^\bullet , from the hydroxyl radical OH^\bullet implies that 1 mol of ozone is consumed. As a result, all the species capable of consuming hydroxyl radicals without regenerating the superoxide radical ion will produce a stabilizing effect on the ozone molecule in water^{32, 33}.

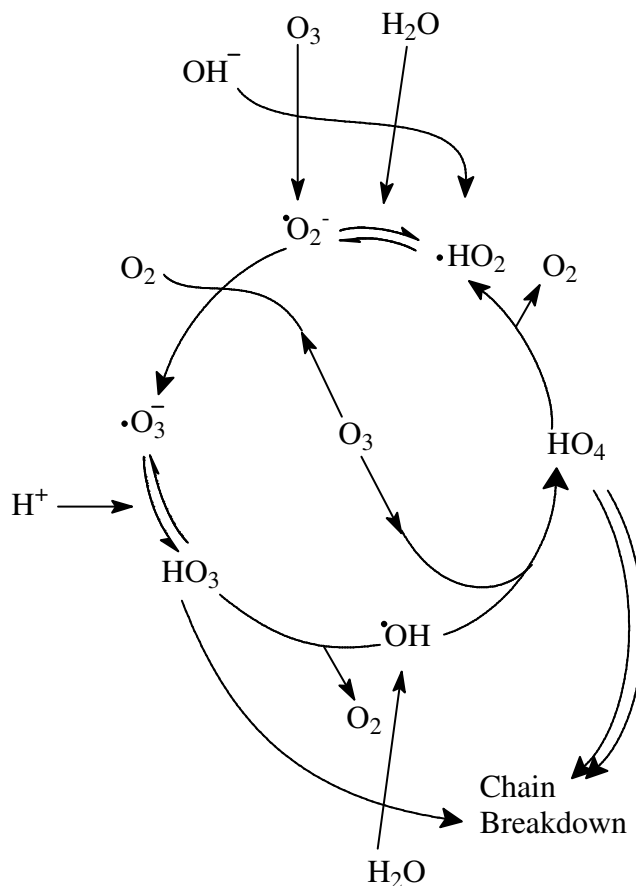


Figure 1.10. Ozone decomposition mechanism^{24, 25}.

1.5.3.1. Initiators, promoters and inhibitors of free-radical reactions:

Ozone is reactive regardless of whether it is in the gas phase or in the liquid phase. There are a wide variety of compounds able to initiate, promote, or inhibit the chain-reaction processes^{27, 29}. The initiators of the free-radical reaction are those compounds capable of inducing the formation of superoxide ion O_2^- from an ozone molecule. Those are inorganic compounds (hydroxyl ions OH^- , hydroperoxide ions HO_2^- and some cations), organic compounds (glyoxylic acid, formic acid, humic substances etc.) and UV radiation at 253.7 nm. Promoters of the free-radical reaction are all organic and inorganic molecules capable of regenerating of O_2^- superoxide (which can promote the decomposition of ozone) anion from the hydroxyl radical. Common promoters that are also organics include aryl groups, formic acid, glyoxylic acid, primary alcohols and humic acids. Among the inorganic compounds, phosphate species are worth special mention²⁷⁻²⁹. The inhibitors of the free-radical reaction are compounds capable of consuming OH^\bullet radicals without regenerating the superoxide anion O_2^- . Some of the more common inhibitors include bicarbonate

and carbonate ions, alkyl groups, tertiary alcohols (e.g. t-butanol) and humic substances. Hoigne and co-workers²⁷⁻²⁹ defined initiators, promoters and inhibitors as in Fig 1.11.

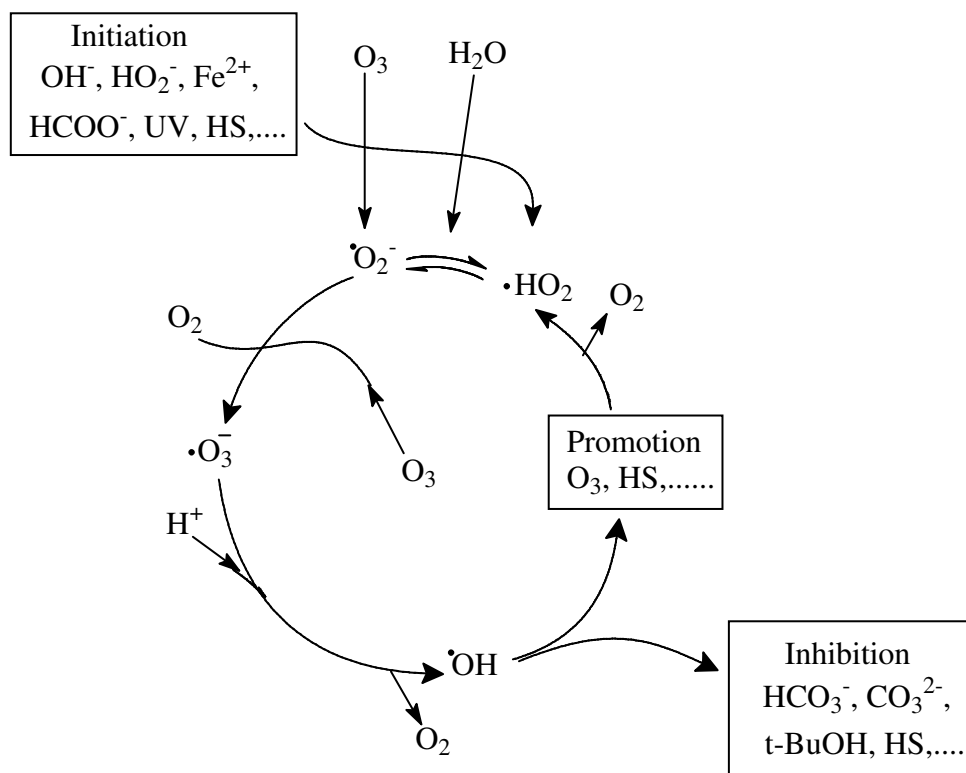
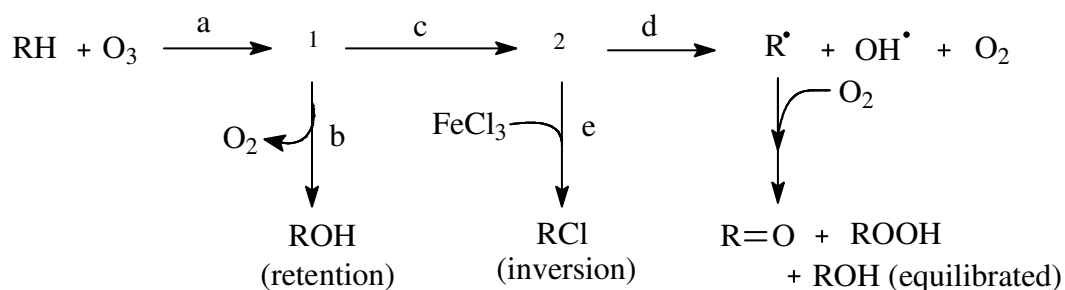


Figure 1.11. Mechanism of ozone decomposition - initiation, promotion and inhibition of radical-type chain reaction²⁷⁻²⁹.

1.5.4. Solvent effect and the carrier gas effect in the ozonation reactions:

Hellman and Hamilton³⁴ observed that there is a slight enhancement in the absolute amounts of products formed with O_2 as carrier gas compared to N_2 during the ozonation of cyclohexane. Their studies reveal that the polarity of the hydrocarbon solvent used in the ozonation reaction doesn't have any effect. The increase in the viscosity of the hydrocarbon solvents (octadecane) resulted in a significant increase in the retention of configuration in the cis-dimethylcyclohexane ozonation. The solvents like ethyl acetate, acetone, and acetonitrile lower the retention of configuration and increase the relative amount of cyclohexanone in the cyclohexane ozonation reactions. It was observed that these solvents react readily with ozone to produce a number of unidentified products. The relative reactivity of primary, secondary, and tertiary hydrogens is not altered significantly, when FeCl_3 is present, is further evidence that FeCl_3 does not change the

ozone reactivity. O_2 is produced in the ozonation of alkane, some of the products characteristic of the $R^\bullet + O_2$ reaction are observed even with N_2 carrier gas. When acetone is present some of the results are complicated due to the reaction of O_3 with the solvent.



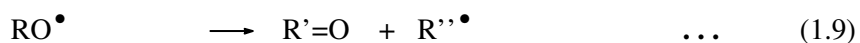
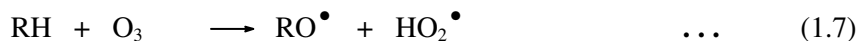
Scheme 1.1. Presence of $FeCl_3$ in ozonation of alkane in acetone solvent³⁴.

The presence of $FeCl_3$, traps the radicals formed from the acetone-ozone reaction before they react with the alkane. The simplest mechanism of ozonation of alkane in acetone solvent reported by Hellman and Hamilton³⁴ is shown in Scheme 1.1.

Since the reactants, alkane and O_3 , are both singlet molecules, compound **1** in Scheme 1.1 would have all its electrons paired. However, because the product, O_2 , can exist in two energetically accessible states (singlet and triplet) it is not surprising that compound **1** could decompose by two pathways to give O_2 . If singlet O_2 is formed, the other fragments must have their electrons paired (spin conservation rule). Then one expects they would collapse directly to alcohol with retention of configuration. On the other hand, if triplet O_2 is formed, the other fragments must have their electrons unpaired and they cannot collapse to give alcohol without spin inversion. Thus, a triplet radical pair compound **2** in Scheme 1.1 would be formed which would eventually diffuse apart to give free radicals, or in the presence of $FeCl_3$ could be trapped to give RCl with inversion of configuration. The conversion of RH to ROH with retention of configuration is an oxygen atom insertion reaction but one in which a free oxygen atom is not involved³⁴. Benson³⁵ estimated that the reaction between the alkane and ozone, where hydrogen is abstracted by ozone from the alkane and forms alkyl radical and hydrotrioxy radical (eqn. 1.6) will be endothermic by at least 20 kcal mol^{-1} .



It was reported that ozone reacted with methane to yield aldehyde at temperatures as low as 15 °C and at 100 °C methane reacted with ozone at such speed that 53% of the introduced ozone disappeared within 2 min. The reaction of methane with ozone gave promise as a means to produce methanol and formaldehyde. Ethanol was reported to result from the action of ozone on ethane and this reaction was noted to proceed with greater rapidity than the reaction of ozone with methane. The reactions of ozone with paraffins proceed with relatively low activation energy and this low value should be associated with the reaction of triplet low lying excited electronic state of the ozone molecule³⁶.

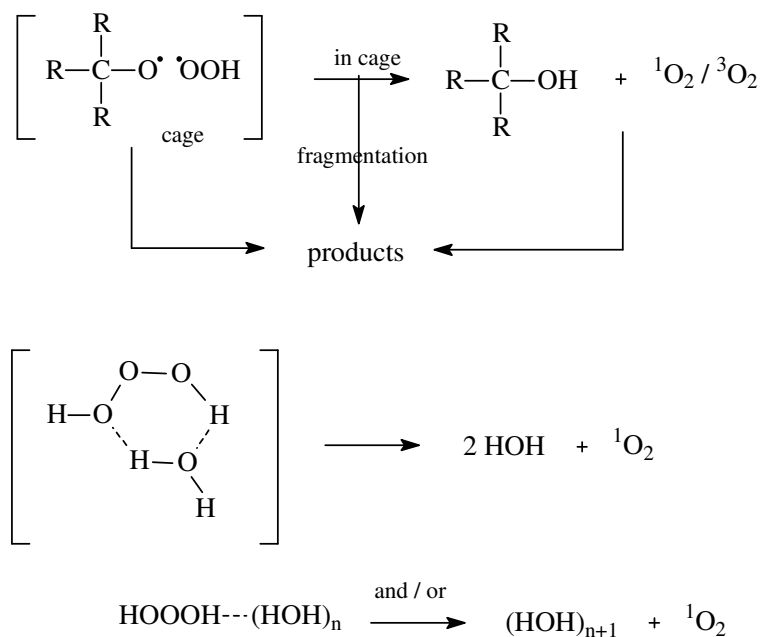


The principal difference between the modes of reaction of normal paraffins relative to that of branched paraffin like isobutene would then reside in the relative stability of the alkoxy radicals, RO^\bullet . In the case of isobutene, t-butoxy radical is sufficiently stable under the reaction conditions to yield, by hydrogen abstraction from RH, t-butyl alcohol. With n-butane and propane the notable absence of alcohols other than methanol is an indication that this reaction (1.8) is of minor importance. Acetone ($\text{R}'=\text{O}$) results from propane by the ejection of a hydrogen atom from the isopropoxy radical, from isobutene by the ejection of a methyl radical (R''^\bullet) from the t-butoxy radical (reaction 1.9, where R = propane). An alternate splitting of the isopropoxy radical to acetaldehyde plus a methyl radical probably occurs with the subsequent rapid oxidation of acetaldehyde^{37, 38}.

Low temperature ozonation of C-H bonds in saturated hydrocarbons with abstractable β -hydrogen atoms produced the corresponding alkyl hydrotrioxides (ROOOH) and hydrogen trioxide (HOOOH). The proposed radical mechanism for the first step of ozonation most probably involves radical pairs in a solvent cage i.e. the species proposed to be formed in the first step of the reaction, that is the abstraction of the hydrogen atom from the R-H bond by ozone, resulting in the formation of the radical pair $\text{R}^\bullet \cdots \text{OOOH}$ with subsequent collapse to ROOOH . HOOOH is formed by the abstraction of hydrogen atom from alkyl radical (R^\bullet) by HOOO^\bullet radical. Hydrotrioxy radical is considerably stabilized by forming intermolecular hydrogen bonded complexes with acetone and dimethyl ether as model oxygen bases³⁹. Plesničar *et al*³⁹

reported theoretical and experimental evidence for the radical mechanism (Scheme 1.2) of the ozonation of isopropyl alcohol and some benzylic alcohols and ethers.

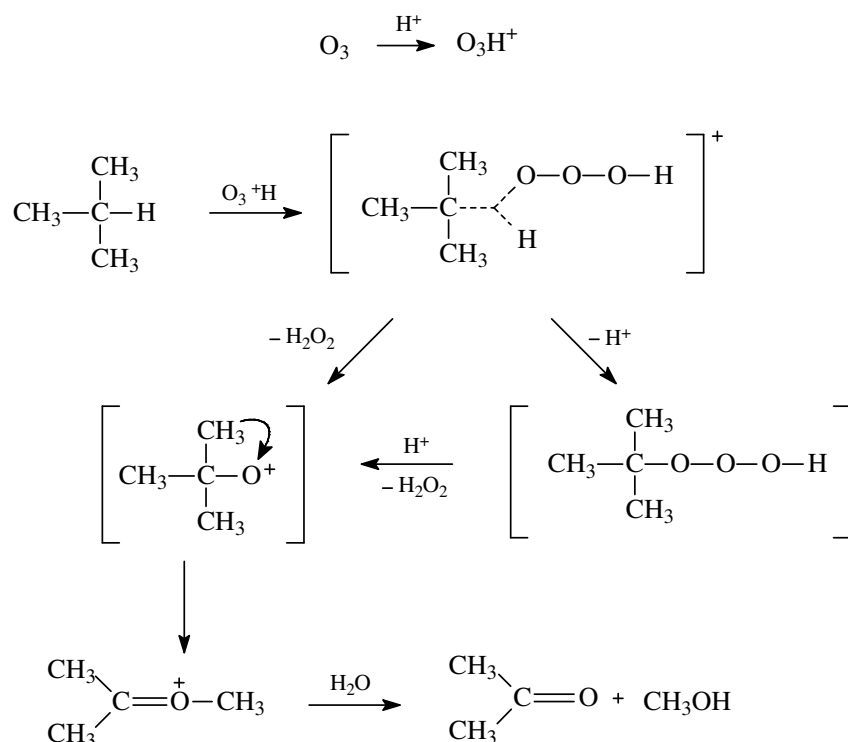
The decomposition of alkyl hydrotrioxides involves a homolytic cleavage⁴⁰ of the RO-OOH bond with subsequent “in cage” reactions of the corresponding radicals, while the decomposition of HOOOH is most likely predominantly a “pericyclic” process involving one or more molecules of water acting as a bifunctional catalyst to produce water and singlet oxygen ($\Delta^1\text{O}_2$) (Scheme. 1.2).



Scheme 1.2. Decomposition of alkyl hydrotrioxides⁴⁰.

Electrophilic nature of protonated ozone in superacidic media in its insertion reactions into the C-H or C-C σ bonds in alkanes⁴¹. Isobutane in superacids [1:1 $\text{FSO}_3\text{H}-\text{SbF}_5$ (magic acid), FSO_3H , $\text{HF}-\text{BF}_3$], or in HF and H_2SO_4 readily reacted with ozone, giving, via the intermediate dimethylmethoxycarbenium ion, acetone and methyl alcohol as shown in the Scheme. 1.3.

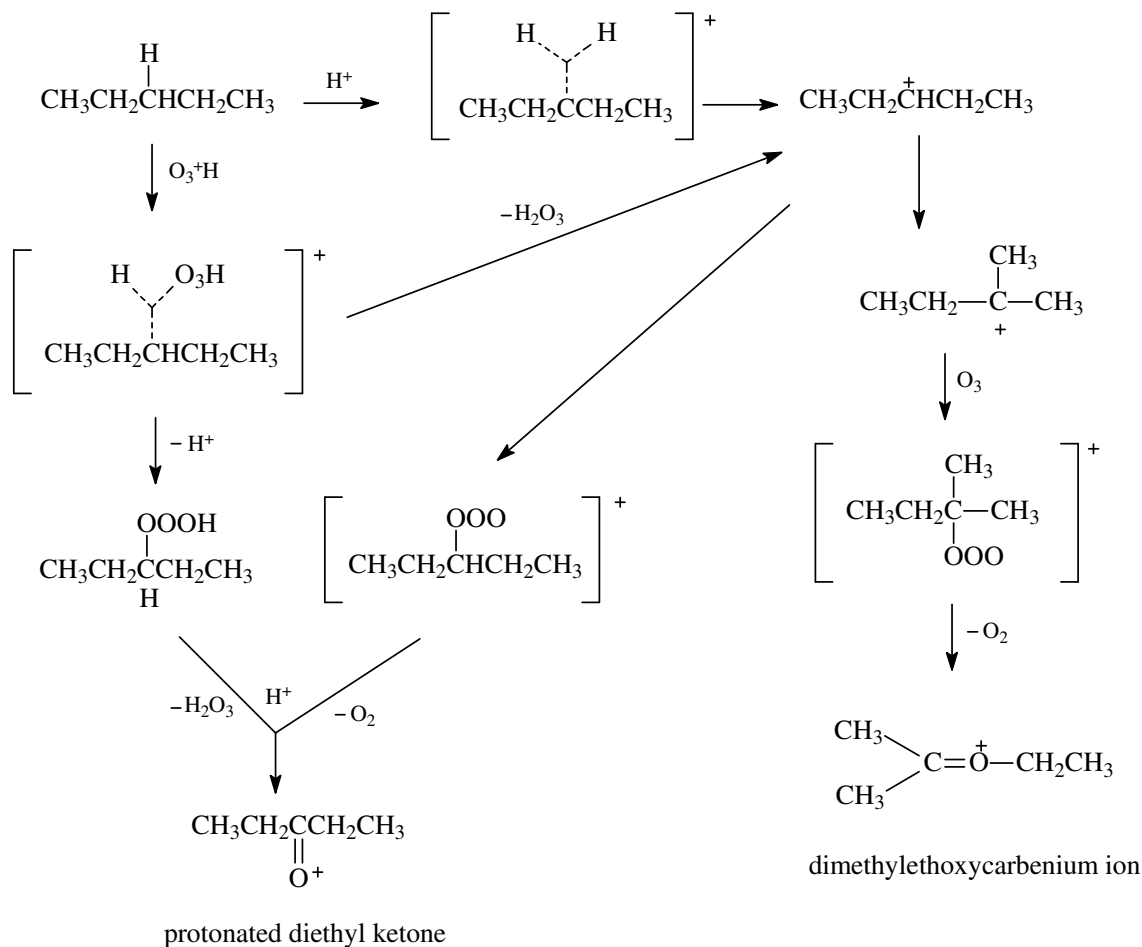
Pentane when treated with ozone in magic acid- SO_2ClF at -78°C gave a complex reaction mixture. The major product was dimethylethoxycarbenium ion and another major identified product was protonated diethyl ketone, which could arise from direct nucleophilic attack by ozone on the diethylcarbenium ion or by electrophilic oxygenation by O_3H^+ at the secondary C-H bond in pentane⁴¹ as shown in the Scheme 1.4.



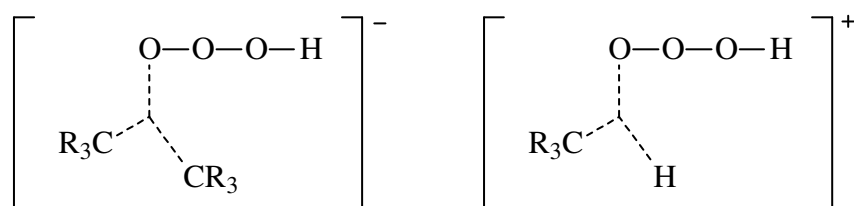
Scheme 1.3. Isobutane ozonation in superacids⁴².

Alkanes reactions with ozone in HF-BF₃, FSO₃H, HF, and H₂SO₄ studied for the further evidence in support of the ozonization reaction through O₃H⁺. Olah *et al*⁴¹ reported that the reaction of alkanes with ozone in the presence of acids weaker than magic acids such as HF-BF₃, FSO₃H, HF, and H₂SO₄, which themselves, at the temperature of -78 °C, do not react with any of the alkanes to give carbenium ions. Ozone in presence of these acids obviously acts as a weaker oxidizing agent than in the presence of magic acid⁴¹.

Olah *et al*⁴¹ reported that the reactions of an electrophilic insertion into the single bonds of the alkane, effected by protonated ozone (O₃H⁺), similarly to such electrophilic reactions as protolysis of alkanes, postulating protonated ozone as an obviously more powerful electrophile than neutral ozone, that the hydrocarbon-ozone complex transition state will be represented by the penta-coordinated ions showed in Scheme 1.5. The concept of penta-coordinated carbonium ion formation, with subsequent cleavage to trivalent carbenium ions and hydrogen trioxide or alkyl hydrotrioxide, satisfactorily explains the results of saturated hydrocarbon reactions with ozone in the presence of strong acid media.



Scheme 1.4. Ozonation⁴¹ of pentane in presence of magic acid-SO₂ClF at -78 °C.

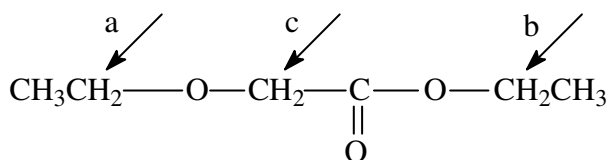


R = alkyl or H

Scheme 1.5. Hydrocarbon-ozone complex transition state represented by pentacoordinated ions⁴¹.

Ozonation of alcohols in trichlorofluoromethane solution was reported to give exclusive products of α oxidation, i.e., carboxylic acids and ketones⁴³. It is assumed that the reactions proceed via

electrophilic oxygenation of the involved C-H bonds of the alcohols with protonated ozone. The relative reactivity of σ bonds in alkanes with protonated ozone⁴¹ was generally found to be $R_3C-H > R_2(H)C-H > R(H_2)C-H > C-C$. Olah *et al*⁴² also studied 3-methyl 1-butanol (with a tertiary C-H bond at the γ position) undergoes reaction more readily than n-butyl alcohol (with a secondary C-H bond at the γ position) with protonated ozone giving oxidation-rearrangement products⁴².



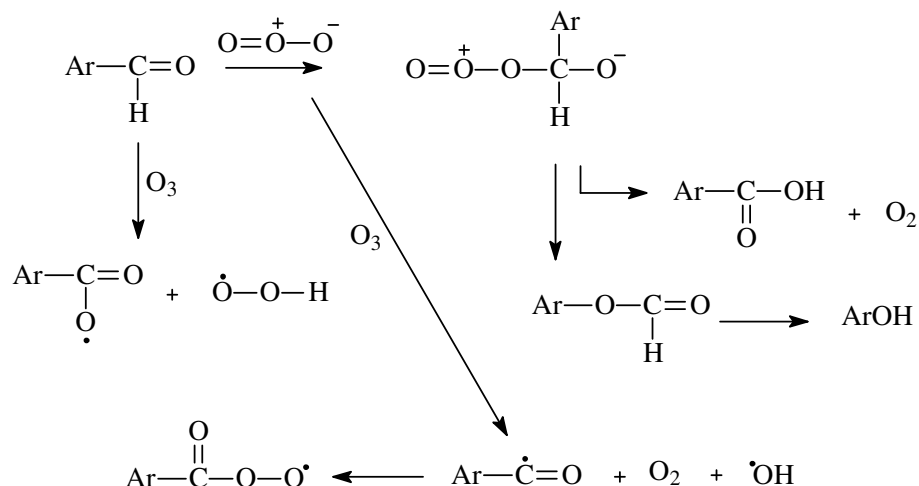
Scheme 1.6. Ozone attack at different hydrogens in ethyl ethoxyacetate⁴⁴.

The tertiary hydrogen of propyl isopropyl ether was found to be, on a statistical basis, 1.7 times more reactive than an α secondary hydrogen. Likewise, for ethyl ethoxyacetate the overall ozone attack (Scheme 1.6) was slow, but occurred at positions a, b, and c, in the proportions 72:22:6. The ozonations were carried out at room temperature with ozone in an oxygen stream. The fact that a maximum of 1.18 mol of ether reacted per mol of ozone consumed indicates that ozone was the major oxidant and that very little autooxidation was involved⁴⁴.

1.5.5. Importance of oxygen in O_3 - O_2 mixture:

White and Bailey⁴⁵ studied the ozonation of aromatic aldehydes, the major product from ozone attack on benzaldehyde is perbenzoic acid both in ozone-nitrogen and ozone-oxygen mixtures. Much more ozone is required per benzaldehyde molecule with ozone-nitrogen than with ozone-oxygen. It is also reported that the perbenzoic-benzoic acid ratio decreased with decreasing oxygen content in the stream, until essentially only benzoic acid resulted when the gas mixture was 1:1:98%, respectively.

Bailey¹³ suggested that in the absence of oxygen ozone attacks the carbonyl group of an aldehyde nucleophilically, whereas in the presence of oxygen ozone serves as a radical initiator. Both acid oxidation and formation of phenols can be explained by the nucleophilic mechanism in Scheme 1.7.



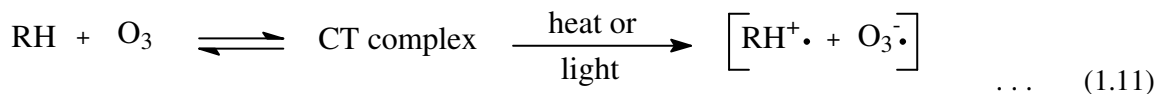
Scheme 1.7. Benzaldehyde ozonation mechanism in absence and presence of oxygen¹³.

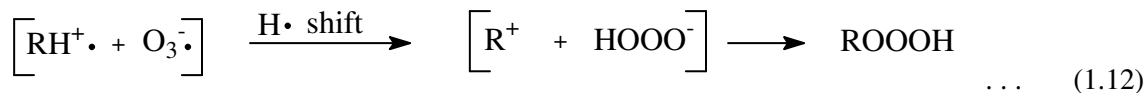
The reaction of a methylene chloride solution of benzaldehyde with ozone from an ozone-nitrogen mixture was found to proceed with essentially quantitative absorption of ozone at temperatures ranging from -20 to 25 °C.

1.6. Mechanisms for the reaction of ozone with hydrocarbons:

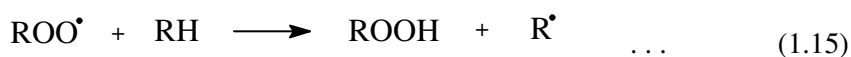
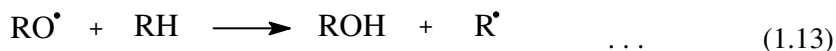
Ozone forms charge transfer (CT) complexes with many types of organic compounds. Mazur *et al*⁴⁶ have suggested that ozone complexes even with saturated hydrocarbons is in accord with the polar nature of ozone, whose tendency to form complexes with aromatic and olefin compounds. Oxygen, which is less electronegative and less polarizable than ozone, forms CT complexes with virtually every organic molecules, including alkanes⁴⁷.

Since photolysis of the CT complex leads to the hydrotrioxide, it appears reasonable to postulate that the CT complex and therefore, polar species leading from cumene to the trioxide. This appears to be strong support for a polar mechanism⁴⁸ rather than for hydrogen atom abstraction. The CT complex of aliphatic hydrocarbons with ozone also has been reported⁴⁶. It appears reasonable to suggest the general reaction pathway for any hydrogen donor, RH, shown in eqns. 1.11 and 1.12.





In the absence of 2,6-tert-butyl-4-methylphenol (BHT), cumyl hydroperoxide is produced during the synthesis of the hydrotrioxide. This probably results from hydrogen abstraction from cumene by any oxy radicals in the system⁴⁹, eqn. 1.13, followed by eqns. 1.14 and 1.15.



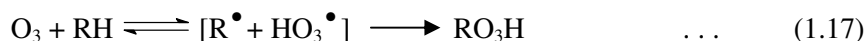
1.7. Reaction of ozone with saturated compounds:

Ozone has been found to react rapidly with alcohols and ethers⁴³ even at -78°C . Durland and Adkins⁵⁰ reported the stereospecific oxidation of decalin (both cis- and trans-) to the corresponding 9-decanol. Whiting *et al*⁴³ later found that the reaction proceed even at -78°C and reported also that adamantane at -78°C is slowly oxidized to the 1-alcohol and ketone in the ratio of 3:1. They further found that CH_3OH reacts at -78°C with O_3 in CFCl_3 solutions with a half-life of minutes while 2-propanol is much faster. The products from $\text{MeOH} + \text{O}_3$ when examined (after warming to 0°C) were about 85% ($\text{HCOOH} + \text{H}_2\text{O}_2$) and about 15% ($\text{CH}_2\text{O} + \text{O}_2$). Ethanol gave about 70% ($\text{CH}_3\text{COOH} + \text{H}_2\text{O}_2$) with about 27% (CH_3CHO) and 2% of ($\text{CH}_2\text{O} + \text{CH}_3\text{CO}_3\text{H}$) and about 18% of O_2 was evolved. Hamilton *et al*⁵¹ reported that initial products of O_3 with cyclohexane as cyclohexanol and cyclohexanone in the ratio of about 3.5:1. It was postulated that hydrotrioxides, RO_3H , were very likely the unstable intermediates in the ozonolysis of various organic substrates, the spectroscopic evidence for their existence become available⁵².

1.7.1. Mechanism of saturated hydrocarbons ozonation:

Reactions of ozone with unsaturated hydrocarbons have been investigated very extensively. Much less work has been done on the corresponding reactions with saturated hydrocarbons. The unusual reactivity of O_3 at low temperatures suggests a radical pathway for its behaviour. This can take either of two paths, a chain reaction initiated by O atoms formed from the reversible dissociation of O_3 or a H-atom abstraction reaction followed by cage recombination of fragments.

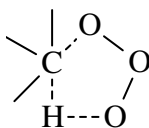




The chain reaction (eqn. 1.16) can be easily discounted. Under usual conditions, the fastest reaction of O atoms will be the reverse combination with O₂, which in solution should be close to the diffusion-controlled limit. Competing reactions with O₃ have E_{act} ~4.5 kcal and with saturates might be fast enough to support a chain in concentrated solutions (> 0.1 M), the products would be alcohols and water, not trioxides, and the rates would be prohibitively slow at -78 °C.

The atom abstraction path (eqn. 1.17) had been earlier discounted as being too endothermic^{35, 43} at -78 °C. With the new Δ*H*_f^o (HO₃•), the H-O₃ bond strength is raised to 68.5 kcal. This would lead to measurable attack on RH at 300 K if the R-H bond strength were not in excess of 87 kcal, which would exclude all the substrates described. At -78 °C, no measurable reaction is possible except for R-H bond strength less than 80 kcal, again much lower than the bond strengths in the compounds discussed. Nangia and Benson⁴⁸ affirm the earlier conclusions that the reaction cannot follow a radical pathway. If free-radical pathways are not available, then only concerted or ionic reaction mechanisms are left as possibilities.

The concerted reaction would amount to insertion of ozone into the C-H bond. The transition state for this reaction would be a five-membered ring with a pentavalent carbon atom as shown in Scheme 1.8. It is estimated that the intrinsic activation energy for pentavalent carbon formation is about 15-20 kcal, while there is an estimated additional 6 kcal for ring strain yielding a minimum expected value of 20-26 kcal.

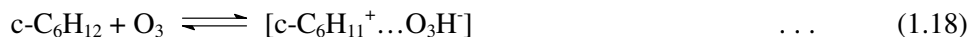


Scheme 1.8. Transition state five-membered ring after ozone insertion into the C-H bond.

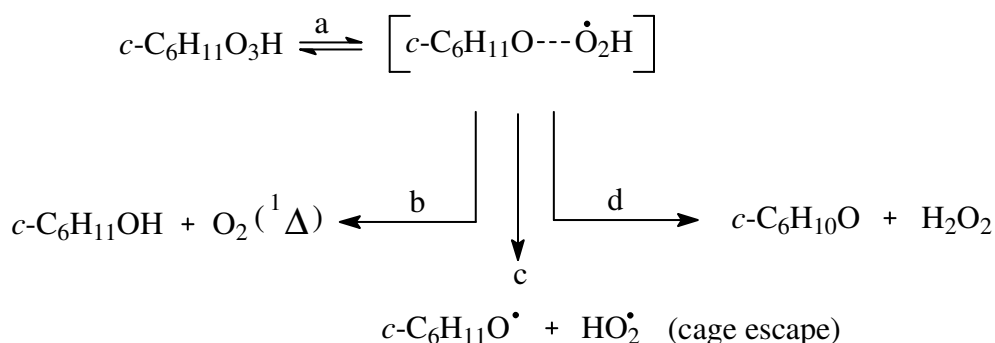
In actual fact there are no true examples of insertion reactions into a σ C-H bond. The very rapid reactions which have been observed for the apparent insertion of such excited species as ¹CH₂ and O (¹D) into C-H bonds are more readily interpreted as abstractions followed by insertions⁴⁸.

Cyclohexane ozonation is typical of the secondary CH₂ group, the initial products are cyclohexanol and cyclohexanone in an estimated ratio of 3.5:1. Nangia and Benson⁴⁸ showed that the hydrotrioxide is most likely to be the initial product formed by the ion-pair (eqn. 1.18)

route and is subsequently followed by the radical decomposition of the hydrotrioxide to alcohol and ketone. For the initial step:



At 25 °C this would predict a half-life for O₃ in cyclohexane of about 2 days. Nangia and Benson⁴⁸ discussed the decomposition of alkyl trioxides of the general formula RO₃R', where R' is either an alkyl group or H atom.



Scheme 1.9. Different paths involved in the ozonation of cyclohexane⁵³.

The radical decomposition would produce a singlet caged radical pair, which could disproportionate in either of two directions as in Scheme 1.9. The nascent radical pair is formed in a singlet state so that the disproportionation will produce singlet O₂ or singlet ketone (path **d**). The radicals which escape the cage can initiate a chain reaction. Both disproportionation paths **b** and **d** are very exothermic, 55 and 75.7 kcal mol⁻¹ respectively, the products formed with large excitation energies⁵³.

Williamson and Cvetanović⁵⁴ determined the second-order rate constants of ozonation in carbon tetrachloride solution at 25 °C for nine paraffins: isobutene, n-pentane, isopentane, neopentane, 3-methylpentane, 2,3-dimethylbutane, n-octane, cyclopentane, and cyclohexane. Their studies showed that different types of C-H bonds in the paraffin molecules show large differences in reactivity, with primary < secondary < tertiary. The values of the ratio (mmol paraffin consumed) / (mmol O₃ absorbed) was found smaller than it could be, as the result of reaction of O₃ with

product alcohols in these high conversion experiments in which about 20-25% of the paraffin reacted. The stoichiometry of some ozone-paraffin reactions are reported in Table 1.4

Table 1.4. Stoichiometry of some ozone-paraffin reactions⁵⁴.

	O₃ added, mmol	O₃ absorbed, mmol	Paraffin reacted, mmol	mmol of paraffin reacted/mmol of O₃ absorbed
Iso pentane	6.32	2.20	1.98	0.90
	5.79	1.46	1.87	1.28
	5.83	2.16	1.92	0.89
3-Methylpentane	6.73	2.98	2.03	0.68
	1.42	0.29	0.20	0.69

The ozonation of paraffins and alcohols in CCl₄ solution gave many orders of magnitude less rapidly than olefins. Their reactivities are approximately comparable to that of benzene and are strongly structure sensitive. Williamson and Cvetanović⁵⁴ showed the order of reactivity is in good agreement with the Hamilton *et al*⁵¹, tertiary > secondary > primary.

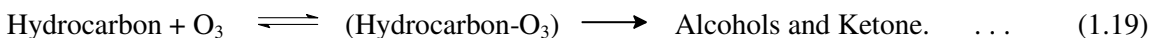
The possibility of slow reactions of ozone with paraffins are subjected to a large solvent effect and the larger differences in reactivity observed may be due to an increased discrimination of ozone attack on paraffin in CCl₄ solution⁵⁴. Another possibility is that neopentane does not provide a true measure of reactivity of primary H atom in general. Small amounts of some rapidly reacting free radicals alkoxy or [•]OH are formed, they have a large effect on the experiments carried out by Hamilton *et al*⁵¹, since they would abstract more indiscriminately primary H atoms and lead indirectly to the formation of corresponding alcohols. Such a contribution, even if relatively minor, could affect the calculated ratios of the initial attack of ozone at various positions in the molecule since ozone itself reacts very slow with primary H atoms⁵⁴.

1.7.2. Complex formation in between ozone and saturated hydrocarbons:

The initial step in the ozonization of a hydrocarbon is formation of a complex between the two reactants. Saturated hydrocarbons are oxidized slowly by ozone, forming alcohols and ketones with a high regio- and stereo-specificity. Although some aspects of these oxidations have been

discussed, their mechanism still remains unclear. Mazur *et al*⁵⁵ reported the ozonation results which suggest an initial formation of a complex between ozone and the saturated hydrocarbons.

Hydrocarbons lacking tertiary C atoms, such as pentane and cyclopentane, are already oxidized at -80 °C, at which temperature hydrocarbons possessing tertiary C atoms such as methylcyclohexane, 2, 3-dimethylbutane, and cis- and trans-decalins are unreactive. These results can be accommodated by assuming formation of a complex between the ozone and the saturated hydrocarbons at low temperatures, which reacts with the reducing agents to give the oxidation products. At higher temperatures the complex decomposes to the oxidation products as shown in eqn. 1.19.



The comparative selectivity in the formation of the tertiary alcohols is consistent with the preference of the electrophilic ozone to form complexes with tertiary C atoms, while the high degree of configurational retention is indicative of an insertion reaction, which may occur by a concerted decomposition of the complex. Furthermore the lower temperatures at which hydrocarbons lacking tertiary C atoms react with ozone points to higher reactivity of complexes with these hydrocarbons.

The increase of the regiospecificity and the decrease of the stereospecificity with raising the temperature may be explained by an additional mechanism which becomes more significant as the temperature increases and which may involve ionic or free-radical intermediates. Mazur *et al*⁵⁵ suggested the complex formation between ozone and saturated hydrocarbons is in accord with the polar nature of ozone, which has the tendency to form complexes with aromatic compounds, olefins and hydrosilanes is well known.

1.7.3. Formation of singlet oxygen from hydrotrioxides in the ozonation of hydrocarbons:

Murray *et al*⁵⁶ reported that the ozonation of relatively unreactive substrates including hydrocarbons, ethers and alcohols, where oxygen rich intermediates, possibly hydrotrioxides are formed, can also be expected to lead the sources of singlet oxygen. Hydrotrioxides have been postulated as intermediates or unstable products in the ozonation of such diverse substrates as hydrocarbons, ethers, alcohols, amines, aldehydes. Evidence has been presented confirming the

existence of trioxides. In many of these cases the oxidized substrate is postulated as arising from decomposition of the hydrotrioxide with a concomitant release of molecular oxygen.

Ozone is a reactant of considerable interest in organic chemistry. Special attention has been paid to the reactions of ozone at activated C-H bonds, such as the α hydrogens of saturated hydrocarbons, alcohols, ethers and aldehydes. In a number of cases, the initial products have been shown to be hydrotrioxides, which are generally stable below about $-40\text{ }^{\circ}\text{C}$. The reaction of ozone with C-H bonds has been shown to occur with net retention of configuration to have a pronounced kinetic isotope effect, and to have a relative reactivity of $3^{\circ} > 2^{\circ} > 1^{\circ}$ for both saturated hydrocarbons and ethers.

The mechanism for the ozonation of C-H bonds has not been clearly established. The proposed mechanisms include initial attack at an oxygen atom, and abstraction of either hydride or a hydrogen atom. A hydride abstraction and the concerted insertion of ozone into a C-H bond are most consistent with the kinetic data by Pryor *et al*⁵⁷. Ozone reactions exhibit greater selectivity between primary, secondary, and tertiary alkanes than do the radicals as shown in Table 1.5. The greater sensitivity of ozone reactions to changes in ring substituents suggests that the transition state for the ozonation of alkanes is more polar than that of a hydrogen-atom abstraction by a free radical.

Table 1.5. Reactivities of some alkanes towards ozone and some radical species.

Type of alkane	Ozone ^a	radicals ^b		
		Br [•]	ROO [•]	RO [•]
Primary	0.003	0.02	0.024	0.08
Secondary	1.00	1.00	1.00	1.00
Tertiary	87.00	40.00	10.00	3.70
Ar-CH ₃ (p) ^c	-2.07	-1.88	-0.76	-0.34

^a Reference 54, (at $25\text{ }^{\circ}\text{C}$ in CCl_4)

^b & ^c Reference 57.

Ozone reacts slowly with saturated hydrocarbons inserting oxygen atoms into their C-H bonds, resulting in alcohols and ketones⁵⁷. This insertion occurs preferentially at the tertiary carbon

atoms, with retention of configuration. One of the factors limiting the use of ozone as reagent for hydroxylation of saturated hydrocarbons is its low solubility in organic solvents. Even at low temperatures at which ozone forms stable solutions in saturated hydrocarbons and no reaction is observed, its solubility is slightly low (~0.1-0.3% by weight at -78 °C). At higher temperatures necessary for reaction to proceed at reasonable rate, the solubility of O₃ is even smaller, necessitating prolonged ozonation periods⁵⁷.

The reactivity of ozone towards most of the organic solvents limits its practical use as a hydroxylation reagent only to neat hydrocarbons. Mazur *et al*⁴⁶ have studied the ozonation reactions by pre-adsorbing the silica gel with hydrocarbons by direct mixing or impregnating by using a volatile solvent. They used the stream of ozone to pass through the silica gel containing ~1% by weight of the hydrocarbon at -78 °C until it becomes saturated with ozone. It was then allowed slowly to room temperature, followed by elution of the organic material. Mazur *et al*⁴⁶ observed quantitative conversions of the hydrocarbons, resulting in a very high yield of the tertiary alcohols. Under the same conditions secondary alcohols are oxidized to ketones.

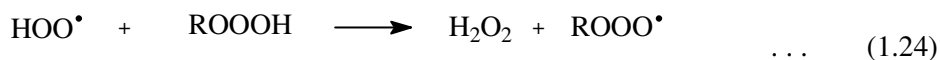
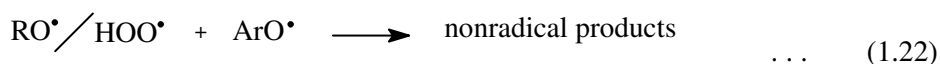
The reaction of ozone with C-H bonds either in solution or by the dry ozonation method, exhibits marked preference for attack at tertiary positions. In solution methylene groups undergo slow oxidation but the conversion of -CH₂- groups into >C=O by dry ozonation appears not to have been observed except in the special case of cyclopropane compounds when cyclopropyl ketones are formed. Beckwith *et al*⁵⁸ reported that the dry ozonation can introduce the carbonyl group at positions remote from functional groups.

The hydroxylation reaction of cyclododecanone by incubation with various fungal cultures is confirmed to the 5-, 6-, and 7- position, demonstrates an interesting similarity between dry ozonation and microbiological oxidation⁵⁸. Dry ozonation of dodecyl acetate gave a complex mixture of keto-acetates⁵⁸. The results obtained by Beckwith *et al*⁵⁸ describes about the particularity of the high regioselectivity of the reaction, consistent with that of dry ozonation which involves attack by gaseous ozone at positions remote from the binding site on substrate adsorbed as a monolayer. There is a remarkable similarity between the results of dry ozonation and biological oxidation indicates that ozonation may have considerable utility for the synthesis of a variety of natural products⁵⁸.

1.7.4. Mechanism for decomposition of the hydrotrioxide:

The fact that 2,6-tert-butyl-4-methylphenol (BHT) and the trioxide decompose with same rate constant indicates that a quantitative yield of radicals is obtained from the decomposition of the trioxide⁵⁹. Hydrotrioxides^{3, 52} that have been studied decompose either to give radicals or by a nonradical path giving $^1\text{O}_2$.

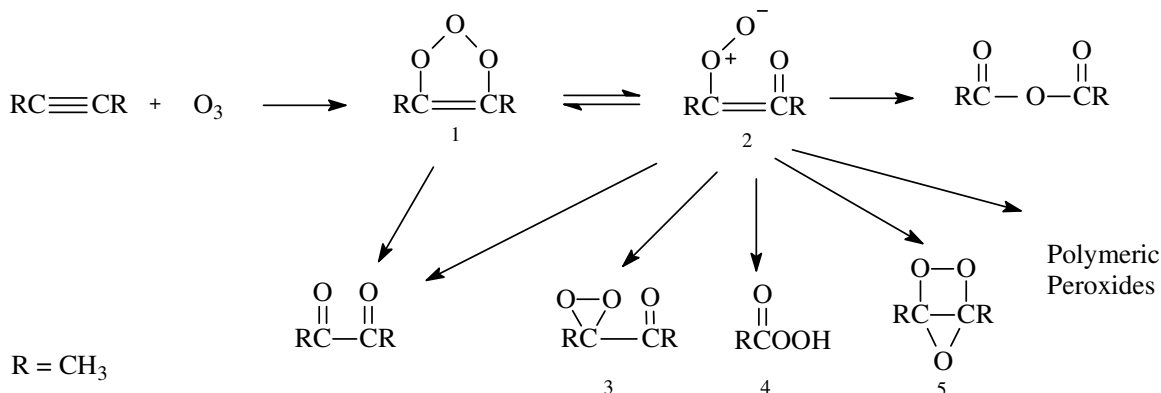
Pryor *et al*⁴⁹ formulate the decomposition of ROOOH as homolysis in eqn. 1.20, in the presence of BHT is followed by eqns. 1.21 and 1.22. In the absence of BHT, chain decomposition shown in eqns. 1.23-1.25 occur leading to cumyl alcohol, additional expected products are hydrogen peroxide⁵³ and oxygen (probably singlet^{52, 53}).



Mechanistic studies of the ozonolysis of acetylenes¹³, unlike the ozonolysis of olefins, have been very limited. The reaction of olefins with ozone is believed to proceed via the intermediacy of the carbonyl oxide **2** as shown in Scheme 1.10. All the products (α -dicarbonyls, acid anhydrides, and polyperoxides) are believed to arise by the rearrangement or reactions of carbonyl oxide **2** in Scheme 1.10. On the basis of their ability to epoxidize olefins, three species (**1**, **3**, and **4** in Scheme 1.10) identified as major intermediates or products formed from carbonyl oxide **2** during the ozonolysis of dimethylacetylene⁵⁹.

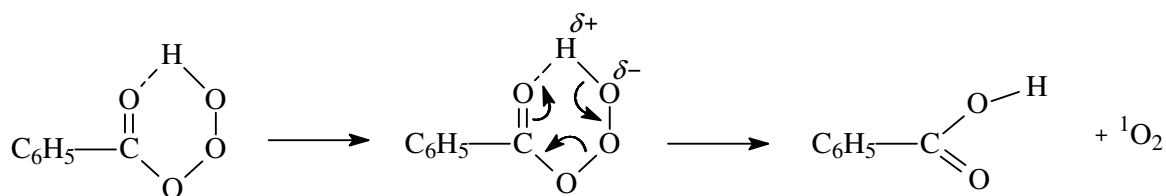
Ozonization of benzaldehyde, 2-methyltetrahydrofuran, and methyl isopropyl ether leads to intermediates which have been characterized as hydrotrioxides. The decompositions give singlet oxygen which was characterized by its reactions with typical singlet oxygen acceptors⁵². Organic

hydrotrioxides are a class of compounds which are related to trioxides in the same manner as hydroperoxides are related to peroxides⁵². Hydrotrioxides appear to be reasonable structures for ozonization intermediates, little experimental evidence has been available to confirm their existence, and arguments have been put forth against their intermediacy in some hydrocarbon ozonizations. There is some evidence for the existence of the parent, nonorganic compound, and hydrogen trioxide⁵².



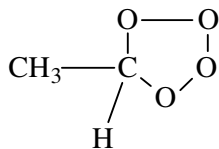
Scheme 1.10. Intermediates formation in ozonolysis of dimethylacetylene⁵⁹.

Sary *et al*⁵² studied the reactions of ozone with organic substrates as possible sources of singlet oxygen. In a number of cases they provided evidence that singlet oxygen is produced in the ozonization reaction, and in some cases such ozonizations are very convenient and efficient sources of singlet oxygen for chemical oxygenation reactions. In the case of benzaldehyde hydrotrioxide gave benzoic acid and singlet oxygen as shown in Scheme 1.11.



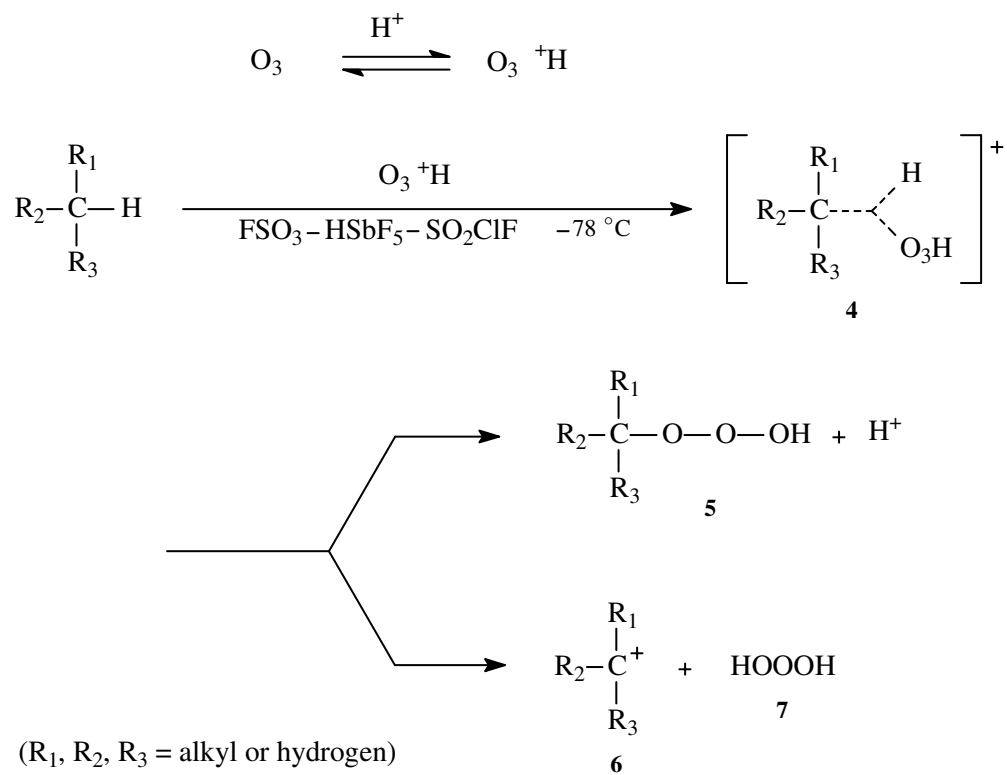
Scheme 1.11. Benzaldehyde ozonation as a source for singlet oxygen formation⁵².

Syrov and Tsyskovskii⁶⁰ observed the mechanism of ozonization of acetaldehyde and considered the possibility that a cyclic tetroxide could be formed as shown in Scheme 1.12, it is unstable and would rapidly rearrange to the hydrotrioxide.



Scheme 1.12. Cyclic tetroxide intermediate in acetaldehyde ozonation⁶⁰.

Yoneda and Olah⁴¹ reported the electrophilic oxygenation of alkanes with ozone in superacid media. They reported that the reaction proceeds via electrophilic insertion of protonated ozone, i.e., $^+\text{O}_3\text{H}$, into the involved single σ bonds of the alkanes, similarly to such electrophilic reaction as protolysis of alkanes⁶¹. The reaction of alkanes with ozone in $\text{FSO}_3\text{H-SbF}_5\text{-SO}_2\text{ClF}$ solution can be best described by the electrophilic attack of protonated ozone into the C-C or C-H σ bonds of the alkanes as shown in Scheme 1.13.



Scheme 1.13. The electrophilic attack of protonated ozone into the C-C or C-H σ bonds of the alkanes⁶².

Ozone has a strong 1, 3 dipole, it is strongly polarizable and it is readily protonated in superacids. Protonated ozone, $^+\text{O}_3\text{H}$, once formed seems to have a significant affinity (i.e. powerful

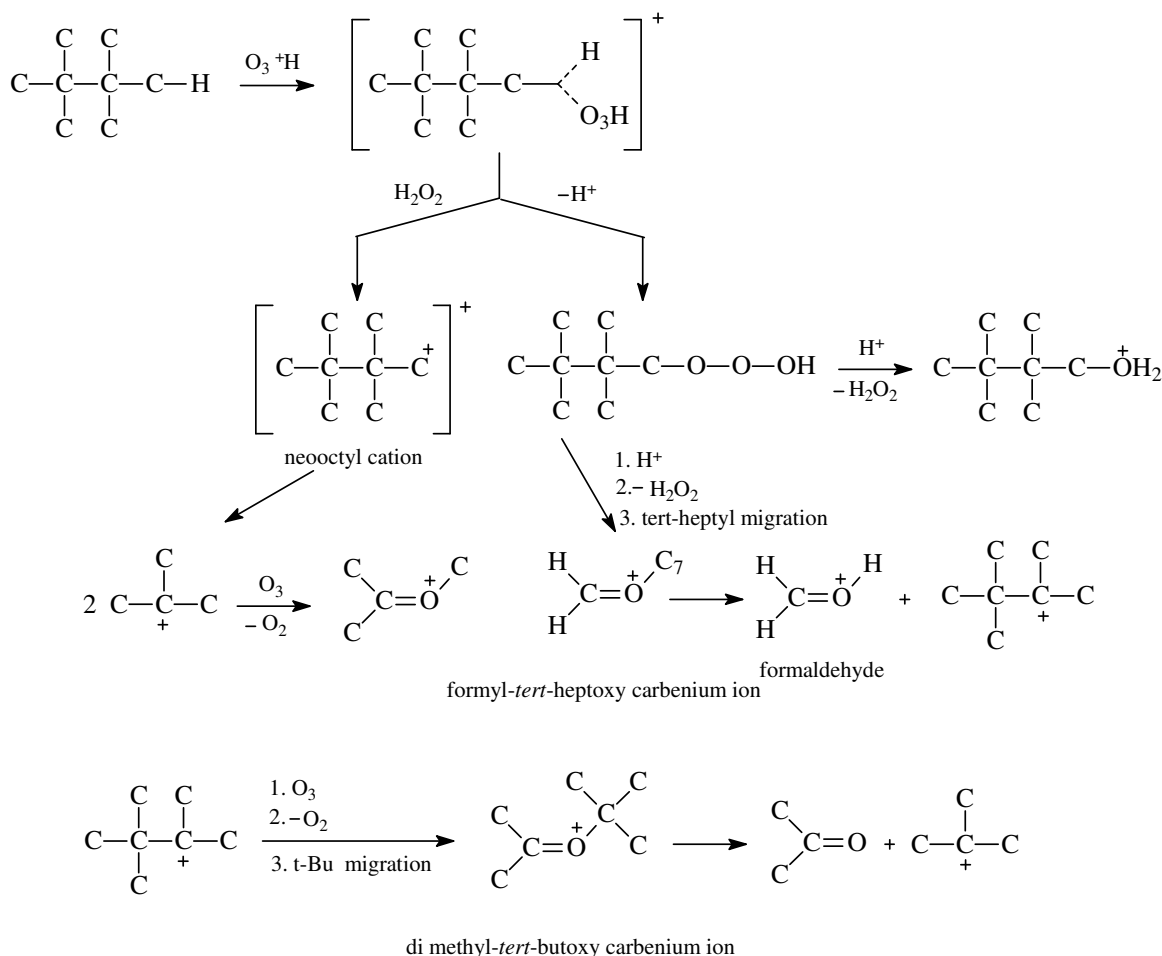
[illegible]

Scheme 1.14. Ozonation of alkanes in strong acid media (superacids)⁶².

Hydrogen trioxide is reported to be an extremely unstable species, decomposing into water and oxygen. In superacids, it can be considered to have the ability to act as a hydroxylating agent. Alkyl trioxides also been considered as hydroxylating agents in an analogous way⁶³.

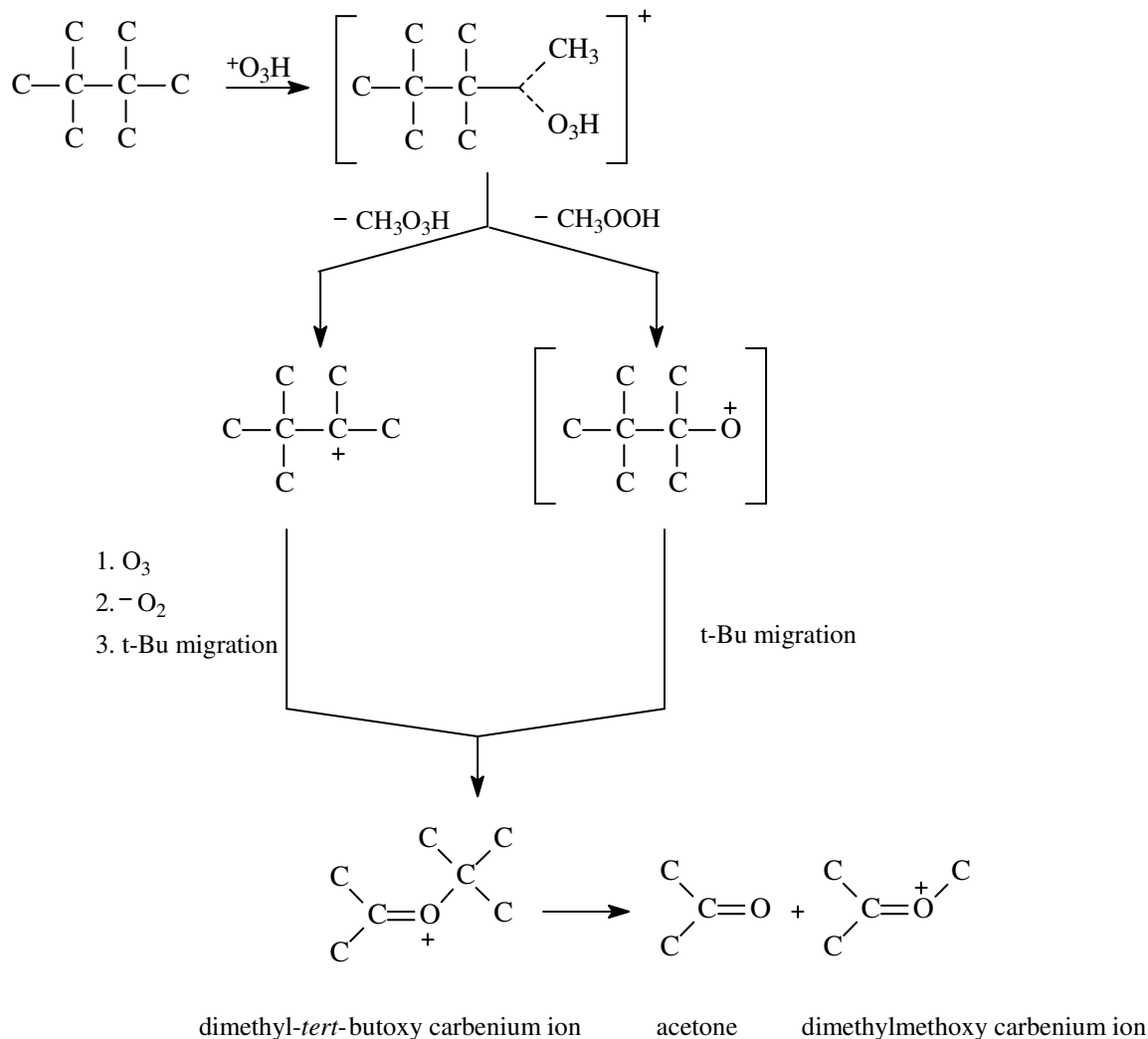
34

Formaldehyde, methyl ethyl ketone, acetylium ion $\text{CH}_3\text{C}\equiv^+\text{O}$, and carbon dioxide in small amounts were identified in the product mixture⁶³.



Scheme 1.15. C-H Bond ozonolysis⁶³.

Olah and co-workers⁴¹ felt that the reaction taking place initially through electrophilic insertion of protonated ozone into the single σ bond of the alkane as shown in the Schemes 1.15 and 1.16. The third possible route, i.e. direct $\text{C}_2\text{-C}_3$ bond ozonolysis, is improbable for steric reasons. Instead formation of the tert-butyl cation can take place through initial attack on the C-H bond with the neo-octyl cation undergoing β -cleavage, subsequent reaction with ozone to yield dimethylmethoxy carbenium ion⁴¹.



Scheme 1.16. C₁-C₂ Bond ozonolysis⁶³.

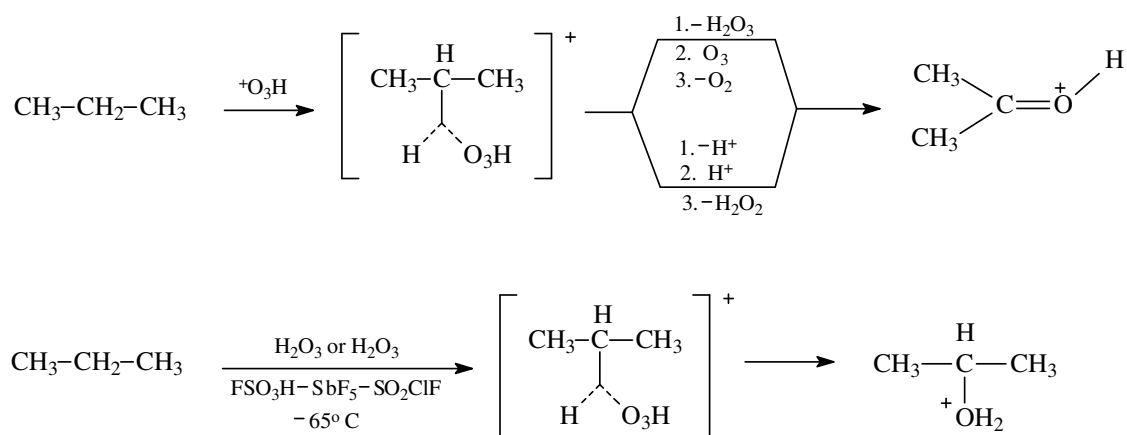
In principle it is considered that the reaction takes place by attack of protonated ozone into the C-H or C₁-C₂ σ bonds as shown in the Schemes 1.15 and 1.16. The reactivity of C-H bonds is much higher than that of the C-C bonds. The product distribution showed that there is no direct C₂-C₃ bond reaction (owing to the steric reasons). The C₁-C₂ and/or C-H bond cleavage were in the good accordance with the experimental results (product ratio of dimethylmethoxy carbenium ion and acetone is about equal), suggesting the attack of protonated ozone preferentially took place with the C-H bonds (being more accessible). The nature of system (particularly steric hindrance) can influence the reactivity of δ bonds. The bulkiness of protonated ozone may cause the higher reactivity of C-H over C-C bonds⁶³.

Olah and co-workers⁴¹ described the reaction of straight chain alkanes with ozone in FSO₃H-SbF₅-SO₂ClF solution at -78 °C. Their detailed studies by changing the temperature with an equimolar amount of ozone, formation of alcohols were observed, suggesting the initial attack of protonated ozone on the involved δ bonds of alkanes. Formation of acetone (protonated) was observed when propane was reacted with similar conditions, with about 30% conversion of propane. By raising the temperature of the solution to -65 °C with no further introduction of ozone and keeping it for about 2 h, the formation of isopropyl alcohol was observed. A similar observation was made for ethane at -40 °C and butane at -65 °C (Table 1.6).

Table 1.6. Secondary hydroxylation of straight chain alkanes by H₂O₂ (or H₂O₃) formed in their ozonolysis in superacids⁶³.

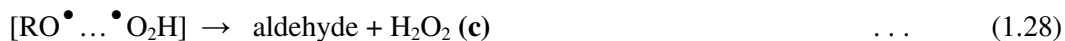
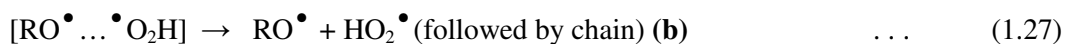
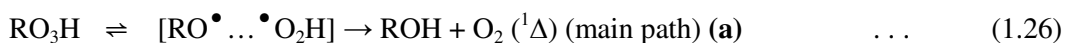
Alkane	Temperature, °C	Reaction Time, min	Product distribution, %
CH ₃ CH ₃	-78	< 1	CH ₃ (H)C=O ⁺ H (~95%)
CH ₃ CH ₃	-78	120	CH ₃ (H)C=O ⁺ H (~95%)
CH ₃ CH ₃	-40	60	CH ₃ (H)C=O ⁺ H (90%), CH ₃ CH ₂ ⁺ OH ₂ (10%)
CH ₃ CH ₂ CH ₃	-78	< 1	(CH ₃) ₂ C=O ⁺ H (~95%)
CH ₃ CH ₂ CH ₃	-78	120	(CH ₃) ₂ C=O ⁺ H (~95%)
CH ₃ CH ₂ CH ₃	-65	60	(CH ₃) ₂ C=O ⁺ H (85%), CH ₃ CH(O ⁺ H ₂)CH ₃ (15%)
CH ₃ CH ₂ CH ₂ CH ₃	-78	< 1	CH ₃ CH ₂ (CH ₃)C=O ⁺ H (40%), CH ₃ (H)C=O ⁺ CH ₂ CH ₃ (60%)
CH ₃ CH ₂ CH ₂ CH ₃	-78	120	CH ₃ CH ₂ (CH ₃)C=O ⁺ H (40%), CH ₃ (H)C=O ⁺ CH ₂ CH ₃ (60%)
CH ₃ CH ₂ CH ₂ CH ₃	-65	60	CH ₃ CH ₂ (CH ₃)C=O ⁺ H (30%), CH ₃ (H)C=O ⁺ CH ₂ CH ₃ (50%), CH ₃ CH ₂ CH(O ⁺ H ₂)CH ₃ (20%)

The results can be best explained proceeding in two steps: primary ozonolysis followed by hydroxylation with H₂O₂ (H₂O₃) formed in the former reaction. The reaction of propane with H₂O₂ in FSO₃H-SbF₅-SO₂ClF at -65 °C confirmed the suggested path, giving isopropyl alcohol (protonated) as shown in Scheme 1.17. On the other hand, tertiary isoalkanes did not give any observable alcohols under the reaction conditions⁶³.



Scheme 1.17. Propane ozonation mechanism⁶³.

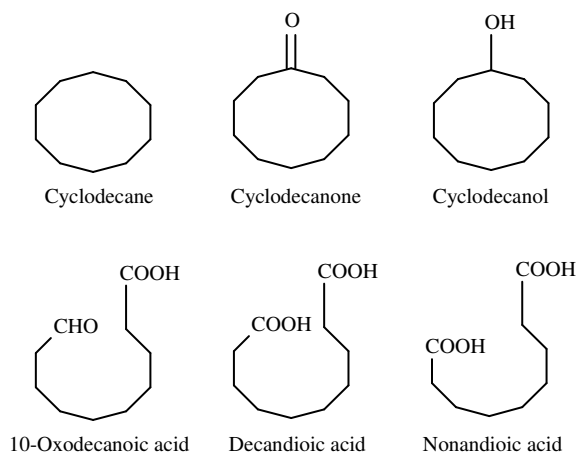
Ozone reactions with saturated compounds are shown by contrast to all proceed via hydride ion transfer to form an intimate ion pair $[\text{R}^+\text{HO}_3^-]$ in a solvent cage which can exothermically collapse to the observed products RO_3H . Solvation enthalpies were calculated from the Kirkwood formula for dipole solvation and shown to lead the reasonable activation energies for ozonation of alkanes, alcohols, and acetals, all of which produce the hydrotrioxides. The kinetics of the subsequent decomposition of these species were shown to proceed via radical processes, including cage disproportionation, which was proposed as the source of the observed high yields of singlet O_2 as shown in step **a** (eqn. 1.26).



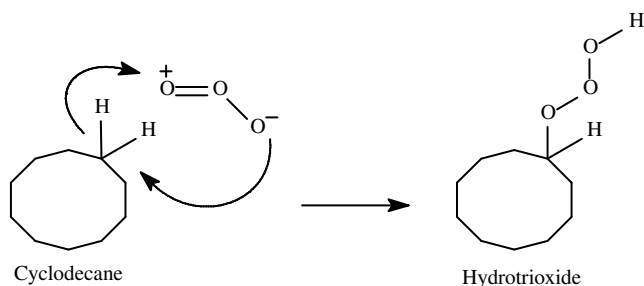
Rate constants were derived for these decompositions and also for the subsequent chain reactions initiated by the radicals, which escape the cage (step **b**, eqn. 1.27) in good agreement with observed data⁴⁸.

1.8. Ozonation of cycloalkanes (cyclohexane and cyclodecane):

The selective oxidation of alkanes at room temperature is one of the important objectives of synthetic chemistry. Cyclodecane and cyclohexane were converted to the corresponding cycloalkanones and cycloalkanols upon ozonation at acidic pH, also some ring cleavage to dicarboxylic acids or aldehydoacids⁵ observed. Ozone has been used for the oxidation of cycloalkanes³ and the formation of hydrotrioxides has been reviewed⁵. These studies suggest that the use of ozone for these processes require improvement of both conversion and selectivity. Barletta *et al*⁵ reported that some cycloalkanes (cyclodecane and cyclohexane) with ozone gave oxygenated products. The ozonation of suspension of cyclodecane in a pH 3 buffer, after 1 h at 25 °C gave a 66.3% conversion of the starting material, the main product was cyclodecanone (28.7% selectivity) and small amount of cyclodecanol. Cyclodecanol is an intermediate in the ring cleavage reaction leading to decandioic acid and also is an intermediate in the formation of cyclodecanone as shown in Scheme 1.18.



Scheme 1.18. Ozonation products of cyclodecane⁵.

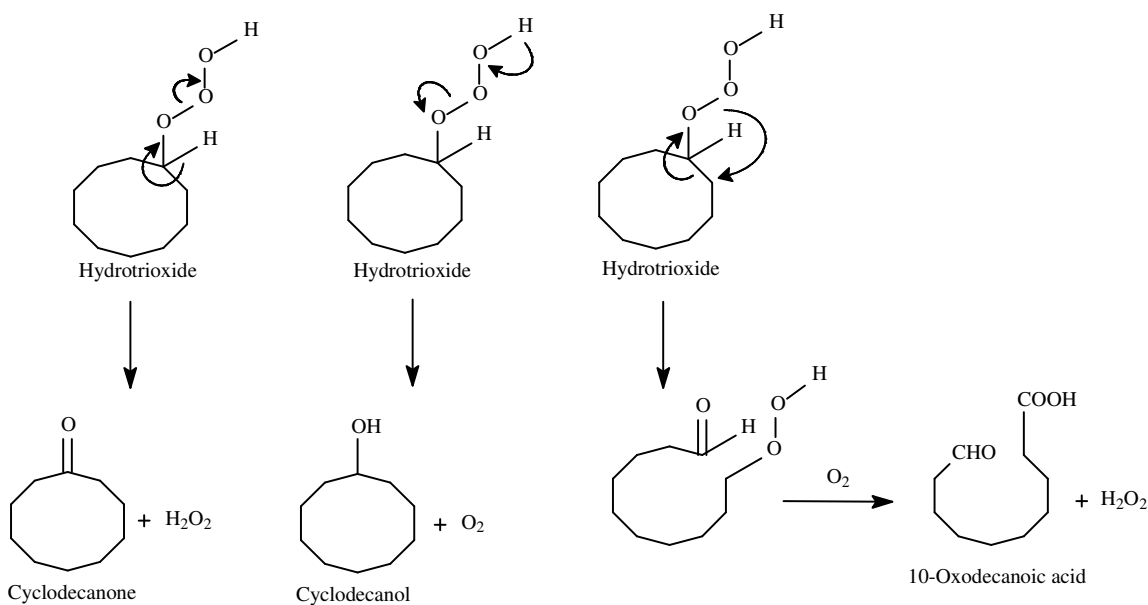


Scheme 1.19. Hydride transfer from the alkane forming hydrotrioxide⁵.

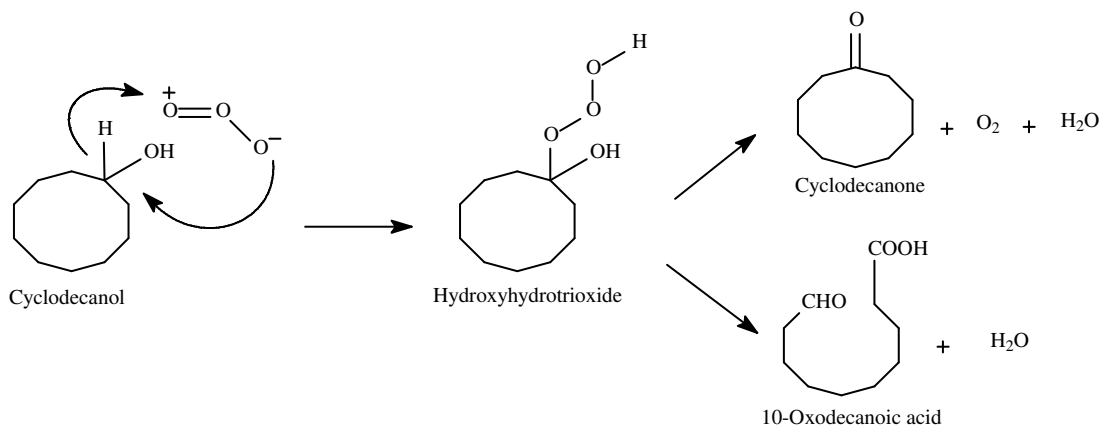
A possible reaction mechanism of hydride transfer from the alkane forms a hydrotrioxide as shown in Scheme 1.19. This mechanistic detail has been suggested²⁷⁴ to account for the oxygenation of some ethers and is in agreement with the fact that oxygen is inserted into the methylene group adjacent to the heteroatom both in the oxygenation of ethers to esters and in the oxygenation of amines to amides⁵⁷.

The key intermediates in the reaction are as shown in Scheme 1.20.

1. Dissociate to cyclodecanone and hydrogen peroxide.
2. Dismutate to cyclodecanol and dioxygen.
3. Rearrange to decandioic acid.



Scheme 1.20. Dissociation, dismutation and rearrangement of hydrotrioxide⁵.



Scheme 1.21. Analogous reaction of ozone with cyclodecanol⁵.

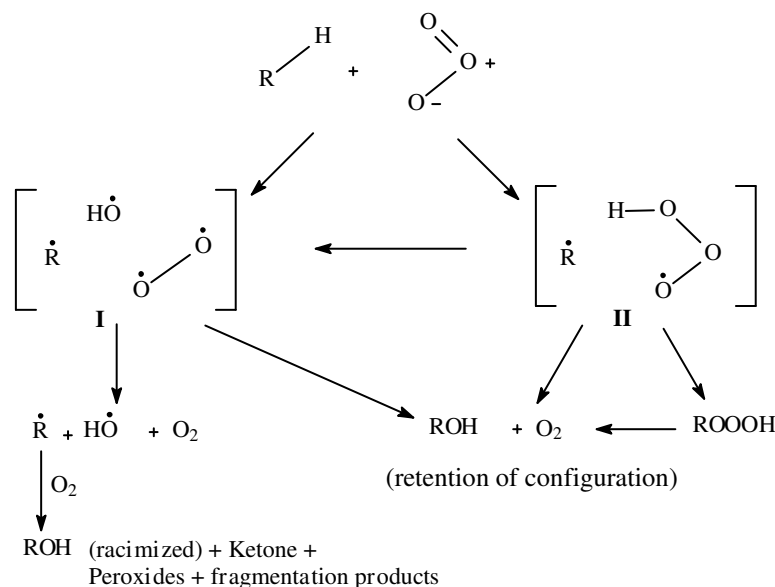
The analogous reaction with cyclodecanol will form a hydroxyhydrotrioxide. This is the second key intermediate in the reaction as shown in Scheme 1.21. The alternative ozonation at pH 7 is probably less effective in the conversion of cyclodecane into cyclodecanone because of its fast further oxidation⁵.

1. Dismutate to cyclodecanone and dioxygen.
2. Dissociate to 10-oxodecanoic acid.

The initial alkane oxidation products are more reactive towards ozone than the alkane, the observed products frequently arise as the result of several steps⁵¹. Ozonation of cyclohexane for short periods at room temperature gave cyclohexanol and cyclohexanone as products, the ratio reported as increased rapidly after several minutes. The result indicates that even after very low conversion the initially formed cyclohexanol is oxidized further by ozone¹³. However, not all the cyclohexanone obtained in the cyclohexane ozonation arised from further oxidation of cyclohexanol. When the observed ratio of cyclohexanone to cyclohexanol was plotted vs time, the extrapolated value to zero time, a ratio of cyclohexanone to cyclohexanol at time zero of 0.25 to 0.3 indicates that some of the cyclohexanone is formed directly from an intermediate in the ozonation⁵¹.

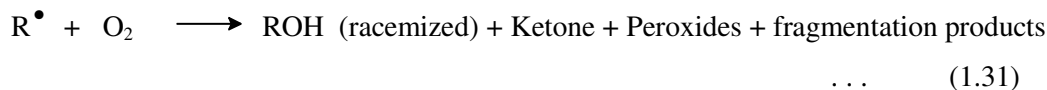
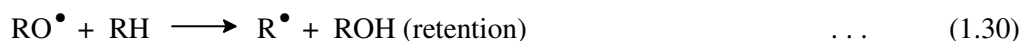
The controlled experiments of cyclohexane oxidation requires the presence of ozone, where unozonized oxygen was passed through the cyclohexane with all other conditions the same, it was reported⁵¹ that no detectable amounts of oxidation products. Hamilton *et al*⁵¹ noticed the formation of peroxide in the ozonation of saturated hydrocarbons at room temperature.

The alkane and ozone react to give a transition state (or solvent caged intermediate) **I** or **II** was suggested as shown in Scheme 1.22, which has considerable radical character. If there is no partial bonding among the various radicals of **I** and **II**, then thermodynamic considerations³⁵ indicate that **I** is more likely than **II**. If the R[•] partially bonded to an oxygen species either **I** or **II** seem possible. Retention of configuration in the alcohol product would be expected if **I** or **II** collapsed directly to alcohol and oxygen (**II** possible reacting with ROOOH as an intermediate). To account for the formation of some racemized alcohol, ketone, peroxides, and fragmentation products, it is suggested that **I** and **II** can also be separate into the radicals R[•] and HO[•]. Alkyl radicals are known to react with oxygen in a series of steps to give these other product as shown in Scheme 1.22.



Scheme 1.22. Radical nature of transition state in the ozonation of saturated hydrocarbons⁵¹.

Mechanisms for the formation of racemized alcohol, which involve the RO^\bullet radical's abstracting a hydrogen atom from the alkane as, for example, in the following sequence (eqns. 1.29-1.31):



It was reported⁵¹ that the initial step in the oxidation is an insertion type reaction in which the transition state has radical character.

1.9. Ozone in the treatment of water and wastewaters:

Ozone application has increased enormously both in number and diversity since the first full scale application of ozone for the disinfection of drinking water in Nice (1906). It is used for the treatment and purification of ground and surface waters, for domestic and industrial wastewater as well as in swimming pools and cooling tower systems. It has also been integrated into production process that utilizes its oxidizing potential, e.g. bleaching in the pulp and paper industry, metal oxidation in the semiconductor industry.

In the industrial wastewater treatment, ozone is used extensively in recycling marine aquaria waters, and other aqueous systems housing zoo animals. It is also used to oxidize cyanide-

containing wastewaters from metal finishing industries by itself and in simultaneous combination with ultraviolet radiation or hydrogen peroxide, and to recycle rinse waters used in electronic chip manufacturing. Ozone is used in many Japanese textile plants in combination with granular activated carbon adsorption, in at least 60 Italian textile-dyeing plants to treat wastewaters, and at least one full-scale combined municipal/industrial treatment plant in the UK, treating primarily coloured wastewaters from local textile dyeing plants. A petroleum refinery in Canada uses ozone to lower levels of phenols in its discharges to a freshwater lake upstream of a potable water intake. Although ozone can be made to treat pulp bleaching plant wastewaters, it has a more productive use in replacing chlorine as the bleaching agent. In this manner, not only is formation of chlorinated organics eliminated, but significant portion of the water used can be recycled to the process³⁰.

Generally, the main areas where ozone is used are:

- ❖ Disinfection
- ❖ Oxidation of inorganic compounds
- ❖ Oxidation of organic compounds, including taste, odour, colour, removal and
- ❖ Particle removal.

1.9.1. Drinking water treatment:

Due to its high oxidation and disinfection efficiency, ozone has been applied in water treatment for many years^{24, 25, 64}. Drinking water supplies are based on natural ground waters, on artificially recharged ground waters or bank filtered surface waters, on lakes and dam reservoirs and on river waters. Ozone is typically applied as a pre-disinfectant for the control of algae and inactivation of bacteria and viruses in direct filtration processes, and as a pre- and/or intermediate oxidant for inorganic and organic matter to eliminate taste, odour, and color compounds; remove turbidity, metal ions; and reduce levels of trihalomethane (THM) and related organic precursors; other disinfection by-products (DBPs) while improving flocculation. In general, ozone may react with water impurities by means of direct or indirect reactions. Reaction between a substrate and ozone molecule is referred to as a direct reaction while the indirect reactions are referred to as those reactions which involve a substrate and radicals derived from decomposition of ozone (Table 1.7). Ozone molecule is highly selective of species it will react with and when a reaction does take place it is relatively slow when compared with radical reactions. On the contrary, radicals are highly reactive and the reaction period is short. Ozone reacts with both organic and inorganic substances in natural waters. Some inorganic substrates⁶⁵ that can be oxidized directly by ozone

are Fe^{2+} , Mn^{2+} , Br^- and NH_3 . Organic compounds such as glyoxylic acid, formic acid, humic acid, primary alcohols and benzene have been found to initiate and promote ozone decomposition while acetone and aliphatic alcohols stop the decomposition chain^{27, 32}.

Table 1.7. Typical initiators, promoters and inhibitors for decomposition of ozone by radical type chain reaction, encountered in natural waters and wastewaters³².

Initiators	Promoters	Inhibitors
OH^\cdot	$\text{R}-\text{C} \begin{matrix} \nearrow \text{H} \\ \searrow \text{OH} \end{matrix}$	$\text{CH}_3-\text{C} \begin{matrix} \nearrow \text{O} \\ \searrow \text{O}^\cdot \end{matrix}$
$\text{H}_2\text{O}_2 / \text{HO}_2^\cdot$	Aryl – (R)	Alkyl – (R)
Fe^{2+}	Formate	$\text{HCO}_3^- / \text{CO}_3^{2-}$
Formate	Humics	Humics
Humics	O_3	TOC
TOC	-	-

* TOC and R represent Total Organic Carbon and Radical respectively.

During ozonation, dissolved organic compounds in water are only partially oxidized. Higher molecular weight organic compounds are transformed into lower molecular weight compounds, leaving dissolved organic carbon concentration (DOC) substantially unaffected^{66, 67}. The reaction of ozone with natural organic matter (NOM) may result in the formation of numerous by-products. Among these by-products epoxides, organic peroxides and aldehydes are of particular concern in drinking water. The formation of aldehydes^{24, 25, 68-75} and carboxylic acids⁷⁶ upon ozonation is well established. The literature provides several examples of aldehyde formation vs. ozone dose^{68, 70}, aldehyde formation vs. pH^{68, 70}, as well as aldehyde formation vs. hydrogen peroxide dose⁷⁰. According to Schechter and Singer⁶⁸ the formation of aldehydes (formaldehyde, acetaldehyde and glyoxal) depends on the ozone, total organic carbon (TOC) ratio of 1.

Kusakabe *et al*⁷⁷ have shown the importance of carboxylic acid formation - virtually the whole organic matter can be oxidized by ozone, e.g. formic acid, acetic acid and particularly oxalic acids are the most significant. Aldehydes are usually observed at the levels of 10 mg L^{-1} after the ozonation, while carboxylic acids are usually present at concentrations of hundreds of micrograms per liter^{75, 78}. A short contact time (4-6 min) is sufficient for the reaction of ozone with organic matter. Carboxylic acids are formed at much higher quantities than aldehydes during the ozonation of natural organic matter⁷⁹.

1.9.1.a. Disinfection: The introduction of ozone in water treatment started about a century ago and was directed at the disinfection of microbial-polluted water. Ozone is very effective against bacteria because even concentrations as low as 0.01 ppm are toxic to bacteria⁸⁰. Ozone is a more effective broad-spectrum disinfectant than chlorine-based compounds. Whereas disinfection of bacteria by chlorine involves the diffusion of HOCl through the cell membrane, disinfection by ozone occurs with the rupture of the cell wall. The disinfection rate depends on the type of organism and is affected by ozone concentration, temperature, pH, turbidity, oxidizable substances, and the type of contactor employed. In the design of chemical disinfection, the concept of $c-t$ (free disinfectant concentration c multiplied by the available contact time t) is frequently applied, based on the law of Chick/Watson (1908). Very often, a $c-t$ value of 1.6 - 2 $\text{mg L}^{-1} \text{ min}^{-1}$ (e.g. 0.4 mg L^{-1} ozone for 5 min) is considered to be sufficient for effective disinfection, after particulate matter is removed down to low turbidities⁸⁰.

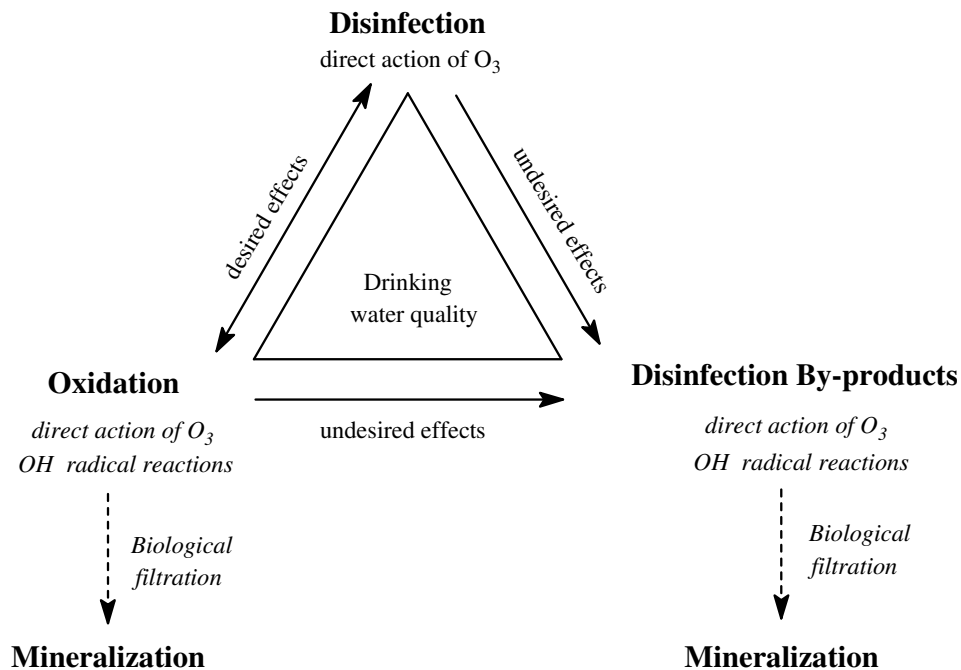


Figure 1.12. Desired and undesired effects of ozone⁶⁴.

The main reasons for the use of ozone are disinfection and oxidation (e.g. taste and odour control, decoloration, elimination of micropollutants) or a combination of both⁸¹⁻⁸³. Similar to other disinfectants for water treatment (e.g. chlorine or chlorine dioxide), ozone is unstable in water

and undergoes reactions with some water matrix components. However, the unique feature of ozone is its decomposition into $\bullet\text{OH}$ radicals which are the strongest oxidants in water⁸⁴. Therefore, the assessment of ozonation processes always involves the two species ozone and $\bullet\text{OH}$ radicals. However, for different applications of ozone the two species are of differing importance. While disinfection occurs dominantly through ozone, oxidation processes may occur through both oxidants, ozone and $\bullet\text{OH}$ radicals^{24, 25, 83, 85} (Fig. 1.12). Ozone is a very selective oxidant; $\bullet\text{OH}$ radicals react fast with many dissolved compounds and the water matrix. For ozone reactions more than 500 rate constants have been measured^{29, 84, 86-88} for $\bullet\text{OH}$ radical reactions the database is even larger and contains a few thousand rate constants^{89, 90}. The most prominent exception is ammonia which is only slowly oxidized by ozone and $\bullet\text{OH}$ radicals. In turn, ammonia also does not affect disinfection's efficiency⁶⁴.

1.9.1.b. Oxidation of inorganic compounds: The reactions of ozone with inorganic compounds in drinking water are typically fast and occur by an oxygen atom transfer reaction. The use of ozonation to oxidize metal surfaces in the semiconductor industry is growing, ozonation for the oxidative removal or transformation of inorganic constituents of drinking and waste waters is a rather rare application, because other methods exist for most of the target compound. However, inorganic compounds may be oxidized as a secondary effect of ozonation for other purposes (particle removal, organics oxidation). Ozone is achieving great interest as a replacement of chlorine and its derivatives in the bleaching of paper pulp, minimizing the organic halogenated compounds formation. Ozone is a highly oxidizing reagent which reacts with lignin but also with carbohydrates, resulting in a decreased viscosity and therefore in a decreased fiber strength⁹¹.

1.9.1.c. Oxidation of organic compounds: The oxidation of organic micropollutants can be divided into compounds that can be directly oxidized by ozone and those which do not react with ozone. For the compounds that can be directly oxidized, ozonation is very efficient. For these compounds, their speciation is decisive for their oxidizability. Organic micropollutants are oxidized with ozone selectively. Ozone reacts mainly with double bonds, activated aromatic systems and non-protonated amines. In general, electron donating groups enhance the oxidation of ozone whereas electron withdrawing groups reduce the reaction rates⁶⁴.

Depending on the water quality, the half-life of ozone is in the range of seconds to hours. The major secondary oxidant formed from ozone decomposition in water is the $\bullet\text{OH}$ radical. The

stability of ozone largely depends on the water matrix, especially its pH, the type and content of natural organic matter (NOM) and its alkalinity⁸³. All water sources may contain NOM, but concentrations (usually measured as dissolved organic carbon, DOC) differ from 0.2 to more than 10 mg L⁻¹. The tasks of NOM-ozonation⁸² are:

Removal of colour and UV-absorbance: Surface waters generally are coloured by naturally occurring organic materials such as humic, fulvic, and tannic acids. Such colour-causing compounds contain multiple conjugated double bonds, some of which are readily split by ozone (specific ozone consumptions in the range below 1.0 g O₃ g⁻¹ DOC).

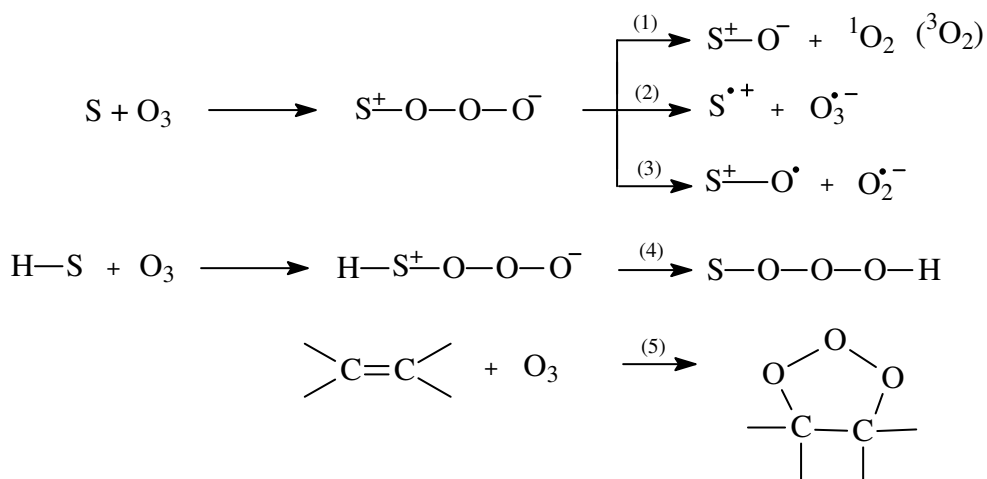
Increase in biodegradable organic carbon ahead of biological stages: For optimal production of biodegradable DOC specific O₃ consumptions of about 1.0-2.0 g O₃ g⁻¹ are advised.

Reduction of potential disinfection by product formation, including trihalomethanes: Trace concentrations of organic materials in treated water with chlorine produce THMs. Because some of these compounds are carcinogenic, the EPA (Environmental Protection Agency) in the USA has set the maximum contaminant level for total THMs at 0.1 mg L⁻¹. The main strategy for controlling THMs is to reduce their precursors. In preozonation, ozone is added in low dosage levels at the front of the plant to aid the coagulation and partial removal of THM precursors. The reduction in DBP formation also depends on the specific ozone consumption. Typical reductions are in the range of 10 to 60% (compared to no ozonated water), at specific ozone dosages between 0.5 to 2.0 g O₃ g⁻¹ DOC initially present.

Direct reduction of DOC/TOC levels by mineralization: Less relevant and applicable, because of the high ozone demand for direct chemical mineralization, with typically more than 3.0 g O₃ g⁻¹ DOC initially present needed to achieve a removal efficiency of 20% or more.

The primary reactions in the oxidation of inorganic and organic compounds with ozone are discussed in the Scheme 1.23. An electrophilic addition of ozone with compound S leads to an intermediate adduct (S-O₃), which then decomposes by formation of primary products⁶⁴.

$S + O_3 \rightarrow \text{Products}$ (where S is the inorganic or organic compound)



Scheme 1.23. Primary reactions of ozone with a compound S: This electrophilic addition⁶⁴ leads to an intermediate adduct (S-O₃) which then decomposes by formation of primary products. Reaction (1) oxygen atom transfer to anionic, uncharged and cationic species; reaction (2) electron transfer; reaction (3) formation of an oxyl radical; reaction (4) ozone insertion; reaction (5) ring formation.

The reaction products of the oxidation of aromatic compounds with ozone are not well covered in literature. The reactivity fuel (additives) viz. benzene, toluene, ethylbenzene and xylene (BTEX) with ozone increases with the degree of substitution with methyl groups. While benzene is relatively unreactive, xylenes have a higher reactivity depending on the position of substitution. Increasing the number of aromatic rings (benzene \rightarrow naphthalene \rightarrow phenanthrene) also leads to an enhanced reactivity, naphthalene²⁹ reacts 1500 and phenanthrene⁹² 10,000 times faster than benzene. Methyl tertbutylether (MTBE) and tertiary butanol (t-BuOH) as fuel additives have a low reactivity with ozone⁹³. In many cases, ethanol is also used as an oxygenate (fuel additive), its reactivity with ozone is very low. In recent studies, it has been shown that traces of pharmaceuticals can be present in water resources used for drinking water production⁹⁴. Diclofenac contains an amino group and carbamazepine (antiepileptic) a double bond, both compounds show high reactivity with ozone. Ethers⁹⁵ are studied in detail because the widespread occurrence of methyl tertiary butyl ether (MTBE < (CH₃)₃C-O-CH₃) has become a major concern in the drinking water community. The reactivity of methyl and other alkyl ethers with ozone is very low and can be neglected for the transformation of these compounds in ozonation processes^{29, 93}.

Many of the oxidation reactions that occur during ozonation are beneficial to the overall drinking water quality. The advantage is decolouration of the water, improvement of organoleptic properties and oxidation of micropollutants. During ozonation of drinking water, the two major oxidants ozone and $\bullet\text{OH}$ radicals govern the chemical processes. While ozone is a very selective oxidant which reacts quickly with double bonds, activated aromatic compounds and deprotonated amines, $\bullet\text{OH}$ radicals react with most water constituents with nearly diffusion-controlled rates⁶⁴.

Table 1.8. Degree of removal of the trace organic compounds during ozonation⁸¹.

Substances	Degree of removal, range in %	Remarks
Taste and odour	20 - 90	Source specific
Methylisoborneol geosmin	40 - 95	Improvements by AOPs: $\text{O}_3/\text{H}_2\text{O}_2$ and O_3/UV
Alkanes	<10	
Alkenes and Chlorinated alkenes	10 - 100	Chlorine content important, AOP support oxidation
Aromatics and chloroaromatics	30 - 100	Highly halogenated phenols are difficult to oxidize
Aldehydes, alcohols, carbonic acids	Low	Typical products of ozonation, easily biodegradable
N-containing aliphatics and aromatics	0 - 50	AOP may increase oxidation rate
Pesticides	0 - 80	Very specific to substance, triazines require AOP
Polyaromatic hydrocarbons	High, up to 100	

For ozone resistant compounds, ozone based advanced oxidation processes (AOPs) can be applied for their oxidation. However, in these processes, a large fraction of the oxidation capacity is lost to the matrix. Product studies have been performed for many compounds for the oxidation with $\bullet\text{OH}$ radicals, and only in a few cases they cover ozone. For the reaction with ozone, there is general information available on product formation from olefins, amines and some aromatic compounds.

The reactivity of saturated compounds (e.g. aldehydes, alcohols, ketones and carboxylic acids) with ozone is typically very low^{29, 86}. Many of these compounds are formed as oxidation products from the reaction of ozone with NOM. Even though they will be oxidized by $\bullet\text{OH}$ radicals, their oxidation rate is usually lower than their formation rate.

Organic micropollutants are found in surface and ground waters, always in conjunction with more or less NOM, but at relatively low concentrations in the range of 0.1 g L^{-1} to 100 g L^{-1} (in water sources of sufficient quality for a water supply). In practical ozone applications, trace organic oxidation has not been a primary task, but was considered to be a positive side effect. A qualitative presentation of expected degrees of removal in full-scale drinking water treatment plants is presented⁸¹ in the Table 1.8.

1.9.1.d. Particle removal processes: Turbidity in water is removed by ozonation through a combination of chemical oxidation and charge neutralization. Colloidal particles that cause turbidity are maintained in suspension by negatively charged particles, which are neutralized by ozone. Ozone further alters the surface properties of colloidal materials by oxidizing the organic materials that occur on the surface of the colloidal spherical particles⁸². Optimal dosage exists, typically in the range of 0.5 mg L^{-1} .

1.9.2. High purity water systems:

Breweries ozonate the brewing water to remove any residuals, taste, odour and to ensure the absence of microorganisms. The soft drink industry removes the ozone residual by vacuum stripping in a degassing chamber before bottling. The bottled water industry⁹⁶ requires that ozone residual be included with the water in the bottle. The ozone residual disinfects the inside of the bottle where contact is made with the water: some ozone, however, escapes into the gas phase where it also disinfects the inside of the cap and the container, which is not in contact with water. Finally, the ozone residual disappears as it decomposes to oxygen. In similar applications, the inside of bottles and cans is sprayed with water containing ozone residual for disinfection prior to the introductions of food.

1.9.3. Ozonation in wastewater treatment:

Full-scale ozonation systems have been used to treat wastewaters, such as landfill leachates, as well as wastewaters from the textile, pharmaceutical and chemical industries. The three largest

applications⁸¹ of ozone to industrial wastes are the oxidation of phenol, cyanide and the treatment of textile dye wastewater. The effluents possessing either natural colour bodies, e.g., tannins and lignins from pulp and paper operations, or synthetic colour bodies, can be decolourised by ozone⁸¹. When molecular ozone, O₃ dissolves in water, the molecule can remain as O₃ or it can decompose by a variety of mechanisms. Increase in pH, temperature, or concentrations of natural organic matter increase the rate of decomposition of molecular ozone⁸¹ into its daughter products.

Molecular ozone itself, being a weaker oxidizing agent than hydroxyl free radical, is a rather selective oxidant. It is because of this selectivity that most water and wastewater treatment processes can be performed with relatively low ozone dosages. A more reactive oxidant would be consumed in large amounts in extraneous oxidation reactions. Because of this high selectivity, most industrial wastewater treatment oxidations can be performed with molecular ozone only a relatively few applications require the hydroxyl free radical. The rate of ozone decomposition in aqueous solution is dependent on pH. Ozone decomposes quickly in high pH and forms hydroxyl radicals. Reactions not only with ozone but also with hydroxyl radicals formed by ozone are important for ozonations of organic substances in high and neutral pH⁹⁷.

As discussed in the previous Section 1.9.1, the main areas where ozone is used in the wastewater treatment are disinfection, oxidation of inorganic compounds, oxidation of organic compounds (including taste, odour, colour removal) and particle removal.

Beltran *et al*⁹⁸⁻¹⁰¹ determined the kinetic rate constant of various fast reactions by assuming a pseudo first order irreversible gas liquid (the reaction is assumed to occur in the liquid film) reaction that takes place between ozone and the organic compound. In a gas-liquid system, gas absorption is followed by a chemical reaction, where two steps control the overall reaction rate (1) the mass transfer from the gas phase to the liquid phase, and (2) the chemical reaction in the liquid phase.

1.10. Chemical oxidation:

These are generally used when biological processes have little efficiency. Chemical oxidation is the most effective process for the removal of organic pollutants present as traces in water. Chemical oxidation aims at the mineralization of the contaminants to CO₂, H₂O and inorganics or, at least, at their transformation into harmless products. They can be divided into two classes:

- Classical chemical treatments
- Advanced oxidation processes

Classical chemical treatments consist generally the addition of an oxidising agent to the water containing the contaminant to oxidize. The most widely used treatments are chlorine, potassium permanganate, oxygen and ozone¹⁰². Beside the advantages all these oxidants have their limitations like selectivity is less, toxic byproducts being generated in the process, large investments in installations and being unstable.

It has been frequently observed that contaminants not amenable to biological treatments are treated by strong oxidation processes for completely mineralized¹⁰³. In these cases, it is necessary to adopt reactive systems much more effective than those adopted in conventional purification processes.

1.10.1. Advanced Oxidation Processes (AOPs):

Most organic compounds are resistant to conventional chemical and biological treatments. For this reason, other methods are being studied as an alternative to biological and classical physico-chemical processes. Of these, AOPs will probably constitute the best option in the near future. Water treatment processes at ambient temperature and pressure, which involve the formation of highly reactive $\bullet\text{OH}$ radicals as an oxidant, are generally referred to as AOPs^{83, 104}. In drinking water treatment they are applied to oxidize ozone resistant compounds such as pesticides¹⁰⁵⁻¹⁰⁷, aromatic compounds and chlorinated solvents such as tri- and tetrachloroethene¹⁰⁸⁻¹¹⁰. The ozonation of dissolved compounds in water can constitute an AOP by itself, as hydroxyl radicals are generated from the decomposition of ozone, which is catalyzed by the hydroxyl ion or initiated by the presence of traces of other substances like transition metal cations³².

Hydroxyl radicals are also characterized by a little selectivity of attack, attractive feature for an oxidant to be used in wastewater treatment. Several and different organic compounds are susceptible to be removed or degraded by means of hydroxyl radicals, as it is shown in Table 1.9. Nevertheless, some of the simplest organic compounds, such as acetic, maleic and oxalic acids, acetone or simple chloride derivatives as chloroform or tetrachloroethane, cannot be attacked by $\bullet\text{OH}$ radicals¹¹¹.

The versatility of AOPs is also enhanced by the fact that they offer different ways of $\bullet\text{OH}$ radicals production, thus allowing a better compliance with the specific treatment requirements. It has to be taken into account, though, a suitable application of AOPs to wastewater treatment make use of expensive reactants as hydrogen peroxide and/or ozone, and therefore they should not replace, whenever possible, the more economic treatments as the biological degradation¹⁰⁴.

Table 1.9. Oxidizable compounds by hydroxyl radicals¹¹¹.

Compounds	
Acids	Formic, gluconic, lactic, malic, propionic, tartaric
Alcohols	Benzyl, tert-butyl, ethanol, ethylene glycol, glycerol, isopropanol, methanol, propenediol
Aldehydes	Acetaldehyde, benzaldehyde, formaldehyde, glyoxal, isobutyraldehyde, trichloroacetaldehyde
Aromatics	Benzene, chlorobenzene, chlorophenol, creosote, dichlorophenol, hydroquinone, p-nitrophenol, phenol, toluene, trichlorophenol, xylene, trinitrotoluene
Amines	Aniline, cyclic amines, diethylamine, dimethylformamide, EDTA, propanediamine, n-propylamine
Dyes	Anthraquinone, diazo, monoazo
Ethers	Tetrahydrofuran
Ketones	Dihydroxyacetone, methyl ethyl ketone

The radical mechanism predominates in less reactive molecules, such as aliphatic hydrocarbons, carboxylic acids, benzenes or chlorobenzenes²⁸. Normally under acidic conditions (pH<4) the direct pathway dominates, above pH 10 it changes to the radical. In ground and surface water (pH 7) both pathways can be of importance²⁹. In special waste waters, even at pH 2 the radical oxidation can be of importance, depending much on the contaminants present⁸¹. Both pathways should be always considered when developing a treatment scheme. In Table 1.10, the second order kinetic constants for ozone and hydroxyl radical of a series of organic compounds is presented.

For complete ozone consumption of water, the $\bullet\text{OH}$ radical yield is almost independent of the rate of the ozone decomposition. Therefore, the main advantage of ozone based AOPs is a shorter reaction time which allows the application of higher ozone dosages without causing

excess ozone concentration at the outlet of a reactor. Ozone based AOPs are most commonly applied in drinking water treatment because conventional treatment schemes including an ozonation step can be easily retrofitted for these processes. The simpler solution to convert a conventional ozonation process into an AOP is to increase reaction time after ozone addition, increase the pH, or add hydrogen peroxide. While the first two possibilities can be costly, the addition of hydrogen peroxide is a cheap and most commonly used solution in drinking treatment. Another alternative is combination of ozone with UV irradiation⁸³. In this process, the first step is a photolysis of ozone to oxygen and O (¹D and ³P) atoms¹¹². Whereas O(¹D) is very reactive and reacts with H₂O to hydrogen peroxide, O(³P) reacts either with O₃ to ²O₂ or under certain treatment conditions with organic solutes RH by H-atom abstraction from –CH₃ groups¹¹². Therefore, part of the oxidation capacity of the system is lost through the reaction O₃ → H₂O₂ but some additional effect can be gained from the direct reaction of organic compounds with O(³P). Additional ozone based AOPs include the combination of ozone with activated carbon¹¹³ or with Mn(II) / Mn(IV)¹¹⁴.

Table 1.10. Second order rate for ozone and hydroxyl radical [•]OH for a variety of compounds.

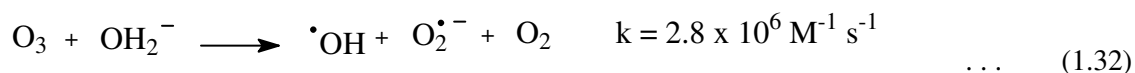
Organic compound	Rate constant (M ⁻¹ s ⁻¹)	
	O ₃ ^(a)	[•] OH ^(b)
Benzene	2.0	7.8 x 10 ⁹
Toluene	14.0	7.8 x 10 ⁹
Chlorobenzene	0.75	4.0 x 10 ⁹
Trichloroethylene	17.0	4.0 x 10 ⁹
Tetrachloroethylene	< 0.1	1.7 x 10 ⁹
n-Butanol	0.6	4.6 x 10 ⁹
t-Butanol	0.03	0.4 x 10 ⁹

^(a) Reference 29 and 86.

^(b) Reference 103

The combination of ozone with hydrogen peroxide is the most commonly applied technical AOP. In this process, the ozone transformation is accelerated by hydrogen peroxide. The reaction of ozone with hydrogen peroxide proceeds through the deprotonated form of hydrogen peroxide according to Staehelin and Hoigne³¹. Hydrogen peroxide initiates the ozone decomposition by formation of an [•]OH radical and superoxide, which further reacts with ozone according to the following equations. The yield of this reaction sequence is on [•]OH radical per decomposed

ozone molecule. This is somewhat higher than the yield achieved in low DOC waters in conventional ozonation processes¹¹⁵. Because the initiation reaction is less important in high DOC waters compared to the promotion reaction, the AOP O₃ / H₂O₂ system does not lead to a better degradation of ozone resistant micropollutants in such waters. However, the main advantage of the O₃ / H₂O₂ lies in the acceleration of the ozone transformation process.

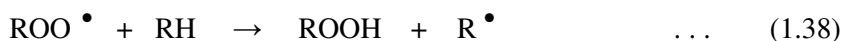
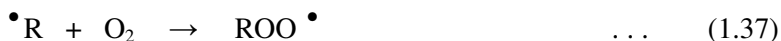
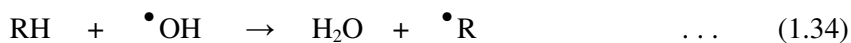


AOPs are alternative to the incineration of wastes¹¹⁶⁻¹¹⁹, which has many disadvantages, and have proceeded along one of the two routes:

- (1) Oxidation with O₂ in temperature ranges between ambient conditions and those found in incinerators Wet Air Oxidation (WAO) processes in the region of 1-20 MPa and 200-300 °C.
- (2) The use of high energy oxidants such as ozone and H₂O₂ and / or photons that are able to generate highly reactive intermediates - $\cdot\text{OH}$ radicals.

Glaze *et al*¹¹⁶ defined AOPs as “near ambient temperature and pressure water treatment process which involve the generation of hydroxyl radicals in sufficient quantity to effect water purification”. The hydroxyl radical ($\cdot\text{OH}$) is a powerful, non-selective chemical oxidant, which acts very rapidly with most organic compounds. Once generated, the hydroxyl radicals aggressively attack virtually all organic compounds. Depending upon the nature of the organic species, two types of initial attack are possible:

- (1). the hydroxyl radical can add itself to the contaminant, as in the case of olefins or aromatic compounds. A common reaction is the abstraction of hydrogen atom to initiate a radical chain oxidation¹¹⁶ (eqns. 1.34-1.38):



(2). the attack by $\bullet\text{OH}$ radical, in the presence of oxygen, initiates a complex cascade of oxidative reactions leading to mineralization of the organic compound. The exact routes of these reactions are still not quite clear.

In general, the AOPs when applied in a right place, give a good opportunity to reduce the contaminants concentration from several hundred ppm to less than 5 ppb. That is why they are called *the water treatment process of the 21st century*¹¹⁶⁻¹¹⁸.

Several methods are available for generating $\bullet\text{OH}$ radicals. These include both non-photochemical and photochemical methods:

- Ozonation at elevated pH (>8.5)
- Ozone + hydrogen peroxide ($\text{O}_3 / \text{H}_2\text{O}_2$)
- Ozone + Catalyst (O_3 / CAT)
- Fenton system ($\text{H}_2\text{O}_2 / \text{Fe}^{2+}$)
- O_3 / UV
- $\text{H}_2\text{O}_2 / \text{UV}$
- $\text{O}_3 / \text{H}_2\text{O}_2 / \text{UV}$
- Photo-Fenton / Fenton like systems
- Photocatalytic oxidation (UV / TiO_2)

1.10.1.1. Ozone + catalyst (Catazone):

Another opportunity to accelerate ozonation reactions is to use heterogeneous or homogeneous catalysts. Several metal oxides and metal ions (Fe_2O_3 , $\text{Al}_2\text{O}_3\text{-Me}$, MnO_2 , Ru/CeO_2 , $\text{TiO}_2\text{-Me}$, Fe^{2+} , Fe^{3+} , Mn^{2+}) have been studied and sometimes a significant acceleration in the decomposition of the target compound has been achieved, although the reaction mechanism in most cases remained unclear¹²⁰.

Advanced oxidation of chlorobenzenes in wastewater as well as in model solutions using iron and manganese ions as heterogeneous catalysts^{120, 121} has been studied. The reduction of total organic carbon (TOC) and chemical oxygen demand (COD) from wastewater was more efficient with the ozone/catalyst system than oxidation with ozone at high pH values. The $\text{O}_3/\text{Mn(II)}$ and $\text{O}_3/\text{Fe(II)}$ systems were more effective in the removal of organochloride compounds than the $\text{O}_3/\text{Fe(III)}$ and $\text{O}_3/\text{high pH}$ systems.

Karpel Vel Leitner *et al*¹²² studied catalytic ozonation of succinic acid using Ru/CeO₂ catalyst, which is barely oxidized by ozone alone. In catalytic ozonation process supports Al₂O₃ and TiO₂ in its anatase form and clay used for metal catalysts¹²³. Salicylic acid was chosen as a model compound. In contrast to unassisted ozonation, TOC measurements showed complete removal of organics in catalytic ozonation. The comparison studies of the efficiency of catalytic ozonation O₃/TiO₂ with plain ozonation and a combination of O₃/H₂O₂ on the model compound oxalic acid¹²⁴, as a result the O₃/TiO₂ system was preferable in terms of process efficiency in TOC reduction.

Ozone-granulated activated carbon systems (O₃/GAC) make a special case of catalytic ozonation. This is quite well known combined system for biorefractory compounds (e.g. pesticides) destruction where the GAC's bed life is prolonged due to the ozonated water¹²⁵. Using GAC as a catalyst for free radicals formation in ozonated water is much less studied. The Ecoclear process - oxidation of biorefractory organics¹²⁶ in the ozonation column filled with the GAC bed by the radicals such as O[•], O₂[•] and O₃[•] (not by [•]OH radicals) formed on the surface of GAC. This process has been in commercial operation since 1992 at an ozone consumption of 1.7 kg ozone per 1 kg COD removed¹²⁶.

Radical-type chain reaction can be initiated by few milligrams of activated carbon or carbon black per liter in ozone-containing water¹¹³, proceeds in the aqueous phase and forms [•]OH radicals.

1.10.1.1.a. Activated carbon:

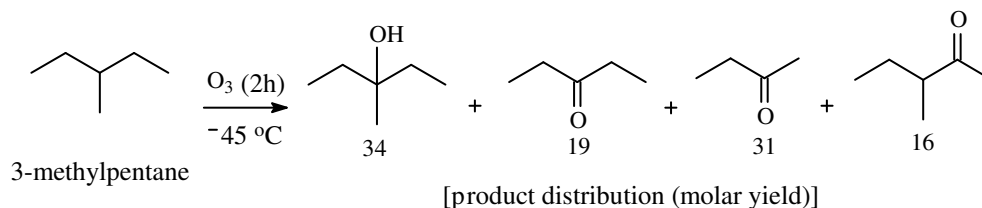
Activated carbon is reported to accelerate ozone decomposition resulting in the formation of [•]OH radicals^{113, 127, 128}. It was demonstrated that incorporated metal centers electrons of the graphenic layers (basal plane electrons) and basic surface groups of the activated carbon, are considered as the main factors responsible for the decomposition of ozone at the activated carbon surface¹²⁹⁻¹³¹.

The presence of activated carbon during the ozonation of organic micro pollutants leads to a reduction in the concentration of DOM increasing the applicability of this treatment system¹²⁹⁻¹³¹. Ozonation in presence of activated carbon can lead to oxidation of micro pollutants either by a direct reaction of the compounds with ozone or by [•]OH radicals that are produced in the interaction of ozone with the surface of activated carbon¹³².

Lake Zurich water treatment with O₃ or O₃/activated carbon indicates that the O₃/activated carbon process leads to an increased transformation rate of ozone and a reduction of the concentration of DOM. Moreover, it was observed that the adsorption of low concentrations of DOC on the surface of activated carbon does not modify its initiating/promoting activity for ozone transformation. This can be explained by (i) the high concentration of surface active sites capable to initiate/promote ozone transformation and/or (ii) initiating/promoting activity of adsorbed DOC¹³³.

1.10.1.1.b. Ozonation with silica gel:

Ozonation of compounds adsorbed on silica gel has become a method of general applicability for the hydroxylation of tertiary C-H bonds in saturated compounds. Ozone cleaves not only C-H bonds but also C-CH₃ bonds. Thus dry ozonation of trans-1,4-dimethylcyclohexane yielded in addition to trans-1,4-dimethylcyclohexanol small amounts of 2,5-dimethylcyclohexanones and 4-methylcyclohexanone¹³⁴.



Scheme 1.24. Product distribution from ozonation of 3-methylpentane¹³⁴.

Mazur *et al*¹³⁴ carried out dry ozonation on a number of aliphatic hydrocarbons and they reported that cleavage of C-C bonds occurs, which caused by a direct insertion of ozone into these bonds. They studied the reactions by adsorbing the substrates on silica gel (1%), passing through it a stream of ozone (3% in oxygen) for 2 h at -45 °C and then removing the excess of ozone by a stream of argon.

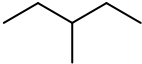
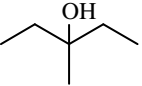
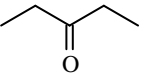
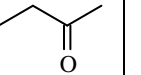
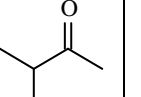
The relative yields of the tertiary alcohols were reported¹³⁴ as considerably lower than those obtained on the ozonation of cyclic hydrocarbons and suggested that the cleavage of alkyl groups resulted large amounts of ketones. The oxidation of aliphatic hydrocarbons is a relatively slow process, resulting in constant product ratios throughout the reaction. Mazur *et al*¹³⁴ noticed that

15% yield in 10 min and 85% yield in 2 h to the same mixture of an alcohol and ketones as shown in Scheme 1.24.

1.10.1.1.c. Formation of ketones in ozonation of 3-methylpentane:

Ozone reacts slowly with saturated hydrocarbons inserting oxygen atoms into their C-H bonds, resulting in alcohols and ketones. This insertion occurs preferentially at the tertiary carbon atoms, with retention of configuration¹³⁵. The significant ratios of ketones¹³⁴ formed by the cleavage of primary, secondary, or tertiary alkyl groups were reported in the same order of magnitude. The product distribution of 3-methylpentane ozonation at different temperature conditions reported by Mazur *et al*¹³⁴ were shown in Table 1.11.

Table 1.11. Product distribution^a from ozonation of 3-methylpentane at various temperatures¹³⁴.

	Temp., °C				
	-45	32	15	20	33
	-23	30	15	20	35
	0	22	13	20	44
	30	8	10	23	60

^a In molar yield (percent).

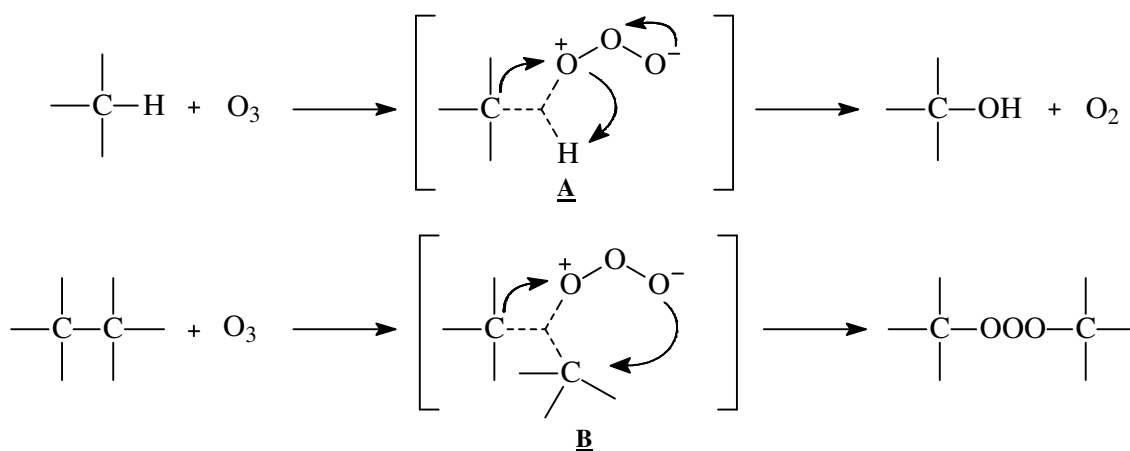
It was reported¹³⁴ that when the ozonation temperature is raised above -20 °C, the respective amounts of the ketones originating from the cleavage of the more highly substituted alkyl groups increases mainly at the expense of the tertiary alcohols as shown by the products distribution in 3-methylpentane at various temperatures. The temperature dependence was found¹³⁴ more pronounced in 2,3-dimethylbutane which at 25 °C gives 70% acetone and 1.5% 2,3-dimethylbutan-2-ol compared with 27% and 31% respectively at -45 °C.

The fragmentation of alkanes into ketones occurs at higher temperatures mainly via tertiary alkoxy radicals generated in the initial cleavage of the tertiary C-H bonds by ozone. The product distribution at low temperatures indicated the fragmentation of the C-C bonds cannot result solely from the attack of ozone on the tertiary C-H bonds. The formation of the cleavage products by an

attack on the primary or the secondary C-H bonds was not probable. It was observed that ozonation of the secondary C-H bonds lead to ketones¹³⁴.

Ozone reactivity toward the primary C-H bonds was found comparatively low (the relative activity toward ozone of primary to secondary and tertiary hydrogens was estimated to be ~0.01:0.1:1), the products formation was mainly due to the corresponding carboxylic acids and to a lesser degree the primary alcohols, but not C-C fragmentation products¹³⁴. Direct insertion of ozone into C-C bonds lead to the highly reactive dialkyl trioxides which decompose to give the cleavage products.

Mazur *et al*¹³⁴ have proposed that the mechanism of C-H bond ozonation involves the formation of an ozone-alkane complex which decomposes electrophilically inserting an oxygen atom into the C-H bond. The transition state for this reaction may be represented by a dipolar structure **A** (Scheme 1.25) containing a penta-coordinated carbon atom analogous to that proposed by Olah⁶³ from ozonations of alkanes in superacids, decomposing with the evolution of a molecule of oxygen. Mazur *et al*¹³⁴ assumed that the reaction of the neutral ozone with the C-C bonds proceeds also by a mechanism similar to that considered by Olah⁶³ for the analogous reaction of protonated ozone, namely through a dipolar intermediate **B** (Scheme 1.25), which collapses forming dialkyl trioxide.



Scheme 1.25. Transition state of dipolar structure and intermediate in ozonation of alkane⁶³.

One of the factors limiting the use of ozone as reagent for hydroxylation of saturated hydrocarbons was its low solubility in organic solvents. Even at low temperatures at which ozone forms stable solutions in saturated hydrocarbons and no reaction was observed, its solubility was

low (~0.1-0.3% by weight at -78 °C). At higher temperatures necessary for reaction to proceed at reasonable rate, the solubility of O₃ was even smaller, necessitating prolonged ozonation periods¹³⁵.

The reactivity of ozone towards most of the organic solvents limits its practical use as a hydroxylation reagent only to neat hydrocarbons. Mazur *et al*¹³⁵ have studied the ozonation reactions by pre-adsorbing the silica gel with hydrocarbons by direct mixing or impregnating by using a volatile solvent. They used the stream of ozone to pass through the silica gel containing ~1% by weight of the hydrocarbon at -78 °C until it becomes saturated with ozone. It was then allowed slowly to room temperature, followed by elution of the organic material. Mazur *et al*¹³⁵ observed the quantitative conversions of the hydrocarbons, resulted a high yield of the tertiary alcohols and noticed that the secondary alcohols were oxidized to ketones at similar conditions.

The reaction of ozone with C-H bonds either in solution or by the dry ozonation method, exhibits marked preference for attack at tertiary positions. In solution methylene groups undergo slow oxidation but the conversion of -CH₂- groups into >C=O by dry ozonation appears not to have been observed except in the special case of cyclopropane compounds when cyclopropyl ketones are formed¹³⁵. Beckwith *et al*⁵⁸ reported that the dry ozonation can introduce the carbonyl group at positions remote from functional groups.

The hydroxylation reaction of cyclododecanone by incubation with various fungal cultures is confirmed to the 5-, 6-, and 7- position, demonstrates an interesting similarity between dry ozonation and microbiological oxidation. Dry ozonation of dodecyl acetate yielded a complex mixture of keto-acetates⁵⁸. The results obtained by Beckwith *et al*⁵⁸ describes the particularity of the high regioselectivity of the reaction, consistent with that of dry ozonation which involves attack by gaseous ozone at positions remote from the binding site on substrate adsorbed as a monolayer. There is a remarkable similarity between the results of dry ozonation and biological oxidation indicates that ozonation may have considerable utility for the synthesis of a variety of natural products.

1.10.1.1.d. Catalytic ozonation processes:

New catalytic ozonation processes are of the most promising directions. Ozone as an oxidant undoubtedly has a number of advantages - high reaction ability allows conducting reactions under mild conditions and low temperatures. Ozonation selectivity could be improved by the catalysts

addition. Ozonation in the presence of metal cations allows changing the rate and pathways of the process. The addition of Fe^{2+} , Mn^{2+} and Cr^{3+} allows one to realize the reactions of hydroxylation, alkyl radicals oxidation, oxidative condensation and other processes without aromatic ring destruction under ozone action¹³⁶.

Catalytic ozonation of different organic compounds is well-investigated area of catalysis, presented by a variety of homo- and heterogeneous systems. However the literature data on catalytic ozonation reactions with higher hydrocarbons (higher alkanes) are practically absent¹³⁶. The catalytic ozonation of higher alkanes makes it possible in the production of a number of useful value added products from it.

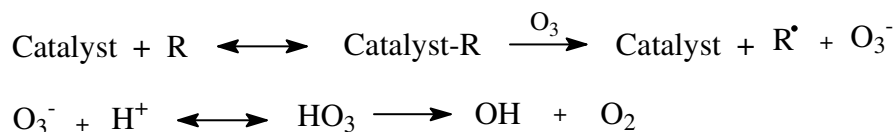
It is widely assumed that ozone reacts in aqueous solution on various organic and inorganic compounds, either by a direct reaction of molecular ozone or through a radical type reaction involving the hydroxyl radical induced by the ozone decomposition in water. The fundamental role played by the hydroxide ions in initiating the ozone decomposition process in water is well known.

Recently, alternative ozonation processes catalyzed by transition metals have been investigated for degradation of organics. Literature data relative to catalytic ozonation can be classified according to (1) activation of ozone by metals in solution and (2) heterogeneous catalytic ozonation in the presence of metal oxides or metals on supports¹³⁷.

Pure metal oxides, mixed metal oxides, and platinum group metals were evaluated as ozonation catalysts. Titanium dioxide, cobalt oxide, nickel oxide, copper oxide, and a mixed metal oxide comprised of copper, zinc, and aluminum did not accelerate the removal of pCBA in deionized water. The mixed metal oxide catalyst may have the most potential as an ozonation catalyst because it was very stable¹³⁷ (i.e., low solubility).

Compounds that do not have any strong nucleophilic sites are not readily oxidized by ozone, many toxic organic compounds fall into this category (e.g., chlorinated solvents and pesticides). Destruction of these compounds requires processes that produce highly reactive hydroxyl radicals. Factors such as intensity of UV radiation, peroxide-to-ozone ratio, pH, and presence of radical scavengers affect these processes. Heterogeneous catalytic ozonation does not require a continuous supply of other reagents or radiation. This makes catalytic ozonation an attractive

alternative to other AOPs. Analyses of natural organic matter have shown that carboxylic acid functional groups are part of its complex structures, and ozonation increases the number of carboxylic acid functional groups^{24, 25}. One possible catalytic reaction pathway explaining the results is as shown in Scheme 1.26, where R is an organic species that has multiple carboxylic functional groups.



Scheme 1.26. Scheme of catalytic ozonation.

Abdo *et al*¹³⁸ studied zinc or copper sulfate, silver nitrate and chromium trioxide to catalyze the bleaching of dye effluents during ozonation. Recent investigation were conducted by Gracia *et al*^{139, 140}, who showed that in the presence of Mn and Ag, ozonation of humic substances in water allows an important reduction in the content of organic matter as compared to ozonation alone.

Andreozzi *et al*¹⁴¹ found that Mn(II) accelerates the oxidation of oxalic acid using ozone under acidic conditions. Consistent with the previous statement from Nowell and Hoigne¹⁴² that no production of $\bullet\text{OH}$ radicals can be directly derived from the transition metals ozonation, the authors proposed that Mn(II)-catalyzed oxidation proceeds through complex formation between oxalic acid and Mn(III), forming an intermediate product which might be oxidized by ozone.

Al-Hayek *et al*¹⁴³ showed the ozonation of phenol in presence of catalysts Fe(III)/Al₂O₃ leads to a significant increase of TOC removal as compared to ozonation alone. The authors suggested the formation of free radicals and/or an increase of nucleophilic sites of adsorbed molecules. Bhat and Gurol¹⁴⁴ studied the ozonation of chlorobenzene in the presence of goethite and found that catalytic ozonation was more effective than ozonation alone. Naydenov and Mehandjiev¹⁴⁵, and Thompson *et al*¹⁴⁶ observed a mineralization of benzene and 1,4-dioxane, respectively, in aqueous solution, obtained by ozonation in the presence of MnO₂.

Ma and Graham¹⁴⁷ showed the formation of MnO₂ in situ by ozonation of atrazine in presence of small amounts of Mn(II), leads to a much greater degree of atrazine oxidation compared to ozone alone. The authors assigned these results to the generation of highly oxidative intermediate species. Andreozzi *et al*¹⁴⁸ reported a significant improvement of oxalic acid ozonation at acidic

pH, induced by the presence of MnO₂. Pines *et al*¹⁴⁹ stated that the combination O₃/metal-TiO₂ was particularly interesting for the oxidation of hydrophilic (biodegradable) compounds. However, the efficiency was found to be weak for hydrophobic compounds. Volk *et al*¹⁵⁰ studied fulvic acid oxidation by O₃, O₃/H₂O₂ and O₃/TiO₂, found that catalytic ozonation induced a smaller BDOC formation than the other two processes and deduced that carboxylic acids (ozonation by-products) could be oxidized preferably by catalytic ozonation.

Bulk of the literature on the catalytic ozonation is focused on the activation of ozone by numerous metals (Fe, Mn, Ni, Co, Zn, Ag, Cr) in solution or by heterogeneous catalysts with metals under various forms (salt of reduced metal, solid oxide, deposited metal on support). It is assumed that these metals are able to enhance the efficiency of ozone for the removal (or the conversion) of different organic compounds in aqueous solution. Catalysts (prepared by impregnation or by the co-gel technique) with given transition metals on various oxides (alumina, anatase, zirconia, clay), can really improve ozonation efficiency and oxidize some polar compounds such as salicylic acid, tripeptide, aquatic fulvic acid and p-toluene sulfonic acid¹³⁷.

There is little information in the literature on the direct catalytic ozonation reactions with organic compounds. Catalytic ozone decomposition at room temperature is advantageous as compared to the thermal decomposition in view of energy saving since there is no need in this case to heat large volumes of air¹⁵. Noble metals like Pt, Rh, Pd and transition metal oxides including Mn, Co, Cu, Fe, and Ni supported on γ -Al₂O₃, SiO₂, TiO₂ have been used to catalyze these organic compounds reaction^{20, 21, 151-155}. Activated carbon is also used for the destruction of ozone by adsorptive decomposition giving oxygen. Both non-catalytic and catalytic routes of ozone decomposition on activated carbon have been reported^{156, 157}. The use of activated carbon is simple and not expensive, but they have low mechanical strength.

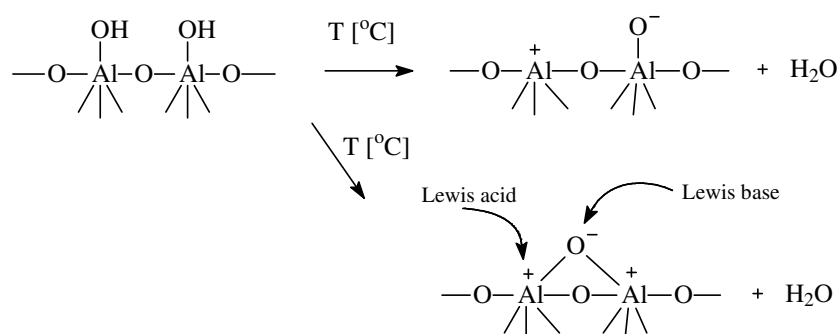
1.10.1.1.e. Catalytic ozonation with Al₂O₃:

Alumina found application in water treatment technology mainly as an ion exchanger for the removal of inorganic anions such as As, Se and F. The usage of alumina as a support for active species, mainly metal or metal oxides in the process of catalytic ozonation of several organic compounds has also been studied^{158, 159}. Parent alumina was shown to be an active catalyst for the ozonation of 2-chlorophenol. γ -Alumina was found to be an effective catalyst for refractory organic compounds such as oxalic, acetic, salicylic and succinic acid ozonation in water.

Several researchers have investigated the possibility of the application of parent alumina or alumina supported with metals or metal oxides as catalysts of the ozonation process¹⁵⁹. Alumina due to its high surface area, mechanical strength and thermal stability has found several applications as an adsorbent and catalyst. The acid-base properties of alumina are the main reason for its wide usage. In water treatment technology, adsorption on several adsorbents such as active carbon, silica gel and zeolites as well as alumina is one of the major processes used mainly for the removal of several and organic compounds from water. Alumina has also been applied as a catalyst for ozonation and wet air oxidation processes^{137, 150, 160}.

At room temperature, alumina adsorbs water as undissociated molecules bonded with strong hydrogen bonds. At higher temperatures, hydroxyl groups are formed on the surface of alumina and, with an increase of temperature, are gradually expelled as H₂O. However, even at 800-1000 °C and in a vacuum, some tenths of a percent of water are still retained in the alumina¹⁵⁸.

The main two parameters determining the catalytic properties of alumina are acidity and basicity. Brønsted acidity-basicity is defined as the ability to proton abstraction-acceptation. Lewis acidity-basicity is the ability to electron acceptance-abstraction. Chemisorption of water on the alumina surface is considered to be a reaction between Al ion, an acceptor of electron pair (Lewis acid), and hydroxyl ion, its donor (Lewis base)¹⁵⁸.



Scheme 1.27. Brønsted and Lewis acid sites as catalytic centers of alumina¹⁵⁸.

Hydroxyl groups formed at alumina surface behave as Brønsted acid sites. However, the dehydration of two neighbouring OH[•] ions from the surface of alumina causes the formation of strained oxygen bridge, active Lewis acid sites. Both Brønsted and Lewis acid sites are thought to be the catalytic centers of alumina¹⁵⁸ (Scheme 1.27).

Lin *et al*¹⁶¹ investigated the average rates of decomposition of aqueous ozone with different metals (Ru, Rh, Pd, Ag, Ni, Pt) on different supports viz. SiO₂, TiO₂, Al₂O₃, SiO₂-Al₂O₃ was illustrated in Table 1.12. Noble metals showed high catalytic activity for the decomposition of aqueous ozone (except Au). It has been reported that supported noble metal and SiO₂ supported catalysts showed highest catalytic activity (except for Ru).

Table 1.12. Comparison of average rates¹⁶¹ of decomposition of aqueous ozone on different metal loaded γ -Al₂O₃.

Catalyst	Average rate (mg _(O3) min ⁻¹ g ⁻¹ _(cat))	Average rate (mg _(O3) min ⁻¹ mol ⁻¹ _(metal))	Specific Surface area (m ² g ⁻¹)
Pd/ γ -Al ₂ O ₃	0.40	851.20	139
Ni/ γ -Al ₂ O ₃	0.16	187.84	-

Reaction conditions: catalyst, 1.5 g; rate of water flow, 0.1751 min⁻¹; reaction temp., 293 K.

Table 1.13. Mechanisms for decomposition of ozone¹⁶¹.

Case of O ₂ not adsorbed on metal	Case of O ₂ adsorbed on metal
O ₃ \longrightarrow O _{3(a)}	O ₃ \longrightarrow O _{3(a)}
O _{3(a)} \longrightarrow O _(a) + O ₂	O _{3(a)} \longrightarrow O _(a) + O _{2(a)}
O _(a) + O ₃ \longrightarrow 2O ₂	O _(a) + O ₃ \longrightarrow O ₂ + O _{2(a)}
	O _{2(a)} \longrightarrow O ₂

(a) – adsorbed

The mechanism of catalytic decomposition of aqueous ozone can be considered as the same as the gaseous ozone¹⁶¹. The mechanism of ozone decomposition on metals or oxides is considered to include the paths shown in Table 1.13. Based on these mechanisms, any of the following factors can be considered for the affective decomposition of ozone on the catalyst surface.

1. *Adsorption ability of O₃*: A catalyst that can easily adsorb O₃.

2. *Decomposition ability of O₃*: A catalyst that can decompose O₃ more easily by producing oxygen species on catalyst surface, which are stable.

3. *Activity of oxygen species*: Two kinds of oxygen active species, lattice oxygen and adsorbed oxygen are possible in the decomposition of O₃. An appropriate activity of oxygen species on catalyst surface is considered to be necessary.

4. *Desorption ability of O₂*: A catalyst which easily desorbs O₂ is advantageous.

Among these factors, the activity of oxygen species was thought to be the determining factor for activity of catalysts.

As the reaction mechanisms of the heterogeneous catalysed reaction with ozone are not clear, several explanations exist. For a proper description, one important question is whether ozone attacks the organic compounds directly or indirectly via the radical mechanism in the presence of the heterogeneous catalyst. The adsorption of organics as well as ozone on the material surface certainly plays an important role. As a result, ozone may decompose on active metal sites of the catalyst's surface¹⁶² or only because of the morphological structure of its support¹⁶³. A majority of authors assume that as a result of this decomposition the acceleration of the indirect radical chain (generation of •OH radicals out of hydroxyl anions) is started¹⁶⁴, even if the ideas of how the initiation takes place differ from author to author. In some papers, the involvement of •OH radicals into the catalyzed reaction is denied because the reaction is not influenced by the presence of radical scavengers like bicarbonates. Other authors consider it possible that the enhancement of direct ozonation could be involved with heterogeneous catalysis.

Legube *et al*¹⁶⁵ suggested as one possible reaction path that alumina may build up chelate complexes with dissolved organics that afterwards can be electrophilically attacked by ozone. The further oxidation of the organic compounds leads to desorption and new vacancy of an adsorption site. In this case, the characteristics of the heterogeneous support can explain the enhanced performance of ozone, but the explanation is not applicable to low adsorbing compounds or supports.

The catalytic effect can be produced by metal deposited, or by the support itself, either due to the structure (pore size, crystal size, and surface) or due to chemical properties (acidity, surface groups, hydrophilic/hydrophobic). The ozone gets adsorbed on the alumina catalyst's surface and then decomposes rapidly due to presence of hydroxyl surface groups. It is known that ozone

catalytically decomposes in gas phase on the surface of metal oxides, especially on the surface of γ -alumina¹⁶⁰ rapidly.

The active atomic oxygen is produced due to the decomposition of ozone and reacts with alumina hydroxyl surface groups to form O_2H^- anions. These anions subsequently can react very fast with another O_3 to form $\bullet\text{O}_2\text{H}$ radicals or these radicals can be produced directly. These radical reacts subsequently with another ozone molecule to generate an O_3^- (ozonide) radical, which decomposes into oxygen and a free $\bullet\text{OH}$ radical which can oxidize organic compounds either in directly or on the surface or in a thin film layer above the catalyst's surface. According to Staehlin and Hoigné¹⁶⁶ a reactivation or closing of the radical chain might not be necessary, because the ozone selective radicals $\bullet\text{O}_2^- \rightleftharpoons \bullet\text{O}_2\text{H}^-$ will be produced by fast decomposition of a new ozone molecule on the catalyst's surface. The adsorption of organics on the catalyst's surface would not be necessary to provide the catalytic effect.

1.10.1.1.f. Metal oxides as catalysts in ozonation reaction:

One of the proposed catalytic mechanisms assumes that the catalyst performs a dual function. Its presence causes both an increase of ozone dissolution and the initiation of the ozone decomposition reaction. Three phases involved in the process of heterogeneous catalytic ozonation were gaseous, liquid and solid phase. In the first stage of the process, the transport of O_3 from gas to liquid takes place. Both ozone and organic molecules are transported to the surface of the catalyst. Generally, the proposed mechanism of the catalytic ozonation on metal oxides as catalysts assumes that the adsorption of organic molecules and ozone takes place simultaneously on the surface of the catalyst. As the result of ozone adsorption and its conversion, O-radicals or $\text{HO}\bullet$ radicals are generated [$\text{O}_2\bullet^-$ transfers an electron to another ozone molecule to form an ozonide anion ($\text{O}_3\bullet^-$), which is the chain reaction promoter and produces $\text{HO}\bullet$ radicals]. Free radicals can initiate a radical chain reaction both on the surface of the catalyst and in the bulk of the aqueous phase. Oxidation proceeds stepwise through several oxidized intermediates whilst radicals are continuously generated by the dissolved ozone that is transferred to the catalyst surface. The affinity of the oxidation products to the catalyst decreases and final products desorb from the catalyst surface.

Gaseous ozone decomposition: gas phase decomposition of ozone show that ozone is adsorbed on the catalyst (e.g. C_{act} , TiO_2 , MnO_2 , Fe_2O_3 , CuO , Al_2O_3 , CeO_2 , sodium chloride, calcite, silica gel and sand) through one of its terminal atomic oxygen.



where S represents the free active centers at the catalyst surface.

In some cases, ozone does not remain in molecular form and dissociates to atomic or diatomic oxygen species. An IR study of low-temperature gaseous ozone adsorption on oxides reveals that at least four forms of ozone adsorption takes place on the surface of metal oxide. These are:

- Physical adsorption.
- The formation of weak hydrogen bonds with surface OH groups.
- Molecular adsorption via coordinative bonding to weak Lewis sites.
- Dissociative adsorption on interaction with strong Lewis sites, resulting in the formation of atomic oxygen atoms, which intermediates the catalytic reactions of ozone decomposition.

Bulanin *et al*¹⁶⁷ proposed the mechanism of dissociative adsorption as follows: Adsorption of ozone molecule on strong Lewis acid sites leads to distortion of the molecule until it becomes unstable against dissociation into a free oxygen molecule and a surface oxygen atom which remains attached to metal oxide, e.g. titanium ion. Oxygen atoms can react with the next ozone molecule with the formation of two oxygen molecules or, if the temperature is high enough for their migration, the recombination of two atoms is also possible.

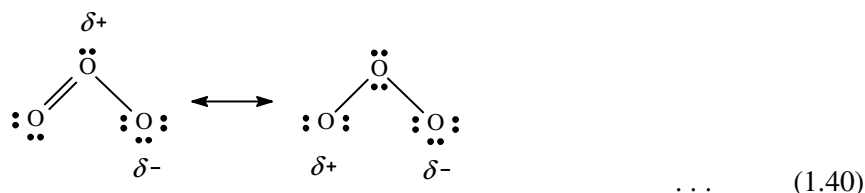
Dissociative ozone adsorption was claimed for several oxides such as Al₂O₃, ZrO₂, MgO and CeO₂. This explains the high activity of γ -alumina, which shows the strong Lewis acidity, as a catalyst of low-temperature ozone decomposition. This is true in the case of γ -alumina as well as ZnO where the Lewis sites are also strong. No bands of molecular oxygen adsorption on Lewis sites were detected¹⁶⁷.

The average rates of aqueous ozone decomposition on several solid phases such as: active carbon, zeolite, Al₂O₃, SiO₂, SiO₂-Al₂O₃ and TiO₂ as reported in Table 1.14. Among the catalysts, AC showed the highest activity, which can be attributed to its reaction with ozone and the formation of carbon dioxide¹⁶¹.

Table 1.14. Average rates of the decomposition of aqueous ozone on solid phase¹⁶¹.
[catalyst, 1.5 g (AC, 1 g); rate of water flow, 0.1751 min⁻¹; temperature 18 °C]

Solid Phase	Average rate (mg _{O3} min ⁻¹ g ⁻¹ _{cat})
AC (activated carbon)	0.25
Zeolite (mordenite)	0.02
Zeolite (HY)	0.00
Al ₂ O ₃	0.01
SiO ₂	0.01
SiO ₂ -Al ₂ O ₃	0.00
TiO ₂	0.00

It has been highlighted that different sites of carbon and metal oxides were involved in the process of ozone decomposition. In the case of carbon, basic sites were regarded as being active. This is in contrast to the case of metal oxides, where ozone is thought to react with strong Lewis acid sites. The ability of ozone to react with both the acidic and basic surface sites of the catalysts was reported as a consequence of its resonance structure¹⁵⁹ (eqn. 1.40).



When discussing the mechanism of catalytic ozonation via ozone and organic adsorption followed by ozone decomposition and final oxidation on the surface of the catalyst, the phenomenon of hard/soft Lewis acids/bases has to be taken into consideration. A soft base is the one in which the valence electrons are easily distorted-polarized or removed. A hard base has the opposite properties, holding on to its valence electrons much more tightly. Hard acid is one of the small sizes, high positive charge and no valence electrons that can be easily distorted or removed. A soft acid is one in which the acceptor atom is of large size, small or zero positive charge, or has several valence electrons which are easily distorted or removed. Generally, hard acids prefer to associate with hard bases and soft acids prefer to associate with soft bases. The stabilities of compounds and complexes are based on this statement “Al³⁺, Ti⁴⁺, which are surface species of frequently applied catalysts-alumina and titania, are hard Lewis acids. They are capable of associating with hard bases such as H₂O, OH⁻ and PO₄³⁻, F⁻, SO₄²⁻, CO₃²⁻. As the bond

formed between hard acids and hard bases is regarded as being strong, it can therefore poison the catalyst used (the catalyst that possesses active sites, which are hard Lewis acids)". The other debatable matter is the possible bond formation between ozone and strong Lewis acid on metal oxides surfaces, as ozone can be treated as Lewis base (whether it is hard or soft base is questionable), it can react with acid surface groups of metal oxide with subsequent decomposition as presented¹⁵⁹.

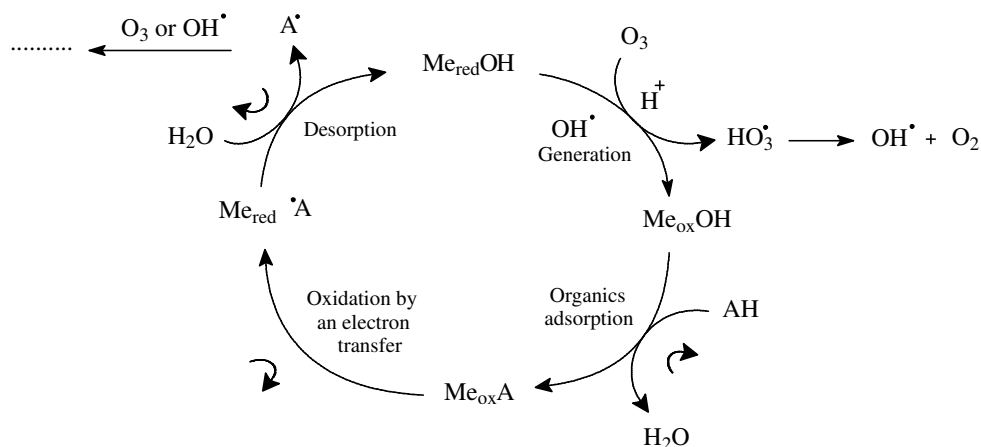
The unique structural properties of ozone have to be taken into consideration as one of its resonance structures, due to the high electron density on one of the oxygen atoms it might show high basicity resulting in strong affinity to Lewis acid sites on the surface of metal oxide. The mechanism of ozone adsorption/decomposition on the surface active sites is acceptable¹⁵⁹. The heterogeneous catalysis is under the influence of many chemical and physical processes such as mass transfer, fluid dynamics, interfacial surface area, surface material, chemical kinetics, temperature, pH of the solution, the composition of water and organic molecule properties. It has to be highlighted that reactions take place in both the liquid and on the surface of the catalyst. Molecular ozone reactions are also possible. Reactions on the catalyst surface might involve several steps such as adsorption, ozone decomposition reaction, surface oxidation reaction and desorption process. The adsorption process is influenced by surface properties of the catalysts such as surface areas, pores volume and surface active sites¹⁵⁹.

The structure of the organic molecule, its pKa, polarity, molecular weight and functional groups determine its affinity to the catalyst surface. All these factors are reported steps that influence the catalytic ozonation process. Depending on the type of the catalyst and organic molecule, either the adsorption / diffusion of organics at the surface of the catalyst or an increased concentration of HO[•] radicals generated due to ozone decomposition at the solid-liquid interface were considered mainly responsible for the improvement of catalytic ozonation¹⁵⁹.

1.10.1.1.g. Metal on support:

On the surface of the reduced Me-catalyst ozone oxidizes metal with the generation of HO[•] radicals. Organic molecules (AH) after adsorption on the catalyst surface were subsequently oxidised by an electron-transfer reaction to give a reduced catalyst (Me_{red}A[•]). The organic radical species A[•] were subsequently desorbed from the catalyst and oxidized by HO[•] or O₃ either in bulk solution or probably within the thickness of an electric double layer as shown in Scheme 1.28. For several catalysts with supported metal studies, the catalyst based on Co(II) ions

were found to be the most efficient for gaseous ozone decomposition due to a facile regeneration of Co(III) by either water vapor or the intermediate radicals having reducing properties¹³⁷.



Scheme 1.28. Possible mechanism for ozonation process in the presence of Me-support (metal oxide) catalyst¹³⁷.

The catalytic activity order of metal supported on Al_2O_3 was found to be $\text{Pt} > \text{Pd} > \text{Ag} > \text{Ru} > \text{Rh} > \text{Ir} > \text{Ni} > \text{Cd} > \text{Mn} > \text{Fe} > \text{Cu} > \text{Zn} > \text{Zr}$. The metals examined such as Pt, Ru, Rh, Pd and Ag were found to be effective in both gaseous and aqueous ozone decomposition. Noble metals (Ru, Rh, Pd, Os, Ir, Ag and Au) are efficient redox catalysts, which are able to decompose O_2 with the formation of oxygen-metal bond strong enough to provide effective ozone decomposition. Generally, the higher activity of the metals deposited on metal oxide for ozone decomposition when compared to metal oxides only probably results from an increase of electron transfer and furthermore, an increase in the rate of redox reaction that takes place in the case of Me-metal oxide catalysts. This on the other hand accelerates the catalytic reactions¹³⁷.

1.10.1.1.h. Zeolites in oxidation of higher hydrocarbons:

Zeolites consist of channels and cages which are only accessible to those molecules with the correct shape and dimensions. Incorporating catalytic sites within such a structure provides the basis of molecular shape-selective catalysts and shape-selective effects have been frequently observed with reactions catalysed by inherent acidic sites, e.g. hydrocarbon cracking and alcohol dehydration¹⁶⁸.

Reactions of n-hexadecane have received particular attention in the past, because n- C_{16} is typical of cracking in long chain paraffins present in gas oils, and because it is readily available.

Reactions of n-hexadecane on HY zeolite have been studied at 300 and 400 °C, found to produce over 140 individual products over the range of conversion studied. It has been reported that in the cracking of n-hexane on HY in the temperature range 350-450 °C increasing amounts of olefins were found in the reaction products as the reaction temperature increases. Abbot and Wojciechowski¹⁶⁹ suggested the occurrence of hydrogen transfer at low temperature oxidations. In the cracking of n-hexadecane, paraffins are the dominant products at 300 °C, whereas olefins were reported to be dominant at 400 °C.

Zeolites have been used in commercial catalytic cracking for about a decade. Reported activities of these zeolites as compared to amorphous silica-alumina ratio have varied widely. Few research groups observed the secondary reactions during the cracking of hexadecane over the silica-alumina catalyst¹⁷⁰.

Shape-selective oxidation of alkanes, catalysed with H₂O₂ and pentasil zeolite titanosilicate, the rates for oxidation of linear alkanes were much higher than those of branched and cyclic alkanes. The oxidation conversion of the linear alkanes hexane, heptane, octane, and nonane by such a zeolite system, the rates decreased in the order hexane > heptane > octane > nonane. This order consistent with the observed large decrease in diffusivity in zeolites with increasing chain length, demonstrating transport restrictions preclude oxidation of molecules of sizes hindered from passing through the crystalline channels. The oxidation of hexane revealed that the ratio of ketone to alcohol increased with time, suggesting that the ketones were secondarily formed from the alcohols³⁷.

There are two distinct classes of hydrocracking catalysts: one containing a strong hydrogenation function, such as Pt or Pd, and the other contains a weak hydrogenation function such as sulfided nickel or tungsten. Hydrocracking of n-hexadecane in the presence of a strong hydrogenation component follows the classical dual functional mechanism: the n-hexadecane on the metal site, followed by cleavage split into two olefins on the acid site, and then is dehydrogenated on the metal site to form paraffinic products. The past studies indicated that the oxidation state of a reducible metal ion in a zeolite depends on the acidity of the zeolite e.g. nickel ion in a Na zeolite is easily reducible, while nickel ion in a hydrogen zeolite is not easily reduced³⁸.

Protonic zeolites find industrial applications as acid catalysts in several hydrocarbon conversion reactions. The activity of these materials is associated with two main properties: shape selectivity

effects due to the molecular sieving properties associated to the well defined crystal pore sizes, where at least a part of the catalytic active sites are located and a strong Brønsted acidity of bridging Si-(OH)-Al sites generated by the presence of aluminium inside the silicate framework. The main factor allowing molecular sieving and, consequently, the shape selectivity is generally considered to be exclusively a sterical effect i.e., only molecules having a critical kinetic diameter lower than the channel diameter are allowed to enter the pores and react on an active site or, to exit them and to be recovered as a product of the reaction. Alternatively, transition state shape selectivity effects limit the formation of bulky transition state intermediates inside the pores and avoid the formation of some unwanted reaction products¹⁷¹.

Catalytic active sites also exist on the external surface and at the pore mouth of zeolite crystals. For shape selective reactions these sites are considered to be responsible for unwanted non-selective catalysis. A possible strategy to avoid unwanted unselective reactivity is to limit the external surface and the extra-framework material by producing large well crystallized zeolite crystals. The possible role of extra-framework species should also be limited by reducing the Al content in the zeolite. Previous studies have been performed on the characterization and on the distinction of internal, external and extra framework acid sites in H-MFI type zeolite structures with usual particle size. Armaroli *et al*¹⁷¹ reported the comparative characterization of a small particle size sample with large particle highly crystalline samples, in order to confirm the previous data and to have additional information on the internal versus external surface acidity in zeolites.

Although some heterogeneous reactions will take place at the external crystal surfaces, most practical zeolite catalysis takes place inside the framework. Here zeolites have the advantage of a very large internal surface about 20 times larger than their external surface for the more open frameworks (e.g. zeolite Y). This internal capacity provides the appropriate surfaces at which catalytic transformations can take place. In the Faujasite zeolites this is typically in the series of large cavities easily available via three-dimensional open-pore networks. Zeolite Y is isostructural with zeolite X (and Faujasite). It differs in its higher Si:Al (in the relatively lower amount of isomorphous substitution of Al for Si into tetrahedral framework position) and this causes a drop in the number of cations present in the framework and an increase in the number of water molecules present.

Zeolite ZSM-5 (MFI) can be regarded as end-members of the pentasil family. This synthetic end-member has three-dimensional pore structures enclosed by 10 oxygen windows but these do not link cavities as such (Fig. 1.18). In ZSM-5 there are two pore systems, one consisting of zig-zag channels of near-circular cross-section and another of straight channels of elliptical shape. All the intersections in ZSM-5 are of the same size. ZSM-5 has a three-dimensional system linked via intersections rather than cavities. These channels have important consequences in the zeolite sorptive and catalytic properties. These zeolites have low aluminium content and consequently few cations are present in them, as yet unresolved, crystallographic sites. Similarly their water contents are low-indeed their frameworks have hydrophobic tendencies, in sharp contrast to the normally highly hydrophilic character of most other known zeolites.

1.11. Zeolites as catalysts in the ozonation of hydrocarbons:

Different sites of carbon and metal oxides are involved in the process of ozone decomposition. In the case of carbon, basic sites are regarded as being active. This is in contrast to the case of metal oxides, where ozone is thought to react with strong Lewis acid sites. The ability of ozone to react with both the acidic and basic surface sites of the catalysts is a consequence of its resonance structure¹⁵⁹.

Zeolites have proved to be valuable technical catalysts in petrochemistry and in oil processing. The characteristic properties of zeolites, such as acidity, shape-selectivity and thermal stability also enable them to be used for highly selective synthesis in the fields of chemical intermediates and fine chemicals. The industrial use of zeolites as catalysts started at the beginning of 1960s with the replacement of cracking catalysts based on amorphous aluminosilicates. Metal-doped Y-zeolites proved successful as bifunctional catalysts in the field of hydrocracking¹⁷². The discovery of ZSM-5, the first representative of the family of pentasil zeolites was a milestone in zeolite chemistry during 1970s. The use of silicone-rich pentasil zeolites as highly acidic, extremely shape-selective and heat-stable catalysts led to new industrial petrochemical processes.

The combination of acidity and shape selectivity in the zeolite catalysts is an important factor for organic chemistry. The tendency to utilize this potential for specific, highly selective syntheses in the field of intermediates and fine chemicals has continued steadily in recent years¹⁷². The numerous modifications of zeolites in respect of the number and strength of acid centers, isomorphous substitution and doping with metals provide an opportunity of employing catalysts that are tailored to suit the reactions desired¹⁷².

Zeolites are crystalline aluminosilicates with a highly ordered crystalline structure. Cavities of a definite size are formed in the rigid, three-dimensional network composed of SiO_4^{4-} and AlO_4^{4-} tetrahedral. The lattice contains cavities of varying diameters, depending on the type of zeolite. A distinction is made between large-, medium-, and small-pore zeolites. In the case of large-pore Y-zeolites, for example a cavity of this type having a diameter of 7.4 \AA is formed by twelve SiO_4 tetrahedra. In the case of small-pore A-zeolites, eight tetrahedral form a ring of diameter 4.1 \AA . The medium-pore pentasil zeolites have a 10-ring system with an ellipsoidal tubular diameter of $5.5 \text{ \AA} \times 5.6 \text{ \AA}$. The structural assembly of uniform channels is an advantageous special feature of zeolites contains larger cavities behind the pore openings¹⁷³.

It is difficult to spend any time in the chemical process industry without hearing about zeolite catalysts. Because of their unique porous properties, zeolites are used in a variety of applications with a global market of several million tonne per annum. In the western world, major uses are in petrochemical cracking, ion-exchange (water softening and purification), and in the separation and removal of gases and solvents. Other applications are in agriculture, animal husbandry and construction. They are often also referred to as *molecular sieves*¹⁷³.

The zeolites encompass materials comprised of the aluminosilicates, aluminophosphates and germanates. The pore sizes can vary from $\sim 3 \text{ \AA}$ to 30 \AA - more than enough to permit the diffusion of atoms and small molecules into the macromolecular structure. The microporous structure is important as it is this which allows the materials to act as catalysts. Other applications include gas separation and ion exchange. Zeolites are designated by three capital letters, following IUPAC rules. These codes are not dependant upon atomic composition, cell dimensions or geometry. They are derived from the names of the types of the materials¹⁷³.

Ozonation with mesoporous materials, which have relatively small pore size ($\sim 4\text{-}5 \text{ nm}$) will only be active towards small molecules. As adsorption plays a significant role in the catalytic ozonation process, it will not be effective towards large molecules that will not undergo adsorption and is therefore expected to be diffusion controlled. The diffusion process in aqueous solution is twice as low as in gaseous phase¹⁵⁹.

1.11.1. Oxyfunctionalisation of alkanes with catalysts:

The literature⁴ shows that the introduction of oxygen containing functional groups in alkanes proceeds with low selectivities over most homogeneous and heterogeneous catalysts. The

catalysts used in alkene oxidation are ineffective for alkanes⁴. Many transition metal complexes were found very effective in C-C bond cleavage, lead to complete oxidation to respective acids. The use of zeolites and molecular sieve based catalysts in oxidation reactions assumed to have a lot of importance in recent times. Titanium silicates exhibiting a pentasil structure (both TS-1 and TS-2), particularly, have been found to catalyse the oxidation of a variety of organic substrates with an aqueous solution of H₂O₂ and were found to be very selective in the oxidation of alkanes.

Hari Prasad Rao and Ramaswamy¹⁷⁴ reported that vanadium silicate molecular sieves can oxidise unactivated alkanes under mild conditions with aqueous hydrogen peroxide, unlike titanium silicates, vanadium analogues were able to oxidise the primary carbon atoms of alkanes to corresponding alcohols and aldehydes. The oxidation of linear saturated hydrocarbons¹⁷⁴, viz., n-hexane, n-heptane, n-octane and cyclohexane were summarized in Table 1.15. The major products of the reaction were reported as the corresponding alcohols, aldehydes and ketones. Small quantities of other products with more than one functional group (e.g. dihydroxyalkanes) and lactones were also detected.

The interesting observation is the formation of primary alcohols and aldehydes. The product distribution showed the activation of carbon atoms at the second position is preferred to others and follows the order 2 > 3 > 4 > 1. The ability of the vanadium silicates to activate the primary carbon atom was also demonstrated in the oxidation of other organic substrates e.g. toluene was oxidised to benzyl alcohol, benzaldehyde and cresols in presence of H₂O₂ at 353 K, with an H₂O₂ selectivity of ca 50%. In addition, a higher aldehyde and ketones to alcohols ratio in the product distribution indicates a greater oxidation ability of vanadium silicates compared to titanium silicates. Vanadium silicate molecular sieves can catalyse the oxyfunctionalization of alkanes to corresponding alcohols, aldehydes, ketones and were able to oxidise the primary carbon atom as well¹⁷⁴.

Table 1.15. Product distribution in the oxidation of linear alkanes¹⁷⁴.

Reactant	Turn-over	H ₂ O ₂ Selectivity	Product distribution (wt. %)									
			1-ol	2-ol	3-ol	4-ol	1-al	2-one	3-one	4-one	Others	Product Selectivity
n-Hexane	1198	57.1	3.7	9.2	8.2	-	7.2	26.3	25.0	-	21.4	79.5
n-Heptane	1030	50.1	3.1	6.8	5.8	2.1	.42	25.1	21.7	7.0	24.2	75.8
n-Octane	821	43.4	4.6	5.9	4.6	3.8	3.2	21.7	18.0	13.8	24.4	75.6
Cyclohexane	706	32.7	-	-	33.3	-	-	-	60.7	-	6.0	94.0

1.11.2. Zeolites as catalysts:

Zeolites have the ability to act as catalysts for chemical reactions which take place within the internal cavities. Zeolites are extremely useful as catalysts for several important reactions involving organic molecules. An important class of reactions is that catalysed by hydrogen-exchanged zeolites, whose framework-bound protons give rise to very high acidity. This is exploited in many organic reactions, including crude oil cracking, isomerisation, fuel synthesis and hydrocarbon synthesis. Zeolites can also serve as oxidation or reduction catalysts, often after metals have been introduced into the framework. Examples are the use of titanium ZSM-5 in the production of caprolactam, and copper zeolites in NO_x decomposition¹⁷⁵.

Zeolites can promote a diverse range of catalytic reactions including acid-base and metal induced reactions. The reactions can take place within the pores of the zeolite, which allows a greater degree of product control. Underpinning all these types of reaction is the unique microporous nature of zeolites, where the shape and size of a particular pore system exerts a steric influence on the reaction, controlling the access of reactants and products. Thus zeolites are often said to act as *shape-selective catalysts*. Increasingly, attention has focused on fine-tuning the properties of zeolite catalysts in order to carry out very specific syntheses of high-value chemicals e.g. pharmaceuticals and cosmetics¹⁷⁵.

"Zeolite" is the broad term used to describe a family of minerals called tectosilicates. These minerals contain small pores, which provide a generous surface area. Zeolites are constructed of tetrahedral AlO_4^{5-} and SiO_4^{4-} molecules bound by oxygen atoms. The versatility of zeolites as catalysts are, they can be custom made by manipulating the structure, silica-alumina ratio, pore size, and density. Other metals can also be incorporated into zeolites to obtain specific catalytic properties¹⁷³.

1.11.3. Classification of zeolite molecular sieves:

Molecular sieves are broadly classified as macroporous, mesoporous, and microporous, based on their pore size^{176, 177} as shown in Table 1.16. Considering the channel size, the microporous molecular sieves can be further divided into ultra large, large, medium, and small pore openings depending on the smallest number of O and T atoms (where O = intersecting channels, T = tetrahedral atom, e.g. Si, Al, or P), which limits the pore openings¹⁷⁷. The development of numerous molecular sieves can also be classified based on their chemical ingredient in the building structure (Fig. 1.13).

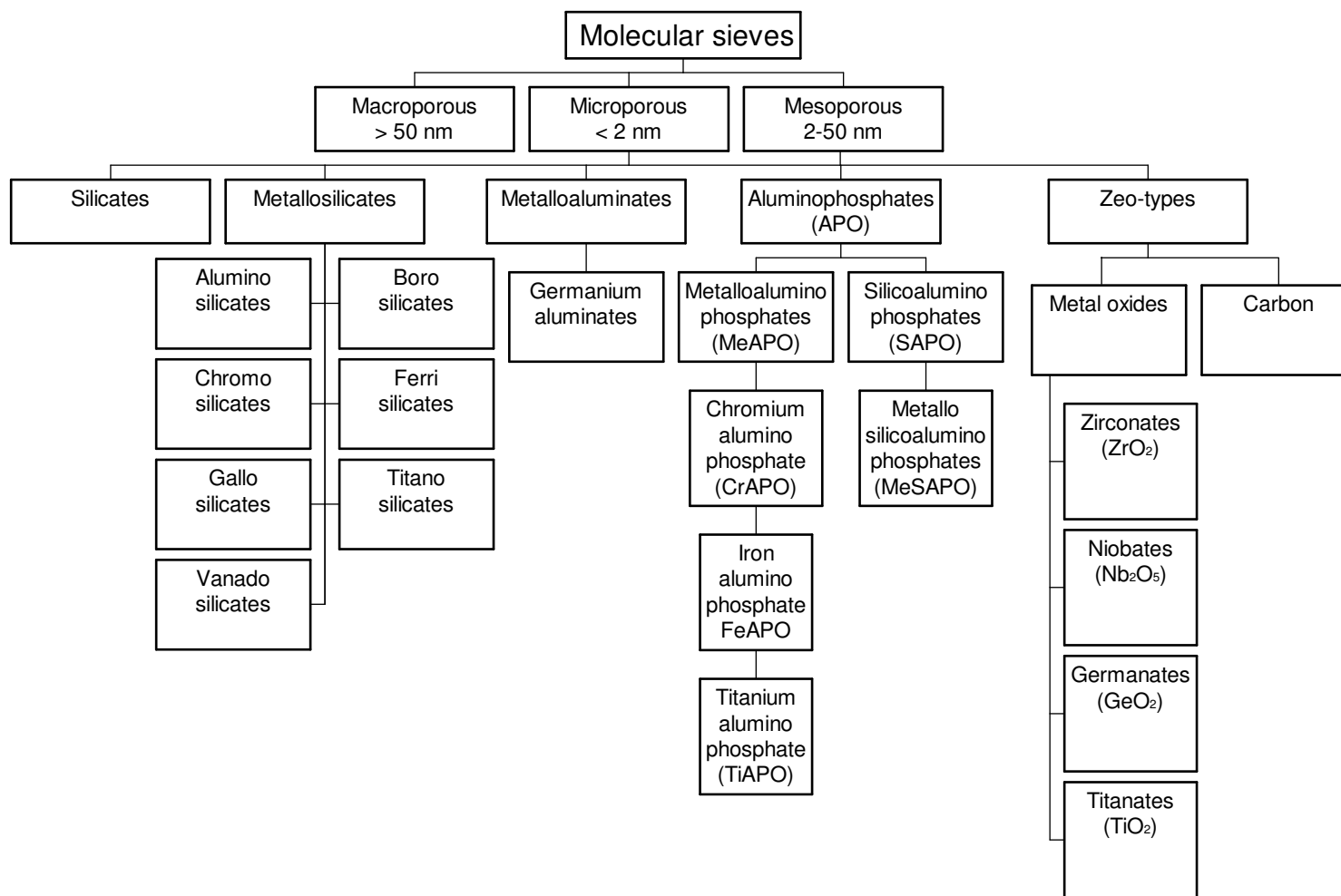


Figure 1.13. Classification of molecular sieves based on chemical component¹⁷⁷.

Table 1.16. Classification of molecular sieves on the basis of pore size^{176, 177}.

Definition	Example	Intersecting Channels	Pore size (Å)	Type of pore accessibility
Macroporous	Porous glasses	–	> 500	–
Mesoporous	MCM-41	–	20-200	1D
	MCM-48	–	20-200	3D
	HMA	–	20-200	1D
Microporous				
<i>Ultralarge</i>	JDF-20	20	6.2-14.5	3D
	VPI-5	18	12.1	1D
	UTD-1	14	7.5	1D
	APO-8	14	7.9-8.7	1D
<i>Large</i>	APO-5	12	7.3	1D
	Zeolite-β	12	6.4-7.6	3D
	ZSM-12	12	5.5-5.9	1D
	Zeolite Y	12	7.4	3D
<i>Medium</i>	ZSM-5	10	5.3-5.5	2D
	ZSM-48	10	5.3-5.6	1D
<i>Small</i>	SAPO-34	8	4.3	2D
	Zeolite-A	8	4.1	3D

1.11.3.1. Framework structure:

A defining feature of zeolites is that their frameworks are made up of 4-connected networks of atoms. One way of thinking about this is in terms of tetrahedral, with a silicon atom in the middle and oxygen atoms at the corners. These tetrahedral can then link together by their corners to form a rich variety of beautiful structures. The framework structure may contain linked cages, cavities or channels, which are of the right size to allow small molecules to enter - i.e. the limiting pore sizes are roughly between 3 and 10 Å in diameter¹⁷⁵ as shown in Fig. 1.14.

In all, over 130 different framework structures are now known. In addition to having silicon or aluminium as the tetrahedral atom, other compositions have also been synthesised, including the growing category of microporous aluminophosphates, known as aluminophosphates¹⁷⁵ (ALPOs).

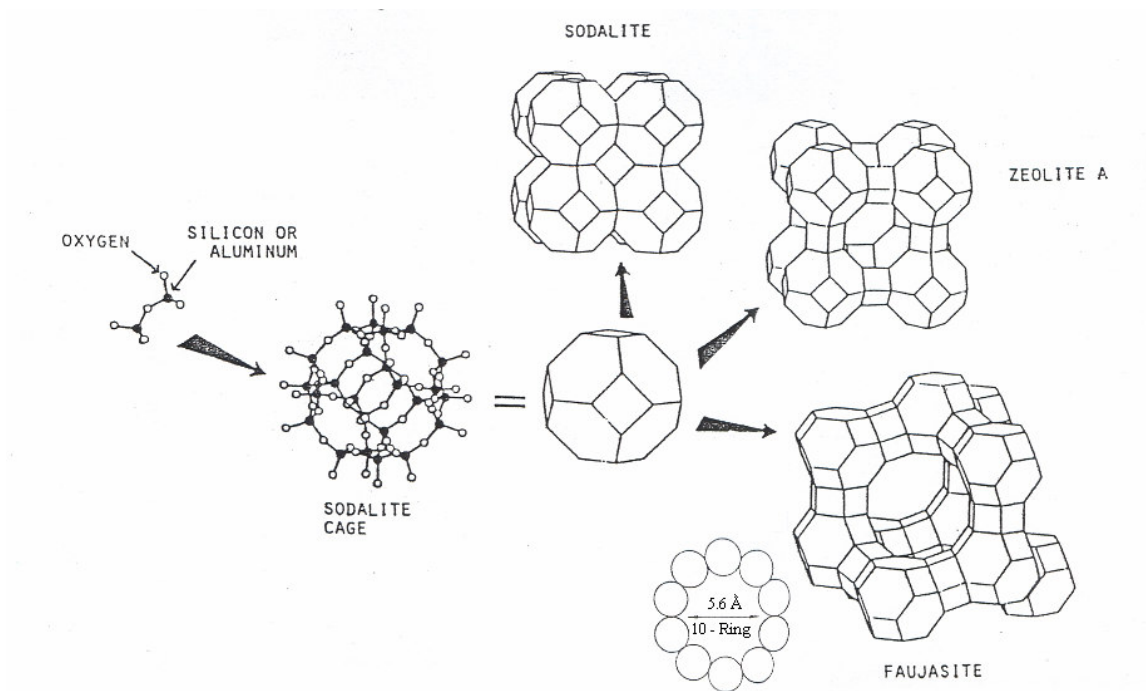


Figure 1.14. Schematic diagram of zeolite frameworks¹⁷⁶.

The advantages in using zeolite as catalysts are profit and environmental regulation compliance. Zeolites can help produce products at milder temperatures and pressures, which lowers operating costs. They also can be applicable to the oxidation processes because of their superior control of reaction selectivity, which saves on feed costs and by reducing waste streams, saves on treatment costs.

1.11.4. Adsorption and separation:

The shape-selective properties of zeolites are also the basis for their use in molecular adsorption. The ability preferentially to adsorb certain molecules, while excluding others, has opened up a wide range of molecular sieving applications. Sometimes it is simply a matter of the size and shape of pores controlling access into the zeolite. In other cases different types of molecule enter the zeolite, but some diffuse through the channels more quickly, leaving others stuck behind, as in the purification of *para*-xylene by silicalite¹⁷⁵ is shown in Fig. 1.15.

Cation-containing zeolites are extensively used as desiccants due to their high affinity for water, and also find application in gas separation, where molecules are differentiated on the basis of their electrostatic interactions with the metal ions. Conversely, hydrophobic silica zeolites preferentially absorb organic solvents. Zeolites can thus separate molecules based on differences of size, shape and polarity¹⁷⁵.

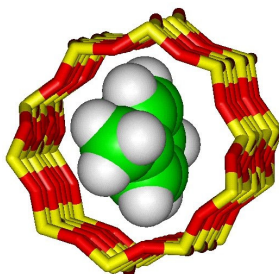


Figure 1.15. The shape of *para*-xylene means that it can diffuse freely in the channels of silicalite¹⁷⁵.

1.11.5. Ion exchange:

The loosely bound nature of extra-framework metal ions (such as in zeolite NaA) (Fig. 1.16) means that they are often readily exchanged for other types of metal when in aqueous solution.

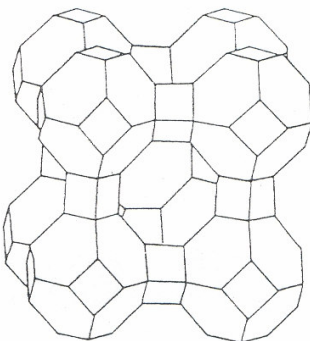


Figure 1. 16. Sodium zeolite A, used as a water softener in detergent powder¹⁷⁶.

This is exploited in a major way in water softening, where alkali metals such as sodium or potassium prefer to exchange out of the zeolite, being replaced by the "hard" calcium and magnesium ions from the water. Many commercial washing powders thus contain substantial amounts of zeolite. Commercial wastewater containing heavy metals and nuclear effluents containing radioactive isotopes can also be cleaned up using such zeolites¹⁷⁵.

1.11.6. Zeolites and the environment:

Zeolites contribute to a cleaner, safer environment in a great number of ways. In fact nearly every application of zeolites has been driven by environmental concerns, or plays a significant role in reducing toxic waste and energy consumption¹⁷⁵.

In powder detergents, zeolites replaced harmful phosphate builders, now banned in many parts of the world because of water pollution risks. Catalysts, by definition, make a chemical process more efficient, thus saving energy and indirectly reducing pollution. Moreover, processes can be carried out in fewer steps, minimizing unnecessary waste and by-products. As solid acids, zeolites reduce the need for corrosive liquid acids, and as redox catalysts and sorbents, they can remove atmospheric pollutants, such as engine exhaust gases and ozone-depleting CFCs. Zeolites can also be used to separate harmful organics from water, and in removing heavy metal ions, including those produced by nuclear fission, from water¹⁷⁵.

Specific zeolite accomplishments¹⁷⁸ are as follows:

- NO_x emission reductions by selective catalytic reduction (SCR).
- Direct oxidation of benzene to phenol, which eliminates cumene as an intermediate and uses nitrous oxide (N₂O) as a reactant. Nitrous oxide is a typical waste stream from adipic acid production.
- Ethylbenzene to styrene conversion at moderate temperatures and pressures. This route also eliminates xylene as a by-product which eliminates several purification steps.
- Caprolactam via oxidation which drastically reduces the number of processing steps as well as waste streams.
- Ability to regenerate/recycle a process' catalyst. Many catalysts must be disposed of after they are spent, but the impregnating of zeolites is a process that can be repeated over and over. Ironically, zeolites themselves help reduce waste.

The technological application of zeolites is based upon the behavior of hydrocarbons within their framework structure and is governed by two factors, (1) the zeolite acid strength and (2) the pore size. It is well known that the former factor is related to both the Brønsted acid sites (catalyst protonation ability) and the bridging hydroxyl groups (the present aluminum ions). A correlation has been proved between the acidity of sites and the aluminum content, as the greatest acidity is achieved by zeolites with relatively low aluminum content. Besides, it was found that zeolite acidity reaches an optimum value at given aluminium content for some zeolite types¹⁷⁹⁻¹⁸¹.

Faujasite-type zeolites have the general formula¹⁷³ $\text{Na}_2\text{O} \cdot \text{Al}_2\text{O}_3 \cdot n\text{SiO}_2 \cdot x\text{H}_2\text{O}$ where $n=2-3$ for zeolite X and >3 for zeolite Y. Zeolite Y, a highly versatile member of the faujasite family, plays a great role in the petrochemical industry^{182, 183}.

Zeolites and related molecular sieves, which contain rigid frameworks and accessible internal channels and/or cages, have been dominating the porous material world for a long time, because of their widespread application in catalytic and separation sciences^{173, 184}. Although there is an increasing demand for materials with tunable structures, the structural design of zeolites is limited by their requirements for tetrahedral oxide skeletons.

The use of heterogeneous catalysts in the industry is determined by their activities in a number of particular chemical reactions. Elucidating the origin of catalytic activity on a molecular level requires understanding the nature, number, strength, and distribution of specific active sites on the surface^{185, 186}.

Zeolites are natural or synthetic aluminosilicates with several properties that make them very useful as heterogeneous catalysts, i.e. they have exchangeable cations in an amount equivalent to the tetrahedral aluminium of the network (which can be substituted by those of catalytic importance or by protons, with the consequent effects on the acidity of the material), their pores (with one or more sizes) have diameters close to molecular dimensions (0.3-1.0 nm, although some have been synthesized with pore sizes up to 1.2 nm) depending on the size of the cations exchanged (typical hydrocarbon dimensions: benzene 0.57 nm x 0.22 nm; n-hexane, 0.35 nm x 0.42 nm). Their hydrophilicity is related to the aluminium content, those with lower Si/Al ratios being more hydrophilic (i.e. zeolite ZSM-5 has an unusual hydrophobicity owing to its high Si/Al ratio.)¹⁸⁷.

Zeolites X and Y have been widely used as catalysts and catalyst supports for processes of fluid catalytic cracking and hydrocracking, due to their structure, which is formed by a central cavity, accessible through twelve-member rings, where linear as well as branched hydrocarbons can penetrate¹⁸⁸.

ZSM-5 is one of the more useful zeolite catalyst¹⁸⁷, which is based on a unit which consists of a five membered ring with one substituent. Zeolite ZSM-5 has two kinds of pores, the first consisting of zig-zag channels of quasi-circular section and the second of straight channels of elliptical cross-section as shown in Fig. 1.17. This zeolite has low aluminium content and

consequently a low ionic exchange capacity. Its water content is also low, having a hydrophobic trend. Its crystalline structure was synthesized including organic molecules with nitrogen, such as tetrapropylammonium bromide in the reaction mixtures in preparations with very high $\text{SiO}_2/\text{Al}_2\text{O}_3$ ratios (20 to more than 8000). This zeolite has been more used in industrial processes, mainly for commodity petrochemicals and to produce gasoline from methanol. The apparent specific surface area of these solids is typically of the order of $500 - 700 \text{ m}^2\text{g}^{-1}$, measured in the conventional way (with nitrogen and analysis by the BET method)¹⁸⁷.

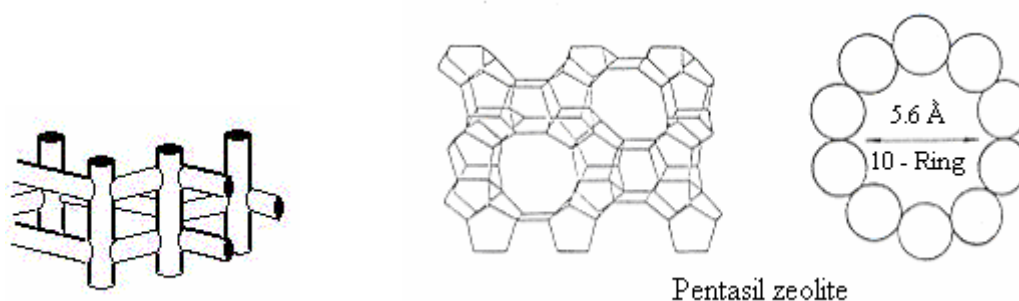


Figure. 1.17. Pentasil zeolites (ZSM-5) structure with emphasized channel systems¹⁸⁹.

The total acidity depends on the amount, strength and position of the acid sites present and can be varied by controlling the Si/Al ratio during the synthesis of the zeolites or in subsequent treatments, the most well known of them being dealuminization¹⁸⁷. The chemical and thermal stability can be increased by gradual leaching of aluminium atoms from the network, by means of strong acid solutions and chelating agents. This treatment also causes other variations in the structure, i.e. the acid properties (because the Si/Al ratio is altered) and the hydrophilic character of the zeolite decreases (when only silicon is present, the structure is hydrophobic, i.e. the zeolite called silicate, Fig. 1.17, in which the amount of aluminium is practically zero). Another way of stabilizing the structure is by exchanging the zeolite with polyvalent cations. This property allows the reproducible preparation and activation of catalysts based on zeolitic materials¹⁸⁷.

Brønsted as well as Lewis, acid sites can be found in these structures¹⁹⁰. Brønsted acid sites are the protons bonded to the oxygen atoms of the network and can be generated by exchange with acid solutions, thermal decomposition of ammonium ions, dissociation of the water molecules present in the structure under strong electrostatic field of the cations. Lewis acid sites are mainly due to the charge-compensating cations, or the trigonal aluminium atoms deficient in oxygen, and can be generated by dehydroxylation of two hydroxyl groups¹⁹⁰.

The structure and catalytic properties of zeolites have been intensively investigated as prototypes of acidic industrial catalysts. Zeolites were first introduced as catalysts for large-scale gas-phase reactions in petrochemistry. Compared to conventional liquid acids, these materials offer significant advantages for processes such as cracking, aromatization, aromatic isomerization, or disproportionation. They are thermally stable and offer convenient reactor design, they are easy to separate from the reaction products, and can be regenerated after the reaction products, and can be regenerated after suffering deactivation, and they offer shape selectivity and control of the reaction outcome. During the past two decades, an ever-increasing volume of research has been carried out promoting the use of zeolites as solid catalysts for organic reactions in the liquid phase e.g., in the production of fine chemicals under environmentally benign conditions. One of the most intriguing properties of acid zeolites is their ability to generate spontaneously organic radical cations upon adsorption of organic electron donors. The rigid microporous solids serves as excellent matrices, stabilizing otherwise reactive or unstable radical cations. The restricted mobility within zeolite pores limits the tendency of free radicals or radical cations to dimerize and prevents access of reagents that typically would cause their decay in solution^{191, 192}.

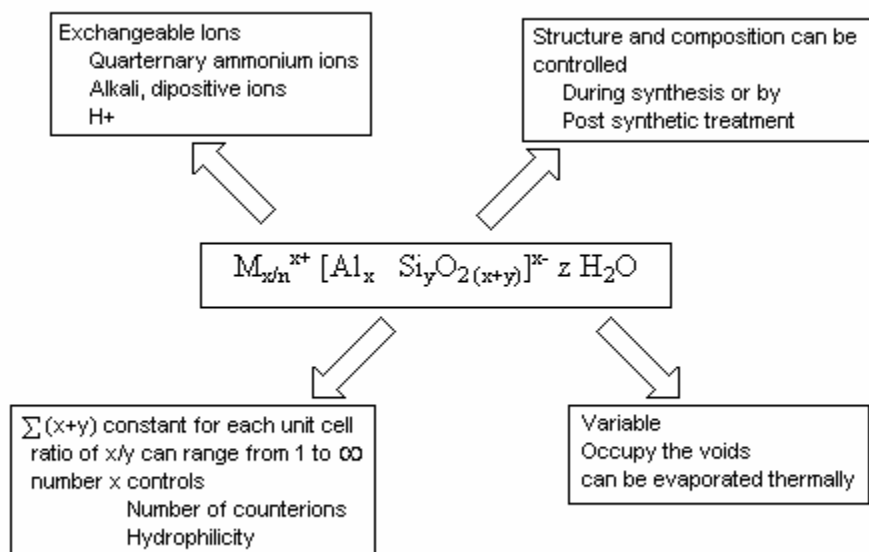


Figure 1.18. Chemical composition of zeolites¹⁹³.

The tetrahedral share the corners or edges; thus the number of oxygens is twice that of Si plus Al atoms. In contrast to amorphous silica or silica-alumina, which lack long-range ordering, zeolites are crystalline; their tetrahedral are spatially arranged in strictly regular fashion. The building

blocks are repeated in the three principal directions of the unit cell. The chemical composition¹⁹³ and some general properties of zeolites are summarized in Fig. 1.18.

1.11.7. Significance of Si/Al ratio:

Zeolites are further grouped into families on the basis of composition, namely the Si/Al ratio. Since the ion exchange capacity is equal to the concentration of Al^{3+} ions in the zeolite, the structures with low Si/Al ratios can have higher concentrations of catalytic sites than the others. There are other transitions in properties exemplified by the acid form zeolites (those incorporating H^+ as the exchangeable ion¹⁹⁴). The zeolites with high concentrations of H^+ are hydrophilic, having strong affinities for polar molecules small enough to enter the pores. The zeolites with low H^+ concentrations (in the limit, silicate, for example) are hydrophobic, taking up organic compounds (e.g. ethanol) from water-organic mixtures; the transition occurs¹⁹⁵ at a Si/Al ratio near 10. The stability of the crystal framework also increases with increasing Si/Al ratios; decomposition temperatures¹⁹⁵ of the different zeolites range from roughly 700 °C to 1300 °C. Zeolites with high Si/Al ratios are stable in the presence of concentrated acids, but those with low Si/Al ratios are not; the trend is reversed for basic solutions^{194, 195}.

The Si/Al ratio of a zeolite unit cell may be varied within a certain range without affecting its crystal structure. The ionic radii of the two elements are very similar, allowing the isomorphic substitution of Si by Al within the tetrahedron units. Though the ratio of Si/Al may vary, the sum of Si+Al atoms remains constant. A network of SiO_4^{4-} tetrahedral is neutral; each AlO_4^{5-} tetrahedron introduces one negative charge in the lattice. The negative charges are balanced by an appropriate number of cations, usually mono- or dipositive, inorganic or organic. Typical cations include alkali metal and quaternary ammonium ions. The latter are usually introduced as templates during the zeolite synthesis to shape the geometry of the lattice during hydrothermal crystallization¹⁹³.

The Si/Al ratio significantly influences the zeolite properties; it may vary from Si/Al = 1 (faujasite X) to Si/Al = ∞ (silicate). The Al content of an aluminosilicate determines the number of cations in the framework, and such properties as the thermal and chemical stability or the polarity of the internal surfaces. Typically with high Al content (zeolite X) are thermally and chemically less stable, so that dehydration at high temperature may cause partial dealumination by water being desorbed with a decrease of crystallinity (“self-steaming”). The polarity of the internal voids is governed by the Al content; it is highly relevant to the ability of zeolites to generate and stabilize

organic radical cations. These parameters control the population and density of cations in the micropores and affect the electron density on the oxygens. Strong electrostatic fields experienced by an organic guest inside zeolite voids have been invoked to explain the remarkable ability of zeolites to stabilize otherwise elusive positively charged organic intermediates as well as charge-transfer complexes^{196, 197}.

The hydrophilicity / hydrophobicity of zeolites is related to the polarity of the pores. Zeolites without framework Al are the most hydrophobic^{198, 199}. All zeolites contain variable amounts of water in the intracrystalline voids, either strongly bound to the solid or more loosely bound by hydrogen bridges. The amount of water adsorbed in a zeolite increases with its Al content. All water has to be removed before guest molecules can be accommodated in the zeolite pores; residual water, even very low concentrations, affects the cation-guest interactions significantly. The chemical composition of the synthetic zeolites can be controlled either during synthesis by varying the composition of the mother gels²⁰⁰ or by post synthetic modifications. Both methods require careful control of experimental conditions²⁰⁰.

As for the crystal structure of zeolites, the long-range ordering of the primary tetrahedral defines nondeformable channels and cavities of strictly uniform dimensions on the molecular (nanometer) scale. They can host organic guest molecules of dimensions smaller than the apertures of the pores. A classification of host-guest chemistry of zeolites is done depending on the dimensions of their micropores as shown in Table 1.17. The apertures are formed by a cyclic array of oxygens alternating with Si or Al; their number determines the diameter of the pore. Zeolites with increasing pore sizes can accept increasingly larger molecules; zeolites are useful for supramolecular chemistry. Besides the pore dimensions, the topology of the internal voids is very important for the incorporation of guest molecules (Fig. 1.19). In this regard, zeolites can be divided into tri-, bi- and mono-directional materials. Faujasites X and Y are typical tri-directional zeolites; their internal space consists of almost spherical cages (“*supercavities*”). 13 Å in diameter, interconnected tetrahedrally through four smaller round openings of 7.4 Å diameter. ZSM-5 is a bi-directional zeolite; its structure is formed by two systems of oval channels, one straight (5.2 X 5.7 Å), and the other sinusoidal (5.3 X 5.6 Å), crossing each other at right angles²⁰¹.

The topology of the zeolite host is crucial for the diffusion of the guest through the interior; it controls the maximum uptake achievable. Zeolites with tri-directional structures are more

accessible and allow diffusion readily, whereas diffusion in the mono-directional zeolites is seriously restricted¹⁹³.

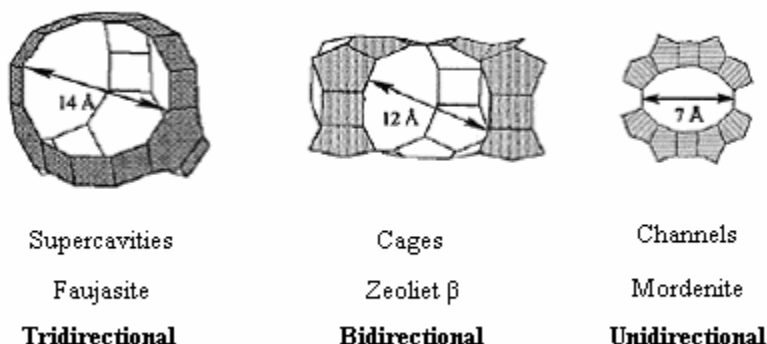


Figure 1.19. Topologies of the internal voids of zeolites²⁰¹.

Zeolites can play a significant role in the adsorption. The guest can be adsorbed on the internal or the external surface. The adsorption of the guest at elevated temperatures is more favourable than the adsorption at room temperature due to the interference of the solvent molecules. The relative polarities of the solute, solvent and zeolite play important role in adsorption. The surface areas of zeolites per unit weight are among the highest for any solid; the internal surface area is much larger than the external one. The representative values are given in the Table 1.17. The ability of zeolites to include organic guests inside the intracrystalline voids is an example of supramolecular chemistry. The host provides a rigid environment containing active sites accessible to the guest. The special role of the zeolite in the resulting supramolecular chemistry has been described by terms such as *molecular sieves*¹⁷³, *microscopic reactor*²⁰², *molecular pocket*²⁰³, or *reaction cavity*²⁰⁴.

The composition and structure of the centers responsible for the electron acceptor ability of zeolites are still subject to controversy and debate. Understanding the nature of these sites may provide control over their population and strength and make it possible to “tune” zeolites to produce optimal yields of radical cations. These features have obvious implications in the area of catalysis, especially for cracking and refining in the petrochemical industry^{205, 206}.

Zeolites are solid acids approaching the acidity of superacids; their application as industrial catalysts is mainly that of heterogeneous acids. Several early studies of organic radical cations on amorphous silica-alumina were undertaken to elucidate the acid properties of these solids. It is

pertinent to summarize the nature and structure of the Brønsted and Lewis acid centers in zeolites^{177, 207}.

Table 1.17. Characteristic properties of selected aluminosilicates^a.

Aluminosilicates	BET area ^b m ² g ⁻¹	Average pore size [Å]	Pore volume ml g ⁻¹
Clay	46	35.7	0.08
Pillared clay	250	13.4	0.18
ZSM-5	375	5.5	0.11
Mordenite	400	7.4	0.16
Zeolite Y	550	12.7	0.32
MCM-41	750	30	0.59

^a References 173, 202-204.

^b Brunauer-Emmett-Teller algorithm.

Protons contained within the zeolite lattice are Brønsted sites¹⁷⁷. The H⁺ forms of zeolites can be prepared from alkali ion containing forms by ion exchange with concentrated hydrochloric acid at elevated temperatures. A milder method employs exchange of alkali ions by NH₄⁺; thermal decomposition eliminates NH₃, leaving H⁺ in the framework. The protons of acidic zeolites are covalently bonded to the oxygen close to a negatively charged aluminum, forming oxonium species. The bridging ≡Si-(OH)-Al≡ hydroxy groups can be monitored by IR spectroscopy (3800-3400 cm⁻¹). Zeolites encompass sites with a wide range of acidities²⁰⁷, whose distribution depends on their chemical composition and crystal structure. The acidity of hydroxy groups in the framework decreases as number of Al centers in the second coordination sphere increases¹⁹³.

Zeolites also contain Lewis sites¹⁷⁶, which are attributed to tricoordinated Al centers. Samples exhibiting Lewis acidity have octahedrally coordinated Al centers, suggesting that extra framework Al species (EFAI), generated during steaming or calcinations of hydrated zeolites, are responsible for the Lewis acidity. The acidity of zeolites can be determined by temperature programmed adsorption/desorption methods¹⁹³ using probe molecules such as NH₃ or CO.

1.11.8. Uranium loaded catalysts:

Uranium (uranyl ions UO₂²⁺ or uranium oxides) may serve as promising oxidizing catalyst owing to its variable valence states vis-à-vis vacant f-orbitals²⁰⁸. Earlier studies in this direction concern dispersion of uranium oxides over dense oxide supports²⁰⁹ such as Al₂O₃, TiO₂, SiO₂, MgO, and

mesoporous molecular sieves²¹⁰. The uranyl ions are known to possess distinctive photo absorption, excitation, and emission characteristics, as compared to any other inorganic cation²¹¹. The lowest excited Eigen value of the uranyl ion (UO_2^{2+}) is a strongly oxidizing species ($E^\circ + 2.6$ V), which is found to be quenched by a variety of organic substrates resulting in the abstraction of their hydrogen atoms^{212, 213}. Number of studies have utilized uranyl ions for homogeneous-phase photooxidation reactions of hydrocarbons^{214, 215}, chlorophenols²¹⁶, and substituted phenols²¹⁷. Suib and co-workers²¹⁸ employed uranyl-exchanged clays and zeolites for the photooxidation of ethanol, isopropyl alcohol, and diethyl ether to yield the corresponding aldehydes and ketones. In another study, Dai *et al*²¹⁹ reported the photocatalytic oxidation of ethanol solution by UO_2^{2+} doped glass, which resulted in the formation of acetaldehyde.

1.11.9. Limitation of microporous molecular sieves:

Despite the diverse applications of microporous molecular sieves, their limited pore opening is a great drawback in the processing of bulkier molecules. For example, from the shape selective catalysis point of view, certain bulkier molecules of agrochemical or pharmaceutical importance are unable to access these micropores. Further, the application of microporous molecular sieves as an ideal host for the development of nanostructured materials is greatly limited. Therefore, the urgent need to design molecular sieves with adjustable porosity came into being after the discovery of the mesoporous molecular sieves.

1.11.10. Mesoporous molecular sieves:

The discovery of mesoporous silicate and aluminosilicate molecular sieves in 1992, designated as the M41S family by the Mobil scientists^{220, 221}, gave a new dimension to material science and catalysis. The M41S family consists of three members, viz., hexagonal MCM-41 with one-dimensional pores, cubic MCM-48 with three-dimensional pore system, and thermally unstable MCM-50 (Fig. 1.20). The M41S family have several advantages such as tunable pore sizes (2-10 nm), high internal surface area ($700\text{-}1500\text{ m}^2\text{g}^{-1}$), large number of internal silanol groups (30-50%), different pore geometry, hydrophilic or hydrophobic nature, high surfactant concentration, and good thermal stability ($\leq 1273\text{ K}$). Thus, it makes them superior than microporous molecular sieves. The growing importance of these mesoporous molecular sieves has been the subject of several recent reviews²²²⁻²²⁹.

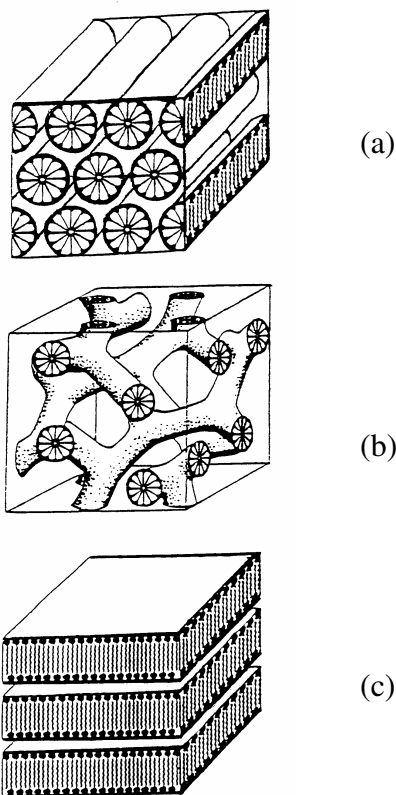


Figure 1.20. Members of M41S family²²⁵: (a) hexagonal MCM-41 (b) cubic MCM-48 and (c) lamellar MCM-50.

1.12. Objectives of the study:

Although, the oxidation of both lower aliphatic and aromatic hydrocarbons has been extensively studied⁴¹, the literature survey shows that little is known about the oxidation of higher aliphatic hydrocarbons. The scope of ozone for oxidation of saturated higher hydrocarbons is among the less explored topics of research³⁹.

The conversion of long-chained saturated hydrocarbons to value added products at moderate temperature and pressure conditions using ozone as the oxidizing agent is the focus of current research. The objective of this study is to investigate the scope of various metals supported on different zeolite material systems (supported metal systems with elements like V, Ni, Pd, and U; Zeolite-Y, ZSM-5, Zeolite Beta (BEA), Al MCM-41 and γ -Alumina) as catalysts for the ozone initiated oxidation of the higher alkanes and to compare their effectiveness. The further objectives are to characterize the catalyst materials and to establish the optimal conditions for better conversion and selectivity efficiencies of the investigated reactions.

CHAPTER – II

MATERIALS AND METHODS

2.0. Introduction:

Compressed air as cheaper source can be used for the ozone synthesis. However, ozone concentration achieved in air-fed generators is low, and the product shows signs of contamination by harmful nitrogen oxides. The nitrogen oxides may be formed during the synthesis of ozone from O₂-N₂ mixtures. The presence of these can be due to the reactions between NO_x and ozone, as well as competitive reactions in which oxygen and nitrogen atoms are consumed. e.g.:



The formation of nitrogen oxides can be avoided by the use of pure oxygen as the substrate gas. In such a case, ozone of high concentration is produced. The use of dielectric packing inside the discharge gap could be another way of increasing ozone concentration²³².

In the current studies ozone was generated by using compressed oxygen (Afrox) and ozonizer (Ozonox), which generates ozone by Corona discharge method. The schematic representation of the experimental setup used during the work is shown in Fig. 2.3. Depending on the voltage applied and oxygen flow rate the amount of ozone generated can be varied between 0.5 to 30.0 mg L⁻¹. For most of the experiments with voltage 140 V, flow rate 1 LPM (Liter per min.) and 20.41 mg L⁻¹ ozone were used. The ozone gas was introduced at the bottom of the column through a sintered porous diffuser with porosity 2 with a gas flow rate 1 LPM. The rotameter is used to monitor and regulate the feed gas (O₂) flow rates.

Prior to the experiments, the ozone generator was always stabilized (20 min.) to reach a steady state production of ozone. During that period the ozone produced was by-passed to the destruction system. Once the instrument was stable, ozone was bubbled through the solution at a fixed flow rate for requisite durations. The amount of ozone in samples was determined by iodometric method and by titrating with standard sodium thiosulfate solution. The amount of ozone produced by changing voltage, O₂ flow rates and temperature were shown in Table 2.1 and 2.2.

2.1. Ozonator instrument calibration:

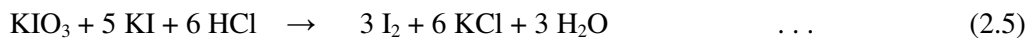
2.1.1. Ozone concentration determination:

Ozone instrument was calibrated by keeping the O₂ flow rate constant and varying the electric potential of the instrument and vice versa (Fig. 2.1). The concentration of ozone at a fixed electric potential, different temperatures and O₂ flow rates was also studied (Fig. 2.2). The determination of ozone concentration by KI method involves oxidation of potassium iodide with ozone to iodine, which gives a blue coloration with starch indicator. Iodine in solution titrated with standard sodium thiosulfate solution²³³. The following reaction takes place during the ozone interaction with KI in alkaline medium:

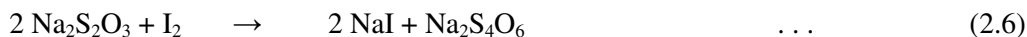


The amount of potassium iodate (KIO₃) formed in solution is proportional to the ozone concentration from the mixture of O₂ and O₃.

At pH 2, iodate ion oxidizes to iodide by releasing iodine, according to the following reaction:



The amount of liberated iodine was determined with sodium thiosulfate (Na₂S₂O₃) solution.



The amount of iodine released is proportional to ozone concentration and can be calculated from the amount of thiosulfate used in the titration.

2.1.2. Preparation of solutions and standardisation:

Potassium iodide solution: The 2% KI solution was prepared by dissolving 20 g of KI (Merck) in 1 L fresh double distilled water. The solution was stored in amber coloured bottle and preserved in refrigerator.

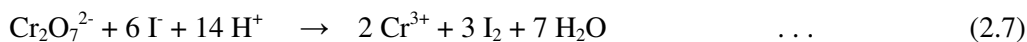
Sulfuric acid, H₂SO₄: The 1.0 M sulfuric acid solution was prepared by diluting 55.5 mL of conc. H₂SO₄ (Merck) to 1.0 L.

Starch indicator solution: To 5.0 g starch (Merck) little quantity of cold water was added and grounded in mortar to a thin paste, then transferred into 1.0 L of boiling distilled water with stirring. The solution was allowed to stand overnight and the clear supernatant was used in the titrations.

Sodium thiosulfate solution: The 0.1 M stock solution was prepared by dissolving 25.0 g of $\text{Na}_2\text{S}_2\text{O}_3 \cdot 5\text{H}_2\text{O}$ (Merck) in 1 L of double distilled water and standardised against potassium dichromate solution. The concentration of the sodium thiosulfate solution was determined each time before the determination of ozone concentration titrimetrically. From the stock solution, 0.0045 M $\text{Na}_2\text{S}_2\text{O}_3$ solution was prepared by dilution and standardised using potassium dichromate solution.

Standardisation of sodium thiosulfate solution (Dichromate method):

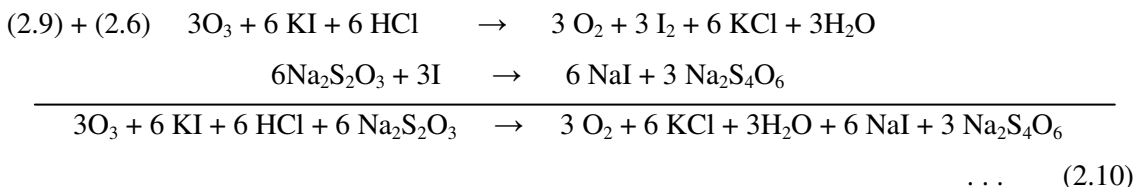
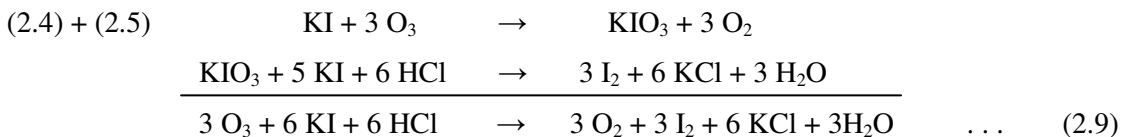
To prepare 0.1 M primary standard solution of dichromate 4.904 g of anhydrous potassium dichromate (Merck) was dissolved in double distilled water and diluted to 1.0 L. To 80.0 mL of distilled water, 1.0 mL of conc. H_2SO_4 , 10.0 mL of 0.1 M and 1.0 g of KI were added and titrated immediately with 0.1 M $\text{Na}_2\text{S}_2\text{O}_3$ solution until the yellow colour of the liberated iodine almost discharged. 1.0 mL of starch indicator solution was added to the flask and continued titration until the blue colour disappeared.



The gas mixture containing ozone and oxygen was bubbled for 2 min into 200.0 mL KI solution. This procedure was repeated using different voltages on the ozone generator. For calibration, the flow rates ranging from 1-10 LPM and voltages of 40-180 V with an interval of 20 V were used. After the absorption of ozone by KI solution, 20.0 mL of the 1 M H_2SO_4 was added to KI solution to reduce the pH below 2. 20.0 mL of the resulting KI solution after the addition of 1 M H_2SO_4 then titrated with 0.0045M $\text{Na}_2\text{S}_2\text{O}_3$ solution until the yellow colour of the liberated iodine almost discharged. At this stage 2.0 mL of starch indicator solution was added and the titration continued to the endpoint at which the blue colour disappeared.

The concentration of ozone can be calculated from the following equation:

From the equations 2.4-2.6,



The stoichiometry of $\text{Na}_2\text{S}_2\text{O}_3$: Ozone is 2:1

$$\text{Mol of Na}_2\text{S}_2\text{O}_3 \text{ used} = \frac{\text{N of Na}_2\text{S}_2\text{O}_3 \times \text{Volume of Na}_2\text{S}_2\text{O}_3}{1000} \quad \dots \quad (2.11)$$

$$\text{Mol of O}_3 = \frac{\text{Mol of Na}_2\text{S}_2\text{O}_3 \text{ used} \times 10 \text{ (dilution factor)}}{2 \text{ (Stoichiometric factor)}} \quad \dots \quad (2.12)$$

$$\begin{aligned}
 \text{Mass of O}_3 &= \text{Mol of O}_3 \times 3 \times 15.999 \quad \dots \quad (2.13) \\
 &= \mathbf{Z}
 \end{aligned}$$

$$\text{Concentration of O}_3 = \mathbf{Z} \times \mathbf{R}^* \text{ (Flow rate per 2 min. time)} \quad \dots \quad (2.14)$$

(* \mathbf{R} is 0.500, 0.250, 0.17, 0.125, 0.100, 0.083, 0.071, 0.063, 0.056, and 0.050 for 1-10 LPM respectively)

$$= \dots \text{ gm L}^{-1}$$

The concentration of ozone calculated above is the concentration of ozone in the mixture of oxygen and ozone, which was bubbled through the KI solution. All the experiments were done in replicate.

Table 2.1. Determination of ozone concentration at room temperature (20 ± 1 °C) and different applied voltages.

O₂ Flow rate L min⁻¹.	[O₃] mg L⁻¹					
	140 V	120 V	100 V	80 V	60 V	40 V
1	20.41	18.37	15.92	11.69	8.97	4.95
2	10.20	9.18	7.96	6.15	4.33	2.47
3	7.00	7.36	5.32	4.10	2.87	1.65
4	5.26	5.20	4.21	3.08	2.01	1.24
5	4.14	4.04	3.55	2.71	1.61	0.99
6	3.45	3.01	3.15	2.05	1.34	0.83
7	3.00	2.89	2.62	1.93	1.15	0.71
8	2.71	2.45	2.08	1.69	1.01	0.66
9	2.44	2.18	1.91	1.44	0.89	0.58
10	2.18	2.11	1.66	1.29	0.74	0.53

Table 2.2. Determination of ozone concentration at 120 V and different temperatures.

O₂ Flow rate L min⁻¹.	[O₃] mg L⁻¹			
	Room Temp. 20 ± 1 °C	15 °C	10 °C	5 °C
1	18.37	17.78	18.09	19.05
2	9.18	8.89	8.57	9.21
3	7.36	5.93	6.24	6.14
4	5.20	4.44	4.36	4.60
5	4.04	3.56	3.68	3.68
6	3.01	2.91	3.07	2.96
7	2.89	2.49	2.63	2.63
8	2.45	2.18	2.23	2.59
9	2.18	1.94	1.98	2.01
10	2.11	1.75	1.78	1.81

From Table 2.1 and Fig. 2.1 it is clear that higher concentration of ozone can be obtained at 140 V and 1 LPM O₂ flow rate. As the O₂ flow rate is increased the concentration of ozone decreased because of the less time of residence of the gas in between the high potential electrodes. Table 2.2 and Fig. 2.2 represent the ozone concentration at different temperatures and O₂ flow rates. It can be noticed that the difference in ozone concentration for most of the cases is little. The temperature has no influence on the ozone concentration as the values are close to one another.

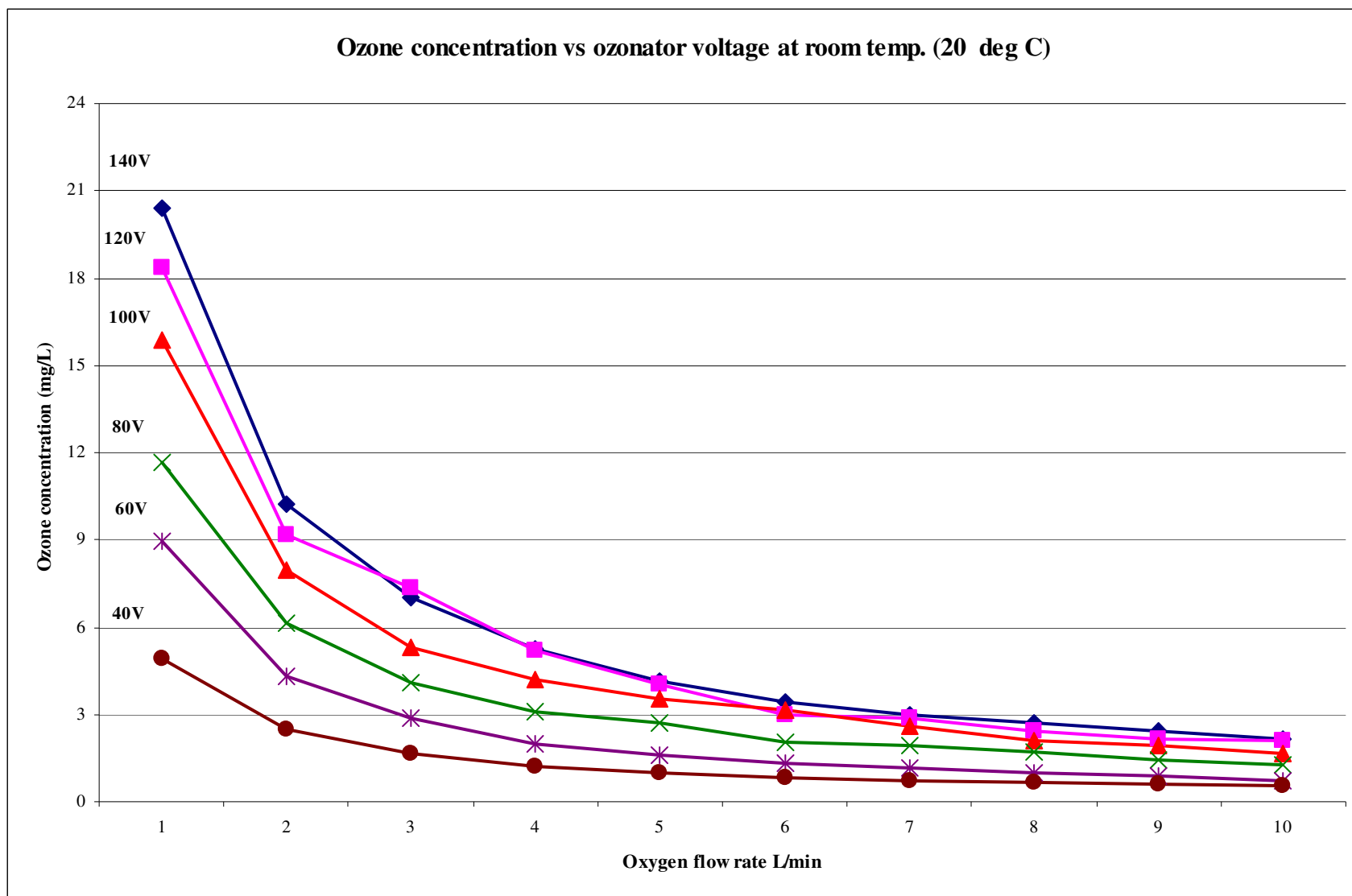


Figure 2.1. Ozone concentration vs ozonator voltage at room temperature (20 ± 1 °C).

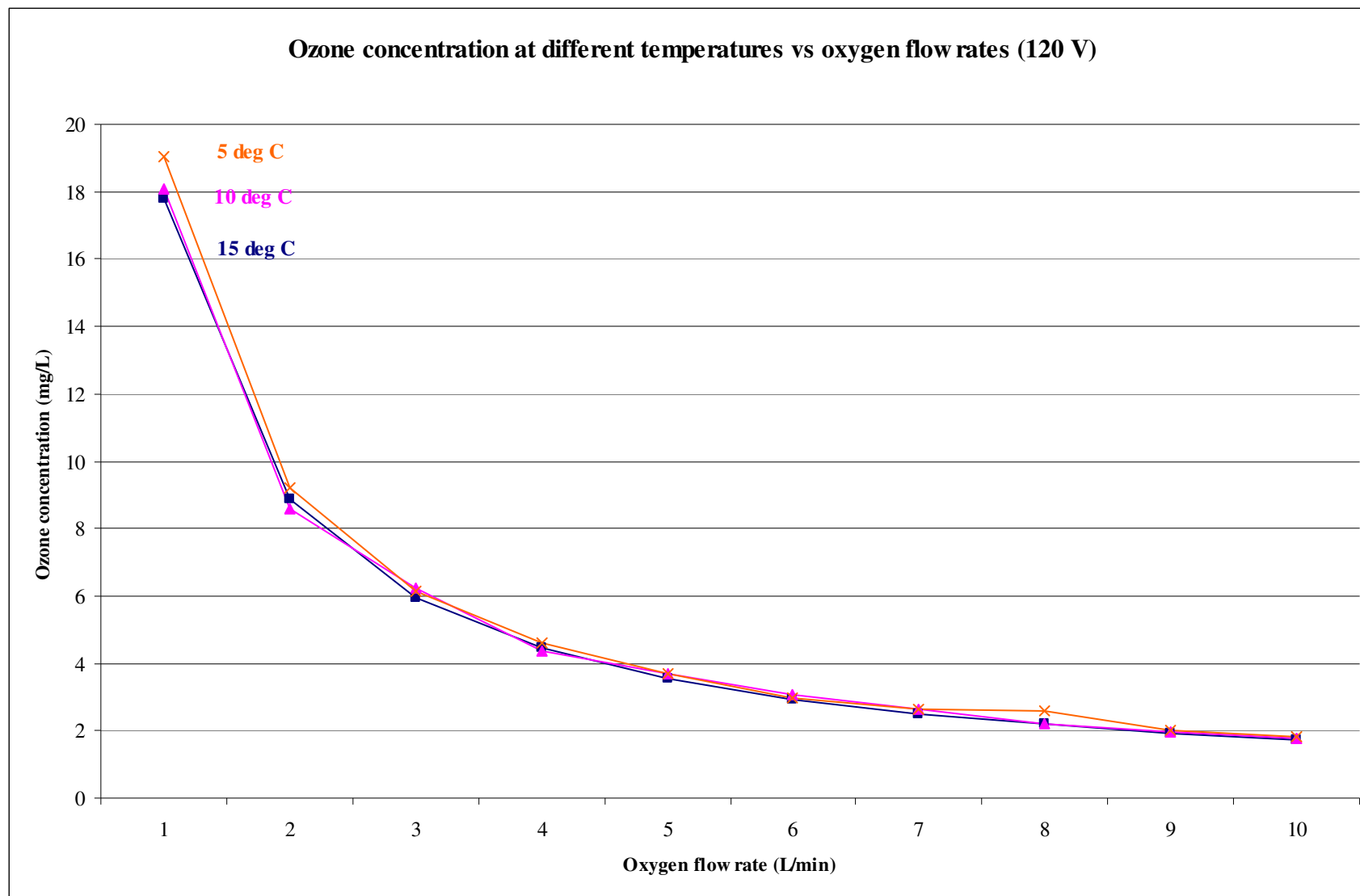


Figure 2.2. Ozone concentration at different temperatures vs oxygen flow rates (120 V).

The ozone content was determined by titration against sodium thiosulfate solution of the iodine released by ozone from a standard iodide solution²³³. All experimental runs were carried out in magnetically stirred flat bottom flask (100.0 mL), with 35.0 mL of n-hexadecane. The resulting ozone and oxygen mixture were bubbled through the substrate with the help of sintered glass bubbler (porosity 2). The gas flow rate with 15.92 mg. L⁻¹ of ozone in oxygen was used for the experiments (flat bottom flask reactions).

2.2. Ozonation of n-hexadecane with different solvents:

Literature survey shows that the ozonation of alkanes were studied in presence of diverse chlorinated solvents, acetone, tetrahydrofuran and benzene³⁴. Various solvents were used mainly to improve the solubility of ozone and to provide suitable reaction conditions. In the current study, the scope of different solvents is investigated for the ozonation of n-hexadecane at temperatures between 0 and 4 °C.

Reactions in methanol:

The ozonation experiments were conducted by saturating MeOH with ozone and then the addition of n-hexadecane to the ozonated MeOH with vigorous mixing. In these experiments 190.0 mL of MeOH was used and 10.0 mL (5% v/v) of n-hexadecane was added to ozonated MeOH. These reactions were studied at voltage range of 40, 80, 120 V and oxygen flow rate of 3, 4 LPM and temperature between 0-4 °C. The low temperature region was chosen for study, due to the stability of ozone. Ozone is known to be more stable at low temperatures and its rate of decomposition increase with rise in temperature. At low temperatures the solubility and activity of ozone increases²³⁴. The oxidation of n-hexadecane in presence of MeOH solvent at low temperature in the range of 0-4 °C was not successful.

Reaction in carbon tetrachloride:

The suitability of CCl₄ as solvent in ozonation reactions was investigated, due to its stability and less reactivity to many oxidizing agents, hydrocarbons are highly miscible. 5% n-hexadecane (v/v) in carbon tetrachloride was used for the ozonation studies in the temperature range 0-4 °C. When ozone was passed through the reaction mixture in CCl₄ at about 0-4 °C, little chemical reaction was observed after 5 h duration of ozonation. Pure CCl₄ was ozonated in the blank runs. The composition of the products of the blank and reaction mixture, it was observed that n-hexadecane remained unreacted, while CCl₄ got oxidised. The aliquots of reaction mixture were

characterized by GC-MS. Based on the products identified, interestingly no oxidation of hexadecane took place and CCl_4 was found oxidized, resulting in a mixture of products. Hexachloroethane and tetrachloroethene were positively identified as the main products of ozone initiated oxidation of carbon tetrachloride.

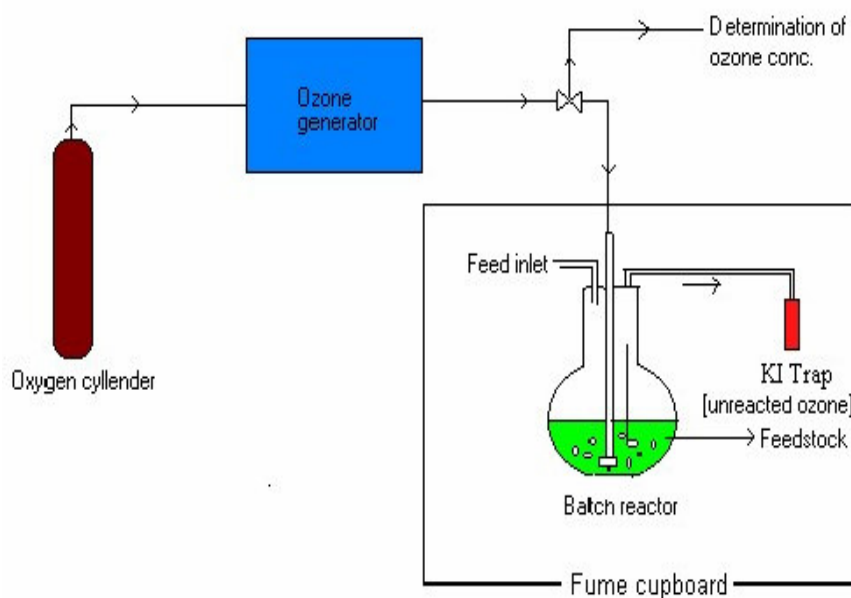


Figure 2.3. Schematic diagram of ozone generation and ozonation reaction in flat bottom flask.

Reaction in tetrahydrofuran:

Ozonation of n-hexadecane was studied using THF as solvent. In these experiments 10.0 mL of n-hexadecane in 190.0 mL of THF (5% v/v) was used. These reactions were studied at voltage range of 40, 80, 120 V and with O_2 flow rate of 3, 4 LPM at room temperature ($20 \pm 1^\circ\text{C}$) and atmospheric pressure. The oxidation of n-hexadecane in presence THF solvent at $20 \pm 1^\circ\text{C}$ temperature was not successful, as THF on ozonation resulted into oxidized products.

Reactions with pure n-hexadecane at about $0-4^\circ\text{C}$:

The oxidation of solvent free n-hexadecane at low temperature in the range of $0-4^\circ\text{C}$ was not successful due to low melting point of the substrate (18°C). Reactants got quickly solidified before the reaction started.

2.3. Reaction in absence of solvent at room temperature:

Hence to overcome the problem of freezing of the substrate at low temperatures 0-4 °C, the reaction was investigated at temperature (20 ± 1 °C). In the preliminary studies at this temperature, a number of separate experiments were conducted by ozonating the reaction mixture for different durations, 1, 2, 3, 4, 5 and 6 h. The reaction products after ozonation were compared by TLC, no appreciable reaction was observed in the first 6 h. In the further investigations, the reaction products were analysed after 9, 12, 15, 18, 21, 24 h of ozonation. 1.0 mL samples from the reaction mixture were used for analysis and characterization of the products by GC-MS. The noticeable reaction occurred only after 5-6 h of ozonation (checked by TLC). The hexadecane was ozonised for 24 h, and during the reaction progress for every 3 h, 1.0 mL samples were drawn from the reaction mixture for characterization by GC-MS.

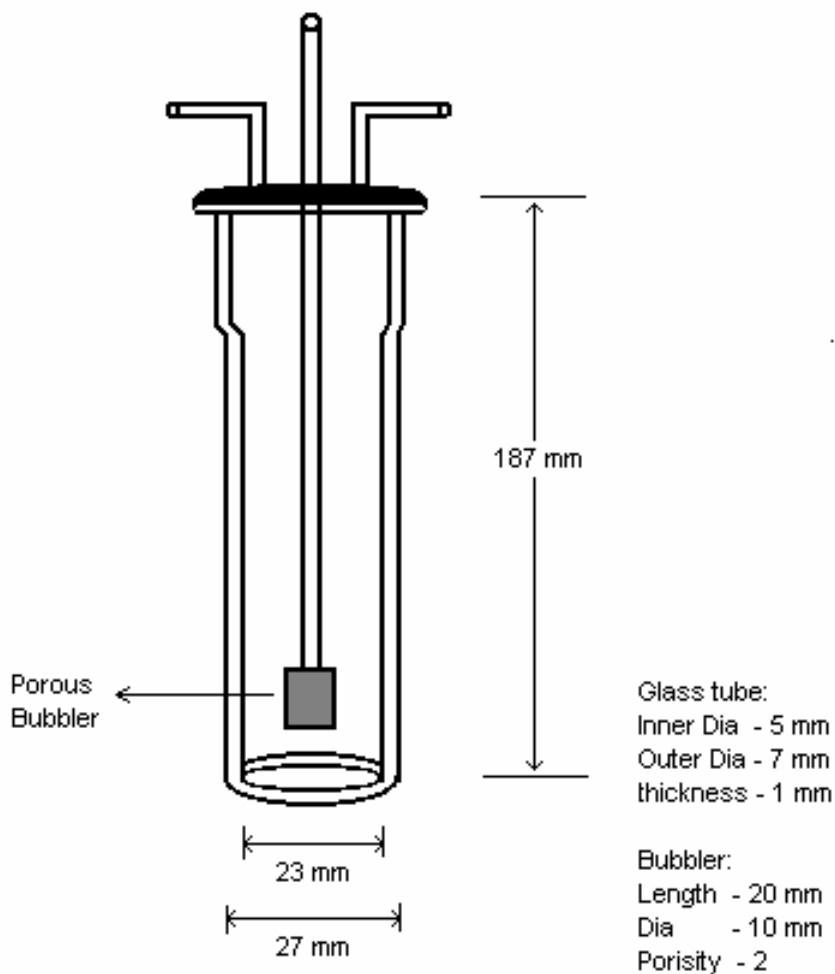


Figure 2.4. Long column dimensions.

To improve the ozone contact and efficiency of the reaction, instead the round bottom flask, a long column was used. The long column dimensions are shown in the Fig. 2.4, with 187.0 mm (column height 160.0 mm + neck height 27.0 mm) height and 25.0 mm internal diameter. The ozone was passed through the glass tube of internal diameter 5.0 mm and outer diameter 7.0 mm and porous bubbler length of 20.0 mm, diameter of 10.0 mm and porosity no. 2. All the experiments with substrate sample (hexadecane, tetradecane or dodecane) of 25.0 mL were carried at normal pressure. The reactions were conducted at temperature 20 ± 1 °C. Ozone was produced by using pure compressed oxygen (Afrox) and ozone generator (Ozonox), which produced the O_3 of concentration, 20.41 mg L^{-1} . The ozone gas was bubbled through a sintered diffuser (porosity 2) with gas flow rate of 1.0 LPM. A rotameter was used to regulate the feed gas (O_2) flow. In all final experiments, the long column was used and ozone concentration was maintained $20.41 \pm 0.08 \text{ mg L}^{-1}$ and O_2 flow rate of 1.0 LPM.

2.4. Thin Layer Chromatography (TLC):

The ozonated samples were drawn at regular intervals of 3 hrs for 24 hrs. The solvent system used for the separation of the products formed in the ozonation of C_{16} , C_{14} and C_{12} compounds was 1: 4 ratio of ethyl acetate and hexane. The stationary phase was Al_2O_3 on aluminum foil support. A finely drawn capillary tube was used for spotting the product mixture and substrate on the TLC plate. Anisaldehyde spray / I_2 vapor was used to identify the products on the TLC plate. The chromatographic plates were exposed to 254 nm UV lamp and a number of products were noticed in the product mixture.

2.5. Gas Chromatography-Mass Spectroscopy (GC-MS):

Further confirmation of all the oxidation products were characterised by GC-MS (ThermoFinnigan Trace GC with AS 3000 autosampler) equipped with Alltech EC-5 (95:5 poly(dimethylsiloxane):poly(diphenylsiloxane) 30 m x 0.23 mm (1 μm film)) capillary column.

Experimental conditions for GC-MS:

GC

Instrument:	ThermoFinnigan Trace GC with AS 3000 autosampler
Column:	Alltech EC-5 [95:5 poly(dimethylsiloxane):poly(diphenylsiloxane) 30 m x 0.23 mm (1 μm film)]
Injector:	200 °C (splitless – time 0.75 min) 0.5 or 1.0 μl injected

Oven: 40 °C (1 min) 10 °C/min to 300 °C (hold 5 min)
Carrier: He at 1 mL/min
MS transfer line: 270 °C

MS

Instrument: ThermoFinnigan PolarisQ (ion trap)
Ion Source: 200 °C
Scan Range: 40-300 (full scan)
Start Time: 4 min

2.5.1. Gas Chromatography (GC):

The identification and the routine analysis of the reaction products were done with the aid of GC-FID (Varian CP-3800 with CP-8400 autosampler) equipped with flame-ionization detector (FID, Nucon) using DB-17 [50:50 poly(dimethylsiloxane):poly(diphenylsiloxane) 15 m x 0.53 mm (1 µm film)] column.

Experimental conditions for GC-FID:

Instrument: Varian CP-3800 with CP-8400 autosampler
Column: DB-17 [50:50 poly(dimethylsiloxane):poly(diphenylsiloxane)
15 m x 0.53 mm (1 µm film)]
Injector: 250 °C (on-column) 0.2 µl injected (rinse solvent: methanol)
Detector: FID 250 °C range 10
Oven: 35 °C (1 min) 20 °C/min to 100 °C; 10 °C to 300 °C (hold 5 min)
Carrier: N₂ at 4 mL/min

To isolate the organic acids from the reaction mixture the reaction products were extracted using sodium bicarbonate 5% solution. The procedures followed are follows:

2.6. Sodium bicarbonate extraction procedure:

A sample of ozonated product was dissolved in methylene chloride (CH₂Cl₂) solvent and was extracted with 5% NaHCO₃ solution. The content was then allowed to stand in a separating funnel for 5-10 min. The sodium bicarbonate layer was separated and acidified with HCl (5%) solution to pH 3. This acidified sample was extracted with methylene chloride (CH₂Cl₂) solvent. The TLC of the extracted CH₂Cl₂ layer using 1:4 ratios of ethyl acetate and n-hexane solvents

showed a good separation of the products. TLC of the organic layer also showed a good separation of products. FT-IR analysis was carried out for these organic layer and sodium bicarbonate layers (with CH_2Cl_2 as background) to confirm the presence of carbonyl and carboxylic acid groups present in the product mixture [Fig. 4.5.1.a and 4.5.1.b, Chapter IV].

2.7. Product separation by column chromatographic technique:

The chromatographic column was prepared with 15 mL of n-hexane in the burette and cotton layer was introduced to pack silica gel (mesh size 0.063-0.200 mm) bed. Silica gel was washed with n-hexane in a beaker to avoid the air bubbles. The silica gel bed length was 20 cc, packed with cotton on the top. Solvent n-hexane was run down 2-3 times to avoid the air bubbles in the column. A 6.0 mL of product mixture was taken and 1.0 mL fractions were collected at the bottom of column. The main products of ozonation were eluted by the addition of ethyl acetate to n-hexane. The purity of the collected fractions was checked by TLC technique. The isolated products were later characterized by GC-MS, FT-IR, NMR, melting point and boiling points.

2.8. Catalytic ozonation:

2.8.1. Zeolites synthesis and impregnation techniques:

For catalytic ozonation studies, the acidic catalysts, zeolites (Micro and Mesoporous molecular sieves) of uni-dimensional and 3-dimensional viz. Zeolite-Y, ZSM-5, Zeolite Beta (BEA), Al MCM-41 and γ -Alumina were identified as suitable catalysts systems for the ozonation of higher hydrocarbons. The classification of the different molecular sieves on the basis of the ring size, pore size and type of pore accessibility is given in the Table 1.14.

The catalysts Zeolite-Y (1D), ZSM-5 (3D) were provided by SÜD-CHEMIE (Mumbai, India), H-Beta 40 (3D), H-Beta 150 (3D) zeolites were provided by SÜD-CHEMIE (Richards Bay, Durban, South Africa), γ -Alumina anhydrous form was purchased from Sarabhai Chemicals (Baroda, India). Al-MCM-41 (1D) was synthesized and characterized by different techniques like powder XRD, Diffuse reflectance UV-VIS spectroscopy, Fourier Transform-IR, SEM, BET analysis for surface area.

Synthesis of zeolite-X catalyst:

The zeolite-X (NaX) was synthesized by hydrothermal crystallization procedure. The initial gel mixture having the molar composition of $3.6\text{Na}_2\text{O} : 3\text{SiO}_2 : \text{Al}_2\text{O}_3 : 144\text{H}_2\text{O}$ was prepared by dissolving 29.2 gm of sodium aluminate (43.65% Al_2O_3 , 39.0% Na_2O) in 125.0 mL of distilled

water and this solution was added with constant stirring to the diluted solution of 78.94 gm sodium silicate (28.5% SiO₂, 8.5% Na₂O, 63% water) with 65.0 mL of water. 14.25 gm of NaOH dissolved in 75.0 mL of water was added drop wise to the above mixture and stirred continuously till the homogeneous mixture was obtained.

This homogeneous mixture was transferred to an autoclave and sealed. The autoclave was placed in the oven and maintained at the temperature of 368 K for 8 h. The autoclave was then removed from the oven and allowed to cool to the room temperature. The solid mass was separated by filtration, washed with warm water until the water wash shows pH 9. The filtered solid was dried at 383 K overnight.

2.9. Synthesis of mesoporous molecular sieves:

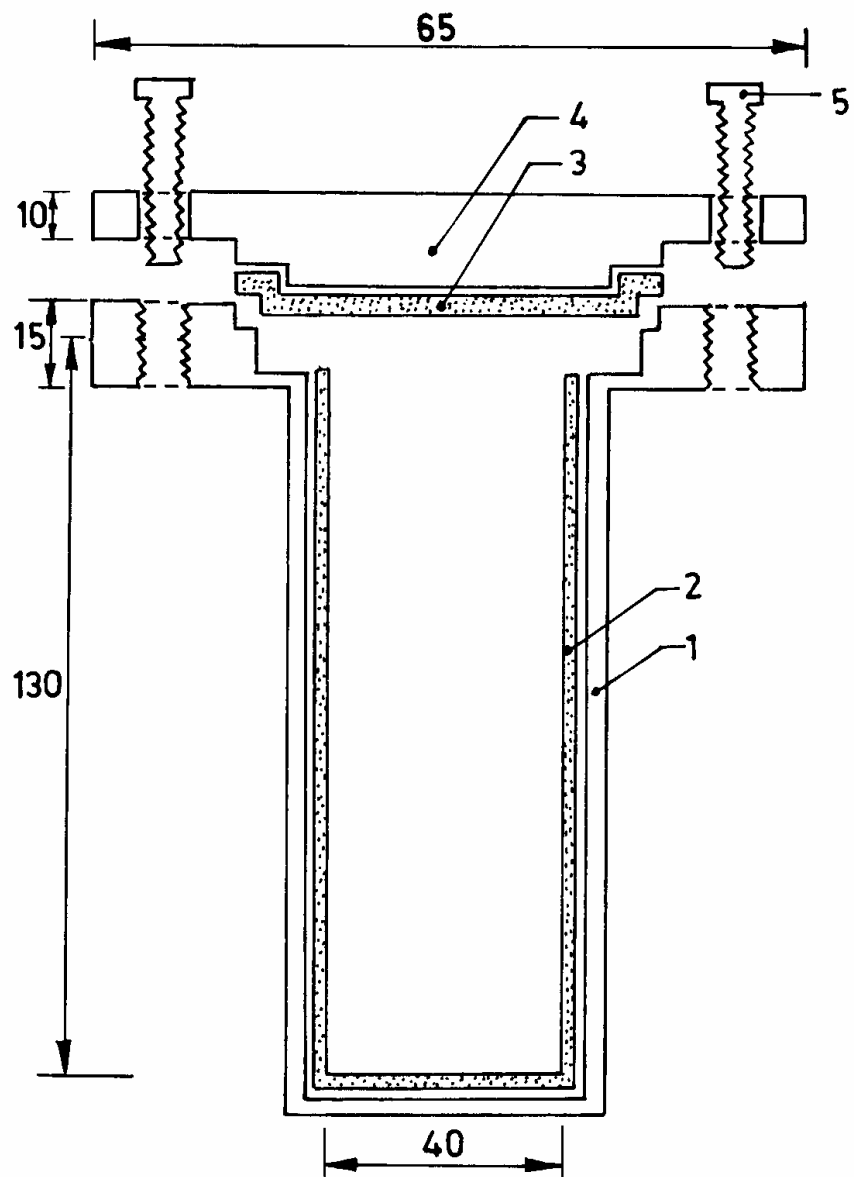
Hydrothermal synthesis:

The natural zeolites are reported to form from volcanic glass and saline water in the temperature range 300-328 K and pH values 9-10. This entire process however, takes as long as 50,000 years. In the 1940s, Barrer *et al*²³⁵ attempted to mimic nature by preparing synthetic zeolites (mordenite and several others) by a hydrothermal method. Later, Breck *et al*²³⁶ of Union Carbide successfully employed this procedure to synthesize a number of zeolites. Over the years, zeolite chemists have extensively adopted the hydrothermal technique for synthesizing a variety of zeolite and zeolite-like molecular sieves^{194, 237-242}. In general, under hydrothermal synthesis conditions, the reaction takes place in superheated water in a closed reactor vessel, which solubilizes the reagents and also helps stabilize the new phase²⁴³. Essentially, water serves two purposes: one as liquid or vapor, it acts as a pressure-transmitting medium and two the reactants that are partially soluble in water can be highly reactive.

The various starting materials, viz., silica, templates, bases, metal sources and bulk metal oxides used for the synthesis of mesoporous MCM-41 molecular sieves are listed in Table 2.3. The various reagents, viz., substrates, standards, oxidants, solvents and gases employed in the present investigation are given in Tables 2.3 and 2.4.

Specially fabricated stainless steel (Grade SS-316) autoclaves were utilized for hydrothermal synthesis of mesoporous silicate, aluminosilicate, titanosilicate, and uranium silicate molecular sieves. In order to avoid the contaminants from the reaction vessel, cylindrical Teflon-containers with lids of appropriate dimensions were employed. Such an assembly, i.e., Teflon-lined

stainless steel autoclaves, is routinely used for the hydrothermal synthesis of zeolite and zeolite-type materials. A simple sketch of the autoclave set-up is depicted in Fig. 2.5



1. Stainless steel jar
2. Teflon container
3. Teflon lid

4. Stainless steel lid
5. Stainless steel bolt

Figure 2.5. Schematic diagram of a stainless steel autoclave (dimensions in mm).

2.10. MCM-41:

The mesoporous (siliceous) MCM-41 molecular sieves were synthesized hydrothermally as per the procedure described²⁴⁴⁻²⁴⁶. Tetramethylammonium hydroxide was diluted with water and stirred for 10 min. To this, fumed silica was added slowly and a homogeneous Solution-A was prepared. Another Solution-B was prepared by mixing cetyltrimethylammonium bromide (CTAB) and NaOH in distilled water, and the solution was stirred for about 30 min. The solutions A and B were mixed together under constant stirring for an hour. The resulting gel was stirred further for 1 h for homogenization.

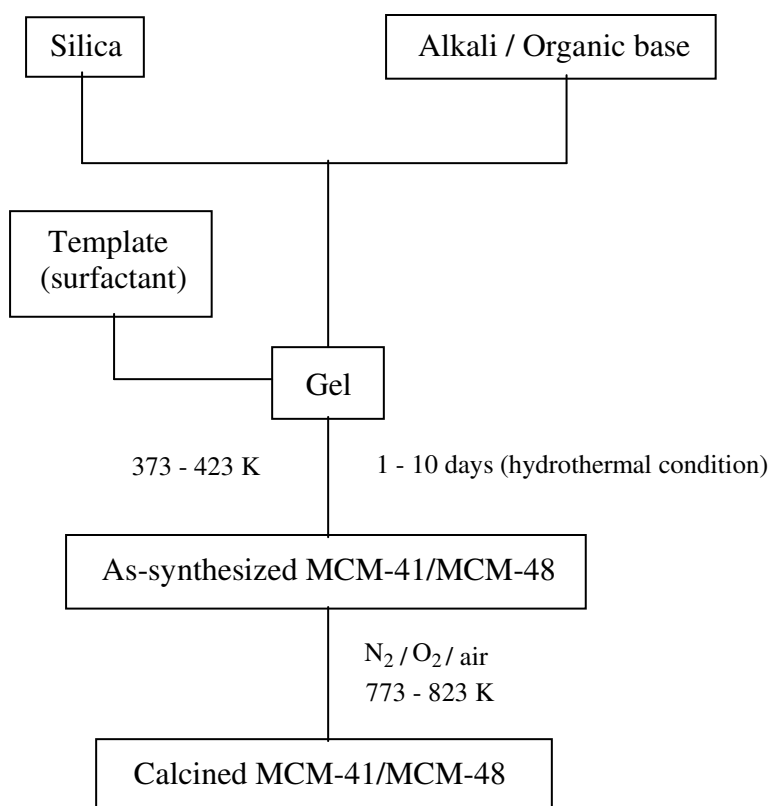
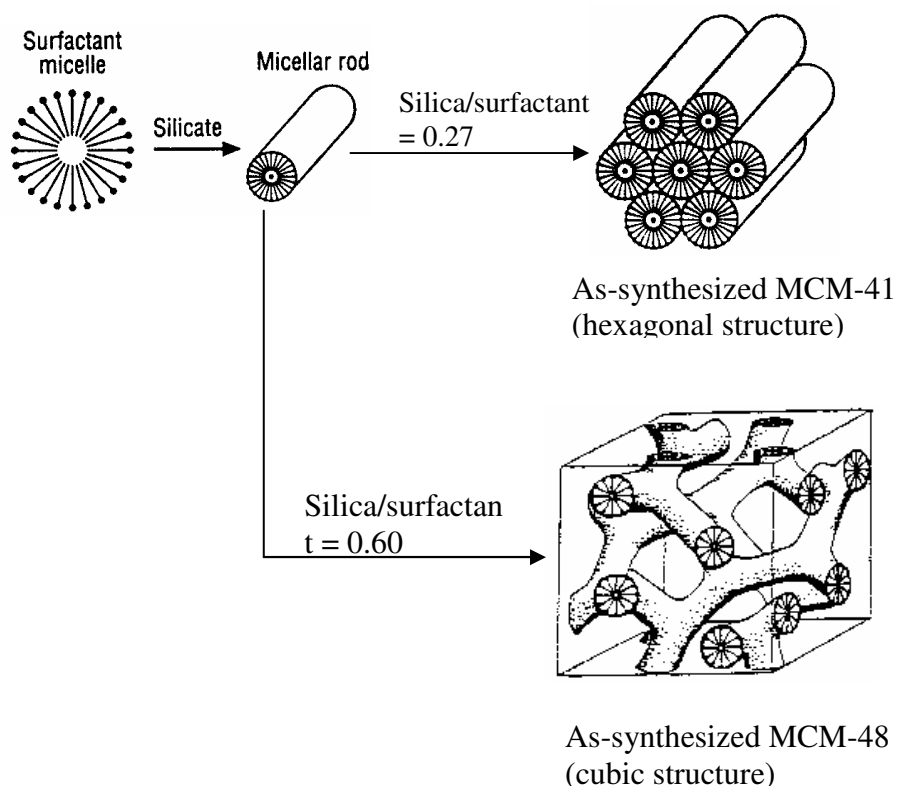


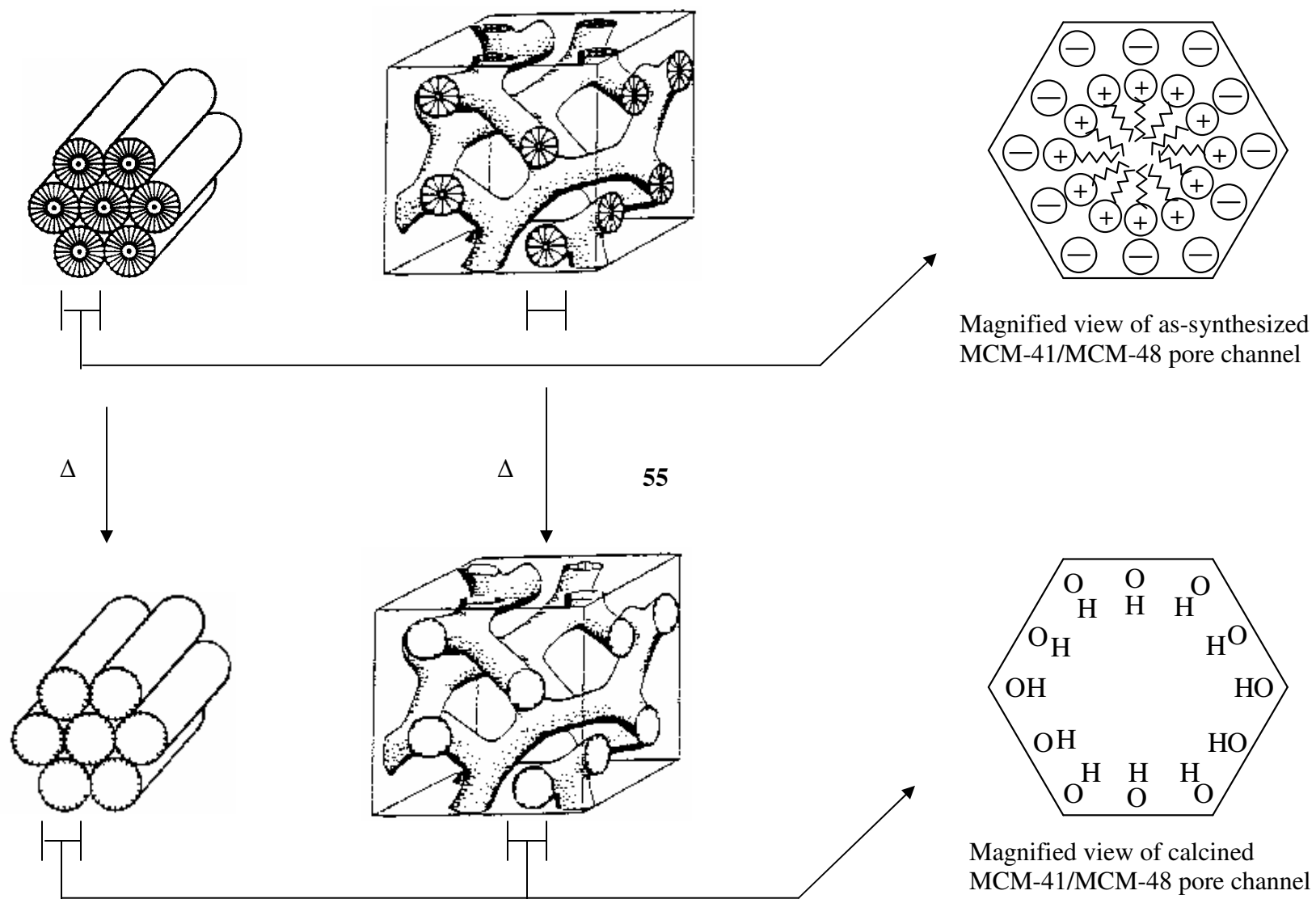
Figure 2.6. Flow chart for the preparation of siliceous MCM-41 and MCM-48 molecular sieves.

The typical gel (molar) composition was: SiO₂ : 0.27CTAB : 0.26TMAOH : 0.13Na₂O : 60H₂O. The pH of the gel was adjusted to 11.5 either by adding dilute H₂SO₄ or aqueous NaOH and was placed in an air oven at 373 K for 1 day in Teflon-lined stainless steel autoclaves (Fig. 2.5). The

solid products obtained were washed, filtered and dried at 353 K. The as-synthesized MCM-41 was then calcined in a tubular furnace at 823 K in a flow of N_2 for 1 h followed by 6 h in air with flow rate 50.0 mL min^{-1} and heating rate of 1 K min^{-1} . The schematic representation of preparation of the siliceous MCM-41 and MCM-48 molecular sieves is shown in the Fig. 2.6. The formation of mesoporous molecular sieves and the schematic representation of the pore channels in MCM-41 and MCM-48 are respectively illustrated in Scheme 2.0 and 2.1.



Scheme 2.0. Formation of MCM-41 and MCM-48 mesoporous molecular sieves.



Scheme 2.1. Schematic representation of the pore channels in MCM-41 and MCM-48.

2.10.1. Al-MCM-41:

Al-MCM-41 molecular sieves were synthesized hydrothermally as per the procedure described earlier (Section 2.10). Aluminum sulphate diluted in distilled water (0.0013 g in 100 mL) was added dropwise with continuous stirring for 30 min. The resulting gel was stirred further for 1 h for homogenization. The typical gel (molar) composition was: $\text{SiO}_2 : 0.27\text{CTAB} : 0.26\text{TMAOH} : 0.13\text{NaOH} : 68\text{H}_2\text{O} : x\text{Al}_2\text{O}_3$, $x = 0.0056\text{--}0.0167$ ($\text{Si}/\text{Al} = 90, 60, 30$).

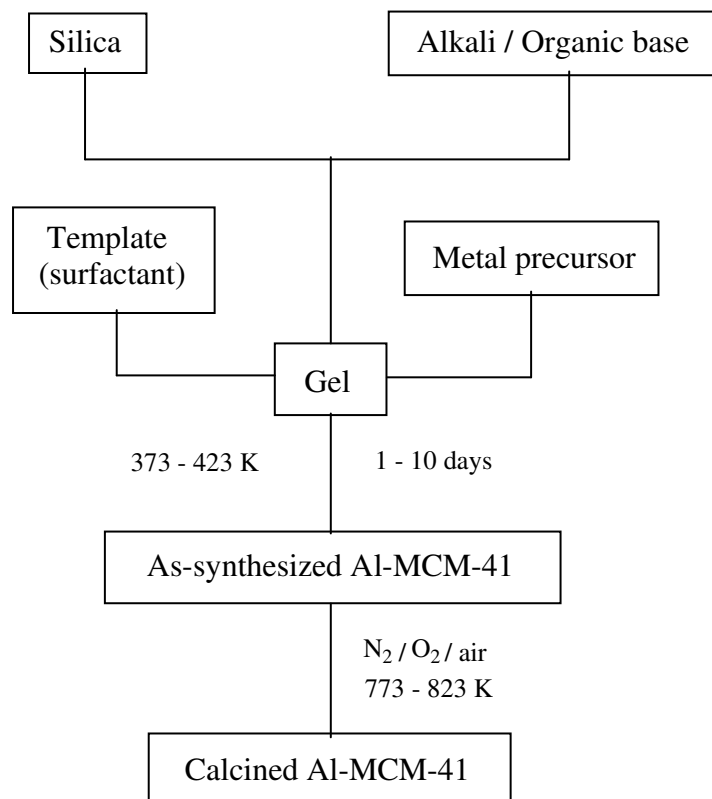
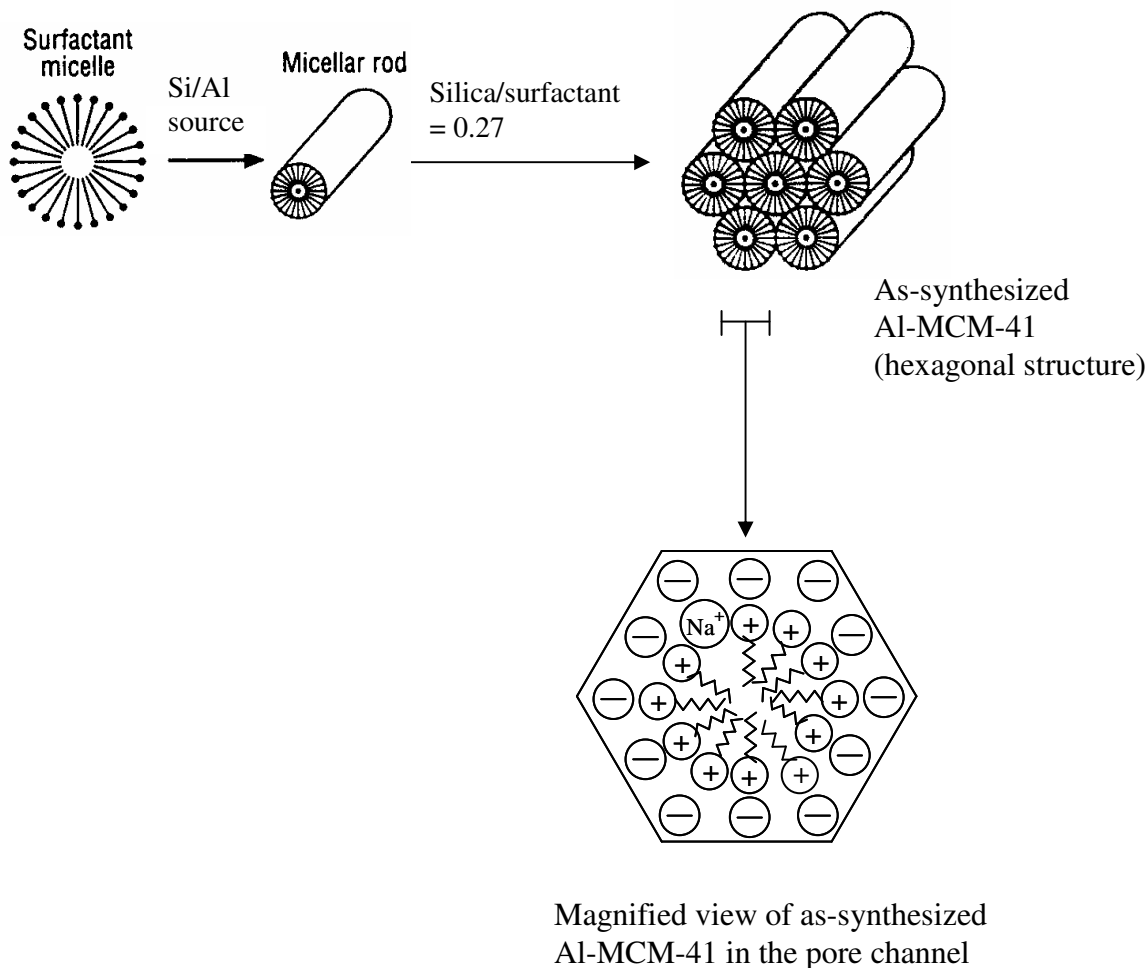


Figure 2.7. Flow chart for the preparation of Al substituted MCM-41 molecular sieves.

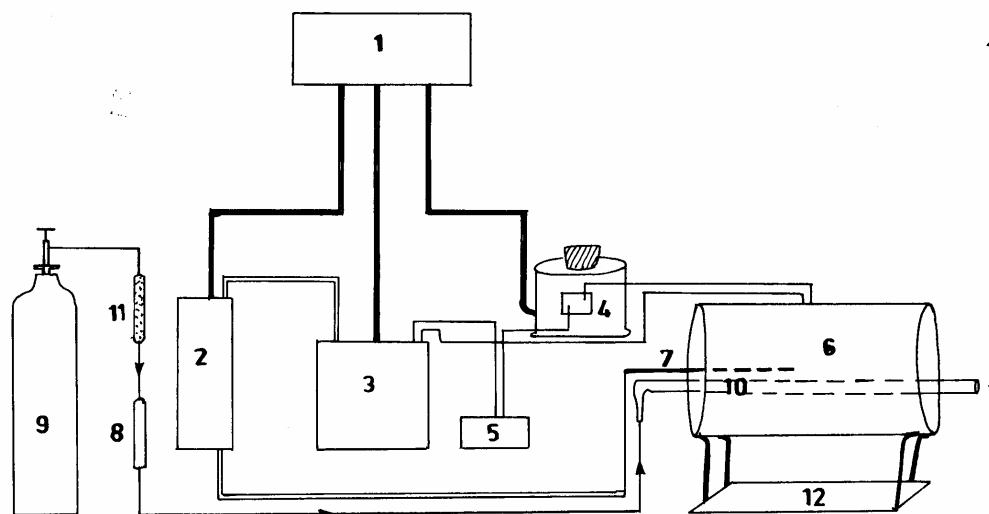
The pH of the gel was adjusted and the solid products obtained were washed, filtered and dried as discussed earlier (Section 2.10). These samples were then calcined in a tubular furnace at 823 K in a flow of N₂ for 1 h followed by 6 h in air with a flow rate 50.0 mL min⁻¹ and a heating rate 1 K min⁻¹ (Fig. 2.7 and Scheme 2.2).



Scheme 2.2. Formation mechanism of as-synthesized Al-MCM-41.

2.11. Calcination:

In order to remove the surfactant, water, and other gaseous molecules from the mesoporous structures, the as-synthesized samples were calcined in a temperature programmed (Indotherm) tubular furnace (Fig. 2.8) under flowing air, nitrogen and/or oxygen atmosphere (40.0–60.0 mL min⁻¹). The heating was carried out from room temperature to 823 K at the rate of 1 K min⁻¹ for 6–22 h. The samples are referred to as calcined materials. About 1.0 g of the as-synthesized sample was placed in the center of the quartz reactor having a thermo-well, which was packed at both ends with ceramic wool. The sample was loaded carefully in the reactor so as to avoid any displacement during the calcination process. A diagrammatic representation of the experimental set-up is presented in Fig. 2.8.



- | | |
|---------------------------|----------------------------|
| 1. Main power supply | 7. Thermocouple |
| 2. Temperature programmer | 8. Flow meter |
| 3. Controller (power) | 9. Gas cylinder |
| 4. Variac | 10. Sample (quartz) tube |
| 5. Ammeter | 11. Silica (moisture) trap |
| 6. Tubular furnace | 12. Stand |

Figure 2.8. Schematic diagram of tubular furnace set-up.

2.12. Metal Impregnation:

The Pd, V and Ni impregnated Na-Y, ZSM-5, H-Beta 150 zeolites and γ -Al₂O₃ catalyst samples were obtained as follows. Firstly, prior to impregnation, the as-synthesized Na-Y, ZSM-5, H-Beta 150 and γ -Al₂O₃ samples were activated at 393 K for 2 h. Aqueous solutions of palladium chloride (0.0835 g in 100.0 mL double distilled water), vanadyl sulphate (0.087 g in 100.0 mL double distilled water), and nickel sulphate (0.224 g in 100.0 mL double distilled water) was added dropwise to 1.0 g of the host and was kept under mild stirring for 1-2 h. The solution was then allowed to stand overnight to ensure maximum loading. The resulting products were then heated gently (~80 °C) on a hotplate to evaporate the water until the catalyst becomes dry, followed by heating at 353 K for 6 h in an oven. The metal (Pd-, V- and Ni-) impregnated zeolites (Na-Y, ZSM-5, γ -Al₂O₃ and H-Beta 150) and U on Na-Y, ZSM-5 catalyst samples were calcined at 823 K for 5-6 h, heating rate of 1 K min⁻¹ and are designated as Pd/Na-Y, Pd/ZSM-5, Pd/ γ -Al₂O₃, V/Na-Y, V/ZSM-5, V/ γ -Al₂O₃, Ni/Na-Y, Ni/ZSM-5, Ni/ γ -Al₂O₃, U/Na-Y and U/ZSM-5. 5% Metal catalysts were also prepared by following the similar impregnation and

calcination procedure like above and are designated as 5% Ni/Na-Y, 5% Ni/ZSM-5, 5% Ni/HB-150, 5% Mn/HB 150, 5% Mo/HB 150 and 5% Co/HB 150.

2.13. Calcination under N₂ flow conditions:

The metal impregnation and calcinations under N₂ flow procedures for these catalysts are described in sections 2.12 and 2.11. A diagrammatic representation of the experimental set-up is presented in Fig.2.9. The samples were designated as Pd/Na-Y N₂ calcined, Pd/ZSM-5 N₂ calcined, Pd/ γ -Al₂O₃ N₂ calcined, V/Na-Y N₂ calcined, V/ZSM-5 N₂ calcined, V/ γ -Al₂O₃ N₂ calcined, Ni/Na-Y N₂ calcined, Ni/ZSM-5 N₂ calcined and Ni/ γ -Al₂O₃ N₂ calcined.

2.14. Characterisation:

Several analytical and spectroscopic techniques were employed to characterise the siliceous and metal-incorporated molecular sieves, and their corresponding metal containing samples. The details of each of these techniques are as follows.

2.14.1. Powder X-ray diffraction (XRD):

In the powder diffraction characterisation of materials, the diffraction pattern is the fingerprint of any crystalline phase and powder diffraction is used extensively to identify the mixture of phases which generally constitutes a catalyst. The dry catalyst samples (as-synthesised, metal impregnated and before and after calcination) were grounded with the help of mortar and pestle. The fine powder of catalysts was packed on the surface of a sample holder. Powder XRD patterns were recorded for all the samples in order to verify the formation and structure of various mesoporous materials. For Al-MCM-41 (60) and Al-MCM-41 (90) the diffraction patterns were recorded in the 2 θ range of 1.5–8.0° using a Rigaku miniflex X-ray diffractometer, equipped with nickel filtered Cu K α radiation ($\lambda = 1.5418 \text{ \AA}$). The scan speed and step size were 0.5° min⁻¹ and 0.02°, respectively. Additional care was taken for the measurements in high angle region (10–80°). For other microporous materials, the diffraction patterns measurements were recorded in the high angle 2 θ range of 2-80°.

2.14.2. Fourier transform-infrared (FT-IR) spectroscopy:

FT-IR spectra of various mesoporous samples were recorded on a Nicolet Impact 400 equipment and Nicolet Impact Model-420 spectrometer with a 4 cm⁻¹ resolution and 128 scans in the mid IR (400–4000 cm⁻¹) region using the KBr pellet technique. About 100.0 mg of dry KBr was mixed

with a little amount (10.0 mg) of the sample and was ground for homogenisation. During the mixing an IR lamp was used for drying. The mixture was then pressed into a transparent, thin pellet at 10 tons cm^{-2} . These pellets were used for the IR spectral measurements.

2.14.3. Diffuse reflectance ultraviolet-visible (DR UV-VIS) spectroscopy:

DR UV-Visible analysis was carried out to identify the charge transfer transitions arising from the metal ions/content present in the matrix of as-synthesised, metal loaded and calcined catalysts. DR UV-Visible spectra of Pd, V and Ni metal containing Na-Y, ZSM-5 and γ -Alumina samples were recorded in the range 200–700 nm on a JASCO-V 570 with BaSO_4 as a reference. DRUV-VIS spectra were also recorded in the range 200–700 nm on an UV-260 Shimadzu spectrophotometer. The procedure adopted for recording the spectra is as follows: A small amount (30.0 mg) of the sample was finely ground prior to recording. It was then spread in the form of a thin and uniform layer on a white filter paper (Whatman 40) and then fitted on the sample holder. A blank filter paper was kept in the reference cell and used as reference.

2.14.4. Thermogravimetry-Differential Thermal Analysis (TG-DTA):

Simultaneous thermogravimetry-differential thermal analysis (TG-DTA) measurements were carried out on a Shimadzu DT-30 TG-DTA system in nitrogen atmosphere (40 ml min^{-1}) with 12.0–15.0 mg of the sample and a heating rate of 10 K min^{-1} in the temperature range 300–1073 K. TG and DTA measurements were also recorded on a Dupont (9900/2100) thermal analysis system.

2.14.5. Scanning Electron Microscopy (SEM):

Morphology and location of metallic species on the surface of the catalysts were revealed by scanning (SEM) electron microscopy. The SEM measurements were carried out using a JEOL JSM-6100 microscope equipped with an energy-dispersive X-ray analyzer (EDX). The images were taken with an emission current = $100 \mu\text{A}$ by a Tungsten (W) filament and an accelerator voltage = 12 kV. The catalysts were secured onto brass stubs with carbon conductive tape, sputter coated with gold and viewed in JEOL JSM-6100 microscope. The pre-treatment of the samples consisted of coating with an evaporated Au film in a Polaron SC 500 Sputter Coater metallizator to increase the catalyst electric conductivity.

2.14.6. Brunauer-Emmett-Teller (BET) surface area analysis:

The Brunauer-Emmett-Teller (BET) surface area analysis for the catalysts was done to find the surface area available, which influences the conversion and selectivity in the ozonation of n-hexadecane. The catalysts were pretreated by degassing under N₂ flow overnight at 250 °C in Micrometrics flow prep 060. The degassed samples were analysed in the Micrometrics Gemini 2360, fully automatic, single- or multi-point BET surface area analyzer under the liquid N₂ conditions. It uses a flowing-gas technique in which the analysis gas flows into a tube containing the sample and into a balance tube at the same time and provides rapid and accurate sample analysis for solid materials.

All these analytical and spectroscopic techniques characterised results, discussion and actual spectra are presented in Chapter 3, Section 3.1 – 3.6.

2.15. Ozonation reactions with microporous and mesoporous molecular sieves:

The selectivity of zeolite catalysts with ozone as oxidant was studied with chosen substrates. All the experiments with substrate samples (hexadecane, tetradecane or dodecane) of 25.0 mL were carried at normal pressure. For the catalytic ozonation studies 5% (w/v) microporous and mesoporous catalysts were employed. The schematic illustration of the long column reactor setup is shown in Fig. 2.9. The substrate in the long column reactor was mixed by a Teflon-coated stirrer at the highest speed using a (HI 190 M magnetic stirrer, Hanna Instruments) scientific magnetic stirrer. Samples of liquid were drawn off using a pasteur pipette from time to time for GC-MS analysis and ozone concentrations were measured. Two 250.0 mL volume of gas washing bottles containing 200.0 mL of 2 % potassium iodide (KI) solution were connected in series to the reactor for collecting all unreacted ozone passing through the reactor. All parts of experimental setup were made of stainless steel, glass or Teflon. Teflon tubing was used for the ozone gas lines. The entire setup was kept in a fume hood for safety, and all connections were reinforced with Teflon tape.

Table 2.3. Specifications of the various starting materials used for the synthesis of various molecular sieves.

Material	Purity (%)	Source
Sodium aluminate (50-55% Al_2O_3 , 40-45% Na_2O)	-	Riedel-deHaën
Sodium silicate (28.5% SiO_2 , 8.5% Na_2O , 63% H_2O) ($\text{Na}_2\text{Si}_3\text{O}_7$)	-	Riedel-deHaën
Sodium hydroxide (NaOH)	99.99	Aldrich
Activated charcoal (100 mesh)	-	Aldrich
Silica gel (particle size 0.063-0.200 mm) Mesh size 70-230 ASTM, BET SA-480-540 $\text{m}^2 \text{g}^{-1}$	-	Merck
Silica		
Fumed silica(SiO_2)	98.80	Aldrich
Tetraethyl orthosilicate (TEOS)	98.00	Aldrich
Template		
Cetyltrimethylammonium bromide (CTAB)	98.00	Aldrich
Tetradecyltrimethylammonium bromide (TDTAB)	98.00	Aldrich
Bases		
Tetramethylammonium hydroxide (TMAOH)	25 wt %	Aldrich
Sodium hydroxide (NaOH)	99.99	Aldrich
Metal precursor		
Aluminium sulfate ($\text{Al}_2(\text{SO}_4)_3 \cdot 18\text{H}_2\text{O}$)	98.00	Aldrich
Vanadyl sulfate ($\text{VOSO}_4 \cdot 3\text{H}_2\text{O}$)	99.99	Aldrich
Sodium metavanadate (NaVO_3)	90.00	Aldrich
Palladium chloride (PdCl_2)	99.00	Aldrich
Nickel sulfate ($\text{NiSO}_4 \cdot 6\text{H}_2\text{O}$)	99.99	Aldrich
Nickel nitrate hexahydrate ($\text{NiNO}_3 \cdot 6\text{H}_2\text{O}$)	≥ 99.00	BDH
Uranyl nitrate ($\text{UO}_2(\text{NO}_3)_2 \cdot 6\text{H}_2\text{O}$)	> 98.00	Sigma-Aldrich

Table 2.4. Specifications of the various reagents and gases used for the ozonation reactions.

Material	Purity (%)	Source
<i>Substrates</i>		
n-Hexadecane	> 99.0	Aldrich
n-Tetradecane	> 99.0	Aldrich
n-Dodecane	> 99.5	Aldrich
1-Dodecanol	≥ 98.0	Merck
<i>Solvents</i>		
Methanol	99.8	BDH
Carbon tetrachloride	99.0	Hopkin & Williams
Tetrahydrofuran	99.0	Unilab
n-Hexane	99.0	BDH
Ethyl acetate	> 99.0	BDH
Dichloro methane	> 99.0	BDH
Chloroform-D	99.8	Aldrich
<i>Gases</i>		
Nitrogen	99.0	Afrox
Oxygen (medicinal grade)	99.0	Afrox
<i>Other chemicals</i>		
Potassium Iodide	99.0	Merck
Sulfuric acid	99.0	Merck
Sodium Thiosulfate pentahydrate	99.0	Merck
Potassium dichromate	99.5	Merck
Starch (soluble)	-	Merck

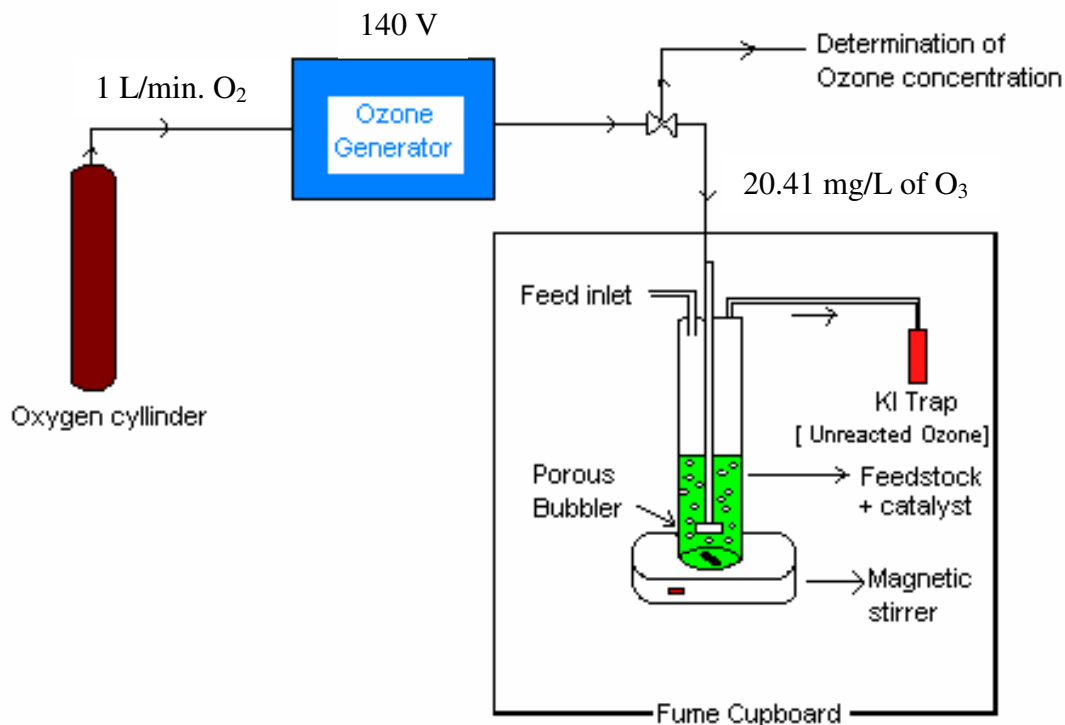


Figure 2.9. Schematic diagram of catalytic ozonation reaction setup.

The catalyst in the fine powder form was dispersed in the reaction medium i.e. n-hexadecane (tetradecane and dodecane) by means of a magnetic stirrer (Hanna Instruments HI 190 M magnetic stirrer). The reaction mixture was kept at a constant room temperature of 20 ± 1 °C and ozone of 20.41 mg L^{-1} was used. The ozone gas was introduced at the bottom of the column through a sintered porous diffuser with porosity 2 with O₂ flow rate of 1 LPM. The rotameter was used to regulate the feed gas (O₂) flow (Fig. 2.9).

All catalytic ozonation results, discussion and actual spectral data are presented in consecutive Chapters 4, 5 and 6.

CHAPTER - III

CATALYSTS CHARACTERISATION

3.0. Introduction:

In this chapter, the characterisation results of various microporous and mesoporous catalyst materials are discussed. Several analytical and spectroscopic techniques viz. X-ray diffraction, Fourier Transform-Infrared spectroscopy, diffuse reflectance ultraviolet-visible spectroscopy, scanning electron microscopy, thermogravimetry-differential thermal analysis and Brunauer-Emmett-Teller surface area analysis were carried out to characterise the siliceous and metal-incorporated molecular sieves, and their corresponding metal containing samples. The catalyst materials viz. Pd- or Ni- or V-loaded γ -Al₂O₃; Pd- or Ni- or V- or U-loaded microporous zeolites, Na-Y, ZSM-5 Si/Al-30, mesoporous Al-MCM-41 Si/Al-90 and Al-MCM-41 Si/Al-60 catalysts are characterised.

3.1. X-ray diffraction studies:

3.1.1. XRD results for Ni-impregnated zeolites:

Nickel-containing solids are known to be active in several catalytic reactions including hydrogenation and oligomerisation. It is usual to find nickel as its oxide or reduced form in such catalytic materials and this constitutes a limitation in terms of selectivities that are achievable with the systems. Supported nickel catalysts prepared with nickel sulfate on Faujasite type zeolites have been scarcely investigated as supports in ozonation reactions. This prompted to employ Ni/zeolite heterogeneous catalyst in the ozonation reactions and to study its preparation and characterisation.

The XRD spectra of the NiSO₄ loaded on γ -Al₂O₃, Na-Y, ZSM-5 material are shown in Figs. 3.1.a, 3.1.b, and 3.1.c respectively. From the XRD spectra, the nature of interaction of NiSO₄ on these materials and crystalline structure were examined. An examination of the XRD patterns in Fig. 3.1.b concerning Na-Y and Ni/Na-Y shows broader baseline (between 20° and 40°) upon the treatment of the zeolite and which is not enhanced after impregnation. This evidence is associated with no loss of crystallinity of the zeolite framework.

The comparison of XRD profiles of zeolite peaks before and after Ni loading (peaks at d values 4.7486, 4.3645 and 3.9020 Å; their corresponding 2θ values 18.670, 20.330 and 22.770) revealed that very small or no loss of crystallinity in the Ni/Na-Y zeolite samples due to loading. Similarly in the Ni/ZSM-5 Si/Al-30 and Ni/ γ -Al₂O₃ samples, no loss of crystallinity was noticed (Figs. 3.1.a and 3.1.c).

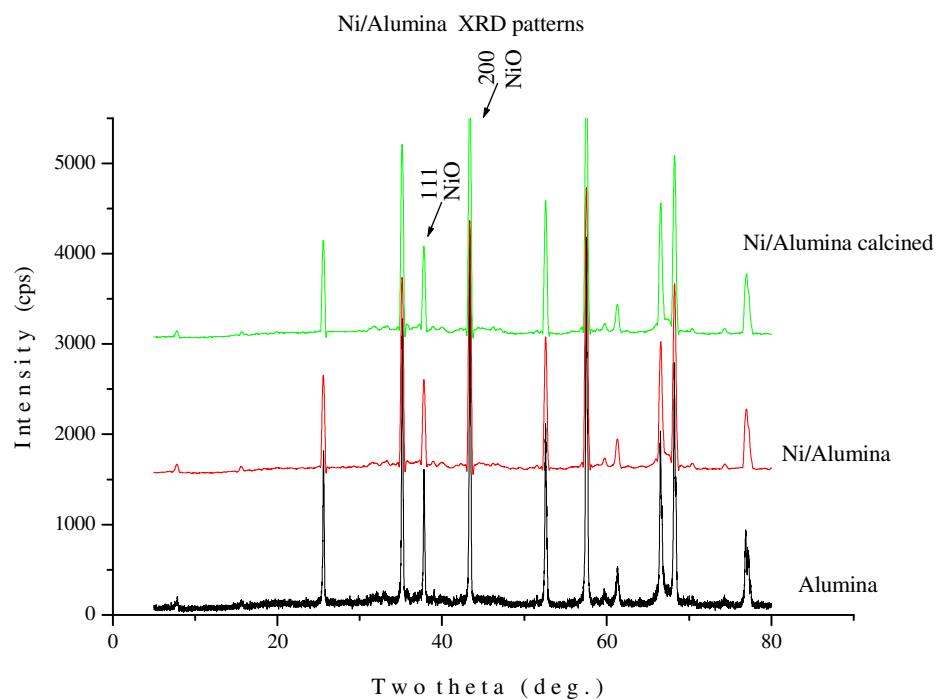


Figure 3.1.a. XRD patterns of Ni loaded γ - Al_2O_3 catalysts (with same intensities in all cases).

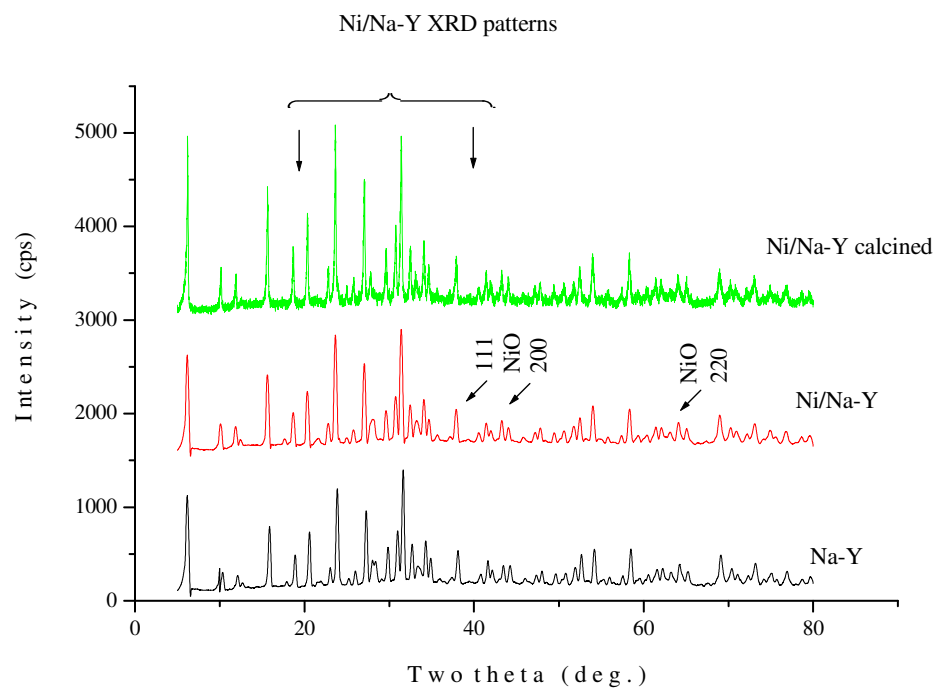


Figure 3.1.b. XRD patterns of Ni loaded Na-Y zeolite catalysts.

The X-ray powder diffraction data were used to identify the Ni^{2+} species formed on the support surface. The X-ray diffraction profiles of the Ni/Na-Y, Ni/ZSM-5 Si/Al-30 zeolites were typical of crystalline FAU (Faujasite family) and ZSM-5 materials. Ni(0.5%)/Na-Y and Ni(5%)/Na-Y samples exhibited diffraction lines of NiO crystals at Cu K α 2θ values of 37.890, 43.270, 63.120; Ni/ZSM-5 catalysts exhibited diffraction lines of NiO crystals at Cu K α 2θ values of 45.060 and 63.590 (Table 3.1). X-ray powder diffraction patterns for the samples in the three figures (3.1.a, 3.1.b, and 3.1.c) showed no appreciable loss in zeolite crystallinity.

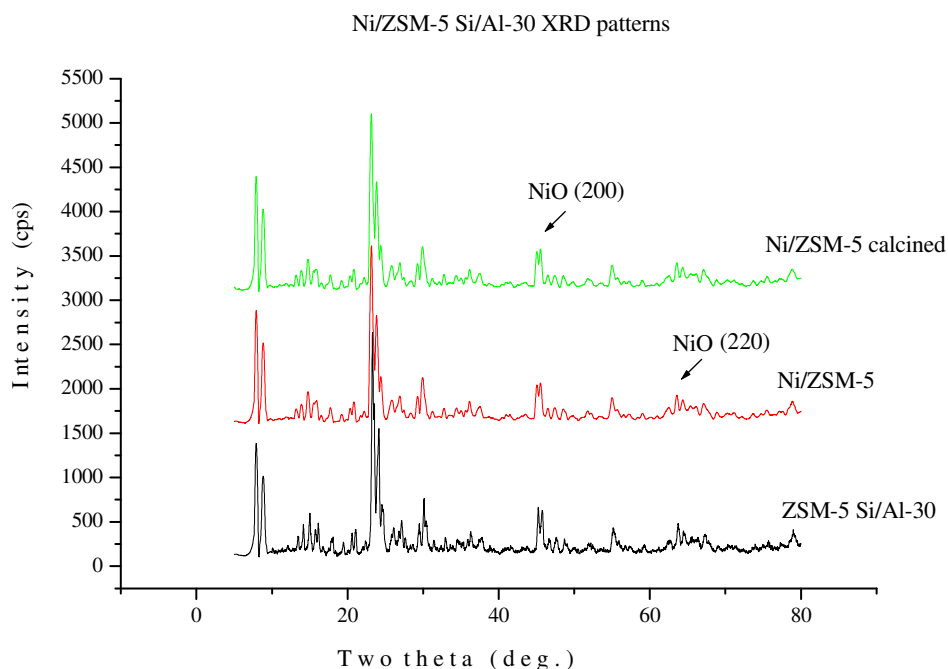


Figure 3.1.c. XRD patterns of Ni loaded ZSM-5 zeolite catalysts.

In the Ni (0.5% and 5%) loaded Na-Y zeolite the d-values at 4.7486, 4.3645, 3.9020 Å peaks are produced by $\text{NiSO}_4 \cdot 6\text{H}_2\text{O}$ as well as Ni deposition on Na-Y zeolite. The d-values at 2.4091 Å (2θ -37.890) (111), 2.0840 Å (2θ -43.270) (200) and 1.4740 Å (2θ -63.120) (220) represent calcined NiO peaks. The NiO peaks are swamped by the zeolite Na-Y characteristic peaks (Table 3.1). To compare respective changes of intensity and absorptions in the XRD, the patterns were plotted one above the other. The units on the Y-axis (ordinate) become arbitrary.

Table 3.1. X-ray diffraction data for Ni-impregnated zeolites.

Compound	2θ	d-value Å	I_{rel}	hkl
NiO^a	-	2.41	91	111
	-	2.088	100	200
	-	1.476	57	220
	-	0.9338	21	420
NiSO₄.6H₂O^a	-	4.900	51	311,002
	-	4.782	24	202
	-	4.367	100	411
	-	4.003	60	411
	-	3.865	60	511
Ni/Na-Y	18.670	4.7486	37	202
	20.330	4.3645	53	411
	22.770	3.9020	28	511
	37.890	2.3725	39	111
	43.270	2.0892	31	200
	63.120	1.4717	22	220
Ni/ZSM-5	45.060	2.0102	26	200
	63.590	1.4619	21	220
Ni/γ-Al₂O₃	37.170	2.4168	7	111
	43.370	2.0846	89	113
γ-Al₂O₃^a	25.560	3.4820	36	012
	35.140	2.5516	70	104
	37.790	2.3785	36	110
	43.370	2.0846	90	113
	52.580	1.7391	50	024
	57.540	1.6004	100	116
	61.300	1.5109	15	018
	66.560	1.4037	49	214
	68.240	1.3732	68	300
	76.960	1.2379	25	1010
	77.260	1.2338	18	119

^a Reference 247.

In the Ni (0.5% and 5%) loaded ZSM-5 zeolite the d-values at 4.900 Å (311,002), 4.367 Å (411), 4.003 Å (411), 3.865 Å (511) refers to the loading of NiSO₄. 6H₂O into the zeolite matrix. The d-values at 2.41 Å (111), 2.088 Å (200) of calcined sample refers to the NiO. The peak with d-value 2.088 Å (200) is a characteristic peak of Ni deposition on ZSM-5 catalyst (Table 3.1).

3.1.2. XRD results for V-impregnated zeolites:

The nature of the interaction of VOSO₄ .3H₂O with γ -Al₂O₃, Na-Y and ZSM-5 were studied with XRD technique and are represented in Figs. 3.2.a, 3.2.b and 3.2.c respectively. The d-values in the V/Na-Y zeolite at 4.3566, 2.1796, and 1.5085 Å represent the VO₂ peaks and the peaks at

1.8440, 1.6963 Å refers to the V_2O_3 . The d-values in the V/ZSM-5 zeolite at 4.351 Å is VO_2 , 3.408 Å is a V_2O_5 and at 1.4719 Å a V_2O_3 peak. The d-values in the V/ γ - Al_2O_3 at 3.391, 2.4789, 1.6101, 1.5107 Å are VO_2 peaks (Table 3.2).

Table 3.2. X-ray diffraction data for V-impregnated zeolites.

Compound	2θ	d-value Å	I_{rel}	hkl
$V_2O_3^a$	-	3.6578	71	012
	-	2.7132	100	104
	-	2.4774	80	110
	-	2.1885	36	113
	-	1.8292	34	024
	-	1.6990	85	116
	-	1.4719	24	214
$VO_4.5H_2O^a$	-	5.43	60	011
	-	5.14	100	210
	-	3.91	70	021
VO_2^a	-	4.35	35	110
	-	3.39	100	120
	-	2.645	50	130
	-	2.479	25	021
	-	2.213	35	121
	-	2.179	25	220
	-	1.610	25	310
	-	1.502	25	151
	-	1.492	25	250
	-	1.426	35	301
$V_2O_5^a$	-	5.768	33	200
	-	4.379	100	001
	-	4.090	27	101
	-	3.408	75	110
	-	2.882	52	301,400
	-	2.6136	25	310
V/Na-Y	20.320	4.3566	53	110
	22.760	3.9037	26	021
	27.020	3.3900	71	120
	34.060	2.6450	48	130
	41.390	2.1796	30	220
	49.380	1.8290	21	024
	54.010	1.6963	42	116
	61.410	1.5085	24	250
	65.120	1.4312	21	301

^a Reference 247.

Table 3.2. X-ray diffraction data for V-impregnated zeolites (contd.).

Compound	2θ	d-value Å	Irel	hkl
V/ZSM-5	20.820	4.351	17	110
	23.150	3.8388	100	-
	25.840	3.408	18	110
	63.580	1.4719	21	214
V/γ-Al₂O₃	25.570	3.391	36	120
	35.160	2.5502	69	-
	37.330	2.4789	7	021
	57.550	1.6101	100	310
	61.310	1.502	15	151

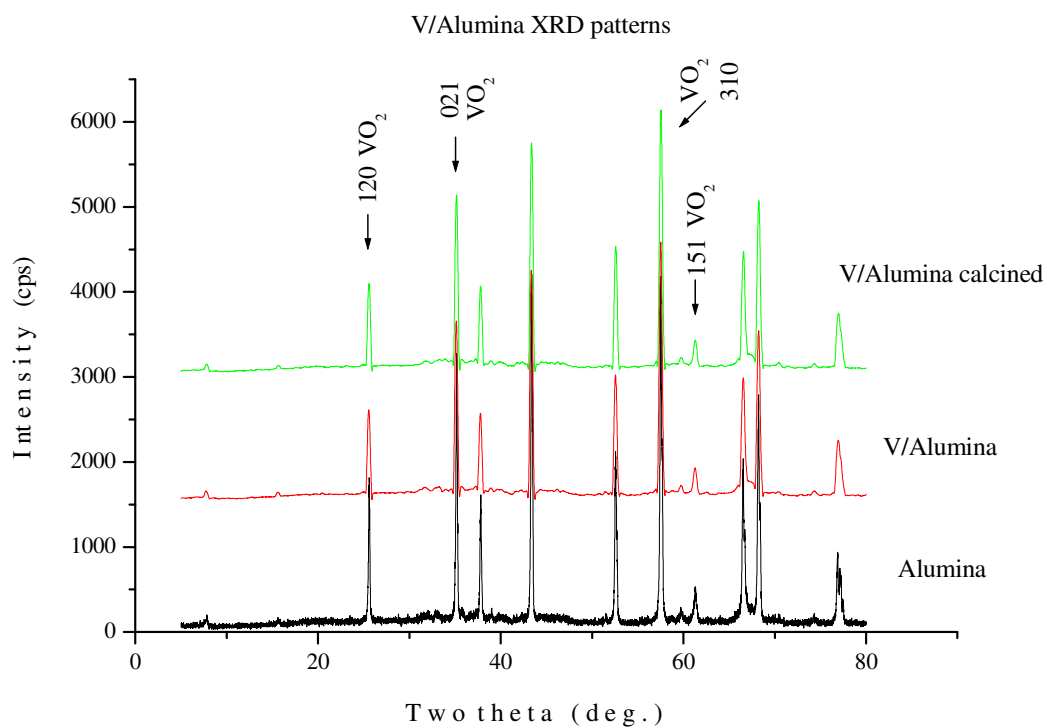


Figure 3.2.a. XRD patterns of V loaded γ -Al₂O₃ catalysts.

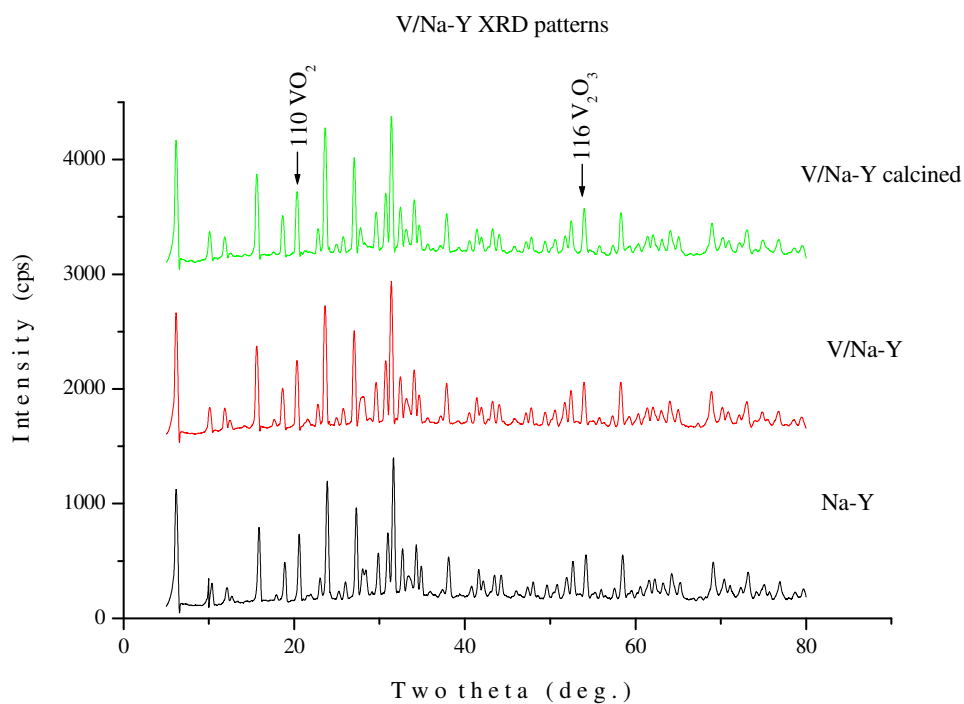


Figure 3.2.b. XRD patterns of V loaded Na-Y zeolite catalysts.

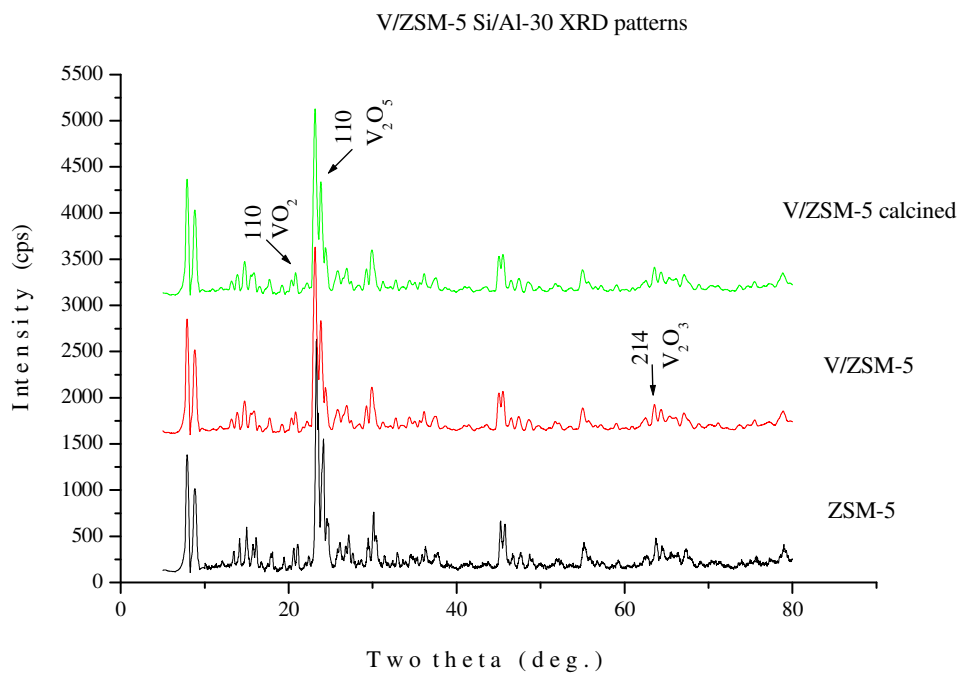


Figure 3.2.c. XRD patterns of V loaded ZSM-5 zeolite catalysts.

3.1.3. XRD results for Pd-impregnated zeolites:

The XRD studies on the nature of the interaction of PdCl_2 with γ -alumina, Na-Y and ZSM-5 are represented in Figs. 3.3.a, 3.3.b and 3.3.c respectively. With the Pd loading, not all the ionic Pd^{2+} can be accommodated at lattice sites, and as a result large tobacco-brown PdO cluster is formed on the external surface of the 0.5 wt% Pd/ZSM-5 and Pd/Na-Y catalysts²⁴⁸. This is apparent from the 2θ Cu $K\alpha=34^\circ$ peak (101) in the XRD diffractogram. Pd^0 clusters are confirmed by the diffraction lines at 2θ Cu $K\alpha=43^\circ$ (d-value 2.239 Å) (111) and 45.5° (d-value 1.9451 Å) (200).

Table 3.3. X-ray diffraction data for Pd-impregnated zeolites.

Compound	2θ	d-value Å	I_{rel}	hkl
Pd^a	-	2.246	100	111
	-	1.945	42	200
	-	1.376	25	220
Pd/Na-Y	43.230	2.239	29	111
	68.930	1.369	36	220
Pd/ZSM-5	45.070	2.2394	26	111
	45.550	1.9451	27	200
	63.580	1.3787	21	220

^a Reference 247.

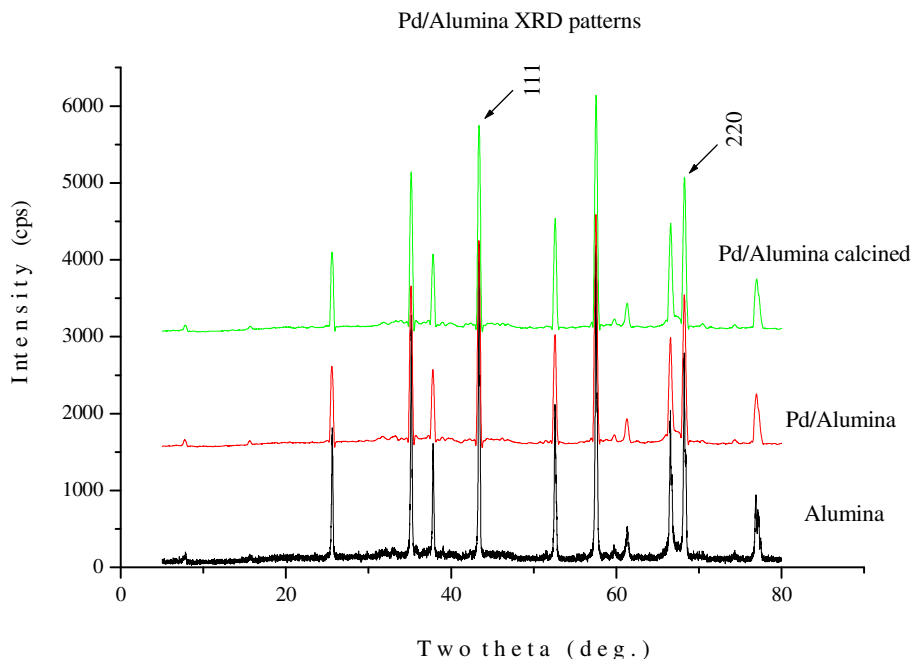


Figure 3.3.a. XRD patterns of Pd loaded $\gamma\text{-Al}_2\text{O}_3$ catalysts.

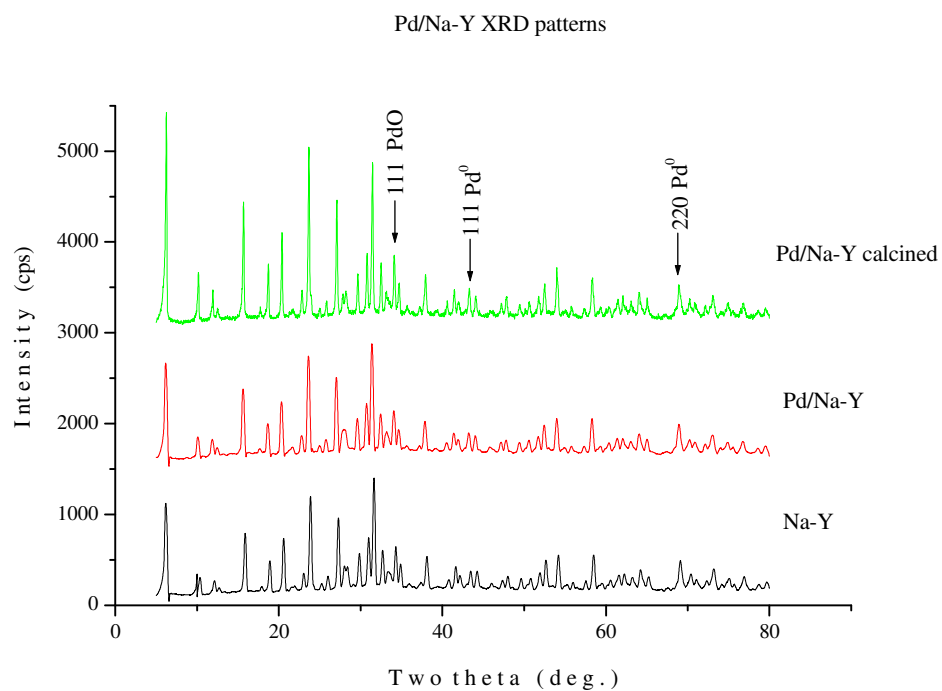


Figure 3.3.b. XRD patterns of Pd loaded Na-Y zeolite catalysts.

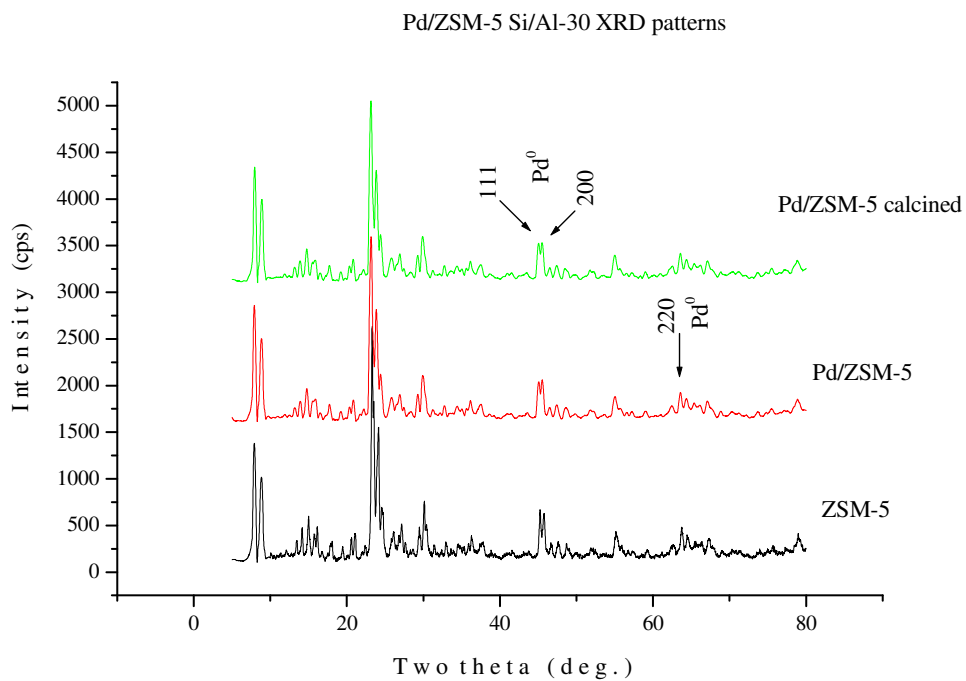


Figure 3.3.c. XRD patterns of Pd loaded ZSM-5 zeolite catalysts.

The d-values of Pd/Na-Y zeolite at 2.2394 and 1.369 Å refer to the planes (111) and (220) respectively. For Pd/ZSM-5 2.2394, 1.9451, 1.3787 Å refers to the planes (111), (200), and (220) respectively (Table 3.3). For Pd-Alumina 2.2399 and 1.3728 Å refer to the (111) and (220) planes respectively.

Considering the XRD diffractograms in Figs. 3.3.a, 3.3.b, and 3.3.c there is evidence that the crystalline ZSM-5 and Na-Y structures remains intact during the impregnation conditions. The XRD patterns of the ZSM-5 samples show well crystallized materials corresponding to the MFI structure in accordance with the reports by Treacy and Higgins²⁴⁹.

3.1.4. XRD results for mesoporous MCM-41 catalysts:

The powder XRD patterns of synthesized MCM-41 sample are illustrated in Fig. 3.4.a. It can be seen that all the samples exhibit four strong reflections, characteristic of hexagonal MCM-41. Figs. 3.4.b and 3.4.c show the XRD patterns of as-synthesized Al-MCM-41 (90) and Al-MCM-41 (60) respectively. It can be seen that all the as-synthesized Al-MCM-41 samples show reflections typical of hexagonal MCM-41 structure^{221, 228, 244}.

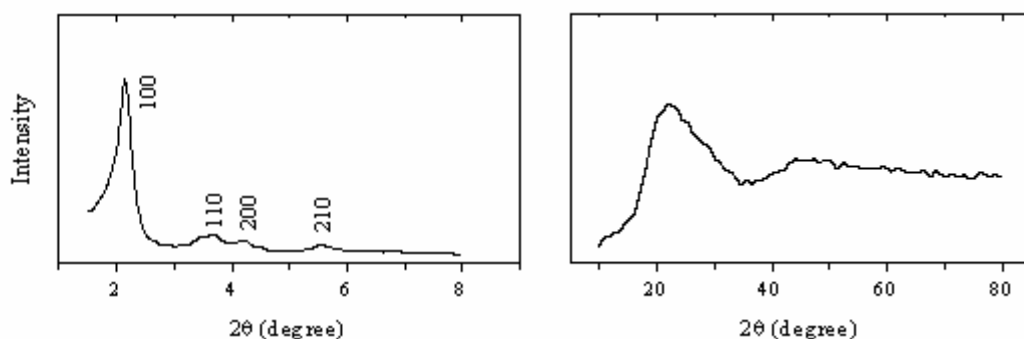


Figure 3.4.a. XRD patterns of as-synthesized MCM-41.

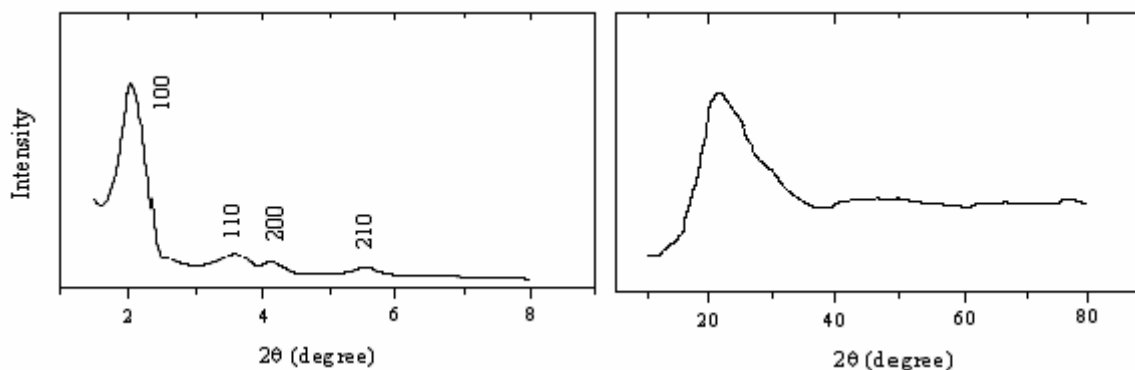


Figure 3.4.b. XRD patterns of as-synthesized Al-MCM-41(90).

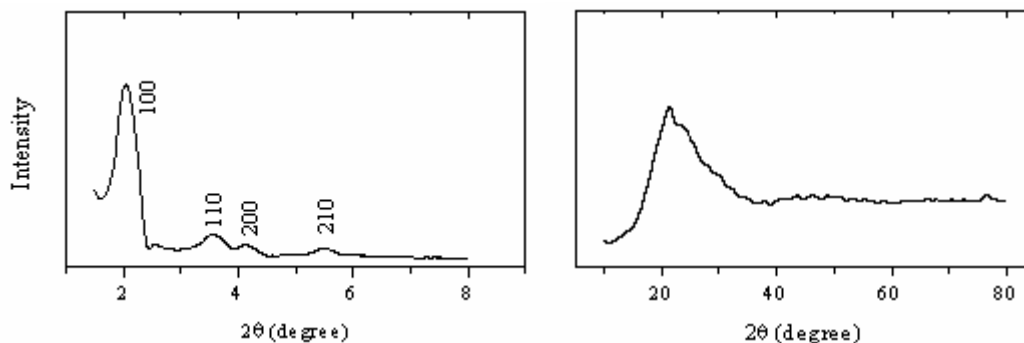


Figure 3.4.c. XRD patterns of as-synthesized Al-MCM-41(60).

Table 3.4. XRD data for Al-MCM-41 samples.

Sample ^a	d_{100} (Å)	a_o (Å) ^b
As-synthesized MCM-41	39.76	45.91
As-synthesized Al-MCM-41 (90)	43.06	49.72
As-synthesized Al-MCM-41 (60)	43.05	49.71

^a The number within parentheses signifies the nominal Si/Al molar ratio in the synthesis gel.

^b $a_o = 2d_{100}/\sqrt{3}$.

The 100 (hkl) reflection of Al-MCM-41 was found to shift towards higher d values as compared to its siliceous analog MCM-41 (Table 3.4 and Figs. 3.4.b-c). The observed shift could be attributed to the framework substitution of Al(III) in the silicate matrix. This is understandable considering that the crystal radius of Al(III) (0.53 Å) is larger than Si(IV) (0.40 Å) in tetrahedral coordination²⁵⁰. In the higher angle region (10-80°), all the as-synthesized samples (Figs. 3.4.a-c) showed a characteristic broad band between 15-35° due to amorphous silica walls²⁵¹.

3.2. Diffuse reflectance UV-Visible spectroscopy:

3.2.1. Ni Loaded zeolites DR UV-Visible spectroscopy:

Diffuse reflectance spectroscopy was employed to investigate the symmetry and the valence of the supported nickel. The DR UV spectra of nickel-loaded zeolites are plotted in the Figs 3.5.a, b, c, d and e. The DR UV baseline function corrected spectra for nickel-loaded γ -Al₂O₃ and Ni-loaded Na-Y zeolite catalysts are represented in Figs. 3.5.b and 3.5.d. The DR UV spectra without baseline corrections are illustrated in Figs. 3.5.a, 3.5.c and 3.5.e. The baseline corrected figures distinctly shows the presence of bands at 400 nm. The attributed bands are highlighted

with arrows in the normal DR UV spectra. The bands can be visualized clearly in the baseline function corrected plots. Due to some technical problems and other limitations the DR UV baseline function data for all the samples couldn't be corrected.

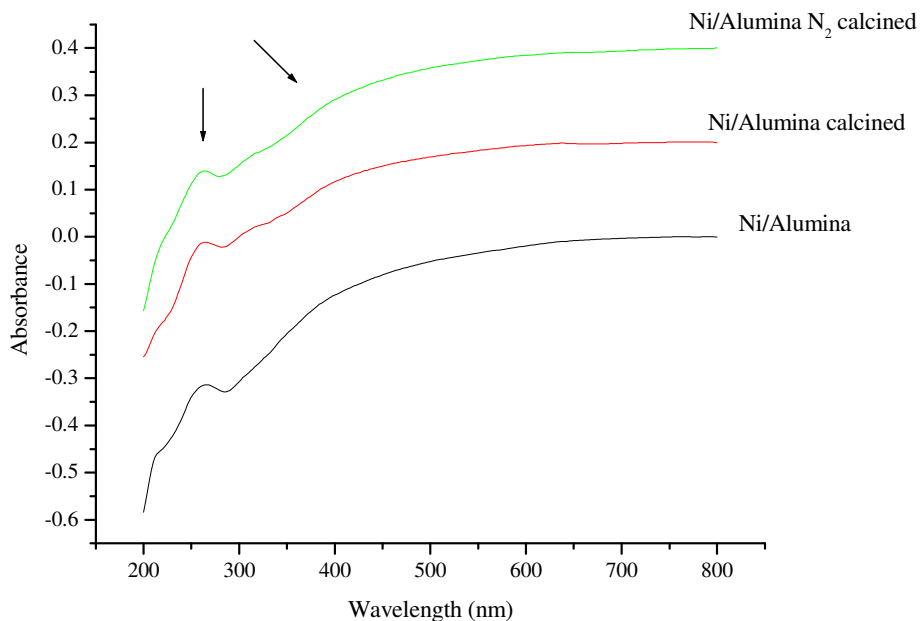


Figure 3.5.a. DR UV spectra of Ni loaded γ -Al₂O₃ catalysts.

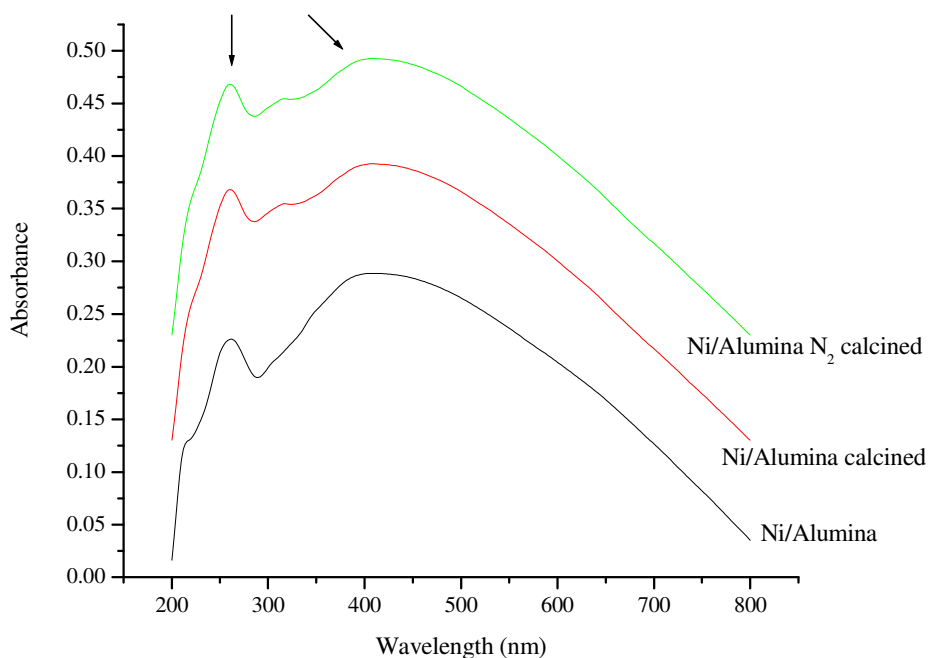


Figure 3.5.b. DR UV spectra of Ni loaded γ -Al₂O₃ catalysts (baseline function corrected).

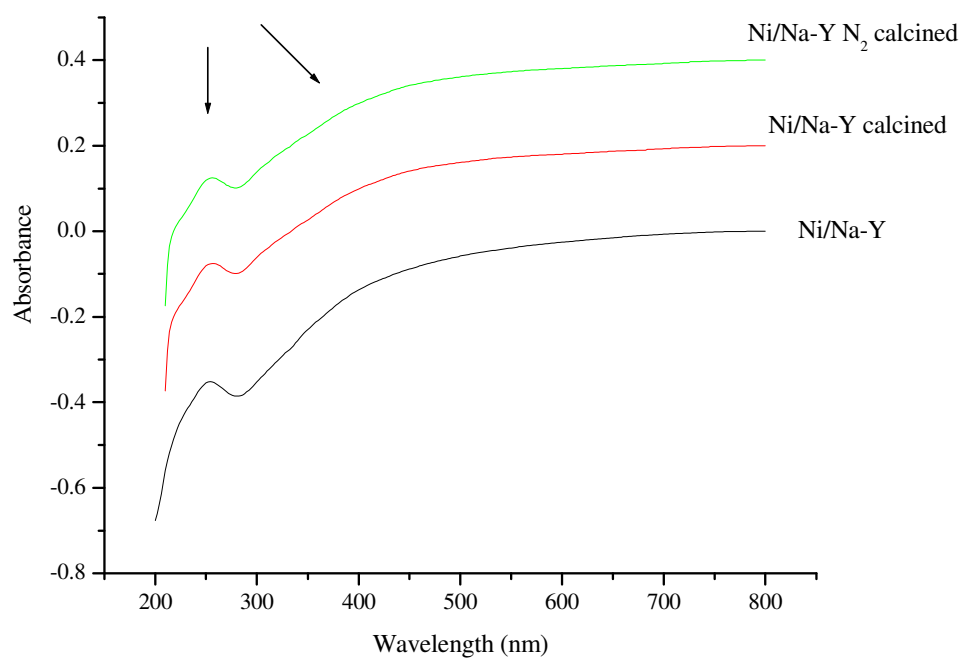


Figure 3.5.c. DR UV spectra of Ni loaded Na-Y zeolite catalysts.

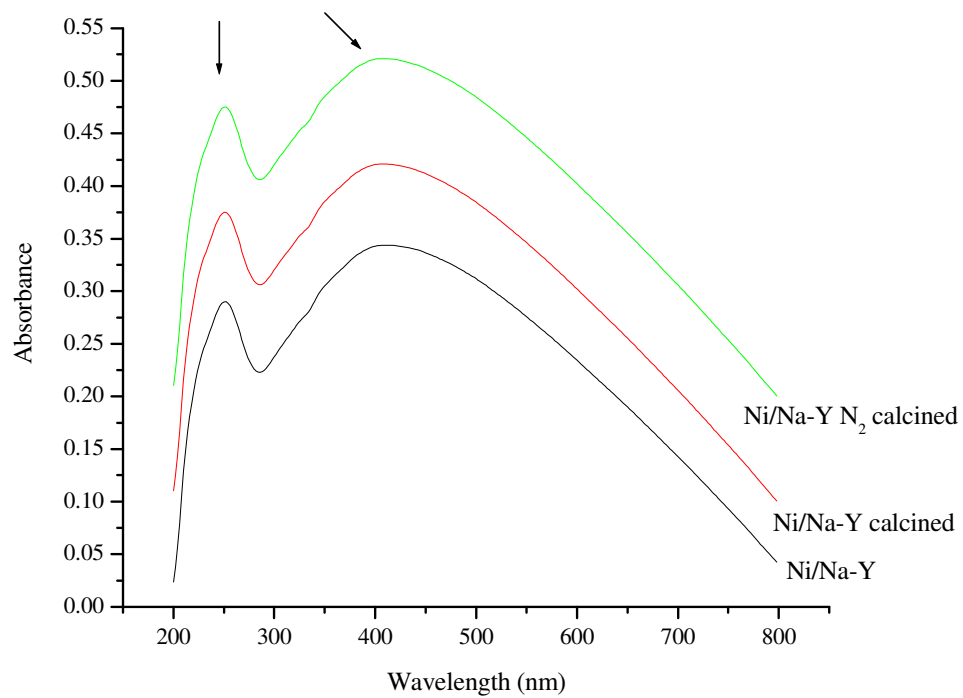


Figure 3.5.d. DR UV spectra of Ni loaded Na-Y zeolite catalysts (baseline function corrected).

The band at 270-290 nm is the characteristic of the catalysts. The DR UV spectra of Ni/Na-Y, Ni/ZSM-5 and Ni/ γ -Al₂O₃ catalysts displayed a major band at 400 nm as illustrated in Figs. 3.5.a-3.5.e. This can be attributed to Ni²⁺ cations in trigonal (D_{3h}) coordination in the sodalite cages²⁵² (S_I cages). The DR UV spectra of Ni/ZSM-5 catalyst displayed a broad band at 400 nm which may be due to Ni²⁺-O charge-transfer transitions²⁵³.

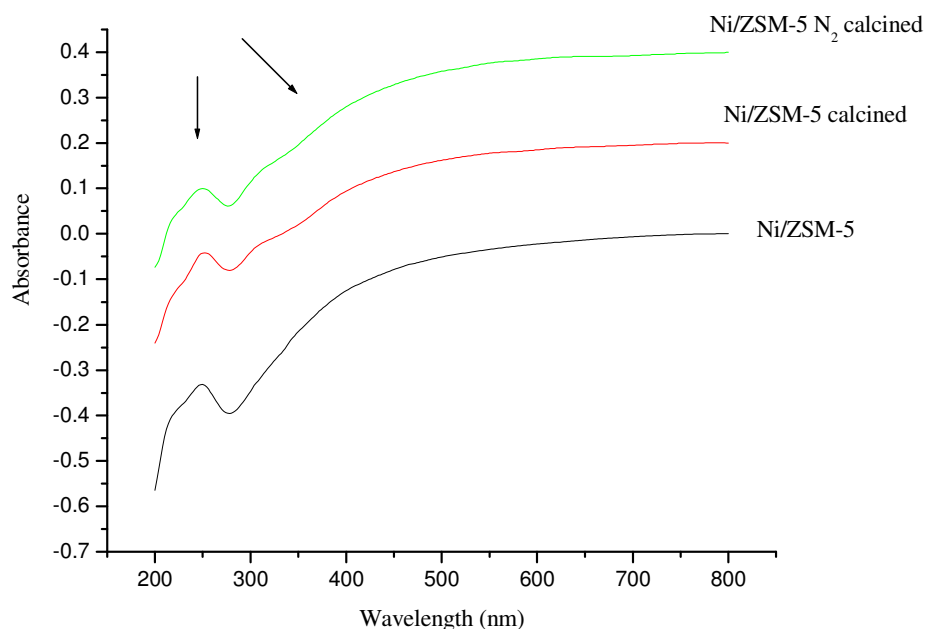


Figure 3.5.e. DR UV spectra of Ni loaded ZSM-5 zeolite catalysts.

To compare respective changes of absorptions in the DR UV, the patterns were plotted one above the other. The units on the Y-axis (ordinate) become arbitrary.

3.2.2. DR UV-Visible spectroscopy for V-containing zeolites:

The DR UV band maxima of freshly prepared 0.5% vanadium containing catalysts depend on the support composition γ -Al₂O₃, Na-Y, ZSM-5, and the impregnation salt VOSO₄. Although the spectra are quite similar, we can notice some important differences both in the d-d region and the UV region. A high intensity charge transfer band in the 300-450 nm region is observed for all samples. The bands located at 320 and 420 nm show that the deposited vanadates maintain the valence and the environment of the initial solution species (Fig. 3.6.a). The absorption band at 400-480 nm is characteristic of V⁵⁺ in octahedral environment (Fig. 3.6.c), while band at 270-300 nm is considered to be due to V⁵⁺ in a highly isolated tetrahedral environment²⁵⁴⁻²⁵⁶ (Fig.

3.6.a). For tetrahedrally co-ordinated V^{5+} the corresponding band occurs between 300 and 350 nm^{255, 256} (Fig. 3.6.b). DR UV-visible spectroscopy for all calcined samples, vanadium retains the oxidation +5 after calcination. However, the band shift towards 400 nm indicates an evolution in the vanadium environment.

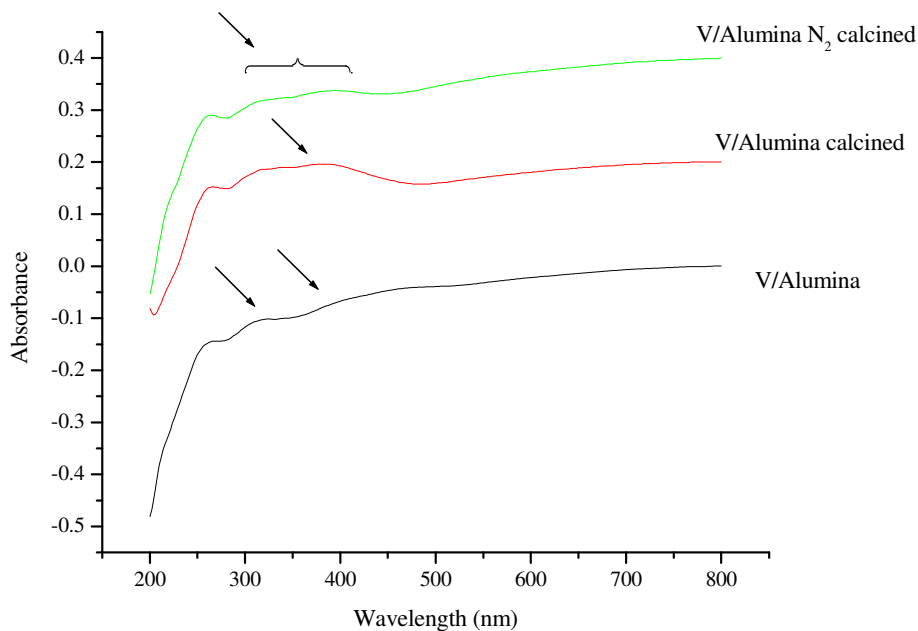


Figure 3.6.a. DR UV spectra of V loaded γ -Al₂O₃ catalysts.

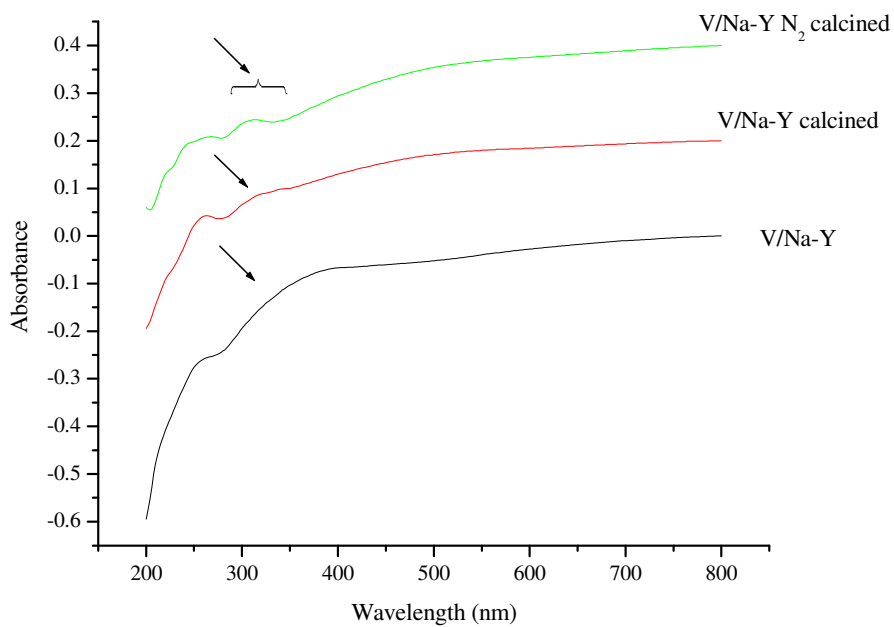


Figure 3.6.b. DR UV spectra of V loaded Na-Y zeolite catalysts.

The DR UV spectra of vanadium are characterized by charge-transfer (CT) transitions of the type $O \rightarrow V^{n+}$ and d-d transitions of V^{n+} , and their energies are dependent on the oxidation state and coordination environment. In Table 3.5, several reference compounds for V^{4+} and V^{5+} are illustrated²⁵⁷. It is clear that the band maxima of the CT transitions of V^{5+} shift to higher energy (lower nanometers) with decreasing coordination number and the band maxima of the CT transitions of V^{5+} is rather limited. Thus, the polymerization of $V^{5+}(Td)$ is only evidenced by a broadening of the absorption bands and/or a small shift of the absorption maxima to lower energy²⁵⁷.

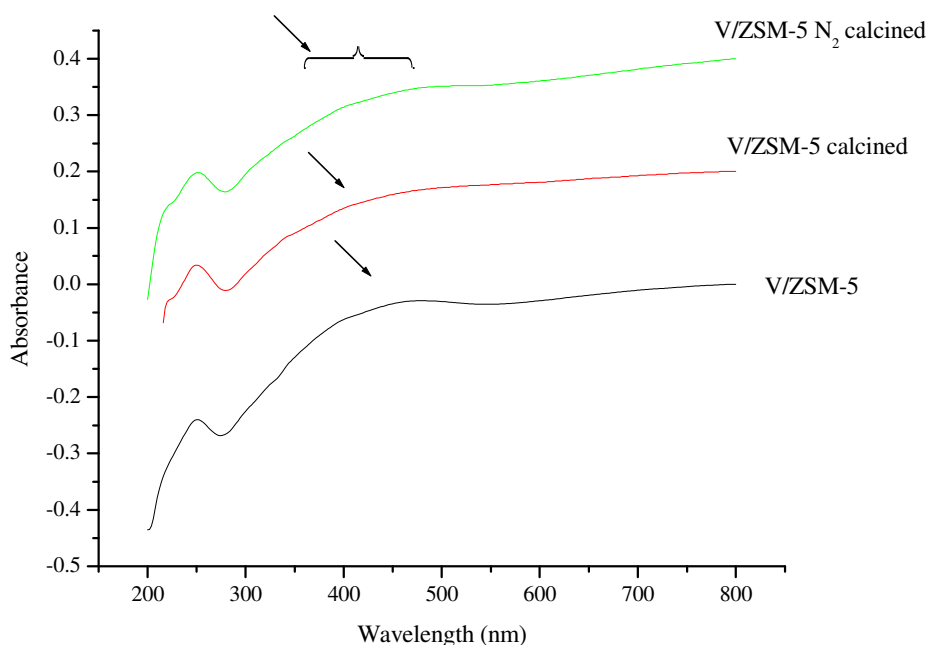


Figure 3.6.c. DR UV spectra of V loaded ZSM-5 zeolite catalysts.

The absorption in the UV region located at 275 nm for $V^{4+}/\gamma\text{-Al}_2\text{O}_3$ is an intense and broad band and is due to the CT transition²⁵⁷ of the support $\gamma\text{-Al}_2\text{O}_3$. In the case of $V^{5+}/\gamma\text{-Al}_2\text{O}_3$, a broad absorption band is visible with a shoulder located at around 370 nm. Thus, V^{5+} is present in tetrahedral coordination on $\gamma\text{-Al}_2\text{O}_3$. V^{4+} is present on $\gamma\text{-Al}_2\text{O}_3$ surfaces as a distorted octahedral species. It is reported that this species has a strong vanadyl character and possesses one coordination vacancy that is filled by a water molecule on the support, both V^{4+} and V^{5+} ions are mobile on hydrated surfaces and preferentially adsorb²⁵⁷ on $\gamma\text{-Al}_2\text{O}_3$.

Table 3.5. The DR UV spectra of vanadium oxides from reference compounds, oxidation state and coordination environment.

Compound	DR UV absorption max (nm) ^a	Oxidation state	Mol. structure
VOSO ₄ .2H ₂ O	747, 654, 266, 210	4+	Square pyramidal and isolated
V ⁴⁺ /γ-Al ₂ O ₃	805, 580, 275	4+	Octahedral and isolated
Na ₃ VO ₄	352, 282, 228	5+	Orthovanadate: Tetrahedral and isolated
V ⁵⁺ /γ-Al ₂ O ₃	370 (sh), 272 (sh)	5+	Tetrahedral

^a sh-shoulder

From Reference 257

The DR UV-Visible spectra for the V/γ-Al₂O₃, V/Na-Y and V/ZSM-5 catalysts clearly display a high intensity band below 400 nm from O-V charge-transfer¹⁷⁴. The presence of V⁴⁺ ions in tetrahedral coordination is doubtful^{174, 258} because the absorption band between 550 and 800 nm is hardly observed.

Impregnation or anchoring of vanadium species gives rise to catalysts which exhibit similar textural and reduction features. After calcinations at 823 K, the DR curve only exhibits two features associated to charge transfer bands at 270 and 340 nm, assigned to V-O transfer $\pi_2 \rightarrow e$ and $\pi_1 \rightarrow e$ respectively, in tetrahedral V(V) species²⁵⁹. The diffuse reflectance spectra of impregnated and anchored vanadium catalysts are quite similar to that of structurally vanadium doped catalysts²⁶⁰.

3.2.3. Pd containing zeolites DR UV-Visible spectroscopy:

The presence of Pd²⁺ cations in the different zeolites is confirmed by an adsorption at approximately 299 nm in the DR UV spectra, which agrees with the earlier literature data²⁶¹. The nature of Pd(II) species obtained by calcinations of Pd²⁺-ZSM-5/Na-Y under air largely depends on the Pd concentration. The 0.5 wt% Pd/ZSM-5 and Pd/Na-Y turns pink upon calcinations; it contains isolated Pd²⁺ cations coordinated to lattice sites, as indicated by an absorption at 477 nm in the DR UV spectrum²⁶¹⁻²⁶³ (Figs. 3.7.a-c).

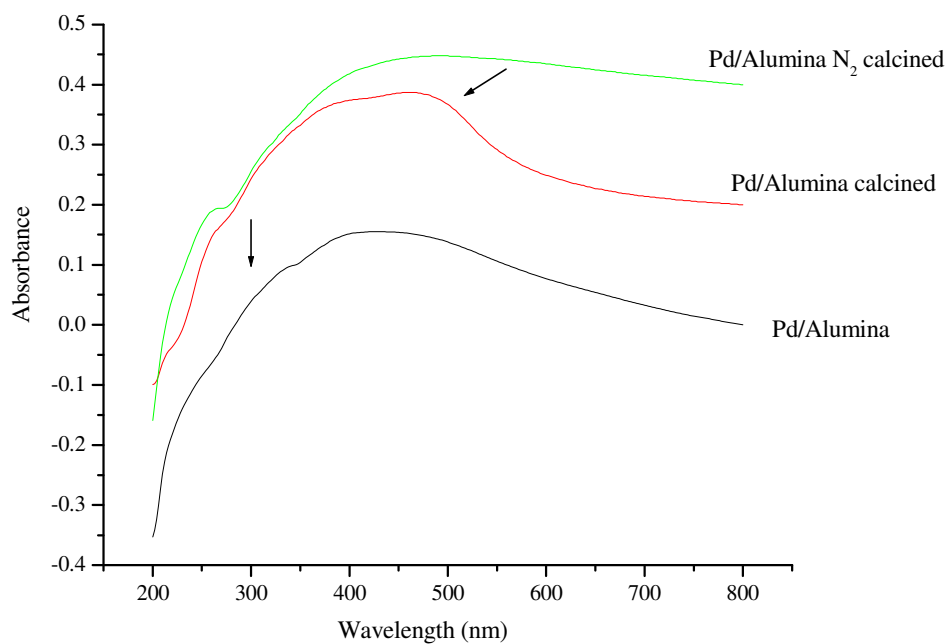


Figure 3.7.a. DR UV spectra of Pd loaded γ -Al₂O₃ catalysts.

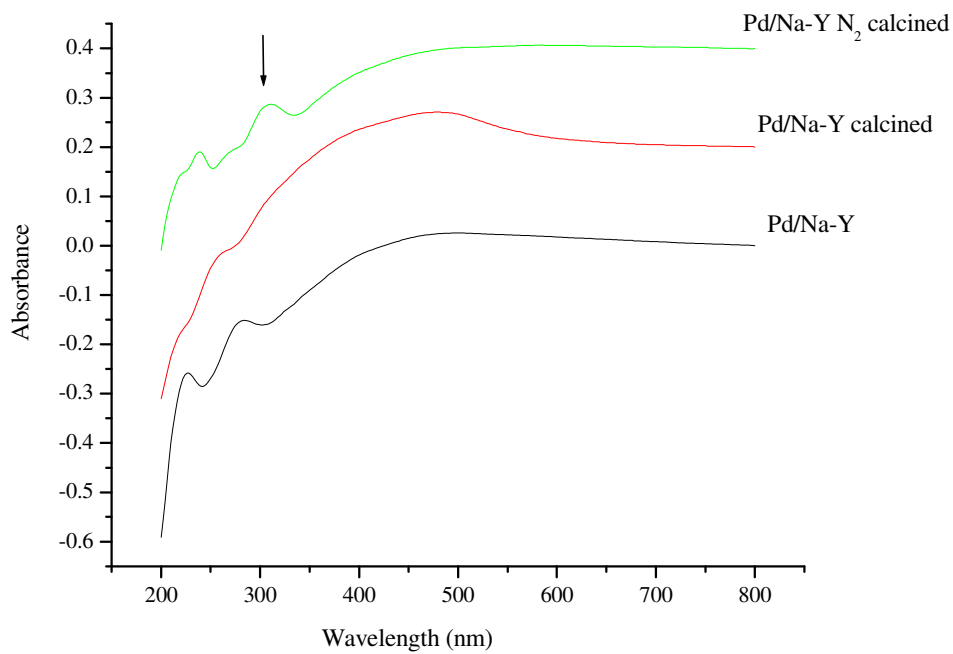


Figure 3.7.b. DR UV spectra of Pd loaded Na-Y zeolite catalysts.

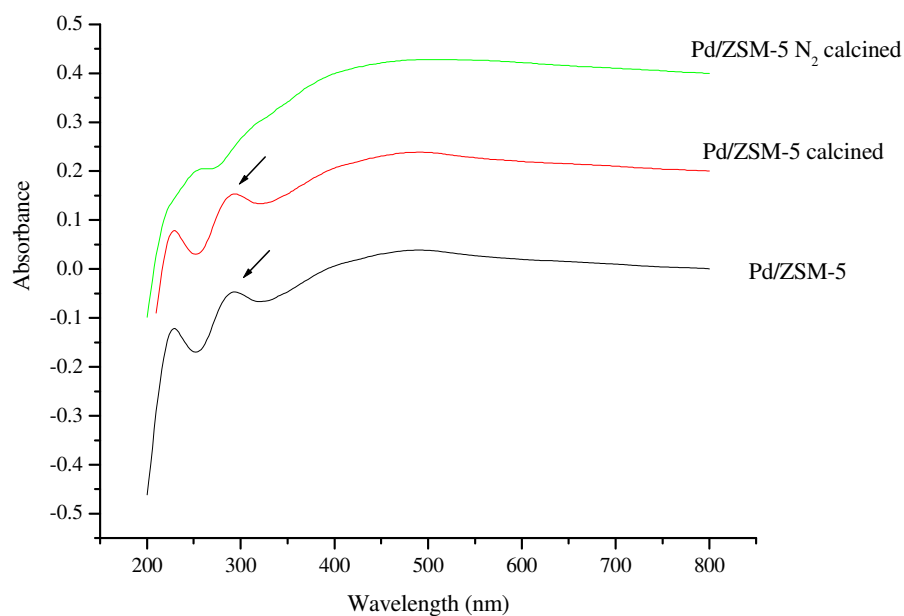


Figure 3.7.c. DR UV spectra of Pd loaded ZSM-5 zeolite catalysts.

3.3. Thermal analysis of mesoporous catalysts (TG-DTA):

Figures 3.8.a and 3.8.b show representative thermograms of as-synthesized Al-MCM-41(90) and Al-MCM-41(60), at varying Si/Al ratios.

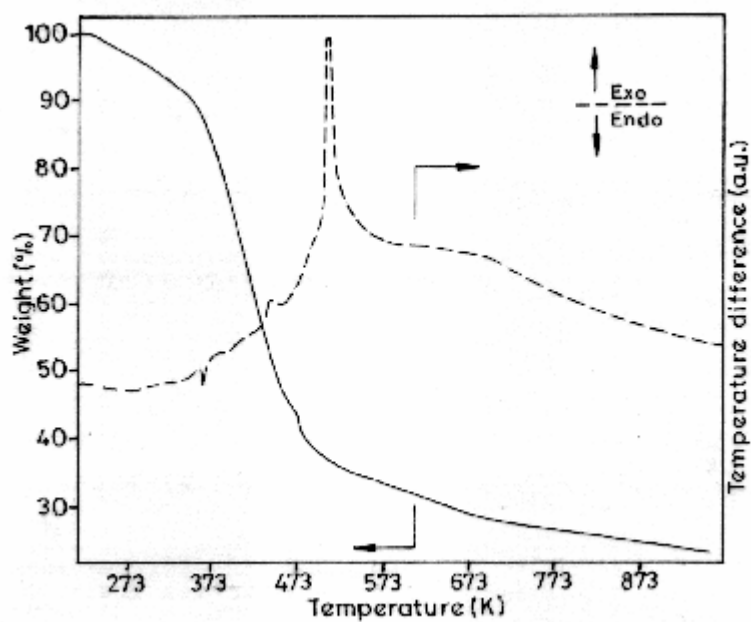


Figure 3.8.a. TG-DTA of as-synthesized Al-MCM-41(90).

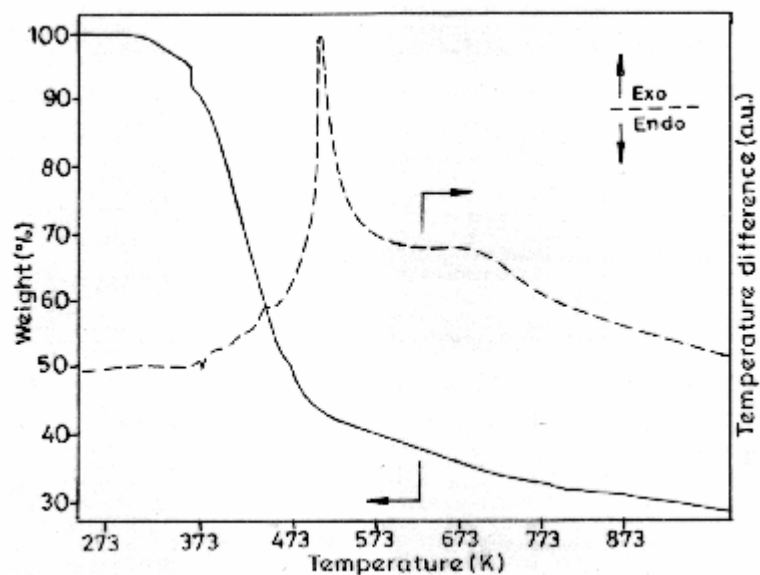


Figure 3.8.b. TG-DTA of as-synthesized Al-MCM-41(60).

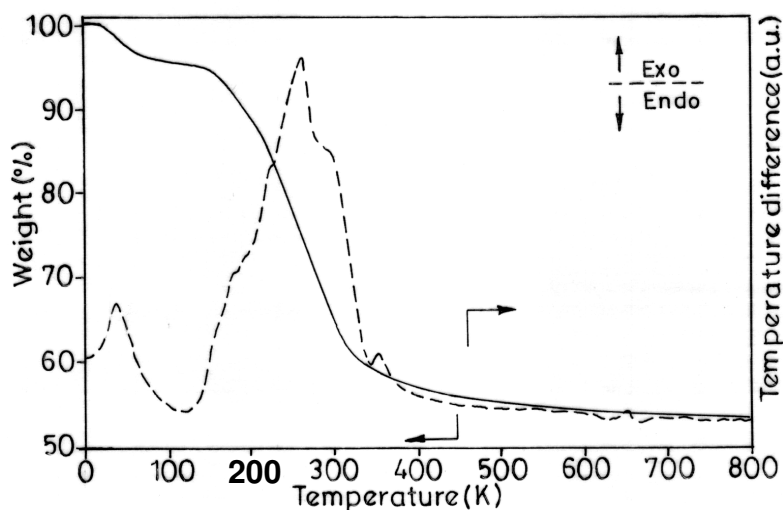


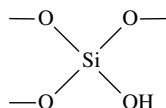
Figure 3.8.c. TG-DTA of as-synthesized MCM-41.

As-synthesized Al-MCM-41 followed a three-stage weight loss, characteristic of mesoporous materials²⁶⁴. The first stage loss is attributed to desorption of water and/or gaseous molecules (4-8 wt%, 300-393 K). The second weight loss corresponds to the oxidative degradation of the surfactant CTA⁺ cations (50-60 wt%; 393-623 K). The third stage weight loss is due to condensation of silanol groups (8-10 wt%; 623-813 K). The respective DTA transitions, viz.,

exothermic and endothermic occurs depending upon the nature of the process. It can be seen that as compared to siliceous MCM-41 (Fig. 3.8.c), which shows ~35-40% weight loss due to surfactant molecules used in preparation of catalyst, as synthesized Al-MCM-41 show a weight loss of ~50-60%. It has been reported earlier that for Al-MCM-41 samples, there is an increased interaction of template molecules with tetrahedral Al- species, apart from the silanol groups and the relative weight loss due to template associated with tetrahedral Al- species increases with increasing aluminium content²⁶⁵.

3.4. FT-IR analysis of zeolites:

Infrared spectroscopy has been responsible for much of the earlier work contributing to the understanding of the mechanisms invoked in zeolite catalysis. The nature of OH groups produced in zeolite structures shows that two major hydroxyl species can be identified in zeolite substrates produced by calcinations. The first has an absorption band at 3740 cm⁻¹ and is diagnostic of terminal hydroxyls of the form:



These are well known from other silicates and silica itself. In a zeolite framework they may arise at the surface or at defect sites in the framework. The second hydroxyl has an absorption band in the 3600-3650 cm⁻¹ region and can be assigned to OH groups associated with a Brönsted site. They are known as ‘bridging’ hydroxyls²³⁹.

The quantification of catalytic sites (Brönsted and Lewis acid sites) can be studied by specific adsorbates of different species sorbed into zeolites relating to framework sorbate and cation sorbate interactions for instance, examination of framework vibrations relating to the nature of SBUs, effect of heat, presence of cations and sorbates, study of zeolite surface hydrolysis and metal aggregate deposition.

Almost all workers reported at least two bands in the hydroxyl stretching region around 3740 and 3610 cm⁻¹. The band around 3740 cm⁻¹ is generally accepted as due to the surface silanol groups. In a zeolite, intensity of this band increases with dealumination of the sample²⁶⁶. The band at 3610 cm⁻¹ is assigned to Brönsted acid sites located inside the zeolite cage²⁶⁷ and corresponds to stronger acidity. This conclusion was supported by Nunan and co-workers²⁶⁸ from the study of deuterated surface of H-ZSM-5. The infrared spectroscopy could also distinguish Brönsted and

Lewis acid sites present on the surface of a solid. Infrared spectra of zeolites such as A, X, and Y provide evidence of –OH groups in various positions. These are associated with neighbouring SiO₄ tetrahedra^{269, 270}.

3.4.1. IR spectra for Na-Y zeolite:

The FT-IR spectrum for Na-Y zeolite sample is shown in Fig. 3.9.a. The peak at 459 cm⁻¹ is assigned to the structure-insensitive internal TO₄ (T=Si or Al) tetrahedral bending peak of zeolite-Y (Na-Y). The peak at 570 cm⁻¹ is attributed to the double ring external linkage peak assigned to zeolite Y in literature¹⁸².

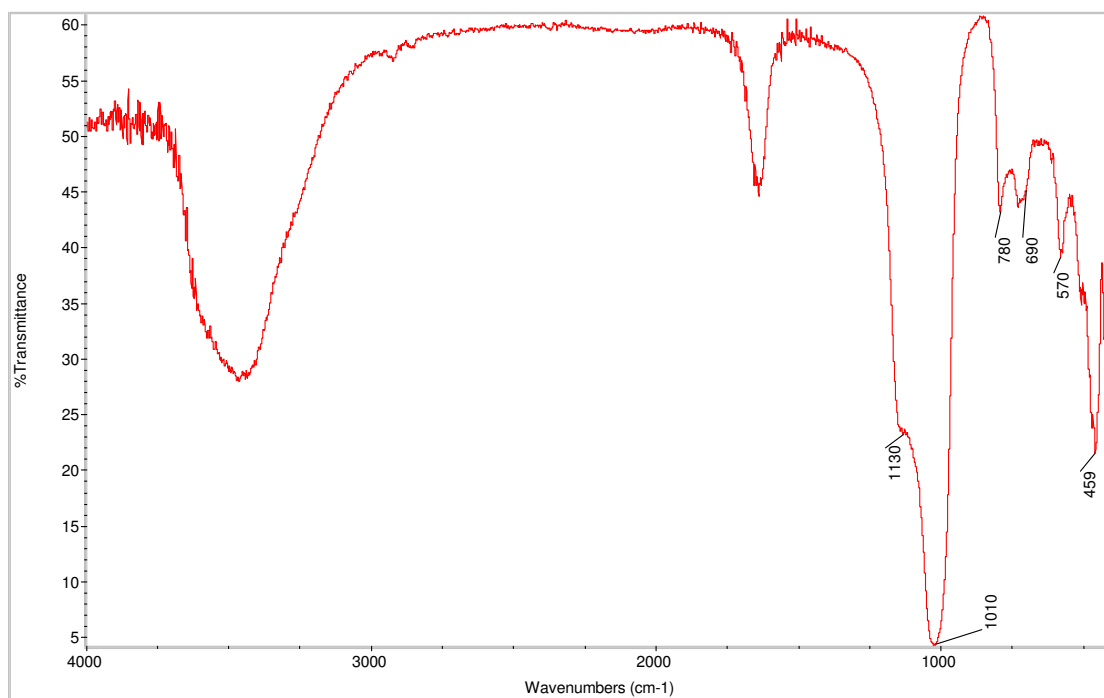


Figure 3.9.a. FT-IR spectrum of Na-Y catalyst.

The peaks at ~685 and ~775 cm⁻¹ are assigned to external linkage symmetrical and internal tetrahedral symmetrical stretchings respectively. The peak at 1010 and shoulder at 1130 cm⁻¹ are assigned to internal tetrahedral asymmetrical and external linkage asymmetrical stretchings respectively. Overall, the FT-IR spectra match well with the characteristic zeolite-Y absorption peaks laid out in past literature¹⁸². A broad band assigned to hydrogen bonded silanols in the range of 3700-3300 cm⁻¹ is observed as shown in Fig. 3.9.a. These findings could be confirmed by thermal analysis TGA-DSC.

3.4.2. IR Spectra for ZSM-5 Si/Al-30:

IR spectrum for ZSM-5 Si/Al-30 is shown in Fig. 3.9.b. In the structure insensitive internal SiO_4 or AlO_4 tetrahedral bending peak of ZSM-5 can be attributed to the peak at 457 cm^{-1} . The peak at 570 cm^{-1} is assigned to the double ring external linkage peak. The peak at $\sim 775\text{ cm}^{-1}$ is assigned to internal tetrahedral symmetrical stretching. The peak at 1120 cm^{-1} is assigned to internal tetrahedral asymmetrical and shoulder at 1226 cm^{-1} to the external linkage asymmetrical stretchings respectively.

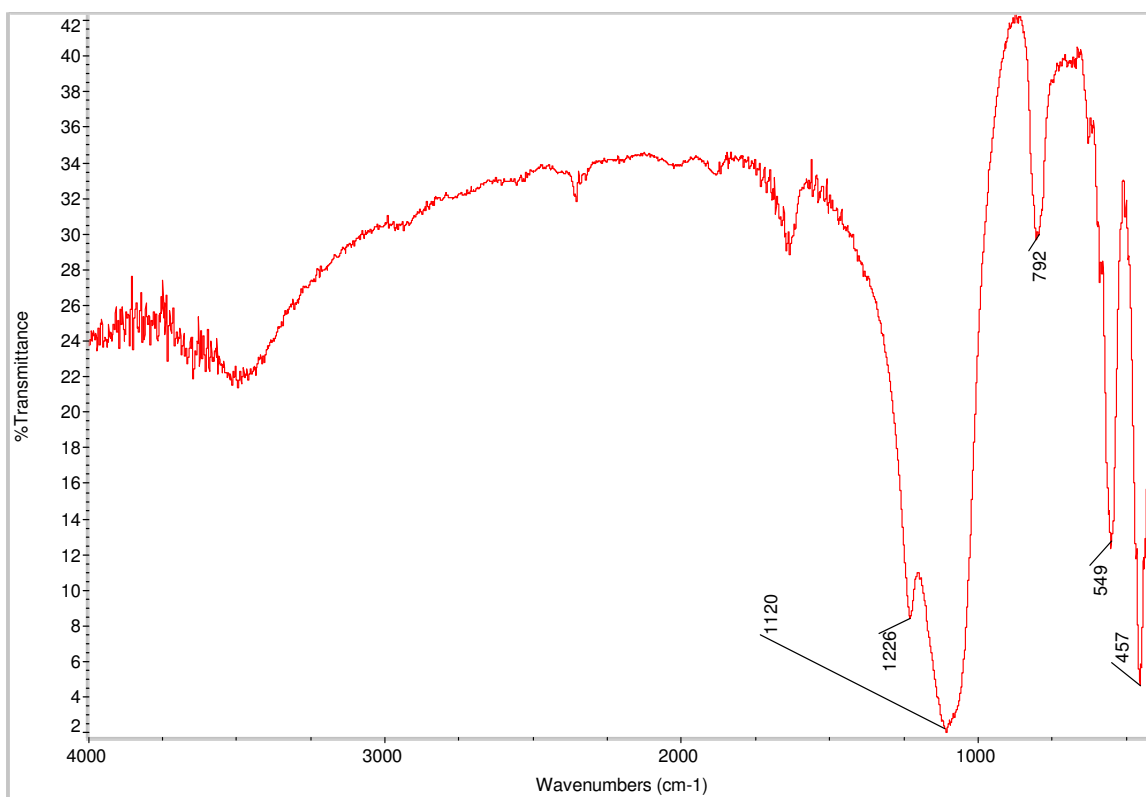


Figure 3.9.b. FT-IR spectrum of ZSM-5 catalyst.

The weak bands around $3400\text{--}3750\text{ cm}^{-1}$ can be assigned to terminal hydroxyl groups, hydroxyl groups on extra lattice alumina, SiOHAl groups (Brønsted acid sites), and to internal hydrogen-bonded silanol groups²⁷¹. The exchange of protons of the SiOHAl groups with metal cations was also reported in the literature²⁷² at around 3610 cm^{-1} .

According to the literature^{273, 274} ZSM-5 samples show a strong and sharp band at 3741 cm^{-1} due to the O-H stretching of the terminal silanol groups located at the external zeolites surface. The weaker band at 3605 cm^{-1} is instead due to the O-H stretching of bridging $\text{Si}(\text{OH})\text{Al}$ groups

located at the internal zeolites surface. These bands are not seen because they are obscured due to the moisture present in the sample.

3.4.3. IR Spectra for zeolite- β :

The peak at 459 cm^{-1} is assigned to the structure insensitive internal SiO_4 or AlO_4 tetrahedral bending. The peak at 570 cm^{-1} is attributed to the double ring external linkage. The peak at 775 cm^{-1} is assigned to internal tetrahedral symmetrical stretching. The peak at 1080 cm^{-1} is assigned to internal tetrahedral asymmetrical stretching. The shoulder at around 1180 cm^{-1} is due to symmetric stretching of Si-O-Al, sensitive to Si/Al ratio are shifted to higher wave numbers for exchanged samples due to an increase in Si/Al ratio. Similar band shifts are reported for others synthetic zeolites with an increase in Si/Al ratio²⁷⁵. IR spectra for different Si/Al ratios can be observed in Figs. 3.9.c and 3.9.d.

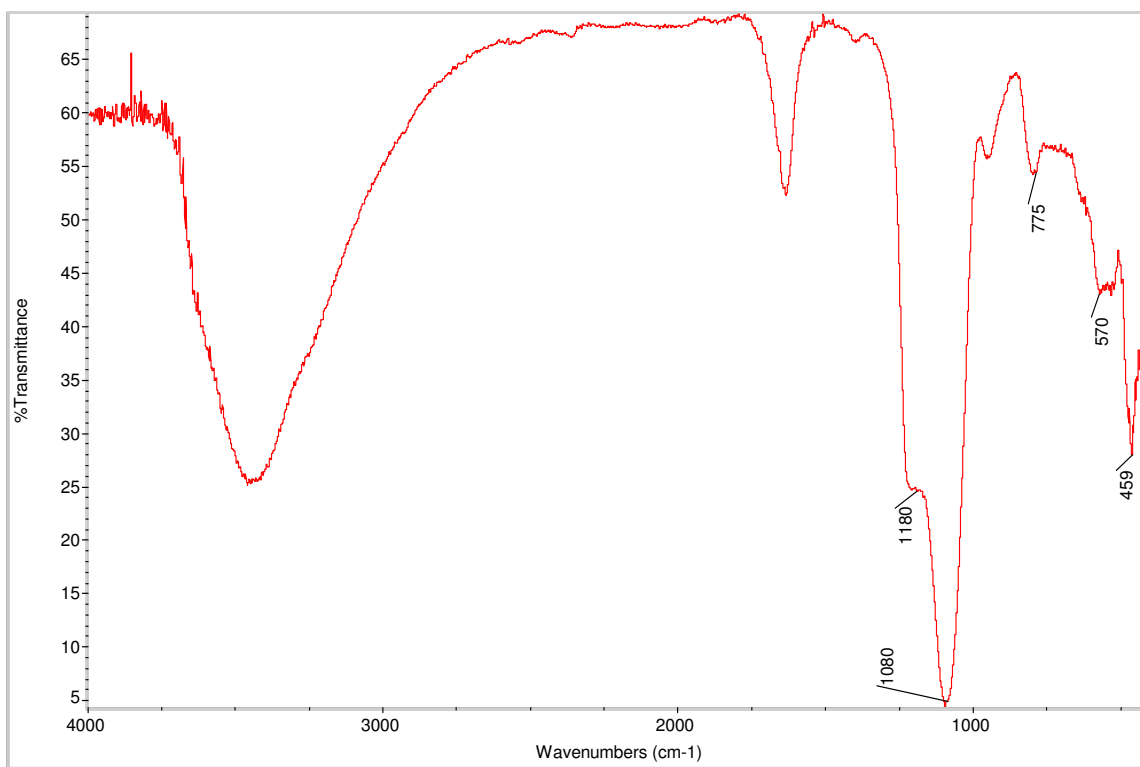


Figure 3.9.c. FT-IR spectrum of HBeta Si/Al-40 catalyst.

A broad band assigned to hydrogen bonded silanols in the range of $3700\text{--}3300\text{ cm}^{-1}$ is observed as shown in Fig. 3.9.d. According to the literature²⁷⁶ the IR spectrum of the hydroxyl region of the activated HBeta zeolite shows five bands, two weaker bands at 3741 cm^{-1} and 3610 cm^{-1} corresponding to terminal SiOH (3741 cm^{-1}) and bridging SiAlOH groups (3610 cm^{-1}). Two

smaller ones at 3782 and 3671 cm^{-1} were attributed to AlOH species near one or two SiOH groups-“transient states of aluminium”- and to extra-framework Al respectively²⁷⁶. These findings could be confirmed by thermal analysis TGA-DSC. All these bands are masked due to the moisture present in the sample. Due to the small particle size of zeolite HBeta, the intensity of the band assigned to the terminal silanol groups is very high, as small particles require more OH groups to close the coordination sphere of Si on the exterior surface²⁷⁷.

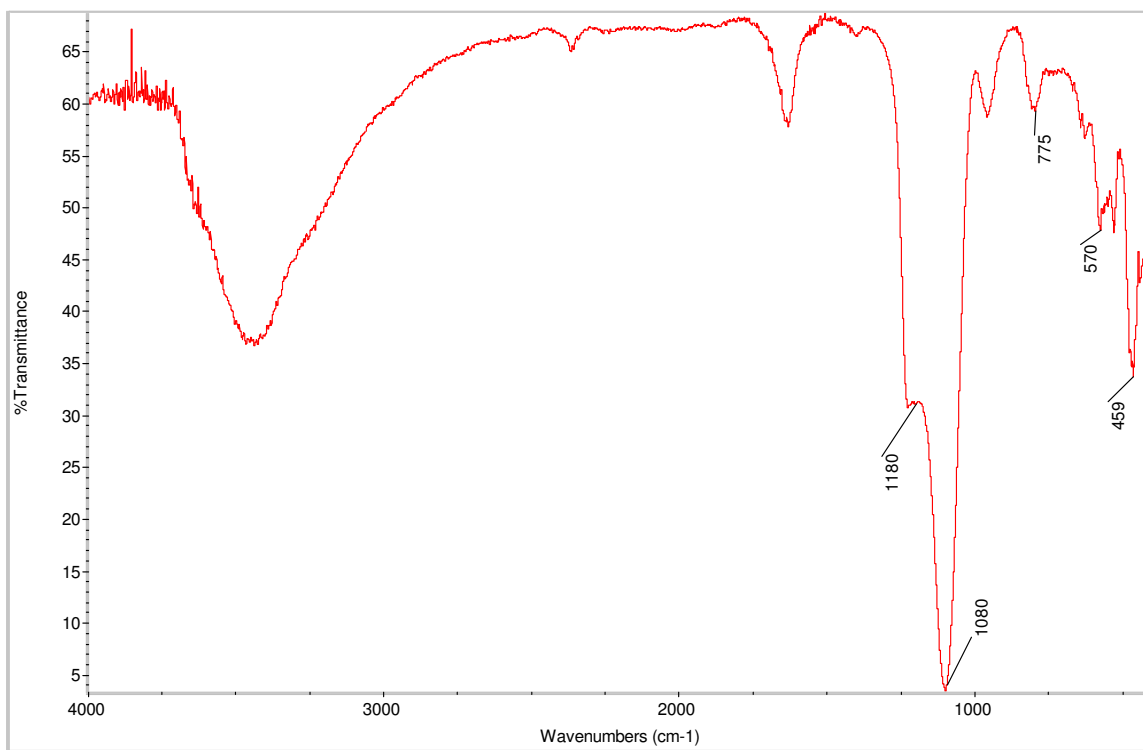


Figure 3.9.d. FT-IR spectrum of HBeta Si/Al-150 catalyst.

3.4.4. IR analysis for Ni Loaded zeolites:

The framework absorption region in the 400-1400 cm^{-1} range includes absorption bands assigned to the vibrations of $\text{Al}(\text{Si})\text{O}_4$ tetrahedra at about 549, 790 and 1068 cm^{-1} , and to internal vibrations at about 461, 1120 and 1222 cm^{-1} as shown in the Fig. 3.10. The bands observed at 549 and 1220 cm^{-1} arise from 5-ring chain and 5-ring block vibrations²⁷⁸, respectively (structure sensitive peaks). For all catalysts, comparison of the positions and intensities of the absorption bands revealed a small decrease in the intensity of the bands corresponding to the vibrations between the tetrahedral.

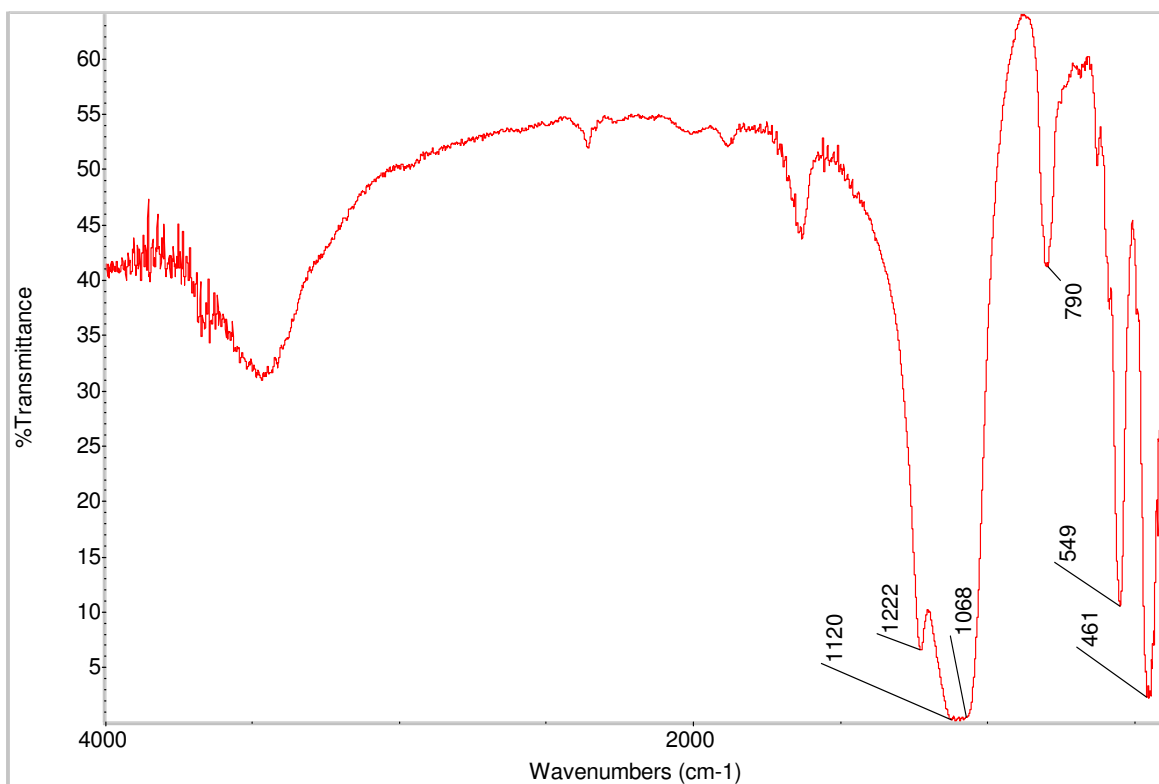


Figure 3.10. FT-IR spectrum of Ni/ZSM-5 catalyst.

The effect of Ni-loading was estimated from the absorption ratio of the 549 and 461 cm^{-1} band. Since for all catalysts, this ratio did not change, it was concluded, in keeping with the XRD data, that the crystallinity was preserved.

3.4.5. IR analysis for V loaded zeolites:

The Fig. 3.11 shows the FT-IR spectrum of V-loaded zeolite Na-Y sample. The spectra of the vanadium loaded aluminosilicates are similar to those of aluminosilicates. The FT-IR spectrum of the vanadium loaded catalysts shows a band at 3665 cm^{-1} , which probably corresponds to OH stretching vibration of VOH groups. The lower energy of this band indicates that these acid groups are stronger than Si-OH groups²⁶⁰.

V-loaded zeolites are active for oxidation reactions while still presenting shape selectivity of the parent zeolite. The FT-IR spectra of zeolites exhibit the bands due to the hydroxyl vibrator of AlO-H and SiO-H groups. A broad peak at 3530 cm^{-1} attributed to H-bonded SiO-H groups.

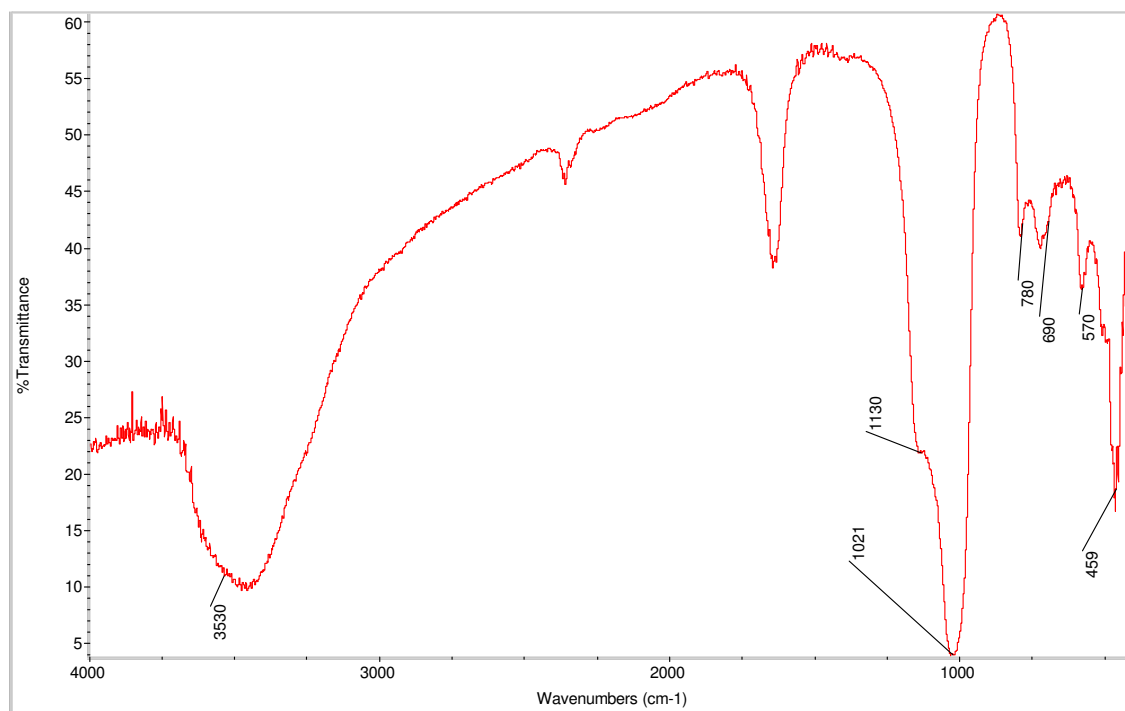


Figure 3.11. FT-IR spectrum of V/Na-Y catalyst.

The intensity of the broad band near 3530 cm^{-1} , associated with hydrogen bonded silanol groups is significantly reduced upon V introduction, showing that silanol groups are consumed. These findings could be confirmed by thermal analysis TGA-DSC. The presence of V is clearly visible with appearance of maxima located at $980\text{--}1050\text{ cm}^{-1}$. Thus, the appearance of band around $980\text{--}1050\text{ cm}^{-1}$ in the vanadium loaded aluminosilicates should be evidence for the incorporation of vanadium into the zeolite framework. Several authors have taken FT-IR peaks appearing around 960 cm^{-1} in silica-based matrices containing transition metal species, as an evidence for the isomorphous substitution of Si atoms by metal atoms²⁷⁹⁻²⁸¹. The intensity of the 960 cm^{-1} band increases along with the vanadium content in the products. A similar peak at 960 cm^{-1} is present in the titanium and vanadium silicate zeolites synthesised by various workers²⁸²⁻²⁸⁶.

3.4.6. IR analysis for Pd loaded zeolites:

The infrared spectra of the Pd loaded samples are shown in Figs. 3.12.a and 3.12.b. Very weak bands at 3745 cm^{-1} and 3610 cm^{-1} are attributed to isolated and terminal silanol groups²⁸⁷ and acidic bridging hydroxyl groups²⁸⁸ respectively. These findings could be confirmed by thermal analysis TGA-DSC. These bands become very weak, indicating that most of the Brønsted acid sites have been replaced by Pd^{2+} ions. Apparently PdCl_2 vapour reacts not only with the strong acid sites, but also with silanol groups.

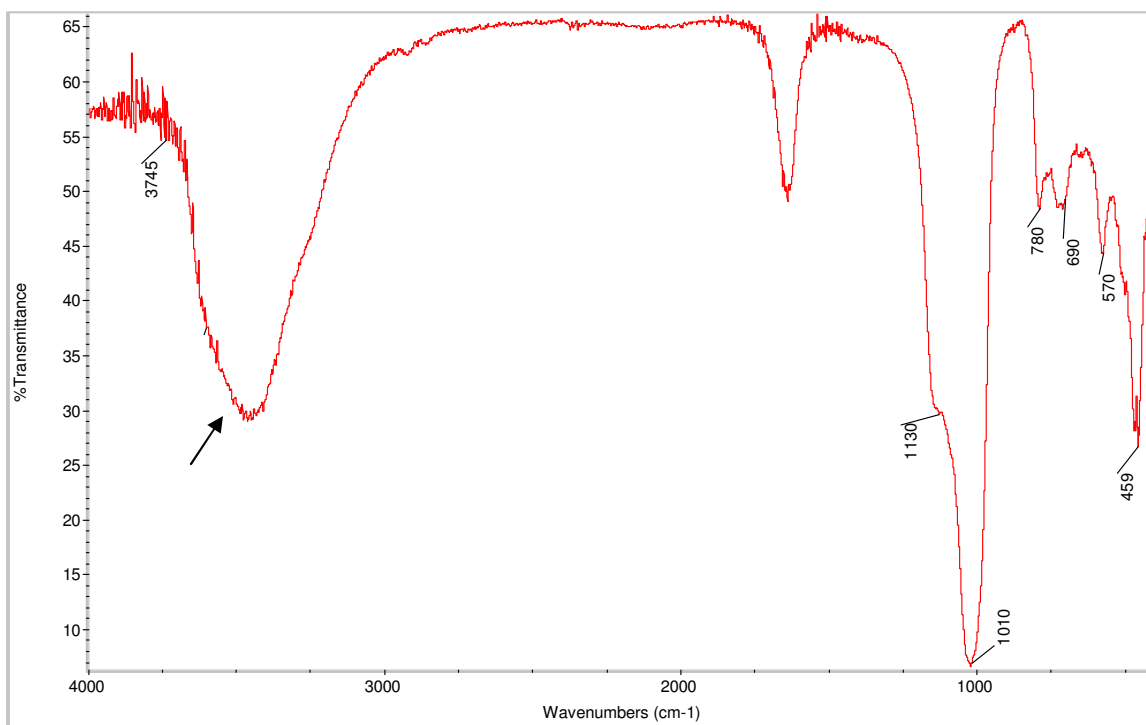


Figure 3.12.a. FT-IR spectrum of Pd/Na-Y N₂ calcined catalyst.

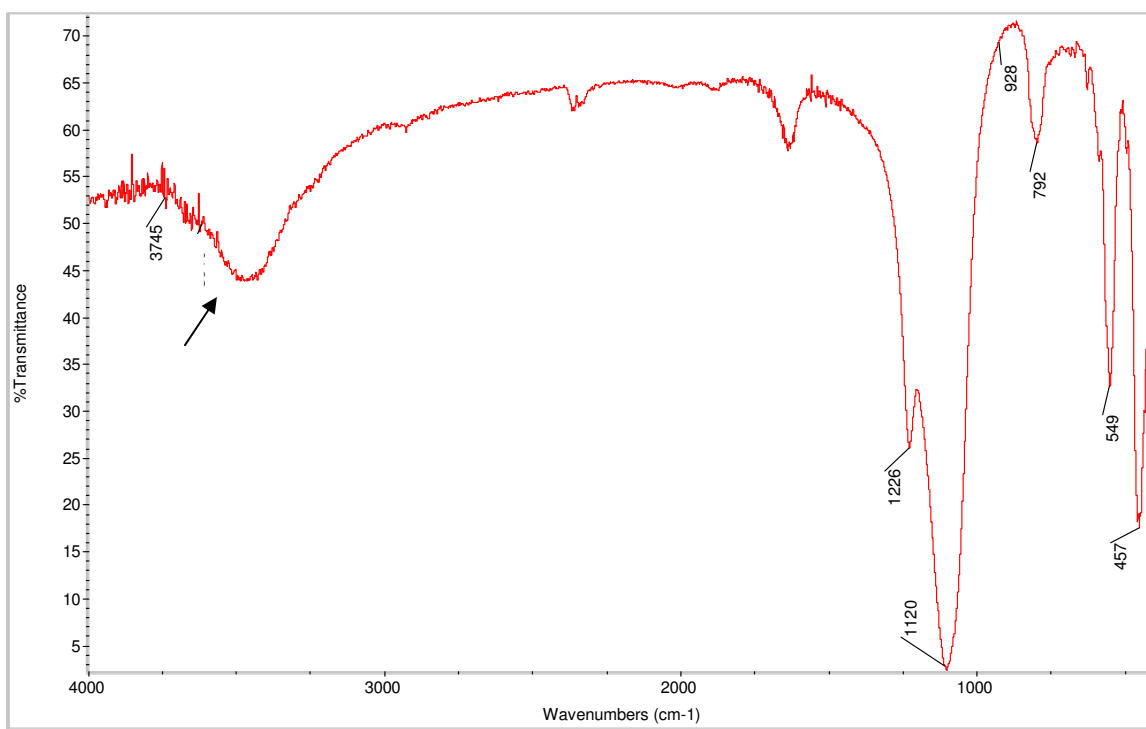


Figure 3.12.b. FT-IR spectrum of Pd/ZSM-5 N₂ calcined catalyst.

Literature^{289, 290} shows that the shoulder at 928 cm⁻¹ assigned to Pd interaction with its neighbouring oxygen induces a severe perturbation of zeolite vibrations. According to several authors the virtual absence of the IR band at 3610 cm⁻¹ proves that the positive charge necessary to compensate the zeolite lattice charge is localized on some Pd entities. They replace the original Brønsted acid sites (and even part of the protons in silanol groups) and will be located at or very near the cation exchange sites of the zeolite^{289, 290}.

3.4.7. IR analysis for U loaded catalysts:

Uranium (uranyl ions UO₂²⁺ or uranium oxides) with its variable valence states vis-à-vis vacant f-orbitals²⁰⁸ may serve as promising oxidizing catalyst. Literature shows that the uranium oxides are dispersed over dense oxide supports such as Al₂O₃, TiO₂, SiO₂, MgO and mesoporous molecular sieves. Compared to any other inorganic cations, the uranyl ions possess distinctive photo absorption, excitation, and emission characteristics. The lowest excited Eigen value (E^o + 2.6 V) of the UO₂²⁺ is a strongly oxidizing species, found to be quenched by a variety of organic substrates resulting in the abstraction of their hydrogen atoms²¹².

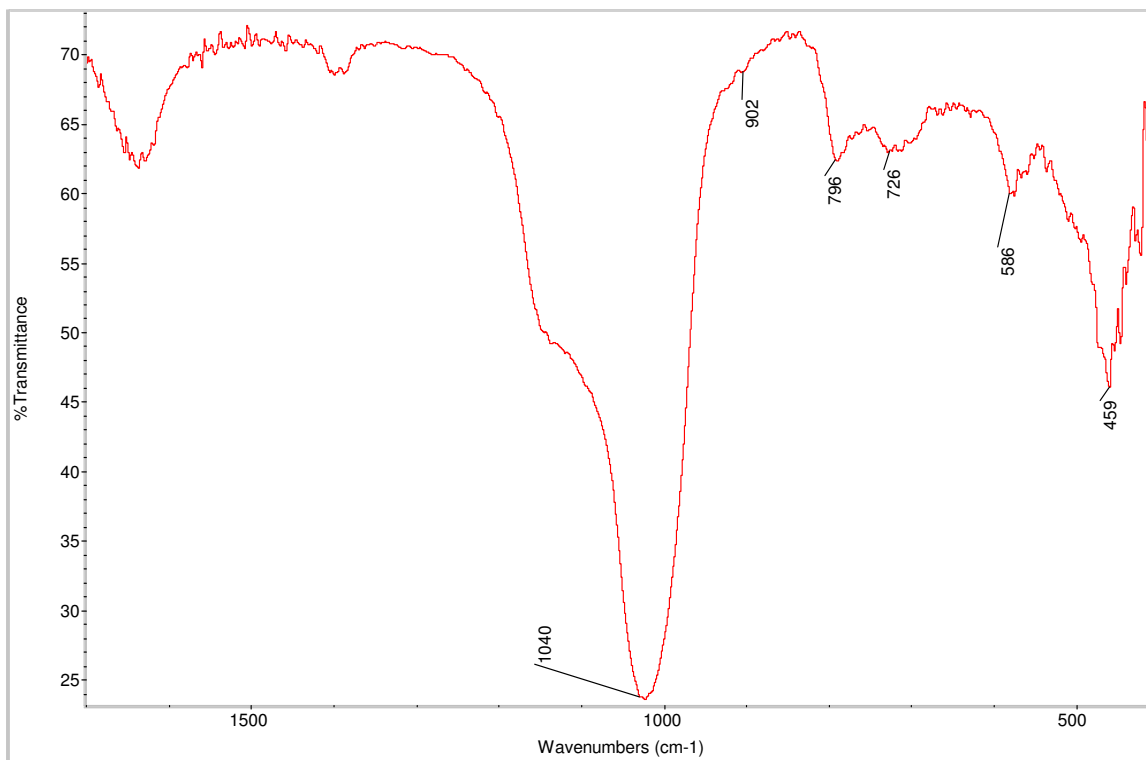


Figure 3.13.a. FT-IR spectrum of U/Na-Y catalyst.

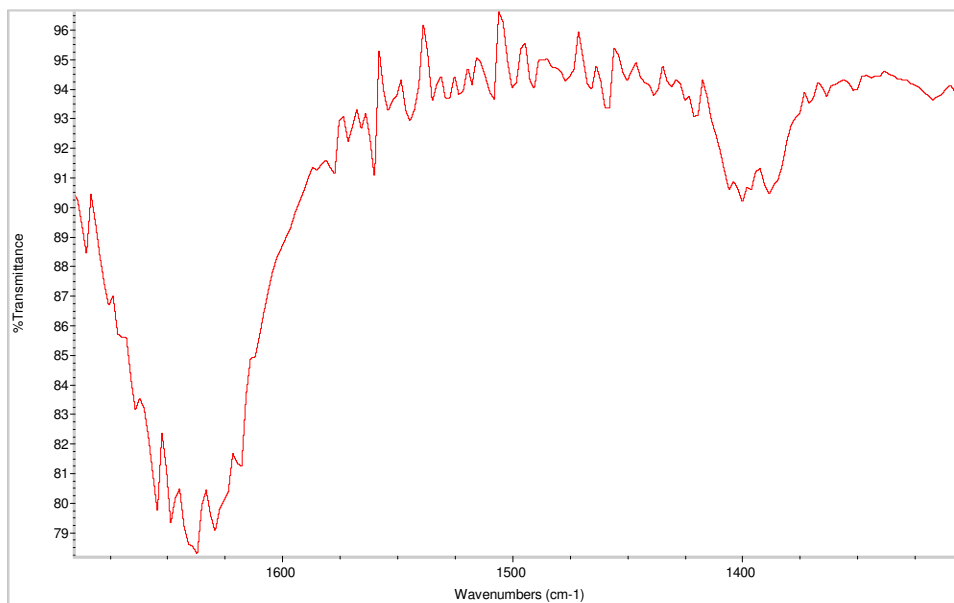


Figure 3.13.b. FT-IR spectrum of U/Na-Y catalyst from 1300-1700 cm^{-1} .

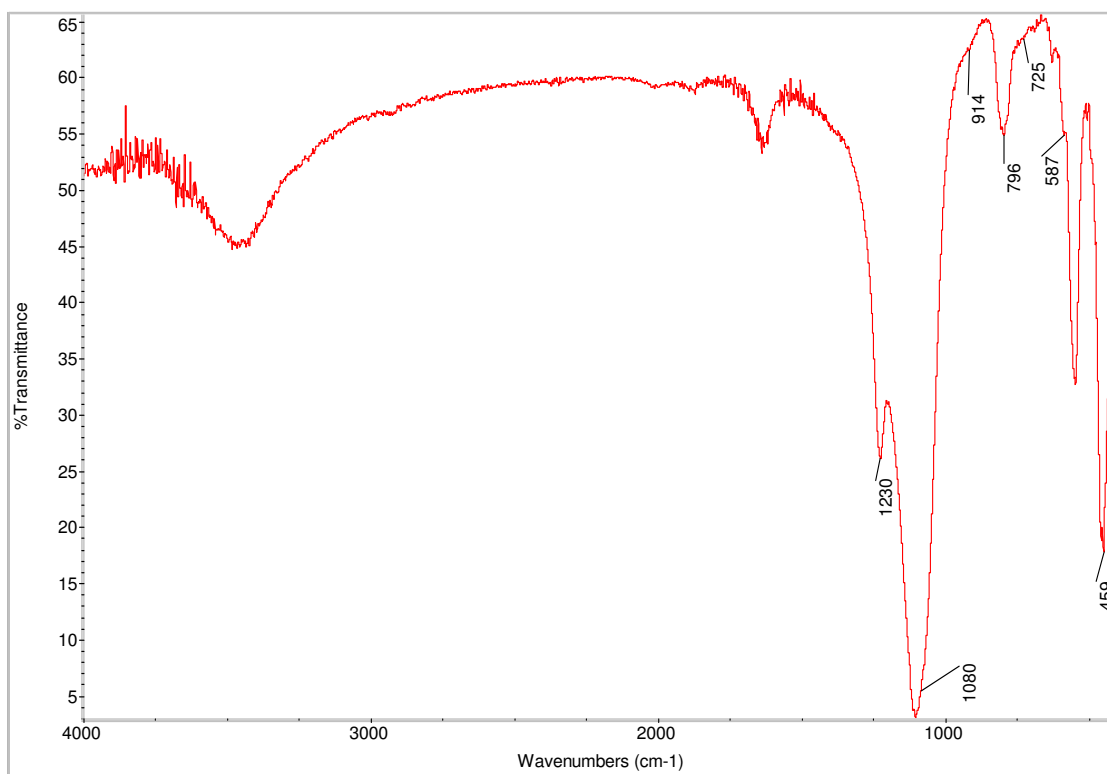


Figure 3.13.c. FT-IR spectrum of U/ZSM-5 catalyst.

Numerous studies have showed that the utilization of uranyl ions for homogeneous-phase photooxidation reactions of hydrocarbons²¹⁴, chlorophenols, and substituted phenols. Suib and co-workers²¹⁸ studied the photooxidation of ethanol, isopropyl alcohol, and diethyl ether by employing uranyl-exchanged clays and zeolites, to yield the corresponding aldehydes and

ketones. Dai *et al*²¹⁹ reported that the photocatalytic oxidation of ethanol solution by UO_2^{2+} doped glass resulted in the formation of acetaldehyde.

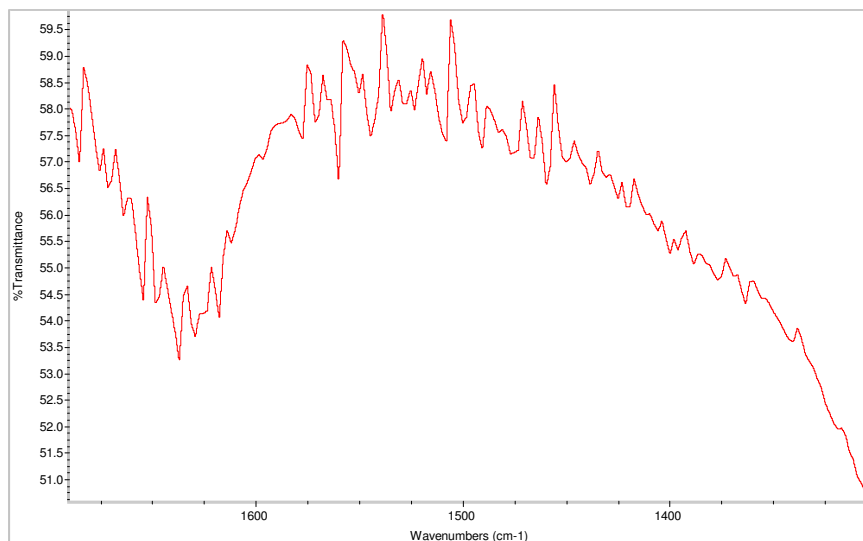


Figure 3.13.d. FT-IR spectrum of U/ZSM-5 catalyst from 1300-1700 cm^{-1} .

The IR bands at ~ 1230 (Fig. 3.13.c), ~ 1080 are attributed to the $\equiv\text{Si-O-Si}\equiv$ asymmetric stretching $\nu_a(\text{Si-O-Si})$, the bands at ~ 794 , 725 (shoulder), and 590 cm^{-1} arise due to $\equiv\text{Si-O-Si}\equiv$ symmetric stretching $\nu_s(\text{Si-O-Si})$ and the bands at ~ 590 , and $\sim 459 \text{ cm}^{-1}$ are assigned to Si-O-Si bending ($\delta_{\text{Si-O-Si}}$) frequencies of $\equiv\text{Si-O-Si}\equiv$ linkages of the aluminosilicates framework. The bands in the range $1700\text{-}1300 \text{ cm}^{-1}$ are due to O-H (Figs. 3.13.b and 3.13.d). The vibrational shoulder at $\sim 902\text{-}914 \text{ cm}^{-1}$ in the UO_2^{2+} loaded samples which may be assigned to asymmetric U=O stretching $\nu_a(\text{U=O})$ of uranyl (UO_2^{2+}) species (Figs. 3.13.a and 3.13.c).

According to the reports of Rabinowitch and Belford²¹¹, the UO_2^{2+} groups are linear and in uranyl acetate they exhibit a strong absorption band at $\sim 930 \text{ cm}^{-1}$ due to asymmetric U=O stretch; the corresponding symmetric vibration expected at 856 cm^{-1} is observed only in very thick samples, well agrees with that of the U=O stretching frequency in a uranyl compound changes with the ligand and a relationship exists between this frequency and the U=O bond distance²⁹¹.

3.4.8. FT-IR analysis for as-synthesized Al-MCM-41 catalysts:

The FT-IR spectra of as-synthesized Al-MCM-41, at varying Si/Al molar ratios, bands ($\nu_{\text{C-H}}$) at ~ 2921 and $\sim 2852 \text{ cm}^{-1}$ are characteristic of the template molecules, which are illustrated in Figs. 3.14.a and 3.14.b.

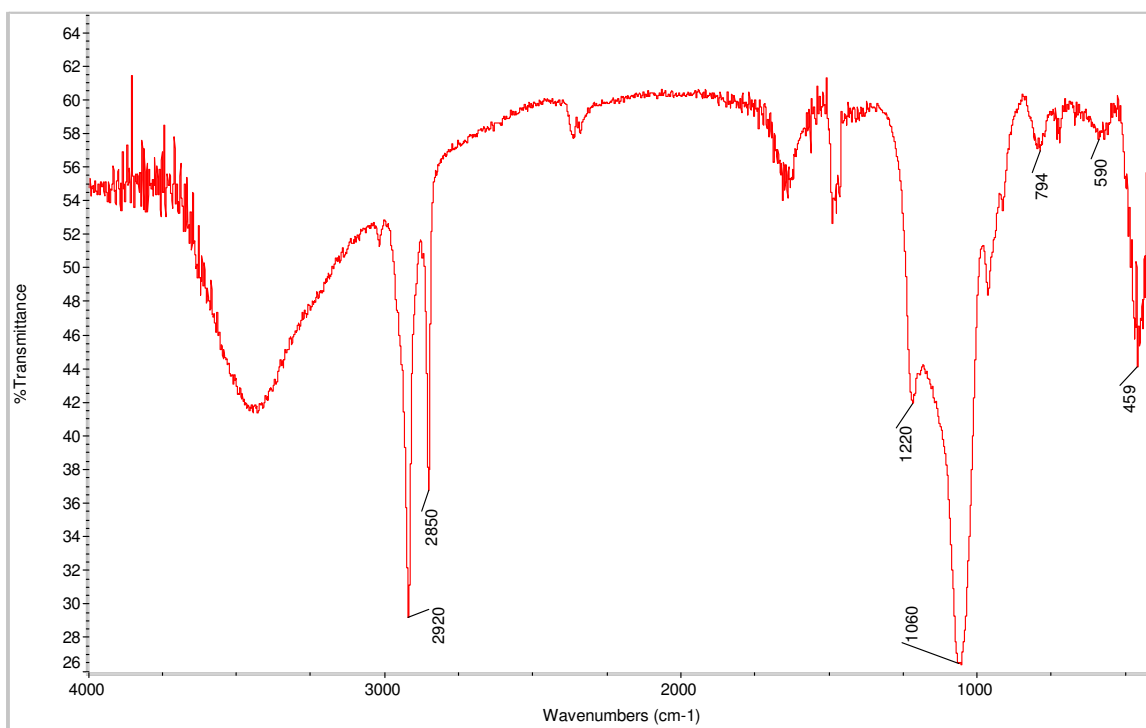


Figure 3.14.a. FT-IR spectrum of as-synthesized Al-MCM-41 (90) catalyst.

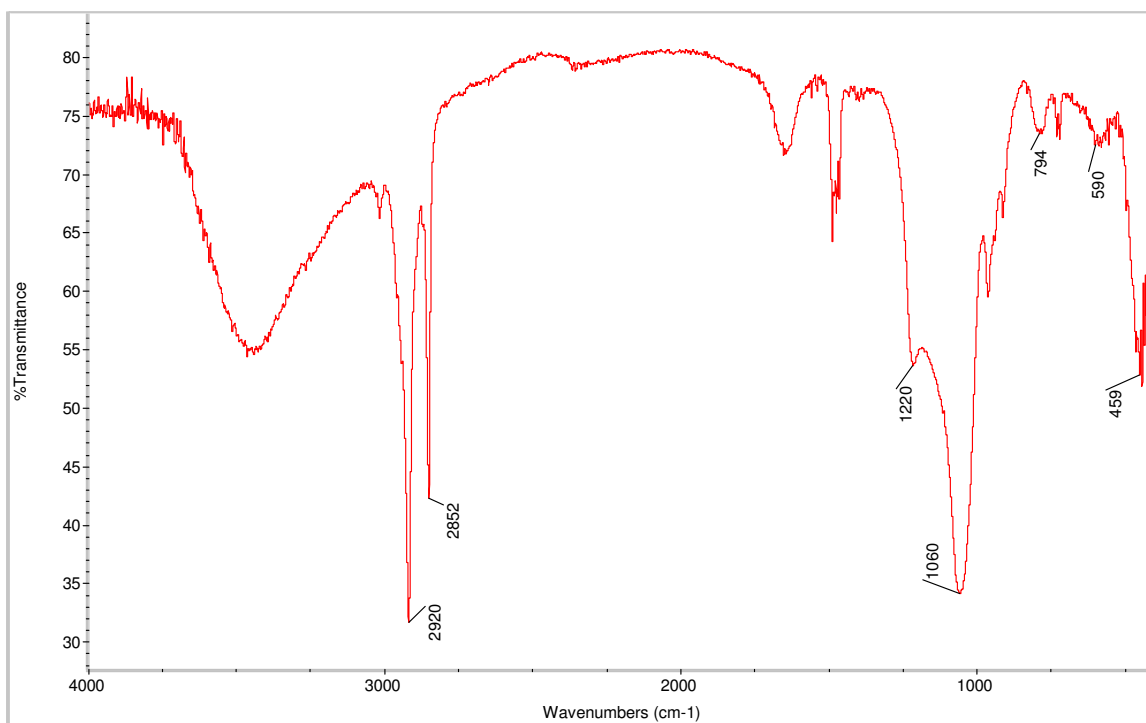


Figure 3.14.b. FT-IR spectrum of as-synthesized Al-MCM-41 (60) catalyst.

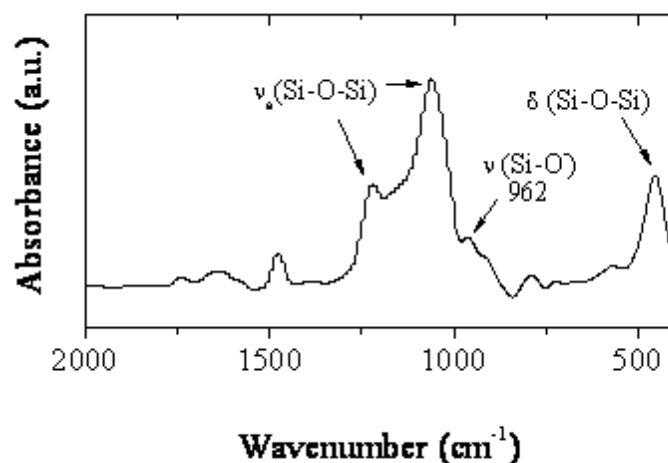


Figure 3.14.c. FT-IR spectrum of as-synthesized Al-MCM-41 (90) catalyst.

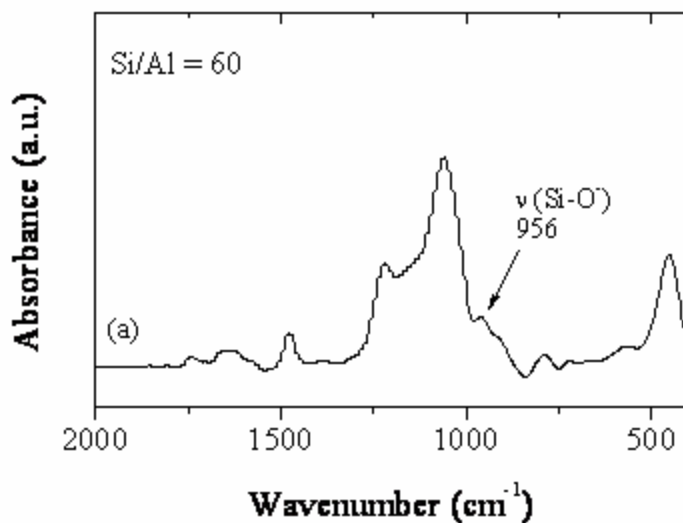
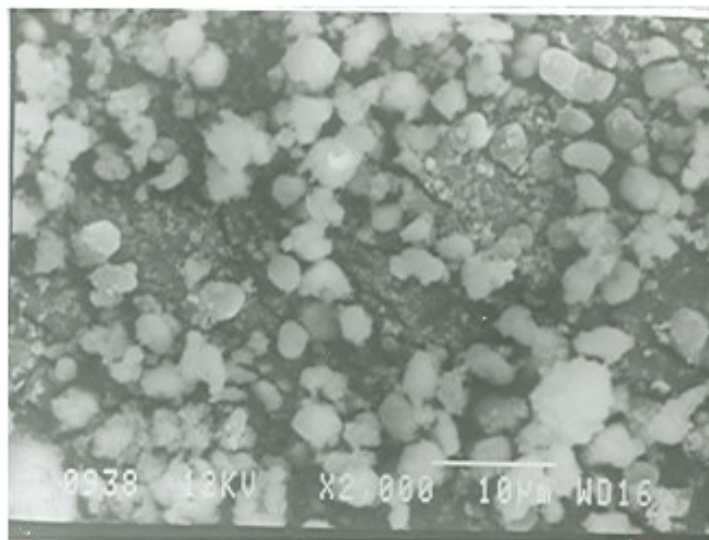


Figure 3.14.d. FT-IR spectrum of as-synthesized Al-MCM-41 (60) catalyst.

The bands at ~ 1220 , ~ 1060 , ~ 794 and ~ 590 cm^{-1} are attributed to the Si-O-Si stretching ($\nu_{\text{Si-O-Si}}$) and the band at ~ 459 cm^{-1} is assigned to Si-O-Si bending ($\delta_{\text{Si-O-Si}}$) frequencies of the mesoporous silicate framework^{292, 293}. However, the framework defect sites, $\equiv\text{Si-O}^-$ and Al-O^- , exhibit stretching frequencies in the same region (800-1100 cm^{-1}) and hence cannot be distinguished (Figs. 3.14.c and 3.14.d).

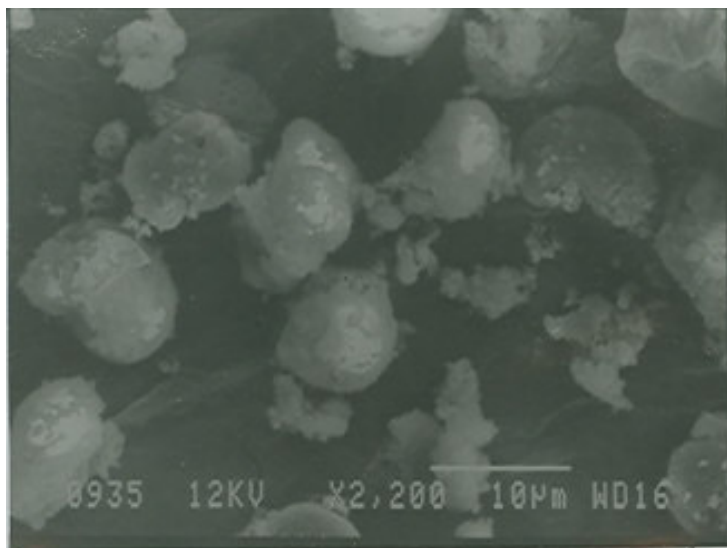
3.5. Scanning Electron Microscopy (SEM) technique:

SEM figures summarise the main features of the metal loaded zeolite-Y (Na-Y), ZSM-5, γ - Al_2O_3 and Al-MCM-41, reflecting morphologies of very crystalline zeolite materials. Magnification in micrographs ranges from X1800 to X3500 with working distance of ~15 and 12 KV. Al-MCM-41 (90) exhibits crystals of approximately 8-9 μm size, whereas Al-MCM-41 (60) exhibit crystals of regular shape with 3 μm size (Figs. 3.15.a and 3.15.b).



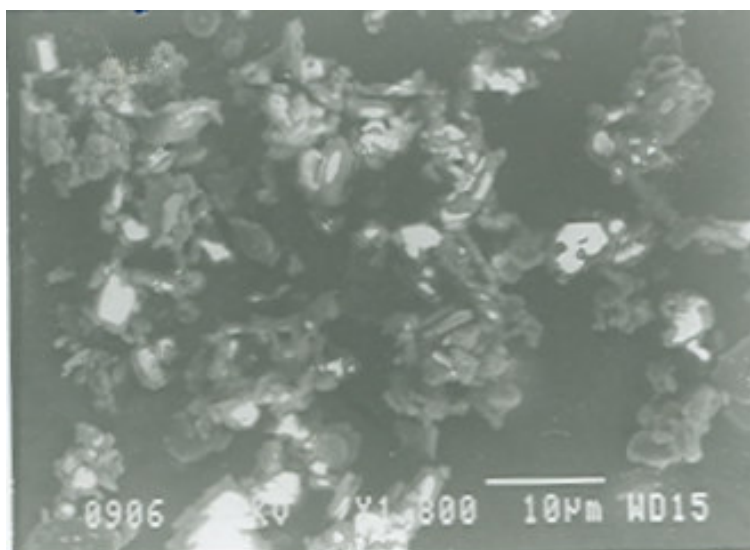
Al MCM 41 (60)

Figure 3.15.a. SEM image of Al-MCM-41 Si/Al-60.



Al MCM 41 (90)

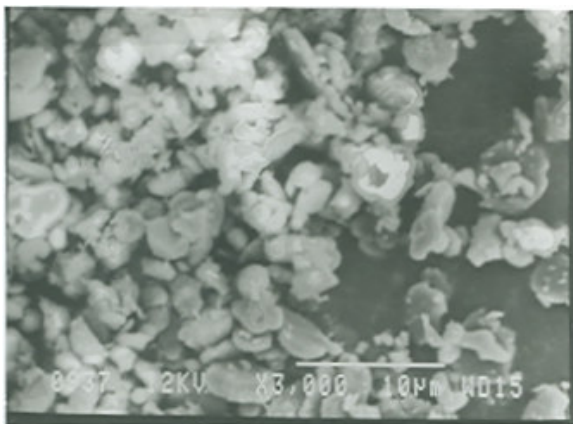
Figure 3.15.b. SEM image of Al-MCM-41 Si/Al-90.



γ -Al₂O₃

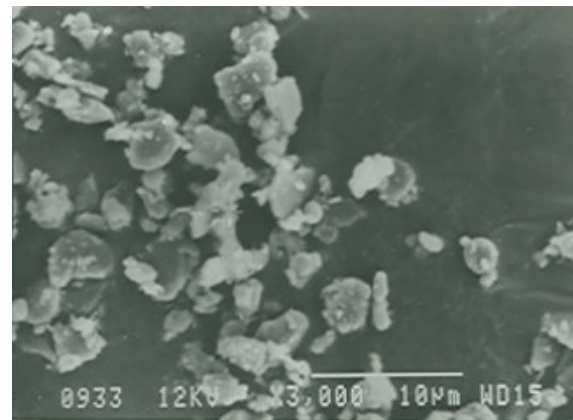
Figure 3.16.a. SEM image of γ -Al₂O₃ support.

Metals with γ -Al₂O₃ support showed the irregular shape while the metals with support calcined under N₂ flow conditions showed regular shapes (Figs. 3.16.a-g). ZSM-5 zeolite shows the features of hexagonal prisms and crystals of size 2-3 μ m. SEM images further reveal a uniform particle size of the sample with a regular shape. From the micrograph the aggregation of the metal particles (Ni, Pd, V, and U) with support particles is also seen. The crystalline nature of ZSM-5 is evident in the electron microscope (Figs. 3.17.a-e).



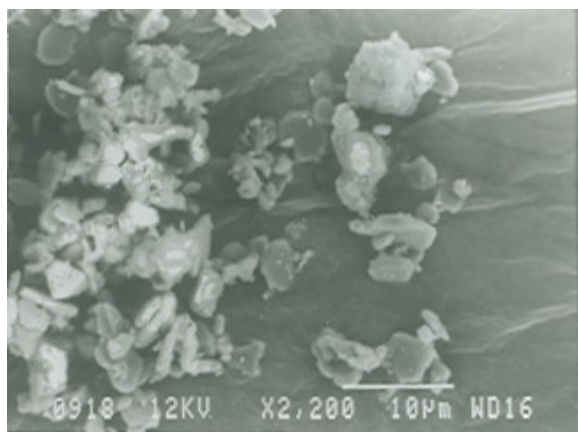
Ni / γ -Al₂O₃

Figure 3.16.b. SEM image of Ni/ γ -Al₂O₃ support.



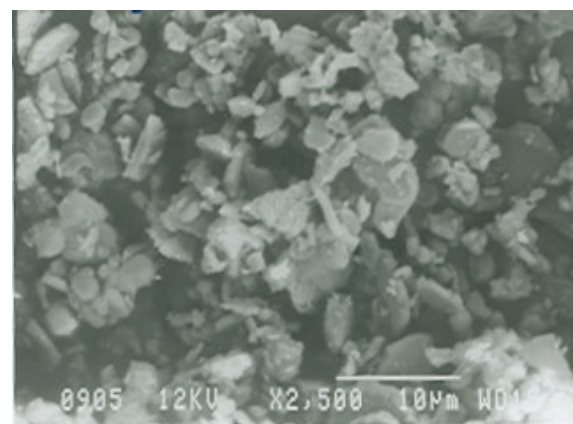
Ni / γ -Al₂O₃ N₂ Calcined

Figure 3.16.c. SEM image of Ni/ γ -Al₂O₃ N₂ calcined.



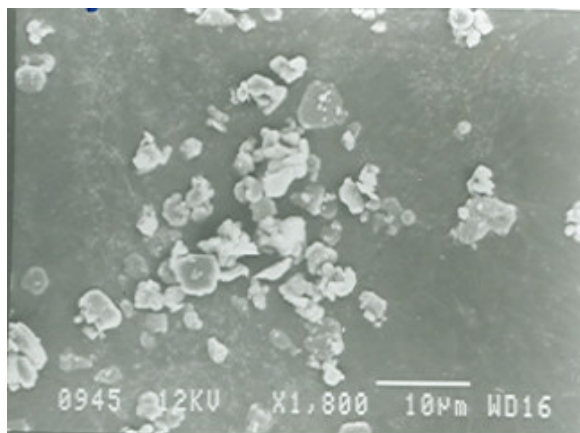
Pd / γ -Al₂O₃

Figure 3.16.d. SEM image of Pd/ γ -Al₂O₃ support.



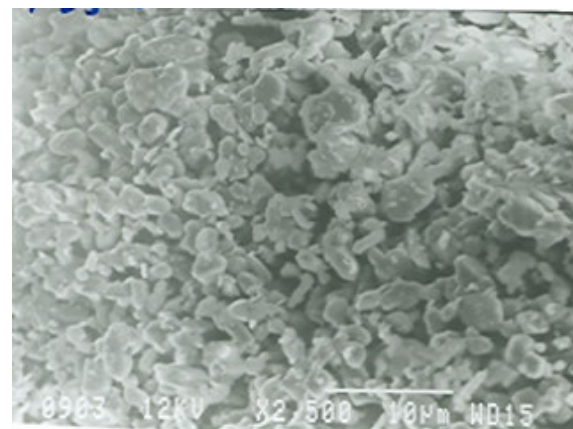
Pd / γ -Al₂O₃ N₂ Calcined

Figure 3.16.e. SEM image of Pd/ γ -Al₂O₃ N₂ calcined.



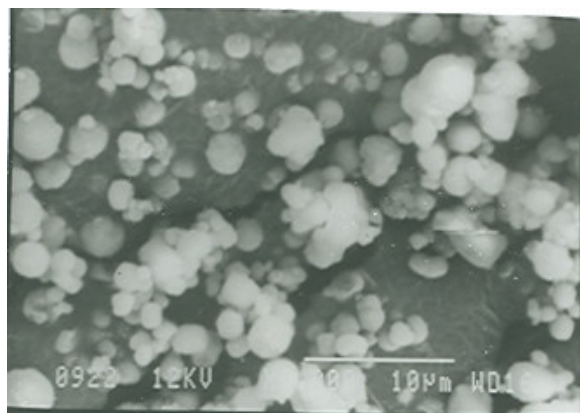
V / γ -Al₂O₃

Figure 3.16.f. SEM image of V/ γ -Al₂O₃ support.



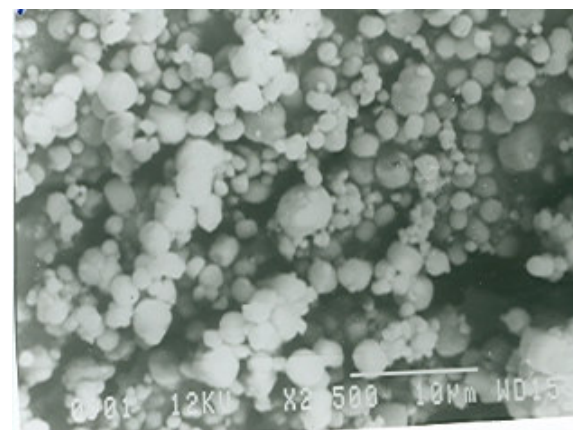
V / γ -Al₂O₃ N₂ Calcined

Figure 3.16.g. SEM image of V/ γ -Al₂O₃ N₂ calcined.



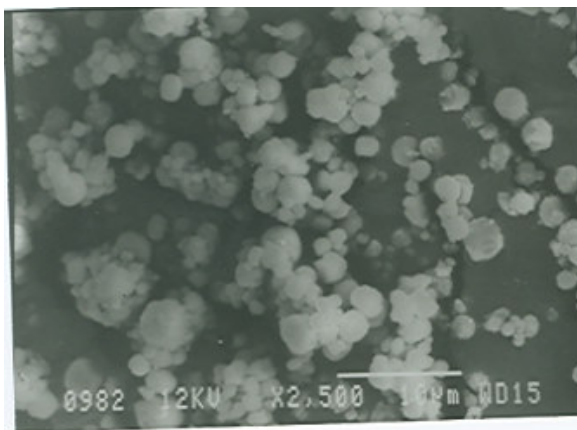
ZSM 5

Figure 3.17.a. SEM image of ZSM-5 support.



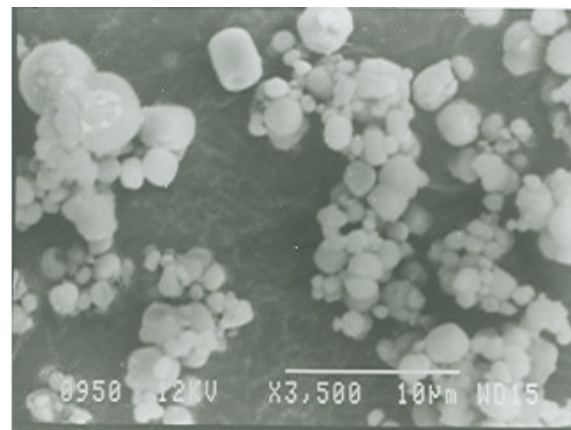
Ni / ZSM 5

Figure 3.17.b. SEM image of Ni/ZSM-5 support.



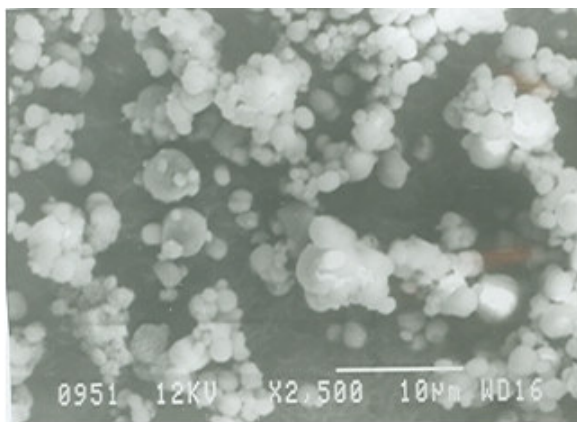
5% Ni / ZSM 5

Figure 3.17.c. SEM image of 5% Ni/ZSM-5 support.



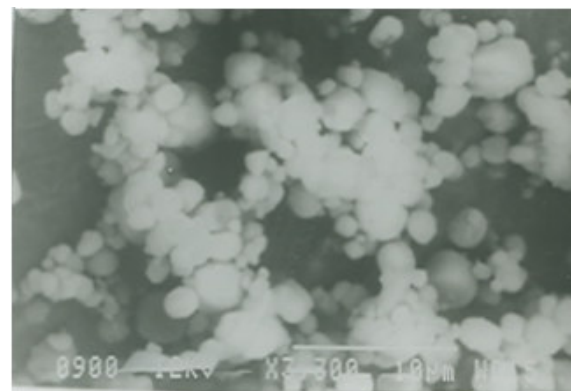
V / ZSM 5

Figure 3.17.d. SEM image of V/ZSM-5 support.



U / ZSM 5

Figure 3.17.e. SEM image of U/ZSM-5 support.



Ni / NaY N₂ Calcined

Figure 3.18. SEM image of Ni/Na-Y N₂ calcined.

Zeolite Na-Y consists of spherulites composed of small blocks stacked in a non-oriented manner. The geometric structural features associated with zeolite-Y are readily apparent while the nature of nickel metal dispersion on the surface is also evident, crystals with a crystal size ranging from 1-3 μm is observed (Fig. 3.18). Regarding the catalyst morphologies, SEM images clearly point out the homogeneity in shapes for all samples, which appear to be highly crystalline in nature.

3.6. BET surface area determination:

BET surface areas of the impregnated solids are reported in Table 3.6. The results are in agreement with the BET surface area measurements that showed a decrease in the surface area upon metal (Ni, V and Pd) impregnation. The BET observations signify that there is a decrease in the surface area for the samples calcined under N_2 flow conditions.

Table 3.6. BET surface area analysis.

Catalyst system	BET Surface Area, $\text{m}^2 \text{g}^{-1}$
Na-Y (Süd Chemie, India)	623
Ni/Na-Y	612
Ni/Na-Y N_2 calcined	592
Pd/Na-Y N_2 calcined	576
V/Na-Y	570
ZSM-5 Si/Al-30 (Süd Chemie, India)	341
V/ZSM-5	330
V/ZSM-5 N_2 calcined	326
UO_2^{2+} /ZSM-5	296
Zeolite H Beta 40 (Süd Chemie, SA)	> 400
H Beta 150 (Süd Chemie, SA)	> 500
Al-MCM-41 Si/Al-60	773
Al-MCM-41 Si/Al-90	774

The zeolite Na-Y catalysts loaded with Pd and V metals showed lower surface area compared to those having Ni metal loadings. Similarly, ZSM-5 catalysts loaded with UO_2^{2+} zeolite showed lower surface area as compared to those having V zeolites. The total surface area of large pore size mesoporous Al-MCM-41 samples was very high ($>770 \text{ m}^2 \text{g}^{-1}$) as it was expected.

The total surface areas of all samples were very high as was expected. The samples even after calcination maintained a very high surface area.

Loading of catalysts with the various metals used in this study does not lead to loss in crystallinity or significant decrease in total surface area. All the zeolite catalyst supports and metal loaded zeolites showed the characteristic bands in the FT-IR spectra and were in good agreement with the literature. The catalysts morphologies (SEM) clearly point out the homogeneity in shapes for all samples. All samples appear to be highly crystalline in nature. Diffuse reflectance spectroscopy results showed the symmetry and the valence of the supported Ni-, V- and Pd-loaded catalysts. The catalysts displayed characteristic bands attributed to Ni^{2+} , V^{5+} and Pd^{2+} cations in different zeolites. Thermal analysis of synthesized Al-MCM-41 catalysts followed a characteristic three-stage weight loss of mesoporous materials.

CHAPTER - IV

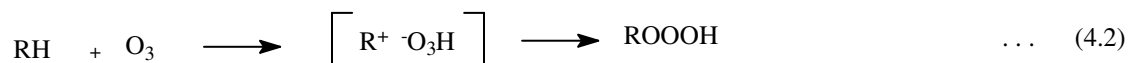
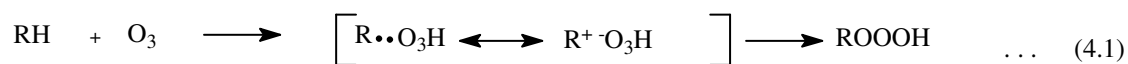
OXIDATION OF HIGHER n -ALKANES WITH OZONE, UNCATALYSED AND IN PRESENCE OF ACTIVATED CHARCOAL

4.0. Introduction:

In this chapter the results for uncatalysed oxidation of three higher alkanes with ozone and in presence of activated charcoal are presented. The ozone initiated oxidation involves several unit operations occurring simultaneously: gas absorption, gas desorption (or stripping), and chemical reaction. Adsorption/desorption may be affected by the mass transfer characteristics of the contacting device as well as flow conditions, and the chemical kinetics may be affected by reaction conditions such as temperature and pH. The rate of reaction are limited or controlled by the rate of mass transfer of ozone into solution²⁹⁴.

Ozone is reported to exhibit variations in its reactivity with different classes of compounds, in non-aqueous solvents under conditions of high temperature, high pressure and high concentrations of ozone and organics^{3, 13}. The alkanes, for example, are relatively unreactive towards ozone because they are saturated compounds. On the other hand, ozone is adept in reacting with alkanes.

The reaction of ozone with C-H bonds has been studied extensively³. The ultimate products formed in such reactions suggest that a hydrotrioxide is an intermediate and these hydrotrioxides have been identified from the reaction of aldehydes, acetals and similar substrates³. The accepted mechanism involves the abstraction of a hydrogen atom in a transition state with appreciable dipolar character³ as the crucial mechanistic step (eqn. 4.1). Benson *et al*⁴⁸ have suggested the hydride abstraction in the mechanism (eqn. 4.2) as the crucial step in the oxidation process.



4.1. Scope of CCl₄ as solvent for ozonation of n-hexadecane:

Literature reports the absorption ozone in carbon tetrachloride and glacial acetic acid reaction mixtures was about 80-90% throughout the reaction⁴⁵. The stability of ozone was influenced by the temperature. Ozone is more stable at low temperatures, with higher solubility and activity²³⁴. Its decomposition rate increases with rise in temperature. Ozone was purged through the pure CCl₄ solvent. Solvent CCl₄ was oxidized resulting into a mixture of products. The positively identified products are the dimerised chloro compounds.

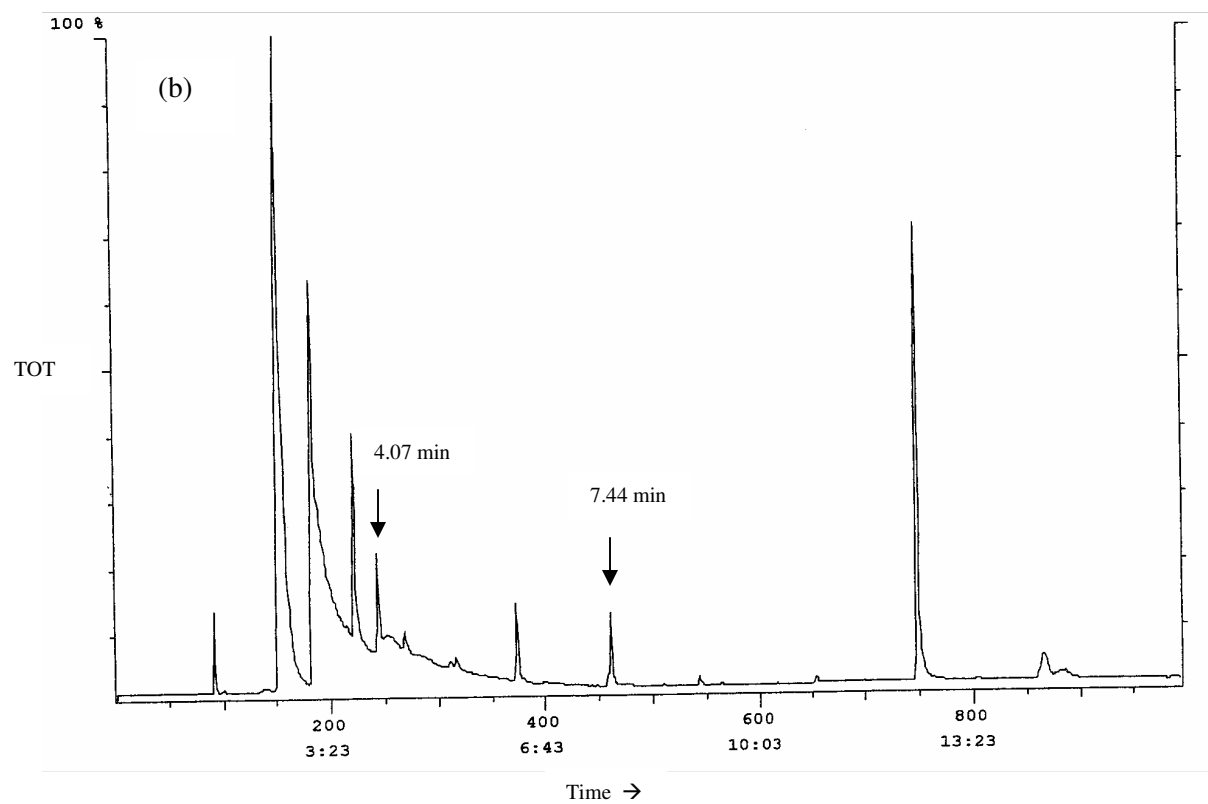
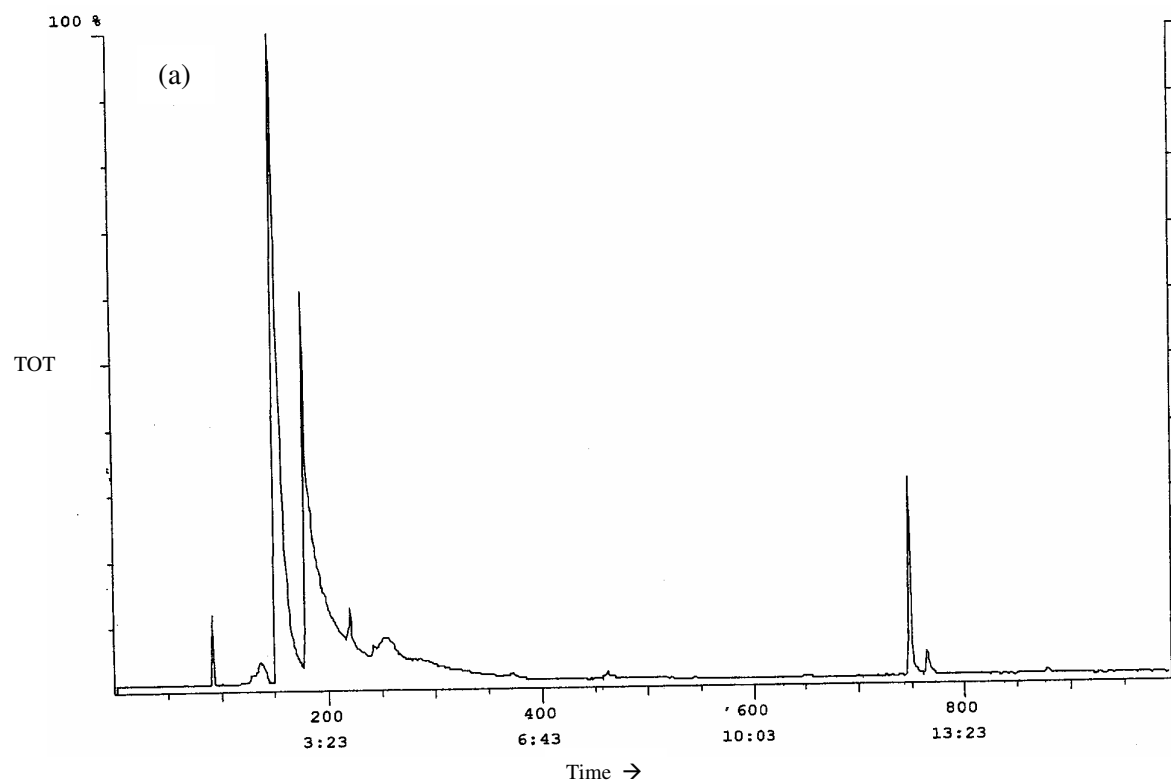


Figure 4.1. Chromatogram of CCl_4 solvent (a) before ozonation (b) after ozonation.

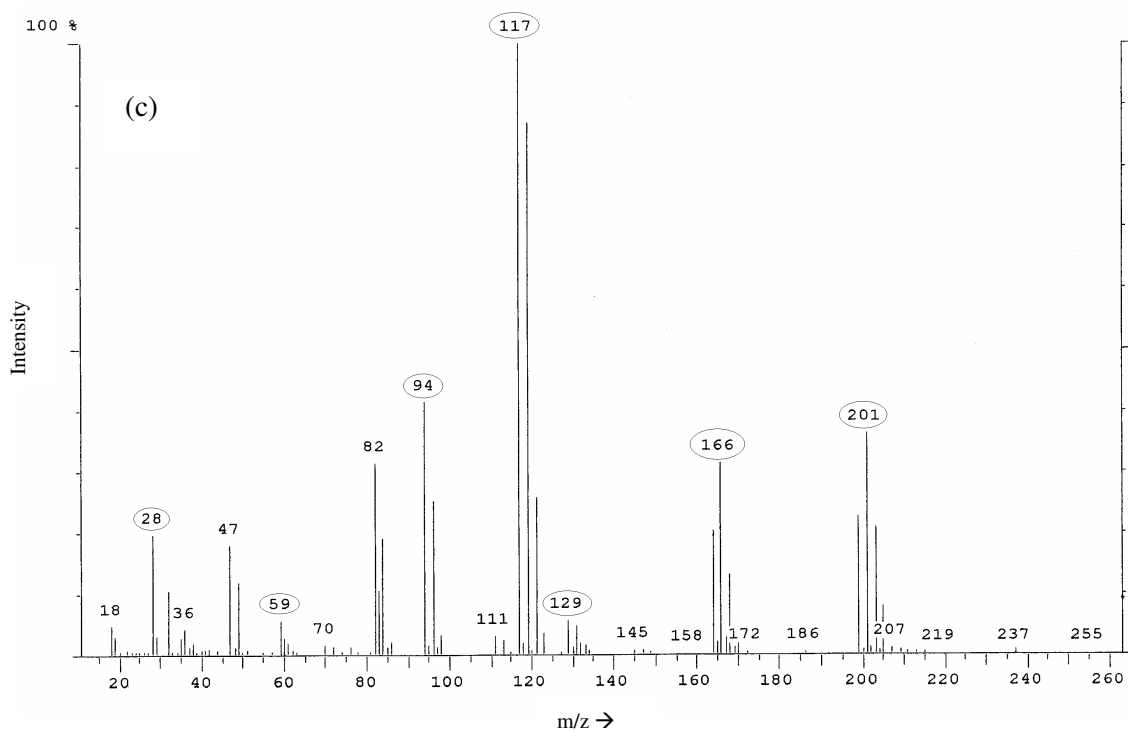


Figure 4.1.c. MS of ozonated CCl₄.

From the chromatogram of the pure CCl₄ and CCl₄ ozonated (Figs. 4.1.a-c), it is observed that the solvent was oxidized. Based on the products identified, carbon tetrachloride was oxidized resulting into a mixture of products. Hexachloroethane and tetrachloroethene were positively identified as the main products of ozone initiated oxidation of carbon tetrachloride.

The base peak at m/z = 117 refers to the trichloro methyl cation (⁺CCl₃). The peak at m/z-237 represents the M⁺ of hexachloroethane. Loss of ³⁵Cl from 236 gives the m/z = 201, corresponding to the pentachloroethane cation (⁺C₂Cl₅). The series of ions detected that corresponds to the fragments (201, 166, 129, 94, 59 and 28) which differ by 35 mass units, formed by the cleavage of -Cl units. This mass pattern represents the peak at retention time 7.44 min. of Fig. 4.1.b.

The mass spectrum shown in Appendix Fig. a, corresponds to the peak with a retention time of 4.07 min on the GC-MS total ion chromatogram shown in Fig. 4.1.b. The mass spectrum indicates the presence of tetrachloroethene. The pattern at m/z-166 represents the M⁺ of tetrachloroethene. Loss of ³⁵Cl from 166 gives the m/z = 129, corresponding to the

trichloroethene cation. The series of ions detected that corresponds to the fragments (94, 60 and 28) which differ by 35 mass units, formed by the cleavage of -Cl units.

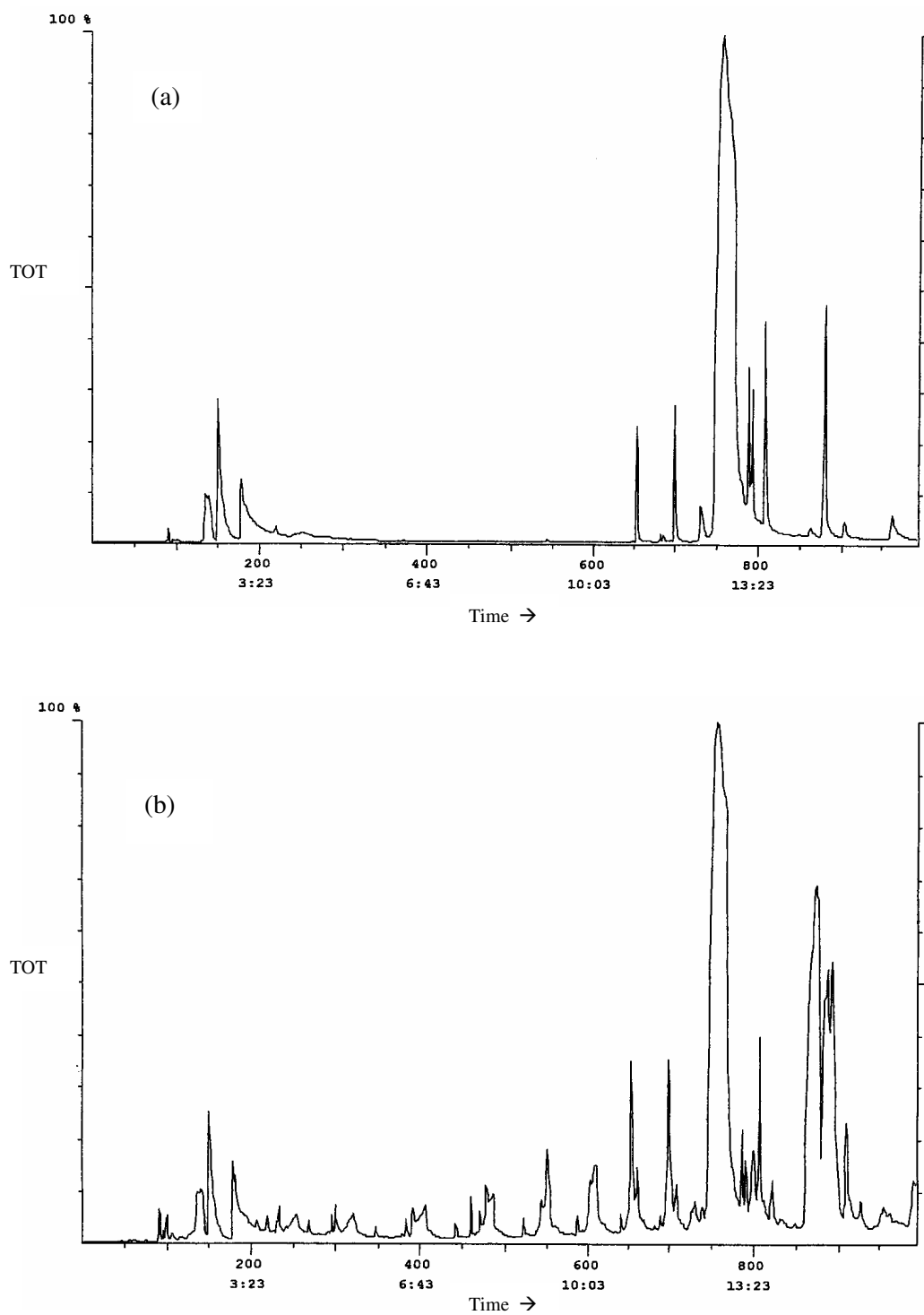


Figure 4.2. Chromatogram of n-hexadecane in CCl_4 solvent (a) before ozonation (b) after ozonation.

Later, 5% n-hexadecane (v/v) in carbon tetrachloride was used for the ozonation studies in the temperature range 0-4 °C. Little reaction was observed even after 5 h of ozonation of the reaction mixture at about 0-4 °C. Noticeable reaction occurred only after about 6 h of ozonation (by TLC). The characterization of reaction mixture by GC/GC-MS (Fig. 4.2) revealed that a small amount of solvent system with hexadecane got oxidized. Solvent CCl₄ was oxidized resulting into a mixture of products. The positively identified products are the dimerised chloro compounds.

4.2. Scope of tetrahydrofuran as solvent for ozonation of n-hexadecane:

Ozonation of n-hexadecane was studied using THF as solvent. In these experiments 5% v/v n-hexadecane (10.0 mL of n-hexadecane in 190.0 mL of THF) was used. These reactions were studied at varied voltage range and O₂ flow rates applied at room temperature (20 ± 1 °C). Ozone was purged through the n-hexadecane in THF solvent. THF solvent was oxidized resulting into a mixture of products.

Fourier transform infrared spectroscopy (FT-IR) was used to characterize the functional groups of the organics. From the literature^{24, 25} it is apparent that the hydroxyl group intensity increases after ozone oxidation, which results in the substitution of functional groups of the organic intermediates associated with the electrophilic reaction by adding into the oxygen atoms. Langlais *et al*^{24, 25} showed that the intensity representing the specific stretch wave numbers of double or triple bond between carbons has been observed to diminish after ozonation mainly due to the mechanism of cyclo addition^{24, 25}.

Upon 5 h ozonation THF got oxidized. The THF on ozonation resulted into oxidized products, the IR spectrum of ozonated THF is shown in the Fig. 4.3. The bands at 1771 and 1721 cm⁻¹ refers to the formation of a keto compound.

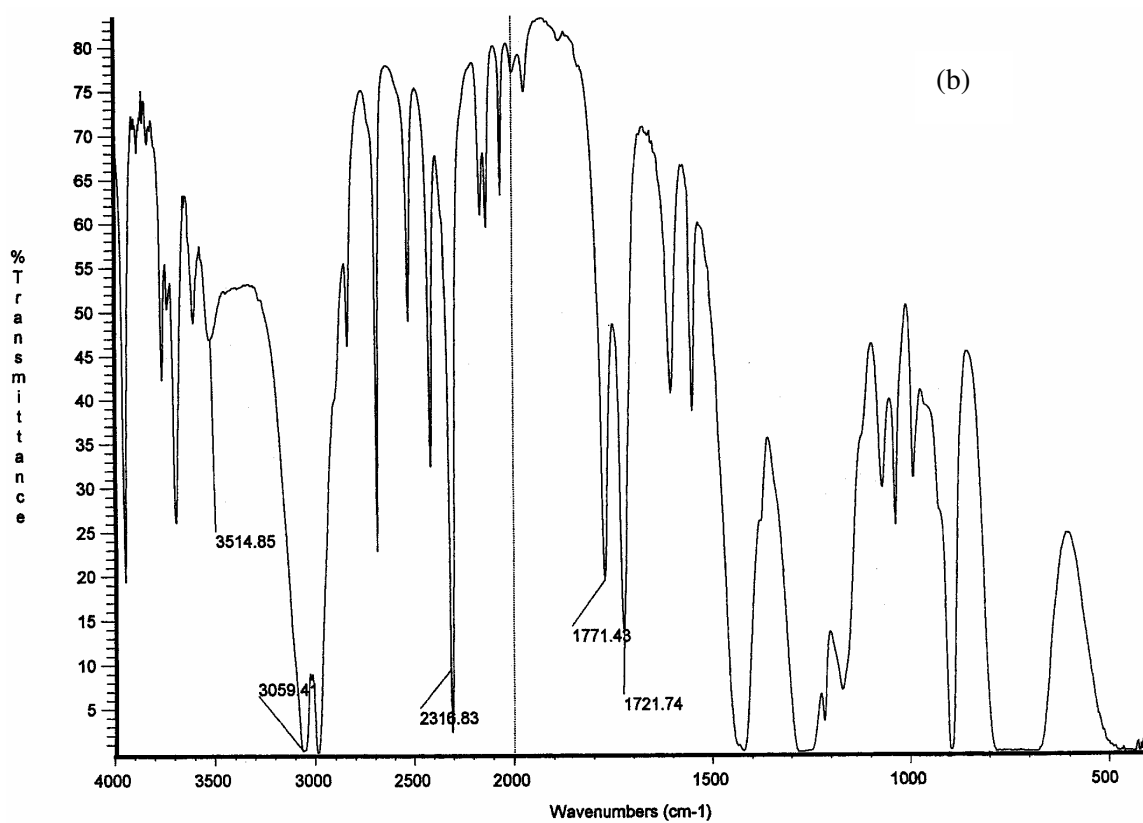
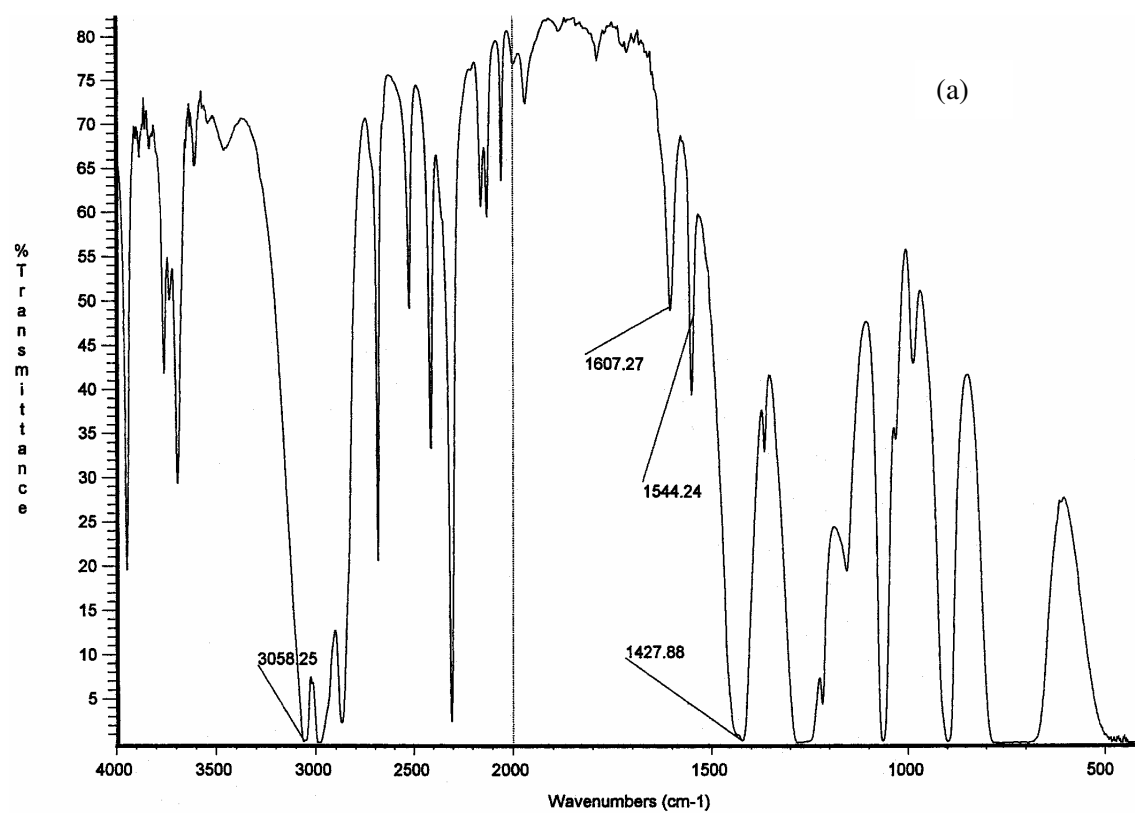


Figure 4.3. IR spectra of THF solvent (a) before ozonation (b) after ozonation.

4.3. Product analysis for ozonation of n-hexadecane in the absence of solvent: The ozonation experimental conditions were similar as discussed in the Chapter II (Section 2.3). All the experiments were carried out in replicate.

4.3.1. Gas chromatography analysis of product mixture:

The chromatograms of the n-hexadecane before and after ozonation are shown in the Fig. 4.4.a and 4.4.b. The peak at retention time 10.8 refers to the unreacted n-hexadecane and group of peaks at the retention time 11.7-12.0 refers to the isomer compounds of hexadecanone, i.e. 4-hexadecanone, 3-hexadecanone and 2-hexadecanone products (Fig. 4.4.b). Further, the unreacted n-hexadecane from the chromatogram is confirmed by injecting the substrate, which elutes at the retention time 10.8 ± 0.2 .

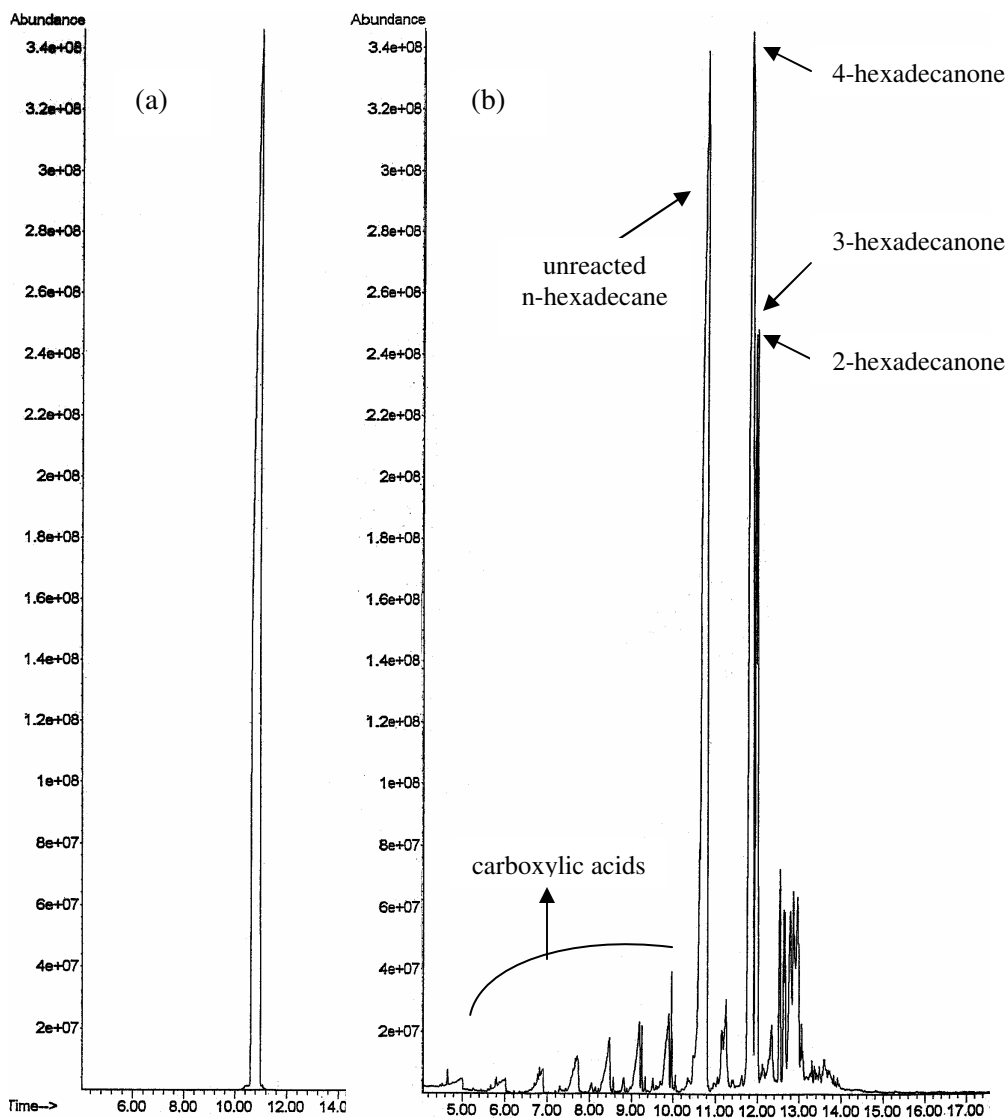


Figure 4.4. Chromatogram of n-hexadecane (a) before ozonation (b) after ozonation.

The small peaks from 4.4-10.0 retention time refer to the different carboxylic acid (detailed discussion in Section 4.4.2) compounds formed due to the further oxidation of the main products of the reaction, hexadecanone isomers.

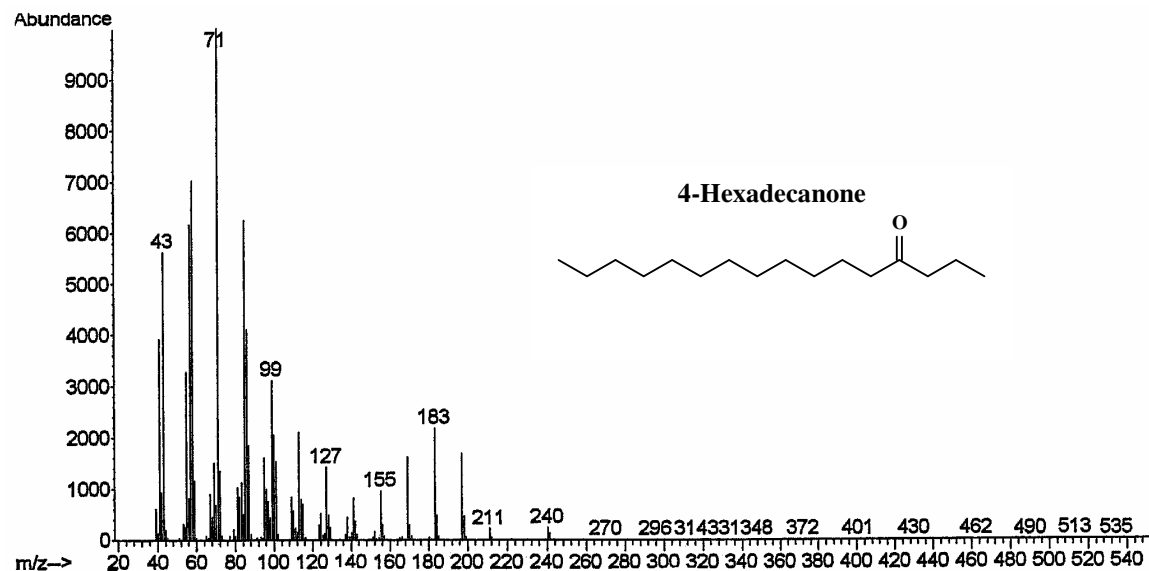


Figure 4.4.c. MS of 4-hexadecanone product.

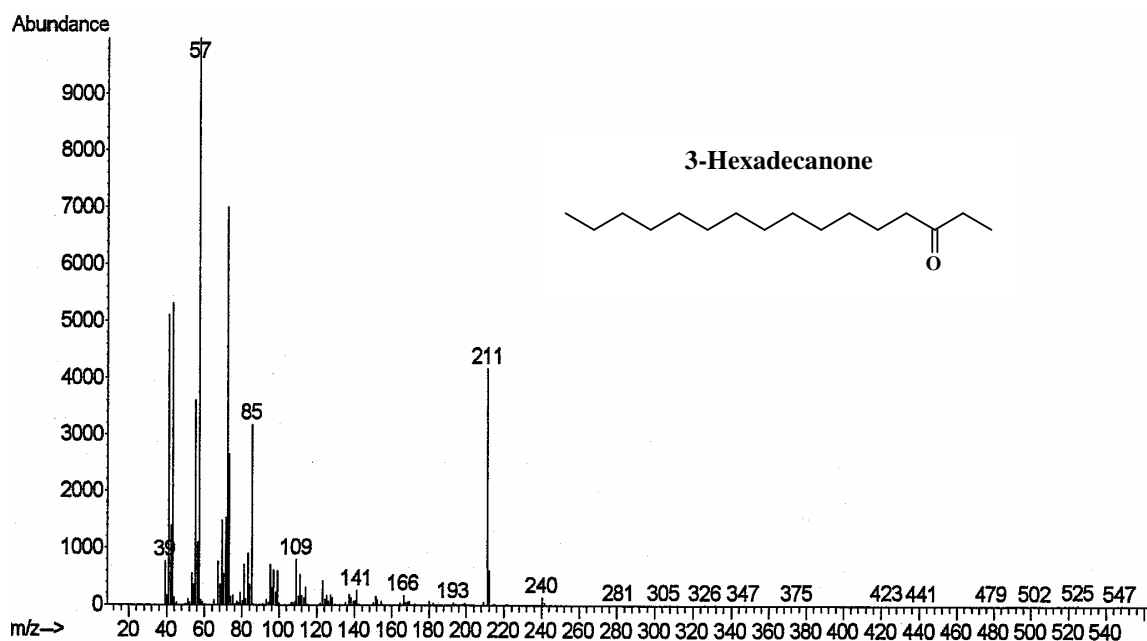


Figure 4.4.d. MS of 3-hexadecanone product.

The base peak at $m/z = 71$ refers to the radical $\text{CH}_3\text{CH}_2\text{CH}_2\dot{\text{C}}=\text{O}$. The molecular ion at $m/z=240$ represents the M^+ of 4-hexadecanone. The series of ions detected that corresponds to the molecular ion, M^+ fragments (43, 58, 71, 85, 99, 114, 127, 141, 155, 169, 183, 197 and 211) that

differ by ~14 mass units, formed by the cleavage of $-\text{CH}_2-$ units (Fig. 4.4.c). This mass pattern represents the peak at retention time 11.70 min on the GC-MS total ion chromatogram shown in Fig. 4.4.b.

The Fig. 4.4.d represents the mass spectra for 3-hexadecanone. The molecular ion at m/z -240 represents the M^+ of 3-hexadecanone. The peak at m/z -57, confirms the position of the keto group at C_3 position. The pattern at m/z - 42, 71, 85, 99, 109, 123, 141, 153, 166, 211 and 240 refer to the molecular ion, M^+ fragments that differ by ~14 mass units, formed by the cleavage of $-\text{CH}_2-$ units of 3-hexadecanone compound. This mass pattern represents the peak at retention time 11.85 min on the GC-MS total ion chromatogram shown in Fig. 4.4.b.

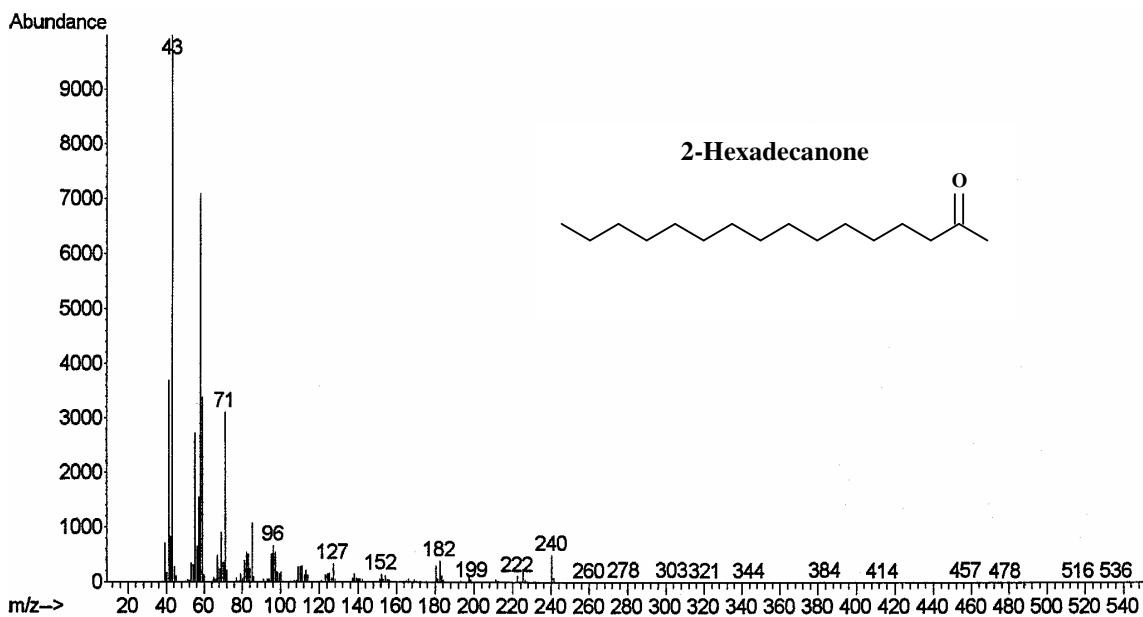


Figure 4.4.e. MS of 2-hexadecanone product.

The solid isomer 2-hexadecanone mass spectrum is showed in the Fig. 4.4.e. The molecular ion at m/z -240 represents the M^+ of 2-hexadecanone. The base peak at m/z - 43 confirms the keto group at C_2 position. The other mass peaks at m/z - 57, 71, 85, 96, 111, 127, 152, 182, 199, 222 and 240 represents the series of ions detected that corresponds to the molecular ion, M^+ fragments that differ by ~14 mass units, formed by the cleavage of $-\text{CH}_2-$ units of 2-hexadecanone, are in good agreement with the literature. This mass pattern represents the peak at retention time 11.95 min on the GC-MS total ion chromatogram shown in Fig. 4.4.b. The mass patterns for 4-, 3- and 2-hexadecanones from literature (NIST98 mass spectra library) are shown in the Appendix Figs. b, c and d.

4.3.2.a. FT-IR analysis of the product mixture:

The peak at 1709 cm^{-1} in the IR spectra refers to the carbonyl group of a keto compound. The peak 1709 cm^{-1} is observed in both extracted layer and organic layer after the bicarbonate extraction (Fig. 4.5.1.a-b), which confirms the presence of carbonyl group of a compound in both layers.

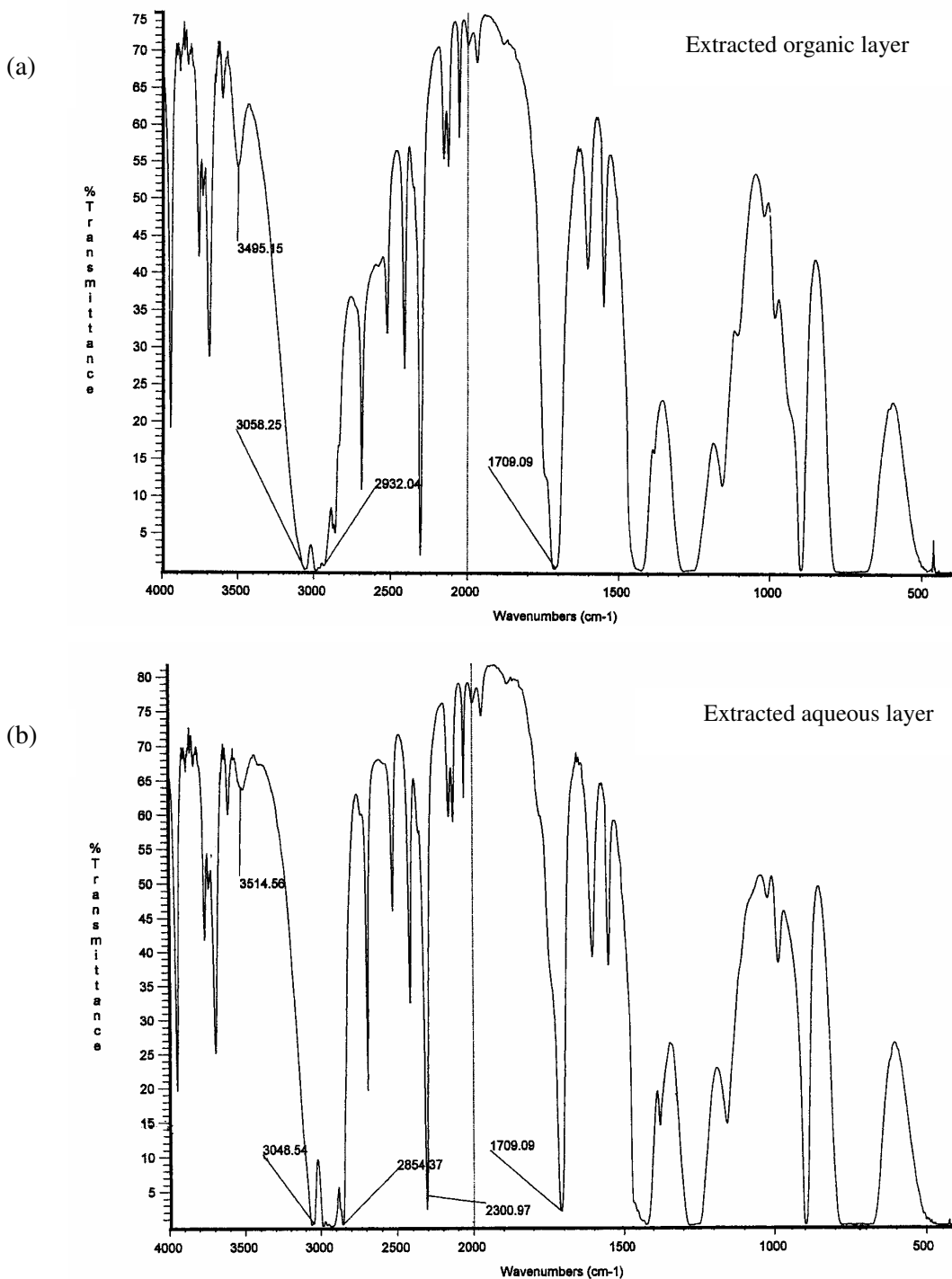


Figure 4.5.1. IR spectra of extracted (a) organic layer (b) aqueous layer.

4.3.2.b. FT-IR analysis of the isolated products:

The FT-IR spectra of the compounds isolated from the column chromatography, the peaks at 1704 cm^{-1} (Figs. 4.5.2.a-b) and 1709 cm^{-1} refers to the carbonyl group of a keto compound (Fig. 4.5.2.c). The FT-IR spectra of the compounds before and after ozonation are shown in Appendix Figs. e and f.

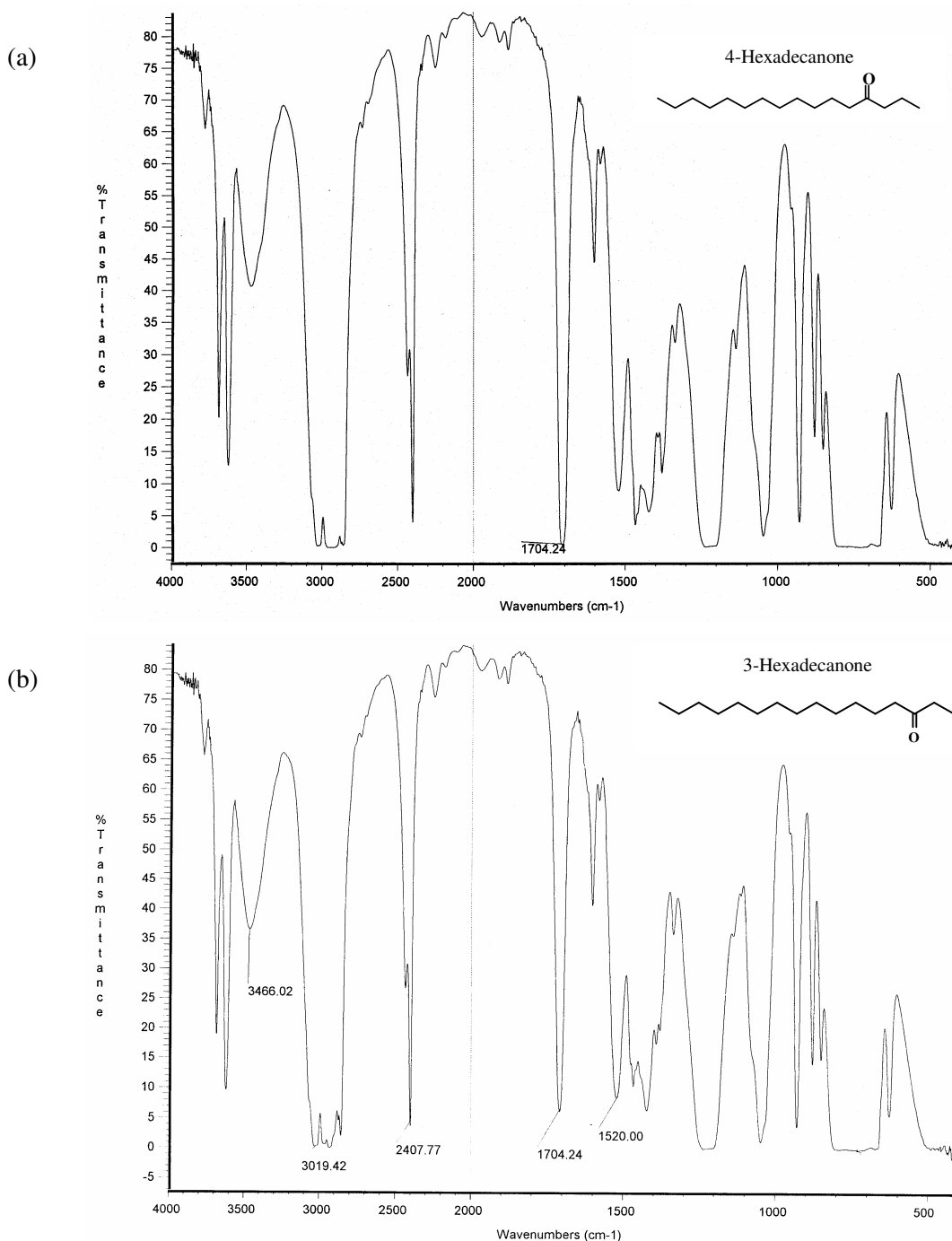


Figure 4.5.2. IR spectra of isolated (a) 4-hexadecanone (b) 3-hexadecanone.

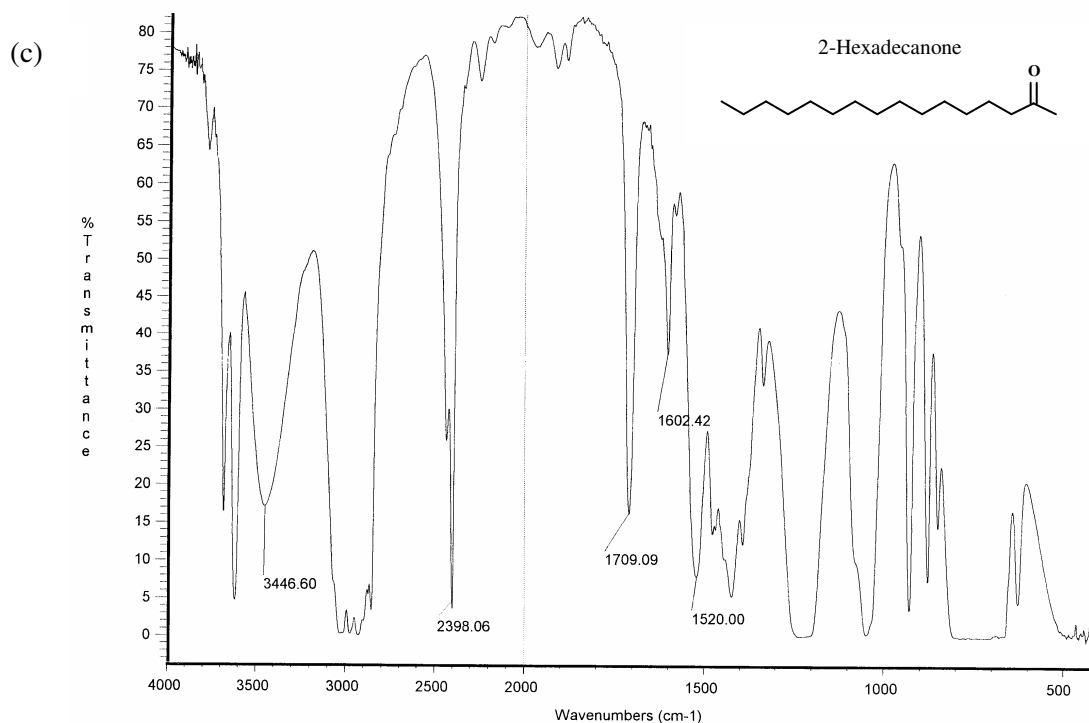


Figure 4.5.2.c. IR spectrum of isolated 2-hexadecanone.

4.3.3. ¹H NMR analysis of 4-, 3- and 2-hexadecanone products:

4-hexadecanone: Signal at 0.8-0.9 δ refers to the 6 protons of methyl ($-\text{CH}_3$) groups, a multiplet. 1.2-1.3 δ represents a signal for 18 protons of methylene ($-\text{CH}_2-$) groups. The signal at 1.48-1.58 δ refers to the 4 protons of methylene ($-\text{CH}_2-$) groups, a multiplet. The deshielded 4 protons of $-\text{CH}_2\text{COCH}_2-$ group can be observed at chemical shift 2.3-2.4 δ , which is a multiplet, refers to 4-hexadecanone (Fig. 4.6).

3-hexadecanone: The signal at 0.8-0.9 δ represents 6 protons of 2 methyl ($-\text{CH}_3-$) groups, refers to a multiplet. The signal at chemical shift 1.2-1.3 δ represents 20 protons of methylene ($-\text{CH}_2-$) groups, which refers to a multiplet. The signal at 1.5-1.6 δ represents 2 protons of methylene ($-\text{CH}_2-$) groups refers to a multiplet. The signal at 2.3-2.4 δ represents 4 protons of $-\text{CH}_2\text{COCH}_2-$ group which is a multiplet, confirms 3-hexadecanone [Appendix Fig. (g)].

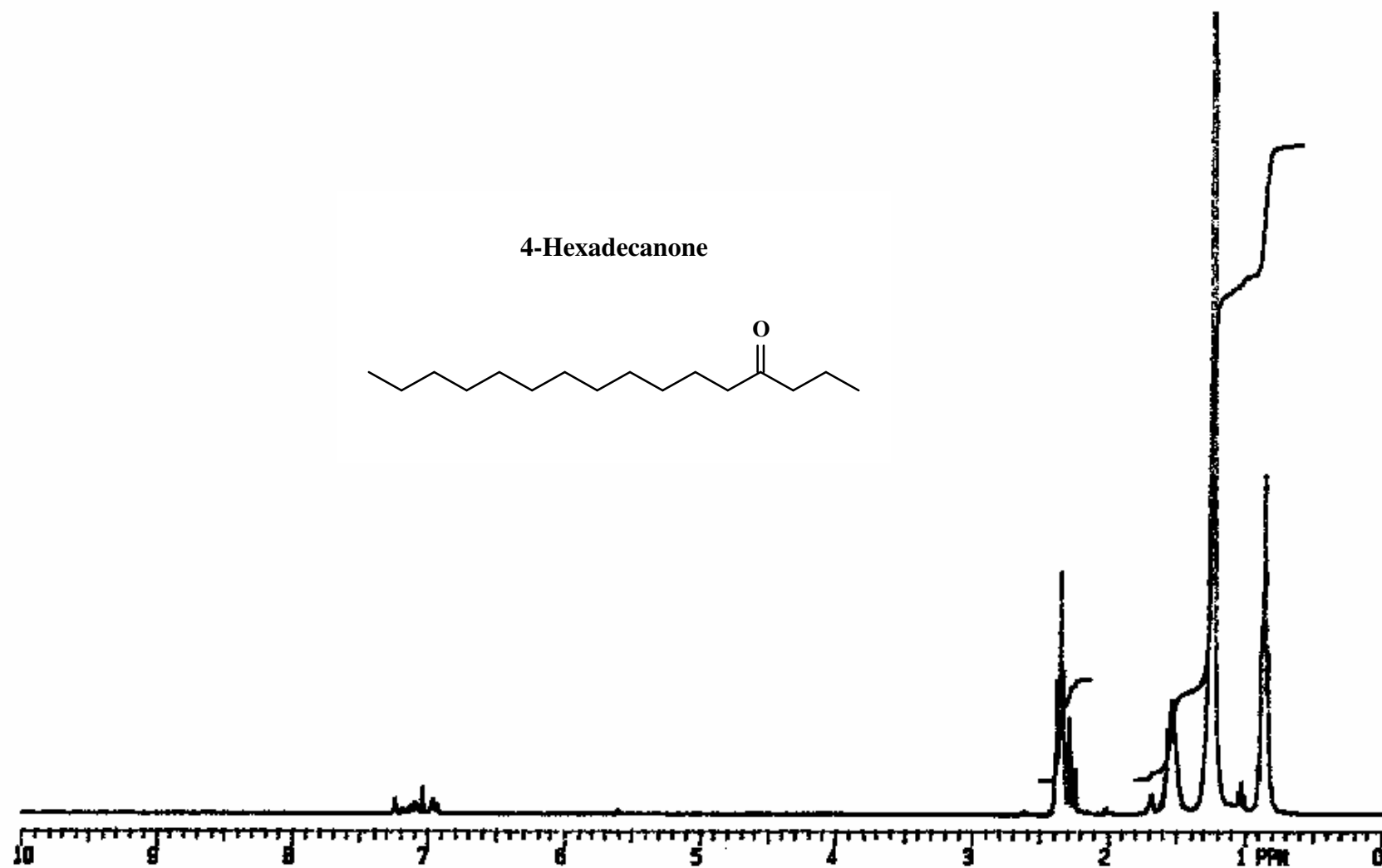


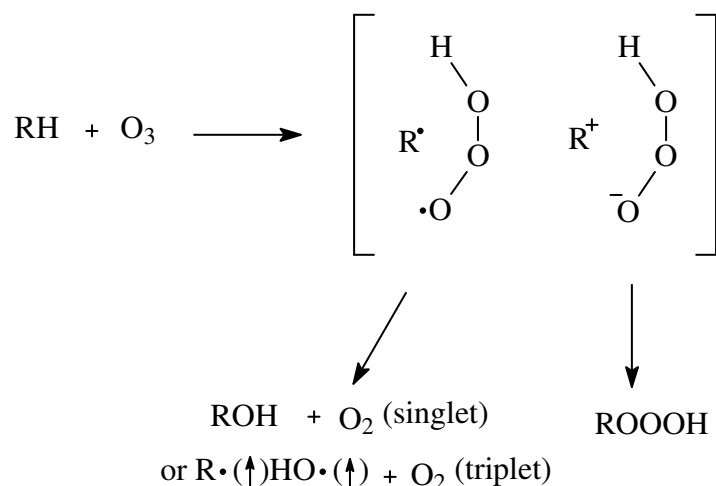
Figure 4.6. ^1H NMR spectrum for 4-hexadecanone.

2-hexadecanone: The solid isomer 2-hexadecanone ^1H NMR spectrum is in good accordance with the literature [Appendix Fig. (h)]. The triplet at 0.87 δ represents 3 protons of $-\text{CH}_3$ group. A broad multiplet is observed at 1.25-1.34 δ , refers to 22 protons of methylene ($-\text{CH}_2$) groups. The signal at 1.50-1.64 δ refers to a multiplet for 2 protons of $-\text{CH}_2$ group. A singlet signal at 2.13 δ refers to 3 protons of methyl ($-\text{COCH}_3$) group and a triplet at 2.38 δ refers to deshielded 2 protons of $-\text{COCH}_2-$ group. The 2-ketone isomer is obtained from the column chromatography is a crystalline compound. The melting point of the 2-hexadecanone (43-45 $^\circ\text{C}$) was determined and it is in good agreement with the literature^{295, 296}.

4.4. Mechanism of the ozone initiated oxidation of higher alkane:

The reactions of ozone with saturated hydrocarbons and alcohols appear to be of at least two distinct types. One involves an electrophilic attack by ozone and the other an ozone-initiated oxidation in which oxygen is the principal reactant. In the latter case ozone behaves as a radical reagent¹³.

Several mechanisms can be envisaged for the oxidation of the C-H bond to form the corresponding hydrotrioxide ROOOH, that is the key intermediates in these reactions, but an unambiguous substantiation of these proposals is, unfortunately, still lacking^{3, 297, 298}. In spite of considerable previous work on the mechanism of the reaction of ozone with various saturated compounds, a number of fundamental questions still remained unanswered.

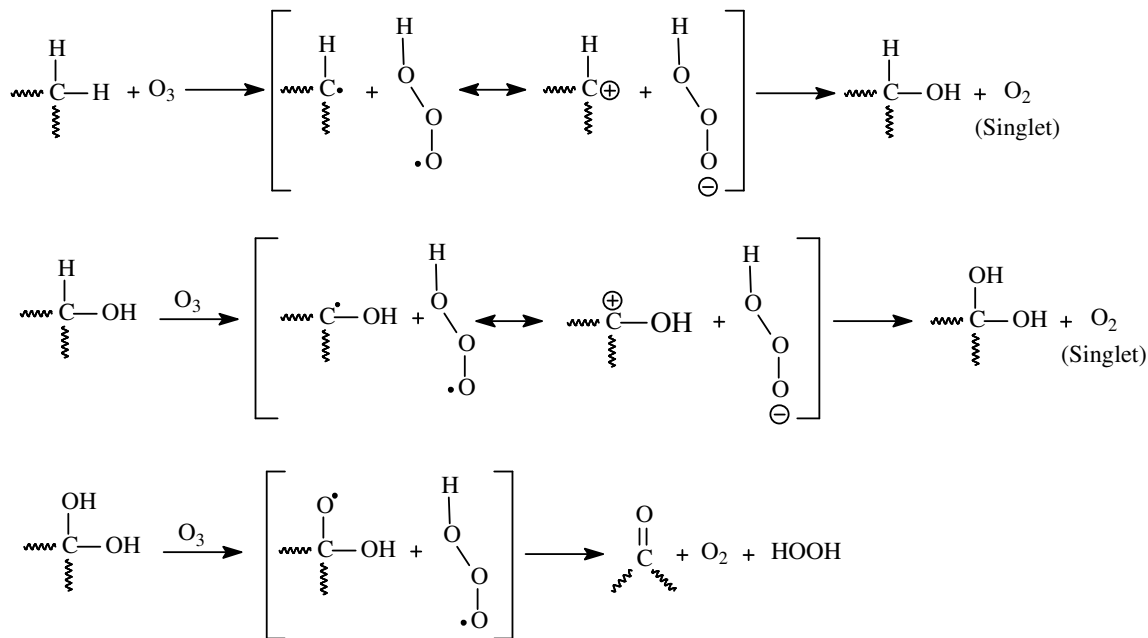


Scheme 4.1. Initial intermediates in ozonation of alkanes.

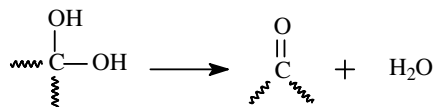
A concerted 1,3-dipolar insertion of ozone into the C-H bond to form ROOOH has been postulated^{134, 299}. A concerted insertion mechanism involving a transition state with the O-H bond formation preceding C-O bond formation was also proposed for ozonations of C-H bonds^{299, 300}. A “radical” mechanism involving hydrogen atom abstraction by ozone to form the radical pair $[R^{\bullet}\cdot\text{OOOH}]$ that collapses to ROOOH has also been suggested³⁴. A hydride ion transfer to form a carbenium ion and hydrotrioxide anion pair $[R^+ \cdot\text{OOOH}]$ was also suggested⁴⁸. The first step in the ozonation of alkanes was reported to have some characteristics of both a radical reaction and some of an insertion reaction. The studies on the ozonation of alkanes still not clear as to the nature of the initial intermediate depicted⁴¹ in the Scheme 4.1.

4.4.1. Formation of alkyl, hydrotrioxide, alkyl hydroxide and alkyl hydroxyl oxide:

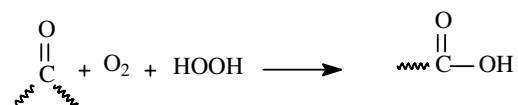
In the ozonation of higher n-alkanes (hexadecane- C_{16} , tetradecane- C_{14} and dodecane- C_{12} compounds), ozone seems to abstract the hydrogen atom from the 4- (or 3- or 2-) positions of the alkanes resulting in the formation of alkyl radical/carbocation with hydrotrioxide radical/ion. The hydrotrioxide formed is highly unstable radical/ion, and dissociates into O_2 and hydroxide radical/ion, which reacts with alkyl radical/carbocation to produce alcohol. The ozone again attacks the carbon atom at which the hydroxide attached and abstracts the remaining hydrogen atom, to form alkyl hydroxide radical/ion. Further the hydrotrioxide, which is unstable gives out oxygen and a hydroxyl radical/ion and combines with alkyl hydroxide to form a dihydroxy compound. The dihydroxy compound can possibly follow two paths. (1) The highly unstable dihydroxy compound can give out water molecule and readily form a ketone with the same number of carbon atoms as the starting material or (2) Ozone abstracts the hydrogen atom from one of the hydroxyl group present and forms the α -hydroxy alkoxide radical/ion. The hydrotrioxide will split into O_2 and hydroxide radical/ion, which further combines with the hydroxide on the carbon atom to form ketone and H_2O_2 . The oxidation of higher alkane with ozone, insertion of an oxygen atom takes place at 4-, 3-, and 2-positions for the higher n-alkanes³⁰¹ (Scheme 4.2).



Conversion of dihydroxy compound to ketone:



Conversion of ketone to carboxylic acid:



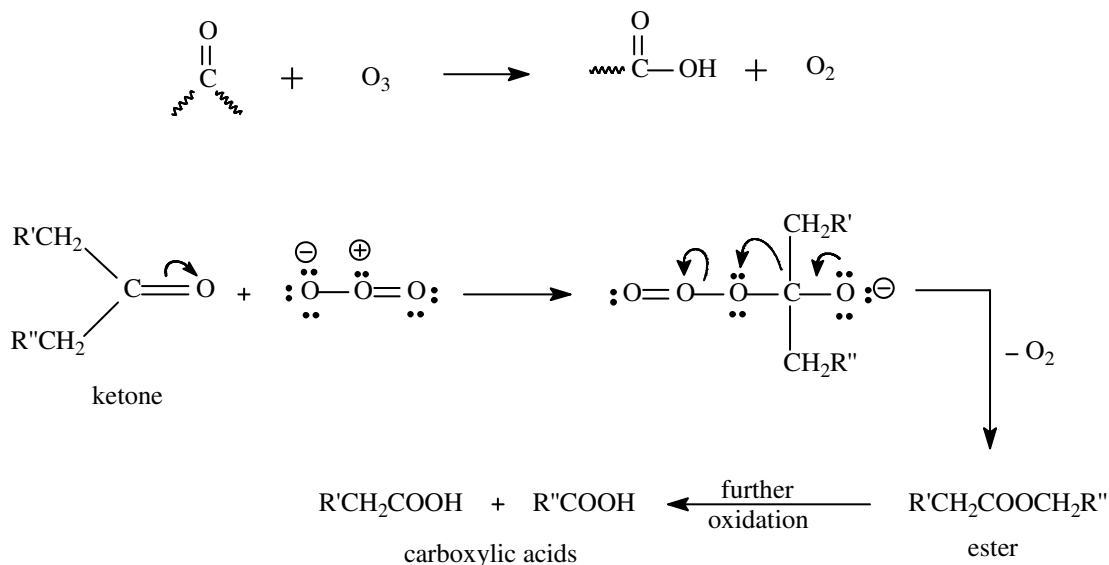
Scheme 4.2. Ozonation mechanism of higher n-alkanes³⁰¹ (C₁₆H₃₄, C₁₄H₃₀ and C₁₂H₂₆).

4.4.2. Formation of carboxylic acids during the ozonation (further oxidation of the products formed):

In presence of strong oxidants, the ketones are known to get oxidized to carboxylic¹³. In current studies too it is noticed from the ozonation of the hexadecane, tetradecane and dodecane that the formation of carboxylic acids follows a similar mechanism to that of the product ketone formed. The carboxylation reactions were slower than the ozonation reactions with aldehydes. Bailey¹³ reported that the formation of adipic acid from cyclohexanone, pentadecanedioic acid from cyclopentadecanone, and acetic acid and propionic acids from diethyl ketone upon ozonation. The possibility of ozone to react as nucleophilic reagent was suggested, nucleophilic attack by

ozone on ketone to produce an ester, followed by the formation of carboxylic acids¹³ (Scheme 4.3).

Briner and coworkers have found that the results of oxidation of propane, butane, hexane, heptane, octane and other alkanes by ozone-oxygen mixtures parallel the results of the similar oxidations of aldehydes¹³, with the exception that higher temperatures are required for the occurrence of reaction (150-400 °C).



where $\text{R}' = \text{R}'' = \text{alkyl group}$

For 4-hexadecanone $\text{R}' = \text{CH}_3(\text{CH}_2)_{10}-$ $\text{R}'' = \text{CH}_3\text{CH}_2-$

For 3-hexadecanone $\text{R}' = \text{CH}_3(\text{CH}_2)_{11}-$ $\text{R}'' = \text{CH}_3-$

Scheme 4.3. Oxidation of ketones to carboxylic acids with ozone.

The product ketone formed from the ozonation reaction on further oxidation with ozone forms a carbonyl radical/ion and hydrotrioxide radical/ion by the attack of ozone on C-C bond (containing oxygen atom). The carbonyl cation is in resonance with acylium ion, which results carboxylic acid by combining with hydroxide radical/ion (which is formed from the dissociation of hydrotrioxide). Tridecanoic (major product, steric effect) and dodecanoic acid formation is possibly due to the further oxidation of 4-ketone / 3-ketone as shown in Scheme 4.3 [Appendix Figs. (i) and (j)]. Similarly in the oxidation of the 3-ketone, ethanoic acid and tetradecanoic acid is observed.

Ozonation of alkanes involves “hydride abstraction” even when tertiary C-H bonds are involved, as protolysis (alkylolysis) of the C-H bond from the front side via formation of a penta-coordinated, three-center bonded carbonium ion. Whereas the process formally results in the transfer of the hydrogen atom with its bonding electron pair, the overall process is better described as just “hydrogen transfer”. Transfer of alkyl groups involving C-C bond protolysis takes place in a similar fashion. The C-C and C-H single bonds of all types (i.e., tertiary, secondary, or primary) show substantial general reactivity in electrophilic reactions such as protolytic processes. Penta-coordinated carbonium ion formation, with subsequent cleavage to trivalent carbenium ions, satisfactorily explains the mechanism of acid-catalysed saturated hydrocarbon transformation reactions. These include isomerizations (involving hydrogen and alkyl shifts), fragmentations, and alkylations. This concept supplements Whitemore’s and Bartlett’s mechanisms where trivalent carbenium ion processes (frequently associated with subsequent deprotonation leading to olefin formation) were exclusively involved. At the same time the work of Olah *et al*⁶¹ substantially extends the scope and understanding of electrophilic reactions based on the realization that the general electron-donor ability of single bonds (shared electron pairs) eventually may equal the importance of lone-electron pairs (unshared electron pairs, Lewis bases)⁶¹.

Under the natural conditions a soil *Arthrobacter* species isolated from Oregon soil was also reported to transform n-hexadecane to a series of ketonic products, the 2-, 3-, and 4-hexadecanones, with evidence for accumulation of 2- and 3- hexadecanols as oxidative intermediates when yeast extract or peptone was used as a growth substrate³⁰².

4.5. Ozonation of n-hexadecane in flat bottom flask under solvent free conditions:

Ozonation of n-hexadecane (25 mL) was carried out at normal temperature (20 ± 1 °C) and pressure conditions using 20.41 mg L⁻¹ of ozone concentration (ozonator voltage at 140 V and 1 LPM oxygen flow rate). Percentage conversion increased with the duration of ozonation, from 4 to 31 (Fig. 4.7). The percent selectivity for the 4-hexadecanone increased during the first 12 h, 57, but decreased with further exposure up to 18 to 24 h due to the oxidation of the starting material and further oxidation of the products 4-, 3- and 2-hexadecanone took place. 3-Hexadecanone percentage selectivity also increased up to 12 h, 12% and decreased from 12 h, 18 h and 24 h continuously. The percentage selectivity for the 2-hexadecanone also decreased during 3 h to 24 h, from 15 to 11 as summarised in Table 4.1.

Table 4.1. Percentage conversion and selectivity in the uncatalysed ozonation of n-hexadecane in flat bottom flask.

Ozonation Time, h	% Conversion ^a	% Selectivity ^b				
		4-Hexa-decanone	3-Hexa-decanone	2-Hexa-decanone	X _{COOH}	Unidentified products ^c
3	4	54	10	15	18	3
6	8	55	12	14	12	5
12	14	57	12	13	11	8
18	24	53	11	12	14	10
24	31	52	11	11	14	12

^a% Conversion – based on the peak areas calculated from the GC/GC-MS chromatogram.

% Conversion = (Peak area of products / Total peak area in the chromatogram) x 100.

^b% Selectivity – based on the amount of product formed in percent out of the total conversion.

% Selectivity = (the amount of the product formed / total amount of substrate converted) x 100.

^c Unidentified Products – The group of compounds which were unidentified.

X_{COOH} – Carboxylic acids.

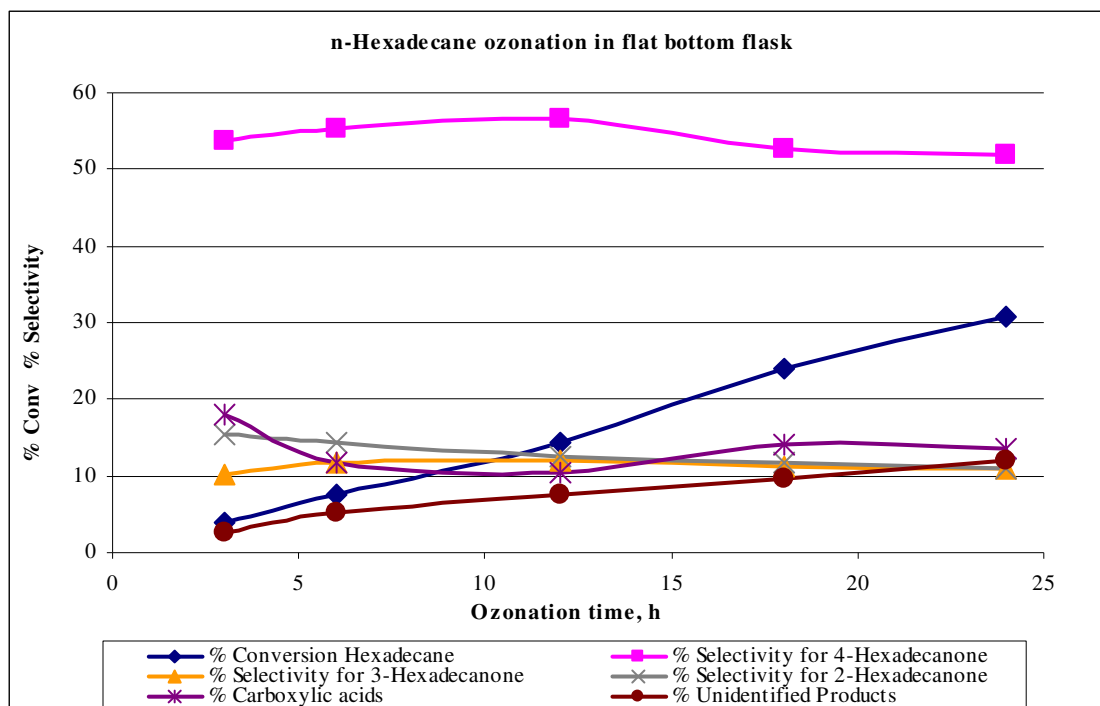


Figure 4.7. n-Hexadecane ozonation in flat bottom flask.

The product ketone forms a carbonyl radical/ion and hydrotrioxide radical/ion on further oxidation with ozone. The attack of ozone on C-C bond (containing oxygen atom) was well explained by Bailey³. The formation of carboxylic acids by further oxidation of products 4-, 3- and 2-hexadecanone is illustrated in Scheme 4.3. The percentage of carboxylic acids (early group of eluted compounds in gas chromatograms) decreased from 3 to 12 h (18-11%) of the starting material, but increased from 12 to 24 h (11 to 14%) as the further oxidation and products took place. The unidentified products (expressed as late group in gas chromatogram) which were not identified, increased with duration of ozonation, 3 to 24 h, from 3 to 12% as the oxidation of the ketone isomer products and the carboxylic acids takes place (Fig. 4.7).

4.6. Ozonation of n-hexadecane in long column reactor:

Ozonation of n-hexadecane (25 mL) was carried out in a long column reactor at room temperature (20 ± 1 °C) with 20.41 mg L^{-1} concentration of ozone (ozonator voltage at 140 V and 1 LPM oxygen flow rate) and with 25 mL of the substrate under solvent free conditions. Table 4.2 summarises the percent conversion and selectivities of different products as function of ozonation time. Figure 4.8 summarises the results for 24 h ozonation of n-hexadecane, it was clear that the percentage conversion increased between 3 to 24 h, from 7 to 48. Using the flat bottom flask, the percentage conversion for the same duration was 31 only. The better yield is due to the ozone contact and efficiency in the reaction was more with the long column reactor (detailed discussion in Chapter II, Section 2.3).

Table 4.2. Percentage conversion and selectivity in the uncatalysed ozonation of n-hexadecane in long column.

Ozonation Time, h	% Conversion	%Selectivity				
		4-Hexa-decanone	3-Hexa-decanone	2-Hexa-decanone	X _{COOH}	Unidentified products ^c
3	7	56	13	13	16	1
6	14	58	13	13	9	8
12	24	57	12	12	10	10
18	42	47	10	10	17	16
24	48	47	10	9	16	17

The initial selectivity of 4-hexadecanone was marginally higher in long column reactor (56%) than the flat bottom flask, which was 54%, but the selectivity towards the 4-hexadecanone decreased with 12, 18 and 24 h ozonation to 47%. 3-Hexadecanone selectivity was decreased during 3 to 24 h of ozonation, from 13 to 10%. The 2-hexadecanone selectivity was also decreased during 3 to 24 h of ozonation (13 to 9%). The overlapped selectivity curves of minor products 3- and 2-hexadecanone was observed in the Fig. 4.8 due to the same percentage conversion during 24 h ozonation. The percentage formation of carboxylic acids was increased from 6 to 24 h (9 to 16) as the ozonation of the products 4-, 3- and 2-hexadecanone with the starting material n-hexadecane took place as illustrated in Scheme 4.3. There was an increase in the unidentified products with the ozonation time, from 1 to 17%, with the oxidation of the ketone isomer products and with the carboxylic acids formation (Table 4.2).

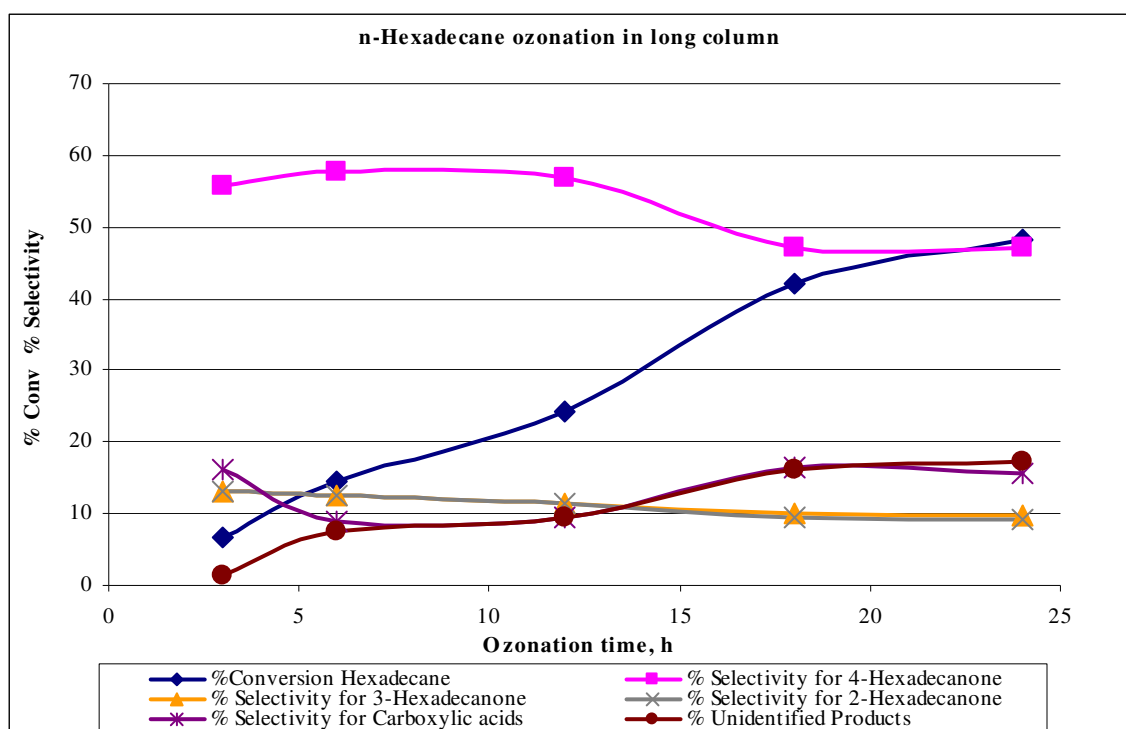


Figure 4.8. n-Hexadecane ozonation in long column.

From the uncatalysed ozonation of n-hexadecane, it was evident that the O_3 is capably attacking the substrate resulting in the formation of 4-hexadecanone, 3-hexadecanone and 2-hexadecanone as main products and it is well documented (illustrated in Scheme 4.3), after 3 h of ozonation the carboxylic group and unidentified products amount also observed increasing. Upon longer duration of ozonation some keto compounds get further oxidised to carboxylic acids and other unidentified products

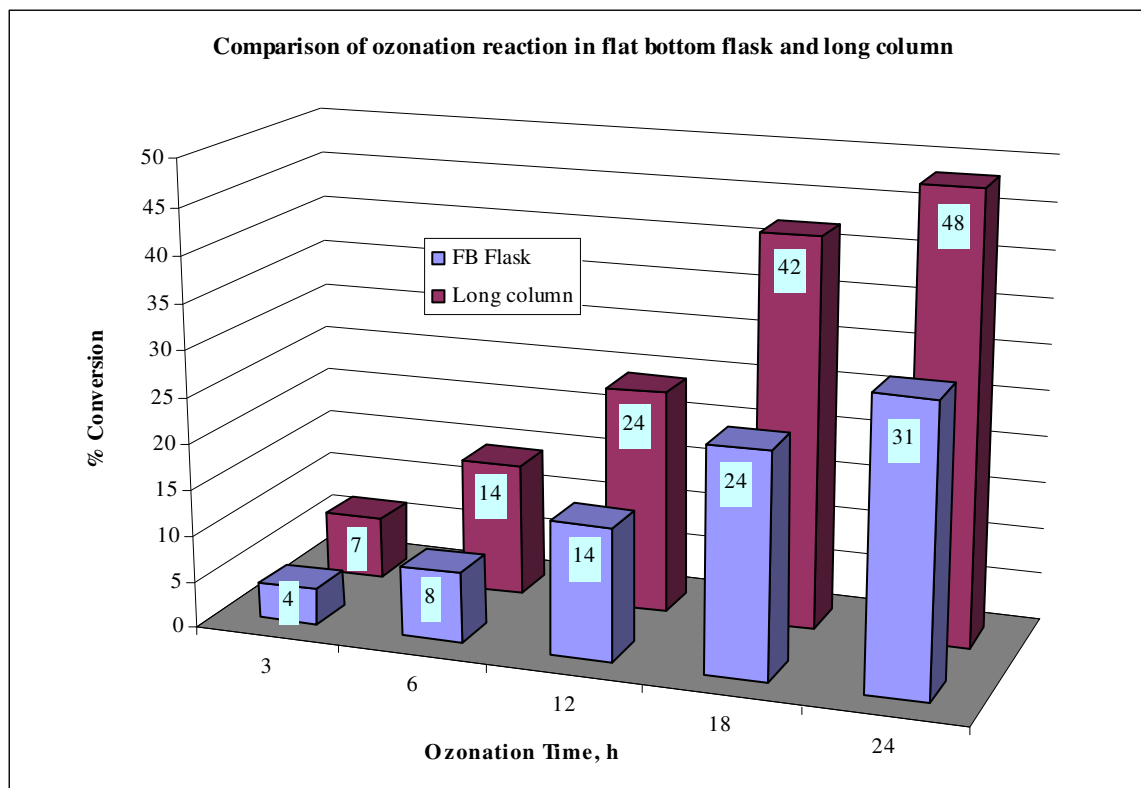


Figure 4.9. Comparison of ozonation reaction in flat bottom flask and long column.

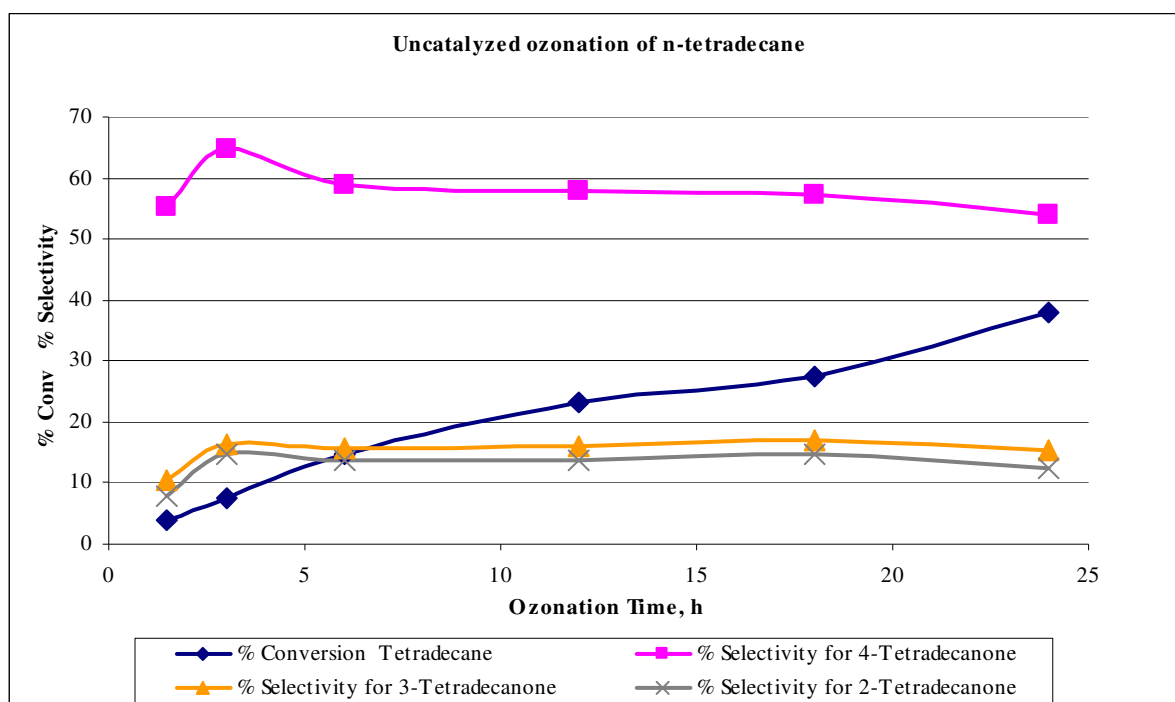
The results of the ozone initiated conversion of n-hexadecane using the flat bottom flask and long column reactors are shown in Fig. 4.9. An observation of the figure shows that higher conversions were achieved in the long column reactor, which was due to enhanced contact between the ozone and reactants. All the rest of experiments were conducted in the long column reactor only.

4.7. Ozonation of n-tetradecane under similar conditions as for n-hexadecane:

Ozonation of n-tetradecane (18 mL) was carried out at room temperature (20 ± 1 °C) with 20.41 mg L^{-1} ozone concentration (ozonator voltage at 140 V and 1 LPM oxygen flow rate). Percentage conversion increased from 7 to 38, for 3 to 24 h ozonation. The main products with n-tetradecane as the substrate were the isomers 4-, 3- and 2-tetradecanones. The selectivity in favour of 4-tetradecanone decreased during 3 to 24 h ozonation, from 65 to 54%, which showed the further oxidation of the product 4-tetradecanone took place as shown in Scheme 4.3 and the ketone oxidation by ozone was well documented³.

Table 4.3. Uncatalysed ozonation of n-tetradecane.

Ozonation Time, h	% Conversion	%Selectivity		
		4-Tetradecanone	3-Tetradecanone	2-Tetradecanone
1.5	4	55	11	8
3	7	65	16	15
6	15	59	16	14
12	23	58	16	14
18	27	57	17	15
24	38	54	15	12

**Figure 4.10.** Uncatalysed ozonation of n-tetradecane.

3-Tetradecanone selectivity was decreased during 3 to 24 h of ozonation (Table 4.3), from 16 to 15%. 2-Tetradecanone selectivity was also decreased during 3 to 24 h ozonation, from 15 to 12% (Fig. 4.10) as the further oxidation of the products took place with 3- and 2-tetradecanone as well.

The formation of 3- and 2-dodecanone was more when compared to that of the hexadecanones, shows the ozone is more skilled in the oxidation of alkanes with lower chain lengths.

4.8. Ozonation of n-dodecane under similar conditions as for n-hexadecane:

Ozonation of n-dodecane (18 mL) was carried out under similar conditions as the other two hydrocarbons. The selectivity for 4-dodecanone decreased during 3 to 18 h, 53 to 40%, which indicated that further oxidation of the product 4-dodecanone. 3-Dodecanone selectivity was also decreased during 6 to 18 h of ozonation, from 21 to 16%, and the selectivity for 2-dodecanone was decreased from 3 to 18 h, 17 to 13% (Table 4.4) as further oxidation of the products took place with 3- and 2-dodecanone as well. The percentage conversion increased with the duration of ozonation from 8 to 54 as shown in Fig. 4.11. Interestingly the conversion efficiency was low initially and increased significantly from 14 to 54% for 6 to 18 h of ozonation. It was observed that the formation of 3- and 2-dodecanone was formed in greater amount as compared to that of the tetradecanones. It indicated that the ozone is more selective in the oxidation of alkanes with lower chain lengths.

Table 4.4. Uncatalysed ozonation of n-dodecane.

Ozonation Time, h	% Conversion	%Selectivity		
		4-Dodecanone	3-Dodecanone	2-Dodecanone
0.75	2	53	20	20
1.5	4	56	22	17
2.3	5	60	20	18
3	8	53	21	17
6	14	50	21	15
18	54	40	16	13

Upon the reaction of ozone with the substrate and the formed products were 4-, 3-, 2-ketones similar to the other two hydrocarbons. The carboxylic acids were formed by the further oxidation of the products (ketones) in the reaction.

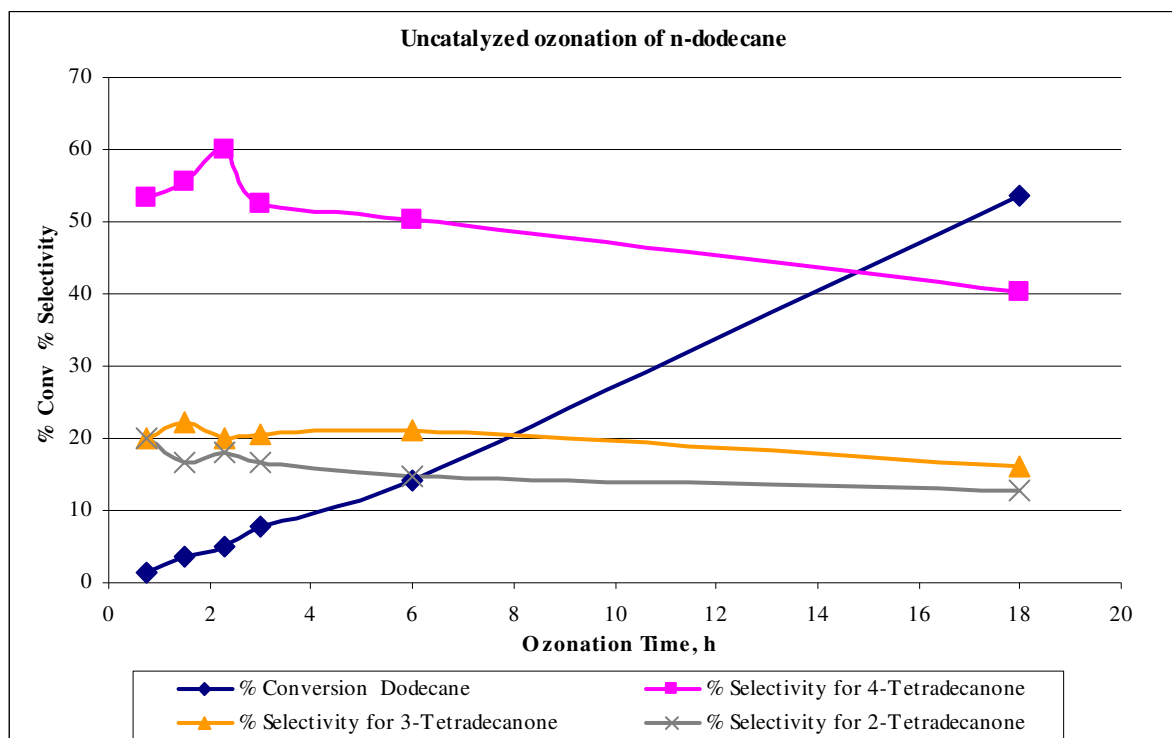


Figure 4.11. Uncatalysed ozonation of n-dodecane.

The carboxylic acid formation possibly follows the mechanism involving ester as an intermediate, followed by the scission of --COOC-- bond with $>\text{C=O}$ on each fragment as illustrated in Scheme 4.3. The formation of different carboxylic acids are probably (Scheme 4.3) due to the breakage of the $\text{--C}_3\text{--O--O--C}_4\text{--}$, $\text{--C}_2\text{--O--O--C}_3\text{--}$ bond and $\text{--C}_1\text{--O--O--C}_2\text{--}$ bonds of 4-, 3- and 2-hexadecanone respectively.

4.9. Ozonation of n-hexadecane with activated charcoal as catalyst:

The ozone initiated oxidation of hexadecane was studied in a long column with 5% w/v of the catalyst activated charcoal. The catalyst was well dispersed in the starting material by means of stirring. The reaction was carried out at temperature 20 ± 1 °C with 20.41 mg L^{-1} ozone concentration (ozonator voltage at 140 V and 1 LPM oxygen flow rate). With the ozonation time the conversion increased during 3 to 24 h, from 4 to 45% as summarised in Table 4.5. Selectivity in favour of 4-hexadecanone was increased for the first 12 h of ozonation, 40 to 42% and then declined to 37% during 24 h ozonation, as the oxidation of the substrate as well as the products occurred, which resulted the decrease in the selectivity for 4-, 3-, and 2-hexadecanones. The selectivity for 3-hexadecanone, first decreased up to 6 h and then increased to 14% on further

ozonation up to 24 h. 2-Hexadecanone selectivity was decreased during first 12 h, and then increased slightly with further ozonation as illustrated in Fig. 4.12.

Table 4.5. Ozonation of n-hexadecane with activated charcoal.

Ozonation Time, h	% Conversion	% Selectivity		
		4- Hexadecanone	3- Hexadecanone	2- Hexadecanone
3	4	40	17	12
6	15	41	11	11
12	25	42	12	10
18	39	38	14	11
24	45	37	14	14

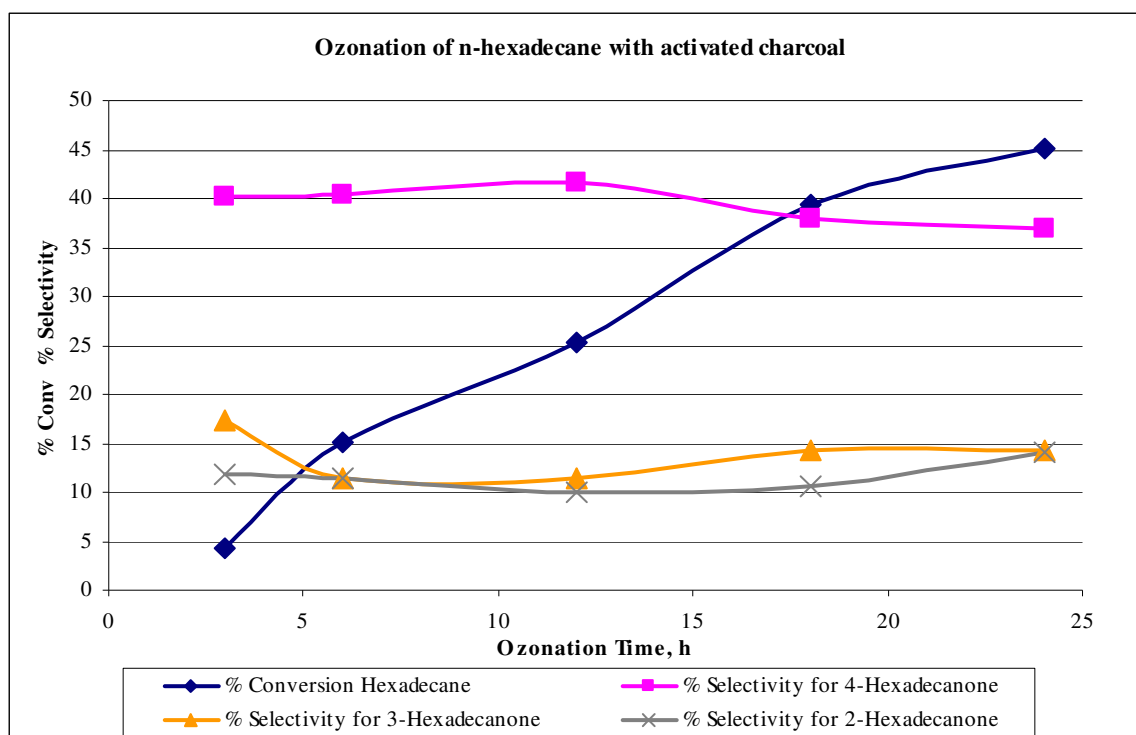


Figure 4.12. Ozonation of n-hexadecane with activated charcoal.

Activated carbon acts not only as the adsorbent, but also as a catalyst by facilitating the reactions between ozone and the substrate on its surface. The catalytic efficiency of activated charcoal for ozone initiated oxidation is reported by Kaptijin¹²⁶, Logemann and Annee³⁰³. They have reported that the radical scavengers such as (bi)carbonates had marginal effect on the charcoal facilitated oxidations. The efficiency of catalytic ozonation¹⁶⁵ was found equally effective under both highly acidic conditions (when HO[•] radicals are not formed) as well as under highly alkaline conditions. This suggests that the catalysis in presence of activated charcoal is through the formation of highly reactive intermediates, other than the HO[•] radicals. The formation of highly active species such as O-radicals on the surface of the catalyst are considered by several researchers^{126, 303}.

The ozone decomposition processes involves different carbon sites and metal sites. The basic Lewis sites are thought to be responsible for ozone decomposition on activated carbon. This is differing with the mechanisms proposed for ozone decomposition on metal oxide surfaces, in which case, strong Lewis acid sites are thought to be active sites. The ability of ozone to react with both the acidic and basic surface sites of the catalysts is a consequence of its resonance structure¹⁵⁹ (Chapter I, eqn. 1.40).

4.9.1. Comparison of uncatalysed n-hexadecane ozonation reaction and reactions in presence of activated charcoal:

The results illustrated in Fig. 4.13 indicate that the presence of 5% (w/v) activated charcoal has exerted only marginal changes, either in the % conversion or in the selectivities of the products compared to the uncatalysed oxidations. The uncatalysed ozonation yielded more conversion upon 24 h (48%), but, activated charcoal gave a conversion for 6 and 12 h (15 and 25%), which were little higher than prior reaction. The conversion rate for the uncatalysed ozonation improved with the increased duration of ozonation (during 18 to 24 h). The ability of ozone to react with the hydrocarbon in presence of activated charcoal is found to be same as in the case of uncatalysed ozonation. Due to the same conversion and selectivities observed in uncatalysed and activated charcoal ozonation reactions, the application of new heterogeneous catalysts for this transformation was studied, which is discussed in the subsequent chapters.

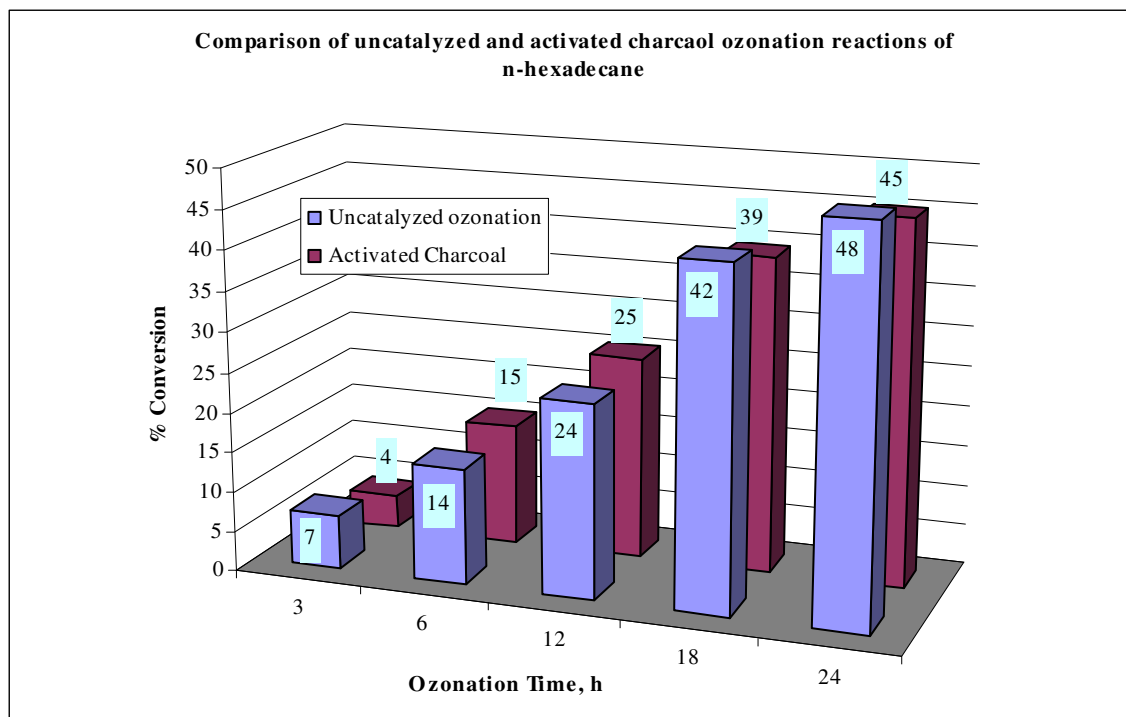


Figure 4.13. Comparison of uncatalysed and activated charcoal ozonation reactions of n-hexadecane.

4.10. Ozonation of n-tetradecane with activated charcoal as catalyst:

The ozonation reaction of n-tetradecane was studied in a long column reactor with 5% w/v of the catalyst activated charcoal under the similar reaction conditions as for n-hexadecane. The catalyst was well dispersed in the starting material by means of stirring.

Table 4.6. Ozonation of n-tetradecane with activated charcoal.

Ozonation Time, h	% Conversion	% Selectivity		
		4-Tetradecanone	3-Tetradecanone	2-Tetradecanone
3	3	61	15	12
6	8	64	17	14
12	18	64	17	15
18	25	61	18	14
24	31	59	17	13

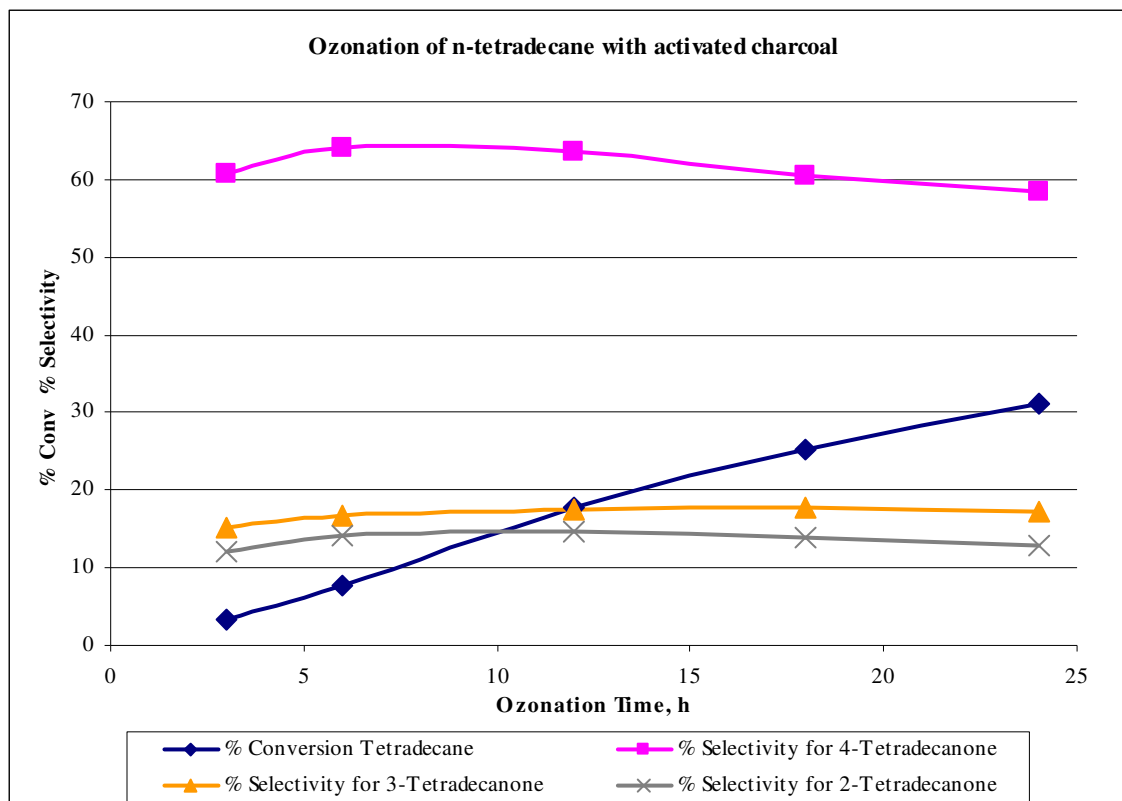


Figure 4.14. Ozonation of n-tetradecane with activated charcoal.

The conversion increased during the reaction time 3 to 24 h, from 3 to 31%. 4-Tetradecanone selectivity was increased for the first 6 h of ozonation, from 61 to 64% as summarized in the Table 4.6. It was observed that selectivity decreased from 12 to 24 h, as the oxidation of the substrate as well as the products took place, as a result the selectivity of the 4-, 3-, and 2-tetradecanone were decreased. 3-Tetradecanone selectivity was increased in the first 18 h (18%) and then decreased to 17% after 24 h. The selectivity in favour of 2-tetradecanone was increased up to 12 h and then decreased up to 24 h as shown in Fig. 4.14.

4.10.1. Comparison of uncatalysed n-hexadecane ozonation reaction and reactions in presence of activated charcoal:

The results illustrated in Fig. 4.15 indicate that the presence of 5% w/v activated charcoal has exerted only marginal changes, either in the % conversion or in the selectivities of the products compared to the uncatalysed oxidations, where the uncatalysed ozonation reaction yielded higher conversion than ozonation with activated charcoal. The conversion of n-tetradecane was more in the uncatalysed reaction (15%) than that of the activated charcoal, which was 8%. The difference

in conversion at 18 h ozonation was identical in both the cases (uncatalysed-27%, activated charcoal-25%).

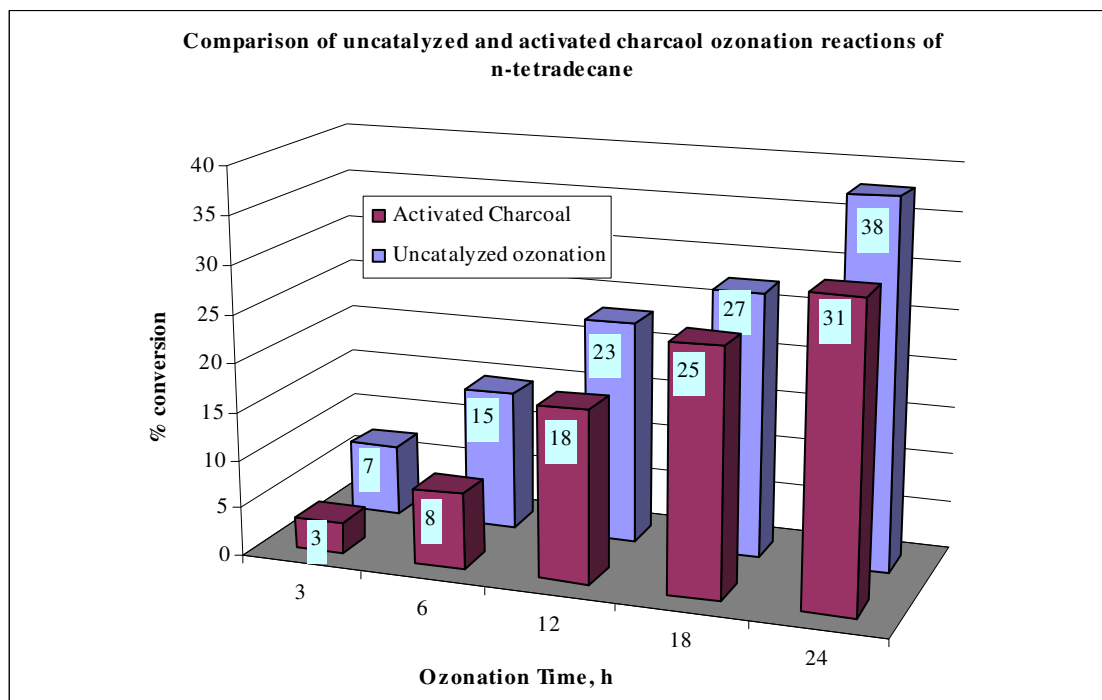


Figure 4.15. Comparison of uncatalysed and activated charcoal ozonation reactions of n-tetradecane.

Ozonation for longer duration up to 24 h resulted lower conversion with activated charcoal, which was 31% than that of the uncatalysed (37.9%). In presence of activated charcoal the reaction was retarded. In the ozonation of tetradecane, the difference between the percentage conversions was more with activated charcoal. In the case of hexadecane ozonation the difference between the conversions was close.

4.11. Ozonation of n-dodecane with activated charcoal as catalyst:

The ozonation reaction of n-dodecane was studied in a long column reactor with 5% w/v of the catalyst activated charcoal under the similar reaction conditions as for n-hexadecane. The catalyst was well dispersed in the starting material by means of stirring. The conversion increased with the ozonation time from 3 to 24 h (3 to 28%) as summarised in Table 4.7. The selectivity in favour of 4-dodecanone was decreased from 6 to 24 h ozonation, 62 to 50%. The selectivities for 3- and 2-dodecanone were increased for the first 12 h of ozonation duration and then decreased up to 24 h as shown in Fig. 4.16. The decrease in the selectivity of 4-, 3- and 2-

dodecanone was because of the oxidation of the substrate as well as the products took place as shown in the Scheme 4.3.

Table 4.7. Ozonation of n-dodecane with activated charcoal.

Ozonation Time, h	% Conversion	% Selectivity		
		4-Dodecanone	3-Dodecanone	2-Dodecanone
3	3	62	19	15
6	5	59	20	17
12	13	57	21	18
18	19	56	20	18
24	28	50	21	15

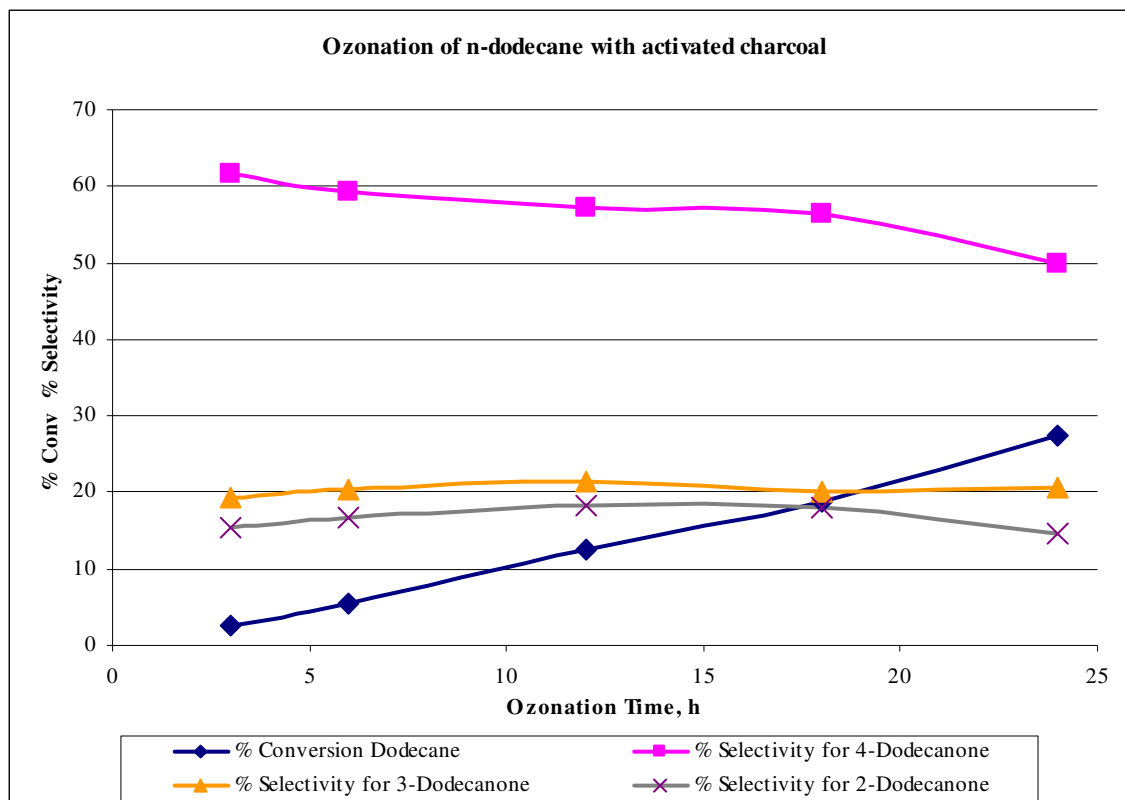


Figure 4.16. Ozonation of n-dodecane with activated charcoal.

The uncatalysed ozonation of higher n-alkanes (hexadecane, tetradecane and dodecane) yielded more conversion than the ozonation reaction with activated charcoal as compared from the Tables 4.2, 4.5; 4.3, 4.6 and 4.4, 4.7.

Beltrán *et al*³⁰⁴ found that the presence of activated carbon during the ozonation process accelerates the ozone decomposition reactions. Activated carbon acts as the adsorbent as well as a catalyst in promoting ozone initiated oxidation. Several researchers^{126, 303} found that the catalytic ozonation process using activated carbon requires little amount of ozone. The reaction mainly takes place on the surface of the catalyst. Legube *et al*¹⁶⁵ found the efficiency of catalytic ozonation is equally effective under both highly acidic conditions where HO• radicals are not formed and in highly alkaline conditions. This suggests that highly active species such as O-radicals are formed on the surface of the catalyst^{126, 303} other than HO• radicals. As discussed in the Section 4.9, it has to be highlighted here that different sites of carbon are involved in the process of ozone decomposition. As ozone exists in resonance structures, it is able to react with both acidic and basic surface sites of the catalysts^{126, 303, 165}.

There are generally three possible mechanisms of catalytic ozonation in heterogeneous systems, which are (1) chemisorption of ozone on the catalyst surface leading to the formation of active species which react with non-chemisorbed organic molecule, (2) chemisorption of organic molecules (associative or dissociative) on the catalytic surface and its further reaction with gaseous or aqueous ozone and (3) chemisorption of both ozone and organic molecules and the subsequent interaction between chemisorbed species.

During oxidation the catalytic activity of the carbon declines by the action of ozone, because of an increase in the number of surface oxygenated groups of acidic character. These functional (electron-withdrawing) groups reduce the reductive properties of the activated carbon and, therefore, its reactivity to ozone, preventing its decomposition. This is in good agreement with the results obtained by Sánchez-Polo and Rivera-Utrilla³⁰⁵.

Guiliano *et al*³⁰⁶ studied the photo-oxidation of n-pentadecane, n-hexadecane, n-dodecane, n-nonadecane, n-eicosane and n-docosane under simulated environmental conditions with anthraquinone as sensitizer, lead to the formation of ketones and alcohols with the same number of carbon atoms as the starting alkane. The formation of the keto-, alcohol isomers and a series of minor products from the saturated hydrocarbons is illustrated in the Scheme 4.4.



The activated charcoal as a catalyst in the ozonation of higher alkanes showed poor activity. Hence the other catalyst materials like silica gel, vanadium phosphorous oxides (VPO), Pd-, Ni- and V- loaded γ -Al₂O₃ catalysts, Pd-, Ni-, V- and U-loaded microporous uni-dimensional and 3-dimensional zeolites like Na-Y, ZSM-5 Si/Al-30, mesoporous Al-MCM-41 Si/Al-90 and Al-MCM-41 Si/Al-60 catalysts were employed to improve the activity on conversion and selectivity of the catalytic ozonation of higher alkanes.

CHAPTER - V

OZONATION OF HIGHER n-ALKANES WITH SILICA GEL, VPO AND METAL SUPPORTED γ -Al₂O₃ CATALYSTS

5.0. Introduction:

The catalysed oxidation of higher alkanes (n-hexadecane, tetradecane and dodecane) with ozone as oxidant is discussed in this chapter. Mazur *et al*¹³⁴ carried out dry ozonation on a number of aliphatic hydrocarbons by adsorbing the substrates on silica gel (1%), ozone passed for 2 h at -45 °C. They showed the cleavage of C-C bonds by a direct insertion of ozone into these bonds and also showed the formation of large amounts of ketones originated from the cleavage of alkyl groups. Mazur *et al*¹³⁴ have proposed that the mechanism of C-H bond ozonation involves the formation of an ozone-alkane complex which decomposes electrophilically inserting an oxygen atom into the C-H bond.

The possibility of the application of parent alumina or alumina supported with metals or metal oxides as catalysts for the ozonation process was investigated by several researchers¹⁵⁹. The properties of alumina like high surface area, mechanical strength and thermal stability has found several applications as an adsorbent and as catalyst. The acid-base properties of alumina are the main reason for its wide usage^{137, 150, 160}.

The scope of different materials namely silica gel, vanadium phosphorous oxides (VPO), Pd-, Ni- and V- loaded γ -Al₂O₃ as catalysts is explored in this chapter. For all the catalytic ozonation studies 5% w/v catalysts were employed. The catalyst in the fine powder form was dispersed well in the reaction medium by means of a magnetic stirrer. The catalytic ozonation experimental conditions and batch reaction setup were similar as discussed in the Chapter II (Section 2.15 and Fig. 2.9). All the experiments were carried out in replicate.

5.1. Ozonation in presence of silica gel or VPO catalysts:

5.1.1. Ozonation of n-hexadecane with silica gel:

The results of ozonation of n-hexadecane in presence of silica gel as function of time are summarised in Table 5.1. Further the main reaction products in presence of silica gel were 4-, 3- and 2-hexadecanones similar to the uncatalysed oxidation reactions. The extent of conversion and selectivities towards various products varied and are illustrated in Fig. 5.1. There is an increase in conversion of hexadecane into isomers of hexadecanones and carboxylic acids relative to that of uncatalysed oxidation. The conversion increased as function of time from 8 (3 h) to 48% (24 h). The selectivity towards the 4-hexadecanone during the first 3 h was 62% and decreased on further exposure to ozone up to 12 h (58%). Further oxidation took place as a result the isomer products formed in the ozonation oxidized into different carboxylic acids depending

on the ketone isomer. 4-Hexadecanone selectivity after 24 h ozonation was decreased to 48%. There was a small difference in the overall selectivities in favour of 3- and 2-hexadecanone during 24 h ozonation as shown in Table 5.1.

Table 5.1. Percentage conversion and selectivities in the ozonation of n-hexadecane with silica gel as catalyst.

Ozonation Time, h	% Conversion	% Selectivity		
		4-Hexadecanone	3-Hexadecanone	2-Hexadecanone
3	8	62	11	10
6	20	58	8	7
12	31	58	12	10
18	40	50	11	9
24	48	48	10	9

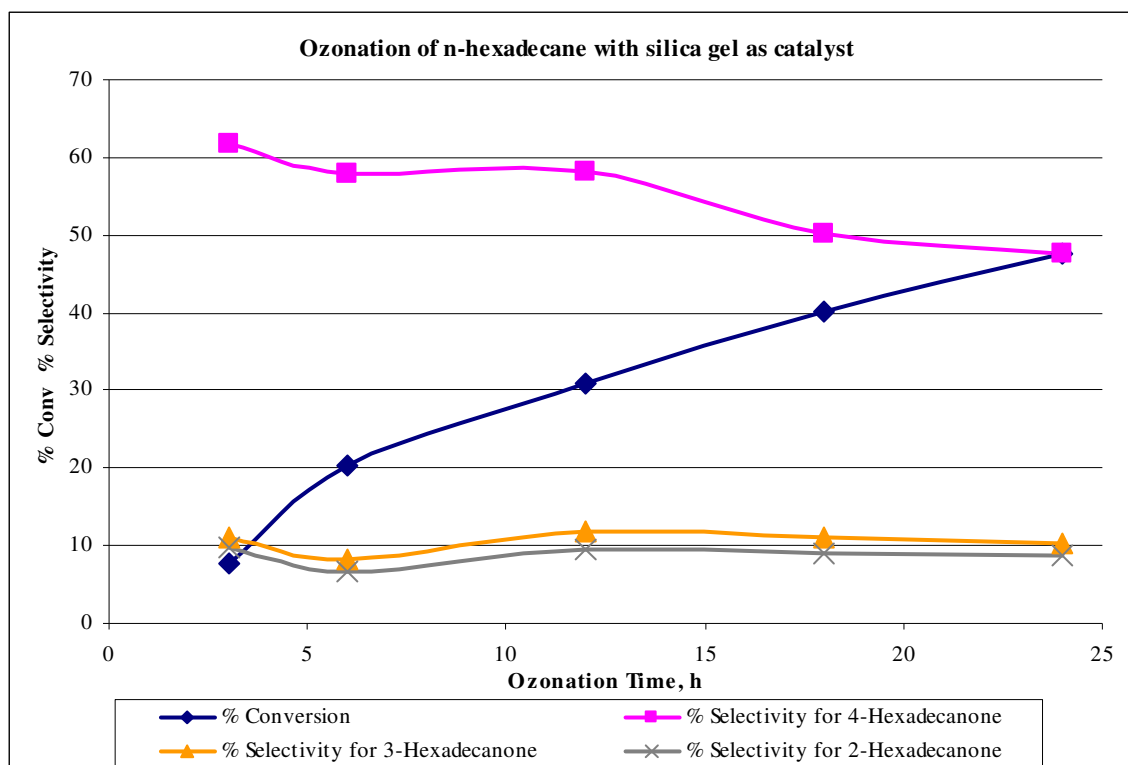


Figure 5.1. Ozonation of n-hexadecane with silica gel as catalyst.

Ozone reacts slowly with saturated hydrocarbons inserting oxygen atoms into their C-H bonds, resulting in alcohols and then to ketones³⁰¹. The mechanism of C-H bond ozonation involves the

formation of an ozone-alkane complex which decomposes electrophilically inserting an oxygen atom into the C-H bond lead to the formation of large amounts of ketones. Mazur *et al*^{41, 134} results also supports the formation of ketones as main products in the ozonation of C-H bonds of saturated hydrocarbons (Schemes 1.4 and 1.25, Chapter I). Beckwith *et al*⁵⁸ described the particularity of the high regioselectivity of the reaction, consistent with that of dry ozonation which involves attack by gaseous ozone at positions remote from the binding site on substrate adsorbed as a monolayer. There is a remarkable similarity between the results of dry ozonation and oxidation in presence of silica gel at normal reaction conditions indicate that ozonation may have considerable utility for the synthesis of an oxygen substituted products.

5.1.2. Ozonation of n-hexadecane with VPO:

During the ozonation of n-hexadecane with VPO catalyst the conversion of n-hexadecane gradually increased with the duration of the reaction. The results are summarised in Table 5.2. The selectivity for the 4-hexadecanone with the VPO catalyst was initially 54%, after 24 h ozonation the percentage selectivity was slightly decreased unlike the silica gel as illustrated in Fig. 5.2. The difference between the selectivities in favour of 3- and 2- hexadecanones was observed as less in between 3 to 24 h ozonation that could be possible due to the attack of ozone only on the n-hexadecane and 4-hexadecanone, which lead to carboxylic acids and further degradation took place. The slight drop in the selectivities for 3- and 2-hexadecanones was due to the formation of carboxylic acids on further oxidation up to 24 h as represented in Table 5.2.

Table 5.2. Percentage conversion and selectivities in the ozonation of n-hexadecane with VPO as catalyst.

Ozonation Time, h	% Conversion	% Selectivity		
		4-Hexadecanone	3-Hexadecanone	2-Hexadecanone
3	7	54	11	10
6	14	47	13	10
12	32	44	10	8
18	40	47	10	8
24	46	47	11	8

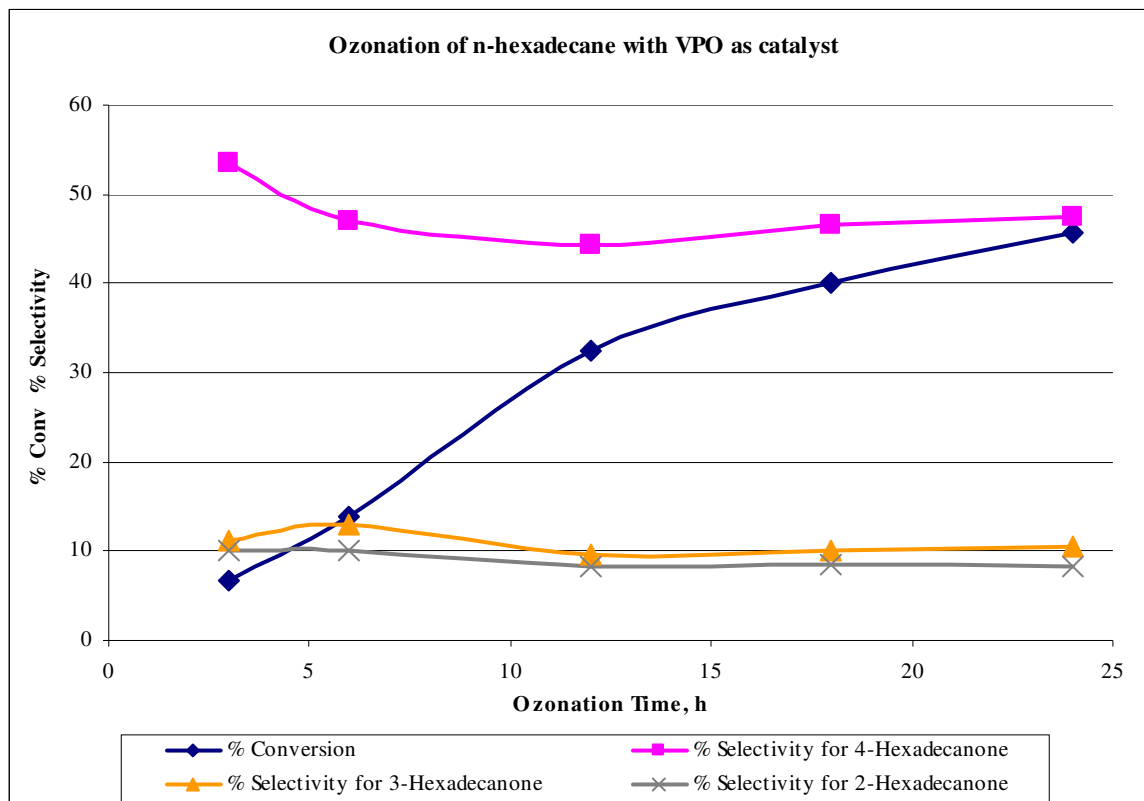


Figure 5.2. Ozonation of n-hexadecane with VPO as catalyst.

The three possible mechanisms in heterogeneous catalytic ozonation are the chemisorption of ozone on the surface of the catalyst leading to the formation of active species which react with non-chemisorbed organic molecule, chemisorbed organic molecules on the catalytic surface and its further reaction with gaseous ozone and the chemisorption of both the ozone/organic molecules with subsequent interaction of the chemisorbed species.

5.1.3. Ozonation of n-tetradecane with silica gel:

The percentage conversion and selectivities in the ozonation of n-tetradecane with silica gel as catalyst are summarised in Table 5.3. During ozone initiated oxidation of the n-tetradecane with silica gel, % conversion increased with ozonation time. Selectivity in favour of 4-tetradecanone increased in the first 6 h of ozonation (69%) and decreased to 60% on 18 to 24 h ozonation duration as shown in Fig. 5.3. Ozone oxidises the adsorbed starting material on the catalyst surface and the direct ozonation of the starting material also takes place. Generally in all the cases after 12 h ozonation duration as the concentration of the products increases, ozone is not being specific about the starting material, it will oxidize the products as well.

Table 5.3. Percentage conversion and selectivities in the ozonation of n-tetradecane with silica gel as catalyst.

Ozonation Time, h	% Conversion	% Selectivity		
		4-Tetradecanone	3-Tetradecanone	2-Tetradecanone
1.5	2	55	10	10
3	4	63	15	13
6	7	69	16	10
18	23	64	17	15
24	30	60	17	13

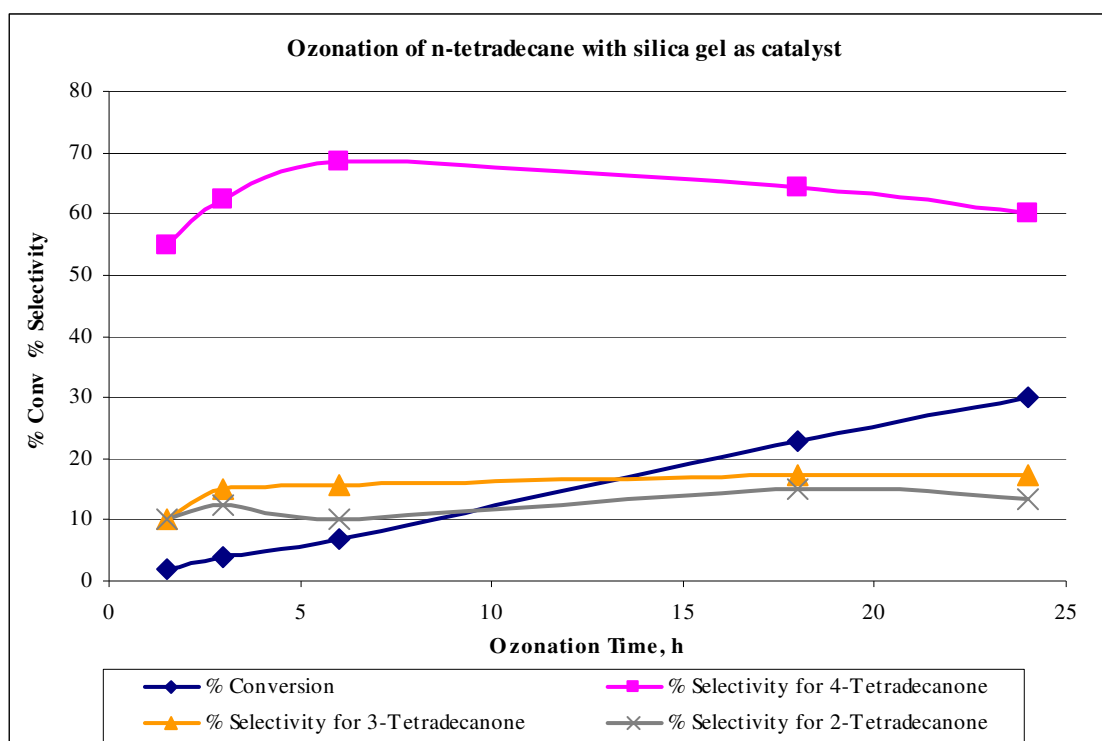


Figure 5.3. Ozonation of n-tetradecane with silica gel as catalyst.

The preference for the 3-tetradecanone was increased gradually on 24 h ozonation to 17% could be due to the chemisorption of both ozone and tetradecane and the subsequent interaction between the chemisorbed species. It can be seen from the Table 5.3, that the formation of 3- and 2-tetradecanones was higher in the case of n-tetradecane than with n-hexadecane ozonation.

5.1.4. Ozonation of n-tetradecane with VPO:

The conversion of n-tetradecane was relatively low when compared with that of silica gel in the ozonation of n-tetradecane with VPO catalyst as the catalyst is being inactive, can be seen from Tables 5.3 and 5.4.

Table 5.4. Percentage conversion and selectivities of the products formed in ozonation of n-tetradecane with VPO as catalyst.

Ozonation Time, h	% Conversion	% Selectivity		
		4-Tetradecanone	3-Tetradecanone	2-Tetradecanone
1.8	2	50	13	13
3	3	63	16	13
12	9	64	17	15
18	15	58	16	14
24	18	61	17	15

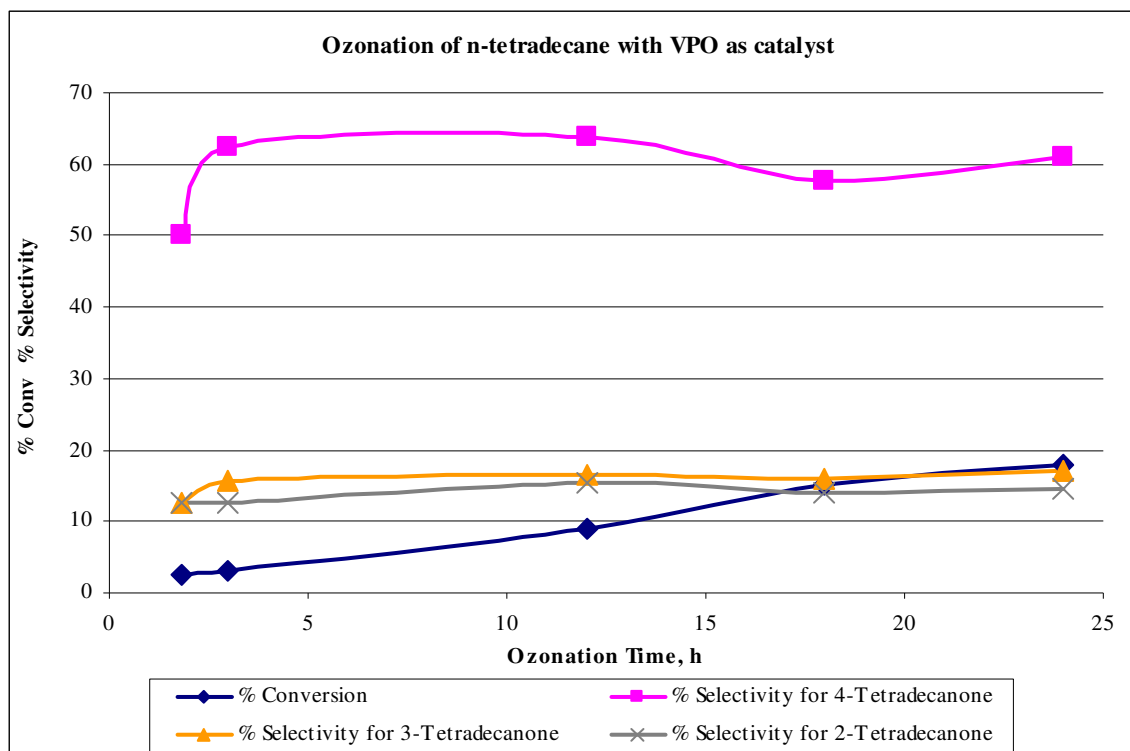


Figure 5.4. Ozonation of n-tetradecane with VPO as catalyst.

Ozonation for a period of 24 h resulted 18% of conversion only, but the selectivities in favour of 4-, 3- and 2-tetradecanone were high when compared with the n-hexadecane results. In the oxidation of alkanes, the lower the chain length of starting material the more efficient is ozone. The selectivities towards 3- and 2-tetradecanone increased steadily up to 24 h ozonation as shown in Fig. 5.4. It can be seen that the formation of the 3- and 2-tetradecanone were much favoured when compared with 3- and 2-hexadecanone on ozonation of hexadecane, ozone is being efficient because of the shorter chain length of n-tetradecane.

5.1.5. Ozonation of n-dodecane with silica gel:

The conversion was gradually increased in the ozonation of n-dodecane with silica gel during 24 h reaction. The percentage conversion and selectivities in the ozone initiated oxidation of n-dodecane are summarised in Table 5.5. The selectivity in favour of 4-dodecanone was observed to be declining from 3 to 24 h ozonation. Whereas, the selectivities for 3-dodecanone were observed to be steady around 20% even after longer exposure to ozone as depicted in Fig. 5.5. From the results in Table 5.5, the selectivities of n-dodecane ozonation with silica gel, it was evident that the formation of isomers 3- and 2-dodecanone were more compared to that of the n-hexadecane. In the oxidation of alkanes, ozone is being efficient with the shorter chain length molecules like n-dodecane.

Table 5.5. Percentage conversion and selectivities in the ozonation of n-dodecane with silica gel as catalyst.

Ozonation Time, h	% Conversion	% Selectivity		
		4-Dodecanone	3-Dodecanone	2-Dodecanone
1.5	2	69	19	13
3	3	62	21	15
6	7	59	21	18
12	15	58	21	17
18	25	58	20	17
24	36	50	20	15

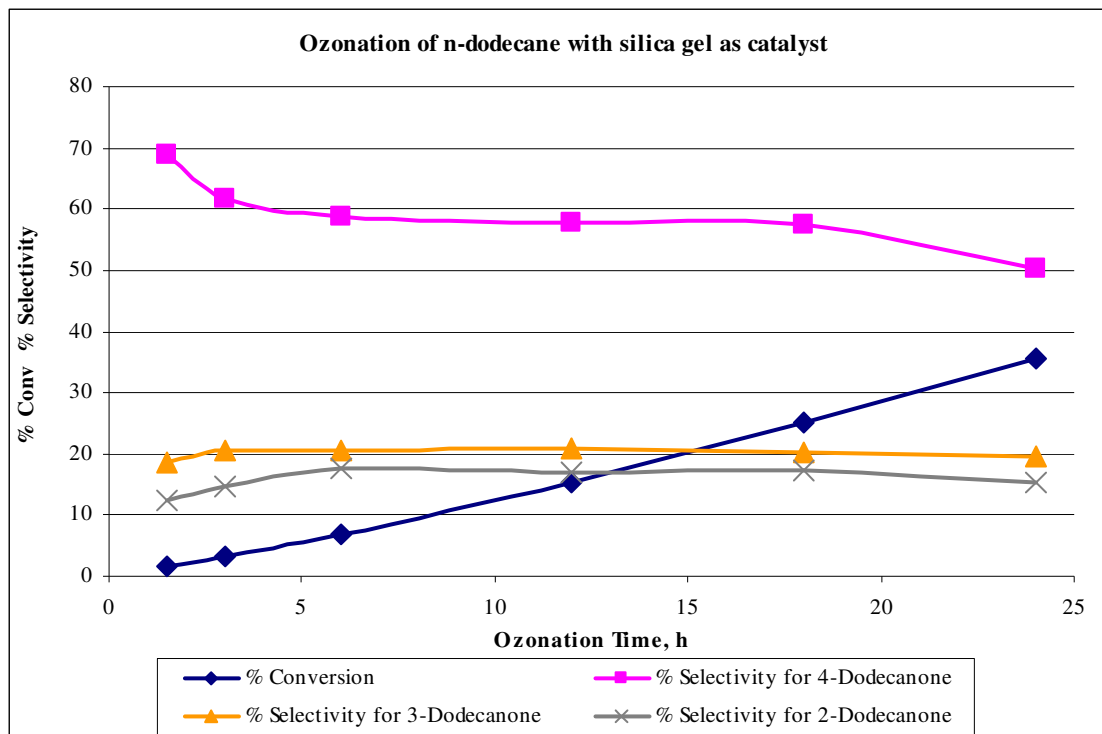


Figure 5.5. Ozonation of n-dodecane with silica gel as catalyst.

In the current studies the oxidation takes place at secondary hydrogens viz. 4-, 3- and 2- positions irrespective of the n-alkane. The formation of the cleavage products due to ozone attack on the secondary C-H bonds leads to ketones. This is also observed by Mazur *et al*¹³⁴ during their studies on the reactivity of ozone towards the primary C-H bonds was comparatively low to the relative activity towards the secondary and tertiary hydrogens, which was estimated as ~0.01:0.1:1.

5.1.6. Ozonation of n-dodecane with VPO:

The conversion of n-dodecane using VPO catalysts increased with time as shown in Table 5.6. The selectivity in favour of 4-dodecanone was decreased during longer exposure to ozone, due to the further oxidation of 4-dodecanone. Initially the formations of 3- and 2-dodecanone were higher and decreased gradually on longer periods of ozonation as represented in Fig. 5.6. As discussed in the previous case with n-tetradecane, n-dodecane yielded higher selectivities towards the 3- and 2- isomers of ketones (more than hexadecane ozonation) with same number of carbon atoms. These results show that ozone is more efficient with the shorter chain length molecules like n-dodecane. As discussed in the Section 5.1.2, the possible mechanisms in the heterogeneous catalytic ozonation are the chemisorption of organic molecules and ozone on the surface of the

catalyst with subsequent interaction of the chemisorbed species, chemisorbed ozone interaction with the non-chemisorbed organic molecules and vice versa. In the current catalytic ozonation reactions it is observed that, if the conversion is higher the selectivities are noted to be low.

Table 5.6. Percentage conversion and selectivities in the ozonation of n-dodecane with VPO as catalyst.

Ozonation Time, h	% Conversion	% Selectivity		
		4-Dodecanone	3-Dodecanone	2-Dodecanone
1.5	3	62	21	17
3	7	57	19	16
6	13	56	21	17
12	24	56	21	17
18	37	54	21	16
24	51	43	17	14

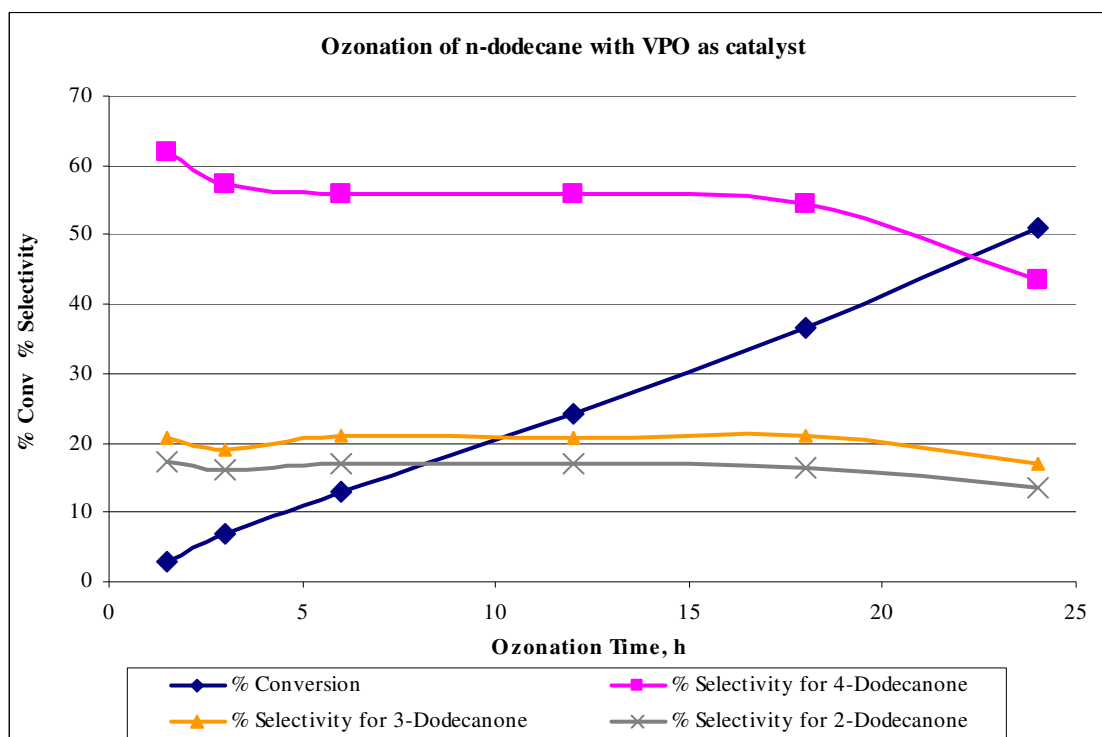


Figure 5.6. Ozonation of n-dodecane with VPO as catalyst.

5.2. Ozonation of n-hexadecane with 0.5% metal (Pd, Ni and V) loaded on γ -alumina catalysts:

Ozonation of n-hexadecane reactions were carried out with 0.5% metal (Pd, Ni and V) loaded γ -alumina catalysts for the oxidation conversion and selectivity studies.

5.2.1. Ozonation of n-hexadecane with 0.5% Pd loaded on γ -Al₂O₃ catalysts:

The application of alumina or metals/metal oxides supported on alumina as catalysts for the ozonation process is well documented¹⁵⁹. The main reasons for the wide usage in several applications of alumina as an adsorbent and as catalyst are acid-base properties, high surface area, mechanical strength and thermal stability^{137, 150, 160}. The % conversion of n-hexadecane with Pd/ γ -Alumina catalyst increased with ozonation time as represented in Table 5.7. Compared to the Pd/ γ -Al₂O₃ N₂ calcined catalyst, conversion of hexadecane was found 50%. The selectivity for 4-hexadecanone decreased with time due to the longer exposure to ozone (56 to 46%) and further oxidation of the product 4-hexadecanone took place. It was observed that the initial amounts of 3- and 2-hexadecanone were high, but gradually decreased upon ozonation for longer duration as illustrated in Fig. 5.7. Further, oxidation of the isomer products 4-, 3-, and 2-hexadecanones took place and an increase in the formation of carboxylic acids and the unidentified products were also observed.

Table 5.7. Ozonation of n-hexadecane with 0.5% Pd/ γ -Al₂O₃ catalyst.

Ozonation Time, h	% Conversion ^a	% Selectivity ^b				
		4-Hexa-decanone	3-Hexa-decanone	2-Hexa-decanone	X _{COOH}	Unidentified products ^c
3	7	55	11	14	13	7
6	15	56	11	13	10	10
12	29	52	11	11	12	14
18	42	49	10	10	14	17
24	50	46	9	9	17	19

^a% Conversion – based on the peak areas calculated from the GC/GC-MS chromatogram.

% Conversion = (Peak area of products / Total peak area in the chromatogram) x 100.

^b% Selectivity – based on the amount of product formed in percent out of the total conversion.

% Selectivity = (the amount of the product formed / total amount of substrate converted) x 100.

^c Unidentified Products – The group of compounds which were unidentified.

X_{COOH} – Carboxylic acids.

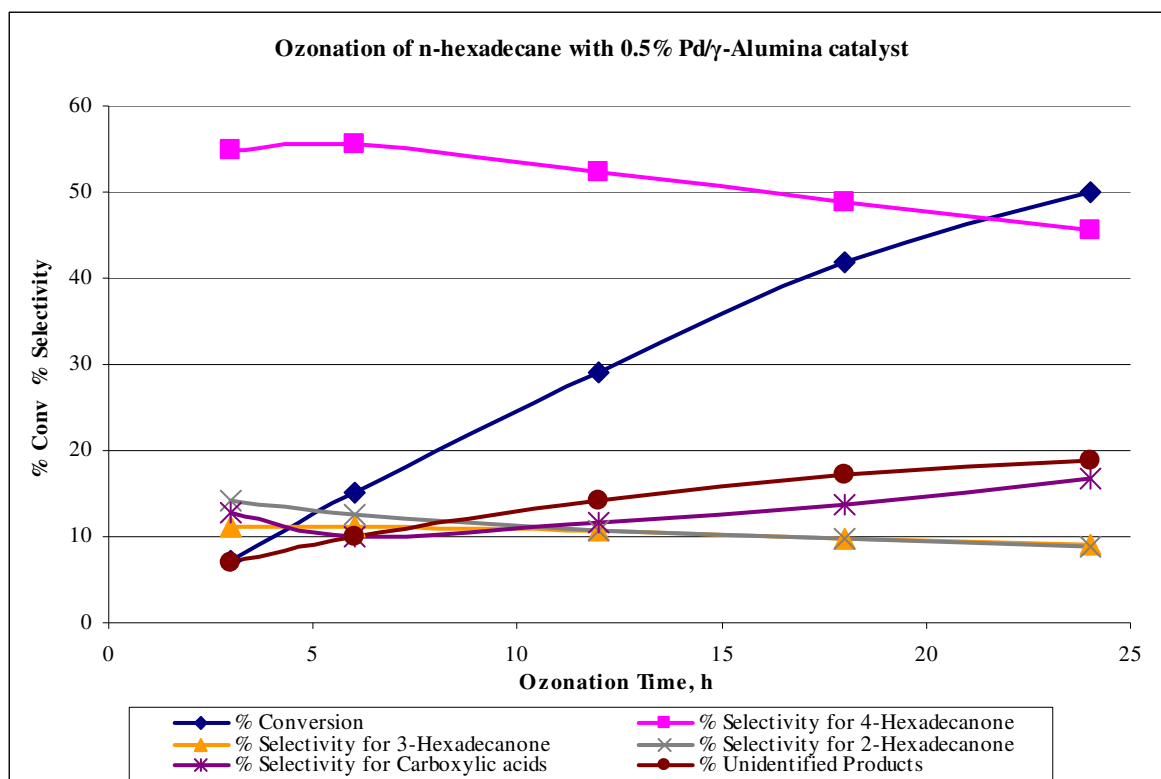


Figure 5.7. Ozonation of n-hexadecane with 0.5% Pd/γ-Al₂O₃ catalyst.

Several explanations on the reaction mechanisms of the heterogeneous catalysed reaction with ozone exist. The proper description of the reaction mechanism is either ozone attacks the organic compounds directly or indirectly via the radical mechanism in the presence of the heterogeneous catalyst. The adsorption of organics as well as ozone on the material surface certainly plays an important role. As a result, ozone may decompose on active metal sites of the catalyst's surface or because of the morphological structure of its support. The decomposition of ozone on the catalyst's surface or due to the support's morphological structure is proposed by Cooper and Burch^{162, 163}. A majority of researchers¹⁶⁴ reported that as a result of this decomposition the acceleration of the indirect radical chain starts, but the ideas of how the initiation takes place differ from one another. Some consider the possible enhancement of direct ozonation with heterogeneous catalysis. Ozonation researchers are taking efforts to design a well conceived mechanism for catalytic oxidation with ozone.

The conversion rate of n-hexadecane with Pd/γ-Al₂O₃ N₂ calcined catalyst increased with time as shown in Table 5.8. The selectivity for 4-hexadecanone was decreased with time due to the longer exposure to ozone (54 to 44%), further oxidation of the product 4-hexadecanone took

place. The initial amounts of 3- and 2-hexadecanone were high and decreased gradually on ozonation for longer periods as illustrated in Fig. 5.8. Further oxidation of the isomer products 4-, 3- and 2-hexadecanones took place and an increase in the formation of carboxylic acids and the unidentified products were also observed.

Table 5.8. Ozonation of n-hexadecane with 0.5% Pd/ γ -Al₂O₃ N₂ calcined catalyst.

Ozonation Time, h	% Conversion	% Selectivity				
		4-Hexa-decanone	3-Hexa-decanone	2-Hexa-decanone	X _{COOH}	Unidentified products
3	8	54	11	15	11	9
7	23	53	11	12	11	12
12	33	51	10	11	14	15
18	43	48	10	10	13	18
24	56	44	9	8	17	21

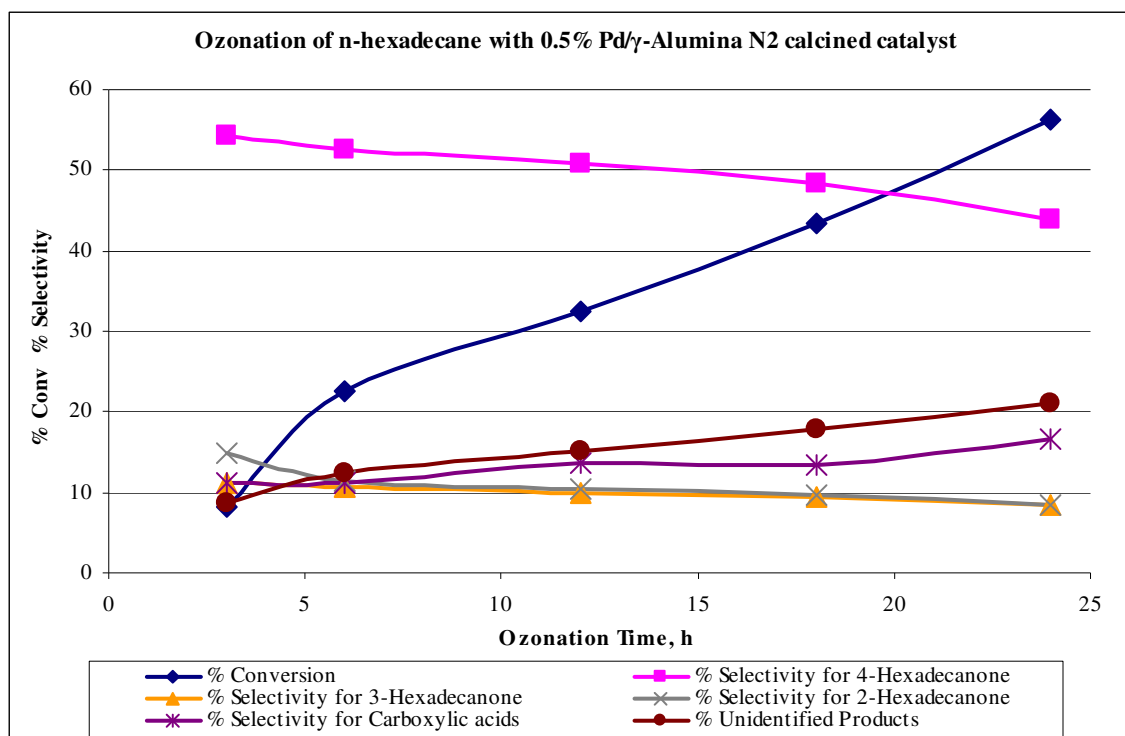


Figure 5.8. Ozonation of n-hexadecane with 0.5% Pd/ γ -Al₂O₃ N₂ calcined catalyst.

The catalytic effect can be produced by metal deposited, or by the support itself, either due to the structure (pore size, crystal size, and surface) or due to chemical properties (acidity, surface groups, hydrophilic/hydrophobic). Legube *et al*¹⁶⁵ suggested one possible reaction path, when alumina build up chelate complexes with dissolved organic molecules, that undergo electrophilic attack by ozone. The further oxidation of the organic compounds leads to desorption and new vacancy of an adsorption site. In this case, the characteristics of the heterogeneous support can explain the enhanced performance of ozone, but the explanation is not applicable to low adsorbing compounds or supports.

Table 5.9. Ozonation of n-hexadecane at higher temperature (~140 °C) with 0.5% Pd/ γ -Al₂O₃ N₂ calcined catalyst.

Ozonation Time, h	% Conversion	% Selectivity				
		4-Hexa-decanone	3-Hexa-decanone	2-Hexa-decanone	X _{COOH}	Unidentified products
1	6	23	5	28	16	26
3	14	39	8	24	9	19
6	31	37	8	15	15	24
12	58	38	8	10	22	20
18	93	10	1	1	46	34

Ozonation of n-hexadecane at temperature ~140 °C was done at controlled conditions. This reaction was carried out in order to compare how the ozone activity is conflicting with the reactions at room temperature 20 ± 1 °C. The conversion rate of n-hexadecane with Pd/ γ -Al₂O₃ N₂ calcined catalyst increased up to 93% during 18 h ozonation as shown in Table 5.9.

The selectivity for 4-hexadecanone was increased during the first 3 h ozonation, then decreased on further exposure to ozone, 10% at 18 h. It was observed that the selectivity in favour of 3-hexadecanone increased for the first 3 h, upon further ozonation the selectivity decreased to 1% during 18 h.

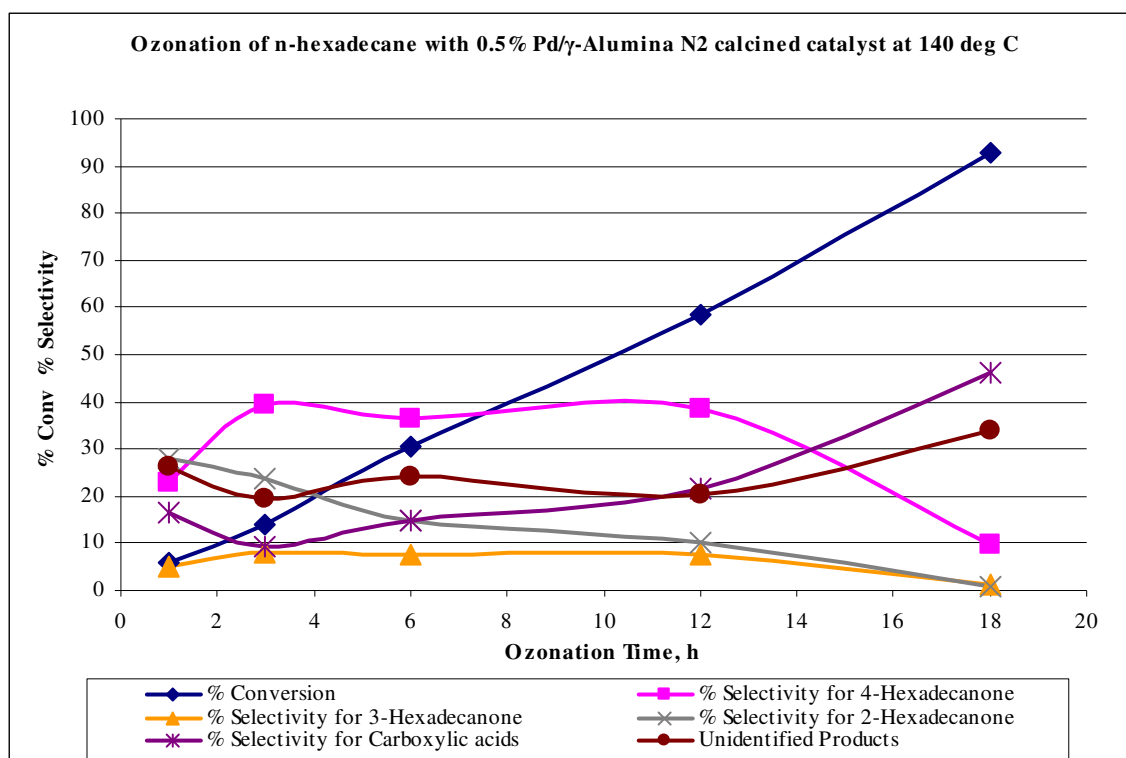


Figure 5.9. Ozonation of n-hexadecane with 0.5% Pd/ γ -Al₂O₃ N₂ calcined catalyst at 140 °C.

2-Hexadecanone selectivity was quite higher in the initial stages of ozonation and later decreased drastically from 3 to 18 h (24 to 1%) ozonation as represented in Fig. 5.9. Further oxidation of the isomer products 4-, 3- and 2-hexadecanones took place and an increase in the formation of carboxylic acids (46%) and the unidentified products (34%) were observed during 18 h exposure. n-Hexadecane ozonation at temperature ~140 °C resulted small amounts of the other isomers 3- and 2-hexadecanone with same number of carbon atoms, but larger amounts of carboxylic acids and unidentified products compared with the ozonation at temperature 20 ± 1 °C. The % conversion is higher and could be ascribed due to the half life of ozone ~140 °C is 90 min., where as at room temperature (20 ± 1 °C) it is 20 min.

5.2.2. Ozonation of n-hexadecane with 0.5% Ni loaded γ -Al₂O₃ catalysts:

Ni/ γ -Al₂O₃ catalyst activity on n-hexadecane ozonation was studied, the conversion rate increased with time up to 48% during 24 h as shown in Table 5.10. The selectivity in favour of 4-hexadecanone increased for the first 6 h, and decreased with time due to the longer exposure to ozone (53%, 49% to 48%) as a result of further oxidation of the ketone isomer products. It was observed that the initial amounts of the products 3- and 2-hexadecanone were high and gradually decreased upon longer durations as illustrated in Fig. 5.10. It was evident that as the products

selectivity decreased and at the same time there was an increase in the formation of carboxylic acids and the unidentified products also. Compared to the Pd/ γ -Al₂O₃ catalysts the conversion rate with Ni/ γ -Al₂O₃ was little lower. According to Lin *et al*¹⁶¹ the average rate of decomposition of ozone on different metals loaded γ -Al₂O₃, Pd/ γ -Al₂O₃ showed more activity than the others.

Table 5.10. Ozonation of n-hexadecane with 0.5% Ni/ γ -Al₂O₃ catalyst.

Ozonation Time, h	% Conversion	% Selectivity				
		4-Hexa-decanone	3-Hexa-decanone	2-Hexa-decanone	X _{COOH}	Unidentified products
3	7	53	11	14	11	7
6	15	55	11	12	11	9
12	27	53	11	11	13	12
18	38	49	10	10	16	15
24	48	48	10	9	14	18

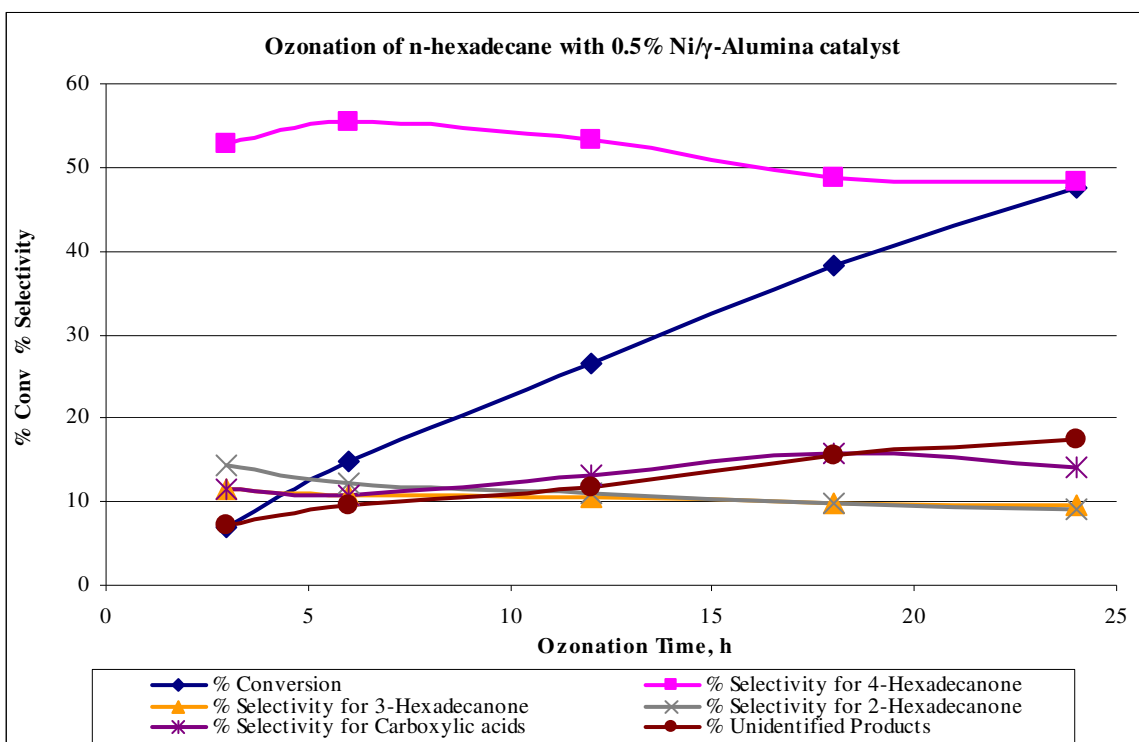


Figure 5.10. Ozonation of n-hexadecane with 0.5% Ni/ γ -Al₂O₃ catalyst.

Table 5.11. Ozonation of n-hexadecane with 0.5% Ni/ γ -Al₂O₃ N₂ calcined catalyst.

Ozonation Time, h	% Conversion	% Selectivity				
		4-Hexa-decanone	3-Hexa-decanone	2-Hexa-decanone	X _{COOH}	Unidentified products
3	6	54	11	16	12	5
6	11	58	11	13	9	8
12	26	52	11	11	12	13
18	36	51	10	10	15	14
24	46	47	9	9	14	19

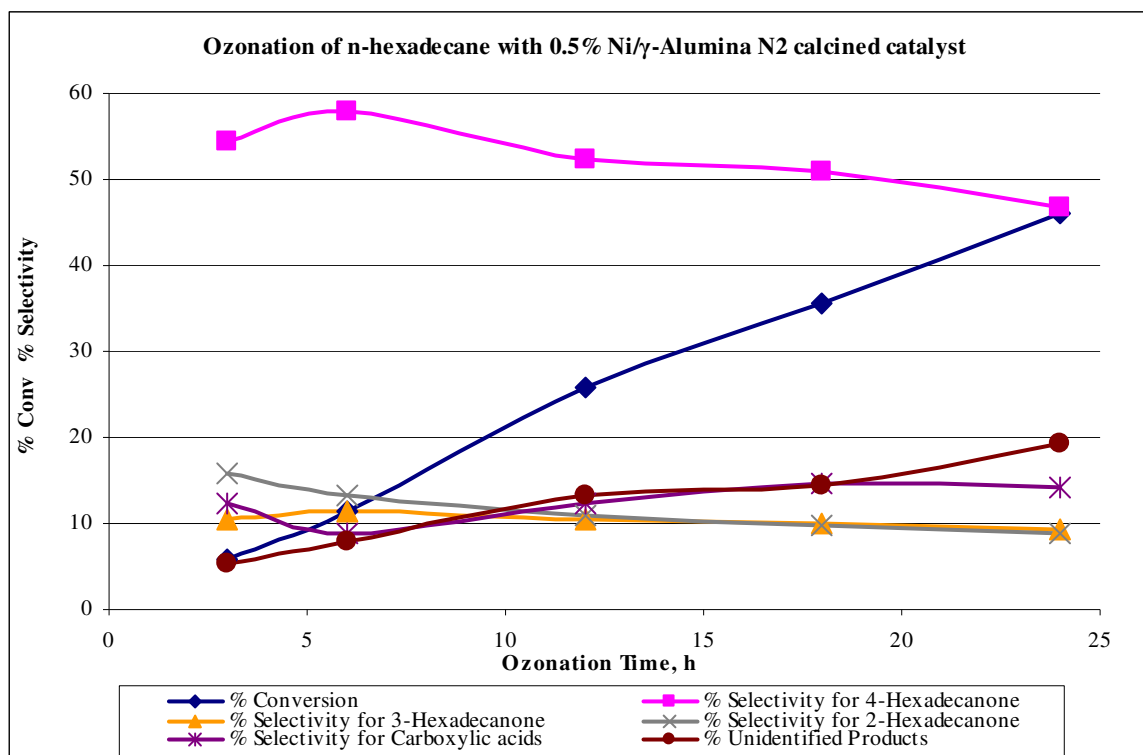


Figure 5.11. Ozonation of n-hexadecane with 0.5% Ni/ γ -Al₂O₃ N₂ calcined catalyst.

Acidity and basicity are the main parameters determining the catalytic properties of alumina. Brønsted acidity-basicity is defined as the ability to proton abstraction-acceptation. Lewis acidity-basicity is the ability to electron acceptance-abstraction. Chemisorption of water on the alumina surface is considered to be a reaction between Al ion, an acceptor of electron pair (Lewis

acid), and hydroxyl ion, its donor (Lewis base) as shown and discussed in Chapter I (Scheme 1.27). Hydroxyl groups formed at alumina surface behave as Brønsted acid sites. The dehydration of two neighbouring OH⁻ ions from the surface of alumina causes the formation of strained oxygen bridge, active Lewis acid sites. Both Brønsted and Lewis acid sites are thought to be the catalytic centers of alumina for this reaction.

Ni/ γ -Al₂O₃ N₂ calcined catalyst activity on the ozonation of n-hexadecane with time was studied. Initial conversion rate of the substrate under study was lower than that of the Ni/ γ -Al₂O₃ catalyst as shown in Table 5.11. Compared to the Pd/ γ -Al₂O₃ catalysts, conversion of the compound under investigation was low. The selectivity for 4-hexadecanone was increased with time due to the longer exposure to ozone. It was observed that the initial amounts of 3- and 2-hexadecanone were high and decreased gradually upon longer duration of ozonation as illustrated in Fig. 5.11. Further oxidation of the isomer products 4-, 3- and 2-hexadecanones took place and an increase in the formation of carboxylic acids and the unidentified products can be observed.

5.2.3. Ozonation of n-hexadecane with 0.5% V loaded γ -Al₂O₃ catalysts:

V/ γ -Al₂O₃ catalyst activity on ozonation of n-hexadecane as function of time was studied. The conversion rate increased with time up to 48% during 24 h as shown in Table 5.12.

Table 5.12. Ozonation of n-hexadecane with 0.5% V/ γ -Al₂O₃ catalyst.

Ozonation Time, h	% Conversion	% Selectivity				
		4-Hexa-decanone	3-Hexa-decanone	2-Hexa-decanone	X _{COOH}	Unidentified products
3	6	55	11	15	13	7
6	11	59	12	14	7	8
12	24	58	11	11	8	12
18	38	49	10	10	13	17
24	48	46	9	9	15	21

The selectivity in favour of 4-hexadecanone was increased during the first 6 h and later decreased with time due to the longer exposure to ozone (55%, 59% and 46%) due to further oxidation of the ketone isomer products. It was observed that the initial amounts of 3- and 2-hexadecanone were higher and gradually decreased upon ozonation for longer duration as described in Fig. 5.12. It is clear from the products pattern that as the products selectivity is decreasing, at the same time

there was an increase in the formation of carboxylic acids and the unidentified products also. Compared to the Pd/ γ -Al₂O₃ catalysts, conversion rate for V/ γ -Al₂O₃ was little lower and similar activity when compared with Ni/ γ -Al₂O₃.

Table 5.13. Ozonation of n-hexadecane with 0.5% V/ γ -Al₂O₃ N₂ calcined catalyst.

Ozonation Time, h	% Conversion	% Selectivity				
		4-Hexa-decanone	3-Hexa-decanone	2-Hexa-decanone	X _{COOH}	Unidentified products
3	9	48	10	13	20	7
6	13	57	12	13	8	9
12	26	55	11	11	9	13
18	37	50	10	10	14	15
24	45	49	10	10	14	17

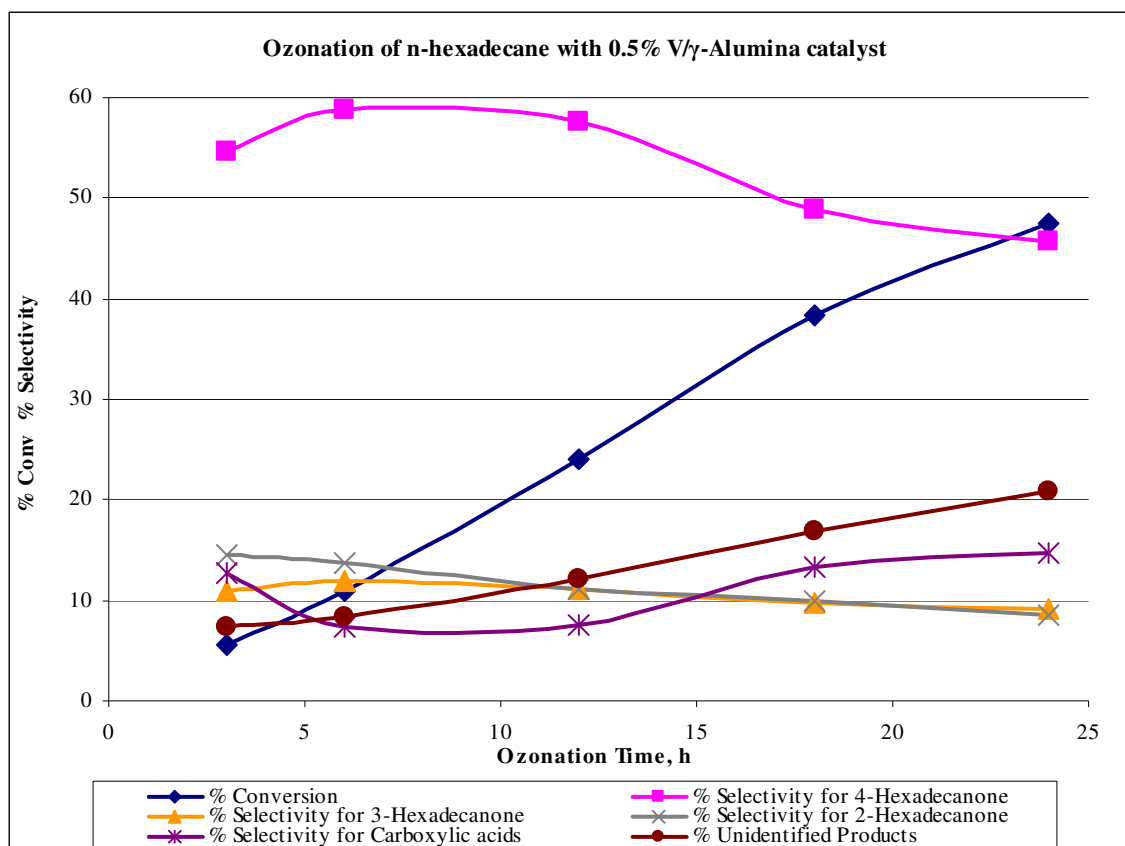


Figure 5.12. Ozonation of n-hexadecane with 0.5% V/ γ -Al₂O₃ catalyst.

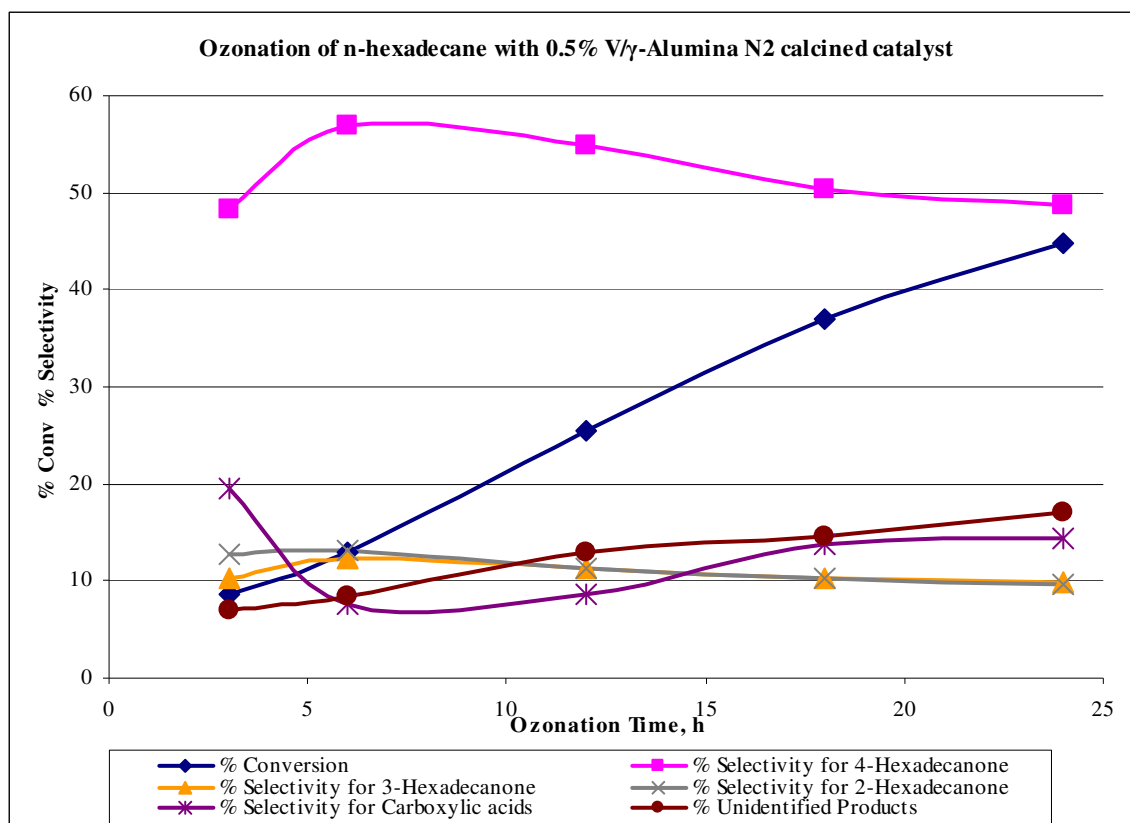


Figure 5.13. Ozonation of n-hexadecane with 0.5% V/ γ -Al₂O₃ N₂ calcined catalyst.

V/ γ -Al₂O₃ N₂ calcined catalyst activity on the ozonation of n-hexadecane with time was studied. The conversion rate of the substrate under study was lower than that of the Ni/ γ -Al₂O₃ catalyst on longer duration as represented in Table 5.13. The selectivity for 4-hexadecanone was increased with time due to the longer exposure to ozone. It was observed that the initial amounts of 3- and 2-hexadecanone were higher and increased up to 6 h ozonation and then gradual decrease of main product 4-ketone can be seen upon ozonation for longer duration as shown in Fig. 5.13. Further oxidation of the isomer products 4-, 3-, and 2-hexadecanones took place and an increase in the formation of carboxylic acids and the unidentified products can be observed. Pd/ γ -Al₂O₃ catalyst was more active compared to Ni- and V/ γ -Al₂O₃ catalysts for ozonation reaction. The activity of the Pd loaded γ -Al₂O₃ was identified as more than the Ni and V metals impregnated γ -Al₂O₃. The comparative conversion results on the activity of the silica gel, VPO and different metals loaded on γ -Al₂O₃ catalysts were shown in Fig. 5.14.

5.3. Comparison of conversion and selectivity of n-hexadecane with silica gel, VPO and 0.5% metal loaded γ -Al₂O₃:

In the heterogeneous catalysed reactions, the understanding of whether ozone attacks the organic molecule directly or indirectly via the radical mechanism is imperative. It is important to note that the adsorption of organics as well as ozone on the surface plays an important role. The catalytic effect can be produced by metal deposited¹⁶², or by the support¹⁶³ itself, either due to the structural properties like pore size, crystal size, and surface or due to chemical properties like acidity, surface groups, hydrophilic/hydrophobic³⁰⁷. The possible enhancement of direct ozonation could also be involved with heterogeneous catalysis.

The main parameters determining the catalytic properties of alumina are acidity and basicity. One possible reaction path is that alumina builds up chelate complexes with dissolved organic molecules, which can be electrophilically attacked by ozone, is also suggested¹⁶⁵. The new vacancy of an adsorption site is provided by desorption of the further oxidized organic compounds. This can explain the enhanced performance of ozone by the characteristics of the heterogeneous support.

In the ozonation of n-hexadecane, different catalysts viz. silica gel, VPO and metal loaded γ -Al₂O₃ were employed. The comparative study on different catalysts activity in the ozonation of n-hexadecane, Pd/ γ -Al₂O₃ N₂ calcined and V/ γ -Al₂O₃ N₂ calcined were noticed to be the best catalysts after 3 h ozonation, during 6 h Pd/ γ -Al₂O₃ N₂ calcined and silica gel catalysts yielded higher conversion as shown in Fig. 5.14. Pd/ γ -Al₂O₃ N₂ calcined, VPO and silica gel were found to be the best catalysts for 12 h ozonation as represented in Table 5.14. Pd/ γ -Al₂O₃ N₂ calcined, Pd/ γ -Al₂O₃, silica gel catalysts conferred higher conversions after 18 and 24 h ozonation (Fig. 5.14). It was observed that the activity of the Pd loaded γ -Al₂O₃ catalyst was more than Ni and V metals impregnated on γ -Al₂O₃ catalysts.

Table 5.14. Percentage conversion in n-hexadecane ozonation with silica gel, VPO and 0.5% metal loaded γ -Al₂O₃ catalysts.

Ozonation Time, h	Silica gel	VPO	Pd/γ-Al₂O₃	Pd/γ-Al₂O₃ N₂ calcined	Ni/γ-Al₂O₃	Ni/γ-Al₂O₃ N₂ calcined	V/γ-Al₂O₃	V/γ-Al₂O₃ N₂ calcined
3	8	7	7	8	7	6	6	9
6	20	14	15	23	15	11	11	13
12	31	32	29	33	27	26	24	26
18	40	40	42	43	38	36	38	37
24	48	46	50	56	48	46	48	45

Table 5.15. Percentage selectivity for the main product, 4-hexadecanone with silica gel, VPO and different 0.5% metal loaded γ -Al₂O₃ catalysts.

Ozonation Time, h	Silica gel	VPO	Pd/ γ -Al ₂ O ₃	Pd/ γ -Al ₂ O ₃ N ₂ calcined	Ni/ γ -Al ₂ O ₃	Ni/ γ -Al ₂ O ₃ N ₂ calcined	V/ γ -Al ₂ O ₃	V/ γ -Al ₂ O ₃ N ₂ calcined
3	62	54	55	54	53	54	55	48
6	48	41	56	53	55	58	59	57
12	58	44	52	51	53	52	58	55
18	50	47	49	48	49	51	49	50
24	48	47	46	44	48	47	46	49

Table 5.16. Normalised percentage selectivity for the main product, 4-hexadecanone with silica gel, VPO and different 0.5% metal loaded γ -Al₂O₃ catalysts.

Ozonation Time, h	Silica gel	VPO	Pd/ γ -Al ₂ O ₃	Pd/ γ -Al ₂ O ₃ N ₂ calcined	Ni/ γ -Al ₂ O ₃	Ni/ γ -Al ₂ O ₃ N ₂ calcined	V/ γ -Al ₂ O ₃	V/ γ -Al ₂ O ₃ N ₂ calcined
3	62	62	63	54	61	72	73	43
6	48	59	75	46	73	105	107	88
12	58	43	56	48	61	62	75	66
18	50	47	47	45	52	57	52	54
24	48	49	44	38	48	49	46	52

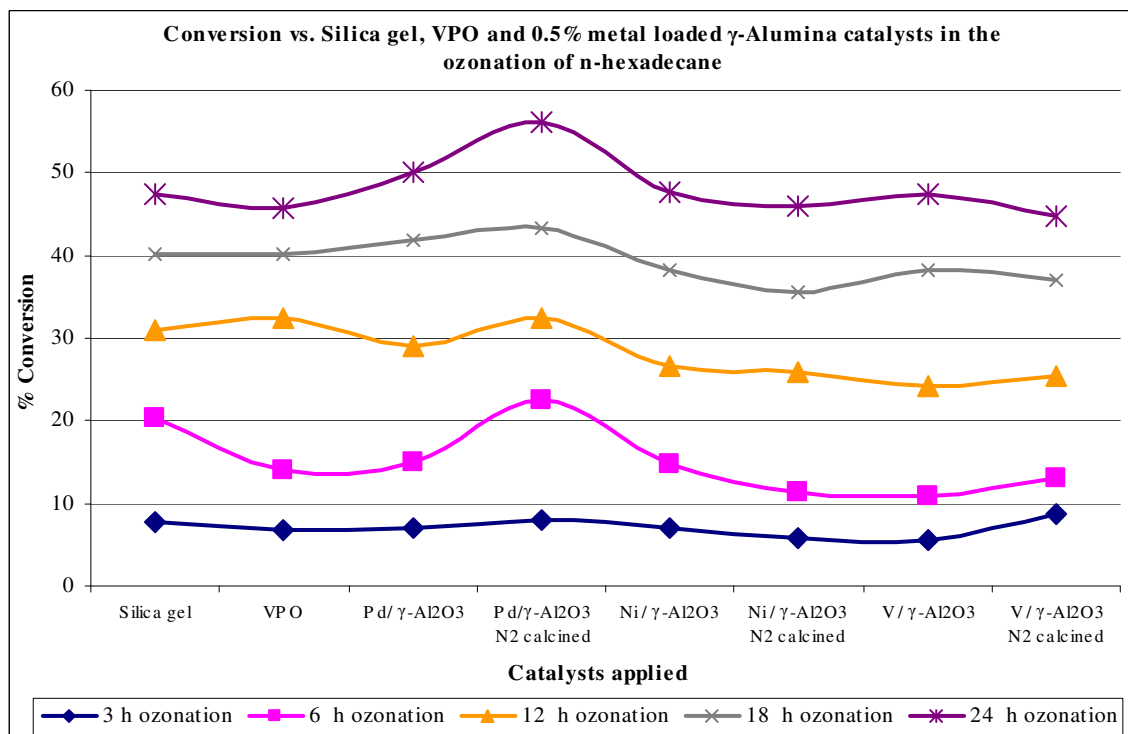
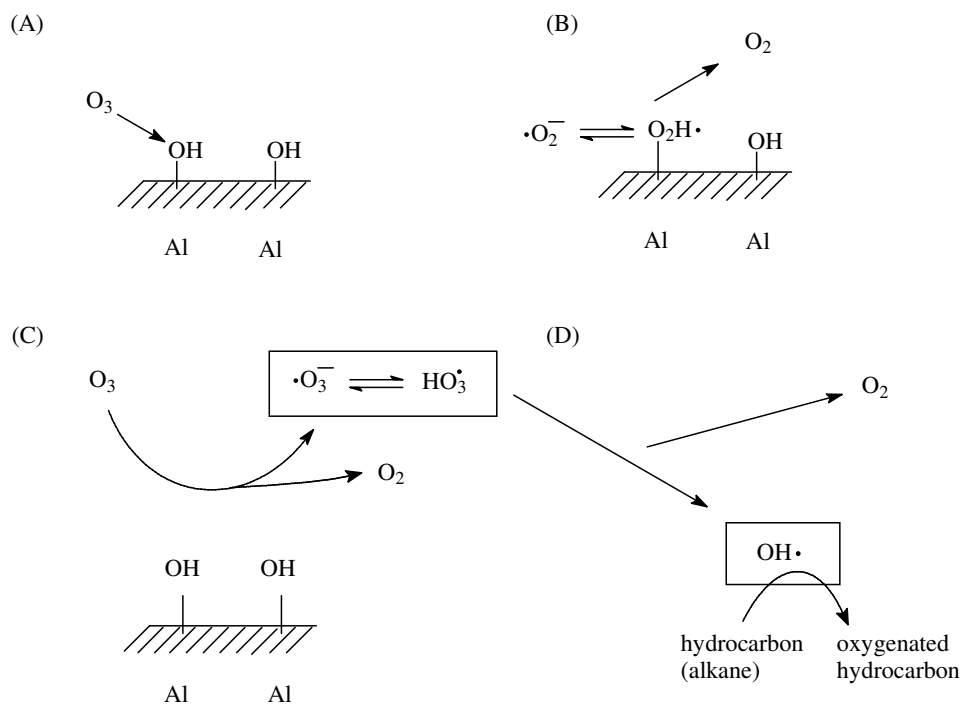


Figure 5.14. Conversion vs. silica gel, VPO and 0.5% metal loaded γ -Al₂O₃ catalysts in the ozonation of n-hexadecane.

In the Scheme 5.1 ozone adsorbs first on the catalyst's surface and then decomposes rapidly due to presence of hydroxyl surface groups. It is known that ozone in gas phase rapidly catalytically decomposes on the surface of metal oxides, especially on the surface of γ -alumina¹⁶⁰.

Due to the decomposition of ozone, active atomic oxygen is produced and reacts with alumina hydroxyl surface groups to O₂H⁻ anions (Scheme 5.1 A), which subsequently can react very fast with another O₃ to O₂H radicals or the O₂H[•] radicals can be produced directly as shown in Scheme 5.1 B. This radical reacts subsequently with another ozone molecule to generate an O₃⁻ radical (scheme 5.1 C). The ozonide radical decomposes into oxygen and a free HO[•] radical which can oxidize the substrate either in directly or on the surface or in a thin film layer above the catalyst's surface (scheme 5.1 D). A reactivation or closing of the radical chain according to Staehlin and Hoigné¹⁶⁶ might not be necessary, because the ozone selective radicals $\cdot\text{O}_2 \rightleftharpoons \cdot\text{O}_2\text{H}$ will be produced by fast decomposition of a new ozone molecule on the catalyst's surface. The adsorption of substrate on the catalyst's surface would not be necessary to provide the catalytic effect.



Scheme 5.1. γ - Al_2O_3 ozonation mechanism.

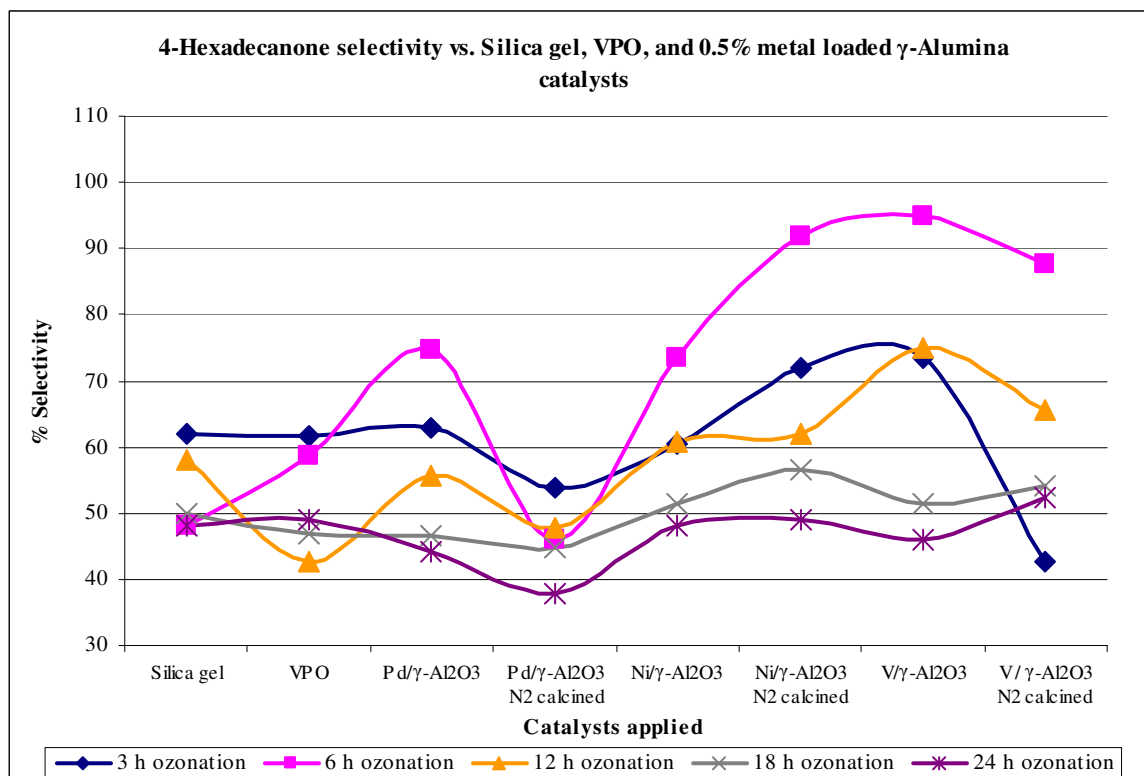


Figure 5.15. 4-Hexadecanone selectivity vs. silica gel, VPO and 0.5% metal loaded γ - Al_2O_3 catalysts.

Table 5.15 summarises the percentage selectivity for the main product, 4-hexadecanone with silica gel, VPO and different 0.5% metal loaded γ -Al₂O₃ catalysts. Whereas, Table 5.16 represents the percentage selectivities from the normalized percentage conversions with all the catalysts employed in the reactions. The selectivity towards 4-hexadecanone in the initial stages of ozonation (3 h) was high with Ni/ γ -Al₂O₃ N₂ calcined and V/ γ -Al₂O₃ catalysts, 72% and 73% respectively. V/ γ -Al₂O₃, Ni/ γ -Al₂O₃ N₂ calcined and V/ γ -Al₂O₃ N₂ calcined catalysts yielded higher activity in the selectivities, 95%, 92% and 88% respectively during 6 h ozonation. V/ γ -Al₂O₃ showed more activity (75%) and V/ γ -Al₂O₃ N₂ calcined also showed selectivity of 66% during 12 h ozonation. The selectivity upon 18 h ozonation, was higher in the case of Ni/ γ -Al₂O₃ N₂ calcined (57%) and V/ γ -Al₂O₃ N₂ calcined (54%) as shown in Table 5.16. In the overall reaction after 24 h V/ γ -Al₂O₃ N₂ calcined yielded higher activity towards the selectivity for 4-hexadecanone as illustrated in Fig. 5.15. Pd/ γ -Al₂O₃ N₂ calcined catalyst which showed the highest conversion, yielded poor selectivity in favour of 4-hexadecanone during the 3, 6, 12, 18 and 24 h ozonation respectively as represented in Fig. 5.15. The catalytic activity order of metal supported on Al₂O₃ was found to be Pd > Ni. The metals examined such as Pd, Ni and also V were found effective in ozone decomposition and in good accordance with Legube and Leitner¹³⁷. The objective of attaining the high selectivities and optimum conversions is achieved with different metal loaded γ -Al₂O₃ catalysts (calcined under N₂ flow conditions also).

CHAPTER - VI

SCOPE OF MESOPOROUS AND MICROPOROUS MOLECULAR SIEVE MATERIAL IN OZONE INITIATED OXIDATION OF HIGHER HYDROCARBONS

6.0. Introduction:

This chapter deals with the oxidation of higher alkanes with ozone as oxidant in presence of various microporous and mesoporous materials. The suitability of the metals supported on mesoporous and microporous molecular sieves in the oxidation of higher hydrocarbons using ozone at normal temperature and pressure conditions is investigated. The utilization of ozone, microporous and mesoporous catalysts in the ozonation of saturated higher hydrocarbons is among the various less explored topics of research in literature.

The characteristic properties of zeolites, such as acidity, shape-selectivity and thermal stability enable them to be used for highly selective synthesis in the fields of chemical intermediates and fine chemicals. Zeolites have proved to be valuable technical catalysts in petrochemistry and in oil processing. The combination of acidity and shape selectivity in the zeolite catalysts is an important factor for organic chemistry¹⁷². The numerous modifications of zeolites in respect of the number and strength of acid centers, isomorphous substitution and doping with metals provide an opportunity of employing catalysts that are tailored to suit the reactions desired¹⁷².

One of the members of M41S family, hexagonal MCM-41 with one-dimensional pores has several advantages such as tunable pore sizes (2-10 nm), high internal surface area (700-1500 m² g⁻¹), large number of internal silanol groups (30-50%), different pore geometry, hydrophilic or hydrophobic nature, high surfactant concentration, and good thermal stability (≤ 1273 K). Thus, it makes them superior than microporous molecular sieves with the growing importance²²²⁻²²⁹.

Various catalyst materials investigated were Pd-, Ni-, V- and U-loaded microporous zeolites Na-Y, ZSM-5 Si/Al-30, mesoporous Al-MCM-41 Si/Al-90 and Al-MCM-41 Si/Al-60 catalysts. To study the activity of zeolite catalysts with ozone as oxidant, 5% w/v catalysts were employed. The fine powder form of the catalyst was dispersed in the reaction medium by means of a magnetic stirrer. These experiments were carried out in a long column reactor, the experimental conditions and batch reaction set-up were similar to experiments with other catalyst materials discussed in Chapter II (Section 2.15 and Fig. 2.9), Chapter III and IV. All the experiments were carried out in replicate.

6.1. Ozonation of n-hexadecane with 0.5% Pd loaded zeolites:

The use of zeolites and molecular sieve based catalysts in oxidation reactions is assuming a lot of importance in recent times. Normally heterogeneous reactions take place at the external crystal

surfaces, while most practical zeolite catalysis takes place inside the framework. Zeolites have the advantage of a very large internal surface, about 20 times larger than their external surface for the more open frameworks such as zeolite Y. This internal capacity provides the appropriate surfaces at which catalytic transformations can take place. In Faujasite zeolites the large cavities are available via three-dimensional open-pore networks. These channels have important consequences in the sorptive and catalytic properties of the zeolites.

The conversion rate and selectivities of ozone initiated oxidation of n-hexadecane in presence of Pd-loaded microporous materials, namely Pd/Na-Y, Pd/Na-Y N₂ calcined, Pd/ZSM-5 and Pd/ZSM-5 N₂ calcined molecular sieves at 6 h intervals are summarised in Tables 6.1 to 6.4. Further the conversion efficiencies of the four catalysts on the said reaction are illustrated in Fig. 6.1. The differences in the conversion efficiencies between the four catalyst materials were broadly minor. Fig. 6.1 shows that Pd/ZSM-5 and Pd/ZSM-5 N₂ calcined catalysts have higher activity for the first 6 h of ozonation. Pd/Na-Y catalyst showed little higher conversion for 12 h (30%). Pd/Na-Y N₂ calcined catalyst had about showed the same conversion up to 12 h (28%) and recorded a highest conversion at 18 h (43%) among all the Pd loaded catalysts.

Table 6.1. Ozonation of n-hexadecane with 0.5% Pd/ZSM-5 zeolite.

Ozonation Time, h	% Conversion ^a	% Selectivity ^b				
		4-Hexa-decanone	3-Hexa-decanone	2-Hexa-decanone	X _{COOH}	Unidentified products ^c
3	7	52	12	15	12	7
6	15	54	11	12	13	9
12	27	56	12	12	8	12
18	38	50	10	10	14	15
24	45	47	10	9	17	16

^a% Conversion – based on the peak areas calculated from the GC/GC-MS chromatogram.

% Conversion = (Peak area of products / Total peak area in the chromatogram) x 100.

^b% Selectivity – based on the amount of product formed in percent out of the total conversion.

% Selectivity = (the amount of the product formed / total amount of substrate converted) x 100.

^c Unidentified Products – The group of compounds which were unidentified.

X_{COOH} – Carboxylic acids.

Pd/Na-Y catalyst showed higher conversion of 48% after 24 h of ozonation (Tables 6.1-6.4). Pd/ZSM-5 N₂ calcined catalyst gave a higher conversion up to 6 h, and later the lowest conversion. Pd/Na-Y N₂ calcined gave a higher conversion of 43% for 24 h (48%). From the BET surface area results (Table 3.6, Chapter III), it is evident that microporous large Na-Y (Table

1.16, Chapter I) zeolite with 12 member ring 3D structure and 7.4 Å pore size has more surface area ~576 m² g⁻¹ available for the oxidation of n-hexadecane with ozone.

Table 6.2. Ozonation of n-hexadecane with 0.5% Pd/ZSM-5 N₂ calcined zeolite.

Ozonation Time, h	% Conversion	% Selectivity				
		4-Hexa-decanone	3-Hexa-decanone	2-Hexa-decanone	X _{COOH}	Unidentified products
3	7	51	12	13	16	7
6	16	58	12	13	8	9
12	25	56	12	12	9	12
18	36	50	10	10	15	15
24	42	51	10	10	13	15

Table 6.3. Ozonation of n-hexadecane with 0.5% Pd/Na-Y zeolite.

Ozonation Time, h	% Conversion	% Selectivity				
		4-Hexa-decanone	3-Hexa-decanone	2-Hexa-decanone	X _{COOH}	Unidentified products
3	5	53	11	15	13	6
6	12	57	12	13	8	9
12	30	51	10	11	12	14
18	39	49	10	10	13	17
24	48	46	9	9	16	18

Table 6.4. Ozonation of n-hexadecane with 0.5% Pd/Na-Y N₂ calcined zeolite.

Ozonation Time, h	% Conversion	% Selectivity				
		4-Hexa-decanone	3-Hexa-decanone	2-Hexa-decanone	X _{COOH}	Unidentified products
3	5	55	10	16	12	4
6	12	52	11	13	15	9
12	28	51	11	11	14	13
18	43	46	10	9	17	16
24	45	52	10	10	10	17

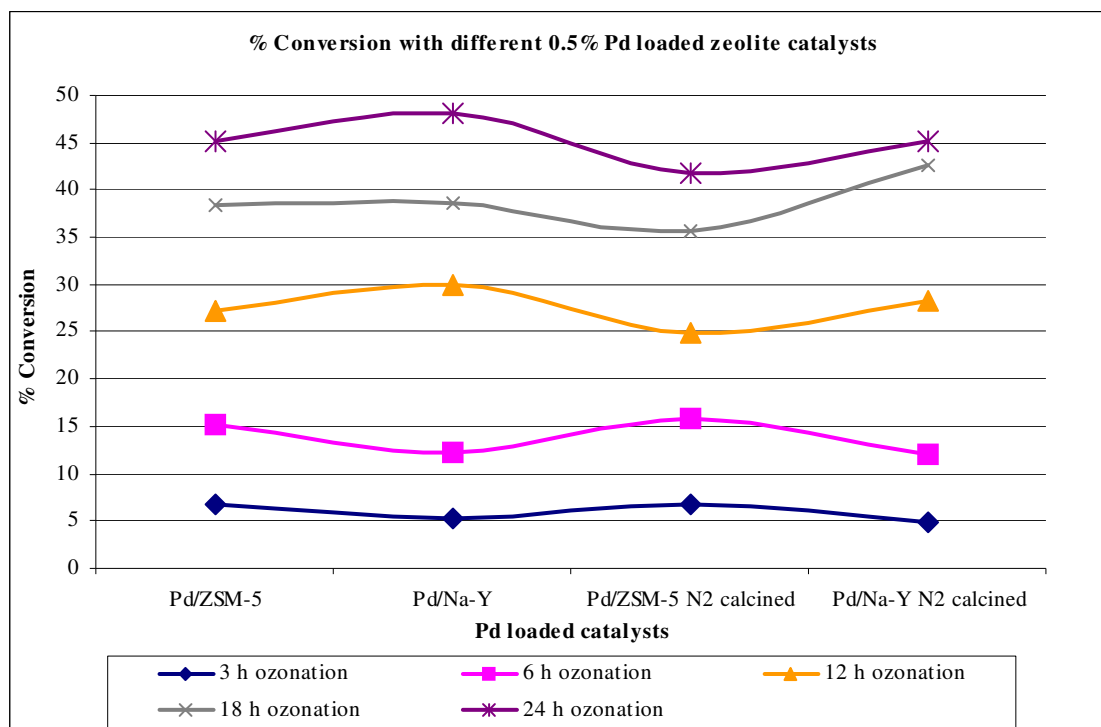


Figure 6.1. Conversion of n-hexadecane with different 0.5% Pd loaded zeolite catalysts.

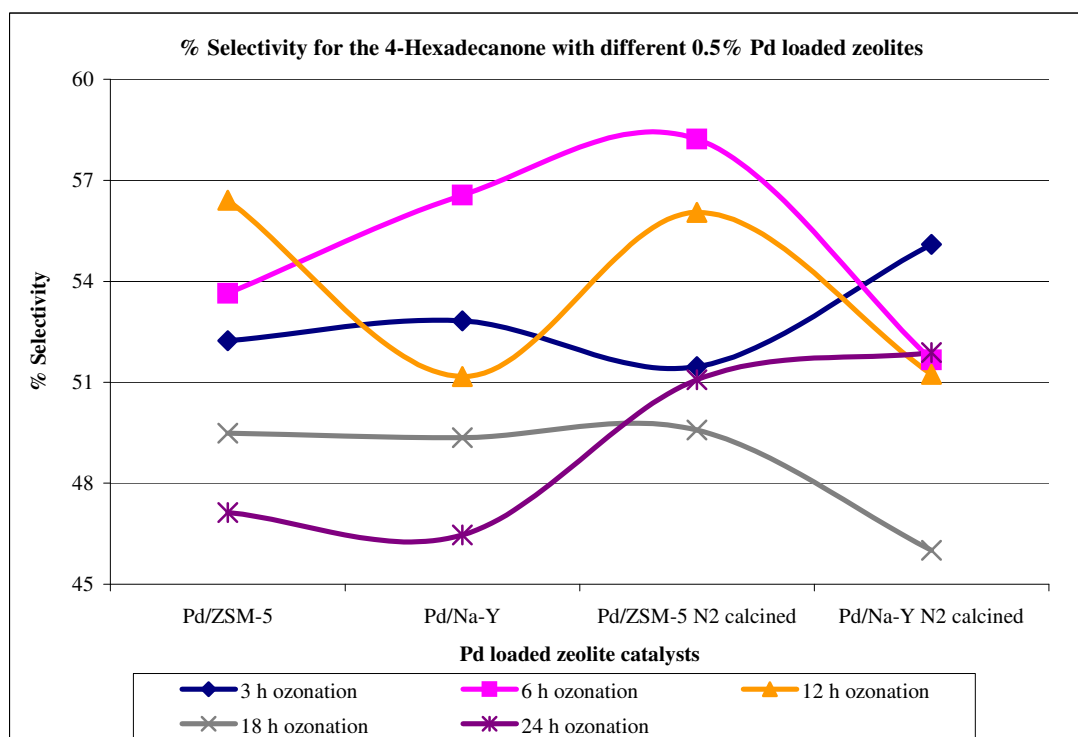


Figure 6.2. Selectivity for the 4-hexadecanone with different 0.5% Pd loaded zeolite catalysts.

The catalyst was active for the first 6 h. With the prolonged ozonation the increase in conversion is marginal, which is possibly due to the active sites occupied by reaction products. When ozone initially attacks the substrate, the products formed remain adsorbed to the catalyst surface. The further reaction of ozone results in oxidation of such products leading to the formation of carboxylic acids. Hence, the active sites of the catalysts were blocked by the products or intermediates restrict the conversion of the substrate. Due to these reasons the catalyst can get deactivated, when the reaction is run for longer duration.

The catalytic mechanism assumes that the catalyst performs a dual function. The presence of catalyst causes both an increase of ozone dissolution and the initiation of the ozone decomposition reaction. In the heterogeneous catalytic ozonation process the three phases involved are gaseous, liquid and solid phase. The transport of O_3 from the gas to liquid takes place in the first stage of the process, and then both ozone and hydrocarbon are transported to the surface of the catalyst. The proposed mechanism of the catalytic ozonation assumes that the adsorption of hydrocarbon and ozone takes place simultaneously on the surface of the catalyst. The O-radicals or HO^\bullet radicals are generated as the result of ozone adsorption and its conversion [$O_2^{\bullet-}$ transfers an electron to another ozone molecule to form an ozonide anion $O_3^{\bullet-}$, which is the chain reaction promoter and produces HO^\bullet radicals]. The free radicals possibly initiate radical chain reaction on both the surface of the catalyst and in the bulk of the substrate phase. The oxidation process proceeds step wise with several oxidized intermediates whilst the radicals are continuously generated by the dissolved ozone, which is transferred to the surface of the catalyst. The affinity of the oxidation products to the catalyst decreases and final products desorb from the catalyst surface.

The selectivities of the four Pd-loaded molecular sieves, namely Pd/Na-Y, Pd/Na-Y N_2 calcined, Pd/ZSM-5 and Pd/ZSM-5 N_2 calcined towards 4-hexadecanone, during the ozone initiated oxidation of n-hexadecane are illustrated in Fig. 6.2. An observation of Fig. 6.2 indicates that selectivity for the 4-hexadecanone with different Pd loaded catalysts, Pd/Na-Y N_2 calcined yielded a high selectivity for the 4-hexadecanone during 3 h (55%) and 24 h (52%). Pd/Na-Y catalyst gave lower selectivity for the 4-hexadecanone after 24 h ozonation. Pd/ZSM-5 N_2 calcined catalyst showed low selectivity for the first 3 h (51%), and gave higher selectivity towards the 4-hexadecanone from 6 to 24 h (58% to 51%) of ozonation.

It is evident from the results (Fig. 6.2) of the four Pd loaded zeolite catalyst materials, Pd/Na-Y catalysts gave a high conversion of 48%, while the Pd/Na-Y N₂ calcined showed a high selectivity for 4-hexadecanone (55%) after 24 h ozonation. Both the Na-Y and ZSM-5, materials calcined under N₂ conditions showed the highest activity for the selectivity towards the 4-hexadecanone. The BET surface area results showed that Na-Y zeolite had large pore size 3D structure, with more surface area available for the selective oxidation of n-hexadecane to 4-hexadecanone. From the results it is clear that the introduction of oxygen atom into the alkanes proceeding with moderate selectivities for all the heterogeneous catalyst systems with increase in oxidation duration. This is in good accordance with the results of Kochi and Sheldon⁴, where the introduction of oxygen containing functional groups in alkanes proceeded with moderate selectivities over most heterogeneous catalysts.

The main factors allowing molecular sieving and the shape selectivity are generally considered to be exclusively a steric effect, only molecules having a critical kinetic diameter lower than the channel diameter are allowed to enter the pores and to react on an active site or, in case, to exit them and to be recovered as a product of the reaction. It is considered that the transition state shape selectivity effects limit the formation of bulky transition state intermediates inside the pores and avoid the formation of some unwanted reaction products¹⁷¹.

6.2. Ozonation of n-hexadecane with 0.5% Ni loaded zeolites:

The reaction conversion and products selectivity data as function of ozonation time in presence of four zeolite materials namely Ni/Na-Y, Ni/Na-Y N₂ calcined, Ni/ZSM-5 and Ni/ZSM-5 N₂ calcined with 0.5% Ni-loading on the ozonation of n-hexadecane are summarised in Tables 6.5-6.8. It was clear that Ni/ZSM-5 and Ni/ZSM-5 N₂ calcined showed high conversion during first 3 h ozonation (6%). The activity of Ni/ZSM-5 catalyst is more (15%) during the first 6 h ozonation. Ni/Na-Y N₂ calcined catalyst yielded the lower conversion after 12 h of ozonation. Whereas, Ni/ZSM-5 and Ni/ZSM-5 N₂ calcined showed the higher conversion rate over 18 h (39%). Further the conversion efficiencies of the four catalysts on the said reaction are illustrated in Fig. 6.3. Ni/Na-Y and Ni/ZSM-5 N₂ calcined catalysts showed the highest conversion of 51% after 24 h as shown in Fig. 6.3. Ni/ZSM-5 also showed better conversion of 50% during 24 h as represented in Tables 6.5-6.8. From 3 to 6 and 18 h ozonation Ni/ZSM-5 catalyst gave the highest conversion. From the ozonation of n-hexadecane with 0.5% Ni loaded zeolites, it was clear that the 2D ZSM-5 and the 3D Na-Y catalysts showed more activity in the oxidation of n-hexadecane with ozone by yielding more conversion.

Table 6.5. Ozonation of n-hexadecane with 0.5% Ni/ZSM-5 zeolite.

Ozonation Time, h	% Conversion	% Selectivity				
		4-Hexa-decanone	3-Hexa-decanone	2-Hexa-decanone	X _{COOH}	Unidentified products
3	6	61	12	14	9	4
6	15	56	11	13	10	10
12	28	59	11	11	7	12
18	39	48	9	10	16	16
24	50	47	9	9	13	20

Table 6.6. Ozonation of n-hexadecane with 0.5% Ni/ZSM-5 N₂ calcined zeolite.

Ozonation Time, h	% Conversion	% Selectivity				
		4-Hexa-decanone	3-Hexa-decanone	2-Hexa-decanone	X _{COOH}	Unidentified products
3	6	56	11	16	11	4
6	12	61	12	13	8	8
12	28	51	11	11	13	13
18	39	50	10	10	14	15
24	51	43	9	8	19	19

Table 6.7. Ozonation of n-hexadecane with 0.5% Ni/Na-Y zeolite.

Ozonation Time, h	% Conversion	% Selectivity				
		4-Hexa-decanone	3-Hexa-decanone	2-Hexa-decanone	X _{COOH}	Unidentified products
3	5	51	10	14	14	8
6	13	57	11	13	8	10
12	27	53	11	11	11	14
18	34	49	10	10	14	16
24	51	45	9	9	15	21

Table 6.8. Ozonation of n-hexadecane with 0.5% Ni/Na-Y N₂ calcined zeolite.

Ozonation Time, h	% Conversion	% Selectivity				
		4-Hexa-decanone	3-Hexa-decanone	2-Hexa-decanone	X _{COOH}	Unidentified products
3	5	57	11	16	12	6
6	9	58	12	14	10	8
12	19	60	12	12	9	10
18	29	56	11	10	9	13
24	38	54	11	10	11	15

The unique structural properties of ozone as one of its resonance structures due to the high electron density on one of the oxygen atoms might show high basicity resulting in strong affinity to Lewis acid sites on the surface of zeolites. The mechanism of ozone adsorption/decomposition on the surface active sites of the catalyst is also possible. In the heterogeneous catalysis, the influence of many chemical and physical processes such as mass transfer, fluid dynamics, interfacial surface area, surface material, chemical kinetics, and temperature and hydrocarbon properties plays significant role. It has to be highlighted here that ozonation reactions take place in both the liquid (n-hexadecane) and on the surface of the catalyst.

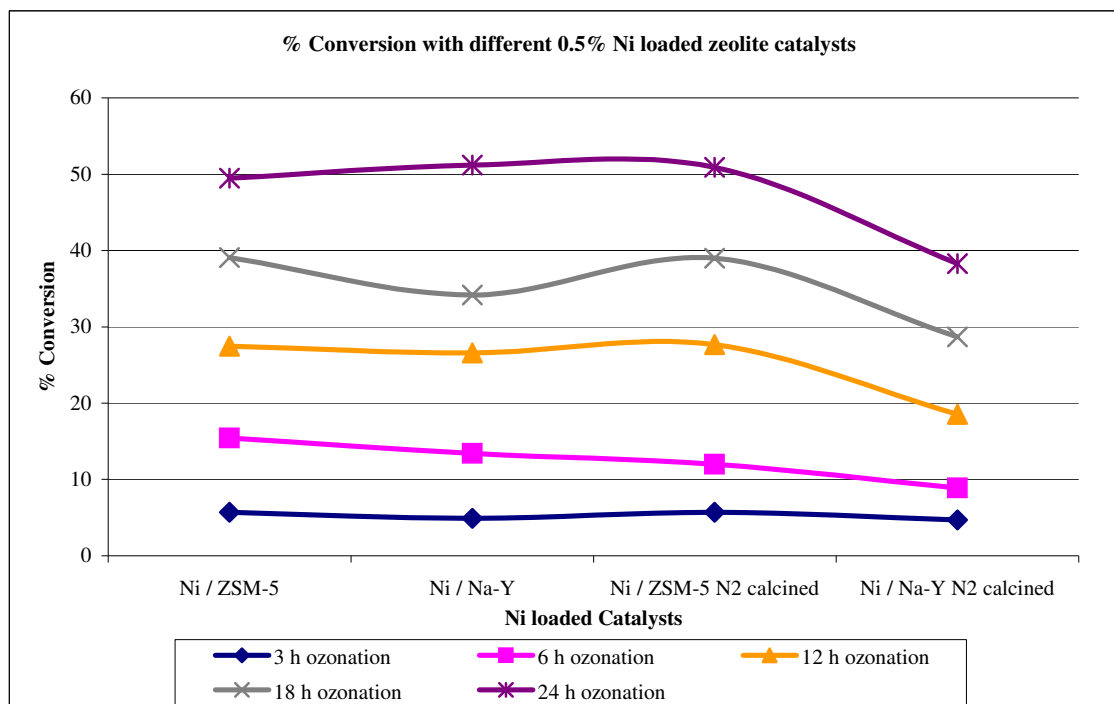


Figure 6.3. Conversion of n-hexadecane with different 0.5% Ni loaded zeolite catalysts.

In the ozone initiated oxidation of n-hexadecane, molecular ozone reactions are also possible. Reactions on the catalyst surface involve several steps such as adsorption, ozone decomposition reaction, surface oxidation reaction and desorption process. The catalytic ozonation process involve the adsorption of ozone on the catalyst, which is influenced by surface properties of the catalysts such as surface area, pore volume and surface active sites.

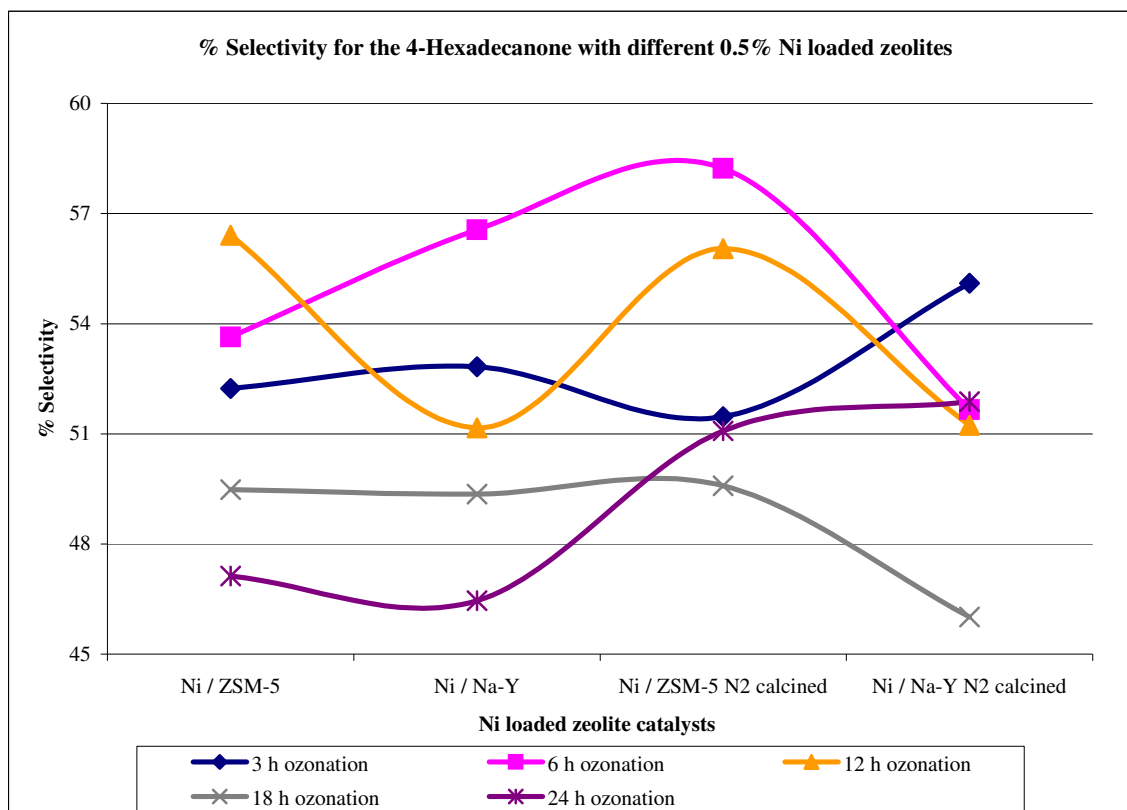


Figure 6.4. Selectivity for the 4-hexadecanone with different 0.5% Ni loaded zeolite catalysts.

It was observed that Ni/ZSM-5 catalyst initially gave highest selectivity of 61% and during 6 h of ozonation Ni/ZSM-5 N₂ calcined and Ni/Na-Y catalysts gave the highest selectivity 61% and 58% respectively, and during 12 h catalysts Ni/ZSM-5 and Ni/Na-Y N₂ calcined yielded better selectivity of 59 and 60% respectively as shown in Fig. 6.4. During 18 h ozonation Ni/Na-Y N₂ calcined showed the lowest selectivity of 56%. After 24 h ozonation Ni/Na-Y N₂ calcined and Ni/ZSM-5 showed the better selectivity towards 4-hexadecanone (54 and 47%). The results show high selectivity with the microporous large Na-Y catalyst, possibly due to more surface area available for the selective oxidation of n-hexadecane. The catalysts prepared under N₂ calcined conditions too yielded appreciable selectivity (Ni/ZSM-5 N₂ calcined-43% and Ni/Na-Y N₂ calcined-54%). Chen and Garwood³⁸ have indicated that the oxidation state of a reducible metal

ion in a zeolite depends on the acidity of the zeolite, e.g. nickel ion in a Na-Y zeolite is easily reducible, while nickel ion in a zeolite with H form is not easily reduced, which agrees well with the current results.

On the surface of the reduced metal-catalyst (Me-catalyst) ozone oxidizes metal with the generation of HO^\bullet radicals. The hydrocarbon (RH) after adsorption on the catalyst surface get subsequently oxidised by an electron-transfer reaction leaving behind a reduced catalyst ($\text{Me}_{\text{red}}\text{R}^\bullet$). The radical species R^\bullet gets subsequently desorbed from the catalyst undergo oxidation by HO^\bullet or by O_3 in bulk hydrocarbon substrate.

6.3. Ozonation of n-hexadecane with 0.5% V loaded zeolites:

The conversion rate and selectivities of ozone initiated oxidation of n-hexadecane in presence of 0.5% V-loaded microporous materials, namely V/ZSM-5, V/ZSM-5 N_2 calcined, V/Na-Y and V/Na-Y N_2 calcined molecular sieves at 6 h intervals are summarised in Tables 6.9-6.12. The differences in the conversion efficiencies between the two V/ZSM-5 and V/ZSM-5 N_2 calcined catalyst materials were broadly minor. V/Na-Y zeolite showed more conversion during 3 to 24 h than the other V loaded catalysts as illustrated in Fig. 6.5. V/Na-Y N_2 calcined catalyst also showed better activity towards the conversion next to V/Na-Y. A higher conversion and the product distribution indicate a greater oxidation ability of vanadium loaded Na-Y compared to that of ZSM-5 catalysts in this reaction, which shows high surface area available for the selective oxidation of n-hexadecane conversion with large microporous Na-Y catalyst. Thus vanadium loaded microporous molecular sieves can catalyse the oxyfunctionalization of alkanes to the corresponding ketones.

Table 6.9. Ozonation of n-hexadecane with 0.5% V/ZSM-5 zeolite.

Ozonation Time, h	% Conversion	% Selectivity				
		4-Hexa-decanone	3-Hexa-decanone	2-Hexa-decanone	X_{COOH}	Unidentified products
3	5	53	11	15	13	6
6	11	58	11	13	9	9
12	22	54	11	11	11	12
18	32	51	10	10	14	14
24	40	51	11	10	11	17

Table 6.10. Ozonation of n-hexadecane with 0.5% V/ZSM-5 N₂ calcined zeolite.

Ozonation Time, h	% Conversion	% Selectivity				
		4-Hexa-decanone	3-Hexa-decanone	2-Hexa-decanone	X _{COOH}	Unidentified products
3	5	58	10	10	13	4
6	10	60	12	14	11	8
12	22	57	12	11	11	10
18	30	55	11	11	13	13
24	39	51	10	10	14	14

Table 6.11. Ozonation of n-hexadecane with 0.5% V/Na-Y zeolite.

Ozonation Time, h	% Conversion	% Selectivity				
		4-Hexa-decanone	3-Hexa-decanone	2-Hexa-decanone	X _{COOH}	Unidentified products
3	6	56	11	16	11	6
6	15	56	11	12	10	10
12	28	55	11	11	10	13
18	45	47	9	10	15	17
24	51	45	9	9	15	21

Table 6.12. Ozonation of n-hexadecane with 0.5% V/Na-Y N₂ calcined zeolite.

Ozonation Time, h	% Conversion	% Selectivity				
		4-Hexa-decanone	3-Hexa-decanone	2-Hexa-decanone	X _{COOH}	Unidentified products
3	4	54	12	16	16	5
6	9	58	12	14	9	7
12	23	54	11	11	12	12
18	37	50	10	10	13	17
24	48	48	9	9	15	19

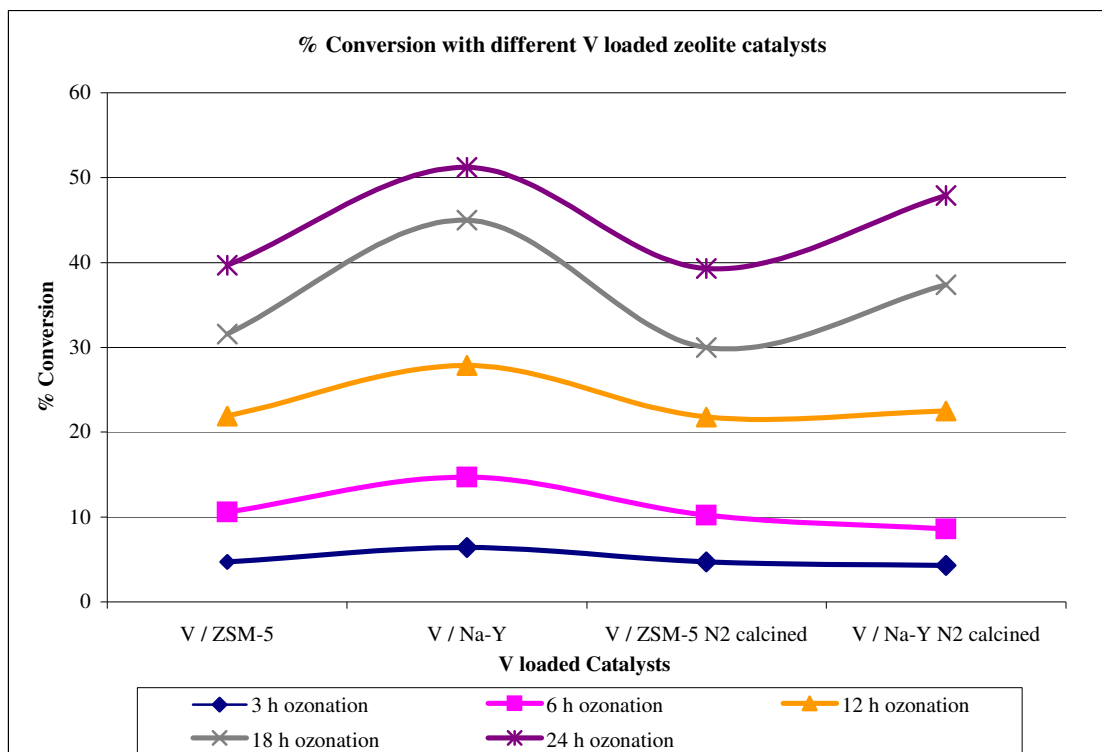


Figure 6.5. Conversion of n-hexadecane with different 0.5% V loaded zeolite catalysts.

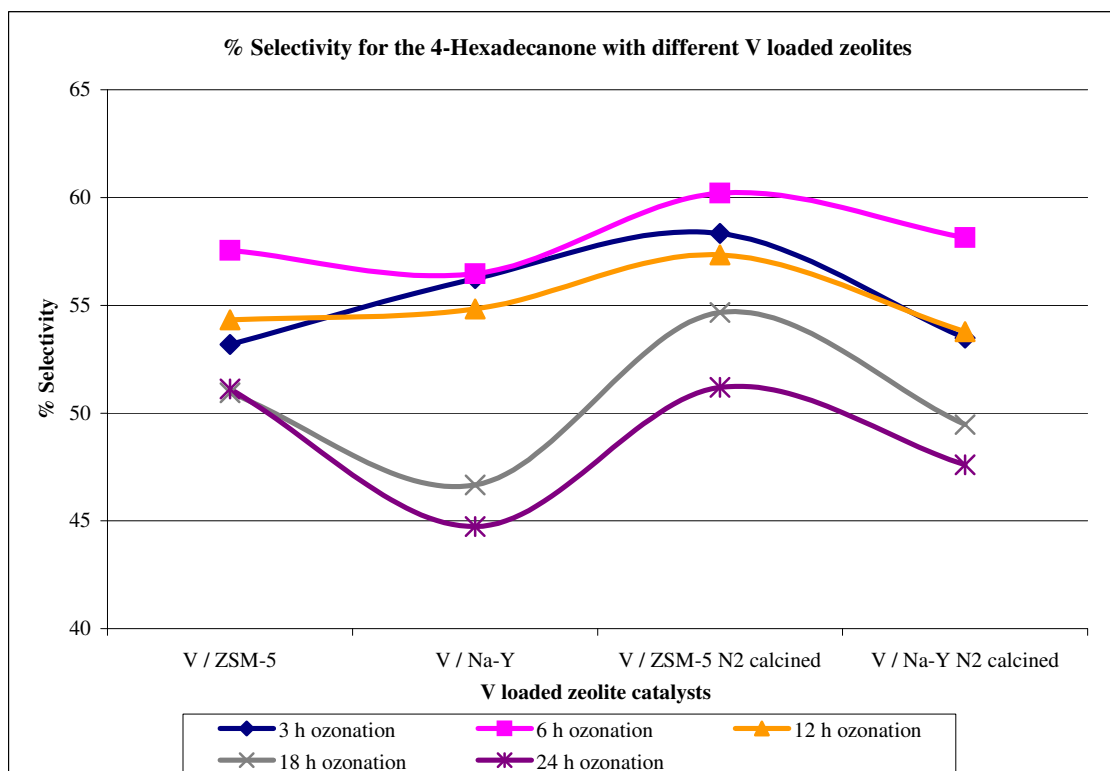


Figure 6.6. Selectivity for the 4-hexadecanone with different 0.5% V loaded zeolite catalysts.

An observation of the results in Fig. 6.6 shows that V/ZSM-5 N₂ calcined catalyst yielded highest selectivity for the 4-hexadecanone. The V/ZSM-5 can be considered as the superior catalyst for 4-ketone selectivity during 24 h ozonation. However, V/Na-Y showed lowest selectivities among all the V loaded molecular sieves up to 24 h ozonation as illustrated in Tables 6.9-6.12. Both the Na-Y and ZSM-5 calcined under N₂ conditions showed the highest selectivity towards the 4-hexadecanone.

From the results it is clear that the introduction of oxygen atom into the alkanes proceeding with moderate selectivities for all the heterogeneous catalyst systems with increase in oxidation duration. This is in good accordance with Kochi and Sheldon⁴ results, where the introduction of oxygen containing functional groups in alkanes proceeded with moderate selectivities over most heterogeneous catalysts.

As discussed in the previous Section 6.2, the oxidation state of a reducible metal ion in a zeolite depends on the acidity of the zeolite³⁸. Ozone oxidizes metal on the surface of the reduced metal-catalyst with the generation of HO[•] radicals. The adsorbed hydrocarbons on the catalyst surface subsequently get oxidized by electron-transfer reaction to give a reduced catalyst. The radical species formed from hydrocarbon are desorbed from the catalyst and oxidized by HO[•] or by O₃ in the substrate.

6.4. Ozonation of n-hexadecane with 0.5% U loaded zeolites:

Literature shows that uranium oxides (uranyl ions UO₂²⁺) dispersed over dense oxide supports serve as promising oxidizing catalysts because of its variable valence states and vacant f-orbitals²⁰⁸. This prompted preparation of the uranium oxide dispersed zeolitic supports for the oxidation of n-hexadecane with ozone in the current studies. Uranyl ions possess instinctive excitation and emission characteristics and are strong oxidizing species. The UO₂²⁺ ions are reportedly quenched by the abstraction of hydrogen atoms from the hydrocarbons²¹². The conversion rate and selectivities of ozone initiated oxidation of n-hexadecane in presence of 0.5% U-loaded supports namely U/silica, U/ZSM-5 and U/Na-Y at 6 h intervals are summarised in Tables 6.13-6.15. The differences in the conversion efficiencies between the U/silica and U/Na-Y catalyst materials were minor. Further the conversion efficiencies and selectivities of the three catalysts on the said reaction are illustrated in Figs. 6.7 and 6.8.

From Fig. 6.7 it can be noticed that U/ZSM-5 catalyst gave highest conversion from 3 to 24 h ozonation. U/Na-Y catalyst showed comparatively low conversion for 3 h, 6 h and 24 h. The two pore system consists of zig-zag channels for near-circular cross-section and straight channels of elliptical shape, responsible in the ZSM-5 zeolites for sorptive and catalytic properties. The other possibility for the higher activity is that all the intersections in ZSM-5 are of the same size.

Table 6.13. Ozonation of n-hexadecane with 0.5% U/Silica.

Ozonation Time, h	% Conversion	% Selectivity				
		4-Hexa-decanone	3-Hexa-decanone	2-Hexa-decanone	X _{COOH}	Unidentified products
3	7	56	13	15	13	4
6	20	46	10	10	28	7
12	27	54	11	11	12	12
18	37	50	10	10	17	13
24	48	44	9	9	20	16

Table 6.14. Ozonation of n-hexadecane with 0.5% U/Na-Y zeolite.

Ozonation Time, h	% Conversion	% Selectivity				
		4-Hexa-decanone	3-Hexa-decanone	2-Hexa-decanone	X _{COOH}	Unidentified products
3	7	56	12	15	11	6
6	15	56	12	12	9	9
12	29	52	11	11	12	13
18	38	51	11	10	13	14
24	45	49	10	10	15	16

Table 6.15. Ozonation of n-hexadecane with 0.5% U/ZSM-5 zeolite.

Ozonation Time, h	% Conversion	% Selectivity				
		4-Hexa-decanone	3-Hexa-decanone	2-Hexa-decanone	X _{COOH}	Unidentified products
3	8	49	12	13	14	12
6	16	57	12	12	9	10
12	33	55	12	11	9	13
18	45	49	10	10	13	17
24	55	44	9	8	17	20

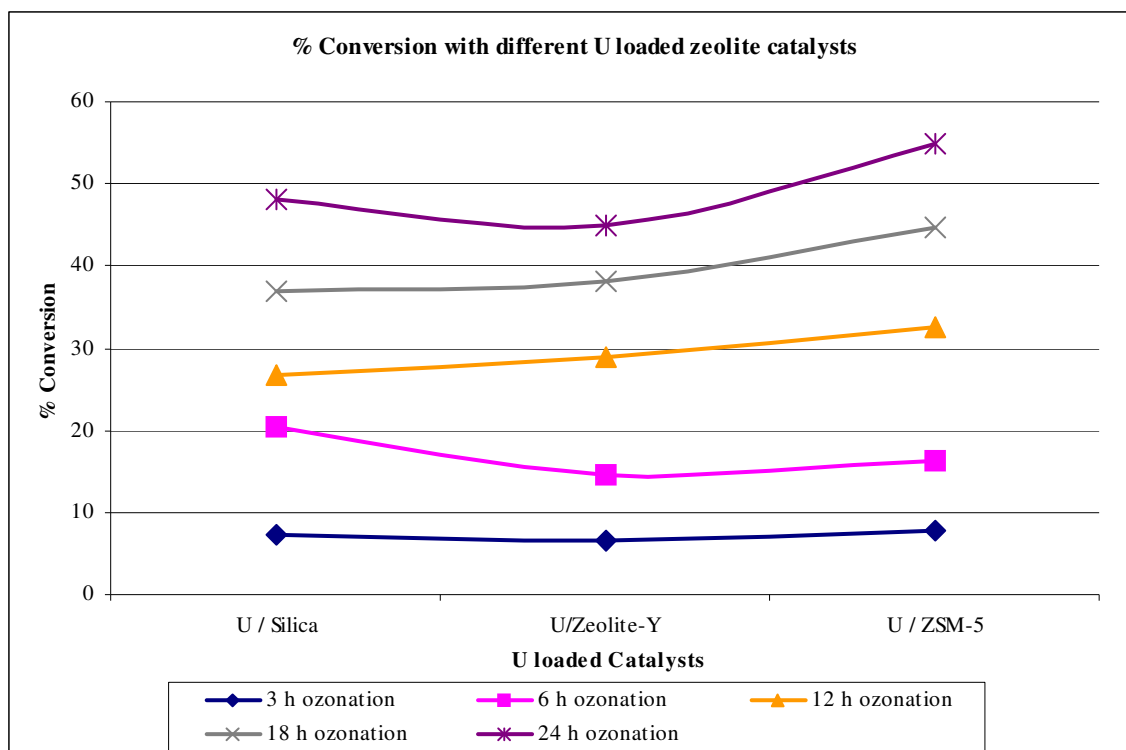


Figure 6.7. Conversion of n-hexadecane with different 0.5% U loaded zeolite catalysts.

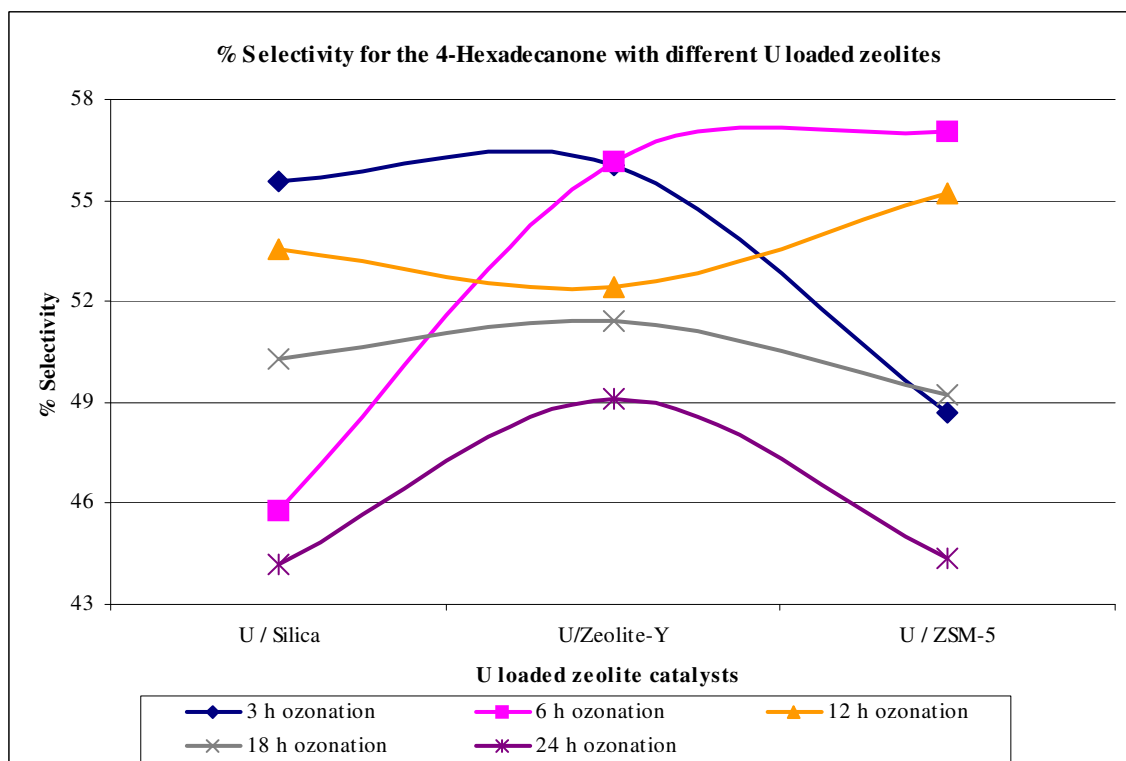


Figure 6.8. Selectivity for the 4-hexadecanone with different 0.5% U loaded zeolite catalysts.

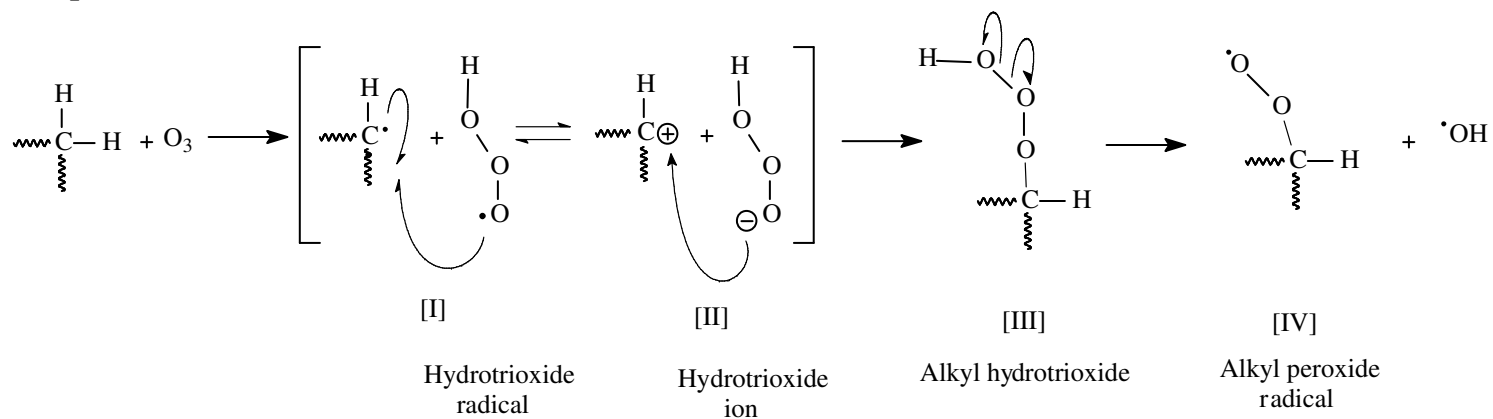
The examination of Fig 6.8 indicates that U/Na-Y catalyst observed as best among the U loaded zeolites for the selectivity towards 4-hexadecanone. During the initial stages of ozonation reaction (3 h) U/Silica and U/Na-Y showed the similar selectivity and from 6 to 24 h ozonation reaction it showed the lowest selectivities as illustrated in Tables 6.13-6.15. UO_2^{2+} /ZSM-5 zeolites observed to be more active towards the selective oxidation product 4-hexadecanone. UO_2^{2+} ions were observed as the more active in both conversion and selectivity in the n-hexadecane oxidation reaction.

6.4.1. Proposed mechanism for the ozonation of n-alkanes with U/ZSM-5:

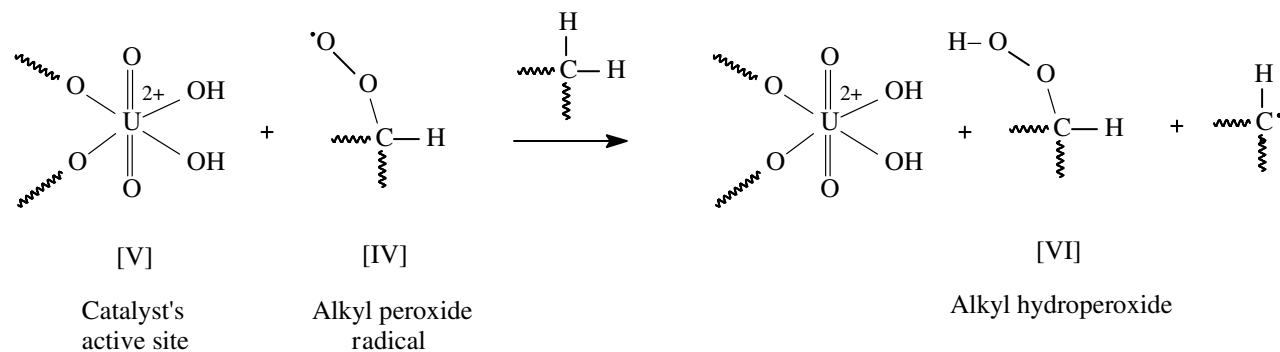
Based on the U-loaded molecular sieves results, a plausible schematic mechanism for the ozonation of higher alkanes with new heterogeneous U/ZSM-5 zeolite catalyst is proposed as shown in Scheme 6.1. In the mechanism, the possibility of chemisorption of ozone on the catalyst surface leading to the formation of active species which react with non-chemisorbed organic molecule, and chemisorption of organic molecule on the catalytic surface and its further reaction with gaseous ozone are illustrated. Ozone abstracts the hydrogen atom from C_4 or C_3 or C_2 position of the n-alkanes (C_{16} , C_{14} and C_{12}) leading to the formation of alkyl radical and hydrotrioxide radical [I] which can interact to give a carbocation and hydrotrioxide ion [II]. The hydrotrioxide radicals and its ions are highly unstable, and combine with the alkyl radical or carbocation to produce alkyl hydrotrioxide [III]. The alkyl hydrotrioxide [III] dissociates into alkyl peroxide [IV] and HO^\bullet radicals by homolytic cleavage as shown in Scheme 6.1, step A.

Near the active site [V] of the catalyst, the alkyl peroxide radical [IV] abstracts a proton from the alkane to produce alkyl hydroperoxide [VI] and an alkyl radical as illustrated in Scheme 6.1, step B. In Scheme 6.1, step C, it is conceivable that the hydroxyl group of uranium active site forms a weak hydrogen bond with the alkyl hydroperoxide [VII], which in turn can react with ozone molecule to give an unstable intermediate, alkyl diperoxo radical [VIII], by losing HO^\bullet radical (similar to step A). The alkyl diperoxo radical [VIII] as shown in Scheme 6.1, step D will be desorbed from the catalyst active site and by losing O_2 (singlet) generates peroxy alkyl radical [IX] by heterolytic cleavage. In Scheme 6.1, step E, the homolytic cleavage of peroxy alkyl radical [IX] takes place and turn into alkoxy diradical [X], which produce 4-ketone [XI] (or 3-ketone or 2-ketone) compound. As described in Scheme 6.1, step F, the alkyl radical (from radical pair [I] or from step B) loses an electron to the active site of the catalyst to form a carbocation. This carbocation then combines with hydrotrioxide ion (from [II]) to generate alkyl hydrotrioxide as shown in Scheme 6.1, step F.

Step A.

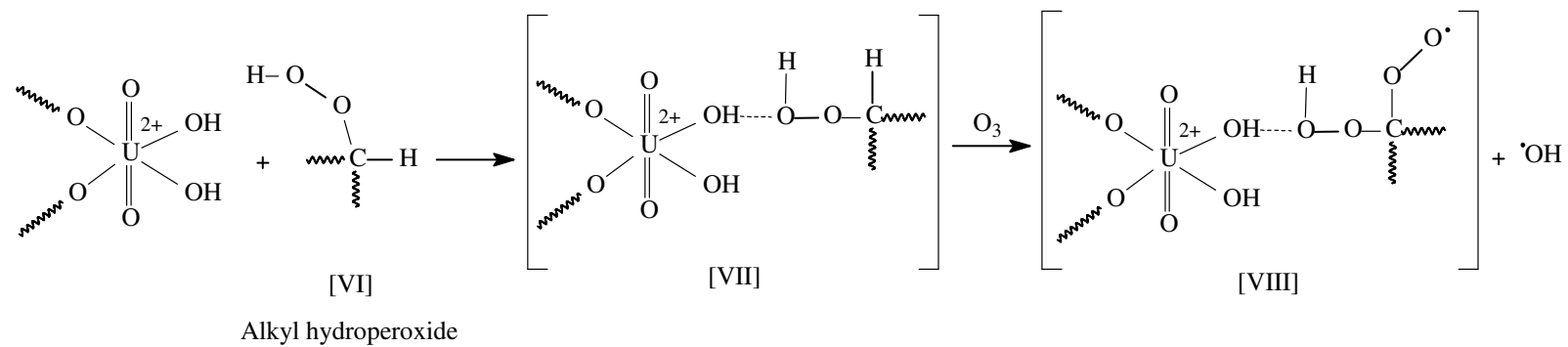


Step B.

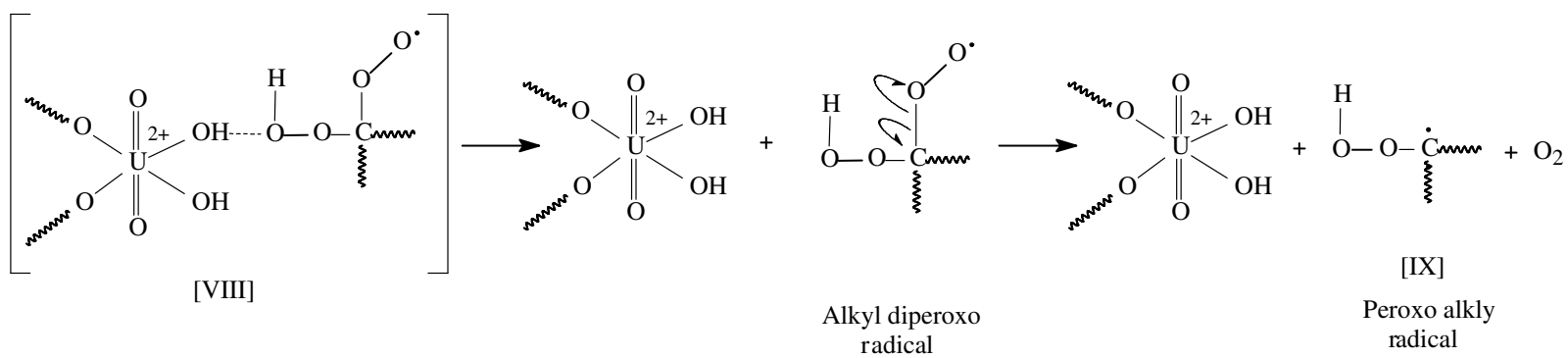


Scheme 6.1. Proposed mechanism in the oxidation of n-alkane with U/ZSM-5.

Step C.

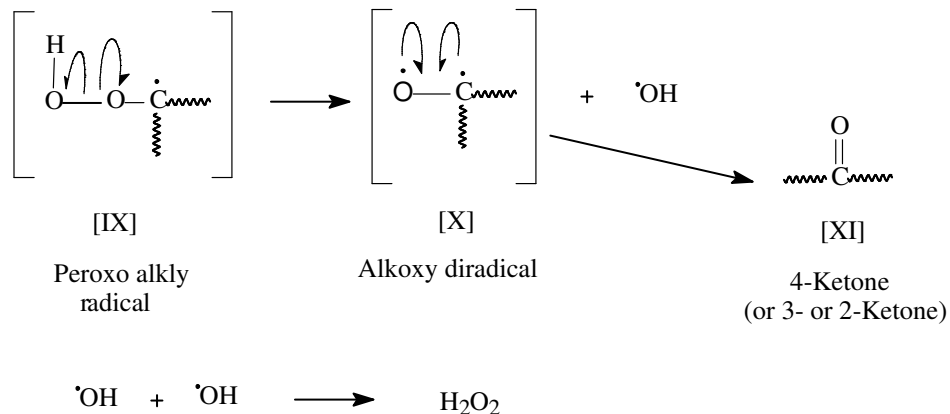


Step D.

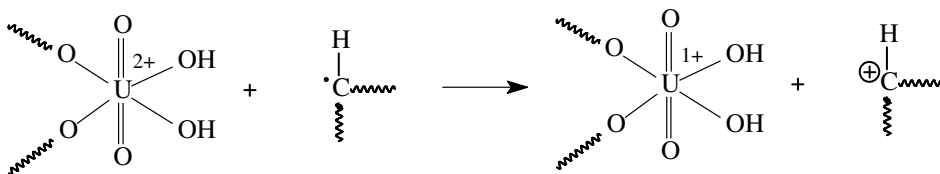


Scheme 6.1. Proposed mechanism in the oxidation of n-alkane with the U/ZSM-5 (Contd.).

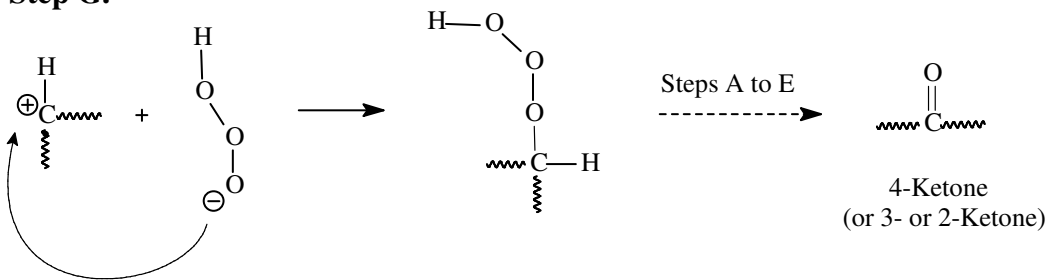
Step E.



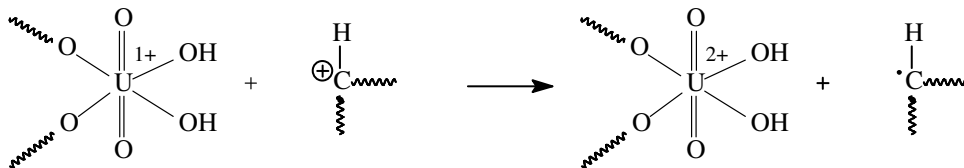
Step F.



Step G.



Step H.



Scheme 6.1. Proposed mechanism in the oxidation of n-alkane with the U/ZSM-5 (Contd.).

This alkyl hydrotrioxide then follows the steps A to E (Scheme 6.1) to produce a ketone compound. Uranium active site of the catalyst loses an electron to the carbocation to generate alkyl radical as illustrated in Scheme 6.1, step H. The alkyl radical generated in step H, then undergoes steps F-G as shown in Scheme 6.1 thereby producing a ketone compound.

6.5. Ozonation of n-hexadecane using Al-MCM-41 with different Si/Al ratios:

The reaction conversion and products selectivity data as function of ozonation time in presence of two mesoporous molecular sieve materials namely Al-MCM-41 Si/Al-60 and Al-MCM-41 Si/Al-90 catalysts on the ozonation of n-hexadecane are summarised in Tables 6.16 and 6.17. The conversion rate and selectivities of ozone initiated oxidation of n-hexadecane in presence of the said mesoporous molecular sieve materials during 3 to 24 h are illustrated in Fig. 6.9. During 24 h ozonation, there is no considerable variation in the conversions observed with the different Si/Al ratios of the Al-MCM-41 catalysts.

Table 6.16. Ozonation of n-hexadecane with Al-MCM-41 Si/Al-90.

Ozonation Time, h	% Conversion	% Selectivity				
		4-Hexa-decanone	3-Hexa-decanone	2-Hexa-decanone	X _{COOH}	Unidentified products
3	6	59	12	12	12	5
6	12	61	13	12	6	8
12	27	58	12	11	4	15
18	39	55	11	10	4	20
24	52	48	10	9	9	24

Table 6.17. Ozonation of n-hexadecane with Al-MCM-41 Si/Al-60.

Ozonation Time, h	% Conversion	% Selectivity				
		4-Hexa-decanone	3-Hexa-decanone	2-Hexa-decanone	X _{COOH}	Unidentified products
3	8	40	8	9	11	4
6	13	54	11	11	10	7
12	28	56	11	11	5	15
18	40	54	11	11	6	18
24	52	48	10	9	10	22

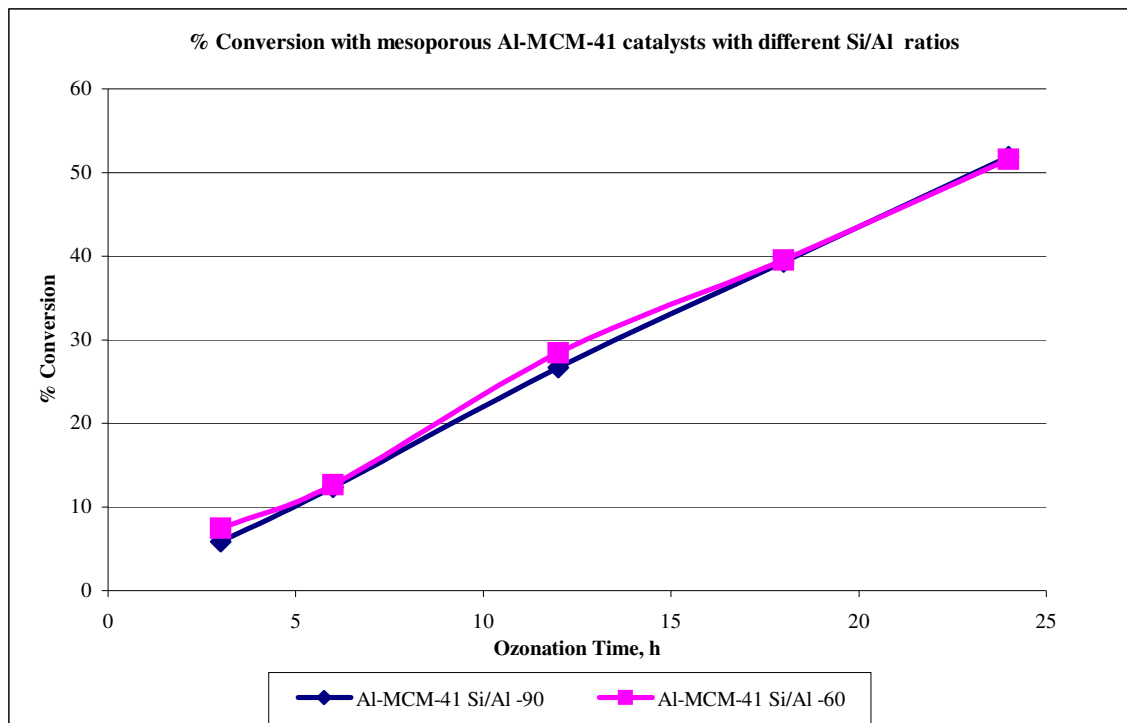


Figure 6.9. Conversion of n-hexadecane with mesoporous Al-MCM-41 catalysts with different Si/Al ratio.

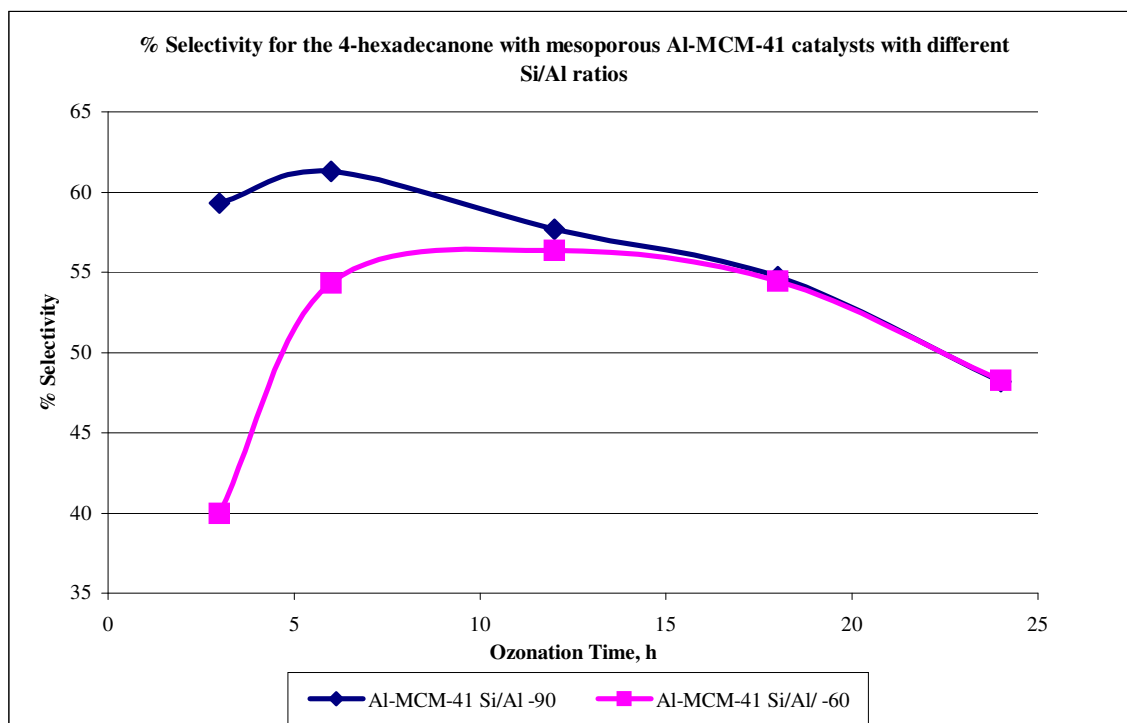


Figure 6.10. Selectivity for the 4-hexadecanone with mesoporous Al-MCM-41 catalysts with different Si/Al ratio.

The observed increase in conversion could be attributed to an increase in moderate and strong acid sites. Flanigen¹⁹⁵ studies reveal that the zeolites structure with low Si/Al ratios can have higher concentration of catalytic sites than the others. The rate of conversion with Al-MCM-41 catalysts was found to be higher than that of the other catalysts employed in the ozonation reactions, this can be ascribed due to the stronger acidic sites and the active catalytic sites available on the surface of the mesoporous material applied in these reactions.

The selectivities of the two mesoporous molecular sieves, namely Al-MCM-41 Si/Al-90 and Al-MCM-41 Si/Al-60 towards 4-hexadecanone, during the ozone initiated oxidation of n-hexadecane are illustrated in Fig. 6.10. An observation of Fig. 6.10 indicates that selectivity for the 4-hexadecanone during 3, 6 and 12 h ozonation, Al-MCM-41 with Si/Al ratio of 90 showed high selectivity towards 4-hexadecanone. After 18 to 24 h ozonation, no appreciable difference in the selectivity was observed with both the mesoporous material having different Si/Al ratios as depicted in Tables 6.16 and 6.17. The increase in aluminium content, i.e., Si/Al = 60, the selectivity was low, possibly due to the low concentration of moderate-to-strong acid sites (Brönsted acid sites). Further, both catalysts showed good structural stability during the reaction. The large pore size (20-200 Å) 1D structure Al-MCM-41 catalysts have large surface area (~770 m² g⁻¹) available for the selective oxidation of n-hexadecane.

It is known that Si/Al ratio affects the acidity of the Al-MCM-41 catalyst. Consequently the higher Si/Al ratio reflects a lower acidity³⁰⁸. The acidity had no effect on the conversion of n-hexadecane with different Si/Al ratio Al-MCM-41 catalysts. Whereas, the selectivity in favour of 4-hexadecanone with the lower acidic catalyst (Al-MCM-41 Si/Al-90) showed higher catalytic activity up to 18 h ozonation. The performance of Al-MCM-41 Si/Al-60 (acidic catalyst) resulted low selectivity for 4-hexadecanone up to 12 h ozonation.

6.6. Ozonation of higher alkanes (n-C₁₆H₃₄, n-C₁₄H₃₀ and n-C₁₂H₂₆) with zeolite beta (H form) catalyst:

The reaction conversion and products selectivity data as function of ozonation time in presence of zeolite beta (H form) materials on the ozone initiated oxidation of n-hexadecane, n-tetradecane and n-dodecane are summarised in Tables 6.18-6.20. An increase in the conversion of n-hexadecane into isomers of hexadecanones and carboxylic acids was observed with zeolite H beta catalyst. The percentage conversion increased as function of time from 5 (3 h) to 36 (24 h). Whereas, the selectivity for the 4-hexadecanone during the first 18 h was increased with time and

on further ozonation up to 24 h decreased to 53%. Further oxidation of the isomer products took place, as a result the ketone isomer products oxidized into different carboxylic acids. A small difference in the selectivities of the 3- and 2-hexadecanone can be observed during the ozonation up to 24 h as illustrated in Table 6.18. In the ozonation of n-tetradecane with zeolite H beta catalysts, conversion of the substrate increased with longer exposure to ozone as shown in the Fig. 6.11. Upon 24 h ozonation 40% of conversion observed and the selectivity towards the main product, 4-tetradecanone was increased during the first 6 h ozonation (67%) as described in Fig. 6.12. One can notice the gradual decrement in the selectivity due to the formation of carboxylic acids, as further oxidation of the products taking place. It was observed that the selectivity towards 3- and 2-tetradecanone increased steadily for the initial 12 h ozonation as represented in Table 6.19. In case of n-dodecane ozonation with zeolite beta (H form) catalyst, conversion rate increased with time as depicted in Table 6.20. Whereas, the selectivity towards 4-dodecanone was decreased gradually with exposure to ozone for longer periods, due to the further oxidation of 4-dodecanone. One can observe the formation of 3- and 2-dodecanone are more compared to that of the hexadecanones and tetradecanones (Tables 6.18-6.20), shows that the ozone is more skilled in the oxidation of alkanes with lower chain lengths (Figs. 6.11 and 6.12).

Table 6.18. Ozonation of n-hexadecane with zeolite beta (H form) catalyst.

Ozonation Time, h	% Conversion	% Selectivity		
		4-Hexadecanone	3-Hexadecanone	2-Hexadecanone
3	5	50	11	13
6	10	56	12	13
12	20	58	12	12
18	28	58	12	11
24	36	53	11	10

Table 6.19. Ozonation of n-tetradecane with zeolite beta (H form) catalyst.

Ozonation Time, h	% Conversion	% Selectivity		
		4-Tetradecanone	3-Tetradecanone	2-Tetradecanone
3	6	61	14	12
6	12	67	17	14
12	24	63	18	14
18	31	59	17	13
24	40	55	16	12

These catalytic ozonation studies reveals that the oxidation takes place at secondary hydrogens viz. 4-, 3- and 2- positions irrespective of the n-alkane. The formation of the cleavage products by ozone attack on the secondary C-H bonds leads to ketones. During the ozonation of the n-alkane there is a possibility that the O₃ can attack the substrate directly and the formed products 4-, 3- and 2-ketones. The carboxylic acids were formed by the further oxidation of the products (ketones) in the reaction. The carboxylic acid formation follows the mechanism involving ester as an intermediate, followed by the scission of –COOC– bond with >C=O on each fragment as illustrated in Scheme 4.3 (Section 4.4.2, Chapter IV).

Table 6.20. Ozonation of n-dodecane with zeolite beta (H form) catalyst.

Ozonation Time, h	% Conversion	% Selectivity		
		4-Dodecanone	3-Dodecanone	2-Dodecanone
3	7	61	21	18
6	13	55	21	16
12	28	46	18	14
18	35	46	19	13
24	41	45	18	12

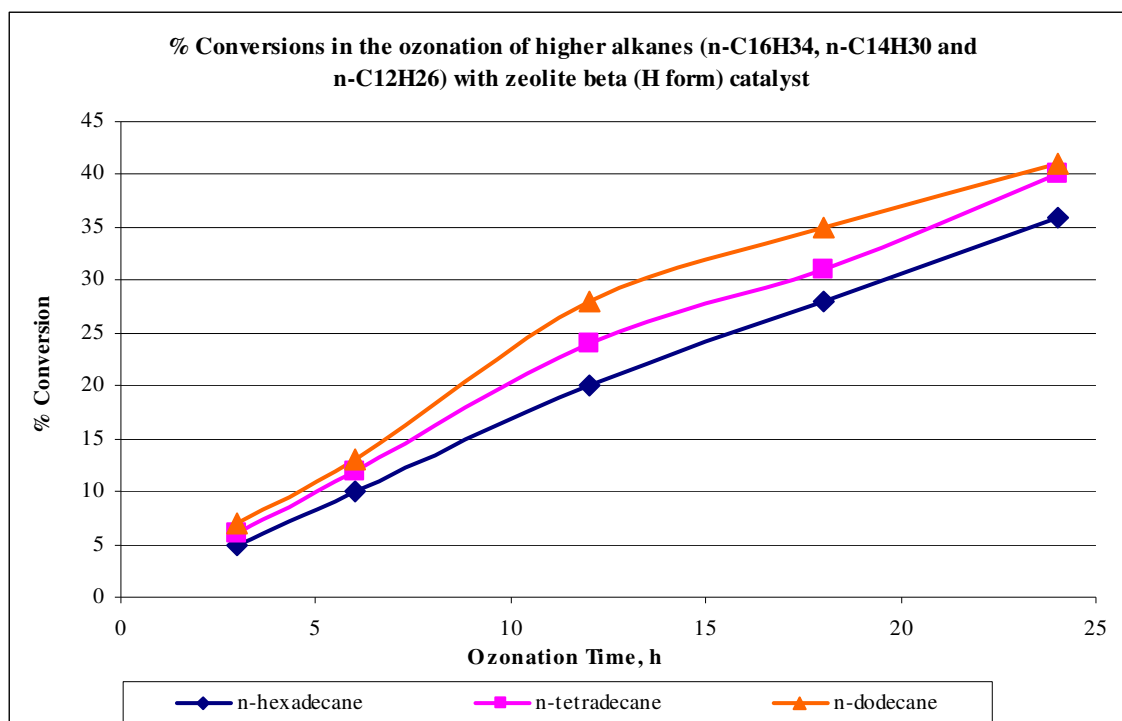


Figure 6.11. Conversions in ozonation of higher alkanes (n-C₁₆H₃₄, n-C₁₄H₃₀ and n-C₁₂H₂₆) with zeolite beta (H form) catalyst.

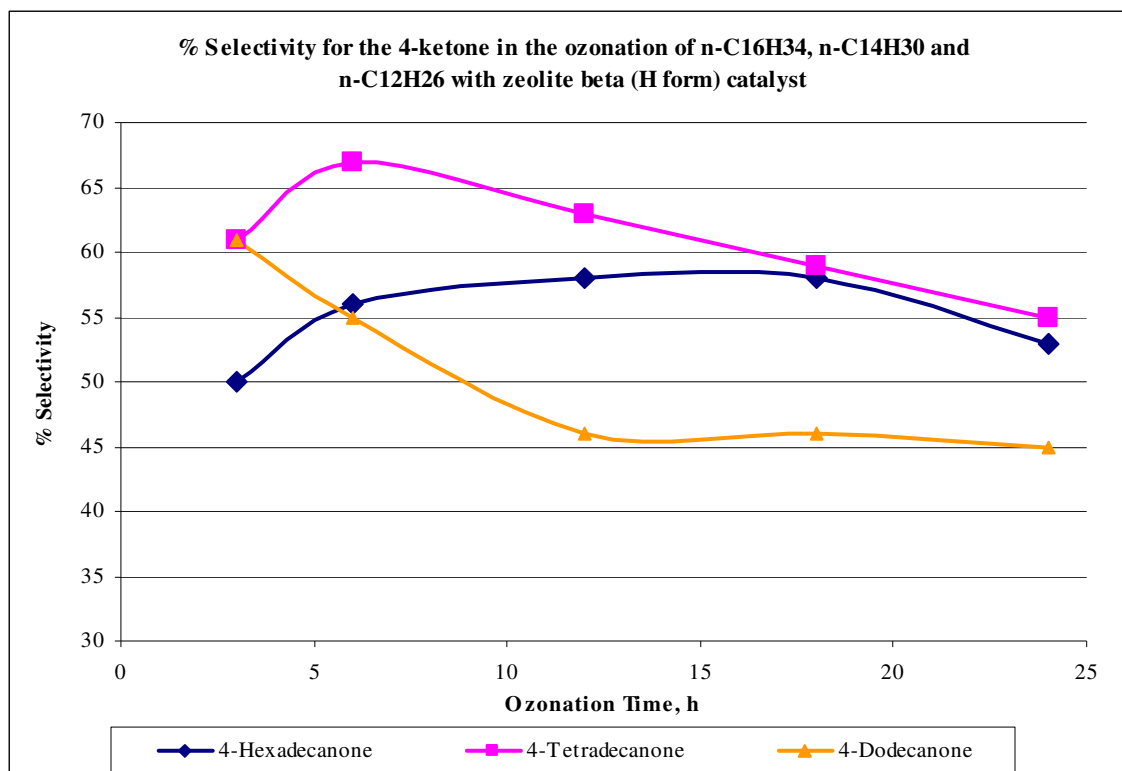


Figure 6.12. Selectivity for the 4-ketone in the ozonation of n-C₁₆H₃₄, n-C₁₄H₃₀ and n-C₁₂H₂₆ with zeolite beta (H form) catalyst.

Generally, the higher activity of the metals impregnated catalysts can be seen for ozone decomposition when compared to the supports itself. This probably results from an increase of electron transfer and, furthermore, an increase in the rate of redox reaction that takes place in the case of metal on support catalysts. This on the other hand, accelerates the catalytic reactions as described by Legube *et al*¹³⁷.

6.7. Ozonation of higher alkanes (n-C₁₆H₃₄ and n-C₁₄H₃₀) with zeolite-X catalyst:

The conversion rate and selectivities of ozone initiated oxidation of n-hexadecane and n-tetradecane in presence zeolite-X at 6 h intervals are summarised in Tables 6.21 and 6.22. Further the conversion efficiencies and selectivities of the catalyst on the said substrates are illustrated in Fig. 6.13. In the catalytic ozonation studies on n-hexadecane with zeolite-X, percentage conversion increased as function of time from 3 to 27 (3 to 24 h). Whereas, the selectivity for 4-hexadecanone during the first 12 h increased with time and on further ozonation up to 24 h decreased to 42% as represented in Fig. 6.13. The ketone isomer products were oxidized to different carboxylic acids on further oxidation of the isomer products. A small

difference in the selectivities towards the 3- and 2-hexadecanone can be observed during the 24 h ozonation as shown in Table 6.21.

Table 6.21. Ozonation of n-hexadecane with zeolite-X catalyst.

Ozonation Time, h	% Conversion	% Selectivity		
		4-Hexadecanone	3-Hexadecanone	2-Hexadecanone
3	3	46	13	11
6	7	53	13	11
12	13	55	12	11
18	20	51	12	10
24	27	42	10	9

Table 6.22. Ozonation of n-tetradecane with zeolite-X catalyst.

Ozonation Time, h	% Conversion	% Selectivity		
		4-Tetradecanone	3-Tetradecanone	2-Tetradecanone
3	6	63	14	14
6	15	68	16	19
12	34	64	15	13
18	47	56	17	15
24	54	45	17	14

n-Tetradecane conversion with zeolite-X catalyst increased with time as illustrated in Table 6.22. The conversion after 24 h ozonation was observed as 54% since the reaction was vigorous with the short chain lengths. Whereas, the selectivity towards 4-tetradecanone was more during the first 6 h ozonation and decreased gradually with longer exposure to ozone, due to the further oxidation of 4-tetradecanone. It was observed that the amounts of 3- and 2-tetradecanone are higher than that of hexadecane ozonation as depicted in Tables 6.21 and 6.22. As discussed in the previous section that the catalytic activity showed by support itself was much lower than that of the metals impregnated catalysts.

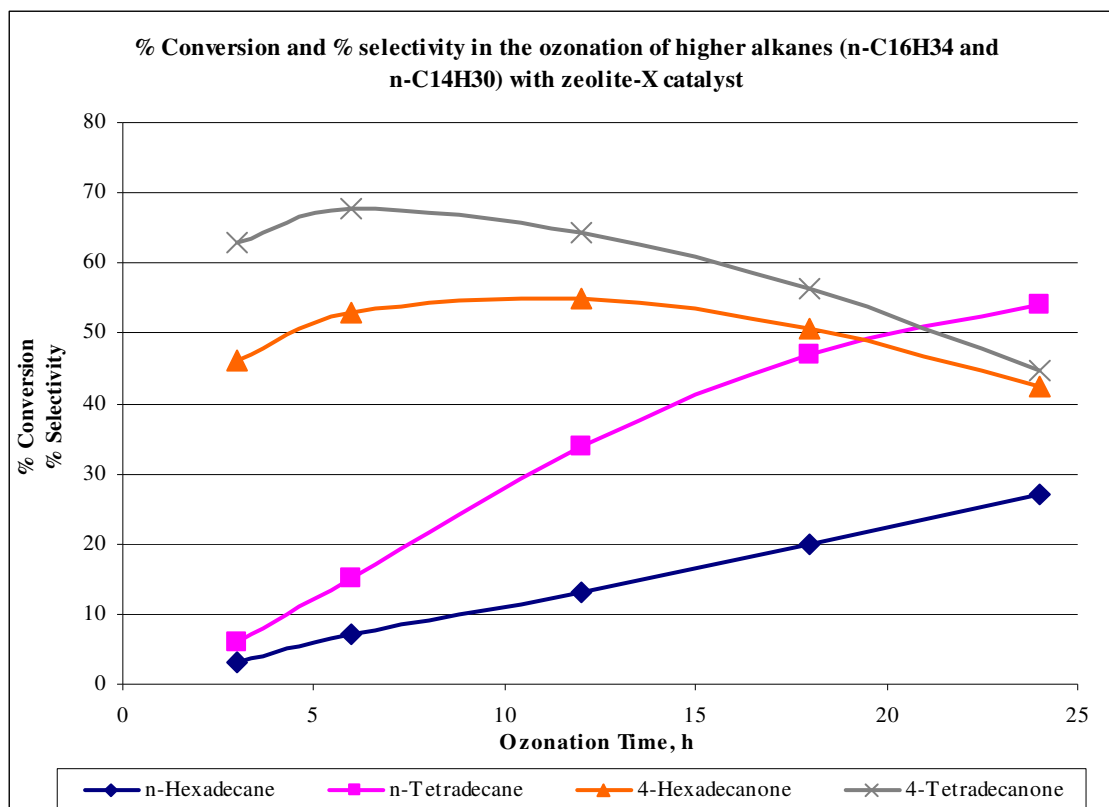


Figure 6.13. Conversion and selectivity in the ozonation of higher alkanes (n-C₁₆H₃₄ and n-C₁₄H₃₀) with zeolite-X catalyst.

6.8. Ozonation of n-hexadecane with 5% metal loaded zeolite catalysts:

Ozonation of n-hexadecane reactions were carried out with 5% metal catalysts for conversion and selectivity studies. The catalyst systems used in these studies were 5% Ni/Na-Y, 5% Ni/ZSM-5, 5% Ni/HB150, 5% Mn/HB150, 5% Mo/HB150 and 5% Co/HB 150.

6.8.1. Ozonation of n-hexadecane with 5% Ni on different zeolite supports:

Ozonation of n-hexadecane with 5% Ni impregnated on different zeolite supports like ZSM-5, Na-Y and HB150 were studied to compare the activity of the Ni metal anchored in different zeolitic framework. Tables 6.23-6.25 summarize the results of ozone initiated oxidation reactions of 5% Ni incorporated microporous material namely 5% Ni/Na-Y, 5% Ni/ZSM-5 and 5% Ni/HB150. The conversion rate and selectivities of ozonation of n-hexadecane in presence of the said 5% Ni-incorporated molecular sieve materials during 3 to 24 h are illustrated in Fig. 6.14 and 6.15. It was clear that 5% Ni/HB150 showed higher conversion during the first 12 h ozonation (28%) and further oxidation up to 24 h the activity of 5% Ni/ZSM-5 catalyst was found higher as

shown in Fig. 6.14. Normally heterogeneous reactions take place inside the framework of the zeolite, these zeolites have large internal surface than their external surface. This can provide the appropriate surface where the catalytic transformations can take place.

Table 6.23. Ozonation of n-hexadecane with 5% Ni/ZSM-5 zeolite.

Ozonation Time, h	% Conversion	% Selectivity		
		4-Hexadecanone	3-Hexadecanone	2-Hexadecanone
3	5	59	12	11
6	10	61	18	11
12	23	55	12	11
18	38	54	10	9
24	45	50	11	9

Table 6.24. Ozonation of n-hexadecane with 5% Ni/Na-Y zeolite.

Ozonation Time, h	% Conversion	% Selectivity		
		4-Hexadecanone	3-Hexadecanone	2-Hexadecanone
3	5	60	12	11
6	10	61	18	11
12	24	44	12	10
18	37	46	10	8
24	41	43	11	9

Table 6.25. Ozonation of n-hexadecane with 5% Ni/HB150 zeolite.

Ozonation Time, h	% Conversion	% Selectivity		
		4-Hexadecanone	3-Hexadecanone	2-Hexadecanone
3	10	56	5	4
6	22	58	5	4
12	28	60	10	8
18	33	59	11	9
24	40	55	11	10

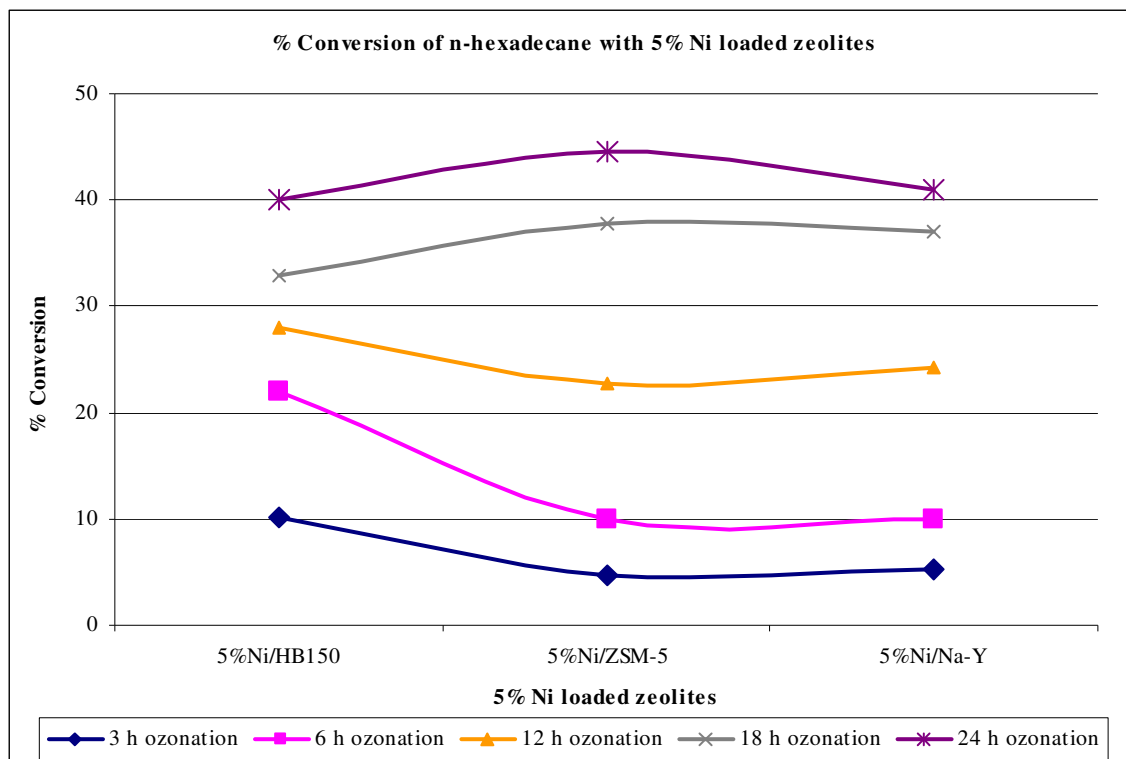


Figure 6.14. Conversion of n-hexadecane with different 5% Ni loaded zeolites.

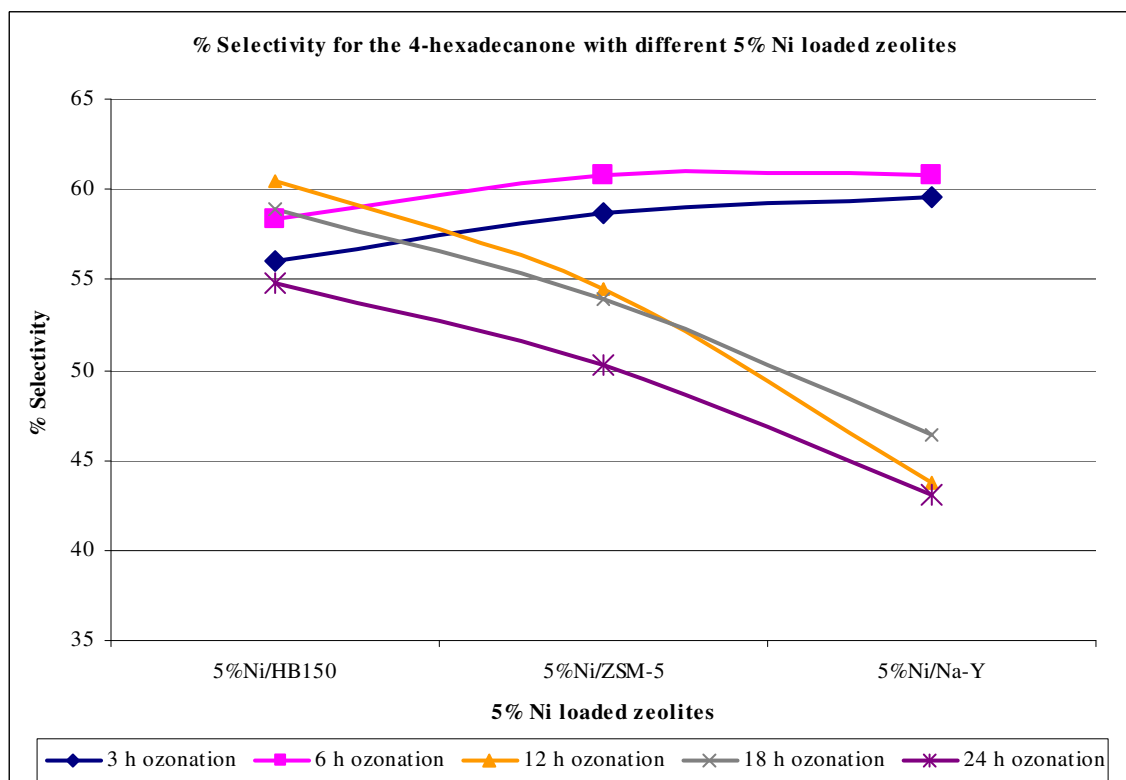


Figure 6.15. Selectivity for the 4-hexadecanone with different 5% Ni loaded zeolites.

The catalyst was found as active during the first 12 h of ozonation and as the duration of reaction is prolonged, the activity was decreased due to the substrate adsorbed on the catalyst surface. The products formed in the ozonation reaction simultaneously reacted with ozone and lead to side products. Hence the active sites of the 3D microporous HB150 catalysts were blocked by starting material and by subsequent products. The catalyst was deactivated due to these reasons when the reaction is run for longer duration of time, as a result the conversion and selectivities were found to be low with the other catalysts. The selectivity with the 5% Ni/HB150 towards 4-hexadecanone was observed higher as represented in Fig. 6.15.

6.8.2. Ozonation of n-hexadecane with 5% metal on HB150 zeolite:

Ozonation of n-hexadecane with 5% metal (Mo, Mn and Co) impregnated on zeolite HB150 supports were studied to compare the activity of different metal incorporated in the framework. Tables 6.26-6.28 summarize the results of these catalytic ozone initiated oxidation reactions using 5% Mo/HB150, 5% Mn/HB150 and 5% Co/HB150 zeolites respectively. The conversion rate and selectivities of these three molecular sieves towards 4-hexadecanone, during the ozone initiated oxidation of n-hexadecane are illustrated in Fig. 6.16 and 6.17.

Table 6.26. Ozonation of n-hexadecane with 5% Mo/HB150 zeolite.

Ozonation Time, h	% Conversion	% Selectivity		
		4-Hexadecanone	3-Hexadecanone	2-Hexadecanone
3	6	56	12	9
6	9	61	13	11
12	20	59	12	10
18	28	55	14	10
24	35	49	14	12

The examination of Fig. 6.16 shows that there is an increase in conversion of n-hexadecane into isomers of hexadecanones and carboxylic acids. The percentage conversion with 5% Mo/HB150 catalyst increased as function of ozonation time from 6 (3 h) to 35 (24 h). Whereas, the selectivity for 4-hexadecanone during the first 6 h was 61% and decreased (49%) as a result of further oxidation of the isomer products into different carboxylic acids upon 24 h ozonation. The formation of 3- and 2-hexadecanones during 24 h ozonation also followed the same trend of 4-hexadecanone (Table 6.26). The conversion and selectivities with 5% Mn/HB150 catalyst

followed the similar trend as 5% Mo/HB150. The formation of 3- and 2-hexadecanone during 24 h ozonation was observed as less than in the case of Mo/HB150 catalyst as shown in Table 6.27.

Table 6.27. Ozonation of n-hexadecane with 5% Mn/HB150 zeolite.

Ozonation Time, h	% Conversion	% Selectivity		
		4-Hexadecanone	3-Hexadecanone	2-Hexadecanone
3	3	52	11	9
6	7	63	13	11
12	17	60	12	11
18	27	56	11	10
24	34	42	11	10

Table 6.28 shows the conversion and selectivity trends with 5% Co/HB150 catalyst. The percentage conversion was increased as function of time from 4 (3 h) to 42 (24 h). The selectivity towards the 4-hexadecanone was increased for the first 6 h was 64% and decreased on further ozonation up to 24 h (43%). The formation of carboxylic acids took place as a result of further oxidation taking place with further oxidation. The 3- and 2- isomers formation for 24 h was less when compared with 5% Mn- and 5% Mo- loaded HB150 catalysts as represented in Fig. 6.17.

Table 6.28. Ozonation of n-hexadecane with 5% Co/HB150 zeolite.

Ozonation Time, h	% Conversion	% Selectivity		
		4-Hexadecanone	3-Hexadecanone	2-Hexadecanone
3	4	61	12	10
6	10	64	13	11
12	23	60	15	9
18	35	50	10	9
24	42	43	11	9

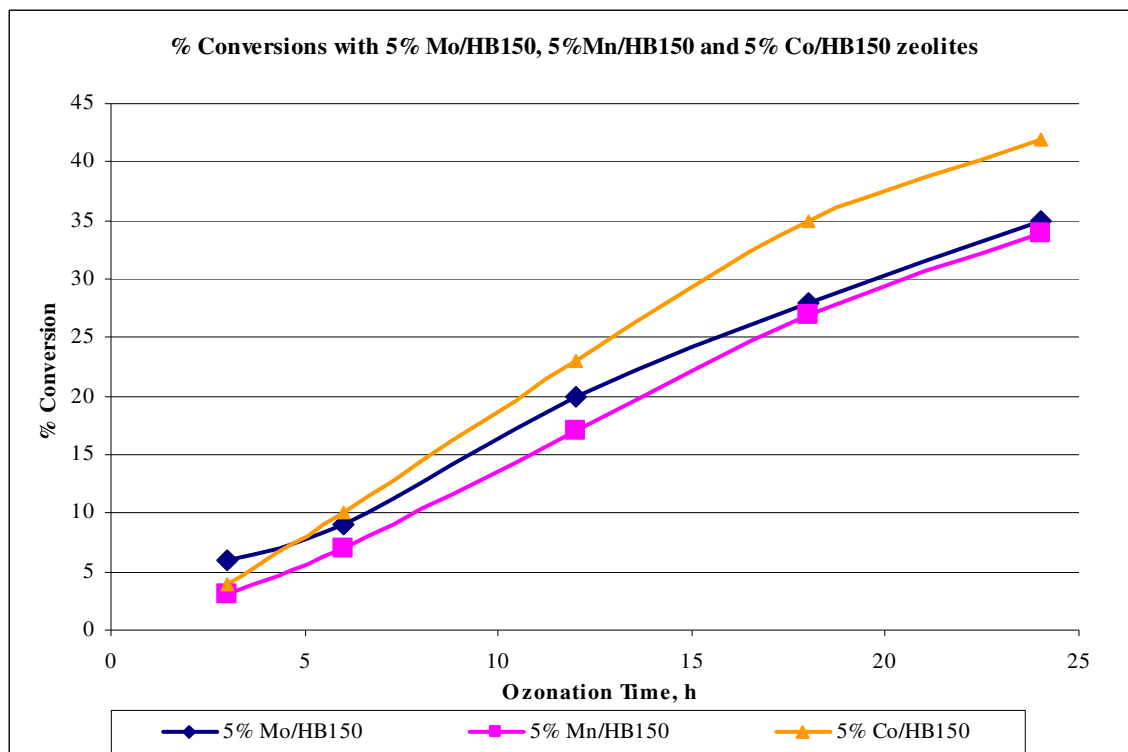


Figure 6.16. Conversions with different 5% metal loaded HB150 (5% Mo/HB150, 5% Mn/HB150 and 5% Co/HB150) zeolites.

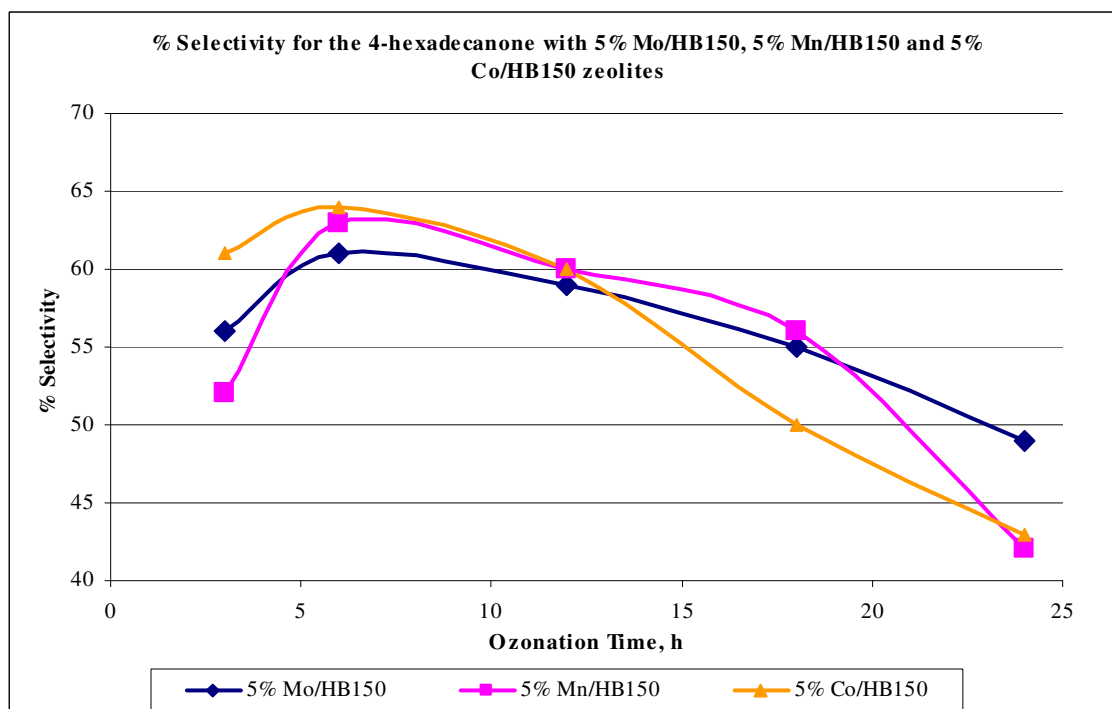


Figure 6.17. Selectivity for the 4-hexadecanone with different 5% metal loaded HB150 (HB150 with 5% Mo/HB150, 5% Mn/HB150 and 5% Co/HB150) zeolites.

The overall conversion was more with 5% Co catalyst, whereas the selectivity towards the 4-hexadecanone was less compared to 5% Mn- and 5% Mo- loaded HB150 catalysts. The selectivity for 4-hexadecanone was observed more with 5% Mn- and 5% Mo- loaded HB150 catalysts during the first 12 h. The selectivity towards the 4-hexadecanone with all the catalysts was more during the first 6 h ozonation and gradually decreased with longer exposure to ozone, due to the further oxidation of 4-hexadecanone.

6.9. Comparison of the efficiency of n-hexadecane conversion with different 5% metal loaded zeolite catalysts:

Comparison of the efficiency of n-hexadecane conversion was done to find the active catalysts among all the 5% metal loaded zeolites in the ozone initiated oxidation reactions. Table 6.29 summarizes the results of conversion patterns of six molecular sieve materials with all the 5% metal loadings, namely 5%Ni/HB150, 5%Ni/ZSM-5, 5%Ni/Na-Y, 5%Mo/HB150, 5%Mn/HB150 and 5%Co/HB150. It is noticed that during the initial ozonation up to 12 h, 5%Ni/HB150 showed highest activity. The catalytic activity at 18 h ozonation was found as more with 5%Ni/ZSM-5 and 5%Ni/Na-Y as shown in Fig. 6.18. Among all the 5% metal catalysts 5%Ni/ZSM-5 showed higher activity, 5%Ni/Na-Y and 5%Co/HB150 catalysts were also yielded considerably higher conversions. The 5% Ni impregnated catalysts showed higher activity than that of the other metal impregnated catalysts, 5% Co also showed convincingly higher activity during the 24 h ozonation.

Table 6.29. Conversion of n-hexadecane with different 5% metal loaded zeolite catalysts.

Ozonation Time, h	5%Ni/HB150	5%Ni/ZSM-5	5%Ni/Na-Y	5%Mo/HB150	5%Mn/HB150	5 % Co/HB150
3	10	5	5	6	3	4
6	22	10	10	9	7	10
12	28	23	24	20	17	23
18	33	38	37	28	27	35
24	40	45	41	35	34	42

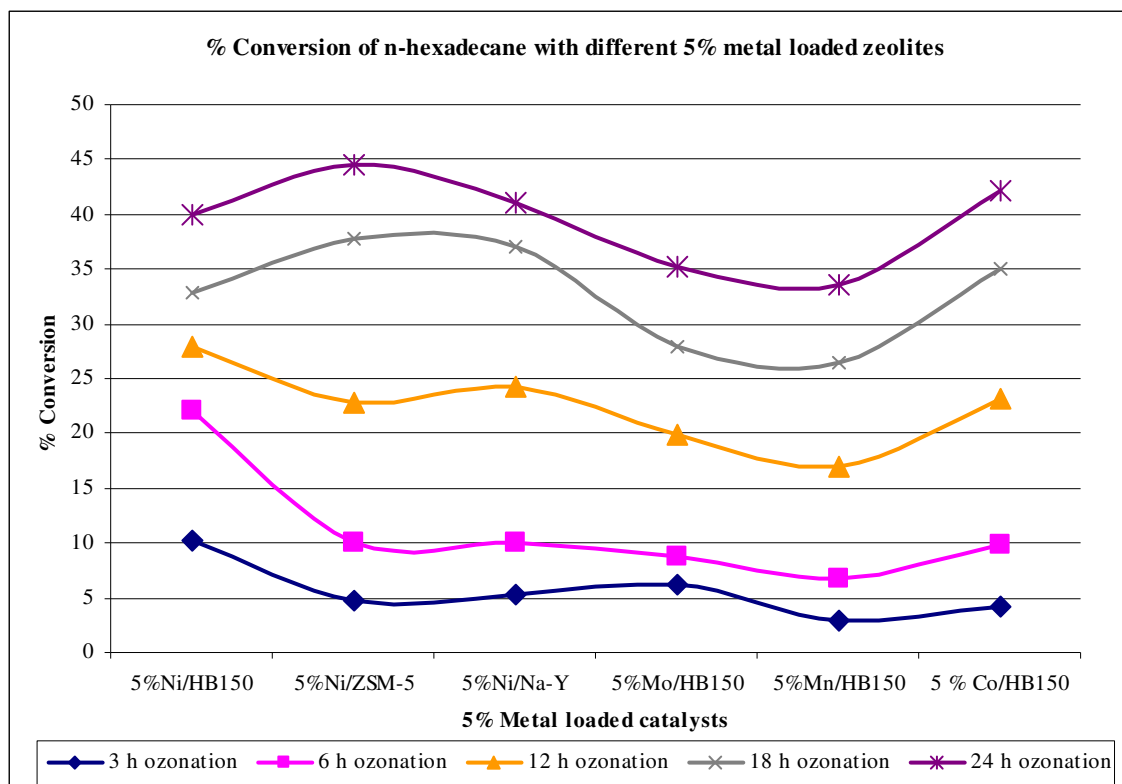


Figure 6.18. Conversion of n-hexadecane with different 5% metal loaded zeolites.

6.9.1. Comparison of the selectivity for 4-hexadecanone with different 5% metal loaded zeolite catalysts:

Comparison of the selectivity for 4-hexadecanone with different 5% metal loaded zeolites was done to find the active catalysts in the ozone initiated oxidation reactions. All the 5% metal catalysts results for the 4-hexadecanone selectivity are summarized in Table 6.30. 5% Co/HB150 catalysts showed higher activity during the first 6 h of ozonation. 5%Ni/HB150 yielded more selectivity towards the 4-hexadecanone up to 24 h ozonation as represented in Fig. 6.19. 5% Mo/HB150 and 5% Ni/ZSM-5 also showed considerable activity towards the 4-ketone product. The 5% Ni impregnated large pore size ~ 7 Å, surface area ~ 500 m² g⁻¹ and 3D pore accessible large microporous HB 150 catalysts showed higher activity than that of the other impregnated metal catalysts, 5% Mo also showed sensibly higher selectivity during the 24 h ozonation.

Table 6.30. Selectivity for the 4-hexadecanone with different 5% metal loaded zeolite catalysts.

Ozonation Time, h	5%Ni/ HB150	5%Ni/ ZSM-5	5%Ni/ Na-Y	5%Mo/ HB150	5%Mn/ HB150	5 % Co/ HB150
3	56	59	60	56	52	61
6	58	61	61	61	63	64
12	61	55	44	59	60	60
18	59	54	46	55	56	50
24	55	50	43	49	42	43

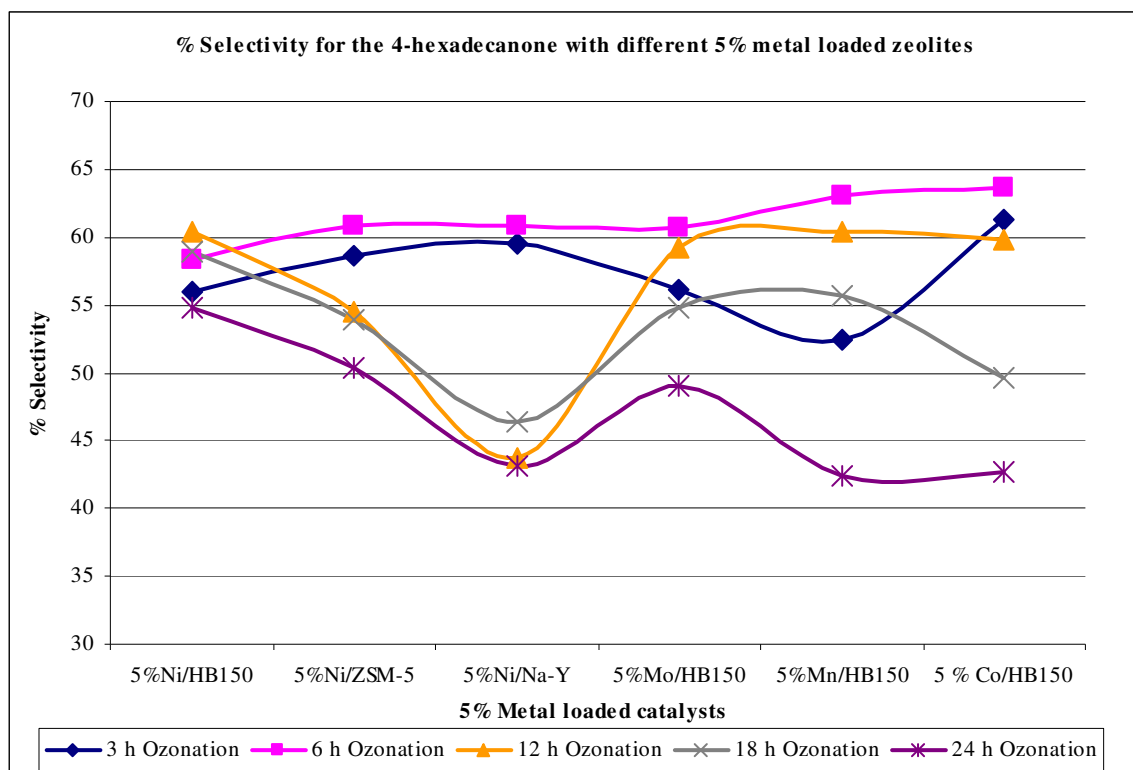
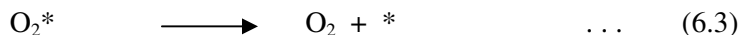
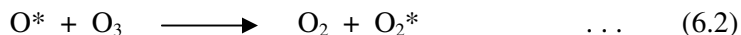
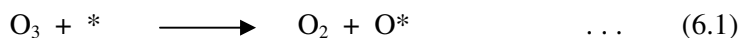


Figure 6.19. Selectivity for the 4-hexadecanone with different 5% metal loaded zeolites.

6.10. Mechanism for ozone decomposition on catalyst sites:

The common mechanism for ozone decomposition on the catalyst's active sites (eqns. 6.1-6.3):



* Active site on the catalyst.

The ozone activity is not only on hexadecane but also the intermediate species formed in the hexadecane oxidation, since the long-lived intermediate species observed on the catalyst surface are not decomposed without ozone feed. The build-up of the intermediate compounds on the catalyst surface steeply decreases the conversions of hexadecane and ozone by blocking the active sites for the ozone decomposition process responsible for hexadecane oxidation.

In the decomposition of intermediate compounds by ozone feed, the decrease of ozone conversion until 12 h implies that they were transformed to other kinds of intermediates that strongly blocked the active sites. The subsequent increase in the ozone conversion after 12 h indicates that these compounds were diminished, resulting in the clean-up of the active sites. By the prolonged ozone feed, the intermediate compounds that were highly resistant to the oxidation with ozone remained on the catalysts surface, giving the bonds containing C-H, C=O and COO- groups.

6.10.1. Mechanism of heterogeneous catalytic ozonation:

As described in the Section 4.11 (Chapter IV) there are three possible mechanisms of catalytic ozonation in heterogeneous systems: chemisorption of ozone on the catalyst surface leading to the formation of active species which react with non-chemisorbed n-alkane molecule ($\text{n-C}_{16}\text{H}_{34}$ or $\text{n-C}_{14}\text{H}_{30}$ or $\text{n-C}_{12}\text{H}_{26}$), chemisorption of n-alkane substrate molecules on the catalytic surface and its further reaction with gaseous or aqueous ozone and chemisorption of both ozone and n-alkane substrate molecules and the subsequent interaction between chemisorbed species.

6.11. Comparison of the efficiency of n-hexadecane conversion with different metal loaded ZSM-5 (Si/Al-30) catalysts:

Table 6.31 illustrates the comparison of the conversion results with different metals loaded microporous ZSM-5 material namely Ni/ZSM-5, Ni/ZSM-5 N_2 calcined, Pd/ZSM-5, Pd/ZSM-5

N₂ calcined, V/ZSM-5, V/ZSM-5 N₂ calcined, U/ZSM-5 and 5%Ni/ZSM-5 catalysts. U/ZSM-5 showed promising results throughout the 24 h ozonation. Ni/ZSM-5, Pd/ZSM-5, Pd/ZSM-5 N₂ calcined showed conversions above 15 % during the first 6 h ozonation. Whereas, U/ZSM-5 showed better conversion results among the other metal loaded ZSM-5 catalysts. Uranyl anchored ZSM-5 zeolite catalysts were found active among all the other metal loaded microporous medium ZSM-5 catalysts as illustrated in Fig 6.20. Uranyl ions, UO₂²⁺ dispersed over dense oxide supports are reported to serve as promising oxidizing catalysts because of its variable valence states and vacant f-orbitals²⁰⁸. Uranyl ions possess instinctive excitation and emission characteristics and are strong oxidizing species as discussed in the previous Section 6.4. It is accepted in the literature that these UO₂²⁺ ions are quenched by the abstraction of hydrogen atoms from the hydrocarbons²¹². The pore systems consisting of near-circular cross-section and straight channels of elliptical shape are accountable for the sorptive and the catalytic properties of ZSM-5. All the intersections in ZSM-5 are of the same size, this could result in high activity of the catalyst.

Table 6.31. Conversions of n-hexadecane with different metal loaded ZSM-5 (Si/Al-30) catalysts.

Ozonation time, h	Ni/ZSM-5	Ni/ZSM-5 N ₂ calcined	Pd/ZSM-5	Pd/ZSM-5 N ₂ calcined
3	6	6	7	7
6	15	12	15	16
12	28	28	27	25
18	39	39	38	36
24	50	51	45	42

Table 6.31. Continued.

Ozonation time, h	V/ZSM-5	V/ZSM-5 N ₂ calcined	U/ZSM-5	5%Ni/ZSM-5
3	5	5	8	5
6	11	10	16	10
12	22	22	33	23
18	32	30	45	38
24	40	39	55	45

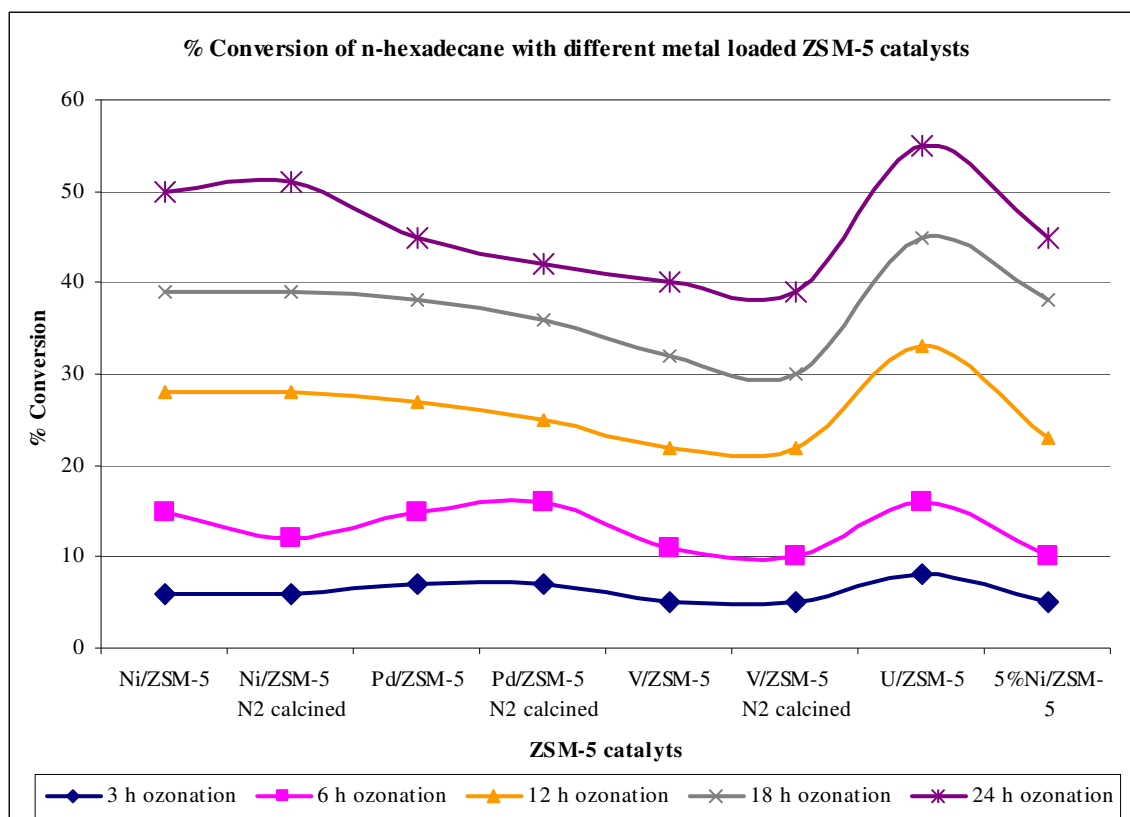


Figure 6.20. Conversions of n-hexadecane with different metal loaded ZSM-5 (Si/Al-30) catalysts.

6.11.1. Comparison of the selectivity for 4-hexadecanone with different metal loaded ZSM-5 (Si/Al-30) catalysts:

The selectivity results for eight ZSM-5 catalysts with different metals namely Ni/ZSM-5, Ni/ZSM-5 N₂ calcined, Pd/ZSM-5 N₂ calcined, V/ZSM-5, V/ZSM-5 N₂ calcined, U/ZSM-5 and 5%Ni/ZSM-5 are recapitulated in Table 6.32. 5%Ni/ZSM-5 and V/ZSM-5 N₂ calcined catalysts showed good selectivity results during the first 3 h ozonation, 59% and 58% respectively. One can notice the increase in the selectivity with all the catalysts during 6 h ozonation. 5% Ni/ZSM-5 and V/ZSM-5 N₂ calcined catalysts were noticed as the highly active after 6 h ozonation, 61% and 60% respectively. V/ ZSM-5 N₂ calcined and 5% Ni/ZSM-5 catalysts showed high selectivity throughout the period of ozonation as shown in Fig. 6.21. Ni/ZSM-5 N₂ calcined, Pd/ZSM-5 N₂ calcined and V/ ZSM-5 also showed promising selectivities during 24 h ozonation reactions. All the metals anchored in the ZSM-5 zeolite were found to be active towards the 4-hexadecanone selectivity.

Table 6.32. Selectivity for the 4-hexadecanone with different metal loaded ZSM-5 (Si/Al-30) catalysts.

Ozonation time, h	Ni/ZSM-5	Ni/ZSM-5 N ₂ calcined	Pd/ZSM-5	Pd/ZSM-5 N ₂ calcined
3	52	51	52	51
6	54	58	54	58
12	56	56	56	56
18	50	50	50	50
24	47	51	47	51

Table 6.32. Continued.

Ozonation time, h	V/ZSM-5	V/ZSM-5 N ₂ calcined	U/ZSM-5	5%Ni/ZSM-5
3	53	58	49	59
6	58	60	57	61
12	54	57	55	55
18	51	55	49	54
24	51	51	44	50

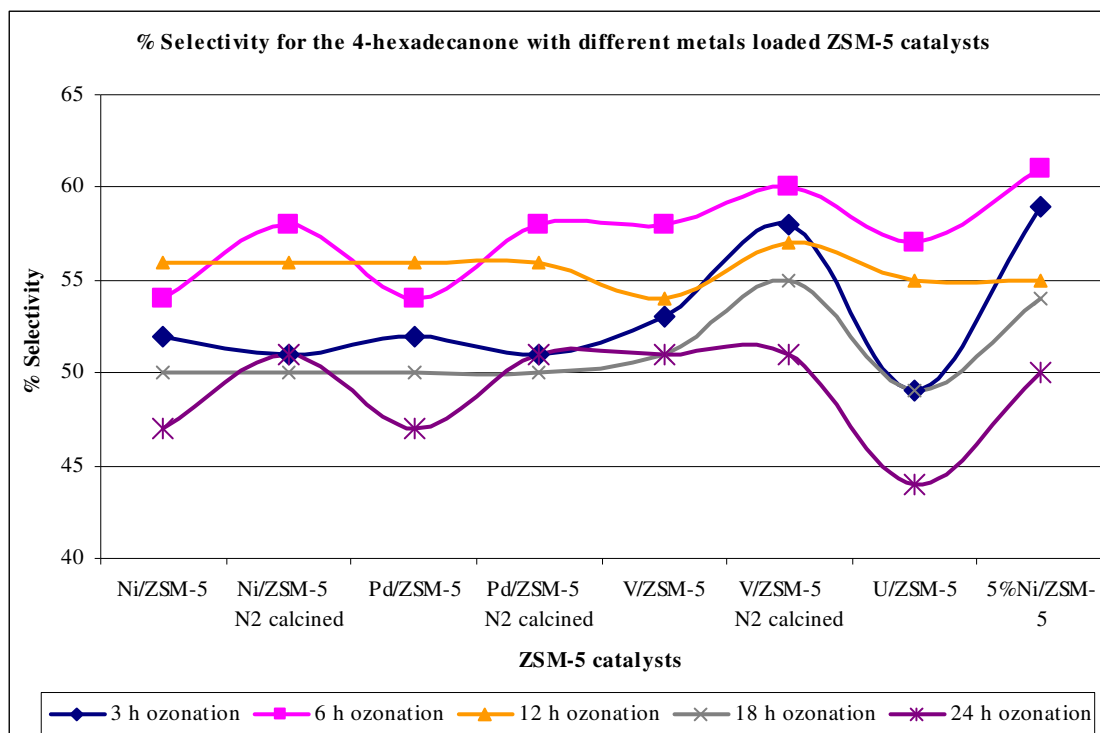


Figure 6.21. Selectivity for the 4-hexadecanone with different metal loaded ZSM-5 (Si/Al-30) catalysts.

6.12. Comparison of the efficiency of n-hexadecane conversion with different metal loaded Na-Y catalysts:

Comparison of the efficiency of n-hexadecane conversion was carried out to find the active metals impregnated on Na-Y zeolite support namely Ni/Na-Y, Ni/Na-Y N₂ calcined, Pd/Na-Y N₂ calcined, V/Na-Y, V/Na-Y N₂ calcined, U/Na-Y and 5%Ni/Na-Y. The activity results of different metals on Na-Y support are summarized in Table 6.33. Ni/Na-Y and V/Na-Y zeolite catalysts showed good conversion during the 24 h ozonation reaction. Nickel and Vanadium metal anchored in large microporous 3D pore accessible Na-Y zeolite support were found active. The results of U metal also found promising during the first 12 h of ozonation as shown in Fig. 6.22. The 5% Ni/Na-Y has no appreciable affect on the ozonation in terms of better conversions. The literature³⁸ indicated that the oxidation state of a reducible metal ion (nickel) in a zeolite depends on the acidity of the zeolite (Na-Y) is easily reducible, while nickel ion in a zeolite (H form) is not easily reduced.

Table 6.33. Conversion of n-hexadecane with different metal loaded Na-Y catalysts.

Ozonation time, h	Ni/Na-Y	Ni/Na-Y N ₂ calcined	Pd/Na-Y	Pd/Na-Y N ₂ calcined
3	5	5	5	5
6	13	9	12	12
12	27	19	30	28
18	34	29	39	43
24	51	38	48	45

Table 6.33. Continued.

Ozonation time, h	V/Na-Y	V/Na-Y N ₂ calcined	U/Na-Y	5%Ni/Na-Y
3	6	4	7	5
6	15	9	15	10
12	28	23	29	24
18	45	37	38	37
24	51	48	45	41

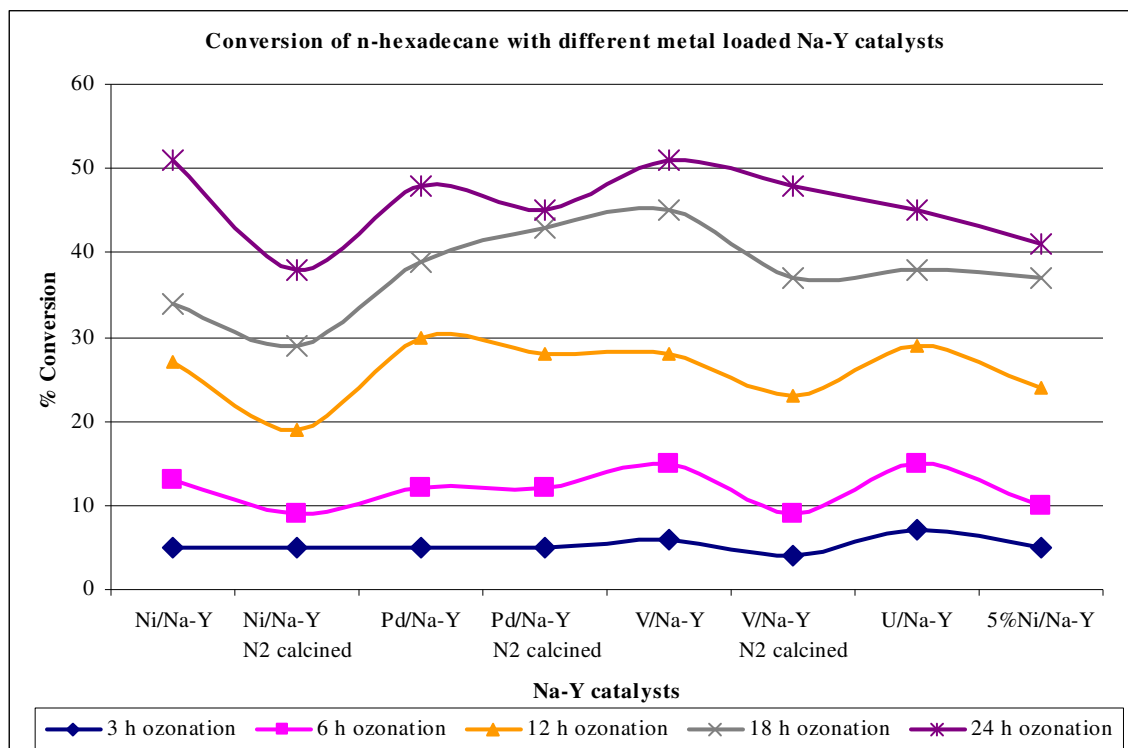


Figure 6.22. Conversion of n-hexadecane with different metal loaded Na-Y catalysts.

6.12.1. Comparison of the selectivity for 4-hexadecanone with different metal loaded Na-Y catalysts:

Comparison of the selectivity for 4-hexadecanone was carried out to find the active metals impregnated on Na-Y zeolite support namely Ni/Na-Y, Ni/Na-Y N₂ calcined, Pd/Na-Y N₂ calcined, V/Na-Y, V/Na-Y N₂ calcined, U/Na-Y and 5%Ni/Na-Y. These selectivity results of Na-Y catalysts with different metals are reviewed in Table 6.34. The selectivity was found more with 5% Ni/Na-Y catalyst during the first 6 h ozonation.

Table 6.34. Selectivity for the 4-hexadecanone with different metal loaded Na-Y catalysts.

Ozonation time, h	Ni/Na-Y	Ni/Na-Y N ₂ calcined	Pd/Na-Y	Pd/Na-Y N ₂ calcined
3	53	55	53	55
6	57	52	57	52
12	51	51	51	51
18	49	46	49	46
24	45	52	46	52

Table 6.34. Selectivity for the 4-hexadecanone with different metal loaded Na-Y catalysts
(contd.).

Ozonation time, h	V/Na-Y	V/Na-Y N ₂ calcined	U/Na-Y	5%Ni/Na-Y
3	56	54	56	60
6	56	58	56	61
12	55	54	52	44
18	47	50	51	46
24	45	48	49	43

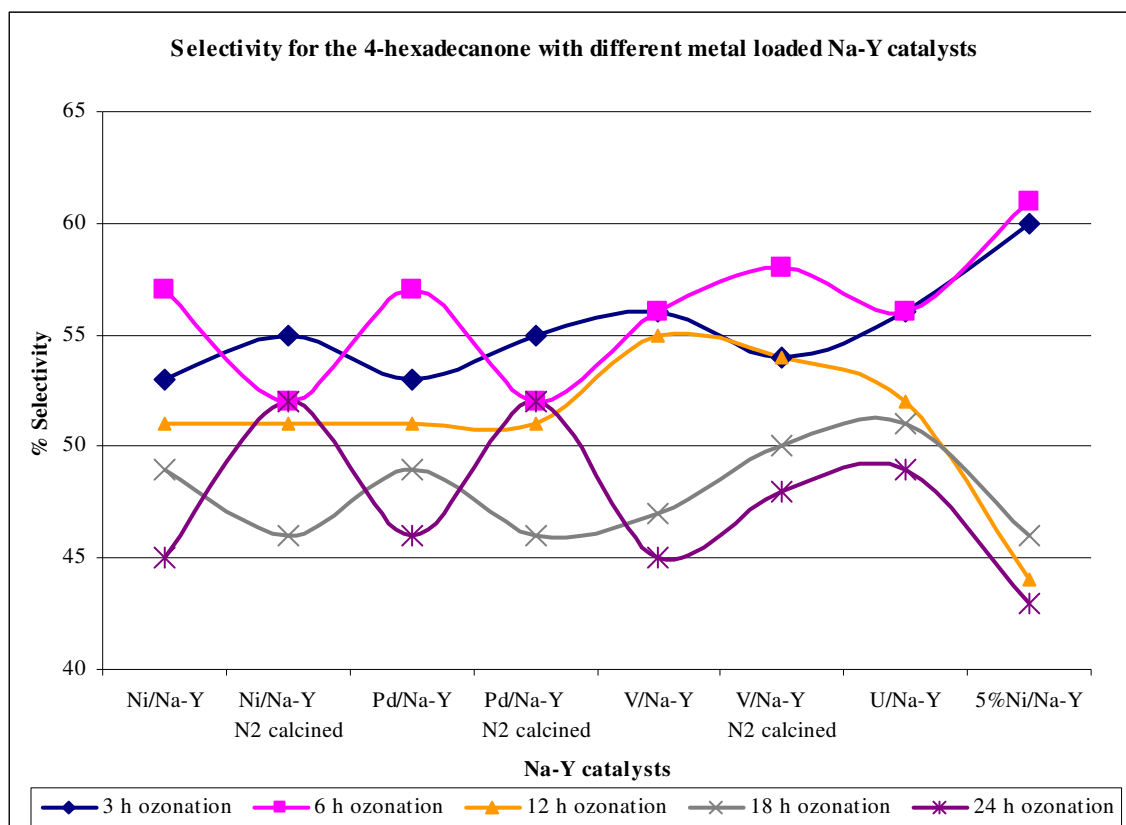


Figure 6.23. Selectivity for the 4-hexadecanone with different metal loaded Na-Y catalysts.

The problem in the functionalisation of saturated hydrocarbons is that their low reactivity due to carbon and hydrogen, not having electron pairs and the molecules do not have orbitals of sufficient energy, that are easily accessible. Thus, highly reactive reagents and/or extreme reaction conditions are typically required in the oxidation of alkanes. However, the initial

products are almost always more reactive than the starting compounds, and undesired side reactions may occur.

An observation of Fig 6.23 shows that the selectivity with most of the catalysts is above 51% during 12 h ozonation, further on oxidation 4-hexadecanone was oxidized into carboxylic acids, resulting decrease in the 4-hexadecanone selectivity. Uranium impregnated Na-Y also showed promising selectivities during the 24 h ozonations as shown in Fig. 6.23. 5% Ni/Na-Y showed less activity compared to 0.5% Ni/Na-Y for the period of 24 h ozonation.

The study indicates that the ozonation of higher alkanes using the zeolite supports alone as a catalyst show poor activity. The metal impregnated microporous uni-dimensional and 3-dimensional zeolites like Na-Y, ZSM-5 Si/Al-30 catalysts; mesoporous Al-MCM-41 Si/Al-90 and Al-MCM-41 Si/Al-60 catalysts have improved activity towards the conversion and selectivity during the catalytic ozonation. Thus the results suggests that optimum conversion of the higher alkanes is achievable with U/ZSM-5, Al-MCM-41 (60), Al-MCM-41 (90) as catalysts and similarly good selectivities are attainable with Ni/ZSM-5, Ni/Na-Y and V/Na-Y as catalysts.

CHAPTER - VII

CONCLUSIONS

7.0. Conclusions:

The use of solvents to enhance the ozone solubility or reactivity towards the higher hydrocarbons is futile and not suitable. Carbon tetrachloride increases the solubility of ozone, but is not apt as solvent for higher hydrocarbon oxidation using ozone, as that itself easily gets oxidised. Hexachloroethane and tetrachloroethene were the main products of ozone initiated oxidation of CCl_4 . The use of tetrahydrofuran as solvent in ozonation also resulted in the formation of a keto compound, butyrolactone oxidized product of THF.

The long column reactor yields better conversions than the flat bottom flask assembly, due to the increased contact between the ozone and reactants. The ozone-initiated oxidation of n-hexadecane, n-tetradecane and n-dodecane is achieved under moderate conditions at $20 \pm 1^\circ\text{C}$ and ambient pressure ($\sim 1\text{ atm}$). The main oxidation products are a mixture of keto- isomers with small amounts of acids. Among the ketones, 4-ketone is the favoured product and 3- and 2-ketones were the minor products. The product ratio of 3-ketone and 2-ketones, increased with the decrease in the chain length of the n-alkane ($n\text{-C}_{16} < n\text{-C}_{14} < n\text{-C}_{12}$). The percentage of conversion increased with reaction time. Further oxidation of the isomers of ketones is observed with longer exposure to the ozone. A plausible mechanism involving the abstraction of hydrogen from the secondary carbon atom at 4- or 3- or 2- positions and the formation of alkyl radical, hydrotrioxide, alkyl hydroxide, and alkyl dihydroxy intermediates is proposed for the ozonation of higher n-alkanes. Possibly, the cleavage is taking place at 4-, 3- and 2- positions of ketone isomers on longer ozonation resulting in formation of the carboxylic acids.

Ozonation results with pure catalysts viz. $\gamma\text{-Al}_2\text{O}_3$ or Na-Y or ZSM-5 Si/Al-30 or zeolite beta (H form) alone showed poor activity. The efficiencies of catalyst materials, namely silica gel, vanadium phosphorous oxides (VPO), $\text{Pd}/\gamma\text{-Al}_2\text{O}_3$, $\text{Ni}/\gamma\text{-Al}_2\text{O}_3$, $\text{V}/\gamma\text{-Al}_2\text{O}_3$, $\text{Pd}/\gamma\text{-Al}_2\text{O}_3$ (N_2 calcined), $\text{Ni}/\gamma\text{-Al}_2\text{O}_3$ (N_2 calcined) and $\text{V}/\gamma\text{-Al}_2\text{O}_3$ (N_2 calcined), microporous uni-dimensional and 3-dimensional zeolite material viz. U/Na-Y, U/ZSM-5 Si/Al-30, U/silica, $\text{Pd}/\text{Na-Y}$, $\text{Pd}/\text{Na-Y}$ (N_2 calcined), $\text{Pd}/\text{ZSM-5 Si/Al-30}$, $\text{Pd}/\text{ZSM-5 Si/Al-30}$ (N_2 calcined), $\text{Ni}/\text{Na-Y}$, $\text{Ni}/\text{Na-Y}$ (N_2 calcined), $\text{Ni}/\text{ZSM-5 Si/Al-30}$, $\text{Ni}/\text{ZSM-5 Si/Al-30}$ (N_2 calcined), $\text{V}/\text{Na-Y}$, $\text{V}/\text{Na-Y}$ (N_2 calcined), $\text{V}/\text{ZSM-5 Si/Al-30}$, $\text{V}/\text{ZSM-5 Si/Al-30}$ (N_2 calcined), mesoporous Al-MCM-41 Si/Al-90 and Al-MCM-41 Si/Al-60 were investigated. All the catalyst materials gave identical products similar to the uncatalyzed and activated charcoal mediated reactions, namely 4-, 3- and 2- ketone isomers with same chain length as parent hydrocarbon and smaller amounts of the different carboxylic acids. The oxidative conversions and the selectivity decreased in the order, $n\text{-C}_{12} > n\text{-C}_{14} > n\text{-C}_{16}$,

consistent with the decrease in the diffusivity of these alkanes in the zeolites. The conversion of the reactant with different catalyst systems varied between 27% and 56% during 24 h ozonations, and the selectivity towards 4-ketone was between 37% and 55% over the same period of ozonation.

Most of the microporous and mesoporous synthesized and commercial catalyst materials used were positively characterized by various spectroscopic techniques. The results illustrate that these materials are of highly crystalline and exhibited the characteristic bands in FT-IR, DR UV-visible spectra, and homogeneity in shapes and high surface areas with SEM and BET techniques. The results are in agreement with the BET surface area measurements that showed a decrease in the surface area upon metal (Ni, V and Pd) impregnation. The BET observations signify that there is a decrease of the surface area for the samples calcined under N₂ flow conditions. The crystallinity of micro and mesoporous support structure has remained intact during the metal (Pd or V or Ni) impregnated conditions. The results showed the characteristic bands in the FT-IR spectra, SEM images confirming the homogeneity in shapes and crystallinity for all samples. The samples after calcination maintained a high BET surface area.

For the ozonation of higher n-alkanes with microporous and mesoporous catalysts, Ni/Na-Y, Ni/ZSM-5 N₂ calcined, V/Na-Y, Al-MCM-41 Si/Al-60 and Al-MCM-41 Si/Al-90 catalysts showed conversion activity above 50%. U/ZSM-5 zeolite is the most promising catalyst in the ozonation of n-hexadecane with a conversion of 55%. The plausible mechanism for the ozonation of higher hydrocarbons with new heterogeneous U/ZSM-5 zeolite catalyst is proposed. In the proposed mechanism, the probability of chemisorption of ozone on the catalyst surface leading to the formation of active species which react with non-chemisorbed organic molecule, and chemisorption of organic molecule on the catalytic surface and its further reaction with gaseous ozone are illustrated. The reaction proceeds through several steps involving the radicals/ions, hydrotrioxide, alkyl hydrotrioxide, alkyl peroxide, HO[•], alkyl hydroperoxide, alkyl diperoxo radical, peroxo alkyl radical, alkoxy diradical to give corresponding 4-, 3-, and 2-ketones. The 3-dimensional pore geometry catalysts showed better activity towards the conversion and selectivity. There is no significant variation observed with the different Si/Al ratios of the Al-MCM-41 catalysts, same conversion rates were observed after 24 h ozonation. The Si/Al ratio of the catalyst material had no or little effect on the ozonation reaction.

The higher activity of the metals impregnated catalysts for ozone decomposition was observed compared to the supports itself. This probably results from an increase of electron transfer and, furthermore, an increase in the rate of redox reaction that takes place in the case of metal on support catalysts, which accelerates the catalytic reactions.

It can be concluded from the catalytic ozonation, that the catalysts that gave the high conversions showed poor selectivity towards the major product 4-hexadecanone, while the catalyst with good selectivity exhibited poor conversions. Pd/ γ -Al₂O₃ N₂ calcined, U/ZSM-5, Zeolite-X and Al-MCM-41 are the promising catalysts for better conversions in the ozonation of higher alkanes. The selectivity of 4-hexadecanone with 5%Ni/HB150, HBeta-40, Pd/Na-Y N₂ calcined and Ni/Na-Y N₂ calcined catalysts was superior. The 3D zeolite catalysts, Na-Y and HB150 showed the efficient selectivity towards the 4-hexadecanone formation.

The calcination of the catalysts under N₂ flow conditions had no effect on the activity of the catalysts towards the conversion and selectivity. Catalysts with 3-dimensional pore geometry showed better activity towards both the conversion and selectivity. No significant variations with the different Si/Al ratios of the Al-MCM-41 catalysts were observed over the 24 h ozonation. It is hoped that these findings will be of great use in the petroleum industry to achieve value added products from the hitherto un-reactive higher hydrocarbons.

As the future work, it will be of interest to investigate the scope of ozone initiated catalytic oxidation of higher hydrocarbons in water, as aqueous systems provide opportunity to investigate the reactivity and selectivity under varied pH conditions and in presence oxidation enhancers. The oxidative reactions occurring at the aqueous/non aqueous interface at moderate reaction conditions will be of curiosity.

REFERENCES

1. US Energy Information Agency, International Energy Annual Report, World Crude Oil Production and Consumption, **2003**.
2. A chart of the IEA figures for world oil production can be found at the following URL: <http://www.dailykos.com/story/2006/1/22/15318/6610> (accessed on 14 Nov 2006)
3. Bailey P.S., "Ozonation in organic chemistry". Academic Press, New York, vol. 2, **1982**.
4. Kochi J.K. and Sheldon R.A., "Metal Catalyzed Oxidations of Organic Compounds", Academic Press, New York, Chapter 1, 3 and 13, **1981**.
5. Barletta B., Bolzacchini E., Fossati L., Meinardi S., Orlandi M., Rindone B., Ozone Sci. Eng., **1998**, 20, 91.
6. Rubin M.B., Bull. Hist. Chem., **2001**, 26, 40.
7. Kotz J.C. and Purcell K.F., "Chemistry and chemical reactivity", 2nd Edition, Orlando, FL: Saunders College Publishing., 1148, **1991**.
8. Heisig C., Zhang W., Oyama S.T. Appl. Catal. B: Environ., **1997**, 14, 117.
9. Rakitskaya T.L., Yu Bandurko A., Ennan A.A., Ya Paina V., Rakitskiy A.S., Micropor. Mesopor. Mater., **2001**, 43, 153.
10. Volz A. and Kley D., Nature, **1988**, 332, 240.
11. Gordon G., Prog. Nucl. Energy, **1995**, 29, 89.
12. Ulmann's "Encyclopedia of Industrial Chemistry", 5th Edition, Verlagsgesellschaft, Germany, 415, **1991**.
13. Bailey P.S., Chem. Rev., **1958**, 58, 925.
14. Atkinson R. and Carter W.P.L., Chem. Rev., **1984**, 84, 437.
15. Naydenov A. and Mehandjiev D., Appl. Catal. A: Gen., **1993**, 97, 17.
16. Mehandjiev D., Cheshkova K., Naydenov A., Georgesku V., React. Kin. Catal. Lett., **2002**, 76, 287.
17. Andreeva D., Tabakova T., Ilieva L., Naydenov A., Mehandjiev D., Abrashev M.V., Appl. Catal. A: Gen., **2001**, 209, 291.
18. Gervasini A., Vezzoli G.C., Ragaini V., Catal. Today, **1996**, 29, 449.
19. Li W. and Oyama S.T., Stud. Surf. Sci. Catal., **1997**, 110, 873.
20. Einaga H. and Futamura S., React. Kin. Catal. Lett., **2004**, 81, 121.
21. Einaga H. and Futamura S., J. Catal., **2004**, 227, 304.
22. L'Air Liquide, French Patent, 1,246,273.
23. Dohan J.M. and Masschelein W.J., Ozone Sci. Eng., **1987**, 9, 315.
24. Langlais B., Reckhow D.A., Brink D.R., Introduction. In "Ozone in Water Treatment: Application and Engineering", Chelsea, Michigan: Lewis Publishers, 317, **1991**.

25. Langlais B., Bellamy W.D., Damez F., Moneiel A., Rakness K.L., Reckhow D.A., Robson C.M., Engineering aspects. In "Ozone in Water Treatment: Application and Engineering", Chelsea, Michigan: Lewis Publishers, 8, **1991**.
26. Beller M., Waide C., Steinberg M., Environmental Protection Agency-W20 report 14010fmh, No 14-12-838, **1970**, 91.
27. Hoigne J. and Bader H., Wat. Res., **1976**, 10, 377.
28. Hoigne J. and Bader H., Ozone Sci and Eng., **1979**, 1, 73.
29. Hoigne J. and, Bader H., Wat. Res., **1983**, 17, 173.
30. Rice R.G., Ozone Sci. and Eng., **1997**, 18, 477.
31. Staehelin J. and Hoigne J., J. Environ. Sci. Technol., **1982**, 16, 676.
32. Staehelin J. and Hoigne J., Environ. Sci. Technol., **1985**, 19, 1206.
33. Tomiyasu H., Fukutomi H., Gordon G., Inorg. Chem., **1985**, 24, 2962.
34. Hellman T.M. and Hamilton G.A., J. Am. Chem. Soc., **1974**, 96, 1530 and the references cited therein.
35. Benson S.W., Adv. Chem. Ser., **1968**, 77, 74.
36. Clarence C., Schubert, S.J., Pease R.N., J. Am. Chem. Soc., **1956**, 2044 and references there in.
37. Tatsumi T., Nakamura M., Negishi S., Tominaga H., Chem. Commun., 1990, 476.
38. Chen N.Y. and Garwood W.E., J. Catal., **1977**, 50, 252.
39. Plesničar B., Cerkovnik J., Tuttle T., Kraka E., Cremer D., J. Am. Chem. Soc., **2002**, 124, 11260.
40. Cerkovnik J., Eržen E., Koller J., Plesničar B., J. Am. Chem. Soc., **2002**, 124, 404.
41. Olah G.A., Yoneda N., Parker D.G., J. Am. Chem. Soc., **1976**, 98, 5261.
42. Olah G.A., Yoneda N., Ohnishi R., J. Am. Chem. Soc., **1976**, 98, 7341.
43. Whiting M.C., Bolt A. J.N., Parish J.H., Adv. Chem. Ser., **1968**, 77, 4.
44. Bailey P.S. and Lerdal D.A., J. Am. Chem. Soc., **1978**, 100, 5820.
45. White H.M. and Bailey P.S., J. Org. Chem., **1965**, 3037.
46. Varkony T.H., Pass S., Mazur Y., J. Chem. Soc., Chem. Commun., **1975**, 709.
47. Pryor W.A., Ohto N., Church D.F., J. Am. Chem. Soc., **1983**, 105, 3614 and the literature cited therein.
48. Nangia G.A. and Benson S.W., J. Am. Chem. Soc., **1980**, 102, 3105.
49. Pryor W.A., Ohto N., Church D.F., J. Am. Chem. Assoc., **1982**, 104, 5813.
50. Durland J.R. and Adkins H., J. Am. Chem. Soc., **1939**, 61, 429.
51. Hamilton G.A., Ribner B.S., and Hellman T.M., Adv. Chem. Ser., **1968**, 77, 15 and the

literature cited therein.

52. Stary F.E., Emge D.E., Murray R.W., J. Am. Chem. Soc., **1976**, 98, 1880.
53. Benson S.W., "Thermochemical kinetics", 2nd Edition, Wiley: New York, **1976**.
54. Williamson D.G. and Cvetanović R.J., J. Am. Chem. Soc., **1970**, 92, 2949 and references cited there in.
55. Varkony H., Pass S., Mazur Y., Chem. Comm., **1974**, 437.
56. Murray R.W., Lumma W.C., Jr. Lin J. W-P., J. Am. Chem. Soc., **1970**, 92, 3205 and references cited therein.
57. Giamalva D.H., Church D.F., Pryor A., J. Am. Chem. Soc., **1986**, 108, 7678 and the references cited therein.
58. Beckwith A.L.J., and Duong T., Chem. Comm., **1978**, 413 and the literature cited therein.
59. Pryor W.A., Govindan C.K, Church D.F., J. Am. Chem. Soc., **1982**, 104, 7563.
60. Syrov A.A. and Tsyskovskii V.K., Zh. Org. Khim., **1970**, 8, 1392.
61. Olah G.A., Halpern Y., Shen J., Mo Y.K., J. Am. Chem. Soc., **1973**, 95, 4960.
62. Olah G.A., Yoneda N., Parker D.G., J. Am. Chem. Soc., **1976**, 98, 2251.
63. Yoneda N. and Olah G.A., J. Am. Chem. Soc., **1977**, 99, 3113.
64. von Gunten U., Wat. Res., **2003**, 37, 1443.
65. Bablon G., Bellamy W.D., Billen G., Bourbigot M., Daniel F.B., Erb F., Gomella C., Gordon G., Hartemann P., Joret J., Knocke W.R., Langlais B., Saplanche A., "Practical application of ozone: principles and case studies. In ozone in water treatment: application and engineering", Edited by Langlais B, Reckhow DA, and Brink DR., Chelsea, MI: Lewis Publishers, 316, **1991**.
66. Amy G.L., Sierka R.A., Bedessem J., Price D., Tan L., J. AWWA, **1992**, 84, 67.
67. Miltner R.J., Shukairy H.M., Summers R.S., J. AWWA, **1992**, 84, 52.
68. Schechter D.S. and Singer P.C., Ozone Sci. Eng., **1995**, 17, 53.
69. Nawrocki J. and Kalkowska I., Toxicol. Environ. Chem., **1999**, 68, 297.
70. Nawrocki J. and Kalkowska I., J. Water SRT – Aqua, **1998**, 47, 50.
71. Glaze W.H., Koga M., Cancilla D., Wang K., McGuire M.J., Liang S., Davis M.K., Tate C.H. and Aieta E.M., J. AWWA, **1989**, 81, 66.
72. Glaze W.H., Koga M. and Cancilla D., Env. Sci. Technol., **1989**, 23, 838.
73. Jacangelo J.G., Patanie N.L., Reagan K.M., Aieta E.M., Krasner S.W. and McGuire M.J., J. AWWA, **1989**, 81, 74.
74. Richardson S.D., "Drinking water disinfection by-products in Meyers RA Ed. The encyclopedia of environmental analysis and remediation", New York, John Wiley & Sons,

- 1998**, 3, 1398.
75. Melin E.S. and Odegaard H., *Wat. Res.*, **2000**, 34, 4464.
 76. Kuo ChK., *J. Chromatogr. A*, **1998**, 804, 265.
 77. Müller M.B., Schmitt D., Frimmel F.H., *Env. Sci. Technol.*, **2000**, 34, 4867.
 78. Xie Y. and Reckhow D.A., *Ozone Sic. Eng.*, **1992**, 14, 269.
 79. Nawrocki J, Swietlik J, Raczyk-Stanislawiak U, Dabrowska A, Bilzor S, Ilecki W. *Ozone Sci. Eng.*, **2003**, 25, 53.
 80. Lechevallier M.W., Welch Nancy J., Smith D.B., *Appl. Environ. Microbiol.*, **1996**, 62, 2201.
 81. Gottschalk C., Libra J.A., Saupe A., "Ozonation of water and wastewater: a practical guide to understand ozone and its application", Wiley-VCH, Weinheim, **2000**.
 82. Camel V. and Bermond A., *Wat. Res.*, **1998**, 32, 3208.
 83. Hoigne J., "Chemistry of aqueous ozone and transformation of pollutants by ozonation and advanced oxidation processes. In: J. Hubrec, Editor. The handbook of environmental chemistry quality and treatment of drinking water", Berlin: Springer, **1998**.
 84. Hoigne J., Bader H., Haag W.R., Staehelin J., *Wat. Res.*, **1985**, 19, 993.
 85. Facile N., Barbeau B., Prevost M., Koudjonou B., *Wat. Res.*, **2000**, 34, 3238.
 86. Hoigne J. and Bader H., *Wat. Res.*, **1983**, 17, 185.
 87. Yao C.C.D. and Haag W.R., *Wat. Res.*, **1991**, 25, 761.
 88. Neta P., Huie R.E., Ross A.B., *J. Phys. Chem. Ref. Data*. **1988**, 17, 1027.
Internet: <http://allen.rad.nd.edu> (dated:14 Nov 2006)
 89. Buxton G.V., Greenstock C.L., Helman W.P., Ross W.P., *J. Phys. Chem. Ref. Data*, **1988**, 17, 513. Internet: <http://allen.rad.nd.edu> (accessed on 14 Nov 2006)
 90. Haag W.R. and Yao C.C.D., *Environ. Sci. Technol.*, **1992**, 26, 1005.
 91. Roncero M.B., Queral M.A., Colom J.F., Vidal T., *Ozone Sci. Eng.*, **2003**, 523.
 92. Trapido M., Veressinina J., Munter R., *Ozone Sci Eng.*, **1994**, 16, 475.
 93. Acero J.L., Haderlein S.H., Schmidt T., Suter M.J.F., von Gunten U., *Environ. Sci. Technol.*, **2001**, 35, 4252.
 94. Ternes T.A., *Wat. Res.*, **1998**, 32, 3245.
 95. Johnson R., Pandow J., Bender D., Curtis P., Zogorski J. *Environ. Sci. Technol.*, **2000**, 34, 210 A-217 A.
 96. Lechevallier M.W., Schulz W., Lee R.G., *Appl. Environ. Microbiol.*, **1991**, 57, 857.
 97. Lawrence J., Tosine H., Onuska F.I., Comba M.E., *Ozone Sci. Eng.*, **1980**, 2, 55.
 98. Beltran F.J., Encinar J.M., Gracia-Araya J.F., *Can. J. Chem. Eng.*, **1992**, 70, 141.

99. Beltran F.J., Encinar J.M., Gracia-Araya J.F., Munoz M.G., *Ozone Sci. Eng.*, **1995**, 17, 355.
100. Beltran F.J., Encinar J.M., Alonso M.A., *Ind. Eng. Chem. Res.*, **1998**, 37, 25.
101. Beltran F.J., Encinar J.M., Alonso M.A., *Ind. Eng. Chem. Res.*, **1998**, 37, 32.
102. Chamarro E., Marco A., Prado J., Esplugas S., *Sociedad Chilena de Quimica*, **1996**, 1/2, 28.
103. Andreozzi R., Caprio V., Insola A., Marotta R., *Catal. Today*, **1999**, 53, 51 and references cited therein.
104. Glaze W.H. and Kang J., *Ind. Eng. Chem. Res.*, **1989**, 28, 1573.
105. Meijers R.T., Oderwald-Muller E.J., Nuhm P., Kruithof J., *Ozone Sci. Eng.*, **1995**, 17, 673.
106. Roche P. and Prados M., *Ozone Sci. Eng.*, **1995**, 17, 657.
107. Beltran J.B., Gonzalez M., Acedo B., Rivas F.J., *J. Hazardous Mater.*, **2000**, B80, 189.
108. Aeita E.M., Reagan K.M., Lang J.S., McReynolds L., Kang J., Glaze W.H. *J. AWWA*, **1988**, 80, 64.
109. Glaze W.H. and Kang J-W. *J. Am. Water Works Assoc.*, **1988**, 80, 57.
110. Karimi A.A., Redman J.A., Glaze W.H., Stolarik G.F., *J. Am. Water. Works Assoc.*, **1997**, 89, 41.
111. Bigda R.J., *Chem. Eng. Prog.*, **1995**, 91, 62.
112. Reisz E., Schmidt W., Schuchmann H.P., von Sonntag C. *Environ. Sci. Technol.*, **2003**, 37, 1941.
113. Jans U. and Hoigne J., *Ozone Sci. Eng.*, **1998**, 20, 67.
114. Ma J. and Graham N.J., *Wat. Res.*, **1999**, 33, 785.
115. Acero J.L. and von Gunten U. *J. Am. Water Works Assoc.*, **2001**, 93, 90.
116. Glaze W.H., Kang J.W., Chapin D.H. *Ozone Sci. Eng.*, **1987**, 9, 335.
117. Carey J.H., "An introduction to AOP for destruction of organics in wastewater", *Water Pollut. Res. J. Can.*, **1992**, 27, 1.
118. TECHNOMMENTARY: Advanced oxidation processes for treatment of industrial wastewater. An EPRI community environmental center Publ. No. 1, **1996**.
119. Reaction rate constants of ozone vs. hydroxyl radical. *UV / Oxidation Handbook*, **1994**.
120. Munter R., *Proc. Estonian Acad. Sci. Chem.*, **2001**, 50, 59.
121. Cortes S., Sarasa J., Ormad P., Gracia R., Ovelheiro J., In *Proc. Int. Reg. Conf. Ozonation and AOPs in Water Treatm.*, Poitiers, France, September 23-25, **1998**.
122. Karpel Vel Leitner N., Gombert B., Legube B., Luck F., *Water Sci. Technol.*, **1998**, 38,

- 203.
123. Legube B., Delouane B., Karpel Vel Leitner N., Luck F., In Proc. Geg. Conf. Ozone, UV-light, AOPs Water Treatm., Setpember 24-26, Amsterdam, Netherlands, **1996**, 509-514.
 124. Pillard H., Dore M., Bourbigot M., In Proc. 10th Ozone World Congress, Monaco, March **1991**, 1, 313-331.
 125. Pinker B. and Henderson W.D., "The effect of ozonation on the performance of GAC", In Proc. Reg. Conf. Ozone, UV-light, AOPs Water Treatm., Amsterdam, Netherlands, September 24-26, **1996**, 307-318.
 126. Kaptijin J.P., Ozone Sci. Eng., **1997**, 19, 297.
 127. Beltran F.J., Rivas J., Alvarez P., Montero de Espinosa R., Ozone Sci. Eng., **2002**, 24, 22.
 128. Ma J., Sui M.H., Chen Z.L., Wang L.N., Ozone Sci. Eng., **2004**, 26, 3.
 129. Rivera-Utrilla J. and Sanchez-Polo M., Appl. Catal. B: Environ., **2002**, 39, 329.
 130. Rivera-Utrilla J. and Sanchez-Polo M., Mondaca M.A., Zaror C.A., J. Chem. Technol. Biotechnol., **2002**, 77, 883.
 131. Rivera-Utrilla J. and Sanchez-Polo M., Langmuir, **2004**, 20, 9217.
 132. Elovitz M.S. and von Gunten U., Ozone Sci. Eng., **1999**, 21, 239.
 133. Sanchez-Polo M., von Gunten U., Rivera-Utrilla J., Wat. Res., **2005**, 39, 3189.
 134. Tal D., Keinan E., Mazur Y., J. Am. Chem. Soc., **1979**, 101, 502 and references cited therein.
 135. Cohen Z., Keinan E., Varkony T. H., Mazur Y., J. Org. Chem., 40, **1975**, 14, 2141 and references cited therein.
 136. Ksenofontova M.M., Mitrofanova A.N., Mamleeva N.A., Pryakhin A.N., Lunin V.V., Ozone Sci. Eng., **2003**, 505 and the literature cited therein.
 137. Legube B. and Karpel Vel Leitner N., Catal. Today, **1999**, 53, 61.
 138. Abdo M.S.E., Shaban H., Bader M.S.H., J. Environ. Sci. Health A, **1988**, 23, 697.
 139. Gracia R., Aragues J.L., Ovelleiro J.L., Ozone Sci. Eng., **1996**, 18, 195.
 140. Gracia R., Aragues J.L., Ovelleiro J.L., Wat. Res., **1998**, 32, 57.
 141. Andreozzi R., Insola A., Caprio V., D'Amore M.G., Wat. Res., **1992**, 26, 917.
 142. Nowell L.H. and Hoigne J., 8th Ozone World Congress, p. E80, Zurich, September **1987**.
 143. Al-Hayek N., Legube B., Dore M., Environ. Technol. Letters, **1989**, 10, 415.
 144. Bhat N. and Gurol M.D., 27th Industrial Waste Mid-Atlantic Conference, Bethlehem, PA, USA, 371, July **1995**.
 145. Naydenov A. and Mehandjiev D., App. Catal. A: Gen., **1992**, 97, 17.

146. Thompson P.E., Sharaatt P.N., Hutchison J., The 1995 ICHIME Research Event, 1st European Conference, **1995**, 297.
147. Ma J. and Graham N.J.D., Ozone Sci. Eng., **1997**, 19, 227.
148. Andreozzi R., Insola A., Caprio V., Marotta R., Tufano V., Appl. Catal. A: Gen., **1996**, 138, 75.
149. Pines D., Humayan .R, Reckhow D.A., Spangenberg C., Water Quality Technology Conference, San Francisco, CA, USA part II - session 4A, 1493, 6-10 November **1994**.
150. Volk C., Roche P., Joret J.C., Pillard H., Wat. Res., **1997**, 31, 650.
151. Dhandapani B. and Oyama S.T., "Gas phase ozone decomposition Catalysts", Appl. Catal.: B-Environ., **1997**, 11, 129.
152. Radhakrishnan R. and Oyama S.T., J. Catal ., **2001**, 199, 282.
153. Li W., Gibbs G.V., Oyama S.T., J. Am. Chem. Soc., **1998**, 120, 9041.
154. Li W. and Oyama S.T., J. Am. Chem. Soc., **1998**, 120, 9047.
155. Li W. and Oyama S.T., "Topics in Catalysis", **1999**, 8, 75.
156. Deitz V.R. and Bitner J.L., Carbon, **1973**, 11, 393.
157. Tekeuchi Y. and Ioth T., Separations Technol., **1993**, 3, 168.
158. Kasprzyk-Hordern B., Adv. Colloid Interface Sci., **2004**, 110, 19 and the literature cited therein.
159. Kasprzyk-Hordern B., Ziolek. M., Nawrocki J., J, Appl. Catal.: B-Environ., **2003**, 46, 639 and the literature cited therein.
160. Ernst M., Lurot F., Schrotter J-Ch., Appl. Catal.: B-Environ., **2004**, 47, 15.
161. Lin J., Kawai A., Nakajima T., Appl. Catal.: B-Environ., **2002**, 39, 157 and the literature cited therein.
162. Cooper C. and Burch R., Wat. Res., **1999**, 33, 3695.
163. Cooper C. and Burch R., Wat. Res., **1999**, 33, 3689.
164. Ma J. and Graham N.J.D., Wat. Res., **1999**, 33, 785.
165. Delanoë F., Acedo B., Karpel Vel Leitner N., Legube B., Appl. Catal. A: Gen., **2001**, 29, 315.
166. Staehlin J. and Hoigné J., Environ. Sci. Technol., **1985**, 19, 1206.
167. Bulanin K.M. Lavalley J.C., Tsyganenko A.A., Colloid Surf. A, **1995**, 101, 153.
168. Derouane E.G., "Intercalation chemistry". Editors Whittingham M.S. and Jacobson M.S., Academic Press, New York, Chapter 4, **1982**.
169. Abbot J. and Wojciechowski B.W., J. Catal., **1988**, 109, 274.
170. Bordley Jr. J.L. and Emmett P.H., J. Catal., **1976**, 42, 367.

171. Armaroli T., Simon L.F., Digne M., Montanari T., Bevilacqua M., Valtchev V., Patarin J., Busca G., *Appl. Catal. A: Gen.*, **2006**, 306, 78 and literature cited therein.
172. Holderich W., Hesse M., Naumann F., *Angew. Chem. Int. Ed. Engl.*, **1988**, 27, 226 and the references therein.
173. Breck D.W., "Zeolite molecular sieves: Structure, Chemistry and Uses", Wiley, New York, **1974**.
174. Hari Prasad Rao P.R. and Ramaswamy A.V., *Chem. Comm.*, **1992**, 1245.
175. <http://www.bza.org/zeolites.html> (accessed on 14 Nov 2006)
176. Davis M.E., *Acc. Chem. Res.*, 1993, 26, 111; *Ind. Eng. Chem. Res.*, **1991**, 30, 1675.
177. Corma A., *Chem. Rev.*, **1995**, 95, 559.
178. Bonnie M.K. and William E C., *Chemical Engineering Progress*, June **1999**, 95, 47.
179. Jia C., Massiani P., Barthomeuf D., *J. Chem. Soc. Faraday Trans.*, **1993**, 89, 3659.
180. Nicolaides C.P., *Appl. Catal. A: Gen.*, **1999**, 185, 211.
181. Dimitrova R., Gunduz G., Dimitrov F.L., Tsoncheva T., Yilmaz S., Urqujeta-Gonzalez E.A., *J. Mol. Catal. A: Gen.*, **2004**, 214, 265.
182. Hobmberg B.A., Wang H.T., Norbeck J.M., Yan Y., *Micropor. Mesopor. Mater.*, **2003**, 59, 13.
183. Wang B. and Ma H.Z., "Micropor. Mesopor. Mater.", **1998**, 25, 131.
184. Barrer R.M., "Zeolites and clay minerals as sorbents and molecular sieves", Academic press, London, **1978**.
185. Gravelle P.C., *Adv. Catal.*, **1972**, 22, 191.
186. Cardona-Martinez N, and Dumesic J.A., *Adv. Catal.*, **1992**, 38, 149.
187. Luengo M. and Yates M., *J. Mat. Sci.*, **1995**, 30, 4483 and literature cited therein.
188. Corma A., "Zeolites: facts, figures and future", *Studies in surface science and catalysis*, Edited by P.A. Jacobs and R. van Santen, Vol. 49, part A, Elsevier Science, Amsterdam, 49, **1989**.
189. Hölderich W., Hesse W., Näuman F., *Angew. Chem. Int.*, **1988**, 27, 226 and literature cited therein.
190. Borade R.B., Adnot A., Kaliaguine S., *J. Chem. Soc. Farad. Trans.*, **1990**, 86, 3949.
191. Hölderich W. F., *Stud. Surf. Sci. Catal.*, **1993**, 75, 127.
192. Corma A. and Garcia H., *Catal. Today*, **1997**, 38, 257.
193. Garcia H. and Heinz D.R., *Chem. Rev.*, **2002**, 102, 3947.
194. Flanigen E.M., *Stud. Surf. Sci. Catal.*, **1991**, 58, 13.
195. Flanigen E.M., "Zeolites: Science and Technology", Editors: Ribeiro F.R., Rodrigues

- A.E., Rollmann L.D., Naccache C., Martinius Nijhoff, The Hague, 3, **1984**.
196. Blatter F. and Frei H., J. Am. Chem. Soc., **1993**, 115, 7501.
 197. Blatter F. and Frei H., J. Am. Chem. Soc., **1994**, 116, 1812.
 198. Camblor M.A, Corma A., Valencia S., Chem. Commun., **1996**, 2265.
 199. Camblor M.A, Corma A, Mifsud A, Pérez-Pariente J., Valencia S., Stud. Surf. Sci. Catal., **1997**, 105, 341.
 200. Camblor M.A, Mifsud A., Pérez-Pariente J., Zeolites, **1991**, 11, 792.
 201. Meier W.M, Olson D.H., Baerlocher C., Zeolites, **1996**, 17, 1.
 202. Turro N.J., Pure Appl. Chem., **1986**, 58, 1219.
 203. Yoon K.B and Kochi J.K., J. Am. Chem. Soc., **1988**, 110, 6586.
 204. Cohen M.D. and Schmidt G.M.J., J. Chem. Soc., **1964**, 1996.
 205. Wojciechowski B.W. and Corma A., "Catalytic Cracking. Catalysts Kinetics and Mechanisms", Marcel Dekker: New York, **1984**.
 206. Scherzer J. and Gruia A.J., "Hydrocracking Science and Technology", Marcel Dekker: New York, **1996**.
 207. Corma A., Rarcia H., Primo J., J. Chem. Res., (S), **1988**, 40.
 208. Collette A., Deremince-Mathien V., Gabelica Z., Nagy J.B., Derouane E.G., Verbist J.J., J. Chem. Soc., Faraday Trans., **1987**, 83, 1263.
 209. Collette A., Maroie S., Riga J., Verbist J.J., Gabelica Z., Nagy J.B., Derouane E.G., J. Catal., **1986**, 98, 326.
 210. Vidya K., Dapurkar S.E., Selvam P., Badamali S.K., Kumar D., Gupta N.M., J. Mol. Catal. A, **2002**, 181, 91.
 211. Rabinowitch E. and Belford R.L., "Spectroscopy and Photochemistry of Uranium Compounds", Pergamon Press, Oxford, **1964**.
 212. Balzani V., Bolletta F., Gandolfi M.T., Maestri M., Top. Curr. Chem., **1978**, 75, 1.
 213. Burrows H.D. and Kemp T.J., Chem. Soc. Rev., **1974**, 3, 139.
 214. Wang W.-D., Bakac A., Espenson J.H., Inorg. Chem., **1995**, 34, 6034.
 215. Bergfeldt T.M., Waltz W.J., Xu X., Sedlak P., Dreyer U., Mockel H., Lilie J., Stephenson J.W., Can. J. Chem., **2003**, 81, 219.
 216. Sarakha M., Bolte M., Burrows H.D., J. Phys. Chem. A, **2000**, 104, 3142.
 217. Sarakha M., Bolte M., Burrows H.D., J. Photochem. Photobiol. A: Chem., **1997**, 107, 101.
 218. Suib S.L., Tanguay J.F., Occelli M.L., J. Am. Chem. Soc., **1986**, 108, 6972.
 219. Dai S., Metcalf D.H., Del Cul G.D., Toth L.M., Inorg. Chem., **1996**, 35, 7786.

220. Kresge C.T., Leonowicz M.E., Roth W.J., Vartuli J.C., Beck J.S., *Nature*, **1992**, 359, 710.
221. Beck J.S., Vartuli J.C., Roth W.J., Leonowicz M.E., Schmidt K.D., Chu C.T.-W., Olson D.H., Sheppard E.W., McCullen S.B., Higgins J.B. and Schlenker J.L., *J. Am. Chem. Soc.*, **1992**, 114, 10834.
222. Davis M.E. and Burkett S.L., *Zeolites*, **1995**, 12, 33.
223. Sayari A., *Chem. Mater.*, **1996**, 8, 1840.
224. Sayari A., *Stud. Surf. Sci. Catal.*, **1996**, 102, 1.
225. Corma A., *Chem. Rev.*, **1997**, 97, 2373.
226. Stein A., Melde B.J., Schrodin R.C., *Adv. Mater.*, **2000**, 12, 1403.
227. Sayari A. and Hamoudi S., *Chem. Mater.*, **2001**, 13, 3151.
228. Selvam P., Bhatia S.K., Sonwane C., *Ind. Eng. Chem. Res.*, **2001**, 40, 3237.
229. Linssen T., Cassiers K., Cool P., Vansant E.F., *Advances Colloid Interface Sci.*, **2003**, 103, 121.
230. Morey M.S., Davidson A., Eckert H., Stucky G.D., *Chem. Mater.*, **1996**, 8, 486.
231. Shin H.J., Ryoo R., Liu Z., Terasaki O., *J. Am. Chem. Soc.*, **2001**, 123, 1246.
232. Jodzis S., *Ozone Sci. Eng.*, **2003**, 25, 63 and the references cited therein.
233. Vogel A., "Textbook of Quantitative Inorganic Analysis", 4th Edition, Longmann, 379, **1978**; Rakness K., Gordon G., Langlais B., Masschelein W., Matsumoto N., Richard Y., Robson C.M., Somiya I., *Ozone Sci. Eng.*, **1996**, 8, 209.
234. Hutchings G.J., Scurrall M.S., Woodhouse J.R., *Appl. Catal.*, **1988**, 38, 157.
235. Barrer R.M., *Disc. Farad. Soc.*, 40, 206, 1944; *J. Chem. Soc.*, **1944**, 2158.
236. Breck D.W., Eversole W.G., Milton R.M., *J. Am. Chem. Soc.*, **1956**, 78, 2338.
237. Breck D.W., "Zeolite molecular sieves: Structure, chemistry and use", Wiley, New York, **1974**.
238. Barrer R.M., *Stud. Surf. Sci. Catal.*, **1985**, 24, 1.
239. Dyer A., "An Introduction into Zeolite Molecular Sieves", John Wiley & Sons, Avon, **1988**.
240. Szostak R., "Molecular Sieves, Principle of Synthesis and Identification", Van Nostrand Reinhold, New York, **1989**.
241. Jacobs P.A. and Martens J.A., (Eds.), *Stud. Surf. Sci. Catal.*, **1989**, 33, 47.
242. Weller M.T. and Dann S.E., *Curr. Opin. Solid State Mater. Sci.*, **1998**, 3, 137.
243. West A.R., "Solid State Chemistry and its Application", John Wiley & Sons, Singapore, **1989**.
244. Kresge C.T., Leonowicz M.E., Roth W.J., Vartuli J.C., Beck J.S., *Nature*, **1992**, 359, 710.

245. Beck J.S., Vartuli J.C., Roth W.J., Leonowicz M.E., Schmitt K.D., Chu C.T.-W., Olson D.H., Sheppard E.W., McCullen S.B., Higgins J.B., Schlenker J.L., *J. Am. Chem. Soc.*, **1992**, 114, 10834.
246. Dapurkar S.E., Badamali S.K., Selvam, P., *Catal. Today*, **2001**, 68, 63.
247. International Centre for Diffraction Data (ICDD), *Mineral Powder Diffraction File Databook* (Sets 1-42), 1601 Park Lane, Swarthmore, Pennsylvania 19081-2389, USA, **1993**.
248. Ali A., Alvarez W., Loughran C.J., Resasco D.E., *Appl. Catal.: B-Environ.*, **1997**, 14, 13.
249. Treacy M.M.J. and Higgins J.B., "Collection of simulated XRD powder patterns for zeolites", 4th Edition, IZA Ed., Elsevier, Amsterdam, 236, **2001**.
250. Shannon R.D. and Prewitt C.T., *Acta Crystallogr. B*, **1969**, 25, 925.
251. Zhang W.H., Shi J.L., Wang L.Z., Yan D.S., *Chem. Mater.*, **2000**, 10, 467.
252. Lepetit C. and Che M., *J. Phys. Chem.*, **1996**, 100, 3137.
253. Pawelec B., Mariscal R., Navarro R.M., Campos-Martin J.M., Fierro J.L.G., *Appl. Catal. A: Gen.*, **2004**, 262, 155.
254. Schraml-Marth M., Wokaun A., Baiker A., *J. Catal.*, **1990**, 124, 86.
255. Concepción P., López Nieto J.M., Pérez-Pariente J., *J. Mol. Catal. A*, **1995**, 99, 173.
256. Balsco T., Concepción P., López Nieto J.M., Pérez-Pariente J., *J. Catal.*, **1995**, 152, 1.
257. Catana G., Ramachandra Rao R., Weckhuysen B.M., Van Der Voort P., Vansant E., Schoonheydt R.A., *J. Phys. Chem. B*, **1998**, 2, 8005.
258. Jhung S.H., Uh Y.S., Chon H., *Appl. Catal.*, **1990**, 62, 61.
259. Chao K.J., Wu C.N., Chang H., Lee L.J., Hu S.F., *J. Phys. Chem. B*, **1997**, 101, 6341.
260. Santamaría-González J., Luque-Zambrana J., Mérida-Robles J., Maireles-Torres P., Rodríguez-Castellón E., Jiménez-López A., *Catal. Lett.*, **2000**, 68, 67.
261. Zhang Z., Sachtler W.M.H., Chen H., *Zeolites*, **1990**, 10, 784.
262. Carvill B.T., Lerner B.A., Zhang Z., Sachtler W.M.H., *J. Catal.*, **1993**, 143, 314.
263. Zhang Z., Mestl G., Knözinger H., Sachtler W.M.H., *Appl. Catal. A: Gen.*, **1992**, 89, 155.
264. Kruk M., Jaroniec M., Ryoo R., Kim J.M., *Chem. Mater.*, **1999**, 11, 2568.
265. Schmidt R., Akporiaye D., Stocker M., Ellestad O. H., *Stud. Surf. Sci. Catal.*, **1994**, 84, 61.
266. Sayed M.B., Kydd R.A., Cooney R.P., *J. Catal.*, **1984**, 88, 137.
267. Ward J.W., *J. Catal.*, **1967**, 9, 225.
268. Nunan J., Cronin J., Cunningham J., *J. Catal.*, **1984**, 87, 77.
269. Gates B.C., "Catalytic Chemistry", Chapter 5, 271, **1992**.

270. Chakrabarty D.K., "Adsorption and Catalysis by Solids", Chapter 8, 172, **1990**.
271. Jacobs P.A. and Von Ballmoos R., J. Phys. Chem., **1982**, 86, 3050.
272. Jentys A., Lugstein A., Vinek H., Zeolites, **1997**, 18, 391 and the literature cited therein.
273. Zecchina A., Bordiga S., Spoto G., Marchese L., Petrini G., Leofanti G., Padovan M., J. Phys. Chem., **1992**, 96, 4991.
274. Jentys A., Tanaka H., Lercher J.A., J. Phys. Chem. B., **2005**, 109, 2254.
275. Gopalakrishnan G. and Krishnasamy V., "Disproportionation of ethylbenzene over lanthanum exchanged zeolite- β ", International series on chemical engineering, Catalysis present & future. Editors. Kanta Rao P and Beniwal R. S., Publications & Information Directorate, New Delhi, Wiley Eastern Limited, New Delhi, 173-188, **1995**.
276. Kiricsi I., Flego C., Pazzuconi G., Parker Jr. W.O., Millini R., Perego C., Bellussi G., J. Phys. Chem., **1994**, 98, 4627.
277. Kinger G., Lugstein A., Swagera R., Ebel M., Jentys A., Vinek H., Micropor. and Mesopor. Mater., **2000**, 39, 307.
278. van der Gaag F.J., Jansen J.C., van Bekkum H., Zeolites, **1984**, 4, 369.
279. Sen T., Rajamohanan P.R., Ganapathy S., Sivasanker S., J. Catal., **1996**, 163, 354.
280. Tuel A. and Ben Taârit Y., Appl. Catal., **1993**, 102, 201.
281. Chien S.H., Ho J.C., Mon S.S., Zeolites, **1997**, 18, 182.
282. Hari Prasad Rao P.R., Ramaswamy A.V., Ratnasamy P., J. Catal., **1992**, 137, 225.
283. Tuel A. and Ben Taârit Y., Zeolites, **1994**, 14, 18.
284. Thanjaraj A., Eapen M.J., Sivasanker S., Ratnasamy P., Zeolites, **1992**, 12, 943.
285. Reddy J.S. and Kumar R., Zeolites, **1992**, 12, 95.
286. Reddy J.S. and Kumar R., J. Catal., **1991**, 130, 440.
287. Zecchina A., Bordiga S., Spoto G., Marchese L., Petrini G., Leofanti G., Padovan M., J. Phys. Chem., **1992**, 96, 4991.
288. Chester A.W., Dessan R.M., Alemani L.B., Woolery G.L., Zeolites, **1986**, 6, 14.
289. Sárkány J., Sachtler W.M.H., Stud. Surf. Sci. Catal., **1995**, 94, 649.
290. Chen H.Y., Wang X., Sachtler W.M.H., Phys. Chem. Chem. Phys., **2000**, 2, 3083.
291. Nakamoto K., "Infrared and Raman Spectra of Inorganic and Coordination compounds", Wiley, New York, **1978**.
292. Serrano D.P., Li H.X., Davis M.E., J. Chem. Soc., Chem. Commun., **1992**, 745.
293. Chen C.-Y., Li H.-X., Davis, M.E., Micropor. Mater., **1993**, 2, 17.
294. Fronk C.A., Ozone Sci. and Engg., **1987**, 9, 265.
295. <http://www.sigmaaldrich.com/spectra/fnmr/FNMR008551.pdf>

(accessed on 14 Nov 2006)

296. <http://www.life.uiuc.edu/hanks/Supplement%20Ginzel%20et%20al%202006.pdf>
(accessed on 14 Nov 2006)
297. Plesničar B., "Organic peroxides", Editor: Ando W, Wiley, Chichester, 479, **1992**.
298. Olah G.A. and Molnar A., "Hydrocarbon chemistry", Wiley, New York, 291, **1995**.
299. Giamalva D.H., Church D.F., Pryor W.A., J. Org. Chem., **1988**, 53, 3429.
300. Plesničar B., Cerkovnik J., Tekavec T., Koller J., J. Am. Chem. Soc., **1998**, 120, 8005.
301. Rajasekhar V.S.R. Pullabhotla and Jonnalagadda S.B., "Catalytic oxidation of higher hydrocarbons with ozone", Carman Symposium, Midrand, Johannesburg, South Africa, 16-18 November **2005**.
302. Klein D.A. and Henning F.A., Appl. Microbiol., **1969**, 17, 676.
303. Logemann F.P. and Annee J.H.J., Water Sci. Tech., **1997**, 35, 353.
304. Beltrán F.J., Rivas J., Alvarez P., Montero-de-Espinosa R., Ozone Sci. Eng., **2002**, 24, 227.
305. Sánchez-Polo M. and Rivera-Utrilla J., Carbon, **2003**, 41, 303.
306. Guiliano M., Anba-Lurot F. El., Doumenq P., Mille G., Rontani J.F., J. Photochem. and Photobiology A: Chemistry, **1997**, 102, 127 and the references cited therein.
307. Jung H. and Choi H., Appl. Catal. B: Environ., **2006**, 66, 288.
308. Antonakou E., Lappas A., Nilsen M.H., Bouzga A., Stöcker M., Fuel, **2006**, 85, 2202.

APPENDIX

Spectrum Plot

C:\GCQ\DATA\CCL4B3

04:48:42

Comment: Ozonated CCl₄ sample

Scan No: 244

Retention Time: 4.07

RIC: 930514

Mass Range: 11 - 290

Peaks: 206 Base Pk: 166 Ioniz: 1319 us Int: 84015

100.00% = 84015

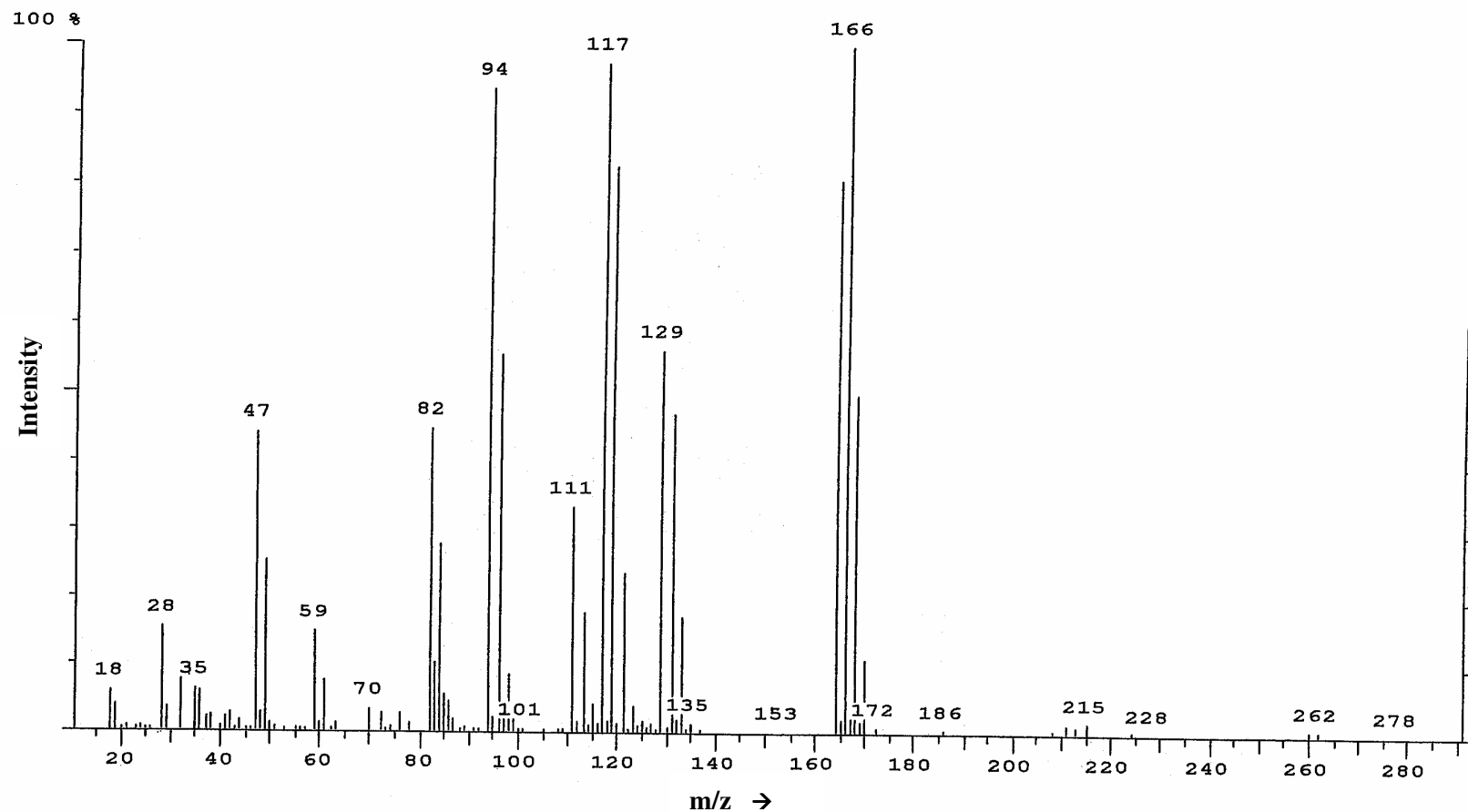


Figure a. MS of tetrachloroethene from ozonated CCl₄ sample.

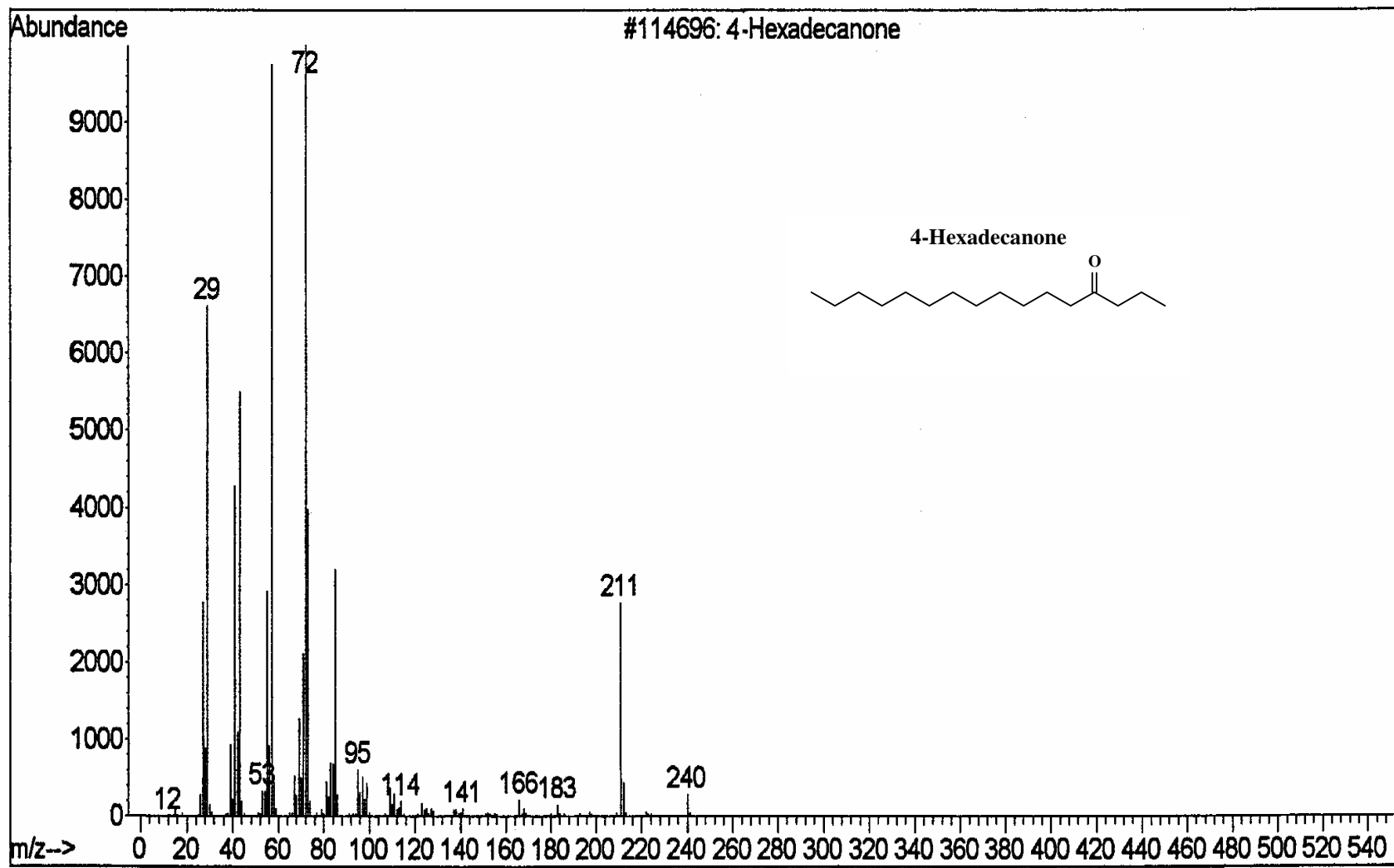


Figure b. MS of 4-hexadecanone.

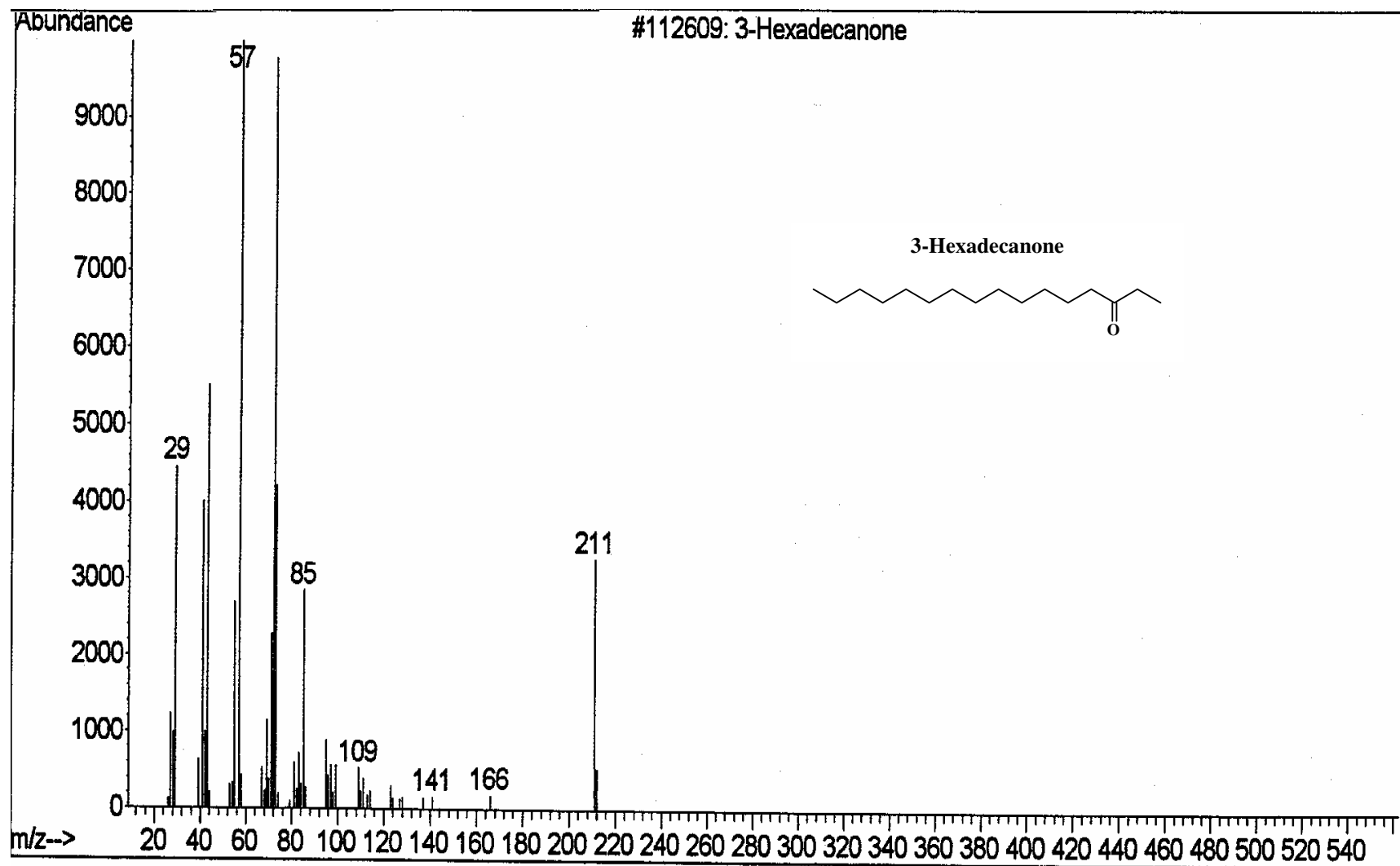


Figure c. MS of 3-hexadecanone.

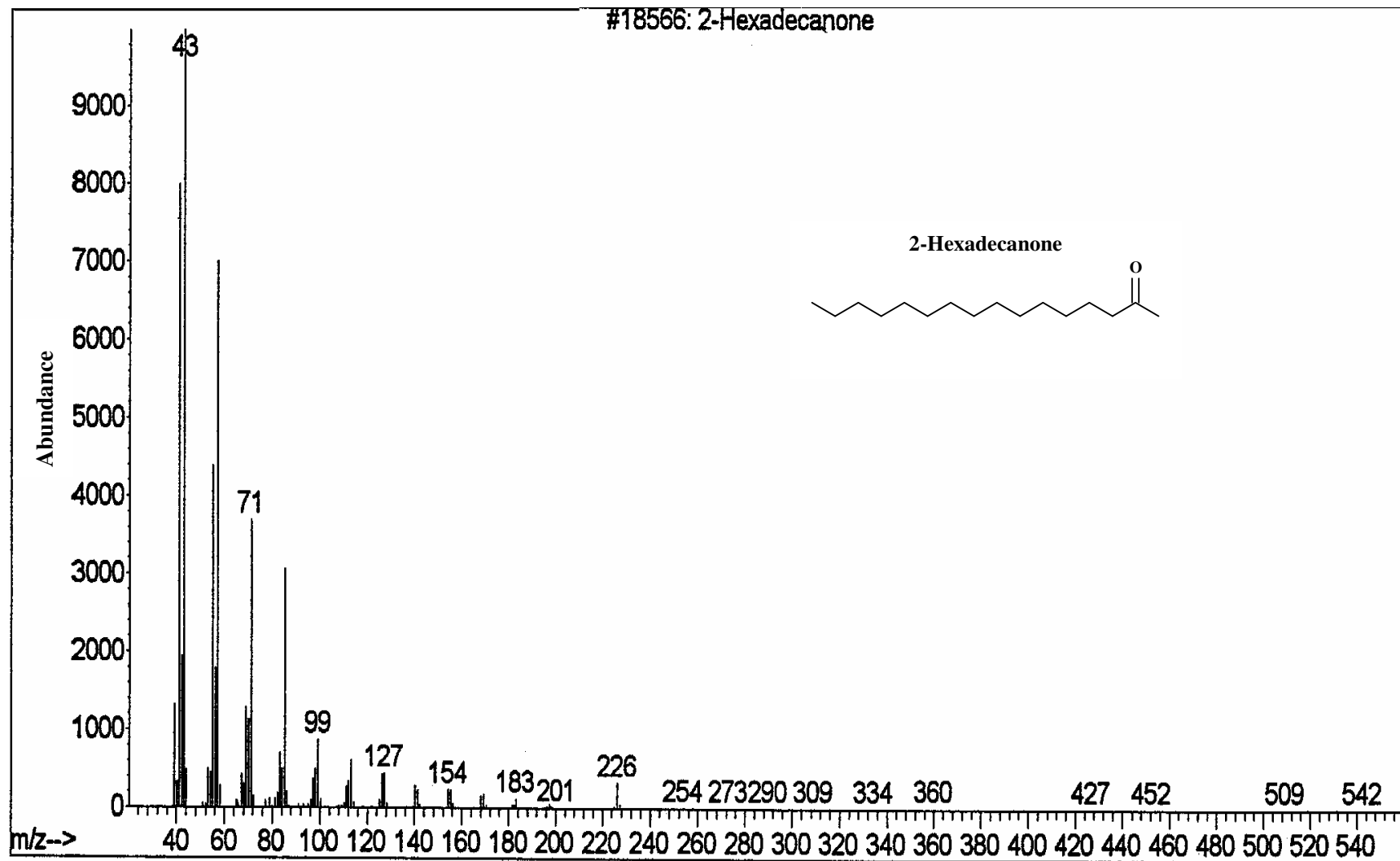


Figure d. MS of 2-hexadecanone.

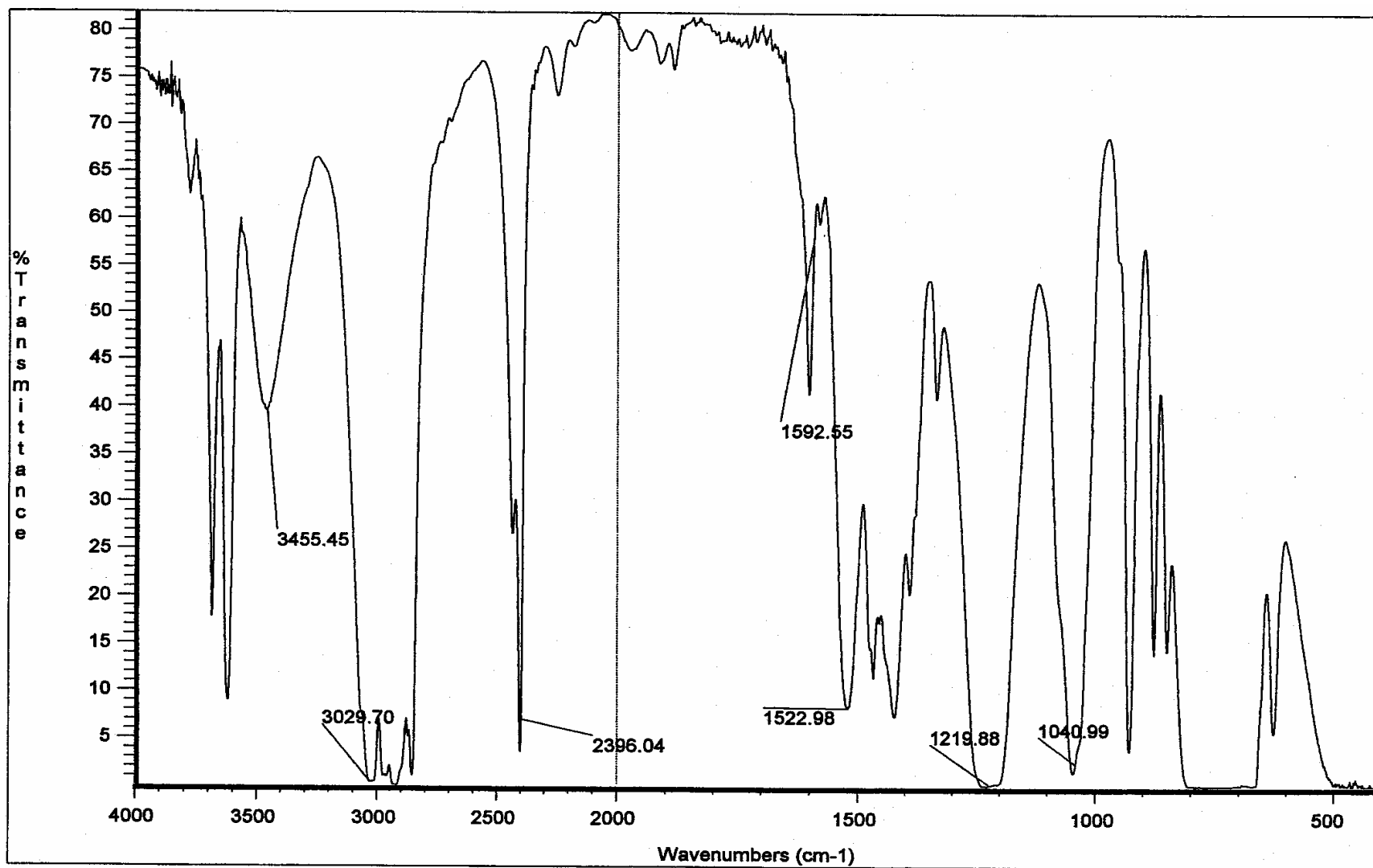


Figure e. IR spectrum of pure n-hexadecane.

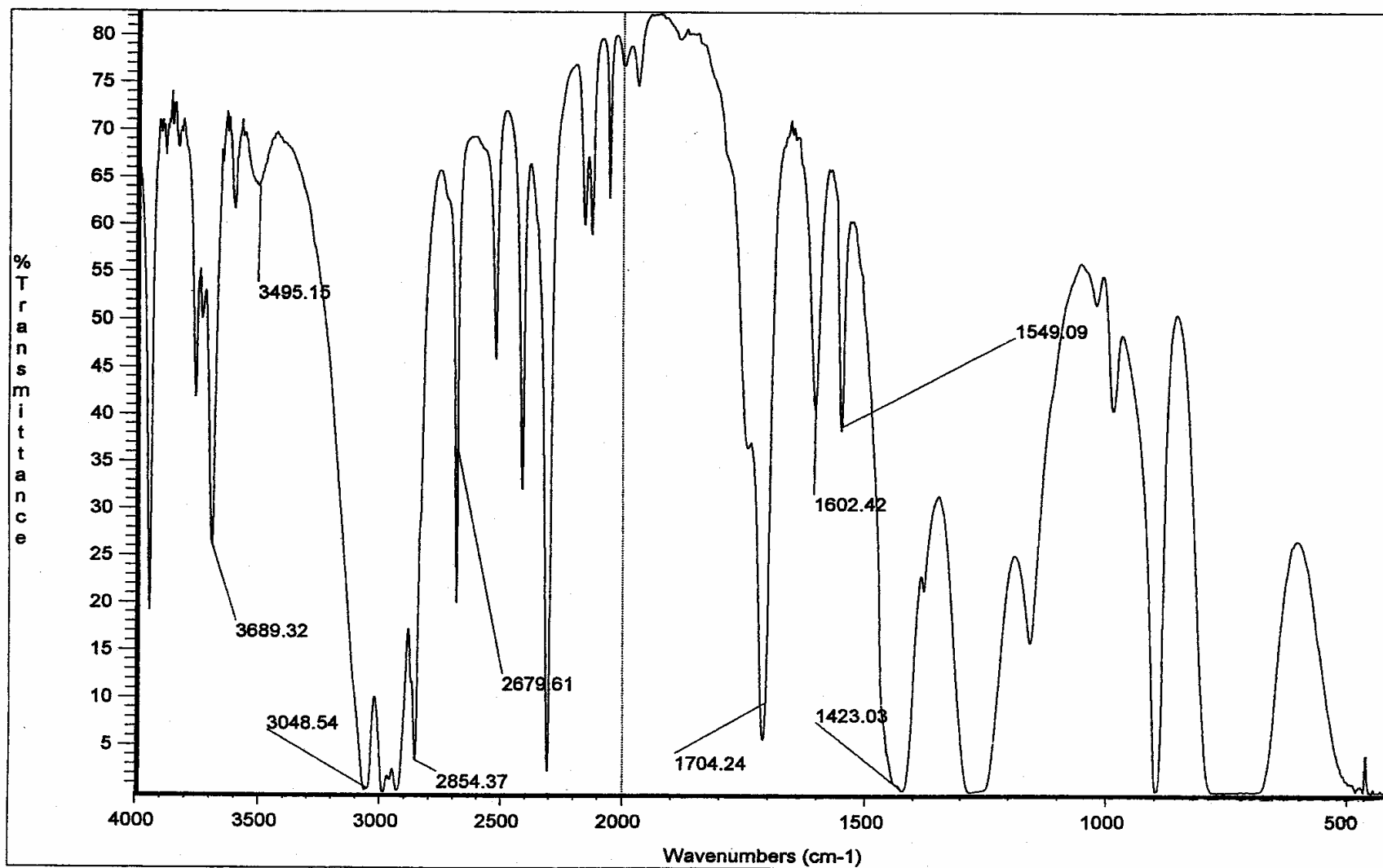


Figure f. IR spectrum of ozonated n-hexadecane.

3-Hexadecanone

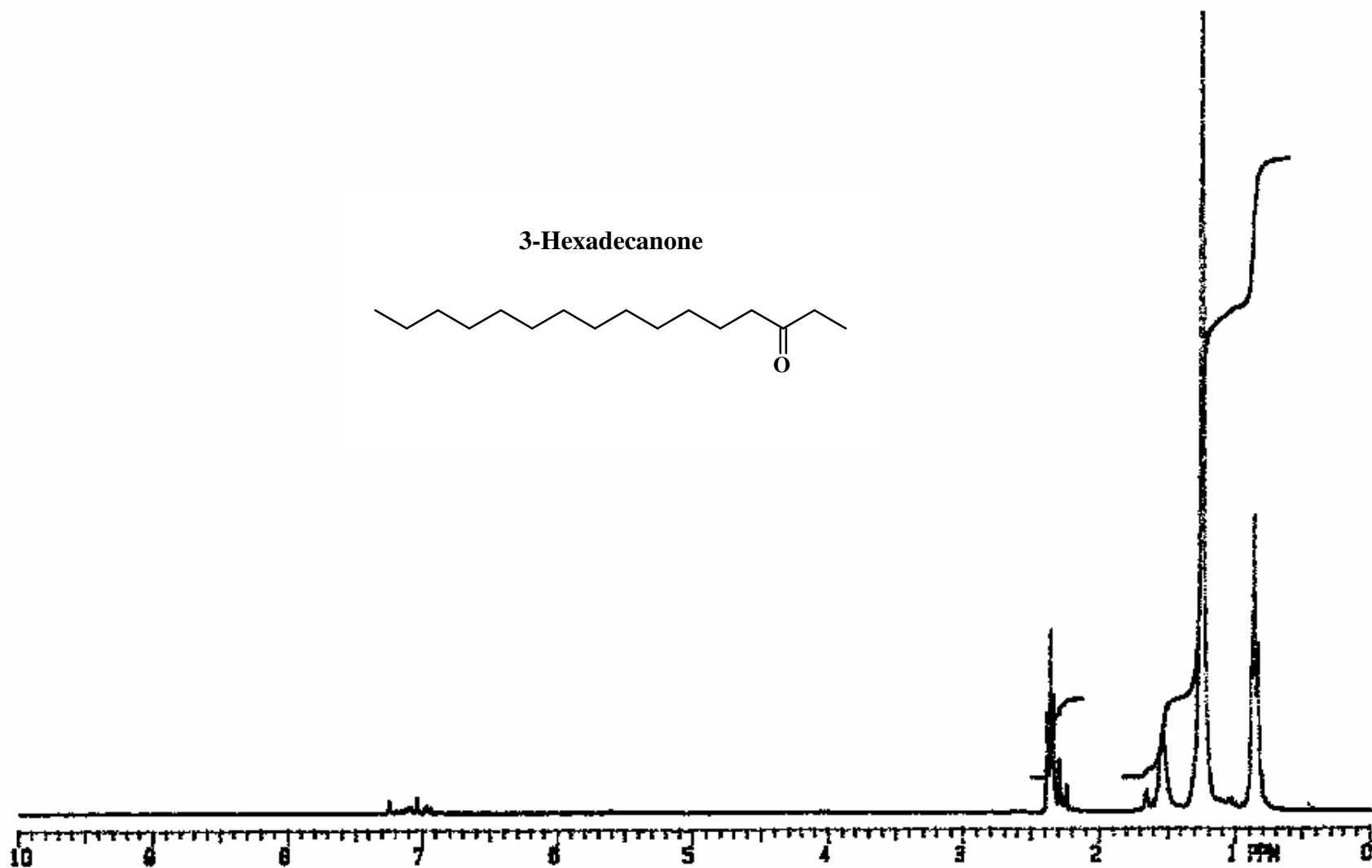
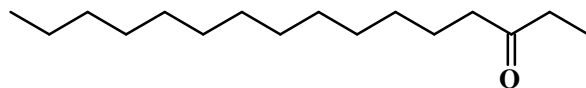


Figure g. ^1H NMR spectrum of 3-hexadecanone.

2-Hexadecanone

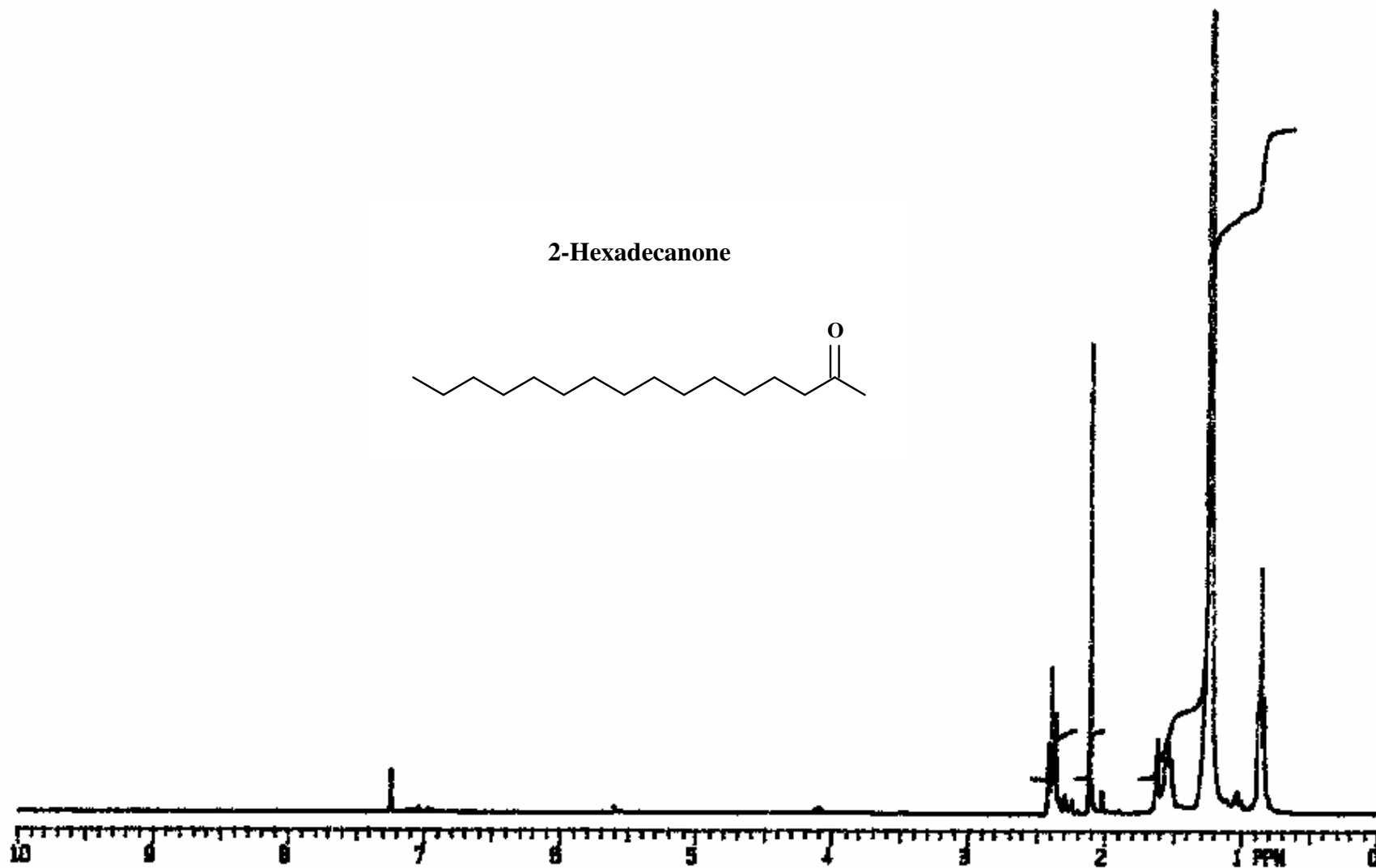
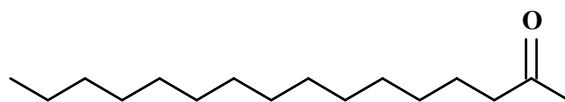


Figure h. ^1H NMR spectrum of 2-hexadecanone.

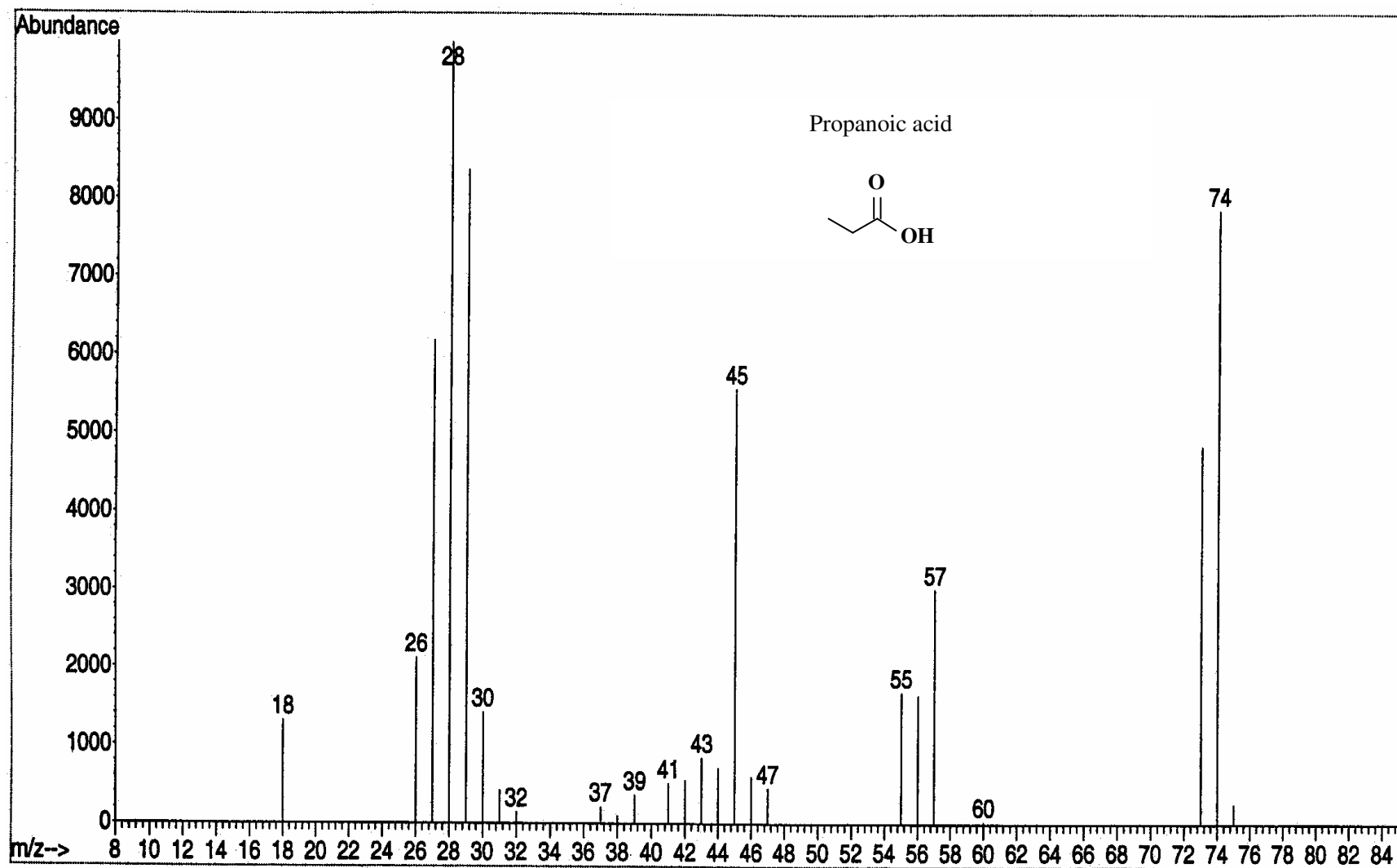


Figure i. MS of Propanoic acid.

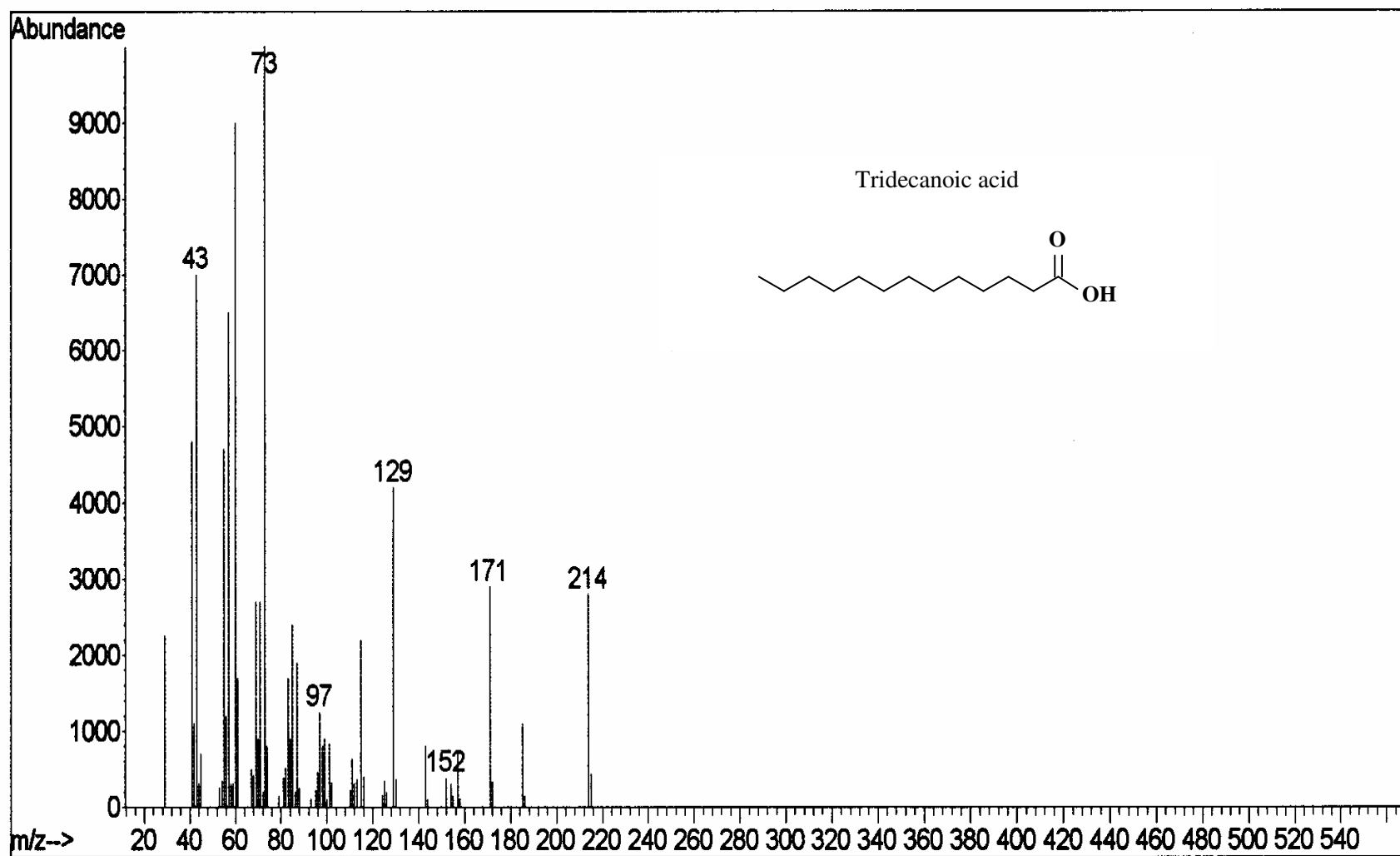


Figure j. MS of Tridecanoic acid.